Copyrighted Material




# ADVANCES IN QUANTUM CHEMISTRY

Volume 23

Per-Olov Löwdin

Copyrighted Material

EDITORIAL BOARD

David P. Craig (Canberra, Australia)
Raymond Daudel (Paris, France)
Ernst R. Davidson (Bloomington, Indiana)
Inga Fischer-Hjalmars (Stockholm, Sweden)
Kenichi Fukui (Kyoto, Japan)
George G. Hall (Kyoto, Japan)
Masao Kotani (Tokyo, Japan)
Frederick A. Matsen (Austin, Texas)
Roy McWeeney (Pisa, Italy)
Joseph Paldus (Waterloo, Canada)
Ruben Pauncz (Haifa, Israel)
Siegrid Peyerimhoff (Bonn, Germany)
John A. Pople (Pittsburgh, Pennsylvania)
Alberte Pullman (Paris, France)
Bernard Pullman (Paris, France)
Klaus Ruedenberg (Ames, Iowa)
Henry F. Schaefer III (Athens, Georgia)
Au-Chin Tang (Kirin, Changchun, China)
Rudolf Zahradnik (Prague, Czechoslovakia)

ADVISORY EDITORIAL BOARD

David M. Bishop (Ottawa, Canada)
Jean-Louis Calais (Uppsala, Sweden)
Giuseppe del Re (Naples, Italy)
Fritz Grein (Fredericton, Canada)
Andrew Hurley (Clayton, Australia)
Mu Shik Jhon (Seoul, Korea)
Mel Levy (New Orleans, Louisiana)
Jan Linderberg (Åarhus, Denmark)
William H. Miller (Berkeley, California)
Keiji Morokuma (Okazaki, Japan)
Jens Oddershede (Odense, Denmark)
Pekka Pyykkö (Helsinki, Finland)
Leo Radom (Canberra, Australia)
Mark Ratner (Evanston, Illinois)
Dennis R. Salahub (Montreal, Canada)
Isaiah Shavitt (Columbus, Ohio)
Per Siegbahn (Stockholm, Sweden)
Harel Weinstein (New York, New York)
Robert E. Wyatt (Austin, Texas)
Tokio Yamabe (Kyoto, Japan)

# *ADVANCES IN*
# QUANTUM CHEMISTRY

EDITOR-IN-CHIEF

**PER-OLOV LÖWDIN**

ASSOCIATE EDITORS

**JOHN R. SABIN AND MICHAEL C. ZERNER**

QUANTUM THEORY PROJECT
UNIVERSITY OF FLORIDA
GAINESVILLE, FLORIDA

## VOLUME 23



ACADEMIC PRESS, INC.

**Harcourt Brace Jovanovich, Publishers**

San Diego New York Boston London Sydney Tokyo Toronto

*Academic Press Rapid Manuscript Reproduction*

Research work for this book performed in part by the Los Alamos National Laboratory under the auspices of the United States Department of Energy.

This book is printed on acid-free paper. ♾

Copyright © 1992 by ACADEMIC PRESS, INC.
All Rights Reserved.
No part of this publication may be reproduced or transmitted in any form or by any means, electronic or mechanical, including photocopy, recording, or any information storage and retrieval system, without permission in writing from the publisher.

Academic Press, Inc.
San Diego, California 92101

*United Kingdom Edition published by*
Academic Press Limited
24–28 Oval Road, London NW1 7DX

Library of Congress Catalog Number: 64-8029

International Standard Book Number: 0-12-034823-3

PRINTED IN THE UNITED STATES OF AMERICA
92 93 94 95 96 97 QW 9 8 7 6 5 4 3 2 1

# Contributors

*Numbers in parentheses indicate the pages on which the authors' contributions begin.*

**Hans Ågren** (4), Institute of Quantum Chemistry, University of Uppsala, S-751 20 Uppsala, Sweden

**L. C. Biedenharn** (129), Department of Physics, Duke University, Durham, North Carolina 27706

**Amary Cesar** (4), Institute of Quantum Chemistry, University of Uppsala, S-751 20 Uppsala, Sweden

**Dieter Cremer** (206), Theoretical Chemistry, University of Göteborg, S-41296 Göteborg, Sweden

**Jürgen Gauss** (206), Theoretical Chemistry, University of Göteborg, S-41296 Göteborg, Sweden

**Christoph-Maria Liegener** (4), Theoretical Chemistry, Friedrich Alexander University, D-8520 Erlangen, Germany

**J. D. Louck** (129), Los Alamos National Laboratory, Theoretical Division, Los Alamos, New Mexico 87545

**Per-Olov Löwdin** (84), Departments of Chemistry and Physics, Quantum Theory Project, University of Florida, Gainesville, Florida 32611

**A. B. Sannigrahi** (302), Department of Chemistry, Indian Institute of Technology, Kharagpur 721302, India

# Preface

In investigating the highly different phenomena in nature, scientists have always tried to find some fundamental principles that can explain the variety from a basic unity. Today they have not only shown that all the various kinds of matter are built up from a rather limited number of atoms, but also that these atoms are constituted of a few basic elements of building blocks. It seems possible to understand the innermost structure of matter and its behavior in terms of a few elementary particles: electrons, protons, neutrons, photons, etc., and their interactions. Since these particles obey not the laws of classical physics but the rules of modern quantum theory of wave mechanics established in 1925, there has developed a new field of "quantum science" which deals with the explanation of nature on this ground.

Quantum chemistry deals particularly with the electronic structure of atoms, molecules, and crystalline matter and describes it in terms of electronic wave patterns. It uses physical and chemical insight, sophisticated mathematics, and high-speed computers to solve the wave equations and achieve its results. Its goals are great, and today the new field can boast of both its conceptual framework and its numerical accomplishments. It provides a unification of the natural sciences that was previously inconceivable, and the modern development of cellular biology shows that the life sciences are now, in turn, using the same basis. "Quantum biology" is a new field which describes the life processes and the functioning of the cell on a molecular and submolecular level.

Quantum chemistry is hence a rapidly developing field which falls between the historically established areas of mathematics, physics, chemistry, and biology. As a result there is a wide diversity of backgrounds among those interested in quantum chemistry. Since the results of the research are reported in periodicals of many different types, it has become increasingly difficult for both the expert and the nonexpert to follow the rapid development in this new borderline area.

The purpose of this serial publication is to try to present a survey of the current development of quantum chemistry as it is seen by a number of the internationally leading research workers in various countries. The authors have been invited to give their personal points of view of the subject freely and without severe space limitations. No attempts have been made to avoid overlap—on the contrary, it has seemed desirable to have certain important research areas reviewed from different points of view.

The response from the authors and the referees has been so encouraging that a series of new volumes is being prepared. However, in order to control production costs and speed publication time, a new format involving camera-ready manuscripts is being used from Volume 20. A special announcement about the new format was enclosed in that volume (page xiii).

In the volumes to come, special attention will be devoted to the following subjects: the quantum theory of closed states, particularly the electronic structure of atoms, molecules, and crystals; the quantum theory of scattering states, dealing also with the theory of chemical reactions; the quantum theory of time-dependent phenomena, including the problem of electron transfer and radiation theory; molecular dynamics; statistical mechanics and general quantum statistics; condensed matter theory in general; quantum biochemistry and quantum pharmacology; the theory of numerical analysis and computational techniques.

As to the content of Volume 23, the Editors would like to thank the authors for their contributions, which give an interesting picture of part of the current state of the art of the quantum theory of matter: from the theory of molecular Auger spectra, over linear algebra and its application to the search fo linear relations in quantum chemistry as well as in other sciences–e.g., econometrics, canonical and non-canonical methods in group theory and group algebra, analytical energy gradient methods in computational quantum chemistry, to *ab-initio* molecular orbital calculations.

It is our hope that the collection of surveys of various parts of quantum chemistry and its advances presented here will prove to be valuable and stimulating, not only to the active research workers but also to the scientists in neighboring fields of physics, chemistry, and biology who are turning to the elementary particles and their behavior to explain the details and innermost structure of their experimental phenomena.

PER-OLOV LÖWDIN

# THEORY OF MOLECULAR AUGER SPECTRA

HANS ÅGREN and AMARY CESAR
Institute of Quantum Chemistry,
University of Uppsala
Box 518, S-751 20 Uppsala, Sweden

CHRISTOPH-MARIA LIEGENER
Chair for Theoretical Chemistry,
Friedrich Alexander University
D-8520 Erlangen, Germany

ADVANCES IN QUANTUM CHEMISTRY
VOLUME 23



Copyright © 1992 By Academic Press, Inc.
All rights of reproduction in any form reserved.

# Contents

**1 Abstract**

**2 Introduction**

**3 Molecular Auger as a Scattering Process**

3.1 Many Channel Scattering Theory

3.2 The Direct Contributions to the Auger Cross Section

3.3 The Resonant Contributions to the Auger Cross Section

3.4 Local Approximation of the Nuclear Motion

3.5 State Interference Effects

3.6 Post-Collision Interaction (PCI)

**4 Vibronic Interaction in Auger Spectra**

4.1 Vertical and Adiabatic Approaches

4.2 Lifetime-Vibrational Interference Effects

4.3 Evaluation of Franck-Condon Factors

**5 Auger Transition Rates**

5.1 Auger Transition Rates From General Many-Electron Wave Functions

5.2 Frozen Orbital Approximation

5.3 Role of Relaxation

5.4 Auger Electron Functions and Transition Moments

**6 Analysis of Molecular Auger Spectra**

6.1 The Many-Body Factor

6.2 The Molecular Orbital Factor

6.3 Comparative Analysis of Auger and Photoelectron Spectra

**7 One-Particle Methods**

**8 Wave Function Methods**

8.1 Open-shell Restricted Hartree-Fock (OSRHF)

8.2 Multi-Configuration Self-Consistent Field (MCSCF)

8.3 Semi-Internal Configuration Interaction (SEMICI)

**9 Green's Function Methods**

9.1 Two-particle Green's Functions

9.2 The Bethe-Salpeter Equation

9.3 Higher Order Irreducible Vertex Parts

9.4 Other Possibilities to Treat the Two-particle Green's Function

9.5 Three-particle Green's Functions

**10 Other Methods**

**11 Applications**

11.1 Chemical Information in Auger Spectra

11.2 Hybridization

11.3 Functional Groups

11.4 Fingerprinting

11.5 Symmetry

11.6 Relation to Solid State Spectra

11.7 Survey of Applications

**12 Sample Analysis: Carbon Monoxide**

12.1 Hole-mixing Auger States

12.2 Assignment

12.3 Satellites

**13 Conclusions and Outlook**

# 1 Abstract

We review theory for molecular Auger spectra, in particular molecular valence Auger spectra. Starting from general scattering equations we display systematically a set of approximations used for computation of Auger spectra. We focus on the consequences of the scattering formulation of the Auger effect for systems with vibrational degrees of freedom, and display the analytical expressions for the vibronic interactions and excitations that can be derived therefrom. The role of direct versus resonant contributions and the descriptions in terms of one- versus two-step processes for the molecular Auger cross sections are formalized and discussed. The role of lifetime-vibrational interference and the state interference effects, and the implications of these effects for interpreting fine structures in molecular Auger spectra is elucidated in some detail.

We discuss the analysis of Auger spectra using many-electron and one-particle theories. The derivation of the cross sections for Auger emission applying general many-electron wave functions is shortly recapitulated. Cross sections for some special cases are derived therefrom; single-determinant approximation of initial states, frozen orbital approximation and the relaxed orbital approximation. The structure of the many-body and the molecular orbital factors derived from the Fermi golden rule expressions are analyzed. The structure of these factors and their consequences for the interpretation of the Auger spectra in different energy regions, viz. inner-inner, inner-outer and outer-outer regions, are discussed. The appearance and character of so-called one-particle states, hole-mixing states, breakdown states, and correlation satellite states are commented in that context. We comment on the use of single versus many-channel approximations for the outgoing Auger wave, and approaches to optimize the outgoing Auger wave in the non-isotropic molecular potential. We also make some brief statements on comparative analysis of photoelectron and Auger spectra, i.e. on similarities in terminology and approximations in deriving properties of valence single- and two-hole states, respectively.

We classify the main computational approaches that have been employed to analyze Auger spectra, namely the one-particle approach, the wave function approach and the Green's function approach. The wave function approach is reviewed with respect to the use of open-shell and multi-configurational self-consistent field, (OSRHF and MCSCF) and semi-internal configuration interaction (SEMICI) methods. We review different possibilities to treat the two-particle and three-particle Greens functions to analyze Auger spectra.

Aspects of Auger studies with respect to electronic structure analysis in general, on local electronic structures that "fingerprint" spectra, molecular orbital analysis, symmetry considerations, role of hybridization and functional groups, and relation to solid state spectra etc., are recapitulated in a separate section. Finally, some of the merits and limitations of these computational approaches are evaluated for Auger spectra of one and the same species, namely, for the oxygen and carbon spectra of carbon monoxide.

# 2 Introduction

Auger electron emission occurs spontaneously from highly excited and ionized states and may be described theoretically as the interaction between a discrete initial and a continuum final state of the same energy. The final state consists of a discrete state with one electron missing and an electron in a continuum orbital. To a first approximation, the expelled Auger electrons have characteristic energies dependent only on the type of sample, but independent of the ionizing agent[1]. Their kinetic energies are therefore direct measures of the energy levels of the final sample ions.

Auger spectra have extensively been used for sample analysis of elements and for surface structure analysis by means of so-called scanning Auger and surface imaging Auger techniques[2]. For molecules the Auger experiment has mostly been used as a spectroscopic tool to obtain information on dicationic state. It is in this respect complementary to other experimental methods, e.g. double-charge-transfer (DCT) spectroscopy[3], charge-stripping mass (CSM) spectroscopy[4], and double coincidence experiments [5,6,7], namely photoion-photoion (PIPICO), photoelectron-photoion (PEPICO) or photoelectron-photoelectron (PEPECO) experiments.

In theoretical research Auger spectra have been analyzed in terms of the electronic and conformational structures of ionic states, but have also been used as probes for the dynamics of electron-molecule scattering processes. For molecules the Auger spectra have mostly been used in the first of these two respects, i.e. for the study of electronic structures of doubly charged molecular ions, in particular of their molecular orbital and the many-body characters. A variety of methods have been proposed with applications that cover a broad range of physically and chemically interesting problems. The analysis of molecular Auger spectra have thus concerned symmetry, delocalization, hybridization and bonding. They have also concerned more subtle effects such as vibronic couplings, fine structures and the associated information on force fields and equilibrium structures of ionic states. The breakdown effect, that is the breakdown of the molecular orbital picture, is known from photoelectron spectroscopy[8,9]. It has been demonstrated and analyzed in that conext in a number of articles [10,11]. Another effect which is known from the photoelectron case is hole-mixing, see e.g. ref. [12], namely the configuraion interaction of one-hole states of equal symmetry. All these effects appear as well for the Auger final states, see e.g. ref. [13].

Three types of molecular Auger spectra can be distinguished, those spectra involving transitions between core shells only, those for which one of the final state vacancies has valence character, and into those spectra in which both final state vacancies are distributed among valence molecular orbitals. The core type spectra are rather straightforward to interpret since they essentially exhibit atomic character. These spectra show an internal invariance with respect to energies and intensities, but respond to different ligand substitutions with small but uniform shifts, the Auger chemical shifts. The second kind of spectra, e.g. KLM spectra of second row molecules are very weak, and have rarely been investigated, neither experimentally nor theoretically. The third kind of spectra, the molecular valence spectra (so-called CVV spectra), are governed by non-radiative emission between initial, well localized, core hole states and final states with holes among the valence orbitals. They are the ones most commonly investigated experimentally and theoretically, partly because they refer directly to electronic structure theory, *viz.* molecular orbital and many-electron theory, but also to the conformation of two-hole ions. The condition for resolving such spectra with respect to molecular

orbital theory and, in particular, with respect to fine structure is that the initial state lifetime width ($\Gamma$) is sufficiently small. Only if the initial state resides in the penultimate main shell, i.e. the outermost core shell, $\Gamma$, is small enough compared to $\omega$ (the MO or vibrational splittings), while $\Gamma \gg \omega$ for all other shells. These spectra are thus the objects for the present review.

The Auger spectra show considerable structure over a wide energy range. The high density of states and the lack of strict selection rules makes the analysis Auger spectra complicated. For smaller species the outermost low kinetic energy part resolves structures that can be described in terms of MO theory and even ni terms of vibronic excitations, while the spectra grow progressively more complicated at higher kinetic energies. To this one should add contributions of inelastic scattering and satellite processes, such as resonance Auger or Auger transitions from initial core excited or core-ionized states.

The final states of molecular Auger transitions are naturally divided into three classes, comprising outer-outer, inner-outer and inner-inner valence states. These three groups of states represent fairly non-overlapping energy regions and have rather different characteristics with respect to relaxation energy, electron correlation, transition amplitudes and vibrational (dissociative) broadenings, etc. Most of the intensity is gathered into the outer-outer group of states, while for the other groups structure is often blurred by dissociative broadening and overlapping satellites. From the theoretical point of view these three spectral regions can roughly be described as one-particle states, hole-mixing states and states with breakdown of MO theory, respectively.

Final state correlation effects and the breakdown of the one-particle picture, i.e. of the orbital description is of great importance in many molecular spectra. It means that one finds more lines than two-hole combinations of orbitals in these spectra. These effects are due to energetic quasi-degeneracies between two-hole states with and without hole-particle (shake-up) excitations, which frequently occur in the inner and intermediate valence regions. Such interactions happen to be more pronounced for molecules than for atoms, the more so the more unsaturated the bonding. This is the reason that these effects are studied more extensively for molecules, although they can, in principle, occur for atoms as well. In fact, for molecules they are likely to arise already for systems containing first-row atoms, whereas for atoms they can be expected only for the heavier ones, starting with Xenon. The development in electronic structure theory has been directed mainly on the evaluation of stationary state properties of the doubly ionized molecules. Not so much work has been dealing with the dynamical aspects of the molecular Auger process, although the physics of this seems to be well understood. The reason for the above choice of priorities is probably to be found in the computational problems inherent to scattering theory for nonspherical systems. The systems for which a detailed analysis of the spectral lineshape beyond the orbital picture has been performed, cover by now a representative cross-section of chemically relevant small molecules and progress is being made toward larger molecules.

The first direct applications of quantum methods on Auger or double hole states were carried in the 60's by Hurley[14]. However, except for this study, very little was accomplished until the mid 70's for the theoretical description of double or multiple-hole states in molecules. The early investigations on molecular Auger were therefore concerned with some basic methodological aspects of the calculation of such states[15,16,17]. The theoretical analysis has focussed on two classes os small molecules; the first and second row hydrides and the first row diatomics, and only few applications on larger molecules have been carried out. The hydrides form a bridge between well-established

atomic Auger spectra with a simple interpretation and the complicated Auger spectra of "electron rich" molecules, and this has made them prototypes for a number of theoretical investigations.

The computational methods fall into two major classes; wave function and Green's functions methods. The former can be further distinguished into one-particle, open-shell self-consistent field (OSSCF,OSRHF), multi-configurational self-consistent field (MCSCF), and semi-internal configuration interaction (SEMICI) approaches. As will be discussed in this review, many calculations of molecular Auger spectra have been performed by ab initio wave function methods, e.g. [13,18]. Apart from ab initio calculations also semiempirical approaches have been frequently employed [19]. Green's function or propagator methods have been widely used in quantum chemical calculations of ionization potentials and excitation energies[10,11,20,21,22,23,24]. However, while particle-particle Green's functions are well-known tools in quantum physics [25,26,27], ab initio correlation calculations of double ionization potentials (and thus relative Auger energies) of finite electronic systems by Green's function methods seem to have performed only in the past decade[28,29,30,31,32,33,34].

The theory of the Auger effect was reviewed in 1982 by Åberg and Howat[35] giving much attention to the aspect of the Auger effect as a one-step resonant scattering process. Although there has been a considerable progress in the theory of Auger spectra in the past 15 years there seems not yet to exist a comprehensive review of this field focussing on molecules. The work presented here concern the theory as well as methods for calculations of molecular Auger spectra, especially molecular valence Auger spectra. We will in particular focus on the implication of the scattering theory formulation of molecular Auger, the one-particle and many-particle interpretations of Auger states and also on computational schemes basing on the one-particle (molecular orbital) and many-particle approximations. Fine structure and interference (lifetime-vibrational- and state interference) effects are derived from the scattering formulation. The various simplified forms for calculating Auger rates are recapitulated, and the "chemical" aspects involved in the analysis of Auger spectra are reviewed, such as interpretations in terms of hybridization and bonding and of local electronic structures in general.

# 3 Molecular Auger as a Scattering Process

Modern formulations of the Auger process follow many-channel resonant scattering theory [35] with roots in the classical work of Fano[36] on the theory for configuration interaction among continuum states. The scattering theory formulation of the Auger process in molecules[37] follows that for the atomic case. The main difference between the two cases is that the nuclear degrees of freedom increase the number of available open scattering channels and create additional vibronic coupling between these channels. The generalization of the conventional analysis of molecular Auger spectra from a two-step to a one-step process is necessary for several reasons. An explicit consideration of the excitation process is required for describing the vibrational and state interference effects, and for the calculation of the Auger lines profiles. There will in general be a contribution from the nuclear degrees of freedom to the core hole state lifetimes and the discrete-continuum interaction energies. There will be inter- and intra-channel couplings in the electronic wave function depending on the nuclear motion. Furthermore, the total scattering cross section includes also the possibility of the direct scattering events for which vibronic coupling may play a role.

The generalization of the scattering theory formulation of Auger to include molecules was earlier given by Cesar et al[37], emphasizing the consequences for the vibronic cross sections and the fine structure analysis. A theory was presented where an explicit assumption of the validity of the Born-Oppenheimer approximation was made for the asymptotic vibronic states of the initial and final states but where the true electronic-vibrational states were assumed to represent the true continuum molecular wave functions. Attention was given to how the vibronic channel coupling is included into the transition amplitudes of the direct and resonant scattering events, and its relative importance for the observed spectral functions.

In the present section we review the scattering formulation of molecular Auger. The presentation assumes a non-relativistic, non-PCI (post-collision interaction) treatment of photon induced molecular Auger spectra. The formulation as such, however, lends itself for an "afterwards" generalization to situations where these restrictions are not appropriate.

## 3.1 Many Channel Scattering Theory

Let us assume a total Hamiltonian $\hat{H}$ that comprises terms due to the molecular target, the radiation field and the the molecule-radiation interaction

$$\hat{H} = \hat{H}_m + \hat{H}_r + \hat{H}_{mr} \tag{1}$$

It can conveniently be splitted into contributions from the usual Hamiltonian for the electronic (including nuclear repulsion) $\hat{H}_{el}$ and nuclear kinetic energy operator $\hat{T}$,

$$\hat{H} = \hat{H}_{el} + \hat{T} + \hat{H}_r + \hat{H}_{mr}. \tag{2}$$

The vector space we choose as domain for the operator $\hat{H}$ contains the basic elements: $|i\omega>$, $|\varphi\varepsilon_1>$ and $|A\varepsilon_1\varepsilon_2>$. The first of these state vectors, $|i\omega>$, represents the molecule in its initial electronic-vibrational ground state and a photon carrying an energy $\hbar\omega$ and linear momentum $k$. The final molecular states in the scattering process are described by the state vectors $|A\varepsilon_1\varepsilon_2>$, specified by the several (vibronic) open

channels collectively labeled by $A$ and by the energies $\varepsilon_1$ and $\varepsilon_2$ of the two electrons in the continuum. These final molecular states are formed as a result of either a direct, one-photon two-electron, scattering event or a resonant scattering event mediated by the intermediate states represented by the state vectors $|\varphi e_1>$. These states contain information on the residual core-hole molecular species in the electronic-vibrational state $\varphi$ and a single (primary) escaping photoelectron with energy $\varepsilon_1 = \omega - I_\varphi$. $I_\varphi$ is the threshold energy for the $\varphi^{th}$ ionization potential of the molecule. The energy of the second electron participating in the process, $\varepsilon_2$, the Auger electron, is under most of the usual experimental conditions a characteristic of the molecular ion. It depends solely on the intermediate and final vibronic states, i.e., $\varepsilon_2 = I_\varphi - I_A$. In this section we will use the simplifying assumption that the resonant events proceed via a single intermediate core-hole state isolated from all other near-lying neighbours. A more complete treatment accounting for several close-lying core-hole states, such as those that are members of a Rydberg series, is given in subsection 3.5. Also, in the rest of this section we review the aspect of the theory which refers to a high excess of energy carried by the primary photoionized electron $e_1$, i.e. to the cases when appreciable post-collision interaction (PCI) between the photoelectron and any of the particles involved in the decay processes can be neglected. The effect of PCI is briefly discussed in subsection 3.6. Furthermore, we will not be discussing the aspects related to the angular distributions neither for the primary photoionized nor for the secondary Auger electrons. For the theory of Auger electron angular distributions for atoms we refer to refs. [38,39,35]. An average on the rotational degrees of motion or rotational interactions are assumed throughout and the final cross sections, eqs. 35 and 39, should thus be interpreted as cross sections for scattering of a particle on a molecule with a fixed orientation in space, averaged over all molecular orientations and integrated for all directions of the emitted particle. In cases where the incoming photons are participating one should also sum over the initial and average over the final polarization states. This last approximation allows the specification of the continuum part of the system by just using one label, namely the excess energy $\varepsilon \equiv \varepsilon_\alpha = \frac{1}{2}k_\alpha^2$ for the particle in the continuum relative to the total energy of the residual ionic species. The latter is defined here as the $\alpha^{th}$ open channel.

We will divide the state vector space into two interacting subspaces and study direct and resonant scattering processes separately. The subspace I, the resonant space, contains only one bound state vector, namely $|\varphi\varepsilon_1>$, while the subspace II, hereafter the background continuum, is spanned by the scattering state vectors $|i\omega>$ and $|A\varepsilon_1\varepsilon_2>$ having at most one particle in the continuum. The reason behind the assumption of just one particle in the background continuum subspace is that we neglect the PCI effects. When this condition is fulfilled it is reasonable to consider the one-electron state vector $|\varepsilon_1>$ as strongly orthogonal to, i.e. decoupled from, the state vectors $|\varphi>$ and $|A\varepsilon_2>$. We can therefore take the state vectors that contain the primary photoelectron $e_1$ formed as a direct product of state vectors of type $|\varphi\varepsilon_1>=|\varphi>\otimes|\varepsilon_1>$, $|A\varepsilon_1\varepsilon_2>=|A\varepsilon_1>\otimes|\varepsilon_1>$.

We introduce now the coordinate representation for the electronic component (or projection) of the states vectors above considered. We associate $\psi_{\alpha\varepsilon}(\mathbf{r};\mathbf{R})$ $(\alpha = i, A)$ and $\varphi(\mathbf{r};\mathbf{R})$ to the wave functions belonging to the background and the resonant subspaces, respectively. In what follows we shall use $\mathbf{r}$ collectively for the spatial coordinates of all electrons and $\mathbf{R}$ for the nuclear coordinates. Following the standard convention we have separated the electronic and nuclear coordinates in the wave functions by a semi-colon, emphasizing the functional dependence on the electronic coordinates, and the parametric dependence on the nuclear coordinates; i.e., for each fixed molecular conformation a set of purely electronic wave functions $\psi_{\alpha\varepsilon}(\mathbf{r};\mathbf{R})$ or $\varphi(\mathbf{r};\mathbf{R})$ are constructed.

The scattering functions $\psi_{\alpha\varepsilon}(\mathbf{r};\mathbf{R})$ are chosen to fulfill the boundary condition for standing scattering waves

$$\psi_{\alpha\varepsilon}(\mathbf{r};\mathbf{R}) \sim_{r\to\infty} \frac{\Omega_\alpha(\mathbf{r}';\mathbf{R})}{r\sqrt{k_\alpha}} \sin(k_\alpha r + \delta_\alpha(\varepsilon)) \tag{3}$$

while the resonant wave function $\varphi(\mathbf{r};\mathbf{R})$ must have a vanishing limit for $r \to \infty$ because it represents a bound state function, i.e.

$$\varphi(\mathbf{r};\mathbf{R}) \longrightarrow 0 \quad \text{as} \quad r \to \infty. \tag{4}$$

$\Omega_\alpha(\mathbf{r}';\mathbf{R})$ denotes the wave functions of the bound electronic state defined by the $\alpha^{\text{th}}$ channel. $r(=|\mathbf{r}|)$ and $\mathbf{r}'$ stands for the spatial coordinates of the escaping particle and the molecular bound electrons, respectively, and $\delta_\alpha(\varepsilon)$ for a phase-shift related to the scattering process. At this stage we introduce the electronic-vibrational wave function for the asymptotic states of the continuum background by imposing the Born-Oppenheimer (BO) approximation that assumes the complete separability of the electronic and nuclear motions present in a molecular system. We write the electronic-vibrational asymptotic wave functions as

$$\Omega_{\alpha n_\alpha}(\mathbf{R},\mathbf{r}') = \Omega_\alpha(\mathbf{r}';\mathbf{R})\chi_{n_\alpha}(\mathbf{R}), \tag{5}$$

where,

$$^N\hat{H}_{el}\Omega_\alpha(\mathbf{r}';\mathbf{R}) = {}^NE_\alpha(\mathbf{R})\Omega(\mathbf{r}';\mathbf{R}); \qquad (\alpha = i), \tag{6}$$

$$^{N-2}\hat{H}_{el}\Omega_\alpha(\mathbf{r}';\mathbf{R}) = {}^{N-2}E_\alpha(\mathbf{R})\Omega(\mathbf{r}';\mathbf{R}); \qquad (\alpha = A), \tag{7}$$

$$[\hat{T} + E_\alpha(\mathbf{R})]\chi_{n_\alpha}(\mathbf{R}) = \mathcal{E}_{\alpha n_\alpha}\chi_{n_\alpha}(\mathbf{R}). \tag{8}$$

$^NE_\alpha^{(R)}$ and $^{N-2}E_\alpha^{(R)}$ are here the electronic BO potential energy surfaces defined for the N and N-2 electronic systems, $\chi_{n_\alpha}$ the respective nuclear wave functions, and $\mathcal{E}_{\alpha n_\alpha}$ is the total energy (electronic plus vibrational) for the molecular system.

## 3.2 The Direct Contributions to the Auger Cross Section

In the derivation above only the asymptotic behaviour of the functions of the continuum background was fully specified. We construct now the set of electronic-vibrational continuum functions $\{\Psi^{\pm}(\mathbf{r},\mathbf{R})\}$ by means of a linear combination of *electronic* standing wave functions $\psi_{\alpha\varepsilon}(\mathbf{r};\mathbf{R})$ of eq. 3,

$$\Psi^{\pm}_{\alpha\varepsilon}(\mathbf{r},\mathbf{R}) = \sum_\beta \int d\varepsilon' \psi_{\beta\varepsilon'}(\mathbf{r};\mathbf{R}) C^{\pm}_{\beta\alpha}(\varepsilon,\varepsilon',\mathbf{R}), \tag{9}$$

where the unknown expansion coefficients $C^{\pm}_{\beta\alpha}(\varepsilon,\varepsilon',\mathbf{R})$ are differentiable functions of the nuclear coordinates $\mathbf{R}$. The sum occurring in eq. 9 is over all energetically allowed discrete electronic states of the final ions or the initial molecule (implicitly also over the vibrational states, however, in the following, if not explicitly stated, we denote the electro-vibrational states with one index, $\alpha$,$\beta$.., instead of $\alpha n_\alpha$,$\beta n_\beta$..). The integration runs over the continuum energy of the colliding or escaping particles. The set of functions $\{\Psi^{\pm}(\mathbf{r},\mathbf{R})\}$ are then required to be non-interacting with respect to the operator $(\hat{H} - E)$, at the energy shell, and to satisfy the outgoing/incoming scattering wave boundary conditions;

$$\Psi_{\alpha\varepsilon}(\mathbf{r},\mathbf{R}) \sim_{r\to\infty} \sum_\beta \frac{\Omega_\beta(\mathbf{r}';\mathbf{R})}{2ir\sqrt{k_\beta}} \begin{cases} [S_{\beta\alpha}(\mathbf{R})e^{i(k_\beta r+\delta_\beta(\varepsilon'))} - \delta_{\beta\alpha}\chi_{n_\beta}(\mathbf{R})e^{-i(k_\beta r+\delta_\beta(\varepsilon'))}] \\ [\delta_{\beta\alpha}\chi^*_{n_\beta}(\mathbf{R})e^{i(k_\beta r+\delta_\beta(\varepsilon'))} - S^{\dagger}_{\beta\alpha}(\mathbf{R})e^{-i(k_\beta r+\delta_\beta(\varepsilon'))}] \end{cases} \tag{10}$$

Notice that the S matrix entering eq. 10 is a function depending on the nuclear coordinates, and therefore projections of the type $< \chi_{n_\beta}(R) \mid S_{\beta\alpha}(R) >$ are necessary for extracting the amplitude of probability of the scattering event $\beta n_\beta \leftarrow \alpha n_\alpha$. To determine the coefficients $C^{\pm}_{\beta\alpha}(\varepsilon, \varepsilon', \mathbf{R})$ we require that

$$(\psi_{\beta\varepsilon'}(\mathbf{r};\mathbf{R})|\hat{H} - E|\Psi^{\pm}_{\alpha\varepsilon}(\mathbf{r},\mathbf{R})) >= |0>, \tag{11}$$

is satisfied for a (matrix element of the) interaction potential $\tilde{V}_{\beta\alpha}(\varepsilon', \varepsilon)$ defined by

$$(\psi_{\beta\varepsilon'}(\mathbf{r};\mathbf{R})|\hat{H} - E|\psi_{\alpha\varepsilon}(\mathbf{r};\mathbf{R})) = [\tilde{H}_\alpha - \varepsilon - E]\delta_{\beta\alpha}\delta(\varepsilon' - \varepsilon) + \tilde{V}_{\beta\alpha}(\varepsilon', \varepsilon). \tag{12}$$

(The tilde is used to indicate that the relevant object acts as an operator on the nuclear space of functions and parentheses $(\cdots|\cdots)$ has the conventional meaning of integrations over the electronic coordinates and the brackets, $<\cdots|\cdots>$, are reserved for integrations over the nuclear coordinates.) The definition for the interaction potential given above is such that the diagonal part of the nuclear kinetic energy operator is entirely included in the nuclear Hamiltonian $\tilde{H}_\alpha$, i.e. we are assuming the adiabatic Born-Oppenheimer approximation. The off-diagonal terms due to the non-adiabatic corrections are included in the interaction potential $\tilde{V}_{\beta\alpha}(\varepsilon', \varepsilon)$ which also includes the molecule-radiation field terms. Below we comment on the importance of the non-adiabatic corrections for the the transition amplitudes for the direct scattering process we are addressing here. To proceed, we substitute $\Psi^{\pm}_{\alpha\varepsilon}(\mathbf{r},\mathbf{R})$ of eq. 9 in eq. 11, imposing the respective boundary conditions for $\Psi^{\pm}_{\alpha\varepsilon}(\mathbf{r},\mathbf{R})$ and $\psi_{\alpha\varepsilon}(\mathbf{r};\mathbf{R})$ and, following closely the method of ref.[36] and [35], solving for the wave function

$$\Psi^{\pm}_{\alpha\varepsilon}(\mathbf{r},\mathbf{R}) = \psi_{\alpha\varepsilon}(\mathbf{r};\mathbf{R})\chi_{n_\alpha}(\mathbf{R}) + \sum_\beta \lim_{\nu\to 0}\int d\varepsilon' \frac{\psi_{\beta\varepsilon'}(\mathbf{r};\mathbf{R})Y^{\pm}_{\beta\alpha}(\varepsilon', \varepsilon, \mathbf{R})}{(E - \tilde{H}_\beta - \varepsilon' \pm i\nu)}. \tag{13}$$

$Y^{\pm}_{\beta\alpha}(\varepsilon', \varepsilon, \mathbf{R})$ is a nuclear coordinate dependent element of the generalized transition matrix for the direct scattering process that satisfies the Lippmann-Schwinger[23] equation

$$Y^{\pm}_{\beta\alpha}(\varepsilon', \varepsilon, \mathbf{R}) = \tilde{V}_{\beta\alpha}(\varepsilon', \varepsilon)\chi_{n_\alpha}(\mathbf{R}) + \sum_\gamma \lim_{\nu\to 0}\int d\tau \frac{\tilde{V}_{\beta\gamma}(\varepsilon', \tau)Y^{\pm}_{\gamma\alpha}(\tau, \varepsilon, \mathbf{R})}{(E - \tilde{H}_\gamma - \tau \pm i\nu)}. \tag{14}$$

There is no ordering problem with the factors in the second term on the right hand side of eq. 13 since the nuclear Hamiltonian is defined to include the diagonal terms in the nuclear kinetic energy operator. Equation 13, better rewritten as

$$\Psi^{\pm}_{\alpha\varepsilon}(\mathbf{r},\mathbf{R}) = \psi_{\alpha\varepsilon}(\mathbf{r};\mathbf{R})\chi_{n_\alpha}(\mathbf{R}) + \tilde{G}(E \pm i0)\tilde{V}\Psi^{\pm}_{\alpha\varepsilon}(\mathbf{r},\mathbf{R}), \tag{15}$$

$$\tilde{G}(E \pm i0) = \sum_\beta \lim_{\nu\to 0}\int d\varepsilon' \frac{|\psi_{\beta\varepsilon'}(\mathbf{r};\mathbf{R}))(\psi_{\beta\varepsilon'}(\mathbf{r};\mathbf{R})|}{(E - \tilde{H}_\beta - \varepsilon' \pm i\nu)} \tag{16}$$

shows a Born perturbation expansion of the the non-adiabatic vibronic interaction included in $\tilde{V}$.

The transition amplitude for the direct scattering process from the initial $(\alpha n_\alpha)$ to the final $(\beta n_\beta)$ electronic-vibrational states is then given by

$$t^{+}_{\beta n_\beta \leftarrow \alpha n_\alpha}(\varepsilon'\varepsilon) = <\chi_{n_\beta}(\mathbf{R})|Y^{+}_{\beta\alpha}(\varepsilon', \varepsilon, \mathbf{R})> = <\chi_{n_\beta}(\mathbf{R})\psi_{\beta\varepsilon'}(\mathbf{r};\mathbf{R})|\tilde{V}|\Psi^{+}_{\alpha\varepsilon}(\mathbf{r},\mathbf{R})> \tag{17}$$

$$t^{-}_{\beta n_\beta \leftarrow \alpha n_\alpha}(\varepsilon', \varepsilon) = t^{+\dagger}_{\beta n_\beta \leftarrow \alpha n_\alpha}(\varepsilon', \varepsilon). \tag{18}$$

It would be instructive to isolate the contributions of the non-adiabatic corrections from the above transition matrix. To this end we consider that the interaction potential $\tilde{V}$ can be split as

$$\tilde{V} = \hat{V}_I + \tilde{V}_{II} = \hat{H}_{mr} + \text{non-adiabatic term} \tag{19}$$

where we assume that the contribution of the potential $\tilde{V}_{II}$ to the scattering transition amplitude is small compared to the contribution due to $V_I$. This approximation seems not to be that drastic for a large group of vibronic transitions in different molecular systems basing on the study of excitation and ionization spectra. We consider, therefore, that the problem is solved exactly for the interaction potential $\hat{V}_I$ in which we find the adiabatic Born-Oppenheimer (ABO) wave function as

$${}^A\Psi^{\pm}_{\alpha\epsilon}(\mathbf{r},\mathbf{R}) = \psi_{\alpha\epsilon}(\mathbf{r};\mathbf{R})\chi_{n_\alpha}(\mathbf{R}) + \tilde{G}(E \pm i0)\tilde{V}_I {}^A\Psi^{\pm}_{\alpha\epsilon}(\mathbf{r},\mathbf{R}), \tag{20}$$

and the element of the transition matrix ${}^AY^{\pm}_{\beta\alpha}(\epsilon',\epsilon,\mathbf{R})$ on the interaction potential $\hat{V}_I$, as

$${}^AY^{\pm}_{\beta\alpha}(\epsilon',\epsilon,\mathbf{R}) = \hat{V}_{I\beta\alpha}(\epsilon',\epsilon)\chi_{n_\alpha}(\mathbf{R}) + \sum_\gamma \lim_{\nu\to 0}\int d\tau \frac{\hat{V}_{I\beta\gamma}(\epsilon',\tau){}^AY^{\pm}_{\gamma\alpha}(\tau,\epsilon;\mathbf{R})}{(E - \tilde{H}_\gamma - \tau \pm i\nu)} \tag{21}$$

and therefore

$${}^At^+_{\beta n_\beta \leftarrow \alpha n_\alpha}(\epsilon',\epsilon) = < \chi_{n_\beta}\Psi_{\beta\epsilon'}(r;R) \mid \hat{V}_I \mid {}^A\Psi^+_{\alpha\epsilon}(r;R) > . \tag{22}$$

Note that it is only at zero order of approximation that the vibronic transition amplitude takes the simple Condon respectively Franck-Condon forms. It then only requires the evaluation of an overlap between the initial and final vibrational states with the electronic transition moment as a weight factor. Now, if we limit ourselves to the first order correction in the non-adiabatic correction, we include the effect of the small potential $\tilde{V}_{II}$ in the transition matrix of eq. 18 by means of the two potential formula[40]

$$t^+_{\beta n_\beta \leftarrow \alpha n_\alpha}(\epsilon',\epsilon) = {}^At^+_{\beta n_\beta \leftarrow \alpha n_\alpha}(\epsilon',\epsilon) + < {}^A\Psi^-_{\beta\epsilon'}(\mathbf{r},\mathbf{R})|\tilde{V}_{II}|\Psi^+_{\alpha\epsilon}(\mathbf{r},\mathbf{R}) > \tag{23}$$

and the distorted wave Born approximation[40] that assumes

$$\Psi^+_{\alpha\epsilon}(\mathbf{r},\mathbf{R}) > \approx {}^A\Psi^+_{\alpha\epsilon}(\mathbf{r},\mathbf{R}) \tag{24}$$

on the second term on the right hand side of eq. 23, to obtain

$$t^+_{\beta n_\beta \leftarrow \alpha n_\alpha}(\epsilon',\epsilon) \approx {}^At^+_{\beta n_\beta \leftarrow \alpha n_\alpha}(\epsilon',\epsilon) + < {}^A\Psi^-_{\beta\epsilon'}(\mathbf{r};\mathbf{R})|\tilde{V}_{II}|{}^A\Psi^+_{\alpha\epsilon}(\mathbf{r},\mathbf{R}) > . \tag{25}$$

In this approximation the non-adiabatic terms correct the adiabatic Born-Oppenheimer waves ${}^A\Psi^+_{\beta\epsilon'}(\mathbf{r},\mathbf{R})$ already distorted by the (stronger) potential $\hat{V}_I$. The relative importance of these corrections for the case of the direct scattering process is expected to be large for the manifold of continuum channels of the final ion since the large number of possible degeneracies or quasi-degeneracies of the electronic states. This implies additional inter- and intra-channel mixings due the nuclear motion. On the other hand channel coupling due to the vibronic interaction of the initial and the doubly charged final electronic states is expectedly weak, because of the large energy separation, which is the case for most Auger events. Therefore, one can ignore any contribution of vibronic interaction to the direct doubly ionization amplitude, and use the (adiabatic) Born-Oppenheimer approximation for the purpose of computing the vibronic transition amplitudes. Quite interesting is, however, the applicability of the above approximation for the case of vibrational excitations accompanying an electronic excitation in electron-molecule collision experiments. With few modifications the theory here presented is also

valid for such phenomena. The initial and final channels may in these cases be very close in energy such that the adiabatic Born-Oppenheimer wave function may not be good enough for calculation of the vibronic transition amplitude. In this case corrections in first order (like eq. 25) or even higher orders may be unavoidable in order for a reasonable estimate of the transition amplitude.

## 3.3 The Resonant Contributions to the Auger Cross Section

Once the scattering wave functions that diagonalize the operator $(\hat{H} - E)$ within the background subspace have been obtained, we are prepared to treat the merged background and resonant subspaces. Let the interaction matrix element between the resonant wave function $\varphi$ and the $\beta^{\text{th}}$ final wave function belonging to the background space be

$$\tilde{M}^{\pm}_{\beta}(\varepsilon', E) = (\varphi(\mathbf{r};\mathbf{R}) \,|\, \hat{H} - E \,|\, \Psi^{\pm}_{\beta\varepsilon'}(\mathbf{r},\mathbf{R})). \tag{26}$$

Like $\tilde{V}_{\beta\alpha}(\varepsilon', \varepsilon)$, this quantity is an operator on the space of the nuclear coordinates. To diagonalize the $(\hat{H} - E)$ operator within the full space, a new linear combination of functions

$$\Phi^{\pm}_{\alpha E}(\mathbf{r},\mathbf{R}) = \varphi(\mathbf{r};\mathbf{R})\Upsilon^{\pm}_{\alpha E}(\mathbf{R}) + \sum_{\beta}\int d\varepsilon' \Psi^{\pm}_{\beta\varepsilon'}(\mathbf{r},\mathbf{R}) B^{\pm}_{\beta\alpha}(\varepsilon', E), \tag{27}$$

is formed. Without loss of generality, the nuclear wave function of the intermediate state $\Upsilon^{\pm}_{\alpha E}(\mathbf{R})$, has been introduced as a multiplicative factor to the BO electronic function $\varphi(\mathbf{r};\mathbf{R})$. From the requirement that the Schrödinger equation and the boundary conditions for the bound, $\varphi(\mathbf{r};\mathbf{R})$, and scattering waves, $\Psi^{\pm}_{\beta\varepsilon'}(\mathbf{r},\mathbf{R})$ and $\Phi^{\pm}_{\alpha E}(\mathbf{r},\mathbf{R})$, are satisfied, we obtain the resonant wave functions

$$\Phi^{\pm}_{\alpha E}(\mathbf{r},\mathbf{R}) = \varphi(\mathbf{r};\mathbf{R})\Upsilon^{\pm}_{\alpha E}(\mathbf{R}) + \Psi^{\pm}_{\alpha\varepsilon}(\mathbf{r},\mathbf{R}) + \sum_{\beta}\lim_{\nu\to 0}\int d\varepsilon' \frac{\Psi^{\pm}_{\beta\varepsilon'}(\mathbf{r},\mathbf{R}) < \tilde{M}^{\pm\dagger}_{\beta}(\varepsilon', E)|\Upsilon^{\pm}_{\alpha E}(\mathbf{R})>}{(E - \mathcal{E}_{\beta} - \varepsilon' \pm i\nu)} \tag{28}$$

and also the wave equation that governs the nuclear dynamics of the system in the intermediate state $|\varphi\varepsilon_1>$.

$$[E - \tilde{H}_{\varphi}(\varepsilon_{e_1}) - \tilde{F}^{\pm}(E)]\,|\,\Upsilon^{\pm}_{\alpha E}(\mathbf{R})> = |\,\tilde{M}^{\pm}_{\alpha}(\varepsilon, E)> . \tag{29}$$

The left hand side of eq. 29 contains a complex, energy dependent, non-local operator $\tilde{F}^{\pm}(\mathrm{E})$ defined by

$$\tilde{F}^{\pm}(\mathrm{E}) = \sum_{\beta}\lim_{\nu\to 0}\int d\varepsilon' \frac{\tilde{M}^{\pm}_{\beta}(\varepsilon', E)\tilde{M}^{\pm\dagger}_{\beta}(\varepsilon', E)}{(E - \mathcal{E}_{\beta} - \varepsilon' \pm i\nu)} = \tilde{\Delta}(E) \mp \frac{i}{2}\tilde{\Gamma}(E). \tag{30}$$

The terms in these two last equations are conveniently interpreted if we consider the background "outgoing waves" $\Psi^{+}_{\alpha\varepsilon}(\mathbf{r},\mathbf{R})$ for the initial scattering state $i$, hereafter renamed as $\alpha$, and the "incoming waves" $\Psi^{-}_{\alpha\varepsilon}(\mathbf{r},\mathbf{R})$ for the final Auger scattering states $\beta$. The molecule-radiation interaction term and electron-electron coulombic repulsion will then constitute the channel interaction potentials. Accordingly, $\tilde{M}^{+}_{\alpha}(\varepsilon, E)$, is interpreted as a source of probability which feeds the intermediate vibronic population from the initial vibronic scattering state $\alpha$ while the imaginary part of $\tilde{F}(E)$, the operator $\frac{1}{2}\tilde{\Gamma}(E)$, is associated to the decay rate of the intermediate state $\varphi$ to alternative final

channels $\beta$. Experimentally, $\tilde{\Gamma}(E)$ corresponds to the width of a band associated to the intermediate state in an excitation-type spectrum. The $\Delta(E)$ term in eq. 29 causes shifts of the BO potential energy surface of the intermediate state. The stationary vibrational states of the intermediate electronic state should therefore be evaluated according to the modified energy dependent "BO potential surface" $\tilde{E}_r = E_\varphi + \varepsilon_1 + \tilde{\Delta}(E)$.

The resonant-transition matrix which is derived in the procedure leading to eq. 28, assumes a simpler form if the final scattering states $\beta$ are represented by an incoming wave boundary condition and the initial scattering state $\alpha$ by the outgoing wave boundary condition. Explicitly, we have

$$T^+_{\beta\alpha}(\varepsilon',\varepsilon,E) = t^+_{\beta\alpha}(\varepsilon',\varepsilon,E) + <\tilde{M}^{-\dagger}_\beta(\varepsilon',E)\,|\,[E-\tilde{H}_\varphi(\varepsilon_1)-\tilde{F}(E)]^{-1}\,|\,\tilde{M}^+_\alpha(\varepsilon,E)> \quad (31)$$

for the element $T^+_{\beta\alpha}$ of the resonant-transition matrix. In a traditional interpretation the elements of this matrix give the amplitude of probability for the system to be found in a final scattering state $\beta$, provided it initially is prepared in the scattering state $\alpha$. $t^+_{\beta\alpha}(\varepsilon',\varepsilon,E)$, as seen before, gives the contribution of a pure direct non-resonant scattering event. From $T^+_{\beta\alpha}(\varepsilon',\varepsilon,E)$ we can then extract useful information on the formation and the decay of the core-hole state, i.e. we can obtain the transition matrix for the photoionization and the Auger emissions processes. We consider this in more detail.

Under ordinary experimental conditions for the recording of the Auger spectra the amplitude for the resonant contribution by far outweighs that of the direct scattering process. Therefore, we proceed our analysis considering only the resonant term as responsible for the scattering transition amplitude. From eqs. 31 and 29 we write an element of the resonant transition matrix,

$$T_{\beta\alpha}(\varepsilon',\varepsilon,E) = <\tilde{M}^{-\dagger}_\beta(\varepsilon',E)\,|\,\Upsilon^+_{\alpha E}(\mathbf{R})>, \quad (32)$$

as a scalar product between the ket $|\,\Upsilon^+_{\alpha E}(\mathbf{R})>$ and the bra $<\tilde{M}^{-\dagger}_\beta(\varepsilon',E)\,|$ vectors. Through $\Psi^-_{\beta\varepsilon'}(\mathbf{r},\mathbf{R})$ the latter object contains all information about the final channel $\beta$ and its interactions. The coupling between the resonant state and the final channel is achieved through the operator $(\hat{H}-E)$ which also is included in the bra $<\tilde{M}^{-\dagger}_\beta(\varepsilon',E)|$. Hence $<\tilde{M}^{-\dagger}_\beta(\varepsilon',E)\,|$ contains all information about the decaying event with the exception, however, of the population of the vibrational levels in the intermediate state. These pieces of information are stored in the ket $|\Upsilon^+_E(\mathbf{R})>$. Let, for a while, $\xi_{Em}(\mathbf{R})$ be a complex, energy-dependent eigenfunction of the optical operator $\tilde{H}_\varphi(\varepsilon_1)+\tilde{F}(E)$, with the corresponding eigenvalue $W_m(\varepsilon_1,E)$, where $m$ denotes vibrational quantum numbers. One sees that

$$T^{phot}_{\alpha m}(\varepsilon_1,\varepsilon,E) = <\xi_{Em}(\mathbf{R})\,|\,\Upsilon^+_{\alpha E}(\mathbf{R})> \quad (33)$$

is a proper element of the transition matrix for the excitation process. The cross section for the primary photoionization process is then given by

$$\sigma^{phot}_\alpha(\varepsilon_1) \propto \sum_m |T^{phot}_{\alpha m}(\varepsilon_1,\varepsilon,E)|^2 \delta(\mathcal{E}_\alpha + \hbar\omega - E) \quad (34)$$

which, when combining with eq. 33 and eq. 29, leads to

$$\sigma^{phot}_\alpha(\varepsilon_1) \propto \sum_m \left| \frac{<\xi_{Em}(\mathbf{R})\varphi(\mathbf{r};\mathbf{R})\,|\,\hat{H}-E\,|\,\Psi^+_\alpha(\mathbf{r},\mathbf{R})>}{E-\tilde{H}_\varphi(\varepsilon_1)-\tilde{\Delta}(E)+\frac{i}{2}\tilde{\Gamma}(E)} \right|^2 \delta(\mathcal{E}_\alpha+\hbar\omega-E). \quad (35)$$

On the other hand,

$$T^{decay}_{\beta m}(\varepsilon', E) = <\tilde{M}^{-\dagger}_{\beta}(\varepsilon', E)|\xi_{Em}(\mathbf{R})> \tag{36}$$

should correspond to the transition amplitude for the decay (Auger) process. If so, we get, consequently, the cross section for Auger emission to all accessible final vibronic states $(\beta n_\beta)$ as

$$\sigma^{emiss}_{\beta\alpha}(\varepsilon', \varepsilon, E) \propto \sum_{n_\beta} \left| \sum_m T^{decay}_{\beta m}(\varepsilon', E) T^{phot}_{m\alpha}(\varepsilon_1, \varepsilon, E) \right|^2 \delta(\mathcal{E}_\beta + \varepsilon' - E) \tag{37}$$

$$\propto \sum_{m_\beta} \left| \sum_n <\tilde{M}^{-\dagger}_{\beta}(\varepsilon', E)|\xi_{Em}(\mathbf{R})><\xi_{Em}(\mathbf{R})|\Upsilon^{+}_{\alpha E}(\mathbf{R})> \right|^2 \delta(\mathcal{E}_\beta + \varepsilon' - E) \tag{38}$$

$$\propto \sum_{n_\beta} \left| \sum_n \frac{<\tilde{M}^{-\dagger}_{\beta}(\varepsilon', E)|\xi_{Em}(\mathbf{R})><\xi_{Em}(\mathbf{R})|\tilde{M}^{+}_{\alpha}(\varepsilon, E)>}{E - \tilde{H}_\varphi(\varepsilon_1) - \tilde{\Delta}(E) + \frac{i}{2}\tilde{\Gamma}(E)} \right|^2 \delta(\mathcal{E}_\beta + \varepsilon' - E). \tag{39}$$

Gel'mukhanov et al[41,42,43], Domcke and Cederbaum[44] and Kaspar et al[45] derived equations for molecular vibronic cross-sections for photoionization and electronic decaying processes equivalent to eqs. 35 and 39. The latter authors[44,45] solved iteratively the equation for the transition operator **T** using a model molecular Hamiltonian which incorporates a linear coupling of the electronic-nuclear motion, the so-called first-order vibronic coupling constant[46,47].

## 3.4 Local Approximation of the Nuclear Motion

In order to derive computable expressions for the photoionization and Auger cross sections given above, one has to address the nuclear motion problem posed by the nuclear Hamiltonians $\tilde{H}_\varphi + \tilde{F}(\mathrm{E})$ of the intermediate state and the nuclear Hamiltonians $\tilde{H}_\gamma$ of the several scattering channels $\gamma$, including the initial one $\alpha$. The solution of the Schrödinger equations for the intermediate state Hamiltonian operator $\tilde{H}_\varphi(\varepsilon_1) + \tilde{F}(E)$ is complicated by its non-local character and the implicit energy dependence brought by the $\tilde{F}(E)$ operator. However, since only a limited spectral range of energy is considered when we are analysing a particular vibronic profile corresponding to a few vibrational levels of the intermediate state, it is reasonable to expect that $\tilde{F}(E)$ is a slowly varying function of $E$. Thus the complexity of the $\tilde{F}(E)$ operator is trivially removed by neglecting its energy dependence. The use of a non-local versus a local operator has been rather extensively discussed in connection with resonant electron scattering, where the 2.3 eV resonance in $N_2$ is the prototype example[48]. An explicit construction of the non-locality of $\tilde{F}$ may be called for in order to describe finer details in core-hole emission spectra. This non-locality problem enters into $\tilde{F}$ through the projector $|\Psi^{-}_{\beta\varepsilon'}(\mathbf{r}, \mathbf{R})><\Psi^{-}_{\beta\varepsilon'}(\mathbf{r}, \mathbf{R})|$ incorporated in the product $\tilde{M}^{-}_{\beta}(\varepsilon', E)\tilde{M}^{-\dagger}_{\beta}(\varepsilon', E)$ of eq. 30. One sees that vibronic (intra-)channel mixing and nonadiabatic corrections to the background subspace of wave functions (eqs. 13 and 14) together with the interchannel mixing and nonadiabatic corrections between the intermediate approximated wave function and those of the background (eq. 26) are the factors which confer the non-locality to $\tilde{F}$. It should be noted that in spite of that the function $\Psi^{\pm}_{\beta\varepsilon'}(\mathbf{r}, \mathbf{R})$ still can be factorized as $\tilde{\Psi}^{\pm}_{\beta\varepsilon'}(\mathbf{r})\chi_{n_\beta}(\mathbf{R})$, the factor $\tilde{\Psi}^{\pm}_{\beta\varepsilon'}$ will not be a simple function of **R** but rather a complicated non-local operator on the nuclear coordinate space (see eqs. 13 and 14).

However, in a first-order approximation, one can obtain $\tilde{F}$ considering only the *electronic* intra- and inter-channel mixings. To do this one recurs to the closure relation for $|\chi_{n_\beta}(\mathbf{R})><\chi_{n_\beta}(\mathbf{R})|$ and ignore all terms where the nuclear kinetic energy operator $\hat{T}$ are involved in eq. 14, then in eq. 13 and finally in eq. 26. At this level of approximation $\tilde{F}$ is transformed to a local function of $\mathbf{R}$ and takes the form

$$F(\mathbf{R}) = \sum_\beta \lim_{\nu\to 0} \int d\varepsilon' \frac{|(\varphi(\mathbf{r};\mathbf{R}) \mid (\hat{H}-\hat{T}) - E \mid \Psi^-_{\beta\varepsilon'}(\mathbf{r};\mathbf{R}))|^2}{(E - E_\beta(\mathbf{R}) - \varepsilon' + i\nu)}, \qquad (40)$$

that is to be compared to the non-local expression of eq. 30. $\Psi^-_{\beta\varepsilon'}(\mathbf{r};\mathbf{R})$ is obtained by equations equivalent to eq. 13 and eq. 14 where $\tilde{V}_{\beta\alpha}(\varepsilon',\varepsilon)$ now is replaced by $V_{\beta\alpha}(\varepsilon',\varepsilon;\mathbf{R})$ that only parametrically depends on the nuclear coordinates $\mathbf{R}$.

## 3.5 State Interference Effects

The expressions for the photoionization and Auger transition amplitudes that have been derived in section 3 are valid for the special case where a single resonance is embedded in a continuum of electronic doubly charged states. The information obtained from the great many studies with core electron spectroscopies for atomic, molecular and solid state samples, suggest that the identification of a main core-hole state as an isolated resonance in the continuum is no that restrictive as it might be thought at first. Either; 1) the core hole states are separated energetically, as when they belong to different elements; or 2) they are spatially separated, as often is the case for chemically shifted species; or 3) only one of the states, the "main" core hole state, receives large amplitude of probability in the excitation process, as most often is the case for core electron shake-up progressions referring to one main core hole state. However, there are situations when one of these conditions fails, i.e. when ionization with high probability produces several close-lying intermediate core-hole states which interfere with each other during the decay process. For the vibronic case, (vibrational-lifetime interference) this is more a rule than exception, see section 4.2. State interference is anticipated in the case of resonance Auger spectra, in cases where there are unusually strong core hole satellites, as for surface-adsorbates, and under certain conditions for chemically shifted species[49,50].

Within a broader context solutions to the problem of configuration interaction between electronic states belonging to the discrete and continuum parts of the spectrum of a Hamiltonian operator have been offered by Fano[36]. He considered the particular cases of (*i*) one discrete state in one continuum state, (*ii*) one discrete state in many continua, (*iii*) many discrete states and one continuum. Solutions for the general case (*iv*) where many discrete states are embedded in many continua were first given by Mies[51] who emphasized the role of the overlap of neighbouring resonances and the spectral line profile for a photoabsorption or a scattering process. Later rederivations and applications for atomic and atomic-like systems in different contexts can be found in ref:s [52,53,54,55]. The general problem of discrete states embedded in continuum states has also been treated in terms of projection operators by Feshbach[56,57], who presented an equivalent solution in the general case (*iv*) in ref. [57].

The theory of multichannel resonant scattering processes for molecular Auger emission for the more general case (*iv*) including a number of electronic states with vibrational degrees of freedom was formulated by Cesar and Ågren[50]. The basic difference

to the treatment in subsections 3.3 is that the solutions for the true continuum function $\Phi^+_{\alpha E}(\mathbf{r},\mathbf{R})$ from the Schrödinger equation

$$(\hat{H} - E)\Phi^+_{\alpha E}(\mathbf{r},\mathbf{R}) = 0 \tag{41}$$

is now sought in the space of functions spanned by $K$ continuum $\{\Psi^+_{\alpha\epsilon}(\mathbf{r},\mathbf{R})\}$ and $N$ discrete $\{\varphi_n(\mathbf{r};\mathbf{R}\}$ linearly independent functions;

$$\Phi^+_{\alpha E}(\mathbf{r},\mathbf{R}) = \sum_n \varphi_n(\mathbf{r};\mathbf{R})\Upsilon^+_{\alpha nE}(\mathbf{R}) + \sum_\beta \int d\epsilon'\, \Psi^+_{\alpha\epsilon}(\mathbf{r},\mathbf{R})B^+_{\beta\alpha}(\epsilon', E). \tag{42}$$

As before, if we impose that

$$<(\Psi^+_{\beta\epsilon'}(\mathbf{r},\mathbf{R})|\hat{H} - E|\Phi^+_{\alpha E}(\mathbf{r},\mathbf{R}))> \;=\; 0 \tag{43}$$

$$\sum_n (\varphi_n(\mathbf{r};\mathbf{R})|\hat{H} - E|\Phi^+_{\alpha\epsilon}(\mathbf{r},\mathbf{R}))> \;=\; |0> \qquad n = 1,2,\ldots,N \tag{44}$$

and also the proper boundary conditions for continuum and bound wave functions, we obtain three fundamental results; a) the continuum wave function

$$\Phi^+_{\alpha E}(\mathbf{r},\mathbf{R}) = \Psi^+_{\alpha\epsilon}(\mathbf{r},\mathbf{R}) + \sum_n \Big[\varphi_n(\mathbf{r};\mathbf{R})\Upsilon^+_{\alpha nE}(\mathbf{R}) + \tag{45}$$

$$\sum_\beta \lim_{\nu\to 0} \int d\epsilon' \frac{\Psi^+_{\beta\epsilon'}(\mathbf{r},\mathbf{R}) < \tilde{M}^{+\dagger}_\beta(\epsilon', E)|\Upsilon^+_{\alpha E}(\mathbf{R})>}{(E - \mathcal{E}_\beta - \epsilon' - i\nu)}; \tag{46}$$

b) the elements of the resonant transition matrix,

$$T_{\beta\alpha}(\epsilon', \epsilon, E) = t^+_{\beta\alpha}(\epsilon', \epsilon, E) + \sum_n < \tilde{M}^{-\dagger}_{n\beta}(\epsilon', E)|\Upsilon^+_{\alpha nE}(\mathbf{R})>; \tag{47}$$

and c) the inhomogeneous integro-differential equation to be satisfied by the nuclear wave functions $\Upsilon^+_{\alpha nE}(\mathbf{R})$:

$$\sum_m [E\mathcal{S}_{nm} - \tilde{H}_{mn} - \tilde{F}^+_{mn}(E)]\,|\,\Upsilon^+_{\alpha nE}(\mathbf{R})> = |\,\tilde{M}^+_{n\alpha}(\epsilon, E)>\,. \tag{48}$$

The interaction matrix element between the functions belonging to the discrete and the continuum subspace, $\tilde{M}^+_{n\beta}(\epsilon', E) = (\varphi_n(\mathbf{r};\mathbf{R})|(\hat{H} - E)|\Psi^+_{\alpha\epsilon}(\mathbf{r},\mathbf{R}))$ has now been given an additional index for the discrete state $n$. The nuclear Hamiltonian and the "level shift" optical operator $\tilde{F}^+_{mn}(E)$ are now $N \times N$ matrix operators on the space of nuclear wave functions. $\mathcal{S}_{mn}$ is an element of the the overlap matrix between the Born-Oppenheimer electronic wave function of the discrete set $\{\varphi_n(\mathbf{r};\mathbf{R})\}$.

Without loss of generality, eq. 48 can be made simpler if the electronic functions of the discrete set are constructed such that they form a set of orthonormalized and non-interacting functions with respect to the *electronic* Hamiltonian matrix $(\hat{H}_{el})_{mn}$, This can be achieved by a pre-diagonalization of the discrete sub-space of functions. Moreover, if we neglect non-adiabatic couplings within this subspace of electronic functions eq. 48 will reduce to set of equations

$$\sum_m [E - \tilde{H}_m - \tilde{F}^+_{mn}(E)]|\Upsilon^+_{\alpha mE}(\mathbf{R})> = |\tilde{M}^+_{n\alpha}(\epsilon, E)>, \tag{49}$$

coupled "by the level shift" $F^{+}_{mn}(E)$. The objects $\tilde{F}^{+}_{mn}(E)$ and $\tilde{M}^{+}_{n\alpha}(\varepsilon, E)$ have here been redefined accordingly. We interpret as before $\tilde{F}^{+}_{mn}(E)$ as a measure of the strength of configuration interaction between the discrete and continuum electronic states. More precisely, the discrete-continuum coupling enters in the effective nuclear optical Hamiltonian $\tilde{H}_{mn} - \tilde{F}^{+}_{mn}(E)$ through the diagonal part of $\tilde{F}^{+}_{mn}(E)$, while the non-diagonal terms give rise to a second-order contribution to the configuration mixing within the subspace of discrete electronic functions $\varphi_n(\mathbf{r};\mathbf{R})$ due the presence of the underlying continuum wherein these discrete electronic states are embedded. The full physical content of the eq. 49 has already been established. For the many core-hole state case we interpret $\Im m\{F^{+}_{mn;\alpha}(E)\} = \tilde{\Gamma}_{mn;\alpha}(E)$ as a partial transition rate for the electronic Auger decay from the $m^{th}$ ($n^{th}$) resonant state into the $\alpha^{th}$ continuum channel once the $n^{th}$ ($m^{th}$) resonant state has been populated by the primary coupling of the initial ground state with the radiation field. Alternatively [51] $\tilde{\Gamma}_{nm}(E)$ is interpreted as a measure of the overlap between the continua underlying different discrete states $n$ and $m$, c.f. discussion below eq. 30.

As for the isolated resonance case of the previous section, the cross section for the Auger process is well approximated as being only due to the resonant contribution to the transition matrix at the energy range of experimental interest. Accordingly, if eq. 49 is formally solved for $\Upsilon^{+}_{\alpha mE}(\mathbf{R})$ and the result taken into eq. 47 we obtain

$$T_{\beta\alpha}(\varepsilon', \varepsilon, E) \approx \sum_{nm} < \tilde{M}^{-\dagger}_{n\beta}(\varepsilon', E)|[E - \tilde{H}_m - \tilde{\Delta}_{mn} - \frac{i}{2}\tilde{\Gamma}_{mn}(E)]^{-1}|\tilde{M}^{+}_{m\alpha}(\varepsilon, E) > . \quad (50)$$

To get an explicit functional expression for the resonant transition amplitude, we insert the spectral resolution of the optical nuclear Hamiltonian.

$$\tilde{H}_n + \tilde{\Delta}_{mn}(E) + \frac{i}{2}\Gamma_{mn}(E) = \sum_{\nu} |\xi^{(n)}_{\nu E}(\mathbf{R})> \mathcal{Z}_{\mathbf{n}\nu}(\mathbf{E}) <\xi^{(\mathbf{n})}_{\nu \mathbf{E}}(\mathbf{R})|, \quad (51)$$

$$\mathcal{Z}_{n\nu}(E) = \mathcal{E}_{n\nu}(E) + \frac{i}{2}\gamma_{n\nu}(E)),$$

to obtain

$$T_{\beta\alpha}(\varepsilon', \varepsilon, E) \approx \sum_{n\nu} < \tilde{M}^{-\dagger}_{n\beta}(\varepsilon', E)|\xi^{(n)}_{\nu E}(\mathbf{R})> [E - \mathcal{Z}_{n\nu}(E)]^{-1} <\xi^{(n)}_{\nu E}(\mathbf{R})|\tilde{M}^{+}_{n\alpha}(\varepsilon, E) > . \quad (52)$$

( $\xi^{(n)}_{\nu E}(\mathbf{R})$ is here assumed to form a complete set of complex discrete and continuum eigenfunctions of $\tilde{H}_n + \tilde{F}^{+}_{mn}(E)$. We should however neglect from our considerations the contribution due to the continuum part of this set of functions.) The energy dependence of the transition matrices $\tilde{M}^{-}_{n\beta}(\varepsilon', E)$ and $\tilde{M}^{+}_{n\alpha}(\varepsilon, E)$, as well of the eigenvalues $\mathcal{Z}_{n\nu}(E)$ of the nuclear optical Hamiltonian, can be removed from our further considerations since the resonances we are addressing are relatively narrow.

The cross-section for the Auger decay will be proportional to the square of the approximated transition amplitude of eq. 52, summed over all final channels and averaged over the initial channels. The symmetry of the electronic and vibrational indices (quantum numbers) in that equation is remarkable. For the case where a pair or more of decaying electronic core-hole states have an energy shift comparable to the displacement between two (populated) adjacent vibrational levels there will be competing electronic-vibrational decay events with equal contributions from the two groups of possible electronic and vibrational interferences. For weak vibrational excitation accompanying the

electronic excitation process we then identify a *state* interference effect. It should be noted, however, that for the ordinary cases where the energy difference between two adjacents vibrational levels is smaller compared with the corresponding difference for the electronic levels, a vibrational rather than state interference is anticipated. The effects of this interference are the distortion and shift of a vibronic band profile from its standard form and position, as has been experimentally observed for several Auger transitions of molecular systems, see section 4.2. It might also be the case that the *state interference* effect changes the line profile of two or more close-lying resonances with an order of magnitude comparable with that for the transition amplitude of the direct doubly ionization processes. This more subtle case requires of course, the full use of the transition amplitude of eq. 47 with both direct and resonant terms entering the analysis of the energy shifts and profiles of the electronic bands.

The treatment beyond the isolated resonance model for the Auger effect indicates thus that resonance Auger spectra require a higher level of theory than "normal" Auger spectra from isolated core hole states. It also indicates that, even for high-energy primary excitation, there will be distortions in measured energy levels and other properties of the core hole states with respect to the corresponding measurements in absorption type spectra.

## 3.6 Post-Collision Interaction (PCI)

Scattering processes involving two or more electrons or other particles in the continuum of the exit channels are subject to post-collision interaction, PCI [58,59,60,61]. PCI accounts for the residual correlation effect of the receding electrons with one another and with the remaining common ion. Experimentally this effect manifests itself by distorting the line profile of an ejected Auger (autoionized, scattered) electron (strong effect) or an emited X-ray photon (weak effect), shifting its maximum to higher energy and asymmetrizing the expected symmetrical Lorentzian profile. In the primary spectrum (e.g. photoelectron spectrum) the PCI effect is expected to change the peak maximum the opposite way.

Classically, in Auger emission, PCI is to a first order of approximation caused by an energy exchange between the escaping particles due to the change in the electric field felt by a slow primary electron when exposed to a different ionic environment after that the Auger decay has taken place. A photoionized electron being in the near threshold continuum with a small excess of energy $\varepsilon = E - I_\varphi$ experiences a comparatively strong PCI effect, while the PCI effect is asymptotically vanishing for large excess of energy $\epsilon$ in the case of photon induced Auger. By contrast, in the case of electron induced Auger emission, there will always be a possibility of producing a slow electron at the neighborhood of the decaying residual ion, the PCI effect therefore never vanishes irrespective the amount of excess of energy given to the primary electron [62,63].

Theoretical treatments of the PCI effect in atoms have been offered by semiclassical approximations [64,65,66,67,68], diagrammatic many-body perturbation [69,70], resonant scattering [71], and complex-coordinate [72] quantum formulations. A key issue in any of these formulations is the explicit or parametric inclusion of the so-called "non-passing" effect, i.e. the inclusion of the time it takes for the Auger electron to overtake a previously emited (photo)electron [73].

The PCI effect is a direct manifestation of the concerted mechanism of core-hole

ionization and decay processes leading to the Auger effect in atoms and molecules, in contrast to the picture where the whole process is considered to proceed as two-step events. Also from this point of view the scattering theory formulation of the Auger effect is essential for interpreting an Auger spectrum. The PCI theory has been generalized to include two outgoing particles in the final continuum channels [71] and has later been refined to also include the "non-passing" effect mentioned above, with good results for the studied atomic systems[74,75,76]. To the best of our knowledge, however, no PCI studies have been applied to Auger spectra of molecules, and we confine therefore this review to the references on atoms given above.

# 4 Vibronic Interaction in Auger Spectra

In this section we derive formulas necessary to construct the spectral functions for Auger emission in molecules including the effects os vibronic interaction. The starting point is given by equation 39 in the previous section for the cross-sections of Auger emission. Any dimensionality for the nuclear motion is accounted for, with a general analytical treatment with respect to force fields and normal modes. The harmonic oscillator approximation will be imposed for all involved states. This has the advantage that closed analytical expressions for the final cross sections can be derived. As shown below this does not imply that anharmonicity contributions to the spectral profiles are neglected !

## 4.1 Vertical and Adiabatic Approaches

The solution for the initial state nuclear motion is expressed in dimensionless normal coordinates $\{\mathbf{q}_\alpha\}$. These coordinates are related to the normal coordinates $\{\mathbf{Q}_\alpha\}$ through $\mathbf{q}_\alpha = (\underline{\omega}^{(\alpha)})^{1/2}\mathbf{Q}_\alpha$, where $\omega_{ij}^{(\alpha)} = \omega_i^{(\alpha)}\delta_{ij}$ are the harmonic frequencies associated to the $i^{th}$ normal mode of the initial electronic state $\alpha$. The solution of the Schrödinger equation for this state is given by the well known wave functions

$$\chi_{\mathbf{n}_\alpha}(\mathbf{q}_\alpha) = \prod_i^N \Big[\frac{1}{2^{n_i} n_i! \pi^{1/2}}\Big]^{1/2} \mathcal{H}_{n_i}(q_{\alpha_i}) e^{-q_{\alpha_i}^2/2}, \tag{53}$$

which we write in short form as

$$\chi_{\mathbf{n}_\alpha}(\mathbf{q}_\alpha) = \sqrt{\frac{1}{2^{\mathbf{n}}\mathbf{n}!\pi^{N/2}}}\,\mathbf{H}_{\mathbf{n}}(\mathbf{q}_\alpha) e^{-\frac{1}{2}\mathbf{q}_\alpha\cdot\mathbf{q}_\alpha}, \tag{54}$$

We use an $N-$dimensional convention for the quantities,

$$\mathbf{q} = \begin{pmatrix} q_1 \\ q_2 \\ \vdots \\ q_n \end{pmatrix} \tag{55}$$

$$\mathbf{n}! = n_1! n_2! \ldots n_N!,$$

$$\mathbf{H}_{\mathbf{n}}(\mathbf{q}) = \mathcal{H}_{n_1}(q_1)\mathcal{H}_{n_2}(q_2)\cdots\mathcal{H}_{n_N}(q_N),$$

where $\mathcal{H}_{n_i}(q_{\alpha_i})$ are the Hermite polynomials. The eigenvalues associated to the initial state are, of course,

$$\epsilon_{n_1,n_2,\ldots}^{(\alpha)} = \sum_i \omega_i^{(\alpha)}(n_i + \frac{1}{2}). \tag{56}$$

For the treatment of the nuclear motion for the other ionic states the nuclear BO potential energy $E_\beta$ ($\beta \neq \alpha$) is expanded in a Taylor series, in terms of the dimensionless coordinates $\mathbf{q}_\alpha$, around the equilibrium geometry of the initial state $\alpha$ defined by $\mathbf{q}_\alpha = \mathbf{0}$. Up to second order, the approximated Hamiltonian $H_\beta$ reads:

$$\tilde{H}_\beta = -\frac{1}{2}\sum_i \omega_i^{(\alpha)} \frac{\partial^2}{\partial q_{\alpha_i}^2} + \sqrt{2}\vec{\kappa}^{\mathrm{t}}\cdot\mathbf{q}_\alpha + \frac{1}{2}\mathbf{q}_\alpha^{\mathrm{t}}\underline{\omega}^{(\alpha)}\mathbf{q}_\alpha + 2\mathbf{q}_\alpha^{\mathrm{t}}\underline{\lambda}\mathbf{q}_\alpha + V_0^{(\beta\alpha)}, \tag{57}$$

where the column vector $\vec{\kappa}$, with elements $\kappa_i = \frac{1}{\sqrt{2}}\partial[E_\beta(\mathbf{q}_\alpha) - E_\alpha(\mathbf{q}_\alpha)]/\partial q_{\alpha_i}|_{\mathbf{q}_\alpha=0}$, and the square matrix $\underline{\lambda}$, with elements $\lambda_{ij} = \frac{1}{4}\partial^2[E_\beta(\mathbf{q}_\alpha) - E_\alpha(\mathbf{q}_\alpha)]/\partial q_{\alpha_i}\partial q_{\alpha_j}|_{\mathbf{q}_\alpha=0}$ are the first- and second-order coupling constants, respectively, as defined by Cederbaum and Domcke[46,47]. $V_0^{(\beta\alpha)} = [E_\beta(\mathbf{q}_\alpha) - E_\alpha(\mathbf{q}_\alpha)]|_{\mathbf{q}_\alpha=\mathbf{0}}$ is the "vertical" electronic transition energy.

The nuclear Hamiltonian of eq. 57 has been shown sucessful for producing vibronic profiles in different types of electronic spectra such as valence- and inner-shell photoelectron, Auger emission, X-ray emission, and electron-molecule resonant scattering spectra[10,44,77,78]. Even when the true potentials have large anharmonic contributions this particular form of Hamiltonian has demonstrated both qualitative and quantitative power for predictions of vibronic band shapes[10,79]. A reason for this is that quadratic expansions of the potential energy surfaces gives reasonable accuracy when the nuclei in the excited state execute small displacements around the center of the expansion $\mathbf{q}_\alpha = \mathbf{0}$. Stating in a more precise way, whenever the final molecular geometry remains within the Franck-Condon zone for times long enough for an experimental measurement the spectrum will "image" the dynamics of the molecular system only at the neighbourhood of $\mathbf{q}_\alpha = \mathbf{0}$. Therefore even if only a harmonic approximation is retained it may give the proper theoretical account of the spectrum, when the expansion point is located to the nuclear geometry where the electronic transition takes place, i.e. the vertical point. With such a local expansion of the potential energy surface the Hamiltonian of eq. 57 can be used to describe the short-time dynamics of the process. This approach will give a proper account for the envelope of an Auger band even for a multidimensional system, i.e. a polyatomic, although the prediction of finer details in spectra of low-dimensional systems, i.e. diatomics, may be poorer. A demonstration of this statement can be found in ref. [10] in terms of analysis of the moments of a vibronic lineshape or in the ref. [80] where a time-dependent description of vibronic transitions is adopted. For a recent time-resolved study on the formation of the spectral function for vibronic emission involving short-lived states we refer to ref. [81].

Contrasting with the choice for the Hamiltonian of eq. 57 which parametrically depends on the gradient and the hessian (first and second derivatives) of the $\beta^{th}$ potential energy surface evaluated at the equilibrium position of the initial state $\alpha$, one can as well make a more traditional choice and take $\tilde{H}_\beta$ defined for parameters refered to small nuclear displacements around a (single) equilibrium molecular conformation:

$$\tilde{H}_\beta = -\frac{1}{2}\sum_i \omega_i^{(\beta)} \frac{\partial^2}{\partial q_{\beta_i}^2} + \frac{1}{2}\mathbf{q}_\beta^t \underline{\omega}^{(\beta)} \mathbf{q}_\beta + T_e^{(\beta\alpha)}. \tag{58}$$

The set of dimensionaless coordinates is now $\mathbf{q}_\beta = (\underline{\omega}^{(\beta)})^{1/2}\mathbf{Q}_\beta$ which conform with the new molecular arrangements. $\underline{\omega}^{(\beta)}$ are the harmonic vibrational frequencies of the molecular system around $\mathbf{q}_\beta = \mathbf{0}$ and $T_e^{(\beta\alpha)}$ the adiabatic electronic transition energy (excluding zero-point energies). This Hamiltonian gives the correct spacing (within the harmonic approximation) between adjacent vibrational lines that build up an absorption or emission band. However, the eigenfunctions of the above Hamiltonian will in general poorly represent the correct behaviour at the Franck-Condon zone, where the vibrational transitions have strong intensities. This implies in general a worse vibrational envelope than by using the Hamiltonian of eq. 57. We refer to ref. [79] for an illustration of these points for the calculation of line profiles in photoelectron spectra. There are several arguments pro and against the Hamiltonians of eqs. 57 and 58, representing the vertical and the adiabatic approaches, respectively. For Auger one should add the argument that the wave packet of the intermediate state is not sufficiently long-lived to

reach the adiabatic point. For polyatomics the construction of the adiabatic Hamiltonian and its eigenvalues is at least an order of magnitude computationally more expensive than the vertical Hamiltonian.

The solution for Schrödinger equation for the Hamiltonian of eq. 57 is easily found. To this end we consider the linear transformation

$$\mathbf{q}_\beta = \underline{J}^{(\beta\alpha)}\mathbf{q}_\alpha + \vec{\sigma}^{(\beta\alpha)} \tag{59}$$

$\mathbf{q}_\beta$ is here a *local* normal coordinate of the $\beta^{th}$ potential energy surface and coincides only with the one of the previous paragraph for the trivial case of a common expansion point. With the definitions

$$\begin{cases} \underline{J}^{(\beta\alpha)} = \underline{\Omega}^{1/2}(\underline{\omega}^{(\alpha)})^{-1/2} \\ \underline{\omega}^{(\alpha)} + 4\underline{\lambda} = \underline{J}^{(\beta\alpha)t}\underline{\Omega}\underline{J}^{(\beta\alpha)}, \\ \vec{\sigma}^{(\beta\alpha)} = \sqrt{2}\underline{\Omega}^{-1}(\underline{J}^{(\beta\alpha)-1})^t\vec{\kappa} \end{cases}, \tag{60}$$

eq. 57 then assumes the form

$$\tilde{H}_\beta = -\frac{1}{2}\sum_i \Omega_i \frac{\partial^2}{\partial q_{\beta_i}^2} + \frac{1}{2}\mathbf{q}_\beta^t\underline{\Omega}\mathbf{q}_\beta + \vec{\kappa}^t\underline{J}^{-1}\underline{\Omega}^{-1}(\underline{J}^{-1})^t\vec{\kappa} + V_0^{(\beta\alpha)}. \tag{61}$$

$\underline{\Omega}$ represents here the curvature of the potential surface around $\mathbf{q}_\alpha = \mathbf{0}$ and is interpreted as the prediction of the excited state harmonic frequencies. The above Hamiltonian is a local representation of the correct harmonic nuclear Hamiltonian for the electronic state $\beta$, eq. 58, because the matrices $\underline{\omega}^{(\beta)}$ and $\underline{\Omega}$ do not match. It is inherent in the method, however, that $\mathbf{q}_\beta$ is the correct set of (dimensionless) normal coordinates associated to $\tilde{H}_\beta$ provided $E_\beta(\mathbf{q}_\alpha)$ has an exact harmonic behaviour within the radius $|\vec{\sigma}^{(\beta\alpha)}|$ of an hypersphere centered at $-\underline{J}^{(\beta\alpha)^{-1}}\vec{\sigma}^{(\beta\alpha)}$. For calculations of a vibronic profile using the Hamiltonian of eq. 57 it is customary to ignore the second order coupling constant $\underline{\lambda}$, i.e. to make the additional approximation of setting $\underline{\Omega} = \underline{\omega}^{(\alpha)}$. It has been argued[10,79] that such a level of approximation does, indeed, include some anharmonic character of the $E_\beta(\mathbf{q}_\alpha)$ surface near the vertical point $\mathbf{q}_\alpha = 0$, i.e. the region where the vibrational transitions with strong intensities reside. Weaker bands at the flanks of the progressions can though be poorly reproduced. See ref:s [10] and [77] for additional illustrations of these points.

The solutions for the eq. 61 is straightforward; the wave functions are

$$\chi_{\mathbf{m}}(\mathbf{q}_\beta) = \sqrt{\frac{1}{2^{\mathbf{m}}\mathbf{m}!\pi^{N/2}}}\mathbf{H}_{\mathbf{m}}(\mathbf{q}_\beta)e^{-\frac{1}{2}\mathbf{q}_\beta\cdot\mathbf{q}_\beta}, \tag{62}$$

with eigenvalues

$$\epsilon^{(\beta)}_{m_1m_2\ldots} = \sum_i \Omega_i\left(m_i + \tfrac{1}{2} - \tfrac{1}{2}|\sigma_i^{(\beta\alpha)}|^2\right) + V_0^{(\beta\alpha)}. \tag{63}$$

The quantity $V_0^{(\beta\alpha)} - \sum_i \Omega_i |\sigma_i^{(\beta\alpha)}|^2$ is readily identified as the difference $T_e^{\beta\alpha}$ between the minima of the two electronic energy surfaces connected by the transition.

An equivalent treatment for the intermediate state Hamiltonian operator $\tilde{H}_\varphi(\varepsilon_1) + \tilde{F}(E)$ closely follows the scheme for the Hamiltonian $\tilde{H}_\beta$ with the additional terms, now included, due to the level shift $\tilde{F}(E)$ operator. Notice that, by virtue of the approximations made in the last part of section 3.4, the $\tilde{F}(E)$ operator will be assumed to be local and energy independent.

## 4.2 Lifetime-Vibrational Interference Effects

In the present section we derive analytical cross sections for vibronic transitions in Auger spectra displaying the lifetime-vibrational interference effects. We then use the set of approximations derived above and assume the zeroeth order "outgoing" and "incoming" wave functions for the initial state $\alpha$ and for all alternative final channels $\beta$. This means that we only consider the first term of the right hand side of eq. 28, and thereby obtain the following expressions for the cross sections 29 and 30, for excitation (photoionization) and emission (Auger-), respectively,

$$\sigma_{n_\alpha}^{phot}(\varepsilon_1) \propto \sum_n \frac{|< \xi_{En}(\mathbf{q}) \mid \mathcal{M}_{el}(\mathbf{q}) \mid \chi_{n_\alpha}(\mathbf{q}) >|^2}{\{\hbar\omega - T_e^{(\varphi\alpha)} - \Delta(\mathbf{0}) - \varepsilon_1 + \sum_i[(\omega_i^{(\alpha)} n_{\alpha_i} - \omega_i^{(\varphi)} n_i) - \frac{1}{2}\Delta\omega_i^{(\varphi\alpha)}]\}^2 + \frac{1}{4}\Gamma^2(\mathbf{0})} \tag{64}$$

and

$$\sigma_{\beta\alpha}^{emiss}(\varepsilon', \varepsilon, E) \propto \sum_{n_\beta} \left| \sum_n \frac{< \chi_{n_\beta}(\mathbf{q})|\mathcal{M}'_{el}(\mathbf{q})|\xi_n(\mathbf{q}) >< \xi_n(\mathbf{q})|\mathcal{M}_{el}(\mathbf{q})|\chi_{n_\alpha}(\mathbf{q}) >}{\{\varepsilon' + T_e^{(\beta\varphi)} - \Delta(\mathbf{0}) + \sum_i[(\omega_i^{(\beta)} n_{\beta_i} - \omega_i^{(\varphi)} n_i) + \frac{1}{2}\Delta\omega_i^{(\beta\varphi)}]\} + \frac{i}{2}\Gamma(\mathbf{0})} \right|^2 \tag{65}$$

The quantities $\mathcal{M}_{el}(\mathbf{q})$ and $\mathcal{M}'_{el}(\mathbf{q})$ correspond to the electronic transition moments, $\Delta(\mathbf{0})$ and $\Gamma(\mathbf{0})$ to the energy shift and the lifetime evaluated at $\mathbf{q}_\alpha = \mathbf{0}$, respectively, and $\Delta\omega_i^{(\mu\nu)} = \omega_i^{(\mu)} - \omega_i^{(\nu)}$. In our treatment the decay process takes place from the same point on the intermediate potential energy surface as where the intermediate electronic state were created. The terms $T^{(\varphi\alpha)} = V_0^{(\varphi\alpha)} + \frac{1}{2}\omega_i^{(\varphi)}|\sigma_i^{(\varphi\alpha)}|^2$ and $T^{(\beta\varphi)} = V_0^{(\beta\varphi)} + \frac{1}{2}\sum_i[\omega^{(\varphi)}|\ \sigma_i^{(\varphi\alpha)}\ |^2 - \omega^{(\beta)}|\ \sigma_i^{(\beta\alpha)}\ |^2]$ represent the predicted difference between the minima of the potential energy surfaces of the initial and intermediate states and the intermediate and final states, respectively. $V_0^{(\mu\nu)} = E^{(\mu)}(\mathbf{0}) - E^{(\nu)}(\mathbf{0})$, as before, correspond to a vertical electronic energy difference between the states $\mu$ and $\nu$ evaluated at the equilibrium geometry of the initial molecular ground state, $\mathbf{q}_\alpha = 0$.

The line profile for the decay processes, eq. 65, differs from the pattern that would be formed by a superposition of a set of displaced Lorentzians, characteristic for the ordinary ionization processes in molecules, eq. 64. One finds instead that the shape of bands is given by a sum of direct and interference terms. The direct contributions are formed, for each $n_\alpha$ and $n_\beta$, as a set of Lorentzians bands

$$\sigma_{\beta\alpha}^{dir}(n_\beta, n_\alpha; \varepsilon', \varepsilon, E) \propto \sum_n \mathcal{L}_n(n_\beta, n_\alpha; \varepsilon', \varepsilon, E) = \sum_n |\mathcal{A}_n(n_\beta, n_\alpha; \varepsilon', \varepsilon, E)|^2 \tag{66}$$

where,

$$\mathcal{A}_n(n_\beta, n_\alpha; \varepsilon', \varepsilon, E) = \frac{< \chi_{n_\beta}(\mathbf{q})|\mathcal{M}'_{el}(\mathbf{q})|\xi_n(\mathbf{q}) >< \xi_n(\mathbf{q})|\mathcal{M}_{el}(\mathbf{q})|\chi_{n_\alpha}(\mathbf{q}) >}{\{\varepsilon' + T_e^{(\beta\varphi)} - \Delta(\mathbf{0}) + \sum_i[(\omega_i^{(\beta)} n_{\beta_i} - \omega_i^{(\varphi)} n_i) + \frac{1}{2}\Delta\omega_i^{(\beta\varphi)}]\} + \frac{i}{2}\Gamma(\mathbf{0})} \tag{67}$$

corresponding to the sequential events of formation and decay of the $n^{\text{th}}$ vibrational levels of the core-hole state. The interference contributions (cross terms) read

$$\sigma_{\beta\alpha}^{interf}(n_\beta, n_\alpha; \varepsilon', \varepsilon, E) \propto \sum_{n \neq m} \mathcal{A}_n(n_\beta, n_\alpha; \varepsilon', \varepsilon, E)\mathcal{A}_m^*(n_\beta, n_\alpha; \varepsilon', \varepsilon, E) \tag{68}$$

and correspond to second-order-like contributions for the combined process of formation and decay of the core-hole state where virtual vibrational transitions $n \leftrightarrow m$ $(m \neq n)$ are possible during the lifetime $(\Gamma^{-1})$ of the intermediate state. Eq. 65 has two interesting limiting cases for the ratio $\gamma_{nm} = \left| \frac{\tau_n(n_\beta) - \tau_m(n_\beta)}{\Gamma(0)} \right|$ $(n \neq m)$. Here

$$\tau_n(n_\beta) = T_e^{(\beta\varphi)}(0) - \Delta(0) + \sum_i [\omega_i^{(\beta)} n_{\beta_i} - \omega_i^{(\varphi)} n_i + \frac{1}{2}\Delta\omega_i^{(\beta\varphi)}] \qquad (69)$$

is the transition energy between the vibronic levels $n\,[\equiv (n_1, n_2, \ldots)]$ of the core-hole $\varphi$ and final $\beta$ states, respectively. If $\gamma_{nm} \gg 1$, then for any choice of $n$ and $m$ $(n \neq m)$, the interference terms (eq. 68) do not appreciably contribute to the total cross section (eq. 65) and one expects well defined Lorentzian shaped peaks forming progressions associated to each individual vibrational level $n_\beta$ of the final electronic state $\beta$. At the opposite extreme one has $\gamma_{nm} \ll 1$, in which case, the intermediate state can be thought of as having a very short electronic lifetime, i.e. $\Gamma^{-1} \ll 1$, so that in the scattering event the intermediate vibrational fine structure can not be discerned from a broad continuum background.

One thus sees that the interference terms, eq. 68, contribute with decreasing degrees of importance for the evaluation of eq. 65, as one passes from the $\gamma_{nm} \ll 1$ to the $\gamma_{nm} \gg 1$ regime. Of special interest are the cases where $\gamma_{nm} \approx 1$. The interference terms, eq. 68, can not be excluded from eq. 65 when there is more than one vibrational level with large population in the intermediate state. The interference results in deformations of the observed Auger bands, sometimes so large in fact as to shift the intensity maximum of the Auger band by many vibrational quantas[42,43,45,82,83,84,37]. This means that the usefulness of the high-resolution inherent in Auger spectroscopy for deriving properties of core hole states, be it energies, force fields or conformations, in a certain sence is compromised by the interference effect.

## 4.3 Evaluation of Franck-Condon Factors

For Auger as for other types electronic spectra full Franck-Condon analyses have been rather scarce in the polyatomic case. This can be referred either to use of costly procedures in the evaluation of the Franck-Condon amplitudes themselves, but also to the mere fact that sufficient input data, viz. equilibrium geometries and force fields often are lacking for ionic or excited states of polyatomics. In some cases, where large amplitude motions are involved, there is also an intrinsic problem of finding appropriate coordinate systems that fulfills rotational invariance between initial and finals states.

In this section we give a solution for the basic overlap integrals over the nuclear coordinates occurring in the numerator of the expressions for the excitation (photoionization) and Auger emission cross-sections eq. 64 and 65. Such integrals are the building stones for either the vertical or adiabatic approaches to the calculation of band shapes in Auger spectra, described in section 4.1. The formulas presented here can thus be seen as the solution of the vibrational part of the Auger spectral function. Expressions for multidimensional harmonic integrals has been offered in the literature either using analytic[85,86] or algebraic[87,88,47,89] methods, with varying degree of efficiency. Here we adopt the first of the above approaches, and derive an efficient recursive procedure for calculating Franck-Condon integrals as they appear in Auger spectra. The procedure is a recursive analogue to the method of Sharp and Rosenstock[85], in which closed analytical expressions in terms of generating functions are used.

According to eq.s 64 and 65, we are looking for the solution for the overlap integral

$$\begin{aligned}\mathcal{I}(\mathbf{n},\mathbf{m}) &= <\chi_{\mathbf{n}}(\mathbf{q}_\alpha)|\mathcal{M}(\mathbf{q}_\alpha)|\xi_{\mathbf{m}}(\mathbf{q}_\beta)> \\ &= \sqrt{\frac{1}{2^{\mathbf{n}+\mathbf{m}}\mathbf{n}!\mathbf{m}!\pi^N}}\int d\mathbf{q}_\alpha \mathcal{M}(\mathbf{q}_\alpha)\mathbf{H}_{\mathbf{m}}(\mathbf{q}_\alpha)\mathbf{H}_{\mathbf{n}}(\mathbf{q}_\beta)\mathrm{e}^{-\frac{1}{2}\mathbf{q}_\alpha^t\mathbf{q}_\alpha - \frac{1}{2}\mathbf{q}_\beta^t\mathbf{q}_\beta} \end{aligned} \quad (70)$$

We assume that the electronic transition matrix $\mathcal{M}(\mathbf{q}_\alpha)$ can be Taylor expanded in the coordinate $\mathbf{q}_\alpha$ about some expansion point $\mathbf{q}_\alpha = \mathbf{0}$ so that, by means of the Hermite polynomial recurrence relations [90], each monomial of degree $p$ contributes for the integral of eq. 70 with a number of terms systematically generated from $H_0(\mathbf{q}_\alpha)$. We concentrate on the case $\mathcal{M}(\mathbf{q}_\alpha) = 1$. If we use the generating functions for the Hermite polynomials[90], and follow Sharp and Rosenstock [85] we write

$$\begin{aligned}\mathcal{I}(\mathbf{s},\mathbf{t}) &= \sum_{\mathbf{n},\mathbf{m}} \frac{\sqrt{2^{\mathbf{n}+\mathbf{m}}\mathbf{n}!\mathbf{m}!\pi^N}}{\mathbf{n}!\mathbf{m}!}\mathcal{A}(\mathbf{n},\mathbf{m})\mathbf{s}^{\mathbf{n}}\mathbf{t}^{\mathbf{m}} \\ &= \int d\mathbf{q}_\alpha \mathrm{e}^{2\mathbf{q}_\alpha^t\mathbf{s} - \frac{1}{2}\mathbf{q}_\alpha^t\mathbf{q}_\alpha - \mathbf{s}^t\mathbf{s} + 2\mathbf{q}_\beta^t\mathbf{t} - \frac{1}{2}\mathbf{q}_\beta^t\mathbf{q}_\beta - \mathbf{t}^t\mathbf{t}}. \end{aligned} \quad (71)$$

Substituting $\mathbf{q}_\beta$ from eq. 61 in the above equation, introducing an $N \times N$ positive defined matrix $\underline{E}$ by

$$\underline{E} = \frac{1}{2}(\underline{1} + \underline{J}^t\underline{J}), \quad (72)$$

with determinant $||\underline{E}||$, the indicated integration gives

$$\mathcal{I}(\mathbf{s},\mathbf{t}) = \sqrt{\frac{\pi^N}{||\underline{E}||}}\mathrm{e}^{-\mathbf{s}^t\mathbf{s} - \mathbf{t}^t\mathbf{t} - \frac{1}{2}\vec{\sigma}^t\vec{\sigma} + 2\vec{\sigma}^t\mathbf{t} + \frac{1}{4}(2\mathbf{s} + 2\underline{J}^t\mathbf{t} - \underline{J}^t\vec{\sigma})^t\underline{E}^{-1}(2\mathbf{s} + 2\underline{J}^t\mathbf{t} - \underline{J}^t\vec{\sigma})}. \quad (73)$$

Rearranging the terms in the exponential, and defining the $2N \times 2N$ matrix $\underline{A}$ and the $2N$ row vector $b$ by

$$\begin{aligned}\underline{A} &= \begin{pmatrix} A_{ss} & A_{st} \\ A_{ts} & A_{tt} \end{pmatrix} = \begin{pmatrix} \underline{1} - \underline{E}^{-1} & \underline{E}^{-1}\underline{J}^t \\ \underline{J}\underline{E}^{-1} & \underline{1} - \underline{J}\underline{E}^{-1}\underline{J}^t \end{pmatrix} \\ b &= \begin{pmatrix} b_s & b_t \end{pmatrix} = \begin{pmatrix} -\frac{1}{2}\underline{E}^{-1}\underline{J}^t\vec{\sigma} & \vec{\sigma} - \frac{1}{2}\underline{J}\underline{E}^{-1}\underline{J}^t\vec{\sigma} \end{pmatrix} \end{aligned} \quad (74)$$

eq. 73 becomes

$$\mathcal{I}(\mathbf{s},\mathbf{t}) = \pi^{\frac{N}{2}}\mathcal{A}(\mathbf{0},\mathbf{0})\mathrm{e}^{2\mathbf{u}^t b - \mathbf{u}^t\underline{A}\mathbf{u}} \quad (75)$$

where,

$$\mathcal{I}(\mathbf{0},\mathbf{0}) = \sqrt{\frac{1}{||\underline{E}||}}\mathrm{e}^{-\frac{1}{2}\vec{\sigma}^t(\underline{1} - \underline{J}\underline{E}^{-1}\underline{J}^t)\vec{\sigma}}; \qquad \mathbf{u} = \begin{pmatrix} \mathbf{s} \\ \mathbf{t} \end{pmatrix}. \quad (76)$$

Now, by analogy with the one dimensional Hermite polynomials, the $2N-$dimensional Hermite polynomials are defined by the exponential generating function [91]

$$\mathrm{e}^{2\mathbf{u}^t b - \mathbf{u}^t\underline{A}\mathbf{u}} = \sum_{\mathbf{n},\mathbf{m}} \frac{\mathbf{s}^{\mathbf{n}}\mathbf{t}^{\mathbf{m}}}{\mathbf{n}!\mathbf{m}!}\mathbf{H}_{\mathbf{n},\mathbf{m}}(\underline{A}|b) \quad (77)$$

With these polynomials the final result for the overlap of eq. 70 is compactly given by

$$\mathcal{I}(\mathbf{n},\mathbf{m}) = \mathcal{I}(\mathbf{0},\mathbf{0})\sqrt{\frac{1}{2^{\mathbf{n}+\mathbf{m}}\mathbf{n}!\mathbf{m}!||\underline{E}||}}\mathbf{H}_{\mathbf{nm}}(\underline{A}|b). \quad (78)$$

In order to be computationally useful the multidimensional Hermite polynomials have to be assigned their operational properties. A close form for the $2N-$dimensional Hermite polynomials, as defined by eq. 77 prove to be very complicated except for the simplest cases of one and two dimensions. However, these polynomials satisfy some interesting recurrence relations which makes the use eq. 78 computationally feasible. It is obvious from eq. 77 that

$$\mathbf{H_{00}}(\underline{A}|b) = 1. \tag{79}$$

If we now differentiate the terms on both sides the equality 77 with respect to the parameter $s_i$ and $t_i$, respectively), the "n" and "m" recurrence relations for $\mathbf{H_{n,m}}(\underline{A}|b)$ are easily found[87,88];

$$\begin{aligned}
&2A_{s_i s_i}(n_i - 1)\mathbf{H_{n_{i-2}m}} + 2A_{s_i t_i} m_i \mathbf{H_{n_{i-1}m_{i-1}}} + \sum_{j\neq i}(A_{s_i s_j} + A_{s_j s_i}) n_j \mathbf{H_{n_{i-1,j-1}m}} + \\
&\sum_{j\neq i}(A_{s_i t_j} + A_{t_j s_i}) m_j \mathbf{H_{n_{i-1}m_{j-1}}} - 2b_{s_i}\mathbf{H_{n_{i-1}m}} + \mathbf{H_{nm}} = 0 \\
&2A_{t_i t_i}(m_i - 1)\mathbf{H_{nm_{i-2}}} + 2A_{t_i s_i} n_i \mathbf{H_{n_{i-1}m_{i-1}}} + \sum_{j\neq i}(A_{t_i t_j} + A_{t_j t_i}) m_j \mathbf{H_{nm_{i-1,j-1}}} + \\
&\sum_{j\neq i}(A_{t_i s_j} + A_{s_j t_i}) n_j \mathbf{H_{n_{j-1}m_{i-1}}} - 2b_{t_i}\mathbf{H_{nm_{i-1}}} + \mathbf{H_{nm}} = 0
\end{aligned} \tag{80}$$

where the indices $\mathbf{n}$ and $\mathbf{m}$ above refer to the sets

$$\mathbf{n} = (\ n_1 \quad n_2 \quad \cdots \quad n_N\ ) \qquad \mathbf{m} = (\ m_1 \quad m_2 \quad \cdots \quad m_N\ ) \tag{81}$$

and, for instance, a substitution in the $i^{th}$ element of this set, $n_i$, by $n_i - 1$ is denoted as

$$\mathbf{n}_{i-1} \equiv (\ n_1 \quad n_2 \quad \cdots \quad n_{i-1} \quad n_i - 1 \quad n_{i+1} \quad \cdots \quad n_N\ ). \tag{82}$$

For the special one-dimensional case, we set $\mathbf{m} = 0$ or $\mathbf{n} = 0$, respectively, in the recurrence relations of eq. 80 and obtain,

$$\begin{aligned}
&2A_{ss}(n-1)\mathcal{H}_{n-2}(A_{ss}|b_s) - 2b_s\mathcal{H}_{n-1}(A_{ss}|b_s) + \mathcal{H}_n(A_{ss}|b_s) = 0 \\
&[2A_{tt}(m-1)\mathcal{H}_{m-2}(A_{tt}|b_t) - 2b_t\mathcal{H}_{m-1}(A_{tt}|b_t) + \mathcal{H}_m(A_{tt}|b_t) = 0]
\end{aligned} \tag{83}$$

This becomes the stantad recurrence relation for the one-dimensional Hermite polynomials;

$$2n\mathcal{H}_{n-1}(y) - 2y\mathcal{H}_n(y) + \mathcal{H}_{n+1}(y) = 0 \tag{84}$$

if we make $y = b_s/\sqrt{A_{ss}}$ and note that

$$\mathcal{H}_n(a|x) = a^{n/2}\mathcal{H}_n(\frac{x}{\sqrt{a}}). \tag{85}$$

The two-dimensional case the Hermite polynomials show a three terms recurrence relation,

$$\begin{aligned}
&2A_{ss}(n-1)\mathbf{H}_{n-2,m}(\underline{A}|b) + 2A_{st}m\mathbf{H}_{n-1,m-1}(\underline{A}|b) - 2b_s\mathbf{H}_{n-1,m}(\underline{A}|b) + \mathbf{H}_{n,m}(\underline{A}|b) = 0 \\
&2A_{tt}(m-1)\mathbf{H}_{n,m-2}(\underline{A}|b) + 2A_{ts}n\mathbf{H}_{n-1,m-1}(\underline{A}|b) - 2b_t\mathbf{H}_{n,m-1}(\underline{A}|b) + \mathbf{H}_{n,m}(\underline{A}|b) = 0,
\end{aligned} \tag{86}$$

first given by Ansbacher[92] and a relatively simple analytic form,

$$\mathbf{H_{n,m}}(\underline{A}|b) = \sum_{k=0}^{min[n,m]} \binom{n}{k}\binom{m}{k} k!(-(A_{st}+A_{ts})^k A_{ss}^{\frac{n-k}{2}} \mathcal{H}_{n-k}(\frac{b_s}{\sqrt{A_{ss}}}) A_{tt}^{\frac{m-k}{2}} \mathcal{H}_{m-k}(\frac{b_t}{\sqrt{A_{tt}}}), \tag{87}$$

already derived for the one-dimensional case in ref. [93], see also ref. [94]. From the recurrence relations given in eq. 80 for the many- dimensional Hermite polynomials, one can easily form equivalent recurrence relations directly for the Franck-Condon amplitudes of eq. 78. To do so it is necessary to associate each memmer of the relations of eq. 80 with a correct normalization factor. If so one obtains;

$$\begin{aligned}
&4A_{s_i s_i}\sqrt{\frac{(n_i-1)}{n_i}}\mathcal{I}(\mathbf{n}_{i-2}\mathbf{m}) + 4A_{s_i t_i} m_i \sqrt{\frac{m_i}{n_i}}\mathcal{I}(\mathbf{n}_{i-1}\mathbf{m}_{i-1}) + \\
&2\sum_{j\neq i}(A_{s_i s_j}+A_{s_j s_i})\sqrt{\frac{n_j}{n_i}}\mathcal{I}(\mathbf{n}_{i-1,j-1}\mathbf{m}) + 2\sum_{j\neq i}(A_{s_i t_j}+A_{t_j s_i})\sqrt{\frac{m_j}{n_i}}\mathcal{I}(\mathbf{n}_{i-1}\mathbf{m}_{j-1}) - \\
&\qquad 2b_{s_i}\sqrt{\frac{2}{n_i}}\mathcal{I}(\mathbf{n}_{i-1}\mathbf{m}) + \mathcal{I}_{\mathbf{nm}} = 0
\end{aligned}$$

$$\begin{aligned}
&4A_{t_i t_i}\sqrt{\frac{(m_i-1)}{m_i}}\mathcal{I}(\mathbf{n}\mathbf{m}_{i-2}) + 4A_{t_i s_i}\sqrt{\frac{n_i}{m_i}}\mathcal{I}(\mathbf{n}_{i-1}\mathbf{m}_{i-1}) + \\
&2\sum_{j\neq i}(A_{t_i t_j}+A_{t_j t_i})\sqrt{\frac{m_j}{m_i}}\mathcal{I}(\mathbf{n}\mathbf{m}_{i-1,j-1}) + 2\sum_{j\neq i}(A_{t_i s_j}+A_{s_j t_i})\sqrt{\frac{n_j}{m_i}}\mathcal{I}(\mathbf{n}_{j-1}\mathbf{m}_{i-1}) - \\
&\qquad 2b_{t_i}\sqrt{\frac{2}{m_i}}\mathcal{I}(\mathbf{n}\mathbf{m}_{i-1}) + \mathcal{I}_{\mathbf{nm}} = 0
\end{aligned} \tag{88}$$

Recurrence relations for multidimensional Franck-Condon amplitudes equivalent to the ones derived above have been obtained by Doktorov et al[87], by Malmquist[89] and very recently by Lerme'[95]. The latter author gives an instructive discussion on the accuracy of these iterative methods when applied to one- and two-dimensional Franck-Condon amplitudes and factors.

# 5 Auger Transition Rates

## 5.1 Auger Transition Rates From General Many-Electron Wave Functions

As mentioned in the introduction, no PCI related effects have been studied nor identified in molecular valence spectra. The experimental reasons for this are given by the comparatively high density of states and the vibronic broadening which smears out or hides possible structures connected to PCI. The theoretical reason is associated to the difficulty in determining continuum waves and associated matrix elements in non-local molecular potentials, and also, from the formal point of view, to formulate a Born-Oppenheimer approximation for infinitely degenerate scattering states. Instead, the implementation of Auger theory for molecules has exclusively been restricted to the framework of Wentzel's ansatz[96] and we confine this section on Auger rates to theoretical studies associated to this ansatz. With this ansatz one assumes the Auger decay as part of a two-step process, i.e. with the decay uncoupled from the excitation of the initial state, and independent of the interaction between primary photoelectron and Auger electron and that interaction with other collisional products is negligible (neglect of PCI). This means that the transition probability for the process will be proportional to the square of the decay transition amplitude of eq. 36, i.e., it may be calculated from Fermi's golden rule in the limit of zero frequency for the external field. A general molecular application at this level of theory has been performed by Colle and Simonucci[97,98], including continuum channel interaction[98], and is further commented below. However, expect for this application it has generally been assumed that the "minus" scattering wave function on the left hand side of eq. 36 is restricted to a zero order of approximation in the iterative Lippmann-Schwinger solution of eq. 14. This corresponds to the complete neglect of final-state continuum inter-channel interactions. Improvements to the last restriction can be obtained by gradually introducing correlation effects in the final channels, discussed in what follows. However, the wave functions do then not strictly satisfy the outgoing boundary conditions for correct scattering waves. Within these approximations the expression for the vibronic transition of probability resembles the usual Condon expression for optical transitions,

$$\sigma_{f_n i_m} \propto |<\chi_n(\mathbf{R})|W_{fi}(\mathbf{R})|\xi_m(\mathbf{R})>|^2 \tag{89}$$

where $W_{fi}(\mathbf{R}$ is the the electronic transition rate. Hereafter in this section we will only be discussing the electronic part of the problem, the vibrational counterpart was addressed previously in section 4.

Originally, Wentzels ansatz[96] was obtained from first order perturbation theory of the interaction between the ionized state and the continuum many-hole final states with the same energy. Its applicability is limited by two conditions; (i) the transition rate is low enough to make the assumption behind Fermi's golden rule valid and; (ii) the initial state $\Psi_i$ is independent of the primary excitation process. When these requirements are not fulfilled a more general scattering formulation is required, as indicated above. In the first requirement lies the assumption that it is meaningful at all to identify an initial state $\Psi_i$. Exceptions are super Coster-Kronig structure in high Z-elements where the strong coupling between discrete and continuum states wipes out any resemblance of a line spectrum. In the second requirement lies the assumption that the Auger decay can be treated as a two-step process and that and that PCI can be neglected.

A derivation of of Wentzel's ansatz for wave functions built on mutually non-orthogonal sets of orbitals and with interacting continuum channels was given explicitly by Howat, Åberg and Goscinski[99] and extended to final many-particle wave functions by Manne and Ågren[100] who, however, retained a single-channel description for the outgoing electron. Other methods within the framework of Wentzel's ansatz are the many-body perturbation method of Kelly[101], and the two-particle Greens function method of Liegener[28]. The latter method have been exploited for a number molecules and is reviewed in section 9. Very recently, Colle and Simonucci proposed a method within Wentzels ansatz, that included discrete and continuum interaction between the final channels of the Auger process. They started from the scattering approach of Åberg and Howat[35] reviewed in section 3, but neglected any coupling to the nuclear motion. The partial and total Auger rates were obtained by solving the Lippman-Schwinger equations, eq. 14. Applications to neon[102] and LiF[97,98] gave very rewarding results.

Wentzels ansatz has normally been applied with a frozen-orbital description of the participating ions. Calculations using more refined wave functions have been performed for several systems. The refinements are of three kinds: (i) the introduction of correlation through the use of configuration interaction wave functions or many perturbation theory; and (ii) the introduction of different orbital bases for the description of initial and final states: (iii) intercation between the continuum parts of the channels Related to the second type of refinement is the introduction of a possible non-orthogonality between the initial and the final states. Below we review the Wentzel ansatz when applied to many-electron wave functions (initial and final state-) but with only a single channel description for the continuum Auger electron, following the derivation based on second quantization by Manne and Ågren[100].

Wentzel's ansatz gives the transition probability as

$$W_{fi} = 2\pi \,|< \Psi_f \mid \hat{H} - E \mid \Psi_i >|^2 \tag{90}$$

where $\hat{H}$ is the electrostatic hamiltonian with the expectation value E for the initial state as well as for the the final state. The final continuum state is assumed normalized per unit energy range. The transition amplitude is defined as the matrix element

$$A_{fi} = < \psi_f \mid \hat{H} - E \mid \Psi_i > \tag{91}$$

The second quantized hamiltonian is expressed as

$$\hat{H} = \sum < p \mid \hat{h}_1 \mid q > \hat{a}_p^+ \hat{a}_q + \frac{1}{2} \sum < pq \mid rs > \hat{a}_p^+ \hat{a}_q^+ \hat{a}_s \hat{a}_r \tag{92}$$

The creation and annihilation operators are defined for an orthogonal orbital set fulfilling the standard anticommutation relations: $\hat{a}_p^+ \hat{a}_q + \hat{a}_q \hat{a}_p^+ = \delta_{pq}$ We write the initial state as

$$\psi_i = \Psi_K = \mid K > \tag{93}$$

and the energy expectation value as $E = E_K$ relating to a vacancy in the K shell. For conveniency of notation the final state we write

$$\Psi_f = \hat{a}_\epsilon^+ \Psi_{LL} = \hat{a}_\epsilon^+ \mid LL > \tag{94}$$

where the notation relates to a double L-shell vacancy (the theory is as such not restricted to these assumptions). It is the spatial and spin symmetry labels of the final residual LL state which normally characterize molecular Auger spectra, i.e. the first

main state on the high kinetic energy side of the water Auger spectrum is denoted as $(3a_1 1b_1)^3B_1$ state, (parenthesis denote orbital labels). It is assumed that the continuum orbital is strongly orthogonal to $\mid LL >$, i.e. that it fulfills the killer condition

$$\hat{a}_\epsilon \mid LL > = 0 \tag{95}$$

The use of strong orthogonality and the killer condition ensures proper normalization and limiting behaviour for $r \rightarrow \infty$ of the final-state wave function. It also confers to the "static exchange" approximation frequently employed in the calculation of photoionization cross sections and shape resonances. The use of the static exchange condition for calculation of Auger continuum orbitals and Auger rates in molecules is given in ref. [103].

Restricting to a single-channel description for the outgoing electron, but keeping the formalism general for any many-electron or orbital description of the initial residual final states. In principle a proper many-channel description and the infinite degeneracy of the final states of the Auger continuum, retaining correct spin and spatial symmetry, can be included by expanding $\Psi_f = \hat{a}_\epsilon \mid LL >$ to $\Psi_f = \sum_i \hat{a}^+_{\epsilon,i} \Psi_{LL} c_i$ where the summation is over states with the energy $E_K$. For calculations under these general assumptions we refer to the recent work of Colle and Simonucci[98].

Assuming the residual final state $\mid LL >$ to be an eigenstate of the full Hamiltonian:

$$\hat{H} \mid LL > = E_{LL} \mid LL > \tag{96}$$

The transition amplitude according to Wentzel's ansatz then takes the form

$$A_{fi} = < \psi_f \mid \hat{H} - E \mid \psi_i > = < \hat{a}^+_\epsilon \Psi_{LL} \mid \hat{H} - E_K \mid \Psi_K > = < LL \mid \hat{a}_\epsilon (\hat{H} - E_K) \mid K > \tag{97}$$

$$= < LL \mid [\hat{a}_\epsilon, \hat{H}] + (\hat{H} - E_K)\hat{a} \mid K > = \tag{98}$$

$$= < LL \mid [\hat{a}_\epsilon, \hat{H}] \mid K > + (E_{LL} - E_K) < LL \mid \hat{a}_\epsilon \mid K > \tag{99}$$

In this formulation the transition amplitude is dependent on the energy difference $E_K - E_{LL} = \epsilon_\epsilon$ for the expelled Auger electron. A final expression using operators defined for the final state is obtained after expanding the commutator

$$[\hat{a}_\epsilon, \hat{H}] = \sum_{pq} < p \mid \hat{h}_1 \mid q > [\hat{a}_\epsilon, \hat{a}^+_p \hat{a}_q] + \frac{1}{2} \sum_{pqrs} [[\hat{a}_\epsilon, \hat{a}^+_p \hat{a}^+_q \hat{a}_s \hat{a}_r] \tag{100}$$

$$= \sum_q < \epsilon \mid \hat{h}_1 \mid q > \hat{a}_q + \frac{1}{2} \sum_{qrs} (< \epsilon q \mid rs > - < \epsilon q \mid sr >) \hat{a}^+_q \hat{a}_s \hat{a}_r \tag{101}$$

as

$$A_{fi} = \sum_r < \epsilon \mid \hat{h}_1 \mid r >< LL \mid \hat{a}_r \mid K > - \epsilon_\epsilon < LL \mid \hat{a}_\epsilon \mid K > \tag{102}$$

$$+ \sum_{qrs} (< \epsilon q \mid rs > - < \epsilon q \mid sr >< LL \mid \hat{a}^+_q \hat{a}_s \hat{a}_r \mid K > \tag{103}$$

This expression was further elaborated on in [100] in the case when sets of mutually non-orthogonal orbitals for initial and final states are chosen, and in the case were single-channel continuum orbitals are optimized in the static potential. The first case is relevant for valence Auger since there is a substantial orbital relaxation between a core hole state (Auger initial state) and states with holes only among valence levels (here Auger final states). The annihilation operators defined for the final state can

be expanded in those of the initial state after a unitary transformation of orbitals as $\hat{a}_\epsilon = \sum_r < \epsilon \mid r > \hat{a}_r$ with the orbital overlap integral $< \epsilon \mid r > = < \phi_\epsilon \mid \phi_r >$, leading to

$$A_{fi} = \sum_r (< \epsilon \mid \hat{h}_1 \mid r > - \epsilon_\epsilon < \epsilon \mid r >) < LL \mid \hat{a}_r \mid K > \tag{104}$$

$$+ \frac{1}{2} \sum_{qrs} (< \epsilon q \mid rs > - < \epsilon q \mid sr >< LL \mid \hat{a}_q^+ \hat{a}_s \hat{a}_r \mid K > \tag{105}$$

This expression contains eq. 103 as a special case when $(< \epsilon \mid r > = \delta_{\epsilon r})$. A second important choice of orbitals are those that take account of *intra*channel intercation within the single continuum channel for the outgoing Auger electron. This requirement is fulfilled by the solution of Hartree-Fock like static exchange equations from which a set of orthogonal and non-interacting orbitals satisfying the killer condition $\hat{a}_v \mid LL > = 0$ can be derived, where v denotes any continuum orbital. The latter condition can be expressed as

$$< LL \mid \hat{a}_\epsilon \hat{H} \hat{a}_v^+ \mid LL > = < LL \mid \hat{a}_\epsilon ([\hat{H}, \hat{a}_v^+] + \hat{a}_v^+ \hat{H}) \mid LL > = \delta_{\epsilon v} E_K \tag{106}$$

Inserting the killer condition (orbital indices $\epsilon$ and v) the Hartree-Fock like equation for the Auger electron are obtained

$$< \epsilon \mid \hat{h}_1 \mid v > + \sum_{qs} (< \epsilon q \mid vs > - < \epsilon q \mid sv >) < LL \mid \hat{a}_q^+ \hat{a}_s \mid LL > = \delta_{\epsilon v} \epsilon_\epsilon \tag{107}$$

It differs from the ordinary Hartree-Fock equations by the inclusion of the density matrix for the residual final state LL that defines the Auger channel of interest.

It is clear that under the normal conditions for Auger spectroscopy with fast excitation particles and fast Auger electrons the energetics of the spectra are given by the spectrum $\mid LL >$ of the two-hole ions. For the spectral function, i.e. intensity versus energy the cross section for each type of Auger event must evidently be considered. From eqs 103 or 105 we see that Auger transition amplitudes contain three parts: (i) a sum involving the one-electron operator; (ii) a term or sum deriving from the non-orthogonality between initial and final states, and (iii) a sum involving the electron-electron interaction. In next section we simplify from these general many-electron expressions for Auger transition amplitudes and give simplified forms that have been used to characterize molecular Auger spectra.

## 5.2 Frozen Orbital Approximation

Using a frozen orbital description for initial and final states one finds that the overlap amplitude $\sum_r \phi_r < LL \mid \hat{a}_r \mid K >$ is zero. The Auger transition amplitude, eeq.105, then reads

$$A_{fi} = \frac{1}{2} \sum_{qrs} (< \epsilon q \mid rs > - < \epsilon q \mid sr >< LL \mid \hat{a}_q^+ \hat{a}_s \hat{a}_r \mid K > = \sum_{qrs} \tau_{qrs} \chi_{qrs} \tag{108}$$

where we denote

$$\tau_{qrs} = < \epsilon q \mid rs > - < \epsilon q \mid sr > \tag{109}$$

as the Auger transition moment and

$$\chi_{qrs} = < LL \mid \hat{a}_q^+ \hat{a}_r \hat{a}_s \mid K > \tag{110}$$

the generalized Auger overlap amplitude (GOA). Like photoelectron spectra one can qualitatively analyze Auger spectra in terms of these orbital transition elements and overlap amplitudes, see sections 6.1 and 6.2. Much of the information inherent in Auger spectra are related to these amplitudes, the complexity of which varies significantly for different species, e.g. between closed-shell or open-shell species, atoms, saturated and unsaturated species etc. Their character differ also in different parts of the spectra, referring to inner-inner, inner-outer, or outer-outer orbital parts, see section 6.3. Approximating furthermore the initial state with a single Slater determinant, that is neglecting initial state correlation, the transition moment reduces to

$$A_{fi} = \sum_{rs} \tau_{rs} c_{rs} \tag{111}$$

where $c_{rs}$ is the expansion coefficient of the main two-hole configuration (holes in r and s orbitals). In this expression the summation was reduced to include one core orbital index only. This is in any case a good approximation due to almost perfect orthogonality between different core orbitals (also two-hole initial ionization is neglected here). $\mid c_{rs} \mid^2$, the weight of the $\Phi_{rs}$ configuration state function is equal to the pole strength of the particle-particle Greens function, see section 9. When there is more than one pair of r,s indices for which $c_{rs}$ is large we talk about *hole mixing Auger states*, see section 12.1.

If one besides frozen orbitals assumes uncorrelated wave functions one obtains the simplest form for the Auger intensities. They relate directly to the least possible combination of determinants that fulfills spatial or spin symmetry, i.e. a CSF. For molecules with non-degenerate point group and closed shell ground states the expression relate to the original formula due to Wentzel's ansatz (see e.g. Assad[104] and Burhop[105]:

$$A_{fi} = 2\pi \mid < \epsilon 1s \mid rs > + < \epsilon 1s \mid sr > \mid^2 \tag{112}$$

$$A_{fi} = 6\pi \mid < \epsilon 1s \mid rs > - < \epsilon 1s \mid sr > \mid^2 \tag{113}$$

For singlet respectively triplet coupled final state vacancies r and s. (1s denotes here the initially emptied core orbital). The generalization to ground-state open-shell cases proceeds by means of spin-coupling theory, see below. For open shell atomic systems general formalisms based on tensor algebra and Racah coefficients have been given by McGuire, Walters and Bhalla and others. For molecular calculations formulas with atomic coupling coefficients are required when atomic Auger transition moments are incorporated into approximate expressions either with the atomic decomposition scheme [106] or in connection with spherical-wave calculations of continuum orbitals in molecular potentials expanded form a single center [107]. In case the Auger intensities are given in the potentials of the molecular point group explicitly, they again "simplifies" according to eq:s 112 and 113.

Estimates of which CSF:s in an open shell system contribute to the spectra can be obtained just by analyzing the final formula for the cross sections in terms of Coulomb, $J = < \epsilon 1s \mid rs >$, and exchange, $K = < \epsilon 1s \mid sr >$, integrals. As seen from eqs. 112 and 113 the singlet coupled final states dominate over the triplet coupled ones for a Auger spectrum of a closed shell molecule. This follows from that the Coulomb and exchange integrals usually are of the same order of magnitude, although this magnitude can vary considerably over a region of energies for the continuum Auger electron[108]. Similar arguments can be made in the open shell case. As shown in ref. [13] the genealogic scheme is suitable for derivation the matrix elements. The different transitions are first ordered according to the spin-coupling of the initial core hole state (i.e. triplet or singlet

spectra for a one-open shell ground state molecule), and then after the spin-coupling of the final state for the residual ion. In the latter case the Auger electron assumes a spin that makes the total spin compatible with that of the core hole state. When the the final state is a three open shell state the relative intensities in the triplet spectrum, i.e. with a triplet coupled core hole state, go as $2 \mid J-K \mid^2$, $\frac{1}{2} \mid J-K \mid^2$ and $\frac{1}{2} \mid J+K \mid^2$ for the final quartet, the triplet and singlet parent coupled doublet, respectively. The corresponding intensities in the singlet spectrum are $\frac{3}{2} \mid J-K \mid^2$ and $\frac{1}{2} \mid J+K \mid^2$ for the triplet parent coupled doublet and the singlet parent coupled states, respectively. In case the Auger transition takes place in the same shell of a one-open shell molecule, the intensities relate simply as $3 \mid J \mid^2$ and $\mid J \mid^2$ for the triplet and singlet initial states respectively. Finally, if the open shell participates in the Auger process the intensities in the two types of spectra will be $3 \mid J \mid^2$ and $\mid J-2K \mid^2$. Without having to compute the J and K integrals explicitly, one may assert that the triplet to triplet parent coupled doublet transition will dominate the one open shell Auger spectrum. Semi-internal CI calculations using the above formulas and the one-center decomposition scheme were carried out in [13] for the nitrogen and oxygen Auger spectra of NO.

## 5.3 Role of Relaxation

If we assume relaxed, state-specific, orbitals instead of frozen orbitals the general equations do not simplify as neatly. The non-orthogonality expression for unrestricted orbitals were derived by Howat et al [99] and applied to the Auger intensities:

$$< \Psi_{xy\epsilon} \mid \hat{H}-E \mid \Psi_{1s} >= \Pi_{j \neq x,y} < j \mid j' > \left[ < \epsilon' 1s' \mid\mid xy > + \begin{vmatrix} < \epsilon' \mid J \mid x > & < \epsilon' \mid J \mid y > \\ < 1s' \mid x > & < 1s' \mid y > \end{vmatrix} \right. \tag{114}$$

$$\left. + \begin{vmatrix} < \epsilon' \mid x > & < \epsilon' \mid y > \\ < 1s' \mid J \mid x > & < 1s' \mid J' \mid y > \end{vmatrix} - \zeta \begin{vmatrix} < \epsilon' \mid x > & < \epsilon' \mid y > \\ < 1s' \mid x > & < 1s' \mid y > \end{vmatrix} \right] \tag{115}$$

$$+ \sum_{j \neq x,y} \left[ \begin{vmatrix} < i' \mid x > & < i' \mid y > \\ < \epsilon' 1s' \mid\mid xi > & < \epsilon' 1s' \mid\mid yi > \end{vmatrix} + \begin{vmatrix} < \epsilon' \mid x > & < 1s' \mid i > \\ < \epsilon' i' \mid\mid xy > & < \epsilon' 1s' \mid\mid xy > \end{vmatrix} \right] \tag{116}$$

where $< ab \mid\mid cd >$ is a short forms for the two-electron direct minus the exchange interaction integrals, and the $\hat{J}$ operator is defined as a sum over the one-electron hamiltonian and two-electron operators as:

$$\hat{J} = \hat{h}_1 + \sum_{j \neq x,y} < j' \mid\mid j > \tag{117}$$

and $\zeta$ energy term is defined as

$$\zeta = E - \frac{1}{2} \sum_{j \neq x,y} (< j' \mid \hat{h}_1 \mid j > + < j' \mid \hat{J} \mid j >) \tag{118}$$

Orbitals with apex are final state orbitals, those without apex initial state orbitals. With separately optimized orbitals we thus introduce matrix elements also over the one-electron part of the hamiltonian. It is is advantageous to keep the orbitals in the spin-restricted form, since we want to distinguish between a singlet spectrum with high intensity and a triplet spectrum with low intensity. Also in this case the intensity expression is quite complex. In the simplest case, i.e. when orbital indices x and y are the same one obtains the following expression, see [103]:

$$< \Psi_{xy\epsilon} \mid \hat{H} - E \mid \Psi_{1s} > = \tag{119}$$

$$\Pi_{j\neq x,1s}(j' \mid j)^2(1s' \mid 1s)\Big[(\epsilon' x \mid 1s' x) + (1s' \mid x)F_{\epsilon' x} + (\epsilon' \mid x)F_{1s' x} - A_x(\epsilon' \mid x)(1s' \mid x) \tag{120}$$

$$\sum_{j\neq x}\left[(j' \mid x)(\epsilon' j \mid 1s' x) + (\epsilon' \mid j)(1s' x \mid j' x)\right] - \tag{121}$$

$$\sum_{j\neq x,1s}\left[(j' \mid x)(\epsilon' x \mid 1s' j) + (1s' \mid j)(\epsilon' x \mid j' x)\right]\Big] \tag{122}$$

where $F_{a'x}$ is the Fock type matrix:

$$F_{a'x} = (a' \mid \hat{h}_1 \mid x) + \sum_{j\neq x,1s}\left[2(j' j \mid a' x) - (j' x \mid a' j)\right] + (1s' 1s \mid a' x) \tag{123}$$

and $A_x$ an energy term:

$$A_x = E - 2\sum_{j\neq x,1s}(j' \mid \hat{h}_1 \mid 1s) - (1s' \mid \hat{h}_1 \mid 1s) - \sum_{i\neq x,1s}\sum_{j\neq x}\left[2(i' i \mid j' j) - (i' j \mid j' i)\right] \tag{124}$$

Both Mulliken notation (round () parenthesis) and Dirac notation (square <> parenthesis) for the two-electron integrals have been used in these formulas.

For atoms and for "electron-poor" saturated systems, like the first and second row hydrides, the effect of relaxation is relatively minor, say 10%. The overlap elements between corresponding orbitals of initial and final states are close to 1.0. For atoms McGuire[109,110] thus concludes that initial versus final state non-orthogonality is not important due to the almost unit overlap matrix. This is also found true for HF[107], $NH_3$[111] and $H_2O$[103]. However, already for the first row diatomics with unsaturated $\pi$ bonds the overlap element between initial and final $\pi$ orbitals may be considerably lower. The $\pi$ bonds conduct a very efficient charge transfer screening of the core hole via electron relaxation through these bonds. This screening and the orbital character is different for different core holes, for example between C and O holes in the CO molecule. Here the carbon core hole takes place within the $\Pi$ manifold of orbitals ($\pi$ and $\pi^*$)while the screening of the oxygen core hole takes place through the $\Sigma$ manifold. The relaxation characteristics thus have a different impact for the cross sections of two-hole derived Auger spectra (as, for instance, also in core hole shake-up spectra). Thus strong screening reaction leads to a large relaxation effect, while weak screening or antiscreening leads to a weak relaxation effect.

## 5.4 Auger Electron Functions and Transition Moments

There are intrinsic difficulties in evaluating the full form of the Auger cross sections, even in the simpler case of frozen orbital "one-particle" wave functions, eq. 111. These difficulties can be referred to the determination of the Auger continuum function $\epsilon$ with high energy and highly oscillatory character. The transition moment, $\tau_{rs} = < \epsilon 1s \parallel rs >$, is a due to a delta energy resonance at high energies in the continuum. A problem in the theoretical description of such resonances lies thus in the explicit construction of continuum electronic wave functions in non-isotropic potentials. Conventional scattering approaches relying on asymptotic boundary conditions have met difficulties in solving this problem, while so-called $L^2$ methods are potentially better in this respect due to the utilization of square integrable basis sets to describe the non-central character of the continuum functions. In the $L^2$ approaches the many-electron continuum is

often approximated by an anti-symmetrized product of a fixed target function for the molecular ion and a continuum orbital for the outgoing electron, the so-called static exchange approximation.

For molecular Auger we know of four applications using $L^2$ methods for calculating Auger rates; Faegri and Kelly for HF[107]; Hihashi, Hiroike and Nakajima for $CH_4$[112,113]; Carravetta and Ågren for $H_2O$[103], and Colle and Simonucci[97,98] for LiF. The latter approach, also commented in section 5.1, used a scattering formalism, and an expansion of the molecular potential in a multi-center $L^2$ basis set. Carravetta and Ågren used a moment theory approach, the Stieltjes imaging method. An appealing feature with moment theory approaches is that they provide a direct generalization of the bound state electronic structure methods and even the very computer codes, with the distinct advantage that both discrete and continuum states can be treated on a common basis, using the same point group symmetry, integral representations of operators, etc. The correct energy normalization of the continuous part of the spectra is obtained from pointwise convergence of the spectral density. The formal motivation for the moment methods origins from the fact that although the solutions of the Schrödinger equation in a square-integrable basis set are proper representations only for the discrete part of the spectrum, they provide proper representations of the *moments* of the spectrum. The great advantage with the scattering $L^2$ methods[98] is that they can account for the important interchannel interactions, and that they fulfill formal boundary conditions and can formally handle the infinite degeneracy of continuum states.

A justification of the Stieltjes imaging, moment theory method, for Auger was given in ref. [103] recalling that the lowest order contribution to the correlation energy of an inner-shell hole (h) can be written as [114,115]

$$E_h^{(2)} = \sum_{x \geq y} E_{hxy}^{(2)} = \sum_{x \geq y} \left[ \sum_{\nu}^{disc} \frac{|< xy \,||\, \nu h >|^2}{\epsilon_x + \epsilon_y - \epsilon_\nu - \epsilon_h} + \int_0^\infty dE \frac{|< xy \,||\, \nu(E) h >|^2}{\epsilon_x + \epsilon_y - E - \epsilon_h} \right] \quad (125)$$

where the two final-state holes, the initial core holes, and the excited orbital are denoted by indices x, y, h and $\nu$, respectively. The excited orbital energy in expression 125 takes discrete ($\epsilon_\nu$) and continuous values; the continuum orbital $\nu(E)$ is considered to be normalized per unit energy interval. The Auger effect occurs for the singularities $E = \epsilon_x + \epsilon_y - \epsilon_h$ of the various functions $E_{hxy}^{(2)}$, and the Auger decay rates are given by the residues of these singularities[114] (c.f. discussion of of the two-particle Greens functions in section 9). Considering the continuum orbital $\nu$ normalized per unit K interval the integral over the continuum-orbital energy E can be written as[103];

$$\int_0^\infty dK \frac{|< xy \,||\, \nu(K) h >|^2}{\epsilon_x + \epsilon_y - \frac{1}{2}K^2 - \epsilon_h} \quad (126)$$

This integral can be seen as a Stieltjes integral where, if compared with the ordinary photoelectron expressions, K and $|< xy \,||\, \nu(K) h >|^2$ correspond to the energy and the oscillator strength distribution, respectively. A discrete spectrum $\{K, |< xy \,||\, \nu h >|^2\}$ forms a basis for the Stieltjes construction of a "K-normalized" continuous functions[103] $Z_{hxy}(K) = |< xy \,||\, \nu(K) h >|^2$ The Auger decay rate is obtained for only one value of this function, corresponding to the resonance energy

$$\Gamma_{hxy} = \frac{2\pi}{K_0} Z_{hxy}(K_0) \quad (127)$$

$$K_0 = [2(\epsilon_x + \epsilon_y - \epsilon_h)]^{\frac{1}{2}} \quad (128)$$

Table 1: Intensities in arbitrary units of Auger transitions in the water molecule. Comparison between results from atomic decomposition, partial-wave, mixed-wave and hole-mixing calculations. From ref [103].

| Channel | Atomic Decomp. | Partial Wave | Mixed Wave | Hole Mixing |
|---|---|---|---|---|
| $2a_1^{-2}$ S | 48 | 98 | 96 | 61 |
| $2a_1 3a_1$ S | 48 | 80 | 76 | 65 |
| $2a_1 3a_1$ T | 11 | 29 | 29 | 29 |
| $2a_1 1b_2$ S | 32 | 52 | 51 | 45 |
| $2a_1 1b_2$ T | 8 | 24 | 23 | 21 |
| $2a_1 1b_1$ S | 55 | 68 | 67 | 58 |
| $2a_1 1b_1$ T | 14 | 32 | 32 | 28 |
| $3a_1^{-2}$ S | 71 | 73 | 71 | 68 |
| $3a_1 1b_2$ S | 58 | 95 | 92 | 96 |
| $3a_1 1b_2$ T | 1 | 1 | 1 | 2 |
| $3a_1 1b_1$ S | 99 | 106 | 101 | 102 |
| $3a_1 1b_1$ T | 2 | 2 | 2 | 2 |
| $1b_2^{-2}$ S | 34 | 59 | 58 | 60 |
| $1b_2 1b_1$ S | 74 | 96 | 89 | 92 |
| $1b_2 1b_1$ T | 0 | 0 | 0 | 0 |
| $1b_1^{-2}$ S | 100 | 100 | 100 | 100 |

In ref. [103] various forms for the Auger electron functions were assumed and optimized in static exchange potentials. One potential was constructed for each separate Auger channel defined by two missing orbitals and the spin coupling. Partial wave, mixed wave and coupled channel calculations were performed for the Auger electron function. From these calculation moments, total and separate channel cross section were obtained. For water the mixing of the partial waves (determined by their (l,m) quantum numbers) was found moderate, while discrete channel interaction is essential towards the high kinetic energy part of the spectrum (see also section 8.3. The results for water for the different forms of the Auger electron function are recapitulated in table 1, together with the corresponding results from the one-center decomposition scheme[106].

With the Stieltjes imaging techniques more exotic effects due to the interaction with the Auger continua can be obtained, such as the geometric dependence of the total Auger rate, and the contribution of discrete-continuum interaction to the inner shell ionization potentials[108]. In ref [116] it was shown that the geometry dependence of the total Auger rate and thus the lifetime was allocated more to the united atom limit than the separate atom limit, and that the "constant resonance width approximation" holds for core ionization of water. The Auger continuum interaction was found to contain considerable structure with respect to energy of the outgoing Auger electron being asymmetric with respect to the resonance points. This interaction leads both to a shift and an asymmetrization of the core spectral band[108,117].

# 6 Analysis of Molecular Auger Spectra

As mentioned in the previous section the starting point for interpretation of molecular Auger spectra, just as other types of core electron spectra of molecules, has mostly been given by Fermi golden rule expressions. One assumes thereby that the non-radiative decay of core hole states occurs as a two-step process, with the deexcitation uncoupled from the excitation and independent of the interaction between primary photoelectrons and Auger electrons.

With a strong orthogonality condition imposed on the scattered electron, fulfilling the killer condition of eq. 95, the leading terms of resulting Fermi golden rule like expressions, eq. 105, take the form:

$$M_{if} = \sum_x \tau_x \chi_x \tag{129}$$

that is a sum of terms, in which each term constitutes a product of a molecular orbital (MO) factor $\tau_x$ and a many-body factor $\chi_x$. For Auger this sum resolves as

$$\sum_x \tau_x \chi_x = \sum_{qrs} < \phi_\epsilon \phi_q \mid \frac{1-P}{r_{12}} \mid \phi_r \phi_s >< \Psi_f(N-2) \mid \hat{a}_q^+ \hat{a}_s \hat{a}_r \mid \Psi_i(N-1) > \tag{130}$$

for which there is a threefold summation of indices: x=q,r,s. However, for all cases it is well motivated to limit the core index q to one item due to the almost perfect orthogonality ($\chi_x \simeq 0$) between states with holes in different core orbitals or with holes in core and valence orbitals. One can note that with, effectively, two indices for annihilation of the initial state orbitals, there is a great number of possibilities for near-degeneracies of the final states of an Auger transition.

With the single-channel and strong orthogonality condition imposed on the continuum electrons a many-body factor is obtained that is only dependent on the characteristics of the residual bound states. A conventional MO analysis of the spectra is entailed only if there is just one large many-body term in the summation and if that term is close to one. In that case one further reduces the MO factor in terms of local decomposition of symmetries and charges, etc. One notes that for Auger a continuum orbital enters explicitly in the MO factor (as it does also in the photoionization case). Starting from the expressions given above one can summarize the various ways electron correlation enters in the interpretation of molecular Auger as follows.

## 6.1 The Many-Body Factor

Concerning the many-body factor $\chi_x$ we distinguish between four different situations:

i. One $\chi_x$ is close to one. This implies that the MO picture and the aufbau principle holds, a "Koopmans theorem" holds, the quasi-particle picture holds. An analysis of $\tau_x$ can be conducted in terms of MO theory, local densities, effective and strict selection rules etc. We denote such states as Koopmans double-hole states.

ii. More than one $\chi_x$ enters in the wave function. One then talks about hole-mixing effects and of electronic interference in the transition cross sections.

iii. Only one $\chi_x$ is large, but this $\chi_x$ is present in more than one state. One can then not associate a one-to-one correspondence between MO:s (or MO factors in eq. 130) and spectral bands (states). The states in question are thus associated with a break-down of the molecular orbital picture.

iv. No $\chi_x$ is large. We have a correlation state satellite.

Although there is no rigorous distinction between these cases, they clearly correspond to observed features in molecular Auger spectra.

The correlation energy contribution to Auger states is model dependent in soo far as there is no unambiguous way to define a many-open shell Hartree-Fock energy. However, whatever definition we choose electron correlation for Auger will be very important. This is also a mere fact because of that Auger spectra exhibit more peaks than can be obtained by combining two orbitals including the appropriate spin-coupling. There is no one-to-one correspondence between states and MO:s and the MO picture breaks down. In contrast to closed shell ground states where the correlation is classified by external single-, double-, excitation schemes, the correlation schemes of one-, two- or many-open shell states must include internal and semi-internal excitations. In fact the configuration interaction due to such excitations is most often the dominant one.

The final states of the Auger transitions can often be characterized as "Koopmans states" with a valid MO description in the outer-outer valence region, as hole-mixing states in the inner-outer region, and as states with break-down of the molecular orbital picture in the inner-inner valence region. The energy limits for these effects are of course system dependent. For atoms and "atom-like" systems such as first row hydrides there is a MO break-down only in the inner-inner valence spectra, the rest being comparatively well described at a one-particle (MO) level. Already for a small species like CO there are hole-mixing states in the outer-outer valence region[18,118], see section 12.1. For larger compounds the role of hole-mixing or break-down of the MO picture is pronounced in the major parts of the spectra.

The correlation types ii and iii can be seen as near-degeneracies, either between Koopmans configurations (hole-mixing) or between eigenstates (MO breakdown). A *static* correlation is then entailed, which in the wave function picture is described by *internal* and *semi-internal* hole-particle excitations. The role of semi-internal CI is pronounced, especially for electron-rich molecules with low symmetry, see section 8.3. In contrast to e.g. valence photoionization states the hole-mixing states for Auger origin often in static correlation for which there are large $\chi_x$:s, and hence large intensities. There are of course a great number of hole-mixing states where the dynamic correlation is leading and with small $\chi_x$:s, corresponding to those appearing in X-ray emission or valence photoionization spectra. However, such weak satellites are generally not observed in the Auger case.

For the correlation state satellites, case iv, the *dynamical* correlation effect is dominating. This is in the wave function picture described by *external* hole-particle excitations. The wave function is then characterized by only one small intermixed $\chi_x$ but is dominated by configurations generated by the hole-particle excitations. It can be noted that also for the outer-most Koopmans states, case i, the correlation (rather

the correlation correction) is of dynamical, i.e. external, origin. In this case, however, it acts only as a modulation to the intermixing of the main Koopmans configuration, with a large $\chi$, and the quasi-particle picture still holds. Since static correlation, just like relaxation, always gives rise to a positive error a "Koopmans" theorem, here the single ionization expression of eq. 138 with $R_{ij}=0$ and $I_i=\epsilon_i$, fails badly for transitions to double inner valence states. In contrast, the dynamical correlation error is negative, thereby counteracting the relaxation error for Koopmans states.

The distinction between static (near-degenerate) or dynamic (non-degenerate) correlation makes it possible to elucidate the role of initial versus final state correlation for the cross sections. For the case when static correlation is dominating for the final state, the initial state correlation can be ignored in a first approximation while, when the dynamic correlation is dominating initial and final state correlation is of equal importance. For correlation state satellite intensities initial and final states should, as a rule, be treated on equal footings.

## 6.2 The Molecular Orbital Factor

The molecular orbital analysis of core hole derived spectra can be carried out at several levels. One can distinguish between three types of orbitals for interpretative purpose; use of canonical Hartree-Fock orbitals (CMO:s); of natural orbitals (NO:s) that diagonalize a density matrix; and of field dependent Dyson orbitals (DO:s). Due to the quite different natures of initial and final states in core hole derived spectra, an NO analysis in terms of e.g. one-center decompositions, should preferably be carried out in terms of bi-natural orbitals that diagonalize a transition density matrix. Most popular is of course the use of canonical Hartree Fock orbitals. Such orbitals have been fundamental in the day-to-day analysis of a number of molecular experiments. This is so also for molecular Auger spectra, even if, as noted above, the use of any single state quantity can be questioned on grounds of the large relaxation. A popular use of CMO:s is to calculate charge and bond order matrices and to perform population analysis. The population numbers are then used in the intensity analysis by means of the use of one-center models. For Auger emission the one-center expression[106] is obtained by decomposing the two-electron orbital transition elements in eq.130. Use of spin-restricted theory leads to the one-center intensity expression

$$I_{pq} = 3\sum_{l,m} \mid J_{lm} - K_{lm} \mid^2, \tag{131}$$

$$I_{pq} = \sum_{l,m} \mid J_{lm} + K_{lm} \mid^2 \tag{132}$$

$$I_{pq} = 2\sum_{l,m} \mid J_{lm} \mid^2 \tag{133}$$

in case of Auger transitions to triplet- and singlet two-hole states and singlet closed shell states, respectively. The summation goes over possible atomic l,m channels with

$$J_{lm} = \sum_{l'm'} \sum_{l''m''} c^{p*}_{nl'm'} c^{q*}_{nl''m''} \delta(m'+m'', m) \times \sum_k d^k(l'm', 00) d^k(lm, l''m'') R^k_{nl'nl'} \tag{134}$$

and correspondingly for the exchange integrals, $K_{lm}$. $c^p$ and $c^q$ denote LCAO expansion coefficients for p and q MO:s pertaining to the atomic orbitals centered on the site of

the core ionization. The $d^k$:s are atomic coupling coefficients, and the $R^k$:s the atomic two-electron integrals involving the Auger (atomic) continuum function, the core orbital and the atomic valence orbitals; $R^k_{nl'nl'} = R^k[\chi_{core}\chi_\epsilon, nl'nl']$ As for XPS this expression gives the intensities as an *incoherent* sum of atomic cross sections.

The one-center model complies with the notion that different core hole derived Auger spectra "map" the the same set of double hole states differently according to the localization character of wave functions and orbitals. The one-center expressions given above have routinely been used to analyze molecular Auger spectra, and much of the "utility" of molecular Auger spectroscopies (as well as of other core electronic spectroscopies) is based on the supply of local information of symmetries and densities through the use of these expressions. Their usefulness derives also from that they are straightforwardly obtained (and computed) from molecular orbital theory. However, the the limits for the range of validity has been tested against higher levels of theory only in a few cases, see table 1.

## 6.3 Comparative Analysis of Auger and Photoelectron Spectra

Due to similarities in experimental techniques Auger and photoelectron spectroscopy are often studied in parallel. The two kinds of spectra can be obtained with same or similar spectrometers, using e.g. identical detectors for monitoring the kinetic energy of the escaping electrons. The excitation system may be different since the Auger electron is an effect of an inner conversion, to a first approximation independent of the ionizing agent, while mono-energetic photons are needed in photoelectron spectroscopy. The intensities are guided by different interacting operators and the initial state is a core hole state for Auger rather than the ground state. Since the initial state core hole is localized some particular simplifications are obtained for the evaluation of the Auger spectra within the one-particle model. For photoelectron spectra, one can at best, at high energies, regard the total cross section as an incoherent sum of contributions for local cross sections. Despite the obvious differences that Auger displays the two-hole- rather than the one-hole spectrum, the notions, the vocabulary and terminology used in analyzing the two types of spectra are analogous, in particular when comparing with high-energy XPS (X-ray photoelectron spectroscopy). These analogies, range from applications of scattering theory approaches, where the Auger effect often is considered merely as a resonant two-electron ionization event, to a coarse level of theory, e.g. the one-particle approximation, where energies of the Auger final states are given by combinations of photoelectron data, namely the single ionization potentials. It can thus be relevant to compare the analysis of the two types of spectra in terms of electronic structure theory, MO theory, the role of relaxation and correlation etc. In order to conduct such a comparison we display a simple scheme used for analysis of XPS in ref. [119], and discuss then the corresponding items for analysis of molecular Auger spectra. It reads as follows

A Radiative (non-radiative) transitions in an N-electron system according to Fermis golden rule

B Static-exchange, strong-orthogonality, approximation for the outgoing electron

C Neglect of conjugate transitions

D Neglect of orbital transition matrix elements (MO-factors)

E Neglect of initial state correlation (ISCI)

F Neglect of final state correlation (FSCI)

G No self-consistent description (orbital orthogonality)

This approximation scheme should be interpreted as follows: Each entry introduces an *approximation*. The corresponding *approximation level* contains this approximation as well as the previous ones. Thus at approximation level F, approximations A to F are employed. Below we employ the same scheme for molecular Auger spectra in order explore similarities.

Starting out from **level A**, we note that the photoelectron transition moment is obtained from Fermi's golden rule as

$$T_{fi} = \sum_r < \epsilon \mid t_1 \mid r >< \Psi_f(N-1) \mid \hat{a}_r \mid \Psi_0(N) > + \sum_r < \epsilon \mid r >< \Psi_f(N-1)\hat{T}\hat{a}_r \mid \Psi_0(N) > \tag{135}$$

A derivation can be found in [120]. $\hat{t}_1$ is here the one- electron and $\hat{T}$ the many-electron transition dipole operator. A basic assumption behind this expression is the strong orthogonality (static exchange) approximation for the final state wave function $\Psi_f(N) = \hat{a}_\epsilon^+ \Psi_f(N-1)$, i.e. with an electron orbital in the continuum added to the correlated final residual state wave function $\Psi_f(N-1)$. The killer condition $\hat{a}_\epsilon \mid \psi_f(N-1) >= 0$ is then fulfilled. We see that the general Fermi's golden rule expression given by eq.135 above and for Auger transitions, eq. 105, rests on the strong orthogonality condition. Comparing the forms of these expressions we see that the photoelectron transition moment contains two terms, the first with a bound continuum one-electron transition element times a many-electron wave function overlap, the second term with a bound continuum orbital overlap times a many-electron transition element. The second term, the so-called conjugate shake" term is a direct consequence of the strong orthogonality condition, and is important when the energy of the expelled photoelectron is low. For intermediate or high energy photoionization the first direct term is dominant. The two factors in this term, the orbital transition moment $< \epsilon \mid \hat{t}_1 \mid r >$ and the generalized overlap amplitude $< \Psi_f(N-1) \mid \hat{a}_r \mid \Psi_0(N) >$ have different significance in different types of spectra and for different energy regions in the same spectrum. The distinction between the two terms is given by the different orbital selection rules. The dipole element $< \epsilon \mid \hat{t}_1 \mid r >$ couples orbitals of different parity and $\Delta l$ (or by selection rules imposed by the point group of the molecule). For the overlap integral there is no change in parity nor in angular momentum. Comparing with Auger[100] one can see that in the intermediate expression in eq. 99

$$A_{fi} =< LL \mid [\hat{a}_\epsilon, \hat{H}] + (\hat{H} - E_K)\hat{a}_\epsilon \mid K > \tag{136}$$

the commutator expression, $< LL \mid [\hat{a}_\epsilon, \hat{H}] \mid K >$, corresponds to the direct term in photoionization. The remaining term, $< LL \mid (\hat{H} - E_K)\hat{a}_\epsilon \mid K >$ however, contains contributions corresponding both due to a "conjugate shake" and a non-orthogonality term, the latter being absent in photoionization. The second term containing these two contributions can be evaluated as

$$-\varepsilon_\epsilon \sum_r < \epsilon \mid r >< LL \mid \hat{a}_r \mid K > \tag{137}$$

which goes to zero with small Auger energies even if the overlap is non-zero in that regime. Furthermore, there are no distinctions based on symmetry properties since

the one-electron integrals $< \epsilon \mid \hat{h}_1 \mid r >$ have the same symmetry properties as the overlap integrals $< \epsilon \mid r >$ which makes it possible to mix various contributions. Thus unlike the photoelectron case it is not possible to uniquely identify a "conjugate-shake" contribution to Auger emission[100].

It is clear that **A** and **B** approximation levels are similar for the two spectroscopies, i.e. one starts out from Fermis golden rule and then perform a strong orthogonality condition in the same manner. At level C we do not identify a conjugate term for Auger, but neglect the non-orthogonality term including also the one-electron hamiltonian contributions. At **level C** we are then left with $M_{if} = \sum_i \tau_x * \chi_x$, eq. 129, where we denoted $\tau_x$ as the orbital element and $\chi_x$ as the generalized overlap amplitude (GOA). At level C one thus finds expressions with the same structure although, evidently, with different contents. However, it is still valid in the two cases to distinguish between the roles of these elements, an analysis which was summarized for photoelectron spectroscopy in ref. [119]. For photoelectron spectra $M_{fi} = T_{fi}$ we have $\tau_x =< \phi_\epsilon \mid \hat{t} \mid \phi_r > \chi_x =< \Psi_f(N-1) \mid \hat{a}_r \mid \Psi_0(N) >$ while for Auger spectra $M_{fi} = A_{fi}$, $\tau_x =< \epsilon q \mid rs > - < \epsilon q \mid sr >$ and $\chi_x =< LL \mid \hat{a}_q^+ \hat{a}_s \hat{a}_r \mid K >$

At next level, **level D**, the orbital transition matrix elements is neglected in photoionization. This confers with the sudden approximation, i.e. that the photoelectron is slowly varying over the small energy region covered by e.g. satellite structure. This holds for high energy ionization of states with the same main-hole (same main orbital) configuration, while for ionization corresponding to different main-hole configurations the orbital element, and therefore the continuum wave for the photoelectron has to be evaluated or at least approximated in some way. For Auger a similar argument holds; for final state Auger satellites corresponding to the same main two-hole configuration, the orbital matrix element can be neglected in a first approximation and then have the intensities guided by the corresponding generalized overlap amplitudes (GOA:s, $\chi_x$:s). For the relative intensities of the different main states (those dominated by their main two-hole configurations), knowledge of the $\tau_x : s$ is always required.

At **level E** one neglects the initial state correlation. Little is known about this in Auger. For photoionization in the valence shell it is more straightforward to pin-point the role of of initial state CI, see e.g. [121,119], basically because neglect of orbital relaxation is a better approximation which makes the Slater-Condon rules apply. Thus when the final photoionization state is governed by a main one-hole (1h) configuration, the GOA:s are governed by the expansion coefficients of this configuration in the final state (corresponding to the pole strengths of the one-particle Green's function). For states dominated by 2h-1p or higher excitations initial state CI is important, by inspection it can be argued in those cases that at least one 2h1p channel have the same strength as the main 1h channel. For unsaturated species where final states contain substantial two- or many-electron excitations, the corresponding higher order excitations are important also for intensities. For Auger spectra the operations are governed by the two-electron annihilator and core creator, but the same overlap arguments apply, although the case is not as clear as for valence photoionization due to orbital non-orthogonality. Thus, irrespective if we denote final Auger states as hole-mixing states or as states with break-down of the orbital picture the final state CI is the important one, while it is, presumably, a good approximation to neglect initial state CI. Thus as shown in section 5.2 the GOA:s are guided by the expansion coefficients of main 2h configurations in the final state.

**Level F** defines neglect of final state correlation. In photoionization this is an appropriate level for two energy regions, the one covering the outer valence or "Koopmans" states and the region for the main core electron ionization. It is not relevant in the inner valence region, i.e. the hole-mixing satellite and the "MO break-down" regions, or the core electron shake-up region. For Auger the role of electron correlation, i.e. final state correlation is decisive, expect maybe for the very outermost levels. With the definition of correlation energy as the difference between one-determinant energy and the exact expectation value of the hamiltonian, final state correlation is always needed for Auger since a correct spin-coupled state needs at least two determinants. For Auger states a better definition is obtained by replacing a single determinant by a proper spin and symmetry adapted least linear combination of determinants, i.e. a configuration state function. It should be stressed that the definition of both correlation and relaxation energies for such states is model dependent. In section 12.1 we described the role of hole-mixing states and the break-down of the orbital picture. For a typical small molecule containing first row species, e.g. the diatomics or triatomics, the energy region can be divided into five energy regions; i) an outer valence region between 10 and 20 eV containing Koopmans states, well described by a one-particle approximation. The leading small correction is given by dynamical correlation. In Auger this corresponds to the outer-outer valence region with $2p^{-2}$ holes for first row molecules. Next is an intermediate satellite region with hole-mixing states, and third an inner valence region (2s holes) in the photoelectron spectrum. For photoionization we have the main core hole and the core electron shake up region with no counterpart in Auger. The valence region in Auger is extended containing except for the outer-outer, also the inner-outer and the inner-inner region. In this region the hole-mixing and the break-down of the MO picture is paramount. In contrast to photoelectron spectra where the hole-mixing only involve main 1h configurations weakly, many of the Auger hole-mixing states have dominant inclusions of main 2h configurations. Only few identifications of Auger satellites with a 3h2p or higher particle-hole excitation have been made, see esction 12.3. For atoms the argon LMM spectrum[122] seems to provide the best example for such satellites.

**Level G** defines no self-consistent description of orbitals. In photoelectron spectra a common set of orbitals can be applied to analyze valence levels since differential relaxation can be picked up by a larger CI expansion. For core ionization, it is important to include relaxation (break-down of Koopmans theorem). Intensities should therefore ideally be evaluated by orbitals that are self-consistently optimized for the initial (core hole) final valence two-hole states. For energies one may trivially avoid the orbital relaxation problem by normalizing the spectrum to the experimental core ionization potential. A separate orbital optimization for all final two-hole states is cumbersome and may not be possible for computational reasons. If a common set of orbitals are chosen for the final states, it is often advantageous to choose a set from optimizing one of the two-hole ionic states rather than the neutral ground state, because the two-hole ionic states all have more contracted wave functions than the neutral species. The differential relaxation between two-hole states can then be picked up by configuration expansions. This has also the advantage that "pure spectroscopic" states are obtained which are both non-overlapping and non-interacting over the hamiltonian, which would not be the case for a state-specific orbital description, unless some extraordinary measures are undertaken[123].

# 7 One-Particle Methods

The one-particle, MO, analysis of Auger spectra starts out from the simple expression for double electron ionization energies;

$$E_{ij} = I_i + I_j - R_{ij} + V_{ij}^S \tag{138}$$

where $I_i$ and $I_j$ denote single ionization energies with holes in orbitals i and j. $R_{ij}$ is a relaxation term and $V_{ij}^S$ a hole-hole interaction term which is dependent on the spin-coupling of the two-hole state. This is an approach that have been much used in rationalizing transition energies for core type Auger spectra[124,125]. It was firstly applied for molecular valence spectra by Jennsion[126,127,13]. Corresponding intensities have in general been evaluated by the one-center intensity model expressed by eqs. 131, 132, 133. In a first approximation, corresponding to the Koopmans level of approximation for photoelectron spectra, $R_{ij}$ is assumed zero, which is correct in the limit of an infinite number of electrons. The double hole ionization potentials are then simply given by sums of two (negative) orbital energies corrected by the hole-hole interaction parameter. For an ordinary molecule this parameter takes values in the order of eV:s. Within the validity of this approximation the Auger spectrum is assigned directly from the photoelectron spectrum provided the hole-hole interaction parameters can be estimated.

Various versions of the one-particle model expressed by eq. 138 have been tested, e.g. using $\Delta SCF$ energies or using experimental energies for $I_i$ and $I_j$. In the latter case the correlation energy is implicitly included for the single ionization steps, however, the change in correlation (and relaxation) going from the first to the second ionization step is not. Also the hole-hole intercation parameters themselves can be obtained in different ways. The intrinsic errors, or relaxation energies, in expression 138 can be formulated as

$$S_{ij} = -\epsilon_i - \epsilon_j - E_{ij}^{SCF} + V_{ij}^{\epsilon} \tag{139}$$

where $\epsilon_i$ and $\epsilon_j$ are the ground state orbital energies and $V_{ij}^{\epsilon}$ is obtained from ground state orbitals, or as

$$D_{ij} = I_i^{SCF} + I_j^{SCF} - E_{ij}^{SCF} + V_{ij}^{SCF} \tag{140}$$

where $I_i^{SCF}$ and $I_j^{SCF}$ denote SCF single ionization potentials and $V_{ij}^{SCF}$ now obtained self-consistently and state specifically (and for appropriate spin-coupling, singlet (S) or triplet (T)). For small molecules containing first row elements it can be seen that the "S" (static) relaxation error increases rather uniformly from a few eV up to 10 eV going from outer to inner double hole states[13]. The "D" relaxation error is smaller in magnitude but shows more irregularities, it can even be negative. This can be understood from the large static correlation of many of the final Auger states and therefore the large difference in correlation energy between first and second ionization steps. Following ref. [13] it can be argued that orbitals optimized for one state in each of the three main inner-inner, inner-outer and outer-outer groups of states can be used to construct D:s and V:s for a "one-particle" spectrum. Such a procedure is better than just using ground state orbitals, but does not require optimization of all states involved. It mimics full $\Delta SCF$ solution quite well, although the correct ordering of states not always is obtained. A numerical evaluation for CO is given in table 2 shown below. Even though the model based on single ionization potentials cannot be used to recapitulate the correct ordering of the different Auger states, it can be used, together with the one-center intensity model, to grossly assign intensity to different parts of the spectra.

Table 2: Auger energies for CO from one-particle calculations compared to SCF and CI calculations and experiment. Taken from ref. [13]

| *Config.* | *Term* | $S^a_{i,j}$ | $D^b_{i,j}$ | $SingleIP:s^c$ | $SCF^d$ | $CI^e$ | $Exper.^f$ |
|---|---|---|---|---|---|---|---|
| GS | | 0 | 0 | 0 | 0 | 0 | 0 |
| $5\sigma^1\pi^3$ | $^3\Pi$ | 4.17 | 0.74 | 36.02 | 38.90 | 42.83 | 41.7 |
| $5\sigma^{-2}$ | $^1\Sigma$ | 4.43 | 4.94 | 43.30 | 41.98 | 43.90 | 43.40 |
| $5\sigma^1\pi^3$ | $^1\Pi$ | 4.19 | 0.75 | 36.77 | 39.64 | 43.40 | |
| $4\sigma^1 5\sigma^1$ | $^3\Sigma$ | 4.34 | 0.68 | 38.50 | 41.44 | 45.17 | 45.5 |
| $1\pi^2$ | $^3\Sigma^-$ | 6.27 | 3.62 | 43.95 | 43.95 | 46.53 | |
| $4\sigma^1 5\sigma^1$ | $^1\Sigma$ | 3.56 | -0.89 | 41.19 | 45.70 | 46.55 | 46.40 |
| $1\pi^2$ | $^1\Delta$ | 7.02 | 4.55 | 45.67 | 44.74 | 48.57 | 47.6 |
| $4\sigma^1\pi^3$ | $^3\Pi$ | 8.32 | 5.79 | 48.48 | 46.31 | 49.04 | |
| $1\pi^2$ | $^1\Sigma^+$ | 5.72 | 3.36 | 46.54 | 46.80 | 50.35 | 50.6 |
| $4\sigma^1\pi^3$ | $^1\Pi$ | 7.81 | 5.78 | 51.40 | 49.24 | 51.96 | 53.5 |
| $4\sigma^{-2}$ | $^1\Sigma$ | 9.28 | 8.94 | 59.69 | 54.37 | 56.64 | 54.5 |
| | | | | | | | 56.6[g] |
| | | | | | | | 57.0[h] |
| | | | | | | | 60.5 |
| $3\sigma^1 5\sigma^1$ | $^3\Sigma$ | 5.25 | 1.29 | 58.62 | 62.45 | 64.91 | |
| $3\sigma^1 5\sigma^1$ | $^1\Sigma$ | 5.90 | 1.98 | 60.36 | 63.50 | 64.99 | 65.5 |
| $3\sigma^1\pi^3$ | $^3\Pi$ | 8.96 | 5.12 | 65.34 | 65.34 | 66.74 | |
| $3\sigma^1 4\sigma^1$ | $^3\Sigma$ | 9.16 | 5.34 | 69.30 | 69.08 | 70.74 | 72.7 |
| $3\sigma^1\pi^3$ | $^1\Pi$ | 8.09 | 4.66 | 72.17 | 72.63 | 76.71 | 74.9 |
| $3\sigma^1 4\sigma^1$ | $^1\Sigma$ | 9.96 | 6.80 | 76.03 | 74.35 | 77.62 | 82.9 |
| | | | | | | | 94.8 |
| $3\sigma^{-2}$ | $^1\Sigma$ | 9.81 | 5.75 | 95.59 | 95.59 | 100.54 | 104.6 |

[a] Static relaxation energy defined by eq. 139. [b] Dynamical relaxation energy defined by eq. 140. [c] Procedure based on three SCF calulations on $3\sigma^{-2\,1}\Sigma$, $3\sigma^1 1\pi^{3\,3}\Pi$ and $1\pi^{-2\,3}\Sigma$ states and single ionization potentials [128]. [d] Full open shell SCF calculations. [e] CI calculations. [f] Experimental results (Auger energies reduced by the core electron ionization potentials). [g] $4\sigma^1 1\pi^{3\,1}\Pi$ CI satellite. [h] $4\sigma^{-2\,1}\Sigma$ CI satellite.

# 8 Wave Function Methods

## 8.1 Open-shell Restricted Hartree-Fock (OSRHF)

Before the advent of modern unconstrained MCSCF optimization algorithms there were considerable difficulties to self-consistently optimize many-open shell states. In particular, the self-consistent optimization of two-open shell states present in Auger spectra were afflicted by some complications that are not present in the Hartree-Fock description of single-hole states. The optimization of two-hole triplets using spin and symmetry restricted SCF theory was straightforward, while singlets were not. In the latter case the fully optimized SCF solution has non-orthogonal open-shell orbitals in the case the two open shell orbitals belong to the same symmetry representation[129]. Two different types of orthogonality constrained approaches were derived to cope with the problem. These were also the two basic open-shell SCF methods that have been applied to molecular Auger spectra. The first is the Roothaan many operator (coupled Fock operator) open shell SCF, implemented in the ALCHEMY program package[130]. The orthogonality constraint was here obtained by the means of Lagrangian multipliers. This method fulfills the generalized Brillouin theorem[131];

$$< 0 \mid \hat{H} \mid 1 > - < 0 \mid \hat{H} \mid 2 > = 0 \tag{141}$$

where 1 and 2 are singly excited configuration states within the space of occupied orbitals with respect to the reference state 0. However, the normal form of the Brillouin theorem is not fulfilled, i.e. singly excited configurations are interacting with the Hartree-Fock reference state (here the OSRHF reference state). Thus two-open shell singlets like $2a_1^{-1}3a_1^{-1}\,{}^1A_1$ state of water were obtained with poorer energies than other two-hole states[16]. This could only be remedied by methods beyond SCF, like limited CI encompassing excitations within the occupied space. The second main OSRHF technique for Auger states was due to Manne and Faegri[17,132] who formulated an alternative Brillouin condition, imposing that second order contributions to the energy from single replacements to the reference state cancel. A significant improvement compared to calculations using the generalized Brillouin theorem was obtained for two open shell singlets of the same symmetry. In general OSRHF has been found appropriate for a gross characteristic of an Auger spectrum. However, it becomes progressively poorer towards the low kinetic energy end of the spectrum.

## 8.2 Multi-Configuration Self-Consistent Field (MCSCF)

With unconstrained multi-configuration SCF (MCSCF) techniques two-hole states can routinely be optimized. The MCSCF wave functions are parametrized as

$$\Psi = \exp(-\hat{\kappa})(\sum_{\mu} c_\mu \mid \Theta_\mu >) \tag{142}$$

where $\hat{\kappa} = \sum_{r>s} \kappa_{sr} \hat{E}^-_{sr}$. $\hat{E}^-_{sr} = \hat{E}_{sr} - \hat{E}_{rs}$ is an antisymmetric operator for rotations of the molecular orbitals within the special orthogonal group and the configuration $\mid \Theta_\mu >$ is either a Slater Determinant (SD) or a Configurational State Function (CSF), i.e. a spin-adapted combination of SD's according to the symmetric group. The orthogonal orbital parametrization allows for full optimization of large classes of wave functions (including so-called CAS and RAS wave functions), in particular those which describe

two-hole states. Calculation of two hole state MCSCF wave functions for the purpose of interpreting Auger spectra can be found in several references, see e.g. ref. [133,18,134]. Results for MCSCF calculations on Auger transition energies in LiF are recapitulated in Table 3 below.

Table 3: MCSCF Auger transition energies of LiF. From ref. [133].

| Config. | Term | MCSCF | Observed |
|---|---|---|---|
| $1\pi^{-2}$ | $^3\Sigma^-$ | 652.04 | 652.18 |
| $4\sigma^{-1}1\pi^{-1}$ | $^3\Pi$ | 651.55 | 650.34 |
| $1\pi^{-2}$ | $^1\Delta$ | 649.16 | 648.47 |
| $4\sigma^{-1}1\pi^{-1}$ | $^1\Pi$ | 648.69 | 647.66 |
| $1\pi^{-2}(4\sigma^{-2})$ | $^1\Sigma^+$ | 648.61 | 646.64 |
| $4\sigma^{-2}(1\pi^{-2})$ | $^1\Sigma^+$ | 646.45 | 644.82 |
| $3\sigma^{-1}1\pi^{-1}$ | $^3\Pi$ | 630.38 | 630.46 |
| $3\sigma^{-1}4\sigma^{-1}$ | $^3\Sigma^+$ | 629.93 | 629.62 |
| $3\sigma^{-1}1\pi^{-1}$ | $^1\Pi$ | 618.78 | 621.85 |
| $3\sigma^{-1}1\sigma^{-1}$ | $^1\Sigma^+$ | | 620.26 |
| $3\sigma^{-2}$ | $^1\Sigma^+$ | 600.27 | 602.62 |

## 8.3 Semi-Internal Configuration Interaction (SEMICI)

Semi-internal configuration interaction (semici) is of profound importance for many spectroscopic problems ranging from deep core hole states to inner valence and hole-mixing valence states. For Auger semici enters in two ways. Firstly as the interaction responsible for the Auger effect itself. The Auger electron can be seen as the external excitation receiving energy from an internal core-valence excitation. For the intial core hole states semici thus represent the interaction with electronic continua. The energetic effect of this interaction has been evaluated with perturbational[135] or Feshbach[108] techniques. The energy computed this way serves as a, usually small, correction to conventional variational schemes. The inclusion of semi-internal excitations make the core hole index very high and unknown a priori, and therefore hard to handle computationally for wave functions of even moderate size. In some cases for higher Z elements however, the semi-internal interaction can lead to a complete break-down of the (core) one-particle or quasi-particle pictures, namely when the conditions for Coster Kronig or super Coster Kronig prevail.

Secondly, semici is responsible for the break-down of the MO picture and the hole-mixing effects among the final Auger states. In this case the semici excitations occur between bound electronic levels only. For molecular states with many valence holes the semi-internal excitations may lead to complete break-down of the one-particle picture. For double hole states, i.e. Auger states, the one-particle picture remains valid in the outer-outer valence region of smaller molecules, while already for three-hole states an orbital interpretation would, probably, be meaningless. For Auger states the internal CI is obtained by redistributing one or two holes among the occupied valence levels, while the semi-internals are obtained as coupled internal-externals, i.e. redistributing one hole in occupied space coupled by an external hole-particle excitation. The importance of semi-internal excitations for Auger states can pictorially be seen from fig. 1. The $4\sigma^{-2}$

hole configuration is quasi-degenerate with the $4\sigma^{-1}5\sigma^{-1}6\sigma^{1}$ configuration, because the negative $5\sigma \rightarrow 4\sigma$ excitation energy is about the same in magnitude as the positive $5\sigma \rightarrow 6\sigma$ excitation energy. From this scheme it is also understood that the quasi-particle picture holds better for atoms and hydrides than for, e.g. $\pi$ electron systems. In the former case the conditions for quasi-degeneracy only exists for the innermost valence state, e.g. for the $2a_1^{-2}$ state $H_2O^{2+}$[136], while for $\pi$ electron systems the availability of low lying $\pi$ to $\pi^*$ excitations makes such degeneracies possible for a number of states, also those of lower energy (such as the $4\sigma^{-2}{}^{2}\Sigma$ configuration states of $CO^{2+}$[128]). Since the number of two-hole states raises with the square of the number of electrons, it is quite clear that the breakdown effect due to semici increases steeply with the size of the molecule, unless the number of excitations is reduced by symmetry. The same holds actually for single-hole photoionization states. As von Niessen and coworkers point out breakdown of the quasi-particle picture may occur also in the outer valence region for those spectra[137]. However the effect is in any case more dramatic for Auger.

Computationally semici poses problems concerning the generation of the (semi-internal) configuration state functions (CSF:s) and concerning the calculation of higher lying roots in the Hamiltonian CI matrix. The latter problem arises because those intensity carrying CSF:s with large intermixing of semi-internals are higher in energy than many multiply excited CSF:s without any Auger intensity (small overlap amplitudes (GOA:s)). These problems are best handled by so-called explicit Hamiltonian approaches, in which the semi-internal configurations can be generated by flexible selection schemes[130]. If the CI Hamiltonian is of moderate size it can of course be diagonalized completely, and all roots corresponding to main and satellite states in the Auger spectra are obtained therefrom. Although flexible the small size of the CI Hamiltonian puts limits to the system that can be handled by explicit CI Hamiltonian techniques. For larger configurational expansions the CI Hamiltonian has to be diagonalized with iterative techniques, i.e. by direct techniques including linear transformations of the CI Hamiltonian on trial vectors. It is, however, often to cumbersome with this technique to diagonalize for all roots in the spectrum. The Lanczos method modified to only extract those roots with large intensities is suitable for constructing a full spectrum[120]. With such schemes configurational expansions of intermediate size can be handled (between 500 and 5000). For even larger sizes of the configurational expansion (and of the CI Hamiltonian) active space techniques have been used with complete (CAS) or restricted (RAS) active spaces, as mentioned in subsection 8.2. In the former case all possible CSF:s within a set of (active) orbitals are generated. For RAS, restrictions are imposed on the excitations, thereby allowing a larger set of active orbitals. The advantage with RAS is that also a larger portion of the dynamical correlation error can be encompassed. However, such wave functions will contain a very large number of configurations in case they are to include the appropriate semi-internals. With large number of CSF:a these methods are again limited to the few lowest roots covering only a part of the Auger spectrum. Computationally efficient variants are given by so-called contracted CI techniques[138], applied in refs. [18,139] to Auger, and by so-called multi-reference selection CI, applied in ref. [140] to Auger. In the latter case the configurational selection is automatized by perturbational or other criteria, which often is an efficient route to calculations of many-hole states or higher excited states.

We conclude this section on wave function methods by stating that for Auger spectra as for other types of spectra involving multiple hole states it is hard to account for the dynamical correlation at the same time as the important static type semi-internal correlation. Exception to this are the very smallest molecules and the outermost two-

hole states for which the dynamical correlation is the dominating correlation effect. On the other hand it is only in the latter cases the experimental spectra show state-specific fine-structure. For intensities, as already pointed out, there is no meaning to dynamically correlate the final state if not the initial core hole state also is dynamically correlated. Although not yet implemented for the Auger case there seems to be ways to go about with such intensity calculations[123]. However, ultimately both the high density of final states with the accompanying breakdown of the BO approximation, and the (neglected) scattering aspects of the problem sets a limit to the effort worth putting into a pure electronic calculation of a molecular Auger spectrum.

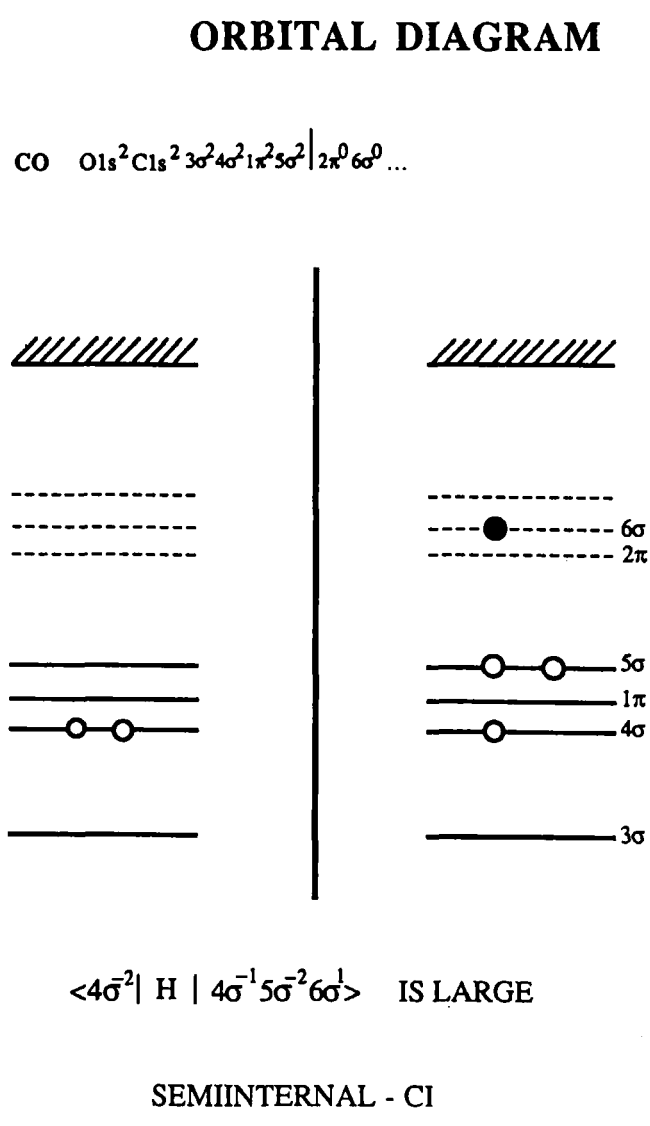



Fig. 1: Pictorial representation of semi-internal configuration interaction (semici) in Auger spectrum of CO.

# 9 Green's Function Methods

## 9.1 Two-particle Green's Functions

A third major branch of calculations of molecular valence Auger spectra is given by the two-particle Green's function method. Two-particle Green's functions are well-known tools in quantum physics [25,26,27]. Ab initio correlation calculations of double ionization potentials (and thus relative Auger energies) of finite electronic systems by means of two-particle Green's functions have been performed by Liegener by an approach based on a renormalized form of the Bethe-Salpeter equation [28], see below, and by several authors by other approximation schemes [29,30,31,32,33,34], see section 9.4. We will first describe the general properties of two-particle Green's functions and then discuss the specific approximations and methods invoked in using them in the actual calculations.

The method uses the fact that the relative Auger kinetic energies are accessible by the double ionization potentials of the system. The kinetic energy is given by $E_{kin} = IP^c - DIP(n)$, where $IP^c$ is the core ionization potential pertinent to the creation of the initial state and DIP(n) is the double ionization potential for the final state under consideration. This means that as long as the primary core ionization potentials of the system are sufficiently different the spectra can be obtained by the DIP:s. This is the case if all the non-hydrogen atoms of the molecule are different. In other cases one has to know the core ionization potentials or at least their chemical shifts.

In the Green's function method the DIP:s are obtained as poles of a two particle Green's function, namely the particle-particle Green's function (2p-GF). This function is defined [25] as

$$\mathcal{G}_{klmn}(\omega) = \int_{-\infty}^{\infty} dt e^{i\omega t}(-i) < \Psi_0^N \mid T[a_l(t)a_k(t)a_m^+a_n^+] \mid \Psi_0^N > \qquad (143)$$

where $\Psi_0$ is the correlated ground state of the neutral molecule in the Heisenberg representation, T is Wick's time ordering operator, $a_l^+$ and $a_l$ are the usual Heisenberg creation and annihilation operators for the canonical Hartree-Fock spin-orbitals.

The particle-particle Green's function has the following spectral resolution, known as the Lehmann representation:

$$\mathcal{G}_{klmn}(\omega) = \sum_{\nu} \frac{< \Psi_0^N \mid a_l a_k \mid \Psi_\nu^{N+2} >< \Psi_\nu^{N+2} \mid a_m^+ a_k^+ \mid \Psi_0^N >}{\omega + DEA_\nu + i\eta} \qquad (144)$$

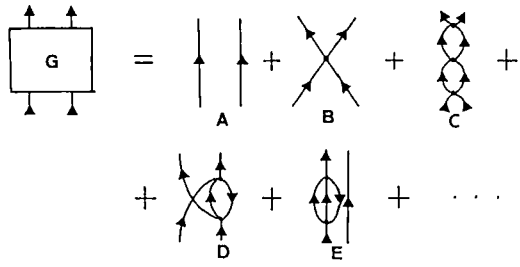
$$- \sum_{\nu} \frac{< \Psi_0^N \mid a_m^+ a_n^+ \mid \Psi_\nu^{N-2} >< \Psi_\nu^{N-2} \mid a_l a_k \mid \Psi_0^N >}{\omega + DIP_\nu - i\eta} \qquad (145)$$

where $\eta$ is the positive infinitesmal tending to zero in the distributional sense and the sums run over all N+2 or N-2 electron states as indicated by the superscripts. The Lehmann representation shows that it is possible to obtain -DIP(n) as poles of the 2p-GF. The 2p-GF is accessible by time-independent perturbation theory. This means that the interacting many-electron ground state is generated by an adiabatic switching process and the terms arising from the series expansion of the time evolution operator are symbolized by diagrams. Partial summation of the diagrammatic series may lead to factorizable equations for the 2p-GF. Instead of using the diagrammatic approach one

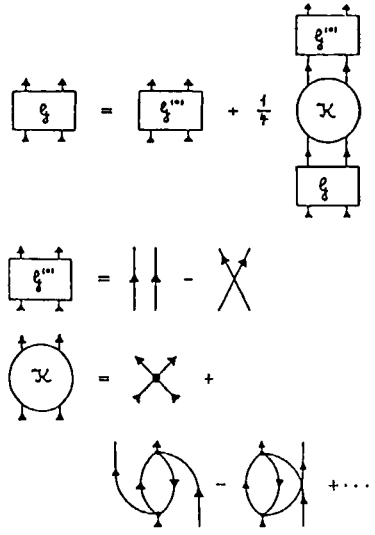
can as well write the 2p-GF as a superoperator resolvent and use algebraic methods for the construction of appropriate approximations, or one can derive matrix equations for the advanced and retarded part of the 2p-GF separately and derive suitable perturbation schemes for them, see section 9.4. We discuss first, in sections 9.2 and 9.3, the case of using a diagrammatic expansion summed via the Bethe-Salpeter equation. This will enable us to establish an explicit connection between one-particle, e.g. photoelectron, spectra and Auger spectra and the breakdown phenomena manifested in both of them.

## 9.2 The Bethe-Salpeter Equation

Constructing the diagrammatic series for the 2p-GF yields an infinite series, each term of which (each diagram) corresponds to an analytic expression which can be evaluated by simple rules. Some representative first terms of the expansion are the following




This series can be easily factorized if one keeps to such diagrams where the two particles interact with each other only simultaneously, as for example in the diagrams A-C of the above expansion. Diagram D contributes to the higher orders of the irreducible vertex part and diagram E contributes to the renormalization of one-particle lines. A partial summation of diagrams is possible and can be described diagrammatically as follows:



Writing this diagram equation, the Bethe-Salpeter equation, for first-order irreducible vertex parts in terms of the actual quantities considered, one obtains in energy representation a matrix equation for matrices over pair indices (k,l) and (m,n), (which cancels the factor 1/4 in front of $\mathcal{K}$), leading to

$$\mathcal{G}(\omega) = \mathcal{G}^0(\omega) + \mathcal{G}^0(\omega)\mathcal{K}\mathcal{G}(\omega), \tag{146}$$

where $\mathcal{K}$ is the first order irreducible vertex part, given by

$$\mathcal{K}_{klmn} = V_{klmn} - V_{klnm} \tag{147}$$

where $V_{klmn}$ denotes two-electron integrals, and $\mathcal{G}^0$ is the interaction-free two-particle Green's function:

$$\mathcal{G}^{(0)}_{klmn}(\omega) = i\int_{-\infty}^{\infty} dt e^{i\omega t}[G^{(0)}_{km}(t)G^{(0)}_{ln}(t) - G^{(0)}_{kn}(t)G^{(0)}_{lm}(t)] = \lambda_{kl}\delta_{kl}\delta_{kn}/(\omega - \epsilon_k - \epsilon_l) \tag{148}$$

where $G^{(0)}(k,l)$ is the interaction-free one-particle Green's function and $\epsilon_k$ the canonical Hartree-Fock orbital energies. Furthermore, the factor $\lambda_{kl}$ is -1 if k and l belong to orbitals occupied in the Hartree-Fock ground state, +1 if k and l refer to virtual orbitals and zero otherwise. Solving the Bethe-Salpeter equation from the inverse of G yields the inverse equation

$$\mathcal{G}^{-1}(\omega) = \mathcal{G}^{(0)-1}(\omega) - \mathcal{K} \tag{149}$$

The above procedure remains valid if one renormalizes the one-particle lines in the diagrams, i.e. replaces the interaction-free one-particle Green's functions $G^{(0)}$ by the exact Green's function $G^{(0)}$ of the interacting system. Then the expression for $G^{(0)}$ has to be modified as:

$$\mathcal{G}^{(0)}_{klmn}(\omega) = i\int_{-\infty}^{\infty} dt e^{i\omega t}[G_{km}(t)G_{ln}(t) - G_{kn}(t)G_{lm}(t)] = \sum_{\mu\nu} \lambda_{k\mu,l\nu} P_{k\mu}P_{l\nu}\delta_{km}\delta_{ln}/(\omega - \omega_{k\mu} - \omega_{l\nu}) \tag{150}$$

where $\omega_{k\mu}$ are the poles of the one-particle Green's function and $P_{k\mu}$ the corresponding pole strengths, i.e. the residue of the eigenvalue of the one-particle Green's function at the corresponding poles. The factor $\lambda_{k\mu l\nu}$ is -1 if both ($k\mu$ and $l,\nu$ are indices describing ionization potentials, +1 if both are electron affinities and zero otherwise. The diagonal approximation for the one-particle Green's function has been assumed in the above expression; the modification for non-diagonal one-particle Green's functions is obvious. Note that in general several poles may exist for a given orbital as is implied by the second index of $\omega_{k\mu}$. This property of the poles of the Dyson equation is a consequence of the pole structure of the irreducible self-energy part. It is a general phenomenon not depending on the particular approximations involved in setting up the Dyson equation, except the correct analytical form of the self-energy part is required. The interpretation of those additional poles, which are not accessible within the one-particle picture, is that they belong to shake-up processes accompanying single-particle ionization and will interact with corresponding configurations. The validity of a quasi-particle picture would in this context mean that one pole-strength is dominating for any one orbital, i.e. is much larger than the other pole-strengths for that orbital. If there are several poles of comparable intensity for one orbital one speaks about a break-down of the quasi-particle picture for that orbital. This happens usually in the inner valence region of molecules, where there exist an approximate near-degeneracy between certain semi-internal (outer-outer) valence shake-up configurations and inner-valence single-hole configurations. That effect has been established in the interpretation of photoelectron spectra [141,11]

The renormalization procedure described above [28] seems to be a natural way to incorporate such effects in the range of Auger spectra, where they can be expected to occur for the same reason as in photoelectron spectra as we have pointed out above in connection with the corresponding wave function methods. One can in the case of a closed-shell system transform the matrix G to decoupled matrices for singlets and triplets. The corresponding expressions fro $K$ are:

$$K^{(S,T)} = V_{klmn} + / - V_{klnm}, \quad if\ k<l\ and\ m<n, \tag{151}$$

$$K^{(S)} = V_{klmn}\ if\ k = l\ and\ m = n, \tag{152}$$

$$K^{(S)} = 2^{1/2}V_{klmn}\ if\ either\ k = l\ or\ m = n, \tag{153}$$

where the upper or lower signs refers to singlets(S) or triplets(T), respectively, and the indices now denote spatial orbitals. (A further blocking of G due to molecular symmetry can also be taken into account in the calculations.)

Solution of the Bethe-Salpeter equation yields not only the poles of the 2p-GF, i.e. the -DIP values, but also the residues of the 2p-GF which are obtained as

$$Res_{DIP_\nu}[-G^{(S,T)}_{ij,i'j'}] = [-[\frac{\delta}{\delta\omega}EVG(\omega)]_{-DIP_\nu}]^{-1}u_{ij\nu}u^*_{i'j'\nu} \tag{154}$$

where EV G denotes the eigenvalues of the 2p-GF matrix having a zero at the solution, and $u(ij\nu)$ are the components of the eigenvectors of the 2p-GF matrix at the pole.

Using the above residues one can get an estimate of the transition rates to the corresponding final state by

$$TR^{(S,T)}_\nu \propto d^{(S,T)}\sum_{lm}\sum_{iji'j'} M^{(S,T)}_{ij}(\phi_{lm})M^{*(S,T)}_{i'j'}(\phi_{lm}) \times Res_{-DIP_\nu}(-G^{(S,T)}_{iji'j'}) \tag{155}$$

where $d^S = 1$, $d^T = 3$. $M_{ijc\phi}$ are the matrix elements between Slater determinants with a core hole or two valence holes and a continuum electron, respectively and are given as

$$M^{(S,T)}_{ij}(\phi) = 2^{-1/2}(V_{ijc\phi} + / - V_{ij\phi c}),\ if\ i \neq j \tag{156}$$

$$M^{(S)}_{ij}(\phi) = V_{ijc\phi},\ if\ i = j \tag{157}$$

The two-particle matrix elements $V_{ijc\phi}$, containing a continuum and a core orbital are usually evaluated in the one-center model discussed above.

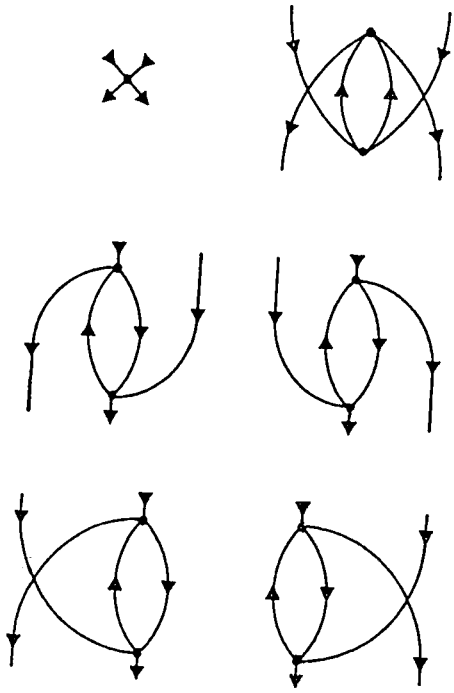
## 9.3 Higher Order Irreducible Vertex Parts

In the previous section a first order approximation for the irreducible vertex part K has been assumed. Extensions beyond this approximation prevent the factorization of the Bethe-Salpeter equation. One possibility to proceed in that case is to consider a modified expansion of the 2p-GF. The most important contributions to the 2p-GF will be expected from those diagrams which have the interaction points situated between the external points of the diagram. Keeping to those diagrams in the expansion will yield a Bethe-Salpeter equation which is factorizable in analogy to the corresponding behaviour of the polarization propagator. The approximation invoked here [142] can be related to the choice of reference state as an uncorrelated one. It can be shown that such

a choice will not affect the position of the poles of the propagator although it may have some influence on the convergence behaviour of its expansion. Renormalization is also possible in that case, but only if the quasiparticle picture is assumed which may be a good approximation in the outer-valence region of many molecules. If an unrenormalized one-particle Green's function is used, the corresponding diagrams containing self-energy parts have to be included in the expression for the irreducible vertex part. In case of using a quasi-particle approximation the expression for $g^{(0)}$ given above simplifies to

$$G^{(0)}_{klmn}(\omega) = -P_{k0}P_{l0}\delta_{km}\delta_{ln}\,/(\omega - \omega_{k0} - \omega_{l0}) \tag{158}$$

where $\omega_{k0}$ and $P_{l0}$ are the quasi-particle poles and correspdonding pole strengths of the one-particle Green's function. The diagrams of K needed in case of using the time-ordered expansion procedure described above are up to second order:



The explicit expressions for Hartree-Fock spin-orbitals are:

$$K_{klmn}(\omega) = V_{kl[mn]} - \sum_{u,v \not\subset occ} \frac{P_{u0}P_{v0}V_{klu v}V_{mn[uv]}}{\omega - \omega_{k0} - \omega_{l0} - \omega_{m0} - \omega_{n0} + \omega_{u0} + \omega_{v}0} \tag{159}$$

$$- \sum_{v \not\subset occ}^{u \subset occ} P_{u0}P_{v0}\left\{ \frac{V_{ku[mv]}V_{vl[un]}}{\omega - \omega_{k0} - \omega_{n0} - \omega_{u0} + \omega_{v0}} + \frac{V_{kv[mv]}V_{ul[vn]}}{\omega - \omega_{l0} - \omega_{m0} - \omega_{n0} + \omega_{v0}} \right. \tag{160}$$

$$\left. - \frac{V_{ku[vn]}V_{vl[mu]}}{\omega - \omega_{k0} - \omega_{m0} - \omega_{n0} + \omega_{v0}} - \frac{V_{kv[un]}V_{ul[mv]}}{\omega - \omega_{l0} - \omega_{n0} - \omega_{u0} + \omega_{v0}} \right\} \tag{161}$$

where $V_{kl[mn]} = V_{klmn} - V_{klnm}$ are the antisymmetrized two-particle integrals. As before one can eliminate the spin dependence of the indices in the case of a closed shell system by transforming to decoupled matrices for singlets and triplets and performing the spin summations.

## 9.4 Other Possibilities to Treat the Two-particle Green's Function

The treatment of second-order irreducible particle-particle vertex parts via the Bethe-Salpeter equation for time-ordered diagrams described above [142] represents a specific choice of a partial summation of diagrams for the particle-particle Green's function. Other choices of partial summations are possible by the "algebraic diagrammatic construction" (ADC) scheme [29] or the superoperator technique [30]. In the ADC scheme suggested by Schirmer and Barth [29] one starts by decomposing the advanced part $G^+$ of the particle-particle Green's function (the second term in the Lehmann representation given in section 8.1) in the following way:

$$G^+(\omega) = f^+(\omega - K - C)^{-1} f \tag{162}$$

where C is a hermitian matrix called the effective interaction matrix, K a diagonal matrix containing the zeroth order DIP's and f is called the matrix of modified transition amplitudes. One assumes to have expansions of the expressions f and C in powers of the electron-electron interaction, inserts those expansions into the binomial expansion of the above expression for the 2p-GF and orders the resulting products according to the order of electron-electron interaction. In this way one obtains for a given order an expression for the 2p-GF which can be compared to the corresponding term of the diagrammmatic expansion. One can then determine the quantities f and C such that the two expressions become equal in a given order. Thus one can use in that order the above expression for $G^+$ which means that the poles can be determined by solving the following eigenvalue problem:

$$(K + C)Y = Y\omega \tag{163}$$

where Y denotes the eigenvector matrix and $\omega$ the diagonal matrix of eigenvalues. It should be mentioned that using a first-order irreducible vertex part and unrenormalized one-particle data and restricting the orbital indices to the occupied space corresponds to the first-order ADC. This is also called the Tamm-Dancoff approximation. Beyond this simplest case ADC will lead to somewhat different levels of approximation than discussed in the previous section. A renormalization seems not yet to have been incorporated in the ADC framework, but the expressions have been formulated for the second [29] and third order [33].

A purely algebraic approach to the 2p-GF suggested by Tarantelli and Cederbaum [32] can be obtained by rewriting the above equation for $G^+$ as

$$G^+(\omega) = f^+(\omega - E + H)^{-1} f \tag{164}$$

where E is a constant term (the ground state energy of the reference system) and H is a hermitian matrix called the effective Hamiltonian matrix. One can derive closed form expressions for a unitary transformation which is constructed in such a way as to allow for an evaluation of the DIP's by means of an eigenvalue problem as small as possible [32]. The explicit working equations are equivalent to those of the ADC up to the third

order (and can be expected to coincide also for the higher order). However, using the unitary transformation can be expected to have computational advantages compared to the ADC because it only requires the expansion at a given order of some closed-form equations and the calculation of the contributions of that order to the exact ground state.

As mentioned above another set of approximations within the framework of Green's function method is possible by writing the particle-particle propagator in superoperator representation, as done by Ortiz [30], and chosing appropriate reference states and inner projection spaces.

The definition of the superoperators [143] is:

$$\hat{I}X = X, \quad , \hat{H}X = [X, H] \tag{165}$$

and the inner product between two operators X and Y is defined by

$$(X \mid Y) = \langle \Psi_0 \mid [Y, X^+]_- \Psi_0 \rangle \tag{166}$$

The particle-particle Green's function becomes in this notation:

$$G(\omega) = (aa \mid (\omega \hat{I} - \hat{H})^{-1} aa) \tag{167}$$

From here one can proceed by the inner projection technique of Löwdin [144] to obtain

$$G(\omega) = (aa \mid h)(h \mid (\omega \hat{I} - \hat{H})h)^{-1}(h \mid aa) \tag{168}$$

where h denotes a complete particle operator manifold. The proper choice of the reference state $\Psi_0$ in this expression is one of the points where approximations take place. It is usually convenient to choose the closed-shell Hartree-Fock ground state here. The choice of a truncated manifold h represents the second possibility to introduce approximations in the context of this formalism. The simplest choice is to use only the space of the products of two particle operators. This case corresponds to using unrenormalized one-particle propagators and first-order irreducible vertex parts in the diagrammatic expansion. Further treatment is possible by using Löwdin's partitioning technique[145], as has been discussed by Ortiz [30].

Furthermore, a multiconfigurational choice for the reference state has been introduced by Graham and Yeager [34]. They used CAS MCSCF and CAS CI reference states and evaluated by means of double commutators symmetrized expressions for the matrices occuring in the above secular problem. For a complete inner projection manifold the symmetrized expressions coincide with the original ones. The multiconfigurational 2p-Gf method is important if nondynamical correlation effects are large in the ground state.

## 9.5 Three-particle Green's Functions

Double-ionization Auger satellites arise if the initial state of an Auger transition is a doubly ionized state with one core hole and one additional valence hole created by shake-off in the primary core-ionization process. The final state is a triply ionized state with three valence holes and permits application of three-particle Green's functions which are well-known in quantum physics [26,27]. They have been applied to the ab initio

treatment of the initial state shake-off problem for molecular Auger as follows [146]. The kinetic energy of the outgoing electron is given by

$$E(kin) = DIP(X) - TIP(Y) \tag{169}$$

where DIP(X) is a double ionization potential (the index X describes a state with a core and a valence hole) and TIP(Y) is a triple ionization potential (Y describes a state with three valence holes). The DIP's can be calculated as above from the two-particle Green's function, and the TIP's can be calculated from a three-particle Green's function which is defined as follows:

$$\begin{aligned} \mathcal{G}_{ijklmn} &= \int_{-\infty}^{\infty} dt\, e^{i\omega t}(-i) \times \langle \Psi_0^N \mid T\left[a_k(t)a_j(t)a_i(t)a_l^{\dagger}a_m^{\dagger}a_n^{\dagger}\right] \mid \Psi_0^N \rangle \\ &= \sum_{\nu} \frac{\langle \Psi_0^N \mid a_k a_j a_i \mid \Psi_\nu^{N+3}\rangle\langle \Psi_\nu^{N+3} \mid a_l^{\dagger}a_m^{\dagger}a_n^{\dagger} \mid \Psi_0^N\rangle}{(\omega + TEA_\nu + i\eta)} \\ &+ \sum_{\nu} \frac{\langle \Psi_0^N \mid a_l^{\dagger}a_m^{\dagger}a_n^{\dagger} \mid \Psi_\nu^{N-3}\rangle\langle \Psi_\nu^{N-3} \mid a_k a_j a_i \mid \Psi_0^N\rangle}{(\omega + TIP_\nu - i\eta)} \end{aligned} \tag{170}$$

The Bethe-Salpeter equation for time-ordered diagrams can be factorized to give

$$\mathcal{G}^{-1}(\omega) = [\mathcal{G}^{(0)}(\omega)]^{-1} - \mathcal{K} \tag{171}$$

where

$$\begin{aligned} \mathcal{K}_{ijklmn} &= -V_{ij[lm]}\delta_{kn} + V_{ik[lm]}\delta_{jn} - V_{jk[lm]}\delta_{in} - V_{jk[mn]}\delta_{il} \\ &+ V_{ik[mn]}\delta_{jl} - V_{ij[mn]}\delta_{kl} - V_{ik[ln]}\delta_{jm} + V_{jk[ln]}\delta_{im} + V_{ij[ln]}\delta_{km} \end{aligned} \tag{172}$$

and

$$\mathcal{G}^{(0)}_{ijklmn}(\omega) = \frac{P_{i0}P_{j0}P_{k0}\delta_{il}\delta_{jm}\delta_{kn}}{\omega - \omega_{i0} - \omega_{j0} - \omega_{k0}} \tag{173}$$

is the interaction-free three-particle Green's function where the quasi- particle approximation has been assumed. This approximation is only valid in the outer-valence region and will yield the satellites on the low kinetic energy side of the leading normal Auger peak. The residues of the three-particle Green's function can be used to estimate the corresponding transition rates, in analogy to the case of the two-particle Green's function. The intensities of the double-ionization Auger satellites are then

$$I(X \rightarrow Y) = N\, Q(X)\, TR(X \rightarrow Y) \tag{174}$$

where $TR(X \rightarrow Y)$ are the transition rates, $Q(X)$ the relative probabilities for the production of the initial state and N a normalization factor. The transition rates are approximated by

$$\begin{aligned} TR(X \rightarrow Y) &= \sum_{mn,ijk} TR(\Phi_{mn}^{S,T} \rightarrow \Phi_{ijk}^{D,Q}) \times \\ &\left[Res_{-DIP_x}(-\mathcal{G}^{S,T}_{mnmn})\, Res_{-TIP_y}(-\mathcal{G}^{D,Q}_{ijkijk})\right] \end{aligned} \tag{175}$$

where $\Phi_{mn}^{S,T}$ and $\Phi_{ijk}^{D,Q}$ are the two-hole and three-hole configurations, transformed to spin eigenstates, and the matrix elements $TR(\Phi_{mn}^{S,T} \rightarrow \Phi_{ijk}^{D,Q})$ can be evaluated in the one-center model by the formulae given in Ågren's work on open-shell molecules[13].

# 10 Other Methods

For the calculation of the Auger spectra of larger molecules semiempirical methods have been developed. Apart from modifications of the one-particle model, e.g. by using the CNDO or INDO approximations for integral evaluation [147,148] the X$\alpha$ method has found several applications [149,150,151,152,153,154,155,156]. In the earliest of those [149] the kinetic energy was simply estimated as the difference of the X$\alpha$ orbital energies for the core hole and the two valence holes. In the later applications the double ionization potential for the final state was obtained as the sum of the orbital energy of the first valence hole plus the orbital energy of the second valence hole calculated in a transition state where the first hole is taken into account by setting its occupancy to 0.5 in the calculation. Thus the calculation of the Auger spectrum requires calculations on only the ground state and n/2 ionized states where n is the number of valence orbitals.

The semiempirical HAM/3 method has also been applied to the calculation of Auger spectra[157]. Here one calculates the ground state of the doubly ionized system and obtains the positions of the other states as the excitation energies of the doubly ionized system using the concept of transition states with 1.5 electrons in each of the four highest orbitals.

On the ab initio level the coupled cluster method should be mentioned as another many-body method that has been applied to the calculation of molecular Auger spectra. Here one adds a cluster operator for the two-hole problem to the cluster operator for the ground state. These two operators act in the exponent of a normal ordered exponential operator on a combination of doubly ionized determinants[158]. One solves for the ground state cluster operator first, using the closed- shell coupled-cluster equations. The one-hole problem is treated next and a corresponding correction for the cluster operator determined. This is used then to obtain the two-hole cluster amplitudes.

# 11 Applications

## 11.1 Chemical Information in Auger Spectra

Auger spectra of molecules in the gas phase have the property that they reflect the local chemical environment of an atom as a part of the molecular system. Since the binding energies are a property of the whole system, the local similarity of spectra is due to local selection rules governing the intensity distribution (transition probability) for the bands corresponding to the manifold of possible final states. In fact, the transition rates are governed by one-center integrals weighted by the populations of the final state hole orbitals at the core ionization site, c.f. eqs. 131, 132, 133 and eq. 134. Therefore, Auger spectroscopy is claimed to contain considerable chemical information on the local electronic structure around the core hole site[159,160]. An example for the site sensitivity of the Auger lineshape is the carbon monoxide molecule, where the $5\sigma$ orbital is a carbon lone pair while $3\sigma$, $4\sigma$ and $1\pi$ are polarized more to the oxygen, a difference which is clearly visible in the two Auger spectra.

An intermediate case between CO and $N_2$ is the $CN^-$ anion which is isoelectronic to both of them, but less polar than CO. There is more resemblance of the nitrogen spectrum of the $CN^-$ anion to that of $N_2$ than of the carbon spectrum to that of CO, an indication that the "perturbation" by polarization takes place mostly on the carbon. In other words, by reducing the polarity of CO the $5\sigma$ lone pair will become more delocalized.

## 11.2 Hybridization

The factors which are most important for the "chemistry" are hybridization and bonding of an atom in the molecule. As is known, hybridization determines a set of atomic orbitals which interact stronger than others (the unhybridized ones) with the orbitals at the surrounding atoms to form bonds which can be characterized in many cases by localized orbitals. The interaction which results in bonding will lower the corresponding orbital energies more than the energies of the orbitals built from unhybridized orbitals. For example, in acetylene the unhybridized p orbitals form a bonding $\pi$-type molecular orbital which is lowered less than the bonding $\sigma$-type orbitals built from the sp hybrids. The bonding will decrease the atomic populations for this orbital at the core ionization site. Since the Auger intensities depend on those valence orbital populations, the intensities should relatively decrease for deeper lying states, i.e. for larger two hole binding energies. In addition, matrix element effects go into the same direction. So, while energy positions are easily connected with transition rates in a qualitative way it remains to specify the two hole binding energies.

For a difference in orbital populations and, therefore, in the lineshape it is, of course, not necessary that the corresponding atoms are different. For example, the Auger spectra of methane, ethylene and acetylene are largely different, corresponding to the different carbon hybridizations in those species, namely sp3, sp2 and sp, respectively[159]. In contrast, for example the carbon spectra of methane, methanol and dimethyl ether are quite similar, in accordance with the fact that the bonding situation for the carbon atom in all three molecules is very similar (sp3 hybridization). Both cases (similar and

different spectra) may occur in one and the same pair of molecules: The carbon spectra of tetramethylsilane and hexamethyldisilane are similar while the silicon $L_2, 3VV$ spectra are different [161].

## 11.3 Functional Groups

Functional group patterns belonging to an atom in different functional groups in the same molecule will be superposed in the corresponding Auger spectrum. An example is methyl cyanide[162] where the carbon spectrum is composed of a methyl group spectrum (sp3) and a cyano carbon spectrum (sp with a triple bond), while the nitrogen spectrum should be similar to that of hydrogen cyanide. In addition to experimental fingerprint identification, theory can resolve composite spectra by being able to calculate them separately, and to predict the missing ones, as e.g. those of hydrogen cyanide[163]. Furthermore, predictions are possible about expected similarities or dissimilarities of spectra. For example, consideration of the carbon spectrum of HCN in comparison to that of $C_2 2H_2$ shows that replacing a terminal CH group by a nitrogen does not have much influence on the lineshape. Even the carbon spectra of $CH_3CN$ and $CH_3CCH$ are expected to be similar although they are composite spectra with different weights[164]. Flipping the CN group around in $CH_3CN$ can be expected to change the carbon lineshape qualitatively as the chemical bonding of the cyano group in $CH_3NC$ is different from that in $CH_3CN$ and also different from the sp carbons in $CH_2CCH$ as has been shown in semiempirical Green's function calculations [164].

Trends in sequences of similar spectra can give hints on changes in the electronic structure of the corresponding molecules if they are reproduced by the calculations. An example is the minor peak at about 250 eV in the nitrogen spectrum at 353 eV which has been assigned to final state correlation effects. The corresponding peak has been shifted with respect to main peaks in the experimental nitrogen spectrum of the $CN^-$ anion as predicted by Green's function calculations on the anion[165].

For sequences of similar spectra belonging to larger molecules identification of group patterns may be complicated by the fact that several components may be superposed with only comparably small chemical shifts and different weights. An example is the sequence of linear alkanes converging ultimately to polyethylene. The superposition of only slightly different methyl and methylene group patterns with different weights leads to interesting changes in the lineshape for intermediate chain lengths, e.g. for propane where the weight for the methyls is double that of the methylene leading to a sharp additional feature on top of the main peak at about 249 eV.

## 11.4 Fingerprinting

In larger molecules local changes of the electronic structure around an atom which occurs in several other place unchanged in the molecule will cause only slight changes in the intensity. For example, in trinitrotoluene there is an additional sp3 carbon in comparison to trinitrobenzene which adds in a 1:6 ratio to the ring-sp2 carbon patterns and explains the difference in the low binding energy region of the carbon spectra of the two substances [166]. Adding instead of the methyl group amino groups to trinitrobenzene populates the amino carbon $\pi$ levels. This leads to dramatic changes in

the energy and intensity of the leading (low DIP) edge of the carbon lineshape for these compounds[166].

Another trend in systematically enlarged chains or clusters is the appearance of shoulders or additional peaks at low binding energy due to the possibility for the final states to more and more delocalize which will reduce the hole- hole repulsion. This can be observed in the alkane sequence [167,168] and in many other cases as e.g. going from ethylene to benzene[166,168] or comparing the fluorine spectra of HF[169] and $CH_3F$[170] (for calculations on $CH_3F$ see Larkins[171,172] and Liegener [173]). The same phenomenon explains some of the differences between solid state (and liquid phase) spectra and gas phase spectra of water, hydrogen fluoride and other hydrogen-bonded substances [159,160,174,175].

## 11.5 Symmetry

For a more general understanding of "chemical" fingerprinting one would need to be able to roughly predict the Auger lineshape for core ionizing a given atom in a molecule already from qualitative considerations on symmetry, hybridization and bonding. If one considers a local model the first factor to be incorporated is symmetry. The simplest case would be a first-row atom surrounded by hydrogens, treating it by starting from the united atom limit and permitting symmetry splitting. For the molecules isoelectronic to neon the procedure is simple and has been used by Økland et al.[176] to estimate the transition rates for such molecules. As in crystal field theory one has in some cases (e.g. ammonia) to distinguish between the strong field and the weak field case. In the strong field case one starts from the configurations of neon letting the orbitals split in the lower symmetry of the molecular point group and then form configurations and terms in the lower symmetry. In the weak field case (which is found to be less appropriate for the present problem) one builds first the atomic double hole terms and then splits these terms in the crystal field of the molecular point group, see Table 4

Table 4: Comparison of configurations and terms in double ionized Ne and $NH_3$. From Økland et al[176].

| Strong Field | | | Weak Field | | |
|---|---|---|---|---|---|
| config:s | config:s | terms | config:s | terms | terms |
| Ne | $NH_3$ | $NH_3$ | Ne | Ne | $NH_3$ |
| $2p^{-2}$ | $3a_1^{-2}$ | $^1A_1$ | $2p^{-2}$ | $^3P$ | $^3E, ^3A_2$ |
| | $1e^{-1}3a_1^{-1}$ | $^3E, ^1E$ | | $^1D$ | $^1A_1, 2^1E$ |
| | $1e^{-3}$ | $^3A_2, ^1E, ^1A_1$ | | $^1S$ | $^1A_1$ |
| $2s^{-1}2p^{-1}$ | $2a_1^{-1}3a_1^{-1}$ | $^3A_1, ^1A_1$ | $2s^{-1}2p^{-1}$ | $^3P^0$ | $^3A_1, ^3E$ |
| | $2a_1^{-1}1e^{-1}$ | $^3E, ^1E$ | | $^1P^0$ | $^1A_1, ^1E$ |
| $2s^{-2}$ | $2a_1^{-2}$ | $^1A_1$ | $2s^{-2}$ | $^1S$ | $^1A_1$ |

## 11.6 Relation to Solid State Spectra

The simplest possible way to relate orbital energies and two hole binding energies comes from solid state theory and is to obtain the density of Auger final states just as the self-convolution of the density of one-particle states[177]. In principle such an approach would imply the assumption of a constant hole-hole repulsion for all final states, because the energy scale for the final states is then frequently assumed as a relative energy scale only. Improvements on this simple approach, still retaining to the concept of density of states, are possible and have been transferred by Hudson and Ramaker[178] from solid state theory to molecular theory.

The self-convolution approach has the advantage of offering the simplest qualitative picture of degeneracy patterns arising from the degeneracies of the single hole states. One can frequently sketch the behaviour of one- particle orbitals for various bonding situations in a Walsh-type diagram. In particular, for a first-row atom in a specified bonding environment this will amount to just four levels. Of these only the three outer-valence levels will lead to characteristic fingerprints. The three outer-valence levels will give rise to six double-hole configurations if triplets are excluded for simplicity. If they are all degenerate as in the $t_2$ level of methane one obtains only one outer-valence Auger peak. If the two highest levels are degenerate as in acetylene one obtains one triply degenerate, one doubly degenerate and one single Auger final state for increasing two-hole binding energy. If all three are non-degenerate and almost equidistant one obtains five Auger peaks the middle of which is doubly degenerate, a pattern which roughly corresponds to the ethylene fingerprint. Including the inner-valence level and the above arguments for intensity changes yields a simple expression for the lineshape which can essentially reproduce the characteristic features for the three molecules methane, ethylene and acetylene[179]. The same considerations are also applicable to other first-row atoms than carbon. For example, for $NH_3$ the degenerate 1e level is situated below $3a_1$. In this case there are three outer-valence Auger peaks with degeneracies increasing from low to high binding energies. The above model can be used to show that the $NH_4Cl$ nitrogen spectrum, the dimethyl ether carbon spectrum and the tetramethylsilane carbon spectrum can be understood as intermediate cases between the methane carbon and the ammonia nitrogen spectrum [179].

## 11.7 Survey of Applications

On the quantitative side the treatment of final state correlation effects represents a necessary further step for an understanding of the chemistry manifested in Auger spectra. We will separately discuss that for the carbon monoxide molecule in the next section. Apart from shifts of the states in the outer valence region, which may often complicate assignment of the features in the spectra, breakdown of the one-particle picture in the inner-valence region is an important result of electron correlation exemplified in the carbon monoxide case.

The nitrogen molecule is another example for strong breakdown effects in molecular Auger specta. The dicationic states of nitrogen have been studied occasionally [14,180,181] and the Auger spectra, recorded experimentally several times [182-188] have been calculated by semi-internal CI[13] and Green's function[189] methods. Final state correlation effects seem to contribute to the ramp-like structure around 331 eV

Table 5: DIPs for the first and last main peak of the $H_2O$ Auger spectrum (eV).

| Method | Singlet $1b_1^{-2}$ | States $2a_1^{-2}$ | Reference |
|---|---|---|---|
| OSRHF | 39.16 | 88.48 | [136,103] |
| CI | 40.54 | 81.62 | [136,103] |
| HAM/3 | 40.86 | 79.04 | [157] |
| GF(ADC) | 39.3 | 83.4 | [31] |
| MRDCI | 40.6 | 84.2 | [31] |
| GF | 40.76 | 83.15 | [173] |
| EXP | 41.33 | 82.23 | [106] |

and to an intensity bump around 352 eV in the spectrum. The 352 eV feature is particularly complex and various other processes must also be expected to contribute to it: Naturally double- ionization satellites will play a role in this region [183,185,186] also satellites due to electron capture in the collision process are possible [186]. Furthermore, transitions involving Rydberg orbitals have been argued to be of importance here[190].

Breakdown effects in molecular Auger spectra have been found in a number of further cases. For example, in the inner-valence region of $H_2O$ semi-internal CI predicts a considerable breakdown of the $2a_1^{-2}$ derived states [136]. In that particular case the state with the main $2a_1^{-2}$ component was shifted as much as 7 eV by the semi-internal interaction. From the many calculations on the water Auger spectrum [106,191,192,136,193,194,157,31,103,174] we give in the following table only a survey of some representative results for the first and last main peak of the spectrum. One can see that there is qualitative agreement of all ab initio calculations, and that the quantitative differences are much less than the 7 eV shift by correlation. The semiempirical HAM/3 results are in line which shows that the parameters used reasonably account for correlation effects.

In the case of the fluorine spectrum breakdown effects of the inner-valence $2\sigma_g$ and $2\sigma_u$ orbitals are important. In a semiempirical analysis of the fluorine Auger spectrum[195] it was noted that interpretation of the midenergy region (the inner-outer region) was more difficult than for the other regions. Subsequent Green's function calculations [196] showed that the inner-valence breakdown effects are responsible for the structures in the midenergy part, explaining in particular a gap in the intensity of the experimental spectrum around 621-626 eV. Furthermore, second order corrections to the irreducible vertex parts have been found to be important in the outer-outer valence part of the spectrum[142]. The fluorine molecule has also been used as a test case for application of the coupled-cluster method[158].

Hydrocarbons are obvious candidates of interest for chemical effects in Auger spectra. For methane a lot of calculations have been reported on semiempirical[126] and ab initio levels, with consideration of correlation effects [191,197] and without [15,17,193,112,113]. However, as can be expected from the analogous photoelectron case [11] breakdown effects are more pronounced for the unsaturated hydrocarbons, e.g. $C_2H_2$, $C_2H_4$, $C_6H_6$[126,157,198,199,200,201,202] because the lowest excitation energy is smaller and the singlet-triplet splitting is larger for unsaturated than for saturated hydrocarbons and these quantities determine the effect of the virtual excitations in the system. In fact, the ramp-like structure in the high DIP region of the ethylene and acetylene spec-

tra can be explained from final state correlation effects and a corresponding structure is much less pronounced in the methane spectrum. For linear alkanes and alkenes ab initio calculations have been extended up to $C_6H_{14}$ and $C_6H_8$[168].

Among the other cases of ab initio studies on electron correlation effects in molecular Auger spectra are NO[13], $CO_2$ [13], HCl[203,204,205,140], HF[191,206,28,146], HCN[163], the $CN^-$ anion[165], LiF[133,97,98], $CH_3F$[173], $SiH_4$[207], $H_2S$[192,134], $N_2O$[208], $C_2H_6$[209], $BF_3$[210], $NH_3$[211], $O_2$[212,139], glycine[213], formaldehyde[214] and formamide[214]. All these calculations find an explicit inclusion of correlation important for a reproduction of experimental spectra. Recent theoretical invesitgations of Auger spectra has also been performed in conjunction with analysis of charge transfer spectra. From the kinetic energy distribution of $H^-$ ions arising from double charge-transfer (DCT) of protons impinging on gaseous molecules several singlet state energies of the double ion are detected that can be associated to band peak energies in Auger spectra[3]. Calculations for the the combined interpretation of DCT and Auger spectra have been performed for HCl[205,140], $H_2S$[134] and $O_2$[212,139].

# 12 Sample Analysis: Carbon Monoxide

Among the Auger spectra of first row diatomics the spectra of carbon monoxide are the most frequently studied. One reason is that CO is one of the simplest cases where two largely different spectra fingerprint the orbital populations in a spectacular way. Furthermore, there has been some interest in the interpretation of som unusual structures in the CO spectra; the intense and uniquely narrow peak (called B3) at about 250 eV in the carbon spectrum and the appearance of "extra" peaks (B9, B11) in the mid region of the oxygen spectrum. Experimental spectra have been recorded by Siegbahn et al[182], Moddeman et al[185], Kelber et al[215], Ungier and Thomas[188], and by Correia et al[18]. In the following discussion of the CO spectra we use the notation of Moddeman et al.[185] given in fig. 2. This figure also shows the results from the Green's function calculations in ref. [118]. The experimental spectra[185] are shown in figs: 3 and 4, together with the interpretation given by the CI calculations[128].

## 12.1 Hole-mixing Auger States

The effect of hole-mixing in Auger spectra maybe best illustrated by the the Auger intensities of the two lowest $^1\Sigma^+$ states of $CO^{2+}$, the X and B states. Hole-mixing Auger states are characterized by that they mix more than one main two-hole configuration into the (final state) wave function. The cross sections for hole-mizing Auger states are given in the frozen orbital approximation by the square of $A_{fi} = \sum_{rs} \tau_{rs} c_{rs}$ (eq. 111). The hole-mixing occurs when there is more than one pair of r,s orbital indices for which $c_{rs}$, the expansion coefficients of the main two-hole configuration (pole strengths of the Green's function), is large. The hole-mixing character of the Auger final state wave functions leads to *electronic interference* for the Auger cross sections. In such a case one needs in addition to the overlap amplitudes also to know the phases and relative magnitudes of the orbital elements $\tau_{rs}$.

Calculations by both the configuration interaction[18] and the Green's function[118] methods have independently shown that interference effects are important and that the proper assignment for the final state of the B3 peak is a superposition of the $4\sigma^1 5\sigma^1$ and $5\sigma^{-2}$ double-hole configurations. It should be mentioned that in previous assignments the B3 peak was attributed mainly to the $4\sigma^1 5\sigma^1$ configuration[191,128] or to the $5\sigma^{-2}$ double-hole configuration alone[215]. The former of those assignments was based on configuration interaction calculations and was supported by the method of Hurley [14] and several $X_\alpha$ calculations[153,155,156]. The second assignment was a semiempirical one, based on a good reproduction of the corresponding binding energy by the semiempirical independent particle model and the hole-hole interaction strength.

A straight application of the intensity model (see section 6.2) which assumes one-center contributions from the leading CSF intensities, a better accordance with experiment was obtained with the second assignment[215], i.e. with the B3 peak (B $^1\Sigma^+$ state) as due to the $5\sigma^{-2}$ configuration. However, taking account of the hole-mixing character of the two states also this argument gives the reverse assignment[18], i.e. the first assignment with a leading $4\sigma^1 5\sigma^1$ configuration, see explanation given below.

Table 6 shows the interpretation of the two lowest $^1\Sigma^+$ states of $CO^{2+}$ from different calculations. As examplified by Correia et al.[18] for the lowest $^1\Sigma^+$ states of the $CO^{2+}$ dications the character of a configuration interaction wave function depends strongly

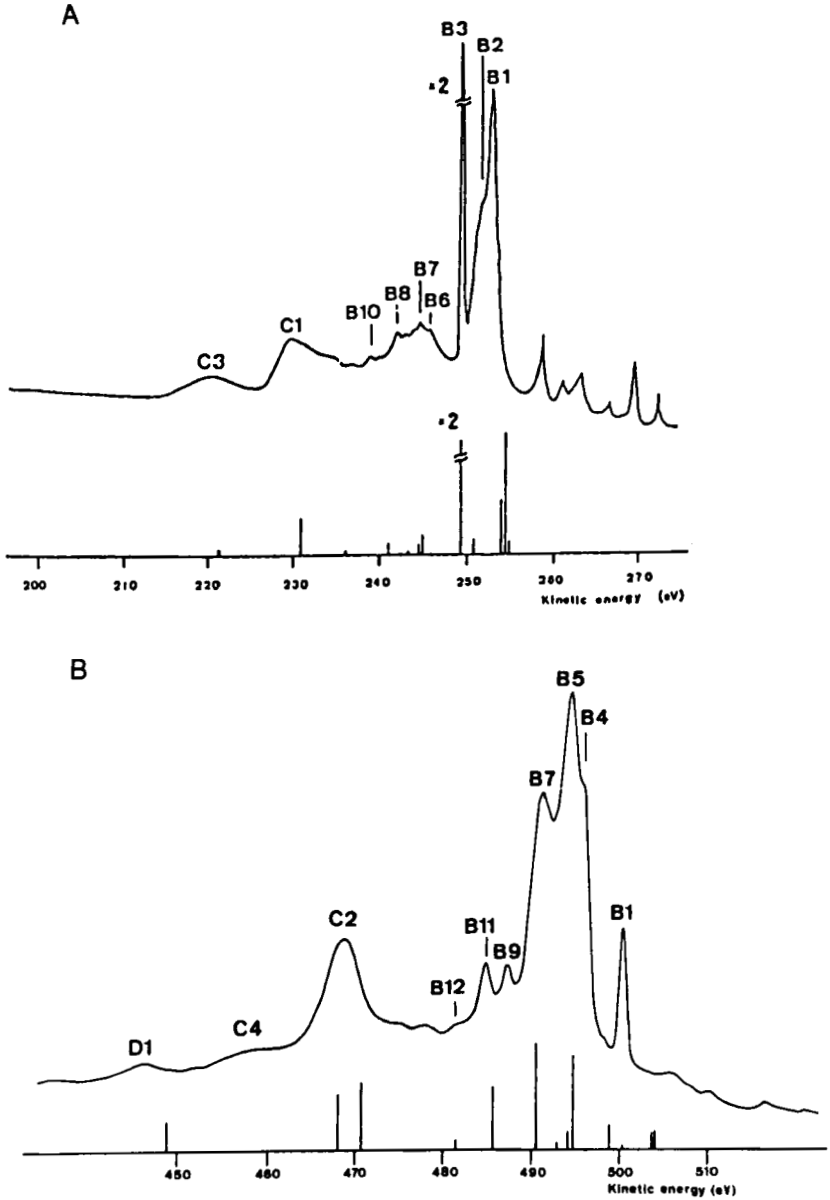



Fig. 2: Theoretical Auger spectra of CO calculated by the Green's function method[118] compared to the experimental spectrum[185]. A) Carbon spectrum; B) Oxygen spectrum. The figure shows also the notation B1-B12, C1-C4, and D1 of Moddeman et al[185] which is used in the text.

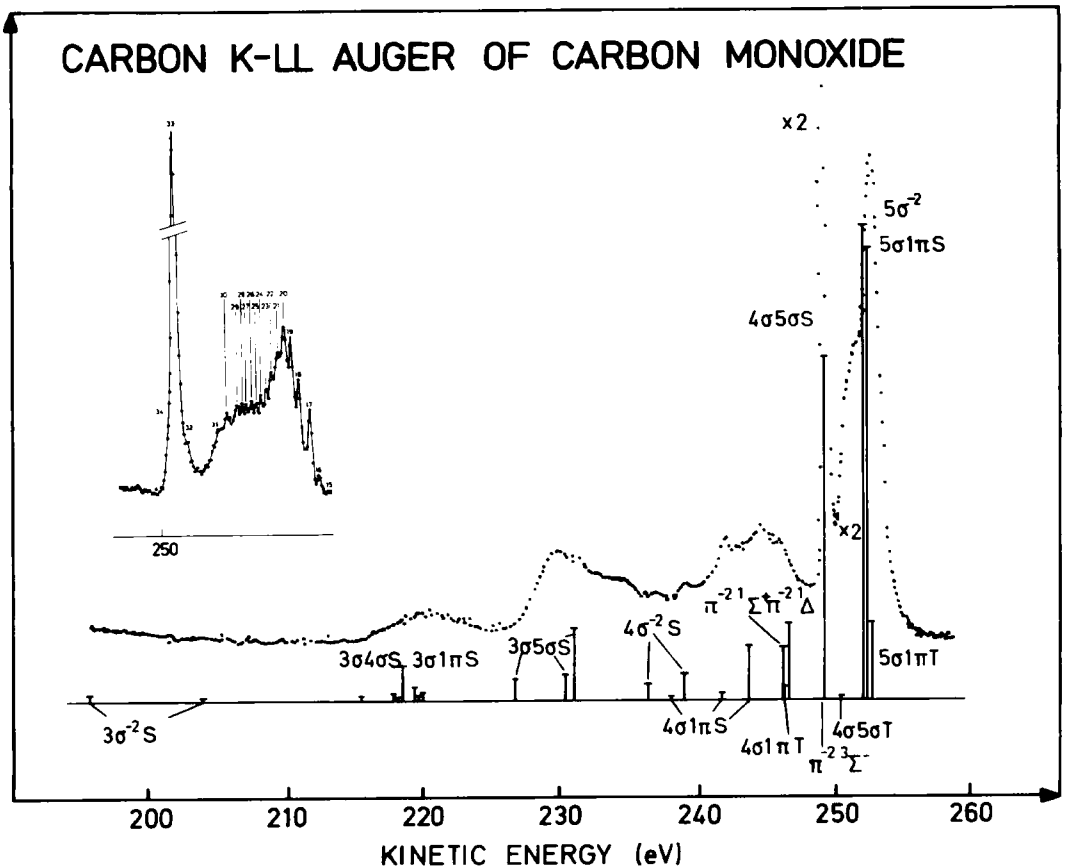



Fig. 3: Theoretical carbon Auger spectrum of CO calculated by the configuration interaction method[128] compared to the experimental spectrum[185].

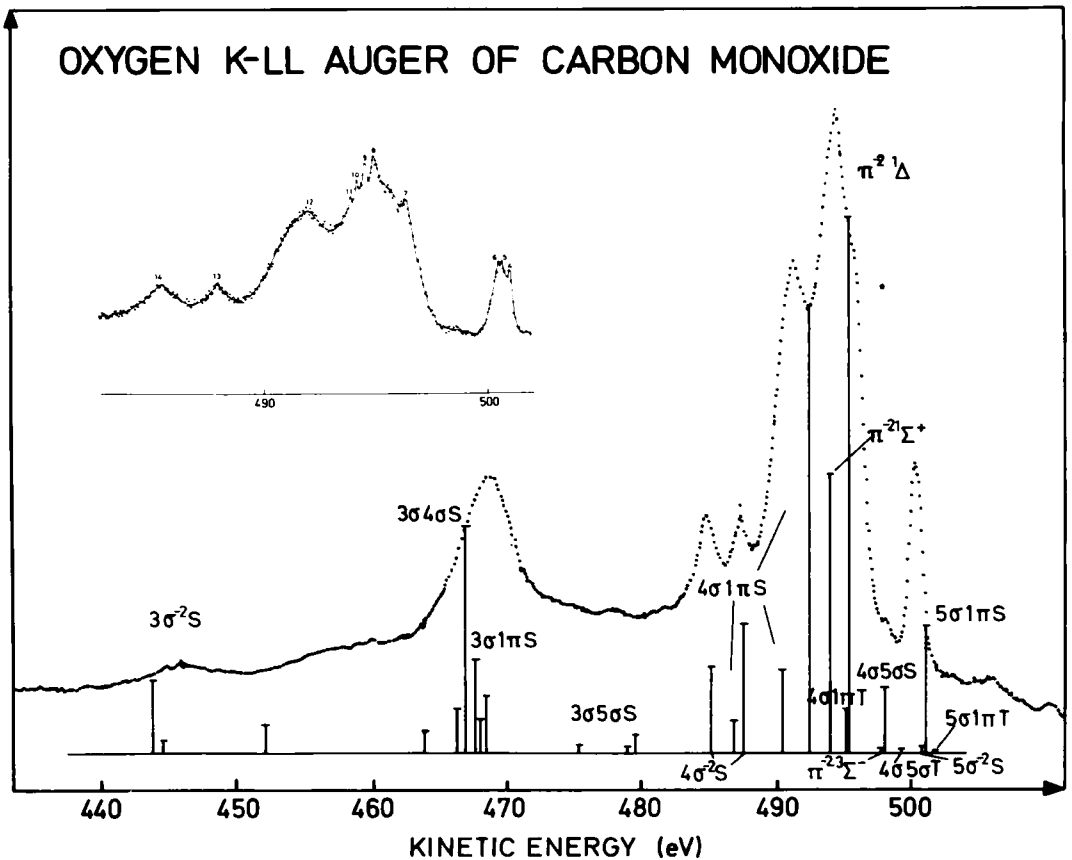



Fig. 4: Theoretical oxygen Auger spectrum of CO calculated by the configuration interaction method[128] compared to the experimental spectrum[185].

Table 6: The two lowest singlet $\Sigma^+$ states in ab initio calculations. From refs. [18] and [?]. "Can." means canonical orbitals.

| Method | State | CI coeff. $5\sigma^{-2}$ | CI coeff. $4\sigma^{-1}5\sigma^{-1}$ | DIP |
|---|---|---|---|---|
| CASSCF | X | 0.92 | -0.12 | 38.53 |
| -"- | B | 0.89 | -0.08 | 43.10 |
| CASCI(can.) | X | 0.80 | 0.40 | 41.58 |
| -"- | B | 0.24 | -0.79 | 44.00 |
| GF | X | 0.76 | 0.39 | 39.38 |
| -"- | B | 0.13 | -0.62 | 44.50 |
| EXP | X | | | 41.70 |
| -"- | B | | | 45.40 |

on the choice of orbitals. The CASSCF results without natural orbital transformation, is shown just to demonstrate that the interpretation becomes arbitrary because of the invariance of the wave functions with respect to unitary transformations among the active orbitals, in fact both the X and the B states become strongly dominated by the same ($5\sigma^{-2}$) configuration. On the other hand the canonical Hartree-Fock CI results are qualitatively similar to the Green's function results of Liegener[118]. The CI coefficients can here be compared to the eigenvector components of the particle-particle Green's function matrix times the square root of the corresponding pole strength. Two other types of CI calculations, so-called semiinternal CI[128] and contracted CI[18] calculations, have been reported for the energies of the X and B states, see Table 8. Note that the energies of the states vary with a couple of eV:s between the calculations. We consider the contracted CI calculation to be the most accurate one, since besides the static correlation due the hole-mixing effect, it also picks up a large portion of the contribution due to the dynamical electron correlation.

One thus finds that both X and B states contain considerable mixing of the $5\sigma^{-2}$ and $4\sigma^{-1}5\sigma^{-1}$ configurations; for the X state they mix as +0.8 and +0.4, for the B state (the B3 peak) as +0.2 and -0.8. Considering only the leading configurations X is a $5\sigma^{-2}$ and B a $4\sigma^{-1}5\sigma^{-1}$, as it should following the one-particle model. However, the hole-mixing by the second configuration is non-negligible in both cases, and furthermore, acts destructively for one state and constructively for the other. This explains the assignment problems using intensity analysis basing on the leading configuration only.

It can be noted that also the Auger lineshapes have been used to assign the X and B states. Thus the reverse ordering[215] (with B state (the B3 peak) assigned to a $5\sigma^{-2}$ configuration) was supported by the argument that the non-bonding character of the $5\sigma$ orbital should explain the narrow lineshape of the peak. It has been pointed out, however, by Correia et al[18] that the fact that the intermediate $C1s^{-1}$ bond length is considerably shortened actually inverts the argument. The unusual lineshape can then be explained from the fact that the corresponding final state is predissociative via an avoided crossing with the next state of the same symmetry. A correspondingly fitted vibronic spectrum of that part of the Auger lineshape can indeed explain the experimental observations[18].

## 12.2 Assignment

The assignments of the other electronic transitions is as follows. The first peak in the experimental spectra belonging to normal (C-VV) transitions is B1 in the terminology of Moddeman [185] which is visible in both the carbon and and the oxygen spectra. There then follows, towards lower kinetic energy, the shoulder B2, visible only in the carbon spectrum. The configuration interaction calculations of Ågren and Siegbahn[128] assign B1 to singlet $\Pi$ ($1\pi^3$,$5\sigma^1$) and B2 to singlet $\Sigma$ ($5\sigma^{-2}$). However, the two states are energetically quite close and their potential energy curves cross at 2.4 bohr[18]. The analysis by Correia et al of the vibronic profiles give a certain assignment of the lowest dicationic singlet state of CO as due to $\Sigma$ symmetry. This level ordering would also be in agreement with all other calculations on these states. B3 is as mentioned above a superposition of $4\sigma^1 5\sigma^1$ and $5\sigma^{-2}$ double-hole configurations which leads by interference to a large intensity for this peak in the carbon spectrum. B5 is assigned to the singlet $\Delta$ and singlet $\Sigma$ $1\pi^{-2}$ double-hole states. It has large intensity in the oxygen spectrum, but is not visible in the carbon spectrum. Jennison et al[216] suggested that this is a result of configuration interaction in the initial state, since the doubly excited $1\pi$ to $2\pi$ shake-up configuration is particularly strong for the $C1s^{-1}$ case.

The peak B7 which appears strongly in the oxygen but weakly in the carbon spectrum is assigned to a singlet $\Pi$ state ($4\sigma^1$,$1\pi^3$). The two peaks B9 and B11 which are visible in the oxygen spectrum are due to a singlet $\Sigma$ ($4\sigma^{-2}$ double hole configuration), and is strongly interacting with shake-up configurations. The splitting of the $4\sigma$ double-hole line is nicely reproduced by the configuration interaction calculations[128]. This is a typical effect of a breakdown of the quasi-particle picture as described in the previous sections. Until now Green's function calculations were not satisfactory in reproducing the splitting in this case, although some less dramatic effects of the kind did occur in the CO calculations, e.g. for the $3\sigma^1 5\sigma^1$ states see Table 7.

Table 7: Breakdown effects for the $3\sigma^{-1}4\sigma^{-1}$ states of the CO dication. Configuration Interaction (CI) and Green's Function (GF) calculations.

| CI DIP | CI weight | GF DIP | GF Pole Strength |
|---|---|---|---|
| 64.99 | 0.45 | 62.39 | 0.25 |
| 65.44 | 0.15 | 62.65 | 0.32 |
| 69.32 | 0.15 | | |

In comparing CI and Green's function calculations for these states one should keep in mind that the CI values were relative energies (this also facilitates for the $4\sigma$ double-hole states comparison with experiment) and that the absolute value of the pole strength of the particle-particle Green's function can be compared to the squared absolute value of the coefficient of the two- hole configuration (in general the sum of the coefficients for all non-shake- up two-hole configurations).

The two peaks B9 and B11 are not visible in the carbon spectrum, due to the small intensity to be expected from the calculations and due to the fact that the features around 239-246 eV in the carbon spectrum are probably superposed by initial state shake-off satellites as pointed out by Ågren and Siegbahn.

Table 8: Assignments of some peaks in the KVV spectrum of CO

| *Peak* | *Exp*[a] | *Exp*[b] | *Exp*[c] | *Assignment*[d] | *CI*[e] | *CI*[f] | *GF*[g] |
|---|---|---|---|---|---|---|---|
| - | | | 39.6 | $5\sigma^1\ 1\pi^1$ (T) | 42.83 | | 38.88 |
| B1 | 42.2 | 41.7 | 40.8 | $5\sigma^1\ 5\sigma^1$,$4\sigma^1\ 5\sigma^1$ | 43.9 | 40.50 | 39.38 |
| B2 | 43.7 | | | $5\sigma^1\ 1\pi^1$ | 43.4 | | 39.71 |
| B3 | 45.8 | 45.4 | | $4\sigma^1\ 5\sigma^1$, $5\sigma^1\ 5\sigma^1$ | 46.55 | 44.67 | 44.50 |
| B5 | 48.1 | | | $1\pi^1\ 1\pi^1\ ^1\Delta$ | 48.57 | | 48.74 |
| " | " | | | $1\pi^1\ 1\pi^1\ ^1\Sigma^+$ | 50.35 | | 49.30 |
| B7 | 51.1 | | | $4\sigma^1\ 1\pi^1$ | 51.96 | | 50.65 |
| B9 | 55.0 | | | $4\sigma^1\ 4\sigma^1$ | 56.64 | | |
| B11 | 57.5 | | | $4\sigma^1\ 4\sigma^1$ | 59.29 | | 57.75 |
| C1 | 65.9 | | | $3\sigma^1\ 5\sigma^1$ | 64.99 | | 62.39 |
| C2 | 73.2 | | | $3\sigma^1\ 4\sigma^1$ | (77.62)[h] | | 72.67 |
| C3 | 75.3 | | | $3\sigma^1\ 1\pi^1$ | 76.71 | | 75.36 |
| D1 | 95.4 | | | $3\sigma^1\ 3\sigma^1$ | 100.54 | | 94.38 |

[a] Experimental Auger results [185,215] [b] Experimental Auger results [18] [c] Experimental photoionization results [7] [d] Final states are singlets unless otherwise indicated (T) [e] Configuration interaction results (semi-internal CI)[128] [f] Configuration interaction results (contracted CI)[18] [g] Green's function results [118] [h] Largest peak of the corresponding breakdown group

The remaining features are formed with strong participation of inner-valence orbitals. C1 is assigned to a singlet $\Sigma$ ($3\sigma^1\ 5\sigma^1$) state, C2 and C3 form together a broad band in the oxygen spectrum (weaker in the carbon spectrum) to which both $3\sigma^1 4\sigma^1$ and $3\sigma^1 1\pi^3$ states contribute. It should be mentioned that the CI calculations predict a breakdown of the quasiparticle picture for the $3\sigma^1 4\sigma^1$ transitions which could explain the broadness of the feature. C4 is not reproduced by the calculations and is probably caused by final state shake-off transitions. D1 is the inner-inner valence peak $3\sigma^{-2}$ ($O2s^{-2}$).

## 12.3 Satellites

There are several satellite transitions which will contribute to the Auger spectrum in addition to the normal processes discussed above. The first group of satellite transitions will appear on the high kinetic energy side of the normal region to which they correspond. They should be expected to be appreciable only for the outer-outer case. They correspond to autoionization transitions and initial state shake-up satellites and are usually denoted according to Moddeman[185] as Ce-V for participant autoionization, Ce-VV for spectator autoionization, and CVe-VV for initial state shake-up.

So, in the high kinetic energy region of electron excited Auger spectra one finds the structures due to autoionization (or deexcitation) of core excited initial states. They will not occur in nonresonant photon excited Auger spectra (this difference actually lead to their identification in the spectrum of molecular nitrogen[185]). One can deliberately excite those spectra if one uses photons carrying just the core to bound state excitation energy. The decay spectra can then be divided within the quasi-particle picture into two components, corresponding on the one hand to final states where the electron in the

virtual orbital participates in the decay so that the final state will have one remaining valence hole, and on the other hand to final states where the electron in the virtual orbital acts only as a spectator so that two additional valence holes are created. The autoionization spectrum can, therefore, be compared to a superposition of photoelectron and normal Auger spectra, the intensities being of course different and the Auger energies accordingly shifted. The assignment and interpretation of these structures for the CO molecule has been discussed several times[185,217,147,218,18,219]. In particular, we mention that for some bands a vibrational analysis has been achieved [18], and that a comparative Green's function study [219] on the three spectra (photoelectron, Auger and autoionization) has been performed.

A corresponding treatment is also possible for the initial state shake-up satellites. However, the consideration of possible final states as either participant, i.e. two hole-, or spectator, three hole- one particle, decay states with respect to the initial shake-up configuration may have to be done for each shake-up state separately if several can be excited. A simplification is possible if one satellite in the XPS spectrum can be treated as dominant. Furthermore, due to the large number of possible states in this process and the complications in spin coupling it may be advisable to treat them approximately by ignoring exchange integrals in an independent particle approximation based on experimental ionization potentials. This semiempirical approach has been found to work qualitatively correct for the case of high- energy satellites in the X-ray excited Auger spectrum of the nitrogen molecule. For CO the corresponding satellites seem not to have been identified. In case there are several close-lying shake-up states appearing the photoelectron spectrum, a semiempirical approach for the Auger decay, or any approach based on separate non-interacting states, must be treated with caution due to state interference effects, see section 3.5. When the ratio between the energy separation and the lifetime broadening is lower than about 5 significant distortions due to these effects can be anticipated as a rule of thumb[81].

The next group of satellite transitions will appear on the low kinetic energy side of the normal outer-outer region and can be classified as initial state shake-off (double-ionization ) satellites, abbreviated as CV-VVV, and double autoionization processes, CVe-VVV. Furthermore, in that part of the spectrum inelastic scattering may obscure the structures. Finally, double Auger transitions, C-VVV, may contribute from the inner- outer region on to lower kinetic energies (starting with the triple ionization potential on the binding energy scale). None of these structures seem to have been theoretically analyzed for the CO case, but there has been an identification of such satellites for other molecules, e.g. for water CV-VVV and C-VVV have been considered in semi-internal CI calculations[136], for hydrogen fluoride CV-VVV satellites have been assigned experimentally [169] and the assignment has been supported by restricted Hartree-Fock calculations[220] and three-particle Green's function calculations [146]. For lithium fluoride CV-VVV and CVe-VV satellites have been identified[133]. Inelastic scattering has been studied experimentally for some molecules, see for example ref:s [169] and [221].

# 13 Conclusions and Outlook

A variety of methods have been applied to the molecular Auger problem and the applications cover by now a representative cross section of chemically and physically interesting molecules and effects. Theory has been found indispensable for interpreting and assigning the spectra. There are several differences in treating the molecular Auger problem as opposed to the atomic one, first of all the breakdown effects which are frequent even for first-row molecules and depending on saturation of bonds and density of states. From the outset of the present state of the art we predict development of theory and calculations of molecular Auger mainly along two lines of research. We may denote these as the "chemistry" the "physics" lines. The former rests basically on the analysis in terms of electronic structure theory, something which has been much advanced lately. The latter will in addition to the electronic structure description also be closely linked to a clever implementation of scattering theory.

The development of the "physics" line for interpretation of molecular Auger effects and spectra was reviewed in sections 3 and 4. Applications have so far focussed on lifetime-vibrational interference effects and fine structures due to vibronic effects, while applications to e.g. PCI have not been undertaken in the molecular case. One can here forsee a development in terms of response and moment theories and of scattering matrix approaches. One can predict further development of these theories more in conjunction with, or as direct generalizations of, the bound state electronic structure methods (and even the very computer codes), rather than by a development on their own. Applications will probably include further studies of vibronic interaction and fine structures on a fundamental basis including the coupling with the continuum as outlined in section 3 of this review, but one might also anticipate studies of threshold effects, angular distributions, post-collision interaction effects and various resonant phenomena in general and vibrationally enhanced resonances in particular. Resonance Auger and shake-up Auger are two particular fields that so far have been rather little studied theoretically in the molecular case, but which probably will be more studied in depth. These type of spectra must be addressed at a higher theoretical level than the "normal" Auger transitions emanating from the well separated core hole states as shown in section 3.5.

It is clear that the presumed theoretical efforts are actualized and motivated by the ever on-going spectroscopic improvements, in particular by the development of synchrotron radiation facilities with energy and polarization variable excitation sources. We believe that first and second row diatomics provide a set of very interesting test cases for the alleged studies. The more simple hydrides are not fully representative, they exhibit "atomic behaviour" in many respects, while molecules with more than two heavy atoms do not show sufficient experimental or "theoretical" resolution. For larger molecules, the number of degrees of freedom for both nuclear and electronic motions, the large number of interacting Auger channels and the break-down of the Born-Oppenheimer approximation are facts that will "smear out" fine structures assigned to vibronic interactions or to resonance effects.

The second line of development, the "chemistry" line of research, refers to a discrete state electronic structure analysis, either by means of advanced many-body methods, or to clever simplifications thereof. The local character of Auger transitions and the entailed local effective selection rules are instrumental in this analysis. Chemical information on symmetry, delocalization, hybridization and bonding can be obtained from

the spectra as described in section 11 of this review. For smaller systems the study of vibronic structures leads to information on the conformational geometries and force fields of two-hole ions. Since larger systems have become tractable systematic trends can be investigated in cluster and oligomer sequences approaching polymers, biomolecules or models of solids or liquids. Thus intermolecular effects will find more interest and the overlap with surface science will become larger as ab initio calculations on adsorbate spectra proceed. The cluster approach is promising in the study of extended systems because of the local probe character of Auger spectra. On the way to ever larger systems more approximate methods will have to be developed. On the ab initio level approaches based on localized orbitals seem to be promising in that respect or, in the case of polymers, localized Wannier functions. In the case of large systems (or polymers) the size consistency of a method becomes important. An example is the two-particle Green's function which will automatically fulfill the size consistency requirement and can be easily transformed to an exciton-like representation in the case of periodic systems. Molecular methods can thus complement solid state methods as well as atomic theory methods in the Auger field.

# References


[1] P. Auger *J. Phys. Radium*, vol. 6, p. 205, 1925.

[2] M. Thompson, M. Baker, A. Christie, and J. Tyson in *Auger electron spectroscopy*, Springer, Berlin, 1985.

[3] P. Fournier, J. Fournier, F. Salama, D. Stärck, S. Peyerimhoff, and J. Eland *Phys. Rev. A*, vol. 34, p. 1657, 1986.

[4] R. Cooks, T. Ast, and J. Beynon *Int.J.Mass Spectrom.Ion Phys.*, vol. 11, p. 490, 1973.

[5] G. Dujardin, L. Hellner, D.Winkoun, and M. Besnard *Chem. Phys.*, vol. 105, p. 291, 1986.

[6] P. Lablanquie, J. Eland, I. Nenner, P. Morin, J. Delwiche, and M. Hubin-Franskin *Phys. Rev. Lett.*, vol. 58, p. 992, 1987.

[7] P. Lablanquie, J. Delwiche, M. Hubin-Franskin, I. Nenner, P. Morin, K. Ito, J. Eland, J. Robbe, G. Gandara, J. Fournier, and P. Fournier *Phys. Rev. A*, vol. 40, p. 5673, 1989.

[8] J. Schirmer, L. Cederbaum, W.Domcke, and W. von Niessen *Chem. Phys.*, vol. 26, p. 149, 1977.

[9] L. Cederbaum, J. Schirmer, W. Domcke, and W. von Niessen *J.Phys B: At. Mol. Phys.*, vol. 10, p. L549, 1977.

[10] L. Cederbaum and W. Domcke *Adv. Chem. Phys.*, vol. 36, p. 205, 1977.

[11] L. Cederbaum, W. Domcke, J. Schirmer, and W. von Niessen *Adv. Chem. Phys.*, vol. 65, p. 115, 1986.

[12] W. von Niessen, G. Bieri, J. Schirmer, and L. Cederbaum *Chem. Phys.*, vol. 65, p. 157, 1982.

[13] H. Ågren *J. Chem. Phys.*, vol. 75, p. 1267, 1981.

[14] A. Hurley *J.Mol.Spectr.*, vol. 9, p. 19, 1962.

[15] I. Ortenburger and P. Bagus *Phys. Rev. A*, vol. 11, p. 1507, 1975.

[16] H. Ågren, U. I. Wahlgren, and S. Svensson *Chem. Phys. Lett.*, vol. 35, p. 336, 1975.

[17] K. Faegri and R. Manne *Mol. Phys.*, vol. 31, p. 1037, 1976.

[18] N. Correia, A. Flores, H. Ågren, K. Helenelund, L. Asplund, and U. Gelius *J. Chem. Phys.*, vol. 83, p. 2035, 1985.

[19] D. Jennison *J. Vacuum Sci. Technol.*, vol. 20, p. 548, 1982.

[20] J. Oddershede *Adv. Quant. Chem.*, vol. 11, p. 275, 1978.

[21] J. Oddershede *Adv. Chem. Phys.*, vol. 69, p. 201, 1987.

[22] Y. Öhrn and G. Born *Adv. Quant. Chem.*, vol. 13, p. 1, 1981.

[23] P. Jörgensen and J. Simons in *Second-Quantization Based Methods in Quantum Chemistry*, Academic Press, New York, 1981.

[24] M. Herman, K. Freed, and D. Yeager *Adv. Chem. Phys.*, vol. 48, p. 1, 1981.

[25] N. Fukuda, F. Iwamoto, and K. Sawada *Phys. Rev. A*, vol. 135, p. 932, 1964.

[26] P. Ring and P. Schuck in *The Nuclear Many-Body Problem*, Springer, Berlin, 1980.

[27] E. Economou in *Green's Functions in Quantum Physics*, Springer, Berlin, 1983.

[28] C. Liegener *Chem. Phys. Lett.*, vol. 90, p. 188, 1982.

[29] J. Schirmer and A. Barth *Z.Physik*, vol. A317, p. 267, 1984.

[30] J. Ortiz *J. Chem. Phys.*, vol. 81, p. 5873, 1984.

[31] F. Tarantelli, A. Tarantelli, A. Sgamelotti, J. Schirmer, and L. Cederbaum *J. Chem. Phys.*, vol. 83, p. 4683, 1985.

[32] A. Tarantelli and L. Cederbaum *Phys. Rev. A*, vol. 39, p. 1639, 1989.

[33] A. Tarantelli and L. Cederbaum *Phys. Rev. A*, vol. 39, p. 1656, 1989.

[34] R. Graham and D. Yeager *J. Chem. Phys.*, vol. 94, p. 2884, 1991.

[35] T. Åberg and G. Howat in *"Theory of the Auger effect" in Handbuch der Physik*, (S. Flügge and W. Melhorn, eds.), Springer, Berlin, 1982.

[36] U. Fano *Phys. Rev.*, vol. 124, p. 1866, 1961.

[37] A. Cesar, H. Ågren, and V. Carravetta *Phys. Rev. A*, vol. 40, p. 187, 1989.

[38] B. Cleff and W.Mehlhorn *Phys. Letters*, vol. 37A, p. 2, 1971.

[39] S. Flügge, W. Mehlhorn, and V. Schmidt *Phys. Rev. Lett.*, vol. 29, p. 7, 1972.

[40] J. Taylor in *Scattering Theory*, Wiley, New York, 1975.

[41] F. Gel'mukhanov, L. Mazalov, A. Nikolaev, A. Kondratenko, V. Smirnii, P. Wadash, and A. Sadovskii *Akad. Nauk SSSR*, vol. 225, p. 597, 1975.

[42] F. Gel'mukhanov, L. Mazalov, and N. Shklyaeva *Sov. Phys. JETP*, vol. 42, p. 1001, 1975.

[43] F. Gel'mukhanov, L. Mazalov, and A. Kontratenko *Chem. Phys. Lett.*, vol. 46, p. 133, 1977.

[44] W. Domcke and L. Cederbaum *Phys. Rev. A*, vol. 16, p. 1465, 1977.

[45] F. Kaspar, W. Domcke, and L. Cederbaum *Chem. Phys. Lett.*, vol. 44, p. 33, 1979.

[46] L. Cederbaum and W. Domcke *J. Chem. Phys.*, vol. 60, p. 2878, 1974.

[47] L. Cederbaum and W. Domcke *J. Chem. Phys.*, vol. 64, p. 603, 1976.

[48] M. Berman, H. Estrada, L. Cederbaum, and W. Domcke *Phys. Rev. A*, vol. 28, p. 1363, 1983.

[49] F. Gel'mukhanov, L. Mazalov, and N. Shklyaeva *Eksp. Teor. Fiz.*, vol. 69, p. 1971, 1975.

[50] A. Cesar and H. Ågren. To be published.

[51] F. Mies *Phys. Rev.*, vol. 175, p. 164, 1968.

[52] C. Davis and L. Feldkamp *Phys. Rev. B*, vol. 15, p. 2961, 1977.

[53] U. Fano and J. Cooper *Phys. Rev. A*, vol. 137, p. 1364, 1965.

[54] L. Armstrong Jr., C. Theodosiou, and M. Wall *Phys. Rev. A*, vol. 18, p. 2538, 1978.

[55] A. Starace *Phys. Rev. B*, vol. 5, p. 1773, 1972.

[56] H. Feshbach *Annals of Physics*, vol. 19, p. 287, 1962.

[57] H. Feshbach *Annals of Physics*, vol. 43, p. 410, 1967.

[58] R. Barker and H. Berry *Phys. Rev.*, vol. 151, p. 14, 1966.

[59] P. Hicks, S. Cvejanovic, J. Comer, F. Read, and J. Sharp *Vacuum*, vol. 24, p. 573, 1974.

[60] V. Schmidt, S. Krummacher, F. Wuilleumier, P., and Dhez *Phys. Rev. A*, vol. 24, p. 1803, 1981.

[61] V. Schmidt *J. de Physique*, vol. C9, p. 401, 1987.

[62] M. Völkel, M. Schnetz, and W. Sandner *J.Phys B: At. Mol. Phys.*, vol. 21, p. 4249, 1988.

[63] W. Sandner and M. Völkel *Phys. Rev. Lett.*, vol. 62, p. 885, 1989.

[64] A. Niehaus *J.Phys B: At. Mol. Phys.*, vol. 10, p. 1845, 1977.

[65] K. Helenelund, S. Hedman, L. Asplund, U. Gelius, , and K. Siegbahn *Phys. Scr*, vol. 27, p. 245, 1983.

[66] M. Kuchiev and S. Scheinerman *Zh. Eksp. Teor. Fiz.*, vol. 90, p. 1680, 1986.

[67] A. Russek and W. Mehlhorn *J.Phys B: At. Mol. Phys.*, vol. 19, p. 911, 1986.

[68] P. van der Straten, R. Morgenstern, and A. Niehaus *Z. Phys. D*, vol. 8, p. 35, 1988.

[69] M. Y. Amus'ya, M. Y. Kuchiev, and S. Nerman *Zh. Eksp. Teor. Fiz.*, vol. 76, p. 470, 1979.

[70] M. Y. Amus'ya, M. Y. Kuchiev, and S. Nerman in *Coherence and Correlation in Atomic Collisions*, (H. Kleinpoppen and J. F. Williams, eds.), Plenum, New York, 1980.

[71] T. Åberg in *Inner-Shell and x-ray Physics of Atoms and Solids*, (D. Fabian, H. Kleinpoppen, and L. M. Watson, eds.), Plenum, New York, 1981.

[72] P. Froelich, O. Goscinski, U. Gelius, and K. Helenelund *J.Phys B: At. Mol. Phys.*, vol. 17, p. 979, 1984.

[73] G. Ogurtsov *J.Phys B: At. Mol. Phys.*, vol. 16, p. L745, 1983.

[74] J. Tulkki, G. Armen, T. Åberg, B. Crasemann, and M. Chen *Z. Physik D*, vol. 5, p. 241, 1987.

[75] G. Armen, J. Tulkki, T. Åberg, and B. Crasemann *J. de Physique*, vol. C9, p. 479, 1987.

[76] J. Tulkki, T. Åberg, S. Whitfield, and B. Crasemann *Phys. Rev. A*, vol. 41, p. 181, 1990.

[77] H. Ågren and J. Müller *J. Electron Spectrosc. Rel. Phen.*, vol. 19, p. 285, 1980.

[78] H. Köppel, W. Domcke, and L. Cederbaum *Adv. Chem. Phys.*, vol. 57, p. 59, 1984.

[79] W. Domcke, L. Cederbaum, L. Köppel, and W. von Niessen *Mol. Phys.*, vol. 34, p. 1759, 1977.

[80] E. Heller *Acc. Chem. Res.*, vol. 14, p. 368, 1981.

[81] A. Cesar and H. Ågren To be published.

[82] T. Carroll, S. Anderson, L. Ungier, and T. Thomas *Phys. Rev. Lett.*, vol. 58, p. 867, 1987.

[83] T. Carroll and T. Thomas *J. Chem. Phys.*, vol. 86, p. 5221, 1987.

[84] T. Carroll and T. Thomas *J. Chem. Phys.*, vol. 89, p. 5983, 1988.

[85] T. Sharp and H. Rosentock *J. Chem. Phys.*, vol. 41, p. 3453, 19614.

[86] H. Kupka and P. Cribb *J. Chem. Phys.*, vol. 85, p. 1303, 1986.

[87] E. Doktorov, I. Malkin, and V. Manko *J. Mol. Spectrosc.*, vol. 56, p. 1, 1975.

[88] E. Doktorov, I. Malkin, and V. Manko *J. Mol. Spectrosc.*, vol. 64, p. 302, 1977.

[89] P. Malmquist UUIP 1058, University of Uppsala, 1982.

[90] W. Magnus, F. Oberhettinger, and R. Soni in *Formulas and Theorems for the Special Functions of Mathematical Physics*, Springer-Verlag, Berlin, 1966.

[91] P. Appel and J. Kampé de Fériet in *Fonctions Hypergéométriques et Hypersphériques, Polynomes d'Hermite*, Gauthier-Villars, 1926.

[92] F. Ansbacher *Z. Naturforschung*, vol. 14a, p. 889, 1959.

[93] W. Wagner *Z. Naturforschung*, vol. 14a, p. 81, 1959.

[94] P. Drallos and J. Wadehra *J. Chem. Phys.*, vol. 85, p. 6524, 1986.

[95] J. Lerme *Chem. Phys.*, vol. 145, p. 67, 1990.

[96] G. Wentzel *Z. Physik*, vol. 43, p. 521, 1927.

[97] R. Colle and S. Simonucci *Phys. Rev. A*, vol. 39, p. 6247, 1989.

[98] R. Colle and S. Simonucci *Phys. Rev. A*, vol. 42, p. 3913, 1990.

[99] G. Howat, T. Åberg, and O. Goscinski *J.Phys B: At. Mol. Phys.*, vol. 11, p. 1575, 1978.

[100] R. Manne and H. Ågren *Chem. Phys.*, vol. 93, p. 201, 1985.

[101] H. Kelly *Phys. Rev. A*, vol. 11, p. 556, 1975.

[102] R. Colle, A. Fortunelli, and S. Simonucci *Nouv. Chim.*, vol. 10, p. 355, 1988.

[103] V. Carravetta and H. Ågren *Phys. Rev. A*, vol. 35, p. 1022, 1987.

[104] W. Asaad *Nucl. Phys.*, vol. 66, p. 494, 1965.

[105] E. Burhop in *The Auger Effect and other Radiationless Transitions*, Cambridge University Press, London, 1952.

[106] H. Siegbahn, L. Asplund, and P. Kelfve *Chem. Phys. Lett.*, vol. 35, p. 330, 1975.

[107] K. Faegri and H. Kelly *Phys. Rev. A*, vol. 19, p. 1649, 1979.

[108] V. Carravetta, H. Ågren, and A. Cesar *Chem. Phys. Lett.*, vol. 148, p. 210, 1988.

[109] E. McGuire *Phys. Rev.*, vol. 175, p. 20, 1968.

[110] E. McGuire *Phys. Rev.*, vol. 185, p. 1, 1969.

[111] D. Jennison *Phys. Rev. A*, vol. 23, p. 1215, 1981.

[112] M. Higashi, E. Hiroike, and T. Nakajima *Chem. Phys.*, vol. 68, p. 377, 1982.

[113] M. Higashi, E. Hiroike, and T. Nakajima *Chem. Phys.*, vol. 85, p. 133, 1984.

[114] R. Chase, H. Kelly, and H. Köhler *Phys. Rev. A*, vol. 3, p. 1550, 1971.

[115] H. Kelly in *Atomic Inner-Shell Processes*, (B. Crasemann, ed.), Academic, New York, 1975.

[116] H. Ågren, V. Carravetta, and A. Cesar *Chem. Phys. Lett.*, vol. 139, p. 145, 1987.

[117] V. Carravetta, H. Ågren, and A. Cesar To be published.

[118] C. Liegener *Chem. Phys. Lett.*, vol. 106, p. 201, 1984.

[119] D. Nordfors, A. Nilsson, S. Svensson, N. Mårtensson, U. Gelius, and H. Ågren *J. Electron Spectrosc. Rel. Phen.*, vol. 00, p. 000, 1991.

[120] R. Arneberg, J. Müller, and R. Manne *Chem. Phys.*, vol. 64, p. 249, 1982.

[121] R. L. Martin and D. A. Shirley *J. Am. Chem. Soc.*, vol. 96, no. 17, p. 5299, 1974.

[122] L. Werme, T. Bergmark, and K. Siegbahn *Physica Scripta*, vol. 8, p. 149, 1973.

[123] P. Malmquist and B. Roos *Chem. Phys. Lett.*, vol. 155, p. 189, 1989.

[124] W. Asaad and E. Burhop *Proc. Phys. Soc. London*, vol. 72, p. 369, 1958.

[125] D. Shirley *Phys. Rev. A*, vol. 7, p. 1520, 1973.

[126] D. Jennison *Phys. Rev. A*, vol. 23, p. 1215, 1980.

[127] D. Jennison *Chem. Phys. Lett.*, vol. 69, p. 435, 1980.

[128] H. Ågren and H. Siegbahn *Chem. Phys. Lett.*, vol. 72, p. 498, 1980.

[129] V. Fock *Z. Physik*, vol. 61, p. 116, 1930.

[130] J. Almlöf, P. Bagus, B. Liu, D. MacLean, U. Wahlgren, and M. Yoshimine *MOLECULE-ALCHEMY program package, IBM Research Laboratory*, 1972. See also IBM Research Report RJ-1077 (1972).

[131] B. Levy and G. Berthier *Int. J. Quant. Chem.*, vol. 2, p. 307, 1968.

[132] R. Manne and K. Faegri *Mol. Phys.*, vol. 33, p. 53, 1977.

[133] M. Hotokka, H. Ågren, H. Aksela, and S. Aksela *Phys. Rev. A*, vol. 30, p. 1855, 1984.

[134] A. Cesar, H. Ågren, A. Brito, P. Baltzer, M. Keane, S. Svensson, L. Karlsson, P. Fournier, and M. Fournier *J. Chem. Phys.*, vol. 00, p. 000, 1990.

[135] L. Cederbaum, W. Domcke, and J. Schirmer *Phys. Rev. A*, vol. 22, p. 206, 1980.

[136] H. Ågren and H. Siegbahn *Chem. Phys. Lett.*, vol. 69, p. 424, 1980.

[137] W. von Niessen *J. Electron Spectrosc. Rel. Phen.*, vol. 51, p. 173, 1990.

[138] P. Siegbahn *J. Chem. Phys.*, vol. 75, p. 2314, 1981.

[139] M. Larsson, P. Baltzer, S. Svensson, B. Wannberg, N. Mårtensson, A. Naves de Brito, N. Correia, M. Keane, M. Carlsson-Göthe, and L. Karlsson *J.Phys B: At. Mol. Phys.*, vol. 23, p. 1175, 1990.

[140] S. Peyerimhoff, M. van Hemert, and P. Fournier *Chem. Phys.*, vol. 121, p. 351, 1988.

[141] L. Cederbaum *Theoret. Chim. Acta*, vol. 31, p. 239, 1973.

[142] C. Liegener *J. Chem. Phys.*, vol. 79, p. 2924, 1983.

[143] O. Goscinski and B. Lukman *Chem. Phys. Lett.*, vol. 7, p. 573, 1970.

[144] P. Löwdin *Phys. Rev. A*, vol. 139, p. 357, 1965.

[145] P. Löwdin *Int. J. Quant. Chem.*, vol. S4, p. 231, 1971.

[146] C. Liegener *Chem. Phys.*, vol. 76, p. 397, 1983.

[147] L. Ungier and T. Thomas *J. Chem. Phys.*, vol. 82, p. 3146, 1985.

[148] F. Larkins *J. Chem. Phys.*, vol. 86, p. 3239, 1987.

[149] M. Barber, I. Clark, and A. Hinchcliffe *Chem. Phys. Lett.*, vol. 48, p. 593, 1977.

[150] N. Lang and A. Williams *Phys. Rev. B*, vol. 20, p. 1369, 1979.

[151] E. Hartmann and R. Szargan *Chem. Phys. Lett.*, vol. 68, p. 175, 1979.

[152] B. Dunlap, P. Mills, and D. Ramaker *J. Chem. Phys.*, vol. 75, p. 300, 1981.

[153] P. Deshmukh and R. Hayes *Chem. Phys. Lett.*, vol. 88, p. 384, 1982.

[154] G. Mikhailov, G. Gutsev, and Y. Borod'ko *Chem. Phys. Lett.*, vol. 96, p. 70, 1983.

[155] G. Laramore *Phys. Rev. A*, vol. 29, p. 23, 1984.

[156] G. Gutsev *Mol. Phys.*, vol. 57, p. 161, 1986.

[157] D. Chong *Chem. Phys. Lett.*, vol. 82, p. 511, 1981.

[158] D. Sinha, S. Mukhopadhyay, M. Prasad, and D. Mukherjee *Chem. Phys. Lett.*, vol. 125, p. 213, 1986.

[159] R. Rye, T. Madey, J. Houston, and P. Holloway *J. Chem. Phys.*, vol. 96, p. 1504, 1978.

[160] R. Rye, J. Houston, D. Jennison, T. Madey, and P. Holloway *Ind. Eng. Chem. Prod. Res. Dev.*, vol. 18, p. 2, 1979.

[161] G. D. Souza, R. Platania, A. D. A. Souza, and F. Maracci *Chem. Phys.*, vol. 129, p. 491, 1989.

[162] R.R.Rye and J. Houston *J. Chem. Phys.*, vol. 75, p. 2085, 1981.

[163] C. Liegener *Chem. Phys. Lett.*, vol. 123, p. 92, 1986.

[164] J. Ortiz *J. Chem. Phys.*, vol. 83, p. 4604, 1985.

[165] H. Pulm, C. Liegener, and H. Freund *Chem. Phys. Lett.*, vol. 119, p. 344, 1985.

[166] J. Rogers Jr., H. Peebles, R. Rye, J. Houston, and J. Binkley *J. Chem. Phys.*, vol. 80, p. 4513, 1984.

[167] R. Rye, D. Jennison, and J. Houston *J. Chem. Phys.*, vol. 73, p. 4867, 1980.

[168] C. Liegener and E. Weiss *Phys. Rev. A*, vol. 41, p. 11946, 1990.

[169] R. Shaw and T. Thomas *Phys. Rev. A*, vol. 11, p. 1491, 1975.

[170] W. Moddeman Thesis, Oak Ridge National Report No.ORNL-TM-3013, 1970.

[171] F. Larkins *J. Chem. Phys.*, vol. 86, p. 3239, 1987.

[172] F. Larkins and L. Tulea *J. Physique*, vol. C9, p. 725, 1987.

[173] C. Liegener *Chem. Phys. Lett.*, vol. 151, p. 83, 1988.

[174] C. Liegener and R. Chen *J. Chem. Phys.*, vol. 88, p. 2618, 1988.

[175] C. Liegener *Phys. Stat. Sol. B*, vol. 156, p. 441, 1989.

[176] T. Økland, K. Faegri, and R. Manne *Chem. Phys. Lett.*, vol. 40, p. 185, 1976.

[177] J. Lander *Phys. Rev.*, vol. 91, p. 1382, 1953.

[178] F. Hutson and D. Ramaker *J. Chem. Phys.*, vol. 87, p. 6824, 1987.

[179] C. Liegener *Phys. Rev. B*, vol. 41, p. 7185, 1990.

[180] S. Fraga and B. Ransil *J. Chem. Phys.*, vol. 35, p. 669, 1961.

[181] E. Thulstrup and A. Andersen *J.Phys B: At. Mol. Phys.*, vol. 8, p. 965, 1975.

[182] K. Siegbahn, C. Nordling, G. Johansson, J. Hedman, P. F. Hedén, K. Hamrin, U. Gelius, T. Bergmark, L. O. Werme, R. Manne, and Y.Baer, "Esca applied to free molecules," 1969.

[183] D.Stalherm, B.Cleff, H.Hillig, and W.Mehlhorn *Z.Naturforsch.*, vol. 24a, p. 1728, 1969.

[184] T. Carlson, W. Moddeman, B. Pullen, and M. Krause *Chem. Phys. Lett.*, vol. 5, p. 390, 1970.

[185] W. Moddeman, T. Carlson, M. Krause, B. Pullen, W. Bull, and G. Schweitzer *J. Chem. Phys.*, vol. 55, p. 2317, 1971.

[186] N. Stolterfoht *Phys. Lett. A*, vol. 41, p. 400, 1972.

[187] W. Eberhardt, J. Stohr, J. Feldhaus, E. Plummer, and F. Sette *Phys. Rev. Lett.*, vol. 51, p. 2370, 1983.

[188] L. Ungier and T. Thomas *Chem. Phys. Lett.*, vol. 96, p. 247, 1983.

[189] C. Liegener *J.Phys B: At. Mol. Phys.*, vol. 16, p. 4281, 1983.

[190] H. Sambe and D. Ramaker *Chem. Phys. Lett.*, vol. 128, p. 113, 1986.

[191] I. Hillier and J. Kendrick *Mol. Phys.*, vol. 31, p. 849, 1976.

[192] R. Eade, M. Robb, G. Theodorakopoulos, and I. Csizmadia *Chem. Phys. Lett.*, vol. 52, p. 526, 1977.

[193] N. Kosugi, T. Ohta, and H. Kuroda *Chem. Phys.*, vol. 50, p. 373, 1980.

[194] S. Polezzo and P. Fantucci *Gazz. Chim. Ital.*, vol. 110, p. 557, 1980.

[195] P. Weightman, T. Thomas, and D. Jennison *J. Chem. Phys.*, vol. 78, p. 1652, 1983.

[196] C. Liegener *Phys. Rev. A*, vol. 28, p. 256, 1983.

[197] O. Kvalheim *Chem. Phys. Lett.*, vol. 86, p. 159, 1982.

[198] C. Liegener *Chem. Phys.*, vol. 92, p. 97, 1985.

[199] E. Ohrendorf, H. Köppel, L. Cederbaum, F. Tarantelli, and A. Sgamelotti *J. Chem. Phys.*, vol. 91, p. 1734, 1989.

[200] F. Tarantelli, A. Sgamelotti, L. Cederbaum, and J. Schirmer *J. Chem. Phys.*, vol. 86, p. 2201, 1987.

[201] L. Cederbaum, F. Tarantelli, A. Sgamelotti, and J. Schirmer *J. Chem. Phys.*, vol. 85, p. 6513, 1986.

[202] L. Cederbaum, F. Tarantelli, A. Sgamellotti, and J. Schirmer *J. Chem. Phys.*, vol. 86, p. 2168, 1987.

[203] O. Kvalheim *Chem. Phys. Lett.*, vol. 98, p. 457, 1983.

[204] H. Aksela, S. Aksela, M. Hotokka, and M. Jaentti *Phys. Rev. A*, vol. 28, p. 287, 1983.

[205] P. Fournier, M. Mousselmal, S. Peyerimhoff, A. Banichevich, M. Adam, and T. Morgan *Phys. Rev. A*, vol. 36, p. 2594, 1987.

[206] O. Kvalheim and K. Faegri *Chem. Phys. Lett.*, vol. 67, p. 127, 1979.

[207] F. Tarantelli, J. Schirmer, A. Sgamelotti, and L. Cederbaum *Chem. Phys. Lett.*, vol. 122, p. 169, 1985.

[208] J. Connor, I. Hillier, J. Kendrick, M. Barber, and A. Barrie *J. Chem. Phys.*, vol. 64, p. 3325, 1976.

[209] E. Ohrendorf, F. Tarantelli, and L. Cederbaum *J. Chem. Phys.*, vol. 92, p. 2984, 1990.

[210] F. Tarantelli, A. Sgamelotti, and L. Cederbaum *J. Chem. Phys.*, vol. 94, p. 523, 1991.

[211] F. Tarantelli, A. Tarantelli, A. Sgamelotti, J. Schirmer, and L. Cederbaum *Chem. Phys. Lett.*, vol. 177, p. 577, 1985.

[212] N. Beebe, E. Thulstrup, and A. Andersen *J. Chem. Phys.*, vol. 64, p. 2080, 1976.

[213] C. Liegener, A. Bakhshi, R. Chen, and J. Ladik *J. Chem. Phys.*, vol. 86, p. 6039, 1987.

[214] N. Correia, A. Naves de Brito, M. Keane, L. Karlsson, S. Svensson, C. Liegener, A. Cesar, and H. Ågren *J. Chem. Phys.*, vol. 00, p. 000, 1991.

[215] J. Kelber, D. Jennison, and R. Rye *J. Chem. Phys.*, vol. 75, p. 652, 1981.

[216] D. Jennison, J. Kelber, and R. Rye *Chem. Phys. Lett.*, vol. 72, p. 604, 1981.

[217] M. Yousif, D. Ramaker, and H. Sambe *Chem. Phys. Lett.*, vol. 101, p. 472, 1983.

[218] W. Eberhardt, C. Chen, W. Ford, E. Plummer, and H. Moser in *DIET2*, (W. Brenig and D. Menzel, eds.), Springer, Berlin, 1985.

[219] H. Freund and C. Liegener *Chem. Phys. Lett.*, vol. 134, p. 70, 1987.

[220] K. Faegri *Chem. Phys. Lett.*, vol. 46, p. 541, 1977.

[221] C. Campbell, J. Rogers Jr., R. Hance, and J. White *Chem. Phys. Lett.*, vol. 69, p. 430, 1980.

# On Linear Algebra, the Least Square Method, and the Search for Linear Relations by Regression Analysis in Quantum Chemistry and Other Sciences

By Per-Olov Löwdin*
Quantum Theory Project, Departments of Chemistry and Physics
University of Florida, Gainesville, Fl 32611.
*Professor Emeritus, Uppsala University, Uppsala, Sweden.

1. Introduction
The abstract Hilbert space and its realizations
Some useful notations
Some properties of the abstract Hilbert space
Properties of linear operators
Operator and matrix inequalities
The main problems in quantum theory

2. The Method of Least Squares
The importance of linear relations
The method of least square and the projector on a subspace
The geometrical structure of a set of elements based on the concept of the norm
Partitioning technique

3. Some Properties of Linear Operators and their Matrix Representations
Some properties of the matrix representation of a linear operator
The characteristic polynomial for a matrix
On the measure of the deviations of points from hyperplanes based on the concept of the norm

4. The Method of Generalized Least Squares
A generalization of the least square method
An alternative formulation of the generalized least square method; the Kalman construction
Some properties of inner projections

5. The Search for Approximate Linear Dependencies in a Finite Basis Set
Orthonormalization procedures: symmetric and canonical orthonormalization
Some theorems about the minors

6. On the Search for Linear Relations by Means of Ordinary and Canonical Regression Analysis
The principles of regression analysis
A "democratic" regression analysis
The canonical regression analysis
A numerical example taken from econometrics
System analysis and the evaluation of errors

ADVANCES IN QUANTUM CHEMISTRY
VOLUME 23

Copyright © 1992 By Academic Press, Inc.
All rights of reproduction in any form reserved.

7. Appendices
A. The inversion of a matrix by partitioning technique
B. Calculation of the characteristic polynomial
C. Rough estimates of the eigenvalues of a matrix
D. Evaluation of the eigenvalues by means of partitioning technique

References

# 1. Introduction

Linear algebra is one of the most important mathematical tools not only in the quantum mechanics but also in many other parts of physics, chemistry, statistics, econometrics, etc. where one deals with a large number of data. A characteristic feature of linear algebra is that it is basically the same in all these fields, and that methods developed in one area may often be applied in other areas. The purpose of this paper is to briefly review some of the basic features of the linear algebra used in the quantum theory of matter, and which to a certain extent may be applied also in other fields.

The abstract Hilbert space and its realizations. -The quantum theory of matter as developed by von Neumann [1] is based on the concept of the existence of an *abstract Hilbert space* , which is an infinite linear space $\mathfrak{H} = \{f\}$ having a binary product $\langle f|g\rangle$ and a norm $\|f\| = \langle f|f\rangle^{1/2}$ with the properties:

$$\langle f|g_1+g_2\rangle = \langle f|g_1\rangle + \langle f|g_2\rangle, \tag{1.1}$$

$$\langle f|g.\alpha\rangle = \langle f|g\rangle.\alpha, \tag{1.2}$$

$$\langle g|f\rangle = \langle f|g\rangle^*, \tag{1.3}$$

$$\langle f|f\rangle \geq 0, \text{ and } =0, \text{ if and only if } f = 0. \tag{1.4}$$

The first two relations imply that the binary product is linear in the second position, the third relation means that it is hermitean symmetric - which also indicates that it is "antilinear" in the first position - whereas the fourth relation shows that the binary product is positive definite. In mathematics, one is instead using the notation $(g,f) = \langle f|g\rangle$, where now the first position is linear and the second antilinear. It is further assumed that $\mathfrak{H} = \{f\}$ contains all its *limit points in the norm* and that the space is separable. The separability axiom implies that there exists an enumerable sequence $\mathfrak{H}'=\{g_k\}$ for $k = 1,2,3,.....$ which is everywhere dense in H, and - by means of Schmidt's successive orthonormal-ization procedure - one may then construct an infinite sequence of *orthonormal* elements $\varphi = \{\varphi_k\}$ which is *complete* in $\mathfrak{H}$. We will return to these concepts below.

A linear operator T is defined in the domain D(T) of the abstract Hilbert space $\mathfrak{H}= \{f\}$, if the element f as well as its image Tf both belong to H. The *adjoint* $T^\dagger$ to the operator T is further defined through the relation

$$\langle T^{\dagger} f | g \rangle = \langle f | T g \rangle . \qquad (1.5)$$

There are two important realizations of the abstract Hilbert space: the $L^2$ Hilbert space with the elements $f = f(X)$ and the binary product

$$\langle f | g \rangle = \int f^*(X)\, g(X)\, dX, \qquad (1.6)$$

where the integral is a Lesbegue integral over all the variables X involved, and the sequential Hilbert space $\mathfrak{H}_0$ consisting of all the infinite column vectors $\mathbf{c} = \{c_k\}$ of complex numbers $c_k$ having a convergent sum

$$||\mathbf{c}||^2 = \langle \mathbf{c} | \mathbf{c} \rangle = \sum_k |c_k|^2 < \infty, \qquad (1.7)$$

and it is evident that the proper treatment of the Hilbert spaces involves a great deal of convergence considerations. This Hilbert space has the binary product

$$\langle \mathbf{c} | \mathbf{d} \rangle = \sum_k c_k^* d_k. \qquad (1.8)$$

Some useful notations. - In the following we will represent rectangular matrices - inclusive quadratic matrices and column and row vectors - by bold-face symbols **A**. If **A** and **B** are two rectangular matrices of order m x p and p x n, then their product **C** = **AB** is a rectangular matrix of order m x n defined by the relation

$$C_{kl} = (\mathbf{AB})_{kl} = \sum_{\alpha} A_{k\alpha} B_{\alpha l}, \qquad (1.9)$$

i.e. one multiplies the rows of the first matrix in order by the columns of the second matrix. Following Dirac [2], we will further consider the abstract binary product or bracket $\langle f | g \rangle$ as the product of a bra vector $\langle f |$ and a ket-vector $| g \rangle$ and introduce the ket-bra operator $K = |g\rangle\langle f|$ through the relation $Kx = g\langle f | x \rangle$:

$$K = |g\rangle\langle f| \qquad \leftrightarrow \qquad Kx = g\langle f | x \rangle. \qquad (1.10)$$

The definition implies that one has $|g\rangle \equiv g$, whereas $\langle f|$ should be interpreted as a linear functional, which maps the element x into the number $\langle f | x \rangle$. One shows immediately that $K^{\dagger} = |f\rangle\langle g|$, $K^2 = \langle f | g \rangle K$, and that K has only one non-vanishing eigenvalue $\lambda = \langle f | g \rangle$, which apparently has the multiplicity one, since the associated eigenfunction g is non-degenerate. An operator of the form

$$P = |x\rangle\langle x | x \rangle^{-1} \langle x|, \qquad (1.11)$$

has the property $P^2 = P$ and is said to be a *projector* associated with the element x; it is apparently also self-adjoint, so that $P^{\dagger} = P$.

Some properties of the abstract Hilbert space. -Let us now consider the orthonormal set $\varphi = \{\varphi_k\}$, which was derived from the enumerable set $\mathfrak{H}' = \{f_k\}$ by the Schmidt procedure. The orthonormality property may be expressed in the form

$$\langle\varphi_k|\varphi_l\rangle = \delta_{kl}. \tag{1.12}$$

It is further easily shown that there is no other element $h \neq 0$ in $\mathfrak{H}$, which is orthogonal to the set $\varphi = \{\varphi_k\}$, i.e. that $\varphi = \{\varphi_k\}$ is a *complete* orthonormal set, and that the completeness is equivalent with the relation

$$1 = \Sigma_k\, |\varphi_k\rangle\langle\varphi_k|, \tag{1.13}$$

which is a *resolution of the identity* in terms of the elementary projectors $P_{kk} = |\varphi_k\rangle\langle\varphi_k|$ ; we note that this sum is convergent in the operator sense. Using fat symbols, one may now condense the orthonormality relation (1.12) and the completeness relation (1.13) into the relations

$$\langle\varphi|\varphi\rangle = \mathbf{1}, \qquad 1 = |\varphi\rangle\langle\varphi|, \tag{1.14}$$

where $\mathbf{1}$ is the unit matrix of infinite order and 1 represents the identity operator. By using the identity operator, one obtains directly for any element f of $\mathfrak{H}$:

$$f = 1.f = |\varphi\rangle\langle\varphi|.\, f = \varphi\, \langle\varphi|\, f\rangle = \Sigma_k\, \varphi_k\langle\varphi_k|\, f\rangle = \Sigma_k\, \varphi_k\, c_k, \tag{1.15}$$

where the infinite sum in the right-hand member is convergent in the norm. This is the *expansion theorem* for the element f in terms of the orthonormal basis $\varphi = \{\varphi_k\}$ and with the Fourier coefficients $c_k = \langle\varphi_k|\, f\rangle$, which we will now arrange in an infinite column vector $\mathbf{c} = \{c_k\}$. One has now the relations

$$f = \varphi\, \mathbf{c} = \Sigma_k\, \varphi_k\, c_k, \qquad f \;\leftrightarrow\; \mathbf{c}\,, \tag{1.16}$$

which means that every element f in the abstract Hilbert space $\mathfrak{H}$ may be represented by a vector $\mathbf{c}$ in the sequential Hilbert space $\mathfrak{H}_0$. We note that, since the basis $\varphi = \{\varphi_k\}$ is defined as a *row vector* , the vector $\mathbf{c}$ will automatically become a *column vector* , which is in agreement with the standard notation.

If $\mathbf{A} = \{A_{kl}\}$ is an arbitrary rectangular matrix - or vector - one defines the adjoint matrix $\mathbf{A}^\dagger$ by the relation $\mathbf{A}^\dagger = \{A_{lk}^*\}$, i.e. one interchanges the rows and columns and takes the complex conjugate. For instance, for a ket-vector $\langle f|$ one gets immediately

$$\langle f| = \langle\varphi\, \mathbf{c}| = \mathbf{c}^\dagger\, \langle\varphi\,| = \tag{1.17}$$

where - in the right-hand member - one multiplies the row vector $\mathbf{c}^\dagger$ by the column vector $\langle\varphi|$ . If one has a second element $g = \varphi\,\mathbf{d}$, one gets hence for the binary product:

$$\langle f|g\rangle = \langle\varphi\,\mathbf{c}|\varphi\,\mathbf{d}\rangle = \mathbf{c}^\dagger\langle\varphi|\varphi\rangle\mathbf{d} = \mathbf{c}^\dagger\,\mathbf{d} = \Sigma_k\, c_k^*\, d_k, \qquad (1.18)$$

where the infinite sum is absolutely convergent. We note that the fat-symbol formalism is a powerful tool for symbolic manipulations, which may later be verified in the standard way. A survey of the various types of convergence used in this section is given elsewhere [3].

Properties of linear operators. - Let us consider a linear operator T. For the sake of simplicity, we will assume that all the basis functions $\varphi_k$ belong to the domain of T, in which case one has the expansion theorem:

$$T\,\varphi_l = \Sigma_k\,\varphi_k\langle\varphi_k|\,T\,\varphi_l\rangle = \Sigma_k\,\varphi_k\,T_{kl}, \qquad (1.19)$$

where the expansion coefficients $T_{kl}$ form a *matrix representation* $\mathbf{T} = \{T_{kl}\}$ of the operator T. We note that, in physics, one is often using a "dummy bar" in the binary product to define the matrix elements, and that one writes $T_{kl} = \langle\varphi_k|\,T\varphi_l\rangle = \langle\varphi_k|\,T\,|\varphi_l\rangle$. One may write relation (1.19) in the more condensed form

$$T\,\varphi = 1.T\varphi = |\varphi\rangle\langle\varphi|T\varphi = \varphi\langle\varphi|T|\varphi\rangle = \varphi\,T, \qquad (1.20)$$

where $\mathbf{T} = \langle\varphi|T|\varphi\rangle$ . If $f = \varphi\,\mathbf{c}$ is an element in the domain of T, one gets further

$$T\,f = T\,\varphi\,\mathbf{c} = \varphi\,T\,\mathbf{c} = \varphi\;\mathbf{c}', \qquad \mathbf{c}' = T\,\mathbf{c}, \qquad (1.21)$$

where the last relation is of conventional character. An important quantity associated with the matrix T is the *trace* of the operator T defined through the relation

$$Tr\,T = Tr\,\mathbf{T} = \Sigma_k\;T_{kk}, \qquad (1.22)$$

i.e. the sum of the diagonal elements, the properties of which will be further discussed below. For the operator itself, one obtains

$$T = 1.T.1 = |\varphi\rangle\langle\varphi|T|\varphi\rangle\langle\varphi| = |\varphi\rangle\mathbf{T}\langle\varphi| = \Sigma_{kl}\,|\varphi_k\rangle T_{kl}\langle\varphi_l| = \Sigma_{kl}\,P_{lk}\,T_{kl}\quad, \qquad (1.23)$$

where the operators $P_{lk} = |\varphi_k\rangle\langle\varphi_l|$ apparently span the operator space $\{T\}$. The operators $\{P_{lk}\}$ form an operator algebra with the multiplication rule

$$P_{kl}\,P_{mn} = \delta_{kn}\,P_{ml}, \qquad (1.24)$$

which indicates that the diagonal elements $P_{kk}$ are *idempotent* (or projectors), whereas the non-diagonal elements $P_{kl}$ are *nil-potent* of order 2. In the operator space it is convenient to introduce the Hilbert-Schmidt binary product:

$$\{T_1|T_2\} = \mathrm{Tr}\, T_1^{\dagger}.T_2 = \\ = \Sigma_{kl} \langle\varphi_k|T_1^{\dagger}|\varphi_l\rangle\langle\varphi_l|T_2|\varphi_k\rangle = \Sigma_{kl} \langle\varphi_l|T_1|\varphi_k\rangle^*\langle\varphi_l|T_2|\varphi_k\rangle, \quad (1.25)$$

and for the norm $\|T\|$ one has then

$$\|T\|^2 = \Sigma_{kl} \ |T_{kl}|^2. \quad (1.26)$$

The Hilbert-Schmidt operator space $\{T\}$ is another realization of the abstract Hilbert space, which is of great importance in the general quantum theory [1]. We note that the operators $P_{kl}$ form an orthonormal basis for this space, which is also complete.

Operator and matrix inequalities. - Another mathematical tool used in the quantum theory of matter is operator inequalitites. If A and B are two self-adjoint operators, one says that $A > B$, if $\langle f|Af\rangle > \langle f|Bf\rangle$ for all f in the common domain of A and B. Putting $f = Tg$, one gets further $\langle g|T^{\dagger}AT|g\rangle > \langle g|T^{\dagger}BT|g\rangle$, i.e.

$$A > B, \quad \rightarrow \quad T^{\dagger}AT > T^{\dagger}BT. \quad (1.27)$$

An operator A is said to be *positive definite*, if $A > 0$. Putting $T = A^{-1}$, one gets immediately $A^{-1} > 0$. Similarly if $A > 1$, one obtains $A^{-1} < 1$. On the other hand, if $A < 1$, one obtains by putting $T = A^{1/2}$ that $A > A^2$. We will now study some consequences of these simple rules.

If $A > B > 0$, one has $B^{-1/2}AB^{-1/2} > 1$, and $B^{1/2}A^{-1}B^{1/2} < 1$, and further $A^{-1} < B^{-1}$. In the same way, one has $1 > A^{-1/2}BA^{-1/2} > (A^{-1/2}BA^{-1/2})^2 = A^{-1/2}BA^{-1}BA^{-1/2}$, and combining the second and fourth member, one gets $B > BA^{-1}B$, which relation is true even if $B \geq 0$. Hence one has

$$A > B > 0, \quad \rightarrow \quad B^{-1} > A^{-1} > 0, \quad (1.28a)$$
$$A > B \geq 0, \quad \rightarrow \quad B > BA^{-1}B, \quad (1.28b)$$

It is evident that the second relation follows from the first whenever $B > 0$.

A special type of inequalities are associated with the self-adjoint projectors P, which satisfy the relations $P^2 = P$ and $P^{\dagger}=P$. Since $P = P^{\dagger}P$, one gets immediately $P \geq 0$. Since further the operator $Q = 1 - P$ is another self-adjoint projector, one has $Q \geq 0$, i.e. $P \leq 1$, and finally

$$0 \leq P \leq 1, \quad 0 \leq T^{\dagger} P\, T \leq T^{\dagger}\, T. \quad (1.29)$$

If $A > 0$, and one chooses $T = A^{1/2}$, one gets immediately

$$0 \leq A^{1/2}PA^{1/2} \leq A, \qquad (1.30)$$

where the operator $A' = A^{1/2}PA^{1/2}$ is known as the *inner projection* of A with respect to P, and it is interesting since it provides a *lower bound* to the operator A; for more details the reader is referred elsewhere [4].

We note the fundamental theorem that, if A and B are two self-adjoint operators which are bounded from below, so that $A > B > \alpha.1$, and the domain of A belongs to the domain of B, then the eigenvalues $a_k$ of A are larger than the eigenvalues $b_k$ of B in order from below, so that $a_k \geq b_k$ ; [5].

In addition to the operator inequalities, one has also *matrix inequalities* of a similar type. If **A** and **B** are two self-adjoint matrices, one says that **A** > **B**, if $\mathbf{c}^{\dagger}\mathbf{A}\mathbf{c} > \mathbf{c}^{\dagger}\mathbf{B}\mathbf{c}$ for all column vectors **c**. One derives then easily the matrix analogues of the inequalities (1.26-30).

The main problems in quantum theory. - In pure quantum mechanics, one of the main problems in studying a physical system with a Hamiltonian operator H is to solve the time-dependent Schrödinger equation

$$H\Psi = - (h/2\pi i)\, \partial\Psi/\partial t, \qquad (1.31)$$

subject to the initial condition $\Psi = \Psi(0)$ for $t = t_o$, where $\Psi = \Psi(t)$ is the wave function describing the physical situation of the system at time t. As a rule, the Hamiltonian H is self-adjoint and bounded from below. The stationary states are obtained by solving the time-independent Schrödinger equation

$$H\,\Psi = E\,\Psi, \qquad (1.32)$$

subject to the boundary condition that $\Psi$ should belong to the $L^2$ Hilbert space or be the derivative with respect to E of a function $\Phi(E)$ in this space. Both problem are most conveniently handled in the Hilbert space formalism using on a complete orthonormal basis $\varphi = \{\varphi_k\}$, and the relation (1.32) may be solved by expressing the eigenfunction $\Psi$ in the form $\Psi = \varphi\,\mathbf{c}$, and by solving a system of linear equations

$$\mathbf{H}\,\mathbf{c} = E\,\mathbf{c}, \qquad (1.33)$$

for the eigenvalues of the Hamiltonian matrix $\mathbf{H} = \langle\varphi|H|\varphi\rangle$. In general quantum theory, one studies instead the behaviour of the system operator $\Gamma = \Gamma(t)$, which is self-adjoint and positive definite and satisfies the Liouville equation

$$- (h/2\pi i)\, \partial\Gamma/\partial t = H\,\Gamma - \Gamma\,H. \qquad (1.34)$$

We note that all possible system operators $\{\Gamma\}$ form a *convex set* , and that the limit points of this set correspond to projectors of the form $\Gamma = |\Psi><\Psi|\Psi>^{-1}<\Psi|$, where $\Psi$ is a wave function in pure quantum mechanics. We note that the problems in general quantum theory are conveniently formulated in the Hilbert-Schmidt space.

A basic assumption in quantum theory is that every physical observable $\mathcal{F}$ corresponds to a linear self-adjoint operator F, the *expectation value* $<F>$ of which is given by the formula

$$<F> = \mathrm{Tr}\, F\, \Gamma\,, \tag{1.35}$$

where $\Gamma$ is the system operator for the physical situation under consideration. For a pure state with the wave function $\Psi$, one gets in particular the standard expression

$$<F> = \mathrm{Tr}\, F\, |\Psi><\Psi|\Psi>^{-1}<\Psi| = <\Psi|\, F\, |\Psi>/<\Psi|\Psi>\,. \tag{1.36}$$

The *width* $\Delta F$ of the operator F is further defined by the relation

$$(\Delta F)^2 = <(\, F^2 - <F>)^2> = <F^2> - \ <F>^2 \geq 0, \tag{1.37}$$

and only when $\Delta F = 0$ does one have a *sharp* expectation value without dispersion. If F and G are two self-adjoint operators, it follows from the properties of quadratic forms that one has the *general uncertainty relations:*

$$\Delta F.\Delta G \ \geq |<FG - GF>|/2. \tag{1.38}$$

We note that the physical results of quantum theory are usually given a *probability interpretation* . The connection between *theory and experiment* is finally given by the assumption that the quantum mechanical expectation value $<F>$ should correspond to the average value $\bar{\mathcal{F}}$ of a a very large number n of *measurements* $\mathcal{F}_i$ over an ensemble of physical systems prepared in exactly the same way:

$$\bar{\mathcal{F}} = (1/n) \sum_{i=1}^{i=n} \mathcal{F}_i, \tag{1.39}$$

In addition to the average or mean value, one studies also the *mean quadratic deviation* $\Delta\mathcal{F}$ which is given by the relation

$$(\Delta\mathcal{F})^2 = (1/n) \sum_i \ (\mathcal{F}_i - \bar{\mathcal{F}})^2 = \bar{\mathcal{F}^2} - (\bar{\mathcal{F}})^2 \ \geq 0\ . \tag{1.40}$$

The experimental quantity $\Delta\mathcal{F}$ corresponds to the theoretical width $\Delta F$, and we note that the necessary and sufficient condition for a *sharp measurement* is $\Delta\mathcal{F} = \Delta F = 0$. The collection and handling of the experimental data $\mathcal{F}_i$ and the study of $\bar{\mathcal{F}}$ and $\Delta\mathcal{F}$ belongs to the field of *statistics*, and in a later section we will return to the problem of the proper treament of large numbers of experimental quantitites not only in physics but also in other sciences.

In concluding this section, we note that even if the problems in the quantum theory of matter are well-fomulated in the abstract Hilbert space, there are obviously great difficulties connected with practical applications due to the fact that one can only use *finite* basis sets, and further that all numbers occurring in the computations have to be truncated to a *finite* number of figures. From the computational point of view, many of the most difficult problems in quantum theory are part of the field of *applied mathematics* in general, and they are then the same as many problems in other sciences. In the following we will try to review how these problems in applied quantum theory are handled by means of the tool of elementary linear algebra.

## 2. The Method of Least Squares

The importance of linear relations. - In many quantum-mechanical calculations, one starts from a set of n linearly independent functions $\mathbf{f} = \{f_1, f_2, f_3, ....f_p\}$ which span a subspace $\mathcal{F}$ of order p with a positive definite binary porduct $\langle f|g\rangle$ satisfying the relations (1.1-4). This subspace may be imbedded in a linar space of higher order or in an infinite Hilbert space $\mathcal{H}$. The basis functions are usually not orthonormal, and they have a *metric matrix* $\Delta = \langle \mathbf{f} \mid \mathbf{f}\rangle$ with the elements $\Delta_{kl} = \langle f_k| f_l\rangle = \langle f_l| f_k\rangle^*$, so that $\Delta$ is positive definite and hermitean:

$$\Delta = \langle \mathbf{f} \mid \mathbf{f}\rangle > \mathbf{0}, \qquad \Delta^\dagger = \Delta . \tag{2.1}$$

The reason for the name "metric matrix" will be explained below. There are two problems related to the *search for linear relations*, which are of fundamental importance in this connection:

1) The expansion of an arbitrary element x - usually not inside the space $\mathcal{F}$ - in terms of the basis $\mathbf{f} = \{f_k\}$ in the best possible way.

2) The search for *approximate linear dependencies* in the basis set $\mathbf{f} = \{f_k\}$ which may influence any secular equation of the type $|\langle \mathbf{f} |H - z.1| \mathbf{f}\rangle| = 0$, so that it becomes satisfied almost identically for all values of the variable z.

In order to attack the first problem, we will first consider two elements x and y situated inside the space $\mathcal{F}$, so that $x = \mathbf{fc}$ and $y = \mathbf{fd}$, respectively. Multiplying

these relations to the left by $\langle \mathbf{f}|$, one obtains $\langle \mathbf{f}|x\rangle = \langle \mathbf{f} \mid \mathbf{f}\rangle \mathbf{c}$ and $\langle \mathbf{f}|y\rangle = \langle \mathbf{f} \mid \mathbf{f}\rangle \mathbf{d}$, i.e.

$$\mathbf{c} = \Delta^{-1}\langle \mathbf{f}\,|x\rangle, \quad \mathbf{d} = \Delta^{-1}\langle \mathbf{f}\,|y\rangle, \tag{2.2}$$

which show that one has a unique isomorphism $x \leftrightarrow \mathbf{c}$ and $y \leftrightarrow \mathbf{d}$ between the elements x and y and the column vectors c and d. For the binary product, one obtains directly $\langle x|y\rangle = \langle \mathbf{fc}|\mathbf{fd}\rangle = \mathbf{c}^\dagger\langle \mathbf{f}|\mathbf{f}\rangle\mathbf{d} = \mathbf{c}^\dagger\Delta\,\mathbf{d}$, i.e.

$$\langle x|y\rangle = \mathbf{c}^\dagger\Delta\,\mathbf{d}, \qquad ||x||^2 = \langle x|x\rangle = \mathbf{c}^\dagger\Delta\,\mathbf{c} = \Sigma_{kl}\, c_k^*\Delta_{kl}c_l\,, \tag{2.3}$$

where the last relation for the square of the length of x shows that the elements $\Delta_{kl}$ form a *metric matrix* of the space - in analogy with the concept defined in the general theory of relativity. The vectors c and d defined by (2.2) are sometimes referred as the *contravariant* representations of the elements x and y.

In addition to the basis f, one may also introduce the *reciprocal basis* $\mathbf{f}_r$, defined by the relation $\mathbf{f}_r = \mathbf{f}\,\Delta^{-1}$. Since one has the relation $\langle \mathbf{f}|\mathbf{f}_r\rangle = 1$, one says that the two sets f and $\mathbf{f}_r$ are *bi-orthonormal*. For the metric matrix of the reciprocal basis, one obtains directly $\langle \mathbf{f}_r|\mathbf{f}_r\rangle = \langle \mathbf{f}\Delta^{-1}|\mathbf{f}\Delta^{-1}\rangle = \Delta^{-1}\langle \mathbf{f}|\mathbf{f}\rangle\,\Delta^{-1} = \Delta^{-1}$. Expanding the elements x and y in terms of the reciprocal basis, so that $x = \mathbf{f}_r\,\mathbf{c}_r$ and $y = \mathbf{f}_r\,\mathbf{d}_r$, one obtains $\mathbf{c}_r = \langle \mathbf{f}|x\rangle$ and $\mathbf{d}_r = \langle \mathbf{f}|y\rangle$, where the vectors $\mathbf{c}_r$ and $\mathbf{d}_r$ are often referred as the *covariant representations* of the elements x and y. One has obviously $\mathbf{c} = \Delta^{-1}\mathbf{c}_r$ and $\mathbf{d} = \Delta^{-1}\mathbf{d}_r$, as well as the relations $\langle x|y\rangle = \mathbf{c}^\dagger\mathbf{d}_r = \mathbf{c}_r{}^\dagger\mathbf{d}$. We note that these ideas are of fundamental importance not only in the theory of relativity but also in solid-state physics, where one uses the concepts of the lattice and its reciprocal lattice.

The method of least square and the projector on a subspace. - We will now return to the first problem in the case when the element x is not situated in the space $\mathcal{F}$, and consider the remainder

$$\mathbf{r} = x - \mathbf{f}\,\mathbf{a}, \tag{2.4}$$

for all possible column vectors a. In the *method of least squares* originally developed by Gauss, one tries to choose the vector a so that one minimizes the norm $||\,\mathbf{r}\,||$ of the remainder. In order to proceed, one observes that the column vector $\mathbf{c} = \Delta^{-1}\langle \mathbf{f}\,|x\rangle$ defined by (2.2) exists even if x is not situated inside the subspace $\mathcal{F}$, and that one has the relations $\langle \mathbf{f}\,|x\rangle = \Delta\,\mathbf{c}$ and $\langle x|\,\mathbf{f}\rangle = \mathbf{c}^\dagger\,\Delta$. For the norm $||\,\mathbf{r}||$, one obtains

$$||\,\mathbf{r}\,||^2 = \langle x - \mathbf{f}\,\mathbf{a} \mid x - \mathbf{f}\,\mathbf{a}\rangle = \langle x|x\rangle - \langle x|\,\mathbf{f}\,\mathbf{a}\rangle - \langle \mathbf{f}\,\mathbf{a}|x\rangle + \langle \mathbf{f}\,\mathbf{a}|\,\mathbf{f}\,\mathbf{a}\rangle =$$

$$= \langle x|x\rangle - \langle x|\,\mathbf{f}\rangle\mathbf{a} - \mathbf{a}^\dagger\langle \mathbf{f}\,|x\rangle + \mathbf{a}^\dagger\langle \mathbf{f}\mid\mathbf{f}\rangle\mathbf{a} = \langle x|x\rangle - \mathbf{c}^\dagger\,\Delta\,\mathbf{a} - \mathbf{a}^\dagger\Delta\,\mathbf{c} + \mathbf{a}^\dagger\,\Delta\,\mathbf{a}$$

$$= \langle x|x\rangle - \mathbf{c}^{\dagger}\,\Delta\,\mathbf{c} + (\mathbf{a}-\mathbf{c})^{\dagger}\Delta\,(\mathbf{a}-\mathbf{c}), \qquad (2.5)$$

where the last term is always positive and zero, if and only if $\mathbf{a} = \mathbf{c} = \Delta^{-1}\langle \mathbf{f}|x\rangle$. Hence one obtains

$$\| r \|^2_{min} = \langle x|x\rangle - \mathbf{c}^{\dagger}\,\Delta\,\mathbf{c} \geq 0, \qquad (2.6)$$

which relation reduces to Bessel's inequality for an orthonormal basis. For the component of x in the subspace $\mathcal{F}$, one gets particularly for $\mathbf{a} = \mathbf{c}$:

$$x_f = \mathbf{f}\,\mathbf{c} = \mathbf{f}\,\Delta^{-1}\langle \mathbf{f}|x\rangle = |\,\mathbf{f}\rangle\,\Delta^{-1}\langle \mathbf{f}|\;x = P_f\,x, \qquad (2.7)$$

where

$$P_f = |\,\mathbf{f}\rangle\,\Delta^{-1}\langle \mathbf{f}\,| \qquad (2.8)$$

satisfies the relations

$$P_f^{\,2} = P_f\,, \qquad P_f^{\,\dagger} = P_f\,, \qquad \mathrm{Tr}\,P_f = p, \qquad (2.9)$$

which means that $P_f$ is a self-adjoint projector of order p, which projects the element x on the subspace $\mathcal{F}$. For the remainder $r = x - x_f = (1-P_f)x$, one obtains directly

$$\langle r|x_f\rangle = \langle (1-P_f)x|P_f\,x\rangle = \langle x|\,(1-P_f)P_f\,|x\rangle = 0, \qquad (2.10)$$

which means that the remainder r is automatically *orthogonal* to the component $x_f$. More generally the remainder r is orthogonal to the entire subspace $\mathcal{F}$, since one has $\langle r|\,\mathbf{f}\rangle = \langle (1-P_f)x|\,\mathbf{f}\rangle = \langle x|\,(1-P_f)\mathbf{f}\rangle = \mathbf{0}$, since $P_f\,\mathbf{f} = \mathbf{f}$, and we note finally that the projector $P_f$ is invariant under non-singular linear transformations $\mathbf{f}' = \mathbf{f}\,\alpha$ of the basis **f**.

Next, we will consider a set $\mathbf{x} = \{x_1, x_2, x_3, \ldots x_q\}$ of q linearly independent elements outside the subspace $\mathcal{F}$ and study the decomposition

$$\mathbf{r} = \mathbf{x} - \mathbf{f}\,\mathbf{A}, \qquad (2.11)$$

where **r** is a row vector with q components and **A** is a matrix of order p x q. The problem is again to find the best matrix **A**, so that the trace of the remainder matrix $\langle r|r\rangle$ becomes as small as possible. We will now introduce the matrix **C** of order p x q through the relation

$$\mathbf{C} = \Delta^{-1}\,\langle \mathbf{f}|\,\mathbf{x}\rangle, \qquad (2.12)$$

which is obtained in the same way as (2.3). For the remainder matrix $\langle r|r\rangle$ of order qxq, one obtains directly by using the relations $\langle \mathbf{f}|\,\mathbf{x}\rangle = \Delta\,\mathbf{C}$ and $\langle \mathbf{x}|\,\mathbf{f}\rangle = \mathbf{C}^{\dagger}\Delta$:

$$\langle \mathbf{r}|\mathbf{r}\rangle = \langle \mathbf{x} - \mathbf{f}\,\mathbf{A}|\mathbf{x} - \mathbf{f}\,\mathbf{A}\rangle = \langle \mathbf{x}|\,\mathbf{x}\rangle - \langle \mathbf{f}\,\mathbf{A}|\mathbf{x}\rangle - \langle \mathbf{x}|\,\mathbf{f}\,\mathbf{A}\rangle + \langle \mathbf{f}\,\mathbf{A}|\,\mathbf{f}\,\mathbf{A}\rangle =$$

$$= \langle \mathbf{x}|\,\mathbf{x}\rangle - \mathbf{A}^{\dagger}\langle \mathbf{f}\,|\mathbf{x}\rangle - \langle \mathbf{x}|\,\mathbf{f}\,\rangle\,\mathbf{A} + \mathbf{A}^{\dagger}\langle \mathbf{f}\,|\,\mathbf{f}\,\rangle\mathbf{A} = \qquad (2.13)$$

$$= \langle \mathbf{x}|\,\mathbf{x}\rangle - \mathbf{A}^{\dagger}\Delta\,\mathbf{C} - \mathbf{C}^{\dagger}\Delta\;\mathbf{A} + \mathbf{A}^{\dagger}\Delta\,\mathbf{A} = \langle \mathbf{x}|\,\mathbf{x}\rangle - \mathbf{C}^{\dagger}\Delta\,\mathbf{C} + (\mathbf{A} - \mathbf{C})^{\dagger}\Delta\;(\mathbf{A} - \mathbf{C}),$$

which leads to a minimum of the trace of $\langle \mathbf{r}|\mathbf{r}\rangle$ for $\mathbf{A} = \mathbf{C} = \Delta^{-1}\langle \mathbf{f}|\,\mathbf{x}\rangle$. For the components in the subspace $\mathcal{F}$, one gets particularly

$$\mathbf{x}_f = \mathbf{f}\,\mathbf{C} = \mathbf{f}\,\Delta^{-1}\langle \mathbf{f}|\,\mathbf{x}\rangle = |\,\mathbf{f}\,\rangle\,\Delta^{-1}\langle \mathbf{f}|\,\mathbf{x} = \mathbf{P}_f\,\mathbf{x}, \qquad (2.14)$$

where the projector $\mathbf{P}_f$ is again given by the relation (2.7). We note that, since $\mathbf{r} = \mathbf{x} - \mathbf{x}_f = (1 - \mathbf{P}_f)\,\mathbf{x}$, the remainder vectors $\mathbf{r}$ are automatically orthogonal not only to the projections $\mathbf{x}_f$ but also to the entire subspace $\mathcal{F}$, since one has $\langle \mathbf{f}|\mathbf{r}\rangle = \langle \mathbf{P}_f\mathbf{f}|(1 - \mathbf{P}_f)\,\mathbf{x}\rangle = \langle \mathbf{f}|\mathbf{P}_f^{\dagger}(1 - \mathbf{P}_f)\,\mathbf{x}\rangle = \mathbf{0}$. One has hence the theorem that self-adjoint porjectors correspond to orthogonal projections, and vice versa.

It is now clear that, since the vectors $\mathbf{x}_f$ are situated in the subspace $\mathcal{F}$, the set $(\mathbf{x}_f,\mathbf{f})$ contains exactly q linear relations, which we will now study in somewhat greater detail. It follows from (2.13) that one has

$$\mathbf{x}_f - \mathbf{f}\,\Delta^{-1}\langle \mathbf{f}|\,\mathbf{x}\rangle = (\mathbf{x}_f,\mathbf{f})\begin{bmatrix} \mathbf{1} \\ -\Delta^{-1}\langle \mathbf{f}|\,\mathbf{x}\rangle \end{bmatrix} = (\mathbf{x}_f,\mathbf{f})\begin{bmatrix} \mathbf{1} \\ \mathbf{K} \end{bmatrix} = (\mathbf{x}_f,\mathbf{f})\,\mathbf{A} = \mathbf{0}. \qquad (2.15)$$

where $\mathbf{1}$ is a unit matrix of order q, whereas the matrix $\mathbf{K}$ is of order p x q. In the following we will also meet linear relations of the more general form $(\mathbf{x}_f,\mathbf{f})\,\mathbf{L}' = \mathbf{0}$, where the matrix $\mathbf{L}'$ is of order n x n with n = p+q. It is then always possible to find a matrix $\mathbf{V}$ of order n x n such that the product $\mathbf{L} = \mathbf{L}'\,\mathbf{V}$ is of the form $\mathbf{L} = (\mathbf{A},\mathbf{0})$, which we will refer to as the *standard form* of the matrix $\mathbf{L}$ describing the linear relation. We note that the matrix $\mathbf{K}$ in the standard form is *unique*, since the coefficients in the expansion theorem (2.13) are unique due to the fact that the elements in the set $\mathbf{f}$ are linearly independent. We will discuss this reduction of the general matrix $\mathbf{L}'$ further below. It follows from these results that the least square method is an excellent tool for finding and studying linear relations.

The geometrical structure of a set of elements based on the concept of the norm.- It is sometimes useful to consider the linear space $\mathbf{A} = \{\mathbf{x}\}$ as a generalization of the ordinary "geometrical space", in which each one of the elements $\mathbf{x}$ is represented by a "point", and the arrow from the zero element to the point $\mathbf{x}$ represents the "geometrical vector" $\vec{\mathbf{x}}$. In this picture, one needs first of all the concept of "distance" $d_{12}$ between two points $\mathbf{x}_1$ and $\mathbf{x}_2$, which is conveniently defined in terms of of the binary product by means of the relation

$$d_{12} = ||\mathbf{x}_1 - \mathbf{x}_2|| = |\langle \mathbf{x}_1 - \mathbf{x}_2|\mathbf{x}_1 - \mathbf{x}_2\rangle|^{1/2}. \qquad (2.16)$$

More specifically one speaks of the quantity $||x|| = \langle x|x\rangle^{1/2}$ as the "norm" of the element x, which measures the "length" of the geometrical vector $\vec{x}$.

There are many norms in linear algebra, and one of the most useful in studying a set of elements $\mathbf{x} = \{x_1, x_2, x_3, .....x_r\}$ is the norm based on a generalization of the relation (2.16). For a single element x, one has $||x|| = \langle x|x\rangle^{1/2}$, and for a set of elements **x**, we will now define the norm $||\mathbf{x}||$ as the positive square root of the determinant of the matrix $\langle \mathbf{x}|\mathbf{x}\rangle$:

$$||\mathbf{x}|| = |\langle \mathbf{x}|\mathbf{x}\rangle|^{1/2} = \tag{2.17}$$

$$= \begin{vmatrix} \langle x_1|x_1\rangle & \langle x_1|x_2\rangle & \dots & \langle x_1|x_r\rangle \\ \langle x_2|x_1\rangle & \langle x_2|x_2\rangle & \dots & \langle x_2|x_r\rangle \\ \dots & \dots & \dots & \dots \\ \langle x_r|x_1\rangle & \langle x_r|x_2\rangle & \dots & \langle x_r|x_r\rangle \end{vmatrix} .$$

The question of the geometrical interpretation of this quantity will be discussed further below. We note that, if the set **x** undergoes a linear transformation $\mathbf{x}' = \mathbf{x}.\alpha$, where $\alpha$ is a quadratic metrix of order r, one gets by determinant rules that $||\mathbf{x}'|| = ||\mathbf{x}||.|\alpha|$, where the last factor is the absolute value of the determinant of $\alpha$. This result implies also that the norm is invariant under unitary transformations of the set **x**.

In the literature, the determinant in (2.17) is known as Gramm's determinant. A well-known theorem says now that the necessary and sufficient condition for the elements in the set **x** to be *linearly independent* is that $||\mathbf{x}||^2 = |\langle \mathbf{x}|\mathbf{x}\rangle| \neq 0$. In the theory of homogeneous equation systems, one has the theorem that the linear equations $\langle \mathbf{x}|\mathbf{x}\rangle.\mathbf{a} = \mathbf{0}$ has a non-trivial solution $\mathbf{a} \neq \mathbf{0}$, if and only if $|\langle \mathbf{x}|\mathbf{x}\rangle| = 0$. Multiplying the relation above to the left by $\mathbf{a}^\dagger$, one gets $\mathbf{a}^\dagger\langle \mathbf{x}|\mathbf{x}\rangle\,\mathbf{a} = \langle \mathbf{xa}|\mathbf{xa}\rangle = \mathbf{0}$, which implies that in this case one has the linear relation $\mathbf{xa} = \mathbf{0}$. On the other hand, if the elements in the set **x** are linearly independent, any relation of the type $\mathbf{xa} = \mathbf{0}$ must imply that one has $\mathbf{a} = \mathbf{0}$. Multiplying the previous relation to the left by $\langle \mathbf{x}|$, one gets $\langle \mathbf{x}|\mathbf{xa}\rangle = \langle \mathbf{x}|\mathbf{x}\rangle\mathbf{a} = \mathbf{0}$, which has only the trivial solution $\mathbf{a} = \mathbf{0}$ whenever $|\langle \mathbf{x}|\mathbf{x}\rangle| \neq 0$. The properties of the norm $||\mathbf{x}||$ are hence of essential importance in studying the occurrence of exact - and later also approximate - linear dependencies.

Before making the geometrical interpretation of the norm (2.17), we will now return to the problem treated in the previous subsection, and study the norm of the set $\mathbf{z} = (\mathbf{x}, \mathbf{f})$ which contains $n = (p+q)$ elements. For the sake of simplicity, we will a first assume that also the combined set is linearly independent. For its metrix matrix, one obtains

$$\langle \mathbf{z}|\mathbf{z}\rangle = \begin{bmatrix} \langle \mathbf{x}|\mathbf{x}\rangle & \langle \mathbf{x}|\mathbf{f}\rangle \\ \langle \mathbf{f}|\mathbf{x}\rangle & \langle \mathbf{f}|\mathbf{f}\rangle \end{bmatrix}. \tag{2.18}$$

For its norm one obtains by ordinary determinant manipulations involving the subtraction of rows and columns:

$$||\mathbf{z}||^2 = \begin{vmatrix} \langle \mathbf{x}|\mathbf{x}\rangle & \langle \mathbf{x}|\mathbf{f}\rangle \\ \langle \mathbf{f}|\mathbf{x}\rangle & \langle \mathbf{f}|\mathbf{f}\rangle \end{vmatrix} = \begin{vmatrix} \langle \mathbf{x}-f\mathbf{C}|\mathbf{x}-f\mathbf{C}\rangle & \langle \mathbf{x}-f\mathbf{C}|\mathbf{f}\rangle \\ \langle \mathbf{f}|\mathbf{x}-f\mathbf{C}\rangle & \langle \mathbf{f}|\mathbf{f}\rangle \end{vmatrix} = \begin{vmatrix} \langle \mathbf{r}|\mathbf{r}\rangle & \langle \mathbf{r}|\mathbf{f}\rangle \\ \langle \mathbf{f}|\mathbf{r}\rangle & \langle \mathbf{f}|\mathbf{f}\rangle \end{vmatrix} =$$

$$= \begin{vmatrix} \langle \mathbf{r}|\mathbf{r}\rangle & \mathbf{0} \\ \mathbf{0} & \langle \mathbf{f}|\mathbf{f}\rangle \end{vmatrix} = ||\mathbf{r}||^2 ||\mathbf{f}||^2, \qquad (2.19)$$

or $||\mathbf{x},\mathbf{f}|| = ||\mathbf{r}||\cdot||\mathbf{f}||$, which means that the norm of the extended set $(\mathbf{x},\mathbf{f}|)$ is the product of the norm of $\mathbf{f}$ multiplied by the norm of the set $\mathbf{r}$ which is *perpendicular* to the set $\mathbf{f}$. This is a generalization of a well-known theorem in elementary geometry, and it implies that if the norm $||x||$ is the length of the element $x$, then the norm $||x_1, x_2||$ is the *area* of the parallelogram spanned by the elements $x_1$ and $x_2$, the norm $||x_1, x_2, x_3||$ is the *volume* of the parallelepiped spanned by the elements $x_1$, $x_2$, and $x_3$, whereas the norm $||x_1, x_2, x_3, \ldots x_r||$ is the *hypervolume* of the hyper-parallelepiped spanned by the elements $x_1$, $x_2$, $x_3$ ...and $x_r$. We will later return to a more detailed discussion of the concept of the norm.

Partitioning technique. - The relation (2.18) gives a natural partitioning of the metric matrix , and we note that *partitioning technique* is a strong tool in linear algebra. If $\mathbf{M}$ is an arbitrary matrix, which may be partitioned in the following way:

$$\mathbf{M} = \begin{bmatrix} \mathbf{M}_{aa} & \mathbf{M}_{ab} \\ \mathbf{M}_{ba} & \mathbf{M}_{bb} \end{bmatrix}, \qquad (2.20)$$

where $\mathbf{M}_{aa}$ and $\mathbf{M}_{bb}$ are quadratic matrices, and $\mathbf{M}_{ab}$ and $\mathbf{M}_{ba}$ are usually rectangular matrices, one obtains - provided that the matrix $\mathbf{M}_{bb}$ is non-singlular - the simple matrix identity:

$$\begin{bmatrix} \mathbf{1}_{aa} & -\mathbf{M}_{ab}\mathbf{M}_{bb}^{-1} \\ \mathbf{0} & \mathbf{M}_{bb}^{-1} \end{bmatrix} \begin{bmatrix} \mathbf{M}_{aa} & \mathbf{M}_{ab} \\ \mathbf{M}_{ba} & \mathbf{M}_{bb} \end{bmatrix} = \begin{bmatrix} \mathbf{M}_{aa}-\mathbf{M}_{ab}\mathbf{M}_{bb}^{-1}\mathbf{M}_{ba} & \mathbf{0} \\ \mathbf{M}_{bb}^{-1}\mathbf{M}_{ba} & \mathbf{1}_{bb} \end{bmatrix}, \qquad (2.21)$$

which is one of the key formulas in the partitioning technique. Taking the determinants of both members of (2.21), one obtains $|\mathbf{M}_{bb}^{-1}| \cdot |\mathbf{M}| = |\mathbf{M}_{aa}-\mathbf{M}_{ab}\mathbf{M}_{bb}^{-1}\mathbf{M}_{ba}|$ or

$$|\mathbf{M}| = |\mathbf{M}_{aa}-\mathbf{M}_{ab}\mathbf{M}_{bb}^{-1}\mathbf{M}_{ba}| \cdot |\mathbf{M}_{bb}|. \qquad (2.22)$$

Applying this identity to the metrix matrix (2.18) and observing the validity of the relation

$$\langle \mathbf{r}|\mathbf{r}\rangle = \langle (1-P_f)\mathbf{x}|(1-P_f)\mathbf{x}\rangle = \langle \mathbf{x}|(1-P_f)\mathbf{x}\rangle = \langle \mathbf{x}|\mathbf{x}\rangle - \langle \mathbf{x}|\mathbf{f}\rangle\langle \mathbf{f}|\mathbf{f}\rangle^{-1}\langle \mathbf{f}| \qquad (2.23)$$

one gets immediately

$$|\langle \mathbf{x},\mathbf{f}|\mathbf{x},\mathbf{f}\rangle| = |\langle \mathbf{x}|\mathbf{x}\rangle - \langle \mathbf{x}|\mathbf{f}\rangle\langle \mathbf{f}|\mathbf{f}\rangle^{-1}\langle \mathbf{f}|\mathbf{x}\rangle| \, |\langle \mathbf{f}|\mathbf{f}\rangle| = |\langle \mathbf{r}|\mathbf{r}\rangle| \, |\langle \mathbf{f}|\mathbf{f}\rangle|, \qquad (2.24)$$

which is identical to (2.19). Partitioning technique is also a strong tool in determining the inverse of a matrix, and one has the formula:

$$\mathbf{M}^{-1} = \begin{bmatrix} \mathbf{M}_{aa} & \mathbf{M}_{ab} \\ \mathbf{M}_{ba} & \mathbf{M}_{bb} \end{bmatrix}^{-1} =$$

$$= \begin{bmatrix} \mathbf{N}_{aa}^{-1} & ; & -\mathbf{N}_{aa}^{-1}\mathbf{M}_{ab}\mathbf{M}_{bb}^{-1} \\ -\mathbf{M}_{bb}^{-1}\mathbf{M}_{ba}\mathbf{N}_{aa}^{-1} & ; & \mathbf{M}_{bb}^{-1}+\mathbf{M}_{bb}^{-1}\mathbf{M}_{ba}\mathbf{N}_{aa}^{-1}\mathbf{M}_{ba}\mathbf{M}_{bb}^{-1} \end{bmatrix} \qquad (2.25)$$

where

$$\mathbf{N}_{aa} = \mathbf{M}_{aa} - \mathbf{M}_{ab}\mathbf{M}_{bb}^{-1}\,\mathbf{M}_{ba}. \qquad (2.26)$$

A brief derivation is given in Appendix A. Inverting the matrix $\langle \mathbf{x},\mathbf{f}|\mathbf{x},\mathbf{f}\rangle$, one gets, for instance:

$$\langle \mathbf{x},\mathbf{f}|\mathbf{x},\mathbf{f}\rangle^{-1} = \qquad (2.27)$$

$$= \begin{bmatrix} \langle \mathbf{r}|\mathbf{r}\rangle^{-1} & ; & -\langle \mathbf{r}|\mathbf{r}\rangle^{-1}\langle \mathbf{x}|\mathbf{f}\rangle\langle \mathbf{f}|\mathbf{f}\rangle^{-1} \\ -\langle \mathbf{f}|\mathbf{f}\rangle^{-1}\langle \mathbf{f}|\mathbf{x}\rangle\langle \mathbf{r}|\mathbf{r}\rangle^{-1} & ; & \langle \mathbf{f}|\mathbf{f}\rangle^{-1}+\langle \mathbf{f}|\mathbf{f}\rangle^{-1}\langle \mathbf{f}|\mathbf{x}\rangle\langle \mathbf{r}|\mathbf{r}\rangle^{-1}\langle \mathbf{x}|\mathbf{f}\rangle\langle \mathbf{f}|\mathbf{f}\rangle^{-1} \end{bmatrix},$$

where one observes that, except for the common factor $\langle \mathbf{r}|\mathbf{r}\rangle^{-1}$ to the right, the elements in the first q columns are identical to the elements in the q columns of the standard matrix $\mathbf{L}$ given by (2.15). We note, however, that if the elements in the remainder matrix $\langle \mathbf{r}|\mathbf{r}\rangle$ tend to zero, the elements in the inverse matrix $\langle \mathbf{r}|\mathbf{r}\rangle^{-1}$ are blowing up, and one has to watch that one is not losing significant figures. From the computational point of view, the standard form (2.15) is hence to be preferred under most circumstances.

## 3. Some Properties of Linear Operators and their Matrix Representations

Some properties of the matrix representation of a linear operator.- Before going into the discussion of a generalization of the least square method, it is useful to briefly review some basic concepts in linear algebra in general. If $\mathbf{T}$ is a linear operator, its matrix representation $\mathbf{T} = \{T_{kl}\}$ in terms of an orthonormal basis $\varphi$ is given by formula (1.19) with $T_{kl} = \langle \varphi_k|\mathbf{T}|\varphi_l\rangle$, and the adjoint operator $\mathbf{T}^\dagger$ is then represented by the adjoint matrix $\mathbf{T}^\dagger = \{T_{lk}^*\}$. The matrix representation of $\mathbf{T}$ in terms of a non-orthonormal basis is slightly more complicated, and we will here concentrate our interest on the case when $\mathbf{T}$ is *stable* with respect to the space $\mathcal{Z}$ or order $n = p + q$ spanned by the elements $\mathbf{z} = \{\mathbf{x},\mathbf{f}\}$. This means that all the image elements $\mathbf{Tz}$ are situated within the subspace $\mathcal{Z}$, so that one has an expansion of the form $\mathbf{Tz} = \mathbf{zT}$, in which case $\mathbf{T}$ is said to be the matrix representation of the operator $\mathbf{T}$. Multiplying this relation to the left by $\langle \mathbf{z}|$, one gets $\langle \mathbf{z}|\mathbf{Tz}\rangle = \langle \mathbf{z}|\mathbf{z}\rangle\mathbf{T}$ and

$$\mathbf{T} = \langle \mathbf{z}|\mathbf{z}\rangle^{-1}\langle \mathbf{z}|\mathbf{Tz}\rangle = \Delta^{-1}\langle \mathbf{z}|\mathbf{Tz}\rangle, \qquad (3.1)$$

where $\Delta = \langle z|z\rangle$ is the metrix matrix for the set **z**. This is the formula desired. For the matrix representation **S** of the adjoint operator $T^\dagger$, one gets immediately

$$\begin{aligned} \mathbf{S} &= \langle z|z\rangle^{-1}\langle z|T^\dagger z\rangle = \langle z|z\rangle^{-1}\langle Tz|z\rangle = \langle z|z\rangle^{-1}\langle zT|z\rangle = \\ &= \langle z|z\rangle^{-1}T^\dagger\langle z|z\rangle = \Delta^{-1}T^\dagger\Delta\,, \end{aligned} \tag{3.2}$$

i.e. **S** is a similarity transformation of the adjoint matrix $T^\dagger$. In the special case, when the operator T is self-adjoint, so that $T^\dagger = T$, one has consequently **S**= **T**, and the relation

$$T = \Delta^{-1}T^\dagger\Delta\,. \tag{3.3}$$

The characteristic polynomial for a matrix. - In order to study the properties of a linear operator T, it is useful to consider its matrix representation **T** and the associated characteristic polynomial P(z) of order n of the form

$$P(z) = |\mathbf{T} - z.\mathbf{1}| =$$

$$= \begin{vmatrix} T_{11}-z & T_{12} & T_{13} & \dots & T_{1n} \\ T_{21} & T_{22}-z & T_{23} & \dots & T_{2n} \\ T_{31} & T_{32} & T_{33}-z & \dots & T_{3n} \\ \dots & \dots & \dots & \dots & \dots \\ T_{n1} & T_{n2} & T_{n3} & \dots & T_{nn}-z \end{vmatrix} =$$

$$= a_0 + a_1 z + a_2 z^2 + a_3 z^3 \,.....\, + a_n z^n, \tag{3.4}$$

where z is a complex variable and

$$\begin{aligned} a_n &= (-1)^n, \\ a_{n-1} &= (-1)^{n-1}\Sigma_k\, T_{kk} = (-1)^{n-1}\mathrm{Tr}\, T, \\ a_{n-2} &= (-1)^{n-2}\Sigma_{k<l} \begin{vmatrix} T_{kk} & T_{kl} \\ T_{lk} & T_{ll} \end{vmatrix} = (-1)^{n-2}\mathrm{Tr}_2\, T, \\ a_{n-3} &= (-1)^{n-3}\Sigma_{k<l<m} \begin{vmatrix} T_{kk} & T_{kl} & T_{km} \\ T_{lk} & T_{ll} & T_{lm} \\ T_{mk} & T_{ml} & T_{mm} \end{vmatrix} = (-1)^{n-3}\mathrm{Tr}_3\, T, \\ &\dots\dots\dots\dots\dots\dots\dots\dots\dots\dots\dots\dots\dots\dots\dots\dots\dots\dots\dots\dots\dots\dots\dots\dots \\ a_0 &= |\mathbf{T}|. \end{aligned} \tag{3.5}$$

It is evident that each coefficient $a_{n-k}$ is the *$k^{th}$ order trace* of the matrix **T**, i.e. the sum of all *principal minors* of order k, multiplied by a sign factor $(-1)^{n-k}$, or:

$$a_p = (-1)^p\, \mathrm{Tr}_{n-p}\, \mathbf{T}. \tag{3.6}$$

An important feature of the polynomial P(z) is that it is independent of the choice of basis, and it is hence characteristic for the operator T itself; we note that, for this reason, the coefficients $a_p$ are sometimes referred to as the *fundamental*

*invariants*. They will be of essential importance in the discussions below. The polynomial $P(z)$ is further characterized by its zero-points $\lambda_1, \lambda_2, \lambda_3, \ldots$ and their multiplicities $g_1, g_2, g_3, \ldots$, etc., and one has the product formula

$$P(z) = \Pi_k \;(\lambda_k - z)^{g_k}, \tag{3.7}$$

where the quantities $\lambda_1, \lambda_2, \lambda_3, \ldots$ are the *eigenvalues* of the operator T. We note that, if the operator T is self-adjoint, the matrix T may always be brought to *diagonal form* by means of a similarity transformation, whereas, if the operator T is of a more general nature, the matrix T may always be brought to *classical canonical form* - consisting of a series of Jordan blocks described by their Segré characteristics - by means of a similarity transformation.

An arbitrary matrix $\mathbf{T}$ of order $n$ is said to have the *rank* $(n - q)$, if all principal minors of order $q$ are identically vanishing, whereas this is not true for all principal minors of order $(q-1)$. In such a case, all the coefficients $a_k$ are vanishing for $k = 0,1,2, \ldots(q-1)$, whereas $a_q$ is the first non-vanishing coefficient. This implies hence that the matrix $\mathbf{T}$ has exactly $q$ eigenvalues which are zero and $p = (n - q)$ eigenvalues which are non-vanishing.

In the following, we will concentrate our interest on a *metric matrix* $\Delta = \langle \mathbf{x}|\mathbf{x}\rangle$ which is hermitian and positive semi-definite and formed from the set $\mathbf{x} = \{x_1, x_2, x_3, \ldots x_n\}$ of order $n$, where the elements are non-vanishing but not necessarily linearly independent. According to (1.23), this matrix corresponds to a self-adjoint *metric operator* D of the form:

$$D = |\mathbf{x}\rangle\langle\mathbf{x}|\mathbf{x}\rangle\langle\mathbf{x}| = \Sigma_{kl} |x_k\rangle\langle x_k|x_l\rangle\langle x_l| = \Sigma_{kl} |x_k\rangle\Delta_{kl}\langle x_l|, \tag{3.8}$$

which has $n$ non-negative eigenvalues $\mu_1, \mu_2, \mu_3, \ldots \mu_n \geq 0$. For the fundamental invariants (3.5), one gets in this particular case:

$$a_n = (-1)^n,$$
$$a_{n-1} = (-1)^{n-1}\mathrm{Tr}\,\Delta = (-1)^{n-1}\Sigma_k \Delta_{kk} = (-1)^{n-1}\Sigma_k \|x_k\|^2,$$
$$a_{n-2} = (-1)^{n-2}\mathrm{Tr}_2\,\Delta = (-1)^{n-2}\Sigma_{k<l} \begin{vmatrix} \Delta_{kk} & \Delta_{kl} \\ \Delta_{lk} & \Delta_{ll} \end{vmatrix} = (-1)^{n-2}\Sigma_k \|x_k, x_l\|^2,$$
$$a_{n-3} = (-1)^{n-3}\mathrm{Tr}_3\,\Delta = (-1)^{n-3}\Sigma_{k<l<m} \begin{vmatrix} \Delta_{kk} & \Delta_{kl} & \Delta_{km} \\ \Delta_{lk} & \Delta_{ll} & \Delta_{lm} \\ \Delta_{mk} & \Delta_{ml} & T_{mm} \end{vmatrix} =$$
$$= (-1)^{n-3}\Sigma_k \|x_k, x_l, x_m\|^2,$$
$$\cdots\cdots\cdots\cdots\cdots\cdots\cdots\cdots\cdots\cdots$$
$$a_0 = |\Delta| = \| x_1, x_2, x_3, \ldots x_n\|^2. \tag{3.9}$$

There is hence a close connection between the fundamental invariants and the norms of the subsets of elements occurring in the set $\mathbf{x} = \{x_1, x_2, x_3, \ldots x_n\}$.

In the case when $\|\mathbf{x}\|^2 = |\langle \mathbf{x}|\mathbf{x}\rangle| = |\Delta| = 0$, one knows that there exists a column vector $\mathbf{c} \neq \mathbf{0}$ having the property that

$$\mathbf{x}.\mathbf{c} = x_1c_1 + x_2c_2 + x_3c_3 + \ldots + x_nc_n = 0, \tag{3.10}$$

and this linear relation is said to define a *hyperplane* of order (n-1) going through the zero-element. If the matrix $\Delta = \langle \mathbf{x}|\mathbf{x}\rangle$ has the rank (n-q), an elementary theorem says further that there exist q essentially different non-trivial solutions $\mathbf{c}_k \neq \mathbf{0}$ for $k = 1,2,3,\ldots q$ which define q different hyperplanes in the linear space. In one approach, one may establish the first hyperplane defined by $\mathbf{c}_1$ with $c_{11} \neq 0$; after leaving out the element $x_1$, one may then consider the reduced set $\mathbf{x}' = \{x_2, x_3, \ldots x_n\}$ and use its matrix $\langle \mathbf{x}'|\mathbf{x}'\rangle$ to determine the next solution $\mathbf{c}_1$ and the associated hyperplane, etc.

In a more direct approach, one may consider all the q eigenvectors $\mathbf{c}_k$ which are associated with the eigenvalue $\mu = 0$ of multiplicity $g = q$ for the matrix $\Delta = \langle \mathbf{x}|\mathbf{x}\rangle$. Multiplying the relation $\Delta\,\mathbf{c}_k = 0$ to the left by $\mathbf{c}_k^\dagger$, one obtains $\mathbf{c}_k^\dagger \Delta\, \mathbf{c}_k = \|\mathbf{x}\mathbf{c}_k\|^2 = 0$, i.e. $\mathbf{x}\mathbf{c}_k = 0$. By choosing the eigenvectors $\mathbf{c}_k$ orthonormal, one can make sure that the q hyperplanes obtained are essentially different. We note also that the entire subspace of order q associated with the eigenvalue $\mu = 0$ may be obtained by using the product projection operator [6]:

$$P = \Pi_{\mu_k \neq 0}\ (D - \mu_k)/(-\mu_k), \tag{3.11}$$

which has the elementary properties $P^2 = P$, $P^\dagger = P$, $\mathrm{Tr}\, P = q$, $DP = PD = 0$. In principle, there are hence no difficulties in treating the exact linear dependencies and the associated hyperplanes.

The difficulties are instead associated with the observation that, even if a given set is strictly *linearly independent* in the sense of mathematics, it may very well show *approximate linear dependencies* in applied mathematics, e.g. when applied to a computer with a given limited accuracy. In this situation, the hyperplanes associated with the very small eigenvalues $\mu \approx 0$ do not go exactly through the points in the set $\mathbf{x} = \{x_1, x_2, x_3, \ldots x_n\}$, and some of these points are then situated *outside* the hyperplanes under consideration - they are "outlyers". It is clear that it is important to find an estimate of the errors involved and to try to minimize them as much as possible.

The mathematical problem of fitting a given set of points in a linear space to hyperplanes with a minimum of errors was first formulated in 1901 in a slightly different way by Karl Pearson [7], and many attempts have then been made to solve this classical problem which is of utmost importance from many practical points of view. It is evident that the nature of the solution depends on the concepts one introduces to measure the errors involved, and in the next subsection we will

limit our interest to error measurements based on the concept of the norm $\|\mathbf{x}\|$ discussed previously.

On the measure of the deviations of points from hyperplanes based on the concept of the norm.- Let us start by considering the deviation $d_1$ of a set of points $\mathbf{x} = \{x_1, x_2, x_3,...x_n\}$ from a given point $x_0$ defined by the relation:

$$d_1^2 = \|x_1 - x_0\|^2 + \|x_2 - x_0\|^2 + \|x_3 - x_0\|^2 +...\|x_n - x_0\|^2 \geq 0, \qquad (3.12)$$

Since the second member is the sum of non-negative terms, one has $d_1 = 0$, if and only if $x_1 = x_2 = x_3 =...x_n = 0$. Next we will consider the deviation $d_2$ of the set $\mathbf{x}$ from a straight line through the point $x_0$ defined by the relation:

$$d_2^2 = \Sigma_{i<j} \|x_i - x_0, x_j - x_0\|^2 \geq 0, \qquad (3.13)$$

Every term in the second member is non-negative, and, if a single one is zero, e.g. $\|x_k - x_0, x_l - x_0\|^2 = 0$, then this implies that there exists a linear relation $x_k - x_0 = \alpha_{kl}(x_l - x_0)$, i.e. $x_k$ and $x_l$ are situated on a straight line through $x_0$, defined by the direction of the geometrical vector from $x_0$ to $x_k$. If another term, say $\|x_k - x_0, x_m - x_0\|^2$ is also zero, it implies that also $x_m$ is situated on the *same* straight line through $x_0$, defined by the direction of the geometrical vector from $x_0$ to $x_k$. If one has $d_2 = 0$, all terms $\|x_i - x_0, x_j - x_0\|^2$ are vanishing, and this implies that all the elements $x_1, x_2, x_3,...x_n$ are situated on the *same straight line* through $x_0$, defined by the direction of the geometrical vector from $x_0$ to any one of the elements $x_i$ involved.

Next, we will consider the deviation $d_3$ of the set $\mathbf{x}$ from a hyperplane through the point $x_0$ defined by the relation:

$$d_3^2 = \Sigma_{i<j<k} \|x_i - x_0, x_j - x_0, x_k - x_0\|^2 \geq 0. \qquad (3.14)$$

In the same way as before, we can conclude that, if a single term in the second member is vanishing, it defines a *hyperplane* through the point $x_0$, whereas - if $d_3 = 0$ - all the terms are vanishing, and the elements in the set $x_1, x_2, x_3,...x_n$ are all situated on the *same* hyperplane through the point $x_0$. In the same way, the quantity $d_{p+1}$ will define the deviation of the set $\mathbf{x}$ from a hyperplane of order p through the point $x_0$. From now on, we will assume that the deviations $d_{p+1}$ are convenient *measures of the errors* involved in fitting the set $\mathbf{x}$ to straight lines and hyperplanes through a given point $x_0$.

In the following, we will consider only the deviations $d_{p+1}$ of the set $\mathbf{x}$ from hyperplanes of order $p = 1,2,3,$ .... through the zero-point, i.e. we will put $x_0 = 0$. In such a case, the deviations $d_1, d_2, d_3,...$ will - except for a sign factor - become identical to the fundamental invariants $a_{n-1}, a_{n-2}, a_{n-3},...$ defined by (3.9), and one gets the general relation

$$d_p = (-1)^{n-p} a_{n-p}. \qquad (3.15)$$

This result implies that it is possible to get a measurement of the errors involved in a hyperplane fitting simply by calculating the secular equation for the metric matrix $\Delta = \langle x|x\rangle$. If the coefficients $a_k$ are vanishing for $k = 0,1,2, \ldots(q-1)$, where $a_q$ is the first non-vanishing coefficient, we have indicated previously that the matrix $\Delta$ has $q$ eigenvalues which are zero and $p = (n - q)$ eigenvalues which are non-vanishing. The fact that the quantities $d_n, d_{n-1}, d_{n-2}, \ldots d_{n-q+1}$ are now also vanishing implies the existence of $q$ hyperplanes of various orders according to the reasoning given above. If further the coefficients $a_q, a_{q+1}, \ldots a_{q+r-1}$ are very small, it means the existence of $r$ more hyperplanes which are not exact but *approximate fits* and which have error measurements given by the absolute values of these coefficients. If finally certain variations are permitted in the given set $x = \{x_1, x_2, x_3, \ldots x_n\}$, the essential problem becomes to adapt these variations so that the error measurements become as small as possible. We will return to this problem in greater detail in a later section.

At this point, we observe that, in the treatment of the remainder vector $\mathbf{r} = \mathbf{x} - \mathbf{fA}$ in Sec. 2, we obtained according to (2.13) for the remainder matrix: $\langle \mathbf{r}|\mathbf{r}\rangle = \langle \mathbf{x}|\mathbf{x}\rangle - \mathbf{C}^\dagger\Delta\,\mathbf{C} + (\mathbf{A} - \mathbf{C})^\dagger\Delta\,(\mathbf{A} - \mathbf{C})$, where the last term for $\mathbf{A} \neq \mathbf{C}$ is positive definite. For the sake of simplicity, we showed that the *trace* of $\langle \mathbf{r}|\mathbf{r}\rangle$ has a minimum for $\mathbf{A} = \mathbf{C}$, but it is now easy to extend the same reasoning to the norm $\|\mathbf{r}\| = |\langle \mathbf{r}|\mathbf{r}\rangle|^{1/2}$. One has obviously the matrix inequality:

$$\langle \mathbf{r}|\mathbf{r}\rangle = \langle \mathbf{x}|\mathbf{x}\rangle - \mathbf{C}^\dagger\Delta\,\mathbf{C} + (\mathbf{A} - \mathbf{C})^\dagger\Delta\,(\mathbf{A} - \mathbf{C}) \geq \langle \mathbf{x}|\mathbf{x}\rangle - \mathbf{C}^\dagger\Delta\,\mathbf{C} \geq \mathbf{0}, \quad (3.16)$$

and a well-known theorem says then that the eigenvalues of $\langle \mathbf{r}|\mathbf{r}\rangle$ are larger than the eigenvalues of the matrix $[\langle \mathbf{x}|\mathbf{x}\rangle - \mathbf{C}^\dagger\Delta\,\mathbf{C}]$ in order from below. Since the determinant $|\langle \mathbf{r}|\mathbf{r}\rangle|$ equals the product of the eigenvalues, it is evident that it also has its minimum for $\mathbf{A} = \mathbf{C}$.

Today there is no problem in calculating all the principal minors of $\mathbf{T}$ and evaluate the coefficients $a_k$ by means of the modern electronic computers, but this was not the case only a couple of decades ago. A large number of methods for calculating the characteristic polynomial, for estimating and calculating the eigenvalues by means of special techniques have been developed over the years, and, even if they have lost most of their importance in modern data analysis, they may still be of essential value in the underlying system analysis which may be performed to understand the theoretical structure of the data available and to make predictions. A brief survey of some of these methods is hence given in Appendices B-D.

## 4. The Method of Generalized Least Squares

A generalization of the least square method. - In the least square method described in Sec. 2 for treating the combined set $\mathbf{z} = \{\mathbf{x},\mathbf{f}\}$, the minimal error $\mathbf{r} = (1-P_f)\,\mathbf{x}$ is described by a self-adjoint projector $P_f$ given by the relation (2.8) and becomes automatically orthogonal to the entire subspace spanned by the elements $\{\mathbf{f}\}$. We will now consider a slight generalization of this approach by studying all possible

projectors P of order p, which are stable on the space $\mathcal{Z} = \{\mathbf{z}\}$, i.e. for which the space $P\mathcal{Z} = \{P\mathbf{z}\}$ is a subspace of $\mathcal{Z}$ of order p. By means of such a projector, one can now write every element in $\mathbf{z}$ as a sum of two components

$$\mathbf{z} = P\,\mathbf{z} + (1-P)\,\mathbf{z} = \hat{\mathbf{z}} + \mathbf{z}_R, \qquad (4.1)$$

where the first term will be considered as the *"main component"* and the second term as the *"remainder"* or residual. In the general case, the projector P is usually not self-adjoint, but we note that the adjoint operator $P^\dagger$ is also a projector, i.e. from $P^2 = P$ follows that $(P^\dagger)^2 = P^\dagger$. For the operator P one has now the decomposition

$$P = (P+P^\dagger)/2 + (P-P^\dagger)/2 = A + iB, \qquad (4.2)$$

where the hermitean operator $B = (P-P^\dagger)/2i$ is an indicator of the deviation from the self-adjointness. In the approach first studied, one obtained a minimum of the trace of $\langle \mathbf{z}_R|\mathbf{z}_R\rangle$ or of the norm $\|\mathbf{z}_R\|$ for the orthogonal projection, i.e. for $B = 0$, and one would anticipate that the same holds even for the general projections. The proof is simple and is based on the identity

$$(1-P)^\dagger(1-P) = 1 - P - P^\dagger + P^\dagger P = 1 - PP^\dagger + (P - P^\dagger)^\dagger(P - P^\dagger), \qquad (4.3)$$

which gives

$$\langle \mathbf{z}_R|\mathbf{z}_R\rangle = \langle \mathbf{z}|(1-P)^\dagger(1-P)|\mathbf{z}\rangle = \langle \mathbf{z}|1 - PP^\dagger|\mathbf{z}\rangle + \langle \mathbf{z}|(P - P^\dagger)^\dagger(P - P^\dagger)|\mathbf{z}\rangle =$$

$$= \langle \mathbf{z}|1 - PP^\dagger|\mathbf{z}\rangle + \langle (P - P^\dagger)\mathbf{z}|(P - P^\dagger)\mathbf{z}\rangle, \qquad (4.4)$$

where the last term is never negative and vanishes, if and only if $(P - P^\dagger)\mathbf{z} = 0$, i.e. if $P = P^\dagger$. The result implies that, if one consider all pairs P and $P^\dagger$, and keeps A fixed and varies B in the decomposition (4.1), one obtains the minimum remainder or residual whenever $P = P^\dagger$. In this case, one has also that $\mathbf{z}_R$ becomes automatically orthogonal to the entire set $\hat{\mathbf{z}}$, i.e. $\langle \mathbf{z}_R|\hat{\mathbf{z}}\rangle = 0$. Let us now consider the matrix representation $\mathbf{P}$ of the projector P, defined by the relation $P\,\mathbf{z} = \mathbf{z}\,\mathbf{P}$. We note that, since $P^2 = P$, one has also $\mathbf{P}^2 = \mathbf{P}$, and we will hence call $\mathbf{P}$ a *projection matrix*. Using (3.1) and the orthogonality property, one gets immediately

$$P\,\mathbf{z} = \mathbf{z}\,\mathbf{P},\quad \mathbf{P} = \langle \mathbf{z}|\mathbf{z}\rangle^{-1}\langle \mathbf{z}|P\mathbf{z}\rangle = \Delta^{-1}\langle \hat{\mathbf{z}} + \mathbf{z}_R|\hat{\mathbf{z}}\rangle = \Delta^{-1}\langle \hat{\mathbf{z}}|\hat{\mathbf{z}}\rangle = \Delta^{-1}\,\hat{\Delta}, \qquad (4.5)$$

where $\hat{\Delta} = \langle \hat{\mathbf{z}}|\hat{\mathbf{z}}\rangle$ is the metrix matrix associated with the main components $\hat{\mathbf{z}}$. We note further that, according to (3.3), the projection matrix satisfies the relation

$$\mathbf{P} = \Delta^{-1}\mathbf{P}^\dagger\,\Delta\,. \qquad (4.6)$$

For the main components $\hat{\mathbf{z}} = P\,\mathbf{z} = \mathbf{z}\,\mathbf{P}$, one gets immediately

$$\hat{\mathbf{z}}\,(1 - \mathbf{P}) = \hat{\mathbf{z}}\,\mathbf{L}' = 0, \tag{4.7}$$

where $\mathbf{L}' = 1 - \mathbf{P}$, and this gives the *linear relation* desired. Let us now make an explicit construction of the projector $\mathbf{P}$ and its associated matrix $\mathbf{P}$. For this purpose, we will consider a linear transformation $\mathbf{z}' = \mathbf{z}\,\alpha$, where $\alpha$ is an arbitrary non-singular matrix of order $n \times n$ of the form $\alpha = (\mathbf{A},\mathbf{B})$, where $\mathbf{A}$ and $\mathbf{B}$ are matrices of order $n \times q$ and $n \times p$ formed by the first $q$ and $p$ column vectors of $\alpha$, respectively. One gets immediately $\mathbf{z}' = (\mathbf{zA},\mathbf{zB}) = (\mathbf{z}_a,\mathbf{z}_b)$, where the sets $\mathbf{z}_a$ and $\mathbf{z}_b$ are again linearly independent. We will now construct the projector $\mathbf{P} = \mathbf{P}_b$ associated with the subspace spanned by the set $\mathbf{z}_b$. According to (2.8) and (3.1), one gets immediately

$$\mathbf{P} = |\mathbf{z}_b\rangle\langle\mathbf{z}_b|\mathbf{z}_b\rangle^{-1}\langle\mathbf{z}_b| = |\mathbf{zB}\rangle\langle\mathbf{zB}|\mathbf{zB}\rangle^{-1}\langle\mathbf{zB}| =$$

$$= |\mathbf{z}\rangle\mathbf{B}\{\mathbf{B}^\dagger\langle\mathbf{z}|\mathbf{z}\rangle\mathbf{B}\}^{-1}\mathbf{B}^\dagger\langle\mathbf{z}|, \tag{4.8}$$

$$\mathbf{P} = \langle\mathbf{z}|\mathbf{z}\rangle^{-1}\langle\mathbf{z}|\mathbf{Pz}\rangle = \mathbf{B}\{\mathbf{B}^\dagger\langle\mathbf{z}|\mathbf{z}\rangle\mathbf{B}\}^{-1}\mathbf{B}^\dagger\langle\mathbf{z}|\mathbf{z}\rangle. \tag{4.9}$$

By using the general theory and the projector P, one can now decompose the set $\mathbf{z}$ into two orthogonal components $\mathbf{z} = \mathbf{Pz} + (1-\mathbf{P})\mathbf{z} = \hat{\mathbf{z}} + \mathbf{z}_R$, where

$$\hat{\mathbf{z}} = \mathbf{Pz} = \mathbf{zP} = \mathbf{z}\;\mathbf{B}\{\mathbf{B}^\dagger\Delta\mathbf{B}\}^{-1}\mathbf{B}^\dagger\Delta\quad, \tag{4.10}$$

and

$$\hat{\Delta} = \langle\hat{\mathbf{z}}|\hat{\mathbf{z}}\rangle = \langle\mathbf{z}|\mathbf{Pz}\rangle = \langle\mathbf{z}|\mathbf{z}\rangle\,\mathbf{P} = \Delta\,\mathbf{B}\{\mathbf{B}^\dagger\Delta\mathbf{B}\}^{-1}\mathbf{B}^\dagger\Delta\quad, \tag{4.11}$$

$$\Delta_R = \Delta - \hat{\Delta} = \Delta\,(1 - \mathbf{P}). \tag{4.12}$$

According to (4.7), one has then the linear relation $\hat{\mathbf{z}}\,\mathbf{L}' = 0$, where $\mathbf{L}' = 1 - \mathbf{P}$. Multiplying to the right by $\alpha = (\mathbf{A},\mathbf{B})$ and observing that $(1 - \mathbf{P})\mathbf{B} = 0$, one gets

$$\mathbf{L}'' = \mathbf{L}'\,\alpha = \{(1 - \mathbf{P})\mathbf{A},0\} = (\mathbf{W}, 0), \tag{4.13}$$

where $\mathbf{W} = (1 - \mathbf{P})\mathbf{A} = \Delta^{-1}\Delta_R\mathbf{A}$ is a matrix of order $n \times q$, which one may write in the form

$$\mathbf{W} = (1 - \mathbf{P})\mathbf{A} = \mathbf{A} - \mathbf{B}\{\mathbf{B}^\dagger\Delta\mathbf{B}\}^{-1}\mathbf{B}^\dagger\Delta\,\mathbf{A} = \begin{bmatrix}\mathbf{W}_{aa}\\ \mathbf{W}_{ba}\end{bmatrix}, \tag{4.14}$$

where $\mathbf{W}_{aa}$ is a matrix of order $q \times q$. Multiplying to the right by $\mathbf{W}_{aa}^{-1}$, one obtains the reduced form desired

$$\mathbf{W}\,\mathbf{W}_{aa}^{-1} = \begin{bmatrix}\mathbf{1}_a\\ \mathbf{W}_{ba}\mathbf{W}_{aa}^{-1}\end{bmatrix}. \tag{4.15}$$

with $\mathbf{K} = \mathbf{W_{ba}W_{aa}^{-1}}$ .Even in the general theory, it is hence easy to find the linear relation associated with the least square method.

An alternative formulation of the generalized least square method: the Kalman construction. - An elegant and forceful formulation of a generalized least square scheme has been given by Kalman [8], and here we will give a brief review of some of the main concepts in terms of the notations and terminology we have used previously. One should observe that Kalman instead of $\mathbf{z_R}$ uses the notation $\tilde{\mathbf{z}}$, and for our metric matrix $\Delta$ - in other connections called the *covariance matrix* - Kalman uses the notation $\Sigma$, and for taking the adjoint (†) he uses the symbol ' . For the three fundamental metrix matrices $\Delta, \hat{\Delta}$, and $\Delta_R$, Kalman hence uses the notations $\Sigma, \hat{\Sigma}, \tilde{\Sigma}$.

In this approach, one starts from the assumption that one has a decomposition $\mathbf{z} = \hat{\mathbf{z}} + \mathbf{z_R}$ into two orthogonal components, so that $\langle \hat{\mathbf{z}} | \mathbf{z_R} \rangle = \mathbf{0}$.

$$\Delta = \langle \mathbf{z}|\mathbf{z}\rangle = \langle \hat{\mathbf{z}} + \mathbf{z_R} \,|\, \hat{\mathbf{z}} + \mathbf{z_R}\rangle = \langle \hat{\mathbf{z}}|\hat{\mathbf{z}}\rangle + \langle \mathbf{z_R}|\mathbf{z_R}\rangle = \hat{\Delta} + \Delta_R, \qquad (4.16)$$

$$\mathbf{1} = \Delta^{-1}\hat{\Delta} + \Delta^{-1}\Delta_R, \qquad (4.17)$$

where one has $\Delta > \mathbf{0}$, $\hat{\Delta} = \langle \hat{\mathbf{z}}|\hat{\mathbf{z}}\rangle \geq \mathbf{0}$, and $\Delta_R = \langle \hat{\mathbf{z}}|\hat{\mathbf{z}}\rangle \geq \mathbf{0}$. Since one has $\Delta > \hat{\Delta} \geq \mathbf{0}$, the inequality (1.28b) gives immediately

$$\hat{\Delta} \geq \hat{\Delta}\Delta^{-1}\hat{\Delta} \ , \qquad (4.18)$$

In the theory of covariance matrices, this inequality is sometimes referred to as Becker's lemma [9]. In this approach, it is observed that if the equality sign in (4.18) holds, the decomposition in (4.16) corresponds to a generalized least square scheme. In such a case, one has the two relations

$$\hat{\Delta} = \hat{\Delta}\Delta^{-1}\hat{\Delta} \ , \quad \Delta_R = \Delta_R\Delta^{-1}\Delta_R, \qquad (4.19)$$

where the second relation is obtained from the first by putting $\hat{\Delta} = \Delta - \Delta_R$. It follows from (4.19) that

$$\Delta^{-1}\hat{\Delta} = \Delta^{-1}\hat{\Delta}\Delta^{-1}\hat{\Delta}, \quad \Delta^{-1}\Delta_R = \Delta^{-1}\Delta_R\Delta^{-1}\Delta_R, \qquad (4.20)$$

which implies that the products $\Delta^{-1}\hat{\Delta}$ and $\Delta^{-1}\Delta_R$ are *projection matrices* adding up to the unit matrix $\mathbf{1}$ according to (4.17). We note that the two projections matrices $\Delta^{-1}\hat{\Delta}$ and $\Delta^{-1}\Delta_R$ are *mutually exlusive* and that one has $\Delta^{-1}\hat{\Delta}(\mathbf{1} - \Delta^{-1}\hat{\Delta}) = \Delta^{-1}\hat{\Delta}\Delta^{-1}\Delta_R = \mathbf{0}$, and the exclusiveness relation

$$\hat{\Delta}\Delta^{-1}\Delta_R = \mathbf{0}. \qquad (4.21)$$

Instead of starting from the first relation (4.19), one may choose the exclusivness relation (4.21) as the fundamental assumption about the three matrices involved. Taking the square of the relation (4.17), one gets immediately

$$\mathbf{1} = \Delta^{-1}\hat{\Delta}\cdot\Delta^{-1}\hat{\Delta} + \Delta^{-1}\Delta_R\cdot\Delta^{-1}\Delta_R, \qquad (4.22)$$

as well as $\Delta^{-1}\Delta_R\cdot\Delta^{-1}\Delta_R = (\mathbf{1} - \Delta^{-1}\hat{\Delta})^2 = \mathbf{1} - 2\,\Delta^{-1}\hat{\Delta} + \Delta^{-1}\hat{\Delta}\cdot\Delta^{-1}\hat{\Delta}$, which together with (4.22) gives $\Delta^{-1}\hat{\Delta}\,\Delta^{-1}\hat{\Delta} = \Delta^{-1}\hat{\Delta}$, or $\hat{\Delta} = \hat{\Delta}\Delta^{-1}\hat{\Delta}$, i.e. the first relation (4.19).

By means of the two projection matrices, it is now possible to verify the decomposition of the elements $\mathbf{z}$ :

$$\mathbf{z} = \mathbf{z}.\mathbf{1} = \mathbf{z}.(\Delta^{-1}\hat{\Delta} + \Delta^{-1}\Delta_R) = \mathbf{z}.\Delta^{-1}\hat{\Delta} + \mathbf{z}.\Delta^{-1}\Delta_R = \mathbf{z}_1 + \mathbf{z}_2, \qquad (4.23)$$

for which one has

$$\langle \mathbf{z}_1|\mathbf{z}_2\rangle = \langle \mathbf{z}.\Delta^{-1}\hat{\Delta}|\,\mathbf{z}.\Delta^{-1}\Delta_R\rangle = \hat{\Delta}\Delta^{-1}\langle \mathbf{z}|\,\mathbf{z}\rangle\Delta^{-1}\Delta_R\rangle = \hat{\Delta}\Delta^{-1}\Delta_R = \mathbf{0}, \qquad (4.24)$$

$$\langle \mathbf{z}_1|\mathbf{z}_1\rangle = \langle \mathbf{z}.\Delta^{-1}\hat{\Delta}\mathbf{z}.\Delta^{-1}\hat{\Delta}\rangle = \hat{\Delta}\Delta^{-1}\langle \mathbf{z}\,|\mathbf{z}\rangle\Delta^{-1}\hat{\Delta} = \hat{\Delta}\Delta^{-1}\hat{\Delta} = \hat{\Delta}, \qquad (4.25)$$

$$\langle \mathbf{z}_2|\mathbf{z}_2\rangle = \langle \mathbf{z}.\Delta^{-1}\Delta_R|\mathbf{z}.\Delta^{-1}\Delta_R\rangle = \Delta_R\Delta^{-1}\langle \mathbf{z}|\mathbf{z}\rangle\Delta^{-1}\Delta_R = \Delta_R\Delta^{-1}\Delta_R = \Delta_R, \qquad (4.26)$$

Hence one has $\mathbf{z}_1 = \hat{\mathbf{z}}$ and $\mathbf{z}_2 = \mathbf{z}_R$, or

$$\hat{\mathbf{z}} = \mathbf{z}.\Delta^{-1}\hat{\Delta}, \qquad \mathbf{z}_R = \mathbf{z}.\Delta^{-1}\Delta_R. \qquad (4.27)$$

The derivations become more transparent, if one introduces the notations $\Delta^{-1}\hat{\Delta} = \mathbf{P}$ and $\Delta^{-1}\Delta_R = \mathbf{1} - \mathbf{P}$ for the two projection matrices involved, and since $\mathbf{P} = \Delta^{-1}\hat{\Delta} = \Delta^{-1}(\hat{\Delta}\Delta^{-1})\Delta = \Delta^{-1}\mathbf{P}^\dagger\Delta$, the matrix $\mathbf{P}$ satisfies the relation (3.3) for a matrix corresponding to a self-adjoint operator P. It is hence evident that the projection matrix $\mathbf{P} = \Delta^{-1}\hat{\Delta}$ defined by the relation (4.19) is identical to the projection matrix in (4.5).

Instead of starting from the first relation (4.19) or the relation (4.21), Kalman has a very simple explicit recipe for the construction of the matrix $\Delta_R$ and hence also for the construction of $\hat{\Delta} = \Delta - \Delta_R$, which is built on the formula

$$\Delta_R = \mathbf{C}\,(\mathbf{C}^\dagger\Delta^{-1}\mathbf{C})^{-1}\mathbf{C}^\dagger, \qquad (4.28)$$

where $\mathbf{C}$ is an arbitrary matrix of order $n \times q$ such that the matrix $\mathbf{C}^\dagger\Delta^{-1}\mathbf{C}$ has an inverse. The proof follows from the fact that the matrix $\Delta^{-1}\Delta_R$ is now

automatically a projection matrix, since one has $\Delta^{-1}\Delta_R.\Delta^{-1}\Delta_R = \Delta^{-1}\mathbf{C}\,(\mathbf{C}^\dagger\Delta^{-1}\mathbf{C})^{-1}\,\mathbf{C}^\dagger\Delta^{-1}\mathbf{C}.\,(\mathbf{C}^\dagger\Delta^{-1}\mathbf{C})^{-1}\mathbf{C}^\dagger = \Delta^{-1}\mathbf{C}\,(\mathbf{C}^\dagger\Delta^{-1}\mathbf{C})^{-1}\mathbf{C}^\dagger = \Delta^{-1}\Delta_R$. From the exclusiveness relation (4.21), one obtains then the linear relation $\hat{\Delta}\,\Delta^{-1}\Delta_R = \mathbf{0}$, which implies that

$$\mathbf{L}' = \Delta^{-1}\Delta_R = \Delta^{-1}\mathbf{C}\,(\mathbf{C}^\dagger\Delta^{-1}\mathbf{C})^{-1}\mathbf{C}^\dagger, \tag{4.29}$$

$$\mathbf{L} = \mathbf{L}'\,(\Delta^{-1}\mathbf{C},\mathbf{0}) = (\Delta^{-1}\mathbf{C},\mathbf{0}) = (\mathbf{A}',\mathbf{0}), \tag{4.30}$$

where $\mathbf{A}' = \Delta^{-1}\mathbf{C}$ , and the linear relation is reduced to its standard form. Putting

$$\Delta^{-1} = \mathbf{d} = \begin{bmatrix} \mathbf{d}_{aa} & \mathbf{d}_{ab} \\ \mathbf{d}_{ba} & \mathbf{d}_{bb} \end{bmatrix}, \qquad \mathbf{C} = \begin{bmatrix} \mathbf{1}_q & \mathbf{0} \\ \mathbf{0} & \mathbf{0} \end{bmatrix}, \tag{4.31}$$

one obtains $\mathbf{C}^\dagger\Delta^{-1}\mathbf{C} = \mathbf{d}_{aa}$, which is a non-singular matrix, and further

$$\mathbf{A}' = \Delta^{-1}\mathbf{C} = \begin{bmatrix} \mathbf{d}_{aa} \\ \mathbf{d}_{ba} \end{bmatrix}, \tag{4.32}$$

which result shows that the matrix $\mathbf{A}'$ may be formed by taking the first q columns of the inverse matrix $\Delta^{-1}$ , in analogy with (2.25), and that the standard form may then be obtained by multiplying to the right by the matrix $\mathbf{d}_{aa}^{-1}$, so that

$$\mathbf{A} = \mathbf{A}'\,\mathbf{d}_{aa}^{-1} = \begin{bmatrix} \mathbf{1}_q \\ \mathbf{d}_{ba}\mathbf{d}_{aa}^{-1} \end{bmatrix}. \tag{4.33}$$

It is evident that it should be possible to derive the simple Kalman formula (4.18) from the generalized least square scheme outlined above. It follows from formula (4.19) that the projection matrix $\mathbf{P}$ for any self-adjoint projector P may be written in the form

$$\mathbf{P} = \langle \mathbf{z}|\mathbf{z}\rangle^{-1}\langle \mathbf{z}|\mathbf{P}\mathbf{z}\rangle = \mathbf{B}\{\mathbf{B}^\dagger\langle \mathbf{z}|\mathbf{z}\rangle\mathbf{B}\}^{-1}\mathbf{B}^\dagger\langle \mathbf{z}|\mathbf{z}\rangle = \mathbf{B}\{\mathbf{B}^\dagger\Delta\mathbf{B}\}^{-1}\mathbf{B}^\dagger\Delta, \tag{4.34}$$

from which one obtains

$$\hat{\Delta} = \Delta\,\mathbf{P} = \Delta\,\mathbf{B}\{\mathbf{B}^\dagger\Delta\mathbf{B}\}^{-1}\mathbf{B}^\dagger\Delta = \mathbf{D}\{\mathbf{D}^\dagger\Delta^{-1}\mathbf{D}\}^{-1}\mathbf{D}^\dagger, \tag{4.35}$$

where we have made the substitution $\Delta\,\mathbf{B} = \mathbf{D}$ ; here $\mathbf{D}$ is a matrix of order n x p. We note that the relation (4.35) has the same structure as the relation (4.28) for $\Delta_R$, and one can then repeat the same reasoning for the projector $\mathbf{Q} = \mathbf{1}\text{-}\mathbf{P}$ defining $\mathbf{z}_R$.

The Kalman scheme seems to be particularly convenient in refining data disturbed by a certain amount of "noise" by constructing a so-called "Kalman filter". For more details, the reader is referred to the original papers.

Some properties of the inner projection.- If A is a positive definite operator, $A > 0$, its *inner projection* A' with respect to a self-adjoint projector P is defined by the relation (1.30) or $A' = A^{1/2}PA^{1/2} \leq A$. If one uses the form (2.8) for the projector P and makes the substitution $\mathbf{g} = A^{1/2}\mathbf{f}$, one gets

$$A' = A^{1/2}PA^{1/2} = A^{1/2}|\mathbf{f}><\mathbf{f}|\mathbf{f}>^{-1}<\mathbf{f}|\,A^{1/2} = |\mathbf{g}><\mathbf{g}|A^{-1}|\mathbf{g}>^{-1}<\mathbf{g}|, \qquad (4.36)$$

where the last expression is very convenient, since it does not contain the square root $A^{1/2}$, and one has only to specify the elements in $\mathbf{g} = \{g_1, g_2, g_3, \ldots g_p\}$. It is easily shown that the expression provides a lower bound to A, even if the operator A has a finite negative part, i.e. has a finite number of negative eigenvalues, provided that the matrix $<\mathbf{g}|A^{-1}|\mathbf{g}>$ reflects this property [10]. It should be observed that the lower bound provided by (4.36) has been frequently used for determining lower bounds to the eigenvalues of the Hamiltonian operator [11]. If one puts $\mathbf{g} = \mathbf{z}\,\mathbf{B}$, one obtains also the alternative formula for the inner projection

$$A' = |\mathbf{z}>\mathbf{B}[\mathbf{B}^{\dagger}<\mathbf{z}|A^{-1}|\mathbf{z}>\mathbf{B}]^{-1}\mathbf{B}^{\dagger}<\mathbf{z}|, \qquad (4.37)$$

which is closely connected with the discussion given above. Putting A= 1 and using (4.36), one sees e.g. that the operator P defined by (4.36) is a lower bound to the identity operator.

## 5. The Search for Approximate Linear Dependencies in a Finite Basis Set

In most quantum-mechanical applications, one starts from a *non-orthogonal* basis $\mathbf{f} = \{f_1, f_2, f_3, \ldots f_n\}$ of order n, formed e.g. from the atomic orbitals of the atoms involved in the system, having a metrix matrix $\Delta = <\mathbf{f} \mid \mathbf{f}> = \mathbf{1} + \mathbf{S}$, where the so-called *overlap matrix* **S** is non-vanishing and not necessarily small. In the following, it is practical to assume that all such bases are normalized to unity, so that, for the diagonal elements, one has $<f_k|\, f_k> = 1$, which also means $S_{kk} = 0$ and that $\mathrm{Tr}\,\Delta = n$. It is an interesting feature of many bases **f** that, even if the elements $f_k$ are linearly independent from a strictly mathematical point of view, they may show *approximate linear dependencies* in a computation with a finite number of significant figures, which means that e.g. the secular equation

$$|<\mathbf{f}|H - z.1|\mathbf{f}>| = 0, \qquad (5.1)$$

is identically vanishing for all values of the variable z , which makes the relation meaningless [12]. In such a case, the eigenvalue problem has to be reformulated [13].

Orthonormalization procedures: symmetric and canonical orthonormalization. - Since any orthonormal basis $\varphi$ with the property $<\varphi|\varphi> = \mathbf{1}$ is free from approximate linear dependencies, the ideal thing would certainly be to work only with an *orthonormalized basis* obtained from the original set **f**. In this

connection, there are three schemes available: the successive, the symmetric, and the canonical orthonormalization procedures. The succesive orthonormalization scheme due to Schmidt may be carried out in practice by *succesive inversion* of the matrix $\langle \mathbf{f}|\mathbf{f}\rangle$ according to formula (2.23) starting out e.g. in the upper left-hand corner, but one finds very quickly that the approximate linear dependencies will show up and destroy the accuracy of the procedure. Another drawback is that the elements are handled successively and not treated "democratically", i.e. on the same footing. In order to avoid this problem, the author constructed the *symmetric orthonormalization* [14] based on the formula

$$\varphi = \mathbf{f}\langle \mathbf{f}|\mathbf{f}\rangle^{-1/2} = \mathbf{f}\,(\mathbf{1}+\mathbf{S})^{-1/2}. \tag{5.2}$$

The proof follows from the fact that

$$\langle \varphi\,|\varphi\rangle = \langle \mathbf{f}\,\Delta^{-1/2}|\mathbf{f}\,\Delta^{-1/2}\rangle = \Delta^{-1/2}\langle \mathbf{f}|\mathbf{f}\rangle\Delta^{-1/2} = \mathbf{1}. \tag{5.3}$$

The last factor in (5.2) may be expanded in a power series in $\mathbf{S}$, provided that the overlap matrix $\mathbf{S}$ is sufficiently small, i.e. $-\mathbf{1} < \mathbf{S} < +\mathbf{1}$, but - in the general case - one has to use the standard definition of a square root. Let $\mathbf{U}$ be the unitary matrix which brings the self-adjoint matrix $\Delta$ to diagonal form $\mu$ with the elements $\mu_k > 0$, so that

$$\mathbf{U}^{\dagger}\Delta\,\mathbf{U} = \mu, \qquad \Delta = \mathbf{U}\mu\,\mathbf{U}^{\dagger}, \qquad \Delta^{-1/2} = \mathbf{U}\mu^{-1/2}\,\mathbf{U}^{\dagger}. \tag{5.4}$$

This scheme is mathematically correct, and it works also in practice provided that all the eigenvalues $\mu_k$ have the number of significant figures required - otherwise it will break down. One usually refers to the smallest eigenvalue $\mu_1$ of the matrix $\Delta = \langle \mathbf{f}|\mathbf{f}\rangle$ as the *measure of linear independence* of the basis $\mathbf{f} = \{f_1, f_2, f_3, \ldots f_n\}$. It is evident that if the number $\mu_1$ is so small that it does not have the number of siginificant figures required in the computation, one is faced with an *approximate linear dependency*. It is clear that the small eigenvalues $\mu_k$ will influence also the symmetric orthonormalization, as may be seen from the relation

$$\varphi = \mathbf{f}\,\Delta^{-1/2} = \mathbf{f}\,\mathbf{U}\mu^{-1/2}\,\mathbf{U}^{\dagger}. \tag{5.5}$$

It is evident that the set $\chi = \varphi\,\mathbf{U}$ is going to be orthonormal, and the relation

$$\chi = \mathbf{f}\,\mathbf{U}\mu^{-1/2}, \quad \text{or} \quad \chi_k = (\mu_k)^{-1/2}\sum_{\alpha} f_{\alpha}\,U_{\alpha k}, \tag{5.6}$$

forms the basis for the method of *canonical orthonormalization* [15]. If the eigenvalues of $\Delta$ are arranged in increasing order, so that $\mu_1 \leq \mu_2 \leq \mu_3 \leq \ldots\ldots \leq \mu_n$, then the orthonormal set $\chi = \{\chi_1, \chi_2, \chi_3, \ldots \chi_n\}$ is arranged in a natural order after decreasing coefficients for $f_{\alpha}$. If $q$ of the eigenvalues $\mu_k$ are so small that

the corresponding functions $\chi_k$ cannot be used in the computations, then they have to be omitted, which means that one replaces the original basis $\mathbf{f}$ or order $n$ by a canonical basis $\chi'$ of order $p = (n-q)$, and in this way one has eliminated the approximate linear dependencies in the eigenvalue problem. Before the time of the large electronic computers, this approach had the drawback that one had to diagonalize the matrix $\Delta$ to find its eigenvalues, and one tried often to construct alternative approaches. The importance of the canonical basis will be further emphasized in the next section. For a review of the orthonormalization procedures, the reader is referred elsewhere [16].

In Sec. 3 we made use of the well-known definition that an arbitrary matrix is said to have the *rank* $(n-q)$ if all its principal minors of order $(q-1)$ are vanishing whereas this is not true for all principal minors of order $q$, which implies that the matrix has exactly $q$ vanishing eigenvalues. Considering the occurrence of the approximate linear dependencies, we will extend this definition and say that the metric matrix $\Delta = \langle \mathbf{f} \mid \mathbf{f} \rangle$ has the *approximate rank* $(n-q)$ provided that $q$ of its eigenvalues $\mu_k$ are either exactly or approximately vanishing. We note that, if the exactly vanishing eigenvalues $\mu_k = 0$ are associated with a number of hyperplanes in the space spanned by the elements $\mathbf{f} = \{f_1, f_2, f_3, \ldots f_n\}$, the almost vanishing eigenvalues $\mu_k \approx 0$ indicate the existence of *approximate hyperplanes* which may also be of essential interest.

Some theorems about the minors. - It is evident that the minors defined in (3.9) must play a fundamental role in the search for exact and approximate linear dependencies. If one considers a specific set $\mathbf{f} = \{f_1, f_2, f_3, \ldots f_n\}$ and its metric matrix $\Delta = \langle \mathbf{f} | \mathbf{f} \rangle$, the norm in square of any selection $\mathbf{g}$ of $m$ elements equals - according to (2.17) - the associated minor of order $m$ : $||\mathbf{g}||2 = |\langle \mathbf{g} | \mathbf{g} \rangle|$.

It is now possible to obtain bounds for these minors. The metric matrix $\langle \mathbf{g} | \mathbf{g} \rangle$ of order $m$ is a self-adjoint matrix, which may be brought to diagonal form $\nu$ by means of a unitary transformation $V$, so that one has

$$V^\dagger \langle \mathbf{g} | \mathbf{g} \rangle V = \nu, \quad \langle \mathbf{g} | \mathbf{g} \rangle = V \, \nu \, V^\dagger, \quad |\langle \mathbf{g} | \mathbf{g} \rangle| = |V| \, |\nu| \, |V^\dagger| = |\nu| , \qquad (5.7)$$

which means that the determinant $|\langle \mathbf{g} | \mathbf{g} \rangle|$ has a value given by the product of the eigenvalues $\nu_1, \nu_2, \nu_3, \ldots \nu_m$. At this point, one observes that the matrix $\langle \mathbf{g} | \mathbf{g} \rangle$ is a submatrix of the matrix $\Delta = \langle \mathbf{f} | \mathbf{f} \rangle$, and one has the well-known theorem [18] that the eigenvalues $\nu_k$ are upper bounds to the eigenvalues $\mu_1, \mu_2, \mu_3, \ldots \mu_m$, in order from below, so that $\nu_k > \mu_k$ for $k = 1,2,3,\ldots m$. For all the minors $|\langle \mathbf{g} | \mathbf{g} \rangle|$ of order $m$ one has hence the inequality

$$|\langle \mathbf{g} | \mathbf{g} \rangle| \geq \mu_1 . \, \mu_2 . \, \mu_3 . \ldots \mu_m , \qquad (5.8)$$

and, in the same way, one shows that all the minors of order m are smaller than the product of the m largest eigenvalues $\mu_k$ of the matrix $\Delta = \langle \mathbf{f}\mathbf{f} \rangle$ . These inequalities will be of value in the next secion.

## 6. On the Search for Linear Relations by Means of Ordinary and Canonical Regression Analysis

The principles of regression analysis. -In this section we will consider *observations* of sets of complex or most often *real numbers* which may occur in physics, chemistry, statistics, econometrics, and other sciences. Each observation is assumed to consist of m numbers $z_{ki}$ for i =1,2,3...m, which are gathered in a column vector $\mathbf{z}_k$ of order m, whereas the total set of data consists of n such vectors $\mathbf{Z} = \{\mathbf{z}_1, \mathbf{z}_2, \mathbf{z}_3, ..., \mathbf{z}_n\}$, where the numbers form a rectangular matrix of order m x n. We note that, since the elements $\mathbf{z}_k$ are now column vectors, we have denoted them by fat symbols, and - in the following - we will change the notations accordingly, even if the principles of the theory are the same. The handling of data associated with a large number of observations belongs to the field of *statistics*, and we note that it is customary to evaluate the average value $\bar{z}_k$ as well as the average quadratic mean $\Delta z_k$,which are defined through the relations:

$$\bar{z}_k = (1/m) \Sigma_i \, z_{ki}, \quad (\Delta z_k)^2 = (1/m) \Sigma_i \, (z_{ki} - \bar{z}_k)^2, \tag{6.1}$$

in analogy with (1.39-40). Instead of the original raw data, we will in the following use only so-called *normalized data* defined through the relation

$$(z_{ki})_{norm} = (z_{ki} - \bar{z}_k)) / (\Delta z_k). \tag{6.2}$$

provided, of course, that $\Delta z_k \neq 0$. A characteristic feature of the normalized data is hence that, if one sums over all the elements of a column vector $\mathbf{z}_k$, then one gets zero, whereas, if one sums over their squares, one gets the number 1 . In the following, we will assume that all data have been normalized in this way in advance. We note further that, in many fields, it is customary to make *probability assumptions* about the distribution of the normalized data around the average value, whereas we will make *no* such assumptions here.

It is evident that the vectors $\mathbf{z}_k$ are elements of a vector space $\mathbf{Z} = \{\mathbf{z}\}$ of order n, and that this space is a subspace of a larger vector space of order m. Hence one has always $n \leq m$ - otherwise one would automatically have (m-n) linear relations. The main problem is now whether there are any exact or approximate *linear relations* between the vectors $\{\mathbf{z}_1, \mathbf{z}_2, \mathbf{z}_3, ..., \mathbf{z}_n\}$, and this problem may now be tackled by means of the methods of linear algebra by investigating the existence of exact or approximate linear dependencies within the set $\mathbf{Z} = \{\mathbf{z}_1, \mathbf{z}_2, \mathbf{z}_3, ..., \mathbf{z}_n\}$. It is clear that, even if this *data analysis* reveals the occurrence of such linear relations, the deeper reason for the existence of such

relations has to be found by *system analysis* of the concepts of the sciences underlying the data themselves, in the same way as quantum theory and its conceptual framework was the underlying science for the data discussed in some of the previous sections.

In studying the subspace $\mathbf{Z} = \{\mathbf{z}\}$ of order $n$, we will assume that it has a binary product defined by the relation

$$\langle \mathbf{z}_1 | \mathbf{z}_2 \rangle = \mathbf{z}_1^\dagger \mathbf{z}_2 = \Sigma_i \; z_{1i} \, z_{2i}, \tag{6.3}$$

in analogy with (2.3), where the index i in the sum goes from 1 to $m$. We note that elements $\mathbf{z}_k$ are normalized so that $\langle \mathbf{z}_k | \mathbf{z}_k \rangle = 1$. In attacking the problem of the existence of exact or approximate linear dependencies, one starts by studying the metric matrix $\Delta = \langle \mathbf{z} | \mathbf{z} \rangle$ of order $n \times n$ with the elements $\Delta_{kl} = \langle \mathbf{z}_k | \mathbf{z}_l \rangle$ and having the exact or approximate rank $p = (n-q)$, where the number $q$ is determined either by one of the methods outlined in the previous section or below. For the sake of simplicity, we will assume that the matrix $\Delta$ is positive definite, so that $\Delta = \langle \mathbf{z} | \mathbf{z} \rangle > \mathbf{0}$, which means that there are no exact linear dependencies. We note that in many fields, as e.g. econometrics, the metric matrix $\Delta$ is referred to as the *covariance matrix*.

In studying the data, we will further assume that the vectors $\mathbf{Z} = \{\mathbf{z}_1, \mathbf{z}_2, \mathbf{z}_3, ..., \mathbf{z}_n\}$ may be divided into two groups $\mathbf{X} = \{\mathbf{x}_1, \mathbf{x}_2, \mathbf{x}_3, ..., \mathbf{x}_q\}$ and $\mathbf{Y} = \{\mathbf{y}_1, \mathbf{y}_2, \mathbf{y}_3, ..., \mathbf{y}_p\}$, where $p = n-q$ and the latter group of vectors is automatically linarly independent. In the *regression analysis* developed during the last hundred years [19] , the vectors in $\mathbf{X}$ are considered as trial vectors or so-called *regressands*, which are going to be expanded in terms of the vectors in the fixed basis $\mathbf{Y}$, called *regressors* . In some problems, e.g. curve fitting by means of the least square method, one knows which vectors should be chosen as the fixed basis $\mathbf{Y}$, and the problem is then easily solved. In other problems, one does not know from the very beginning which vectors in $\mathbf{Z}$ are most conveniently assigned to each group, and, if one tries all possible assignments, one gets a *complete regression analysis*. If the subspace $\mathcal{Y}$ spanned by the basis $\mathbf{Y}$ is described by the projector

$$P_Y = |\mathbf{Y}\rangle\langle\mathbf{Y}|\mathbf{Y}\rangle^{-1}\langle\mathbf{Y}|, \tag{6.4}$$

given by (2.8), then it is possible to divide every trial vector $\mathbf{x}_k$ into a projection $\mathbf{x}_k' = P_Y \mathbf{x}_k$ on $\mathbf{Y}$ and a remainder $\mathbf{r}_k = (1-P_Y)\,\mathbf{x}_k$ . This scheme corresponds to the use of the least square method, and we note that $\mathbf{r}_k$ is automatically orthogonal to $\mathbf{x}_k'$ as well as to the entire subspace spanned by the vectors in $\mathbf{Y}$.

For the set $\mathbf{X} = \{\mathbf{x}_1, \mathbf{x}_2, \mathbf{x}_3, ..., \mathbf{x}_q\}$, one gets in the same way

$$\mathbf{X} = \mathbf{X}' + \mathbf{R} = P_Y \mathbf{X} + (1-P_Y)\mathbf{X}, \tag{6.5}$$

where the remainder $\mathbf{R} = (1-P_Y)\mathbf{X}$ has the metric matrix

$$\langle \mathbf{R}|\mathbf{R}\rangle = \langle (1-P_Y)\mathbf{X}|(1-P_Y)\mathbf{X}\rangle =$$

$$= \langle \mathbf{X}|(1-P_Y)|\mathbf{X}\rangle = \langle \mathbf{X}|\mathbf{X}\rangle - \langle \mathbf{X}|\mathbf{Y}\rangle\langle \mathbf{Y}|\mathbf{Y}\rangle^{-1}\langle \mathbf{Y}|\mathbf{X}\rangle. \qquad (6.6)$$

In practice, this regression analysis is simplified by the fact that, according to (2.25) and (2.27), the columns of the inverse matrix $\mathbf{d} = \Delta^{-1}$ form the linear relations under study, and one has then only to multiply them by the matrix $\langle \mathbf{R}|\mathbf{R}\rangle = \mathbf{d}_{aa}^{-1}$ to get the standard form desired. In the following it is convenient to define the "least square error" $\rho(\mathbf{X},\mathbf{Y})$ corresponding to this particular assignment by the norm of $\mathbf{R}$ in square :

$$\rho(\mathbf{X},\mathbf{Y}) = ||\mathbf{R}||^2 = |\langle \mathbf{R}|\mathbf{R}\rangle| = |\langle \mathbf{X}|\mathbf{X}\rangle - \langle \mathbf{X}|\mathbf{Y}\rangle\langle \mathbf{Y}|\mathbf{Y}\rangle^{-1}\langle \mathbf{Y}|\mathbf{X}\rangle| =$$

$$= ||\mathbf{Z}||^2 / ||\mathbf{Y}||^2 = |\langle \mathbf{Z}|\mathbf{Z}\rangle| \; / \; |\langle \mathbf{Y}|\mathbf{Y}\rangle| \,, \qquad (6.7)$$

where the last transformation is obtained by using the relation (2.24). One sees directly that, since the numerator is the same for all partitions , one gets the smallest "least square error" for the partitioning where the minor $|\langle \mathbf{Y}|\mathbf{Y}\rangle|$ has its *largest* possible value, i.e. when one has chosen the regressors forming the basis in this approach to be as linearly independent as possible. In total there are $\binom{m}{q}$ assignments of the vectors in $\mathbf{Z}$ into two groups $\mathbf{X}$ and $\mathbf{Y}$, and - in a complete regression analysis - one is supposed to calculate all the corresponding errors $\rho(\mathbf{X},\mathbf{Y})$ and select the assignment, which gives the smallest error. For the sake of simplicity, we will assume that this happens only for one special assignment $\mathbf{Z} = (\mathbf{X}_S, \mathbf{Y}_S)$, in which case one has the linear relation

$$\mathbf{X}'_S - \mathbf{Y}_S\langle \mathbf{Y}_S|\mathbf{Y}_S\rangle^{-1}\langle \mathbf{Y}_S|\mathbf{X}_S\rangle = \mathbf{0}, \qquad (6.8)$$

or in the standard form (2.14)

$$(\mathbf{X}'_a, \mathbf{Y}_a)\begin{bmatrix} \mathbf{1} \\ -\langle \mathbf{Y}_S|\mathbf{Y}_S\rangle^{-1}\langle \mathbf{Y}_S|\mathbf{X}_S\rangle \end{bmatrix} = \mathbf{0}. \qquad (6.9)$$

If there are several minimal error quantities $\rho(\mathbf{X},\mathbf{Y})$ which are the same, there are obviously several linear relations possible, and, in this case, the least square method in its original form does not give any clue how one may select one relation which is better than the other(s), and one may then have to consider several possibilities in the succeeding system analysis. It is also clear that, by diving the elements in the set $\mathbf{Z}$ into regressands $\mathbf{X}$ and regressors $\mathbf{Y}$, they are not treated in a "democratic" or equivalent way giving the same importance to all the elements of the set $\mathbf{Z}$.

A "democratic" regression analysis.- In order to approach this problem, we will start by assuming that we will always choose the first $q$ elements of $\mathbf{Z}$ as the regressors, but that we instead change the order of the elements of $\mathbf{Z}$ by means of *permutations* , so that one has $\mathbf{Z}' = \mathbf{ZV}$, where $\mathbf{V}$ is a permutation matrix consisting

only of the elements 1 and 0. Instead of varying the partitions, one can now vary the permutation matrix **V**, and, observing that the permutation matrices **V** are always special cases of unitary matrices **U**, one can now carry out these variations *continuously* by varying the unitary matrix **U** in the relations

$$\mathbf{Z'} = \mathbf{ZU}, \quad \langle \mathbf{Z'}|\mathbf{Z'}\rangle = \mathbf{U}^\dagger\langle \mathbf{Z}|\mathbf{Z}\rangle\mathbf{U}, \qquad |\langle \mathbf{Z'}|\mathbf{Z'}\rangle| = |\langle \mathbf{Z}|\mathbf{Z}\rangle|, \tag{6.10}$$

In this approach, one treats all the elements of **Z** in an equivalent way, and one can now apply the least square method to a partition, where the "regressands" **Y'** are the last p elements of **Z' = ZU**. Again one will get a smallest "least square error", provided that the determinant $|\langle \mathbf{Y'}|\mathbf{Y'}\rangle|$ of the $p = (n-q)$ elements is as large as possible. One can now use the theorem (5.8) and its extension in determinant theory, which says that the largest possible value of a minor of order p is equal to the product of the p largest eigenvalues of the associated matrix. Hence the optimum choice of the unitary transformation **U** is given by the matrix U which brings the matrix $\langle \mathbf{z}|\mathbf{z}\rangle$ to diagonal form, so that

$$\mathbf{U}^\dagger \langle \mathbf{z}|\mathbf{z}\rangle \mathbf{U} = \mu, \tag{6.11}$$

where it is now important that the column vectors in **U** are arranged in such an order that the diagonal elements in $\mu$ are arranged in increasing order $0 < \mu_1 \leq \mu_2 \leq \ldots \leq \mu_n$. According to the generalized least square method developed in Sec. 4, one utilizes the projector **P** associated with the subset **Y'** to decompose the original set **Z** into two orthogonal components. By combining the generalized least square method with the unitary transformations in the eigenvalue theory, it is hence possible to treat all the elements of **Z** in an equivalent way, and we will now study this approach in somewhat greater detail.

The canonical regression ananlysis.- In studying the properties of the metric matrix $\Delta = \langle \mathbf{z}|\mathbf{z}\rangle$, we will now write relation (6.11) in the various forms:

$$\mathbf{U}^\dagger \Delta \mathbf{U} = \mu, \quad \Delta \mathbf{U} = \mathbf{U}\mu, \quad \Delta = \mathbf{U}\mu\mathbf{U}^\dagger, \quad \Delta^{-1} = \mathbf{U}\mu^{-1}\mathbf{U}^\dagger, \tag{6.12}$$

and introduce the following partitionings:

$$\mathbf{U} = (\mathbf{U_a}, \mathbf{U_b}), \qquad \mu = \begin{bmatrix} \mu_a & 0 \\ 0 & \mu_b \end{bmatrix}, \qquad \mathbf{U}^\dagger = \begin{bmatrix} \mathbf{U_a}^\dagger \\ \mathbf{U_b}^\dagger \end{bmatrix}, \tag{6.13}$$

where $\mathbf{U_a}$ consists of the eigenvectors associated with the q lowest eigenvalues, which are gathered in the quadratic matrix of order q. From the second equation (6.12), one gets immediately the relations

$$\Delta \mathbf{U_a} = \mathbf{U_a}\mu_a, \quad \Delta \mathbf{U_b} = \mathbf{U_b}\mu_b. \tag{6.14}$$

From the unitary property $\mathbf{U}\mathbf{U}^\dagger = \mathbf{U}^\dagger\mathbf{U} = \mathbf{1}$, one gets further the two relations

$$U_a U_a^\dagger + U_b U_b^\dagger = 1\,, \quad \begin{bmatrix} U_a^\dagger U_a & U_a^\dagger U_b \\ U_b^\dagger U_a & U_b^\dagger U_b \end{bmatrix} = \begin{bmatrix} 1_a & 0 \\ 0 & 1_b \end{bmatrix}. \tag{6.15}$$

and from the last two equations (6.12) one obtains

$$\Delta = U\mu U^\dagger = U_a \mu_a U_a^\dagger + U_b \mu_b U_b^\dagger\,, \tag{6.16}$$

$$\Delta^{-1} = U\mu^{-1}U^\dagger = U_a \mu_a^{-1} U_a^\dagger + U_b \mu_b^{-1} U_b^\dagger \tag{6.17}$$

Let us now consider the transformation $Z' = ZU = \{zU_a, zU_b\} = \{z_a, z_b\}$, where

$$z_a = zU_a\,, \qquad z_b = zU_b\,. \tag{6.18}$$

In the following we will concentrate our interest solely on the second set $z_b = zU_b$, which form a set of p "regressands" having a maximum norm $||z_b||^2$, which equals the product of the p largest eigenvalues of $\Delta$. For the projector $P = P_b$ associated with the set $\{z_b\}$ of order $p = n\text{-}q$, one gets directly according to (2.8):

$$P = |z_b\rangle\langle z_b|z_b\rangle^{-1}\langle z_b| = |zU_b\rangle\langle zU_b|zU_b\rangle^{-1}\langle zU_b|$$

$$= |z\rangle U_b [U_b^\dagger \langle z|z\rangle U_b]^{-1} U_b^\dagger \langle z| = |z\rangle U_b \mu_b^{-1} U_b^\dagger \langle z|. \tag{6.19}$$

By using (3.1) and (6.16), one gets further for the associated projection matrix $\mathbf{P}$:

$$\mathbf{P} = \langle z|z\rangle^{-1}\langle z|P\,z\rangle = U_b \mu_b^{-1} U_b^\dagger \Delta = U_b U_b^\dagger\,, \tag{6.20}$$

For the projector $(1 - P)$ and its matrix, one obtains from the first relation (6.15) that

$$1 - \mathbf{P} = U_a U_a^\dagger\,, \tag{6.21}$$

and this implies also that the projector $(1 - P)$ is associated with the subset $z_a = zU_a$. In this particular case, one has hence $(1 - P) = P_a$, and we note further that the two projection matrices $\mathbf{P}_b = U_b U_b^\dagger$ and $\mathbf{P}_a = U_a U_a^\dagger$ are not only idempotent, complementary and mutually exclusive, as required by the general theory, but also self-adjoint.

We will now use the generalized least square method outlined in Sec. 4. By means of the projector P, it is then possible to decompose the set $\mathbf{z}$ into two orthogonal components $z = Pz + (1\text{-}P)z = \hat{z} + z_R$, where

$$\hat{z} = Pz = zP = z\,U_b U_b^\dagger\,, \quad z_R = (1\text{-}P)z = z(1\text{-}P)U = zU_a U_a^\dagger\,. \tag{6.22}$$

For the associated metric matrices, one obtains

$$\hat{\Delta} = \langle \hat{z} | \hat{z} \rangle = \langle z\, U_b U_b^\dagger | z\, U_b U_b^\dagger \rangle = U_b U_b^\dagger \langle z | z \rangle U_b U_b^\dagger = U_b \mu_b U_b^\dagger, \quad (6.23)$$

$$\Delta_R = \langle z_R | z_R \rangle = \langle z\, U_a U_a^\dagger | z\, U_a U_a^\dagger \rangle = U_a U_a^\dagger \langle z | z \rangle U_a U_a^\dagger = U_a \mu_a U_a^\dagger, \quad (6.24)$$

and, using (6.16), one checks easily the relation $\hat{\Delta} + \Delta_R = \Delta$. All the linear relations in the regression analysis are now given by the column vectors of the inverse matrix $\mathbf{d} = \Delta^{-1}$:

$$\Delta^{-1} = U_a \mu_a^{-1} U_a^\dagger + U_b \mu_b^{-1} U_b^\dagger , \quad (6.25)$$

where we can now concentrate our interest on the first q column vectors, which in order to give the linear relations in the standard form have to be multiplied by the matrix $\mathbf{d}_{aa}^{-1}$. We note that, according to (6.7), one gets for the associated least square error:

$$\rho_R = ||Z||^2 / ||Y'||^2 = |\langle Z|Z\rangle| / |\langle Y'|Y'\rangle| = |\Delta| / |\mu_b| = |\mu_a| = \mu_1 . \mu_2 . \mu_3 .. \mu_q, \quad (6.26)$$

where the right-hand side is the product of the q lowest eigenvalues of $\Delta$ and is hence *optimal* in the sense we have discussed before.

At this point it is interesting to observe that, if one introduces the canonical orbitals defined by (3.6), one gets directly $\mathbf{Z'} = \mathbf{ZU} = \chi \mu^{1/2}$ and particularly $\mathbf{z'}_b = \chi' \mu_b^{1/2}$, which means that the elements in the basis $\mathbf{z'}_b$ are proportional to the elements in the canonical basis $\chi'$. For each one of the vectors $\mathbf{z'}_k$, one has the relations $\mathbf{z'}_k = \chi_k \mu_k^{1/2}$ , which means that all elements $\mathbf{z'}_k$ are mutually orthogonal but have the norm square $||\mathbf{z'}_k||^2 = \mu_k$:

$$\mathbf{z'}_k = \chi_k \mu_k^{1/2}, \qquad ||\mathbf{z'}_k||^2 = \mu_k, \quad (6.27)$$

There is hence a close connection between the existence of the canonical basis $\chi'$ and the optimal regression analysis and, to emphasize this connection, one should perhaps refer to the latter as the *canonical regression analysis* . It is now clear that, if one of the eigenvalues $\mu_k$ tends to zero, one gets immediately a corresponding linear relation. This means also that, in order to determine the best approximate rank q, one has to study the lowest eigenvalues $0 < \mu_1 \leq \mu_2 \leq \ldots \leq \mu_q \leq \mu_{q+1} \leq \mu_{q+2} \leq \ldots$, and to stop the sequence when the eigenvalue $\mu_q$ is still sufficiently small but the next eigenvalue $\mu_{q+1}$ is too large to correspond to a reasonably small remainder.

It remains to study the linear relations $\hat{\mathbf{z}}\, \mathbf{L'} = 0$ connected with this scheme. Since one has $\hat{\mathbf{z}} = \mathbf{z}\, \hat{\mathbf{P}}$ , one gets directly

$$L' = P_R = U_a U_a^{\dagger}, \tag{6.28}$$

where the right-hand member is a matrix of order n x n. In order to reduce it to standard form, we will multiply it to the right by the matrix $U = (U_a, U_b)$ which gives

$$L'' = L' U = (U_a U_a^{\dagger} U_a, U_a U_a^{\dagger} U_b) = (U_a, 0) = \begin{bmatrix} U_{aa} & 0 \\ U_{ab} & 0 \end{bmatrix}, \tag{6.29}$$

and multiplying once more to the right by $U_{aa}^{-1}$, one gets finally

$$L = L' U \begin{bmatrix} U_{aa}^{-1} & 0 \\ 0 & 0 \end{bmatrix} = \begin{bmatrix} 1_a & 0 \\ U_{ab} U_{aa}^{-1} & 0 \end{bmatrix}, \tag{6.30}$$

which is the standard form desired.

It is remarkable that the linear algebra and the least square method have the same structure in so many different sciences, and that e.g. the *metric matrix* of physics occurs as the *covariance matrix* of econometrics [20] even if in the latter field the researchers have a completely different way of plotting and evaluating the results of their regression analysis [21]. Since the mathematical structure is the same, this diversity in the different approaches should lead to a valuable cross-fertilization between the different areas of the sciences where methods of this type are applicable.

A numerical example taken from econometrics.- In order to illustrate our approach numerically, we will choose an example from econometrics in which field the metric matrices - or covariance matrices - are usually of reasonably low order. Let us consider the example of order n = 5 given by Frisch [20], which has been treated as a test case by many later researchers, e.g. by Los [21]:

$$\Delta = \begin{bmatrix} 0.993576 & -0.121999 & 0.871663 & 1.135675 & -0.223826 \\ -0.121999 & 1.013902 & 0.881726 & -1.117290 & 0.213635 \\ 0.871663 & 0.881726 & 1.772628 & 0.028997 & -0.053500 \\ 1.135675 & -1.117290 & 0.028997 & 2.292407 & -0.424277 \\ -0.223826 & 0.213635 & -0.053500 & -0.424277 & 1.000000 \end{bmatrix} \tag{6.31}$$

which matrix we will treat in its original unnormalized form. For the eigenvalues $\mu$ one gets :

$$\mu = 0.00909508;\ 0.012154;\ 0.890106;\ 2.64503;\ 3.51613; \tag{6.32}$$

and it is clear that, in this case, one has q = 2. For the matrix $U_a$ of order 5 x 2 formed by the first two eigenvectors associated with the two lowest eigenvalues, one obtains

$$\mathbf{U_a} = \begin{bmatrix} -0.473539 & 0.660623 \\ -0.577009 & -0.536009 \\ 0.524104 & -0.0486306 \\ -0.0488635 & -0.589195 \\ 0.0248127 & 0.00991144 \end{bmatrix} \tag{6.33}$$

and, multipying to the right by $\mathbf{U_{aa}}^{-1}$, one gets finally

$$\mathbf{L} = \begin{bmatrix} 1 & 0 \\ 0 & 1 \\ -0.486585 & -0.508982 \\ -0.494137 & 0.490211 \\ -0.0119382 & -0.0332048 \end{bmatrix}, \tag{6.34}$$

which is the canonical and optimal linear relation desired. According to Los [23], there are 10 ordinary linear regressions, and the best one of them having the smallest value of $\rho(\mathbf{X},\mathbf{Y})$ according to (6.7) leads instead to the linear relation

$$\mathbf{L} = \begin{bmatrix} 1 & 0 \\ 0 & 1 \\ -0.484016 & -0.506409 \\ -0.491225 & 0.487522 \\ -0.0110484 & -0.033884 \end{bmatrix}, \tag{6.35}$$

which compares favorably with (6.34). This result depends on the fact that one of the regressions has a considerably smaller value of $\rho$ than the others. The special value of the *canonical regression analysis* becomes particularly clear when one has a very large number of regressions with about the same values of $\rho$.The author is indebted to Lic. Juan José Gonçalves Oreiro for carrying out the calculations reported in eqs. (6.33-35) and for his valuable help in constructing the software programs for performing optimal regression analysis for arbitrary values of $n$ and $q$ of limited orders.

The author would further like to express his sincere gratitude to Drs. Rudolf Kalman, Cornelis Los, Aris Spanos, and Ragnar Bentzel for valuable discussions about the least square method in connection with regression analysis held at a minisymposium at the University of Florida, October 23 -25, 1990.

System analysis and the evaluation of errors. - It has been emphasized above that, in many of the quantum mechanical applications, the approximate linear dependencies arise from the fact that - in the computations - one has to replace the exact numbers occurring in the theory by approximate numbers with a specified number of significant figures, and this means that the calculations are affected by *truncation errors*. It is clear that, in such a case, the least square method may be an excellent tool for studying the occurrence of linear dependencies, and that one may always check the results obtained by going to higher accuracy in the calculations.

In many of the experimental sciences, there are *measurement errors* and the question is how they may be eliminated. In many connections, one tries to consider the remainders or residuals in the least square methods as estimates of the errors

involved and use them to refine the data. However, in physics and chemistry there are both systematic errors and random errors, and the nature of the former may be clarified only by a deep-going study of both the underlying theory and the experimental set-up. The same thing applies also to the errors occurring in many other sciences based on statistics, e.g. medicine, sociology, and econometrics. This means that, in many sciences, one cannot make a reliable *error analysis* without additional basic assumptions. It goes without saying that *data-analysis* based on e.g. the least square method may be a valuable tool to get a first understanding of the structure of the data, but that it can never replace the true *system analysis* dealing with the theories of the system themselves. It should always be remembered that the least square method is a pure mathematical tool for handling data, which is independent of the underlying science, and that this is both the strength and the weakness of this approach.

## 7. Appendices

Appendix A: The inversion of a matrix by partitioning technique. - Let us consider the non-singular matrix $\mathbf{M}$ of order n x n in a partitioned form:

$$\mathbf{M} = \begin{bmatrix} \mathbf{M}_{aa} & \mathbf{M}_{ab} \\ \mathbf{M}_{ba} & \mathbf{M}_{bb} \end{bmatrix} , \qquad (A.1)$$

and let us evaluate its inverse matrix $\mathbf{M}^{-1}$ by solving the equation system $\mathbf{Mx} = \mathbf{y}$ in its partioned form

$$\begin{bmatrix} \mathbf{M}_{aa} & \mathbf{M}_{ab} \\ \mathbf{M}_{ba} & \mathbf{M}_{bb} \end{bmatrix} \begin{bmatrix} \mathbf{x}_a \\ \mathbf{x}_b \end{bmatrix} = \begin{bmatrix} \mathbf{y}_a \\ \mathbf{y}_b \end{bmatrix}, \qquad (A.2)$$

which corresponds to the relations

$$\begin{aligned} \mathbf{M}_{aa}\mathbf{x}_a + \mathbf{M}_{ab}\mathbf{x}_b &= \mathbf{y}_a, \\ \mathbf{M}_{ba}\mathbf{x}_a + \mathbf{M}_{bb}\mathbf{x}_b &= \mathbf{y}_b. \end{aligned} \qquad (A.3)$$

Solving $\mathbf{x}_b$ from the second equation, one obtains $\mathbf{x}_b = - \mathbf{M}_{bb}^{-1}\mathbf{M}_{ba}\mathbf{x}_a + \mathbf{M}_{bb}^{-1} \mathbf{y}_b$, and substituting this expression in the first equation one gets

$$( \mathbf{M}_{aa} - \mathbf{M}_{ab} \mathbf{M}_{bb}^{-1}\mathbf{M}_{ba} )\mathbf{x}_a = - \mathbf{M}_{ab} \mathbf{M}_{bb}^{-1} \mathbf{y}_b + \mathbf{y}_a . \qquad (A.4)$$

Introducing the notation $\mathbf{N}_{aa} = \mathbf{M}_{aa} - \mathbf{M}_{ab} \mathbf{M}_{bb}^{-1}\mathbf{M}_{ba}$, one gets the solution $\mathbf{x}_a = \mathbf{N}_{aa}^{-1}\mathbf{y}_a - \mathbf{N}_{aa}^{-1} \mathbf{M}_{ab} \mathbf{M}_{bb}^{-1} \mathbf{y}_b$, which relation is then substituted in the previous expression for $\mathbf{x}_b$. In this way, one obtains

$$\mathbf{x}_a = \mathbf{N}_{aa}^{-1}\mathbf{y}_a - \mathbf{N}_{aa}^{-1} \mathbf{M}_{ab} \mathbf{M}_{bb}^{-1} \mathbf{y}_b,$$

$$\mathbf{x}_b = - \mathbf{M}_{bb}^{-1}\mathbf{M}_{ba}\mathbf{N}_{aa}^{-1}\mathbf{y} + \mathbf{M}_{bb}^{-1}\mathbf{M}_{ba}\mathbf{N}_{aa}^{-1} \mathbf{M}_{ab} \mathbf{M}_{bb}^{-1} \mathbf{y}_b + \mathbf{M}_{bb}^{-1} \mathbf{y}_b , \qquad (A.5)$$

which gives

$$\mathbf{M}^{-1} = \begin{bmatrix} \mathbf{N}_{aa}^{-1} & ; & -\mathbf{N}_{aa}^{-1}\mathbf{M}_{ab}\mathbf{M}_{bb}^{-1} \\ -\mathbf{M}_{bb}^{-1}\mathbf{M}_{ba}\mathbf{N}_{aa}^{-1} & ; & \mathbf{M}_{bb}^{-1}+\mathbf{M}_{bb}^{-1}\mathbf{M}_{ba}\mathbf{N}_{aa}^{-1}\mathbf{M}_{ab}\mathbf{M}_{bb}^{-1} \end{bmatrix}, \quad (A.6)$$

i.e. the formula we have used in (2.25). If we instead solve for $\mathbf{x}_a$ first, and introduces the notation $\mathbf{N}_{bb} = \mathbf{M}_{bb} - \mathbf{M}\mathbf{M}_{aa}^{-1}\mathbf{M}_{ab}$, one gets the alternative solution

$$\mathbf{M}^{-1} = \begin{bmatrix} \mathbf{M}_{aa}^{-1}+\mathbf{M}_{aa}^{-1}\mathbf{M}_{ab}\mathbf{N}_{bb}^{-1}\mathbf{M}_{ba}\mathbf{M}_{aa}^{-1} & ; & -\mathbf{M}_{aa}^{-1}\mathbf{M}_{ab}\mathbf{N}_{bb}^{-1} \\ -\mathbf{N}_{bb}^{-1}\mathbf{M}_{ba}\mathbf{M}_{aa}^{-1} & ; & \mathbf{N}_{bb}^{-1} \end{bmatrix}. \quad (A.7)$$

Since the two expressions must be identical, one gets four identities of two different types, which are of fundamental importance in the partitioning technique in general:

$$\mathbf{N}_{aa}^{-1}\mathbf{M}_{ab}\mathbf{M}_{bb}^{-1} = \mathbf{M}_{aa}^{-1}\mathbf{M}_{ab}\mathbf{N}_{bb}^{-1}, \quad (A.8)$$

$$\mathbf{N}_{bb}^{-1} = \mathbf{M}_{bb}^{-1}+\mathbf{M}_{bb}^{-1}\mathbf{M}_{ba}\mathbf{N}_{aa}^{-1}\mathbf{M}_{ab}\mathbf{M}_{bb}^{-1}. \quad (A.9)$$

We note that by starting in one of the corners of the diagonal, one may invert a matrix in full by a series of successive use of the relations (A.5) or (A.6).

Appendix B. Calculation of the characteristic polynomial.- We will here briefly review some of the classical methods for calculating the characteristic polynomial $P(z)$, since they form the basis also for parts of the current approaches. In one method, one forms the powers of the original matrix $\mathbf{T}$ by repeated multiplications by $\mathbf{T}$ leading to the sequence

$$\mathbf{T}, \mathbf{T}^2, \mathbf{T}^3, \mathbf{T}^4, \ldots\ldots \mathbf{T}^{n-1}, \mathbf{T}^n, \quad (B.1)$$

evaluates the traces $s_p$ of all these matrices, so that

$$s_p = \mathrm{Tr}\,\mathbf{T}^p, \quad (B.2)$$

and uses the well-known connection formulas [24]:

$$\begin{aligned} &\mathrm{Tr}\;\mathbf{T} = s_1, \\ &\mathrm{Tr}_2\,\mathbf{T} = (s_1^2-s_2)/2, \\ &\mathrm{Tr}_3\,\mathbf{T} = (s_1^3-3s_1s_2+2s_1)/3!, \\ &\mathrm{Tr}_4\,\mathbf{T} = (s_1^4-6s_1^2s_2+8s_1s_3-6s_4-3s_2^2)/4!, \\ &\ldots\ldots\ldots\ldots\ldots\ldots\ldots\ldots\ldots\ldots\ldots\ldots\ldots\ldots\ldots\ldots\ldots\ldots\ldots\ldots \end{aligned} \quad (B.3)$$

We note, however, that the formation of the sequence (B.1) involves $n^4$ multiplications and a storage of $n^3$ results, which becomes a rather formidable computational problem when $n$ increases.

In many quantum-mechanical applications, the number $n$ is very large, and one has then to use a somewhat different approach, in which one does not store

quadratic matrices of order n x n but only column vectors of order n. Starting from an arbitrary vector $\tau$ of order n, one may now form a sequence of vectors

$$\tau_0 = \tau,\ \tau_1,\ \tau_2,\ \tau_3,\ \tau_4,\ \ldots\ldots\tau_n, \qquad (B.4)$$

by successive multiplication by the matrix **T**, so that $\tau_k = \mathbf{T}\tau_{k-1} = \mathbf{T}^k\tau$ . According to the Cayley-Hamilton theorem, one knows that the matrix **T** satisfies its own characteristic equation:

$$P(\mathbf{T}) = a_0.\mathbf{1} + a_1.\mathbf{T} + a_2.\mathbf{T}^2 + a_3.\mathbf{T}^3 + \ldots\ldots\ldots + a_n.\mathbf{T}^n = \mathbf{0}, \qquad (B.5)$$

which also gives the relation $P(\mathbf{T})\,\tau = \mathbf{0}$, or

$$\tau_0.a_0 + \tau_1.a_1 + \tau_2.a_2 + \tau_3.a_3 + \ldots\ldots\ldots + \tau_n.a_n = \mathbf{0}, \qquad (B.6)$$

where $a_n = (-1)^n$. At this point, it is convenient to arrange the first n vectors in the sequence (B.4) into a quadratic matrix $\Omega = \{\tau_0, \tau_1, \tau_2, \tau_3, \tau_4, \ldots\ldots\tau_{n-1}\}$ of order n and the unknown coefficients $a_0,\ a_1, a_2, a_3, \ldots\ldots a_{n-1}$ into a column matrix **a** of order n, in which case one may write relation (B.6) in the form

$$\Omega\,\mathbf{a} = (-1)^{n-1}\tau_n\,, \qquad (B.7)$$

which is an equation system which may be solved by any standard method, e.g. Gaussian elimination.

The vectors (B.4) are said to form a *Kryloff basis* , and the approach is straight-forward provided that the vectors in (B.4) are linearly independent so that $\Omega$ has an inverse; otherwise one does not get all the coefficients $a_k$, and one has to start over again from another trial vector $\tau$.

This approach may be further simplified if the matrix T is self-adjoint, so that $\mathbf{T}^\dagger = \mathbf{T}$. In addition to the vectors (B.4), one now forms the numbers

$$\tau_k^\dagger\,\tau_l = (\tau^\dagger\,\mathbf{T}^k)(\,\mathbf{T}^l\tau\,) = \tau^\dagger\,\mathbf{T}^{k+l}\,\tau = t_{k+l}, \qquad (B.8)$$

which leads to the sequence $t_0, t_1, t_2, t_3, \ldots, t_{2n-1}$ of 2n numbers. Multiplying the relation (B.6) successively by $\tau_0^\dagger, \tau_1^\dagger, \tau_2^\dagger, \ldots, \tau_{n-1}^\dagger$, one gets a series of equations

$$\begin{aligned}
&t_0a_0 + t_1a_1 + t_2a_2 + t_3a_3 + \ldots\ldots\ldots + t_{n-1}a_{n-1} = (-1)^{n-1}\ t_n,\\
&t_1a_0 + t_2a_1 + t_3a_2 + t_4a_3 + \ldots\ldots\ldots + t_n\ a_{n-1} = (-1)^{n-1}\ t_{n+1},\\
&t_2a_0 + t_3a_1 + t_4a_2 + t_5a_3 + \ldots\ldots\ldots + t_{n+1}a_{n-1} = (-1)^{n-1}\ t_{n+2},\\
&\ldots\ldots\ldots\ldots\ldots\ldots\ldots\ldots\ldots\ldots\ldots\ldots\ldots\ldots\ldots\ldots\ldots\ldots\ldots\ldots\\
&t_{n-1}a_0 + t_na_1 + t_{n+1}a_2 + t_{n+2}a_3 + \ldots + t_{2n-2}a_{n-1} = (-1)^{n-1}\ t_{2n-1}, \qquad (B.9)
\end{aligned}$$

which may again be solved by any standard method, e.g. Gaussian elimination. The matrix of the t-coefficients in the left-hand member form a matrix of the type

$$\begin{bmatrix} t_0 & t_1 & t_2 & \dots & t_{n-1} \\ t_1 & t_2 & t_3 & \dots & t_n \\ \dots & \dots & \dots & \dots & \dots \\ t_{n-1} & t_n & t_{n+1} & \dots & t_{2n-2} \end{bmatrix} \qquad \text{(B.10)}$$

which is often referred to as a *Hankel matrix* , and we note that there is a rich literature about these matrices and their determinants.

Today there are special programs for evaluating the characterisitc polynomial of a given matrix **T** available both on the large-scale electronic computers and on the personal computers, which are useful in any form of data analysis, but the methods outlined above may still be of value in a system analysis where numerical results are not yet available.

Appendix C. Rough estimates of the eigenvalues of **T**.- Since the eigenvalues play an essential role in the determination of the exact or approximate rank of an arbitrary matrix **T** of order n, it is often worthwhike to try to give a rough estimate of their positions in the complex plane. Let us denote the eigenvalues of **T** by $\lambda_i$ and the associated eigenvectors by $\mathbf{c}_i$, so that $\mathbf{T}\,\mathbf{c}_i = \lambda_i\,\mathbf{c}_i$ , or $(\mathbf{T} - \lambda_i.\mathbf{1})\,\mathbf{c}_i = \mathbf{0}$. One may write the last relation in the form

$$\Sigma_l\,(T_{kl} - \lambda_i.\delta_{kl})c_{li} = (T_{kk} - \lambda_i)c_{ki} + \Sigma_{l\neq k}\,T_{kl}\,c_{li} = 0, \qquad \text{(C.1)}$$

for all values of k. For each value of i, the vector components $c_{li}$ have one absolutely largest value, which is assumed for l = p, so that $|c_{li}| \leq |c_{pi}|$. Putting k = p in (C.1) and dividing by $c_{pi}$, one obtains

$$T_{pp} - \lambda_i = - \Sigma_{l\neq p}\,T_{pl}\,c_{li} \,/\, c_{ip}, \qquad \text{(C.2)}$$

which gives the rough estimate

$$| T_{pp} - \lambda_i | < \Sigma_{l\neq p}\,|T_{pl}| = r_p, \qquad \text{(C.3)}$$

which is known as *Hadamard's inequality* . The circle $| z - T_{pp}| = r_p$ in the complex plane is called a Hadamard circle and will be denoted by $C_p$. In order to make the theorem really useful, it is necessary to break the connection between the indices i and p, since one does not know the eigenvectors at all. This is accomplished by observing that the eigenvalues $\lambda_i$ are roots to the characteristic polynomial P(z) = 0, and as such continuous functions of the matrix elements $T_{kl}$. In this way, one obtains the Lévy-Hadamard-Gerschgoring theorem saying that all the eigenvalues of **T** lie inside the closed domain formed by the Hadamard circles $C_1$, $C_2$, $C_3$, ..., $C_n$. If the circles are not intersecting, there is exactly one eigenvalue within each circle; if m circles are intersecting, there are exactly m eigenvalues inside the

closed connected domain formed by these circles. This theorem is easily proved by using continuity arguments.

The question is now whether one can improve this estimate in any way. For this purpose, we will consider a matrix $\mathbf{T}$ which - for the sake of simplicity - is assumed to be normal so that $\mathbf{T}^\dagger\mathbf{T} = \mathbf{T}\mathbf{T}^\dagger$. Let $\alpha$ be an arbitrary complex number, and let $\lambda_\alpha$ be the eigenvalue which is closest to $\alpha$. The matrix $(\mathbf{T} - \alpha.\mathbf{1})^\dagger(\mathbf{T}-\alpha.\mathbf{1})$ is self-adjoint and positive definite and has the eigenvalues $|\lambda_i - \alpha|^2$ of which $|\lambda_\alpha - \alpha|^2$ is the smallest one. This implies that one has the matrix inequality

$$(\mathbf{T} - \alpha.\mathbf{1})^\dagger(\mathbf{T}-\alpha.\mathbf{1}) \geq |\lambda_\alpha - \alpha|^2 .\mathbf{1}. \qquad (C.4)$$

Putting $\alpha = T_{pp}$, one gets directly $(\mathbf{T} - T_{pp}.\mathbf{1})^\dagger(\mathbf{T}-T_{pp}.\mathbf{1}) \geq |\lambda_\alpha - T_{pp}|^2 .\mathbf{1}$; for the pp-component of this relation one gets in particular

$$\Sigma_l (T_{pl} - T_{pp}.\delta_{pl})^*(T_{lp} - T_{pp}.\delta_{lp}) \geq |\lambda_\alpha - T_{pp}|^2 , \qquad (C.5)$$

for the eigenvalue $\lambda_\alpha$ which is closest to $T_{pp}$. Hence one gets the inequality

$$|\lambda_\alpha - T_{pp}| \leq ( \Sigma_{l\neq p}|T_{pl}|^2)^{1/2} = w_p, \qquad (C.6)$$

where the so-called *Weinstein radius* $w_p$ is usually considerably smaller than the Hadamard radius $r_p$. The circle $| z-T_{pp}| = w_p$ in the complex plane is often referred to as a Weinstein circle and denoted by $W_p$. The inequality (C.6) says that the eigenvalue closest to $T_{pp}$ must lie within the circle $W_p$. This theorem has the drawback that a particular eigenvalue $\lambda'$ may be the closest one to several diagonal elements $T_{pp}$, $T_{qq}$ , etc., in which case there are eigenvalues $\lambda''$ which are not 'the closest one" to any diagonal element $T_{kk}$ whatsoever, and which are hence not covered by the inequality (C.6). Since some of the Weinstein circles may hence be empty, the study of the Weinstein circles gives the best result if they are treated in combination with the Hadamard circles.

In conclusion it should be observed that by means of Given's method an hermitean matrix $\mathbf{T}$ may be brought to tridiagonal form $\mathbf{T}'$ by means of $n(n-1)/2$ successive unitary transformations of the second order, which is sometimes of value in estimating the eigenvalues.

In connection with the search for approximate linear dependencies, it is, of course, of particular importance to find out if there are any eigenvalues of the matrix $\langle f|f\rangle$ which are close to zero, and sometimes even the rough estimates of the types outlined here may be of value for this purpose. Today there are special programs for evaluating the eigenvalues of a given matrix $\mathbf{T}$ available both on the large-scale electronic computers and on the personal computers, which are useful in any form of data analysis, but the methods described above may still be of some value in a system analysis where numerical results are not yet available.

Appendix D. Evaluation of the eigenvalues by means of partitioning technique. - If the order n of the matrix **T** is very high, it may be worthwhile to try to evaluate some of its eigenvalues by means of the partitioning technique [25]. In this case, one starts from the eigenvalue problem in the form $\mathbf{T}\,\mathbf{c} = \lambda\,\mathbf{c}$, and partitions the matrix **T** and the eigenvector **c** in the following way:

$$\mathbf{T}=\begin{bmatrix} \mathbf{T}_{aa} & \mathbf{T}_{ab} \\ \mathbf{T}_{ba} & \mathbf{T}_{bb} \end{bmatrix}, \qquad \mathbf{c}=\begin{bmatrix} \mathbf{c}_a \\ \mathbf{c}_b \end{bmatrix}, \tag{D.1}$$

which gives

$$\begin{bmatrix} \mathbf{T}_{aa} & \mathbf{T}_{ab} \\ \mathbf{T}_{ba} & \mathbf{T}_{bb} \end{bmatrix}\begin{bmatrix} \mathbf{c}_a \\ \mathbf{c}_b \end{bmatrix}=\lambda\begin{bmatrix} \mathbf{c}_a \\ \mathbf{c}_b \end{bmatrix}, \tag{D.2}$$

or

$$\begin{aligned} \mathbf{T}_{aa}\,\mathbf{c}_a + \mathbf{T}_{ab}\,\mathbf{c}_b &= \lambda\ \mathbf{c}_a\ , \\ \mathbf{T}_{ba}\,\mathbf{c}_a + \mathbf{T}_{bb}\,\mathbf{c}_b &= \lambda\ \mathbf{c}_b\ , \end{aligned} \tag{D.3}$$

Solving $\mathbf{c}_b$ from the second relation in (D.2), one gets $\mathbf{c}_b = -\,(\lambda.\mathbf{1}-\mathbf{T}_{bb})^{-1}\,\mathbf{T}_{ba}\,\mathbf{c}_a$, and substituting this expression in the first relation one obtains

$$[\mathbf{T}_{aa} - \mathbf{T}_{ab}\,(\lambda.\mathbf{1}-\mathbf{T}_{bb})^{-1}\,\mathbf{T}_{ba}]\,\mathbf{c}_a = \lambda\ \mathbf{c}_a\ , \tag{D.4}$$

which is the basic equation in the partitioning technique. We note that it is usually used in the de-coupled form

$$[\mathbf{T}_{aa} - \mathbf{T}_{ab}\,(z.\mathbf{1}-\mathbf{T}_{bb})^{-1}\,\mathbf{T}_{ba}]\,\mathbf{c}_a = z_1\ \mathbf{c}_a\ , \tag{D.5}$$

where the secular equation

$$|\mathbf{T}_{aa} - \mathbf{T}_{ab}\,(z.\mathbf{1}-\mathbf{T}_{bb})^{-1}\,\mathbf{T}_{ba} - z_1.\mathbf{1}| = \mathbf{0}, \tag{D.6}$$

defines a multivalued function $z_1 = f(z)$ having the "bracketing" property that, between z and $z_1$, there is always at least one true eigenvalue $\lambda$. The partitioning method is particularly convenient for evaluating the low-lying eigenvalues of the positive definite matrix $\Delta = \langle \mathbf{f}|\mathbf{f}\rangle$, where one may start from $z = 0$ and then iterate until one obtains $z=f(z)$. It has been programmed for the large-scale electronic computers, and it is particularly useful if one wants to study only a particular set of eigenvalues.

## References


1. J. von Neumann, *Mathematische Grundlagen der Quantenmechanik* (Springer, Berlin, 1932).
2. P.A.M.Dirac, Proc.Roy.Soc. London **A114**, 243 (1927); see also *The Principles of Quantum Mechanics* (4th ed. ClarendonPress,Oxford,1958).
3. P.O. Löwdin, *Concepts of Convergence in Mathematical Chemistry*, in J.Math.Chem. (J.C. Baltzer AG, Basel, Switzerland 1990).
4. P.O. Löwdin, Phys.Rev. **139**, A357 (1965).
5. For a proof, see e.g. ref. 4, particularly p. 359.
6. P.O. Löwdin, Phys.Rev. **139**, A 1509 (1965).
7. K. Pearson, *On Lines and Planes of Closest Fit to Systems of Points in Space*, Phil.Mag **6**, 559 (1901).
8. R.E. Kalman, *Adv. in Econometrics* , 169 (Ed. W.Hildebrand, Cambridge Univ. Press 1982); *Dynamical Systems II* , 331 (Eds. A.R. Bednarek and L. Cesari, Academic Press, New York 1982); Uspheki Mat. Nauk. **40**, 29 (1985); *Recent Adv. in Communication and Control Theory*, 448 (Eds. Kalman, Marchuk, Ruberti, and Viberti, Optimization Software, Inc. 1987); in *Lions Festschrift* (Eds. H. Brezis and P.G. Ciarlet, 1989); *Nine Lectures on Identification* (Springer Lecture Notes on Economics and Mathematical Systems, 1990).
9. P. Becker, A. Kapteyn and T. Wansbeek, *Misspecification Analysis*, 85 (Ed. T.K. Dijkstra, Springer 1984).
10. P.O. Löwdin, Int. J. Quantum Chem. **4S**, 231 (1971). see also P.O. Löwdin, in Proc.**1988** Girona Workshop in Quantum Chemistry (Ed. Ramon Carbo, Elsevier 1989).
11. See e.g. P.O. Löwdin, J.Chem.Phys. **43**, S175 (1965), and numerous papers from the Florida group published in the same volume.
12. R.H. Parmenter, Phys. Rev. **86**, 552 (1952); P.O. Löwdin, Ann.Rev.Phys.Chem. **11**, 107 (1960); J. Appl.Phys. **33**, 251 (1962).
13. P.O. Löwdin, Int. J. Quantum Chem. **1S**, 811 (1967).
14. P.O. Löwdin, Arkiv Mat. Astr. Fysik (Stockholm) **35A**, No. 9 (1947); "*A Theoretical Investigation into some Properties of Ionic Crystals*" (Thesis, Almqvist and Wiksell, Uppsala, Sweden, 1948); J. Chem. Phys. **18**, 365 (1950).
15. P.O. Löwdin, Adv. in Physics **5**, 1 (1956); particularly p. 49.
16. P.O. Löwdin, Adv. Quantum Chem. **5**, 185 (1970).
17. M. Berrondo and P.O. Löwdin, Int. J. Quantum Chem. **3**, 767 (1969).
18. E.A Hylleraas and B. Undheim, Z.Physik **65**, 759 (1930); J.K.L. MacDonald, Phys. Rev. **43**, 830 (1933).
19. T.N. Thiele, Vidsk. Selsk. Skr. 5, Rk. Naturvid. og Mat. Afd. (Copenhagen) **12, 5**, 381 (1880); R. Frisch, "*Statistical Confluence Analysis by Means of Complete Regression Systems*" ( University Institute of Economics, Oslo, Norway, 1934); T. Koopmans, "*Linear Regression Analysis of Economic Time Series*" (Netherlands Econometric Institute, Harlem,1937); T. Havelmoo, Econometrica **11**,1 (1943); O. Reiersöl, Econometrica **9**,1 (1941); "*Confluence Analysis by Means of Instrumental Sets of Variables*", Arkiv Mat. Astr. Fysik (Stockholm) **32**, 1 (1945); E. Malinvaud, "*Statistical Methods of Econometrics*" (North Holland, Amsterdam, 1970).

20. K.G. Jöreskog, Biometrika **57** (1970); reprinted in "*Latent Variables in Socio-Economic Models*" (Eds. D.J. Aigner and A.S. Goldberger, North-Holland, Amsterdam 1977).
21. S. Klepper and E.E. Leamer, Econometrica **52**, 163 (1984); C.A. Los and C. McC. Kell, Proc. 8th IAC/IFORS Symp. Vol. 2, 866 (Beijing 1988); C. A Los, Computer & Mathematics with Applications **17**, 1269, 1285 (1989);
22. See R. Frisch, ref. 4, p.123.
23. C.A. Los, private communication.
24. G. Gallup, Int. J. Quantum Chem. 2, 695 (1968)
25. P.O.Löwdin, J. Mol. Spectrosc. **10**, 12 (1963); **13**, 326 (1964); **14**, 112 (1964); **14**, 119 (1964); **14**, 131 (1964); J. Math. Phys. **3**, 969 (1962); **3**, 1171 (1962); **6**, 1341 (1965); Phys. Rev. **139**, A357 (1965); J. Chem. Phys. **43**, S175 (1965); Int. J. Quantum Chem. **2**, 867 (1968); Int. J. Quantum Chem. **S4**, 231 (1971); **5**, 685 (1971) (together with O. Goscinski); Phys. Scrip. **21**, 229 (1980); Adv. Quantum Chem. (Academic Press, New York, 1980) **12**; Int. J. Quantum Chem. **21**, 69 (1982).

# CANONICAL AND NONCANONICAL METHODS IN APPLICATIONS OF GROUP THEORY TO PHYSICAL PROBLEMS

J. D. LOUCK
Los Alamos National Laboratory
Theoretical Division
Los Alamos, NM 87545, U.S.A.

and

L. C. BIEDENHARN
Department of Physics, Duke University
Durham, NC 27706, U.S.A.

*To Professor F. A. Matsen for his contributions in quantum chemistry*

ADVANCES IN QUANTUM CHEMISTRY
VOLUME 23

Copyright © 1992 By Academic Press, Inc.
All rights of reproduction in any form reserved.

## Table of Contents

1. INTRODUCTION

2. REVIEW OF GENERAL PRINCIPLES
   - 2.1. Left and Right Translations
   - 2.2. Lie Algebras
   - 2.3. Homogeneous Polynomial Spaces
   - 2.4. Boson Operator Realizations
   - 2.5. Irreducible Polynomial Spaces and Representations
   - 2.6. Algebras Associated with the General Linear Group

3. CANONICAL $U(3)$ WCG-COEFFICIENTS

4. FURTHER CANONICAL METHODS
   - 4.1. Group-Subgroup Reductions $G \downarrow U(n)$
   - 4.2. Group-Subgroup Reductions $U(n) \downarrow G$
   - 4.3. The Canonical Solution of the $SU(3) \downarrow SO(3)$ Reduction Problem

   Appendix. The Pattern Calculus Rules

5. NONCANONICAL METHODS: THE $SU(3) \supset SO(3)$ EXAMPLE
   - 5.1. The Build-up Principle
   - 5.2. The Weyl Theorem
   - 5.3. $SO(3)$ and $SU(2)$ Irreducible Sets
   - 5.4. Nonorthogonal Bases I
   - 5.5. Nonorthogonal Bases II

# I. INTRODUCTION

F. A. Matsen was a pioneer in applications of unitary symmetry in quantum-chemistry and in the present paper we survey current applications of unitary group techniques as motivated by physical problems.

The basic problem in quantum chemistry is to find solutions of the many-body Schrödinger equation, and, aside from a few very special cases, the only feasible approach is to truncate the relevant solution space, sometimes even drastically, to obtain simpler models that capture some of the essence of the original problem. Thus, for example, Matsen and Pauncz[1] advocated the approach whereby dynamical spin-effects (but not kinematic effects) were ignored: this gives the model of *spin-free quantum chemistry.* Similarly they discussed[1] the Hückel-Hubbard approach to organic chemistry which drastically truncates the space of relevant degrees of freedom to a single atomic orbital at each site in the molecule. The relevant symmetry group of the system is then the unitary group $U(n)$, for $n$ sites.

Let us indicate briefly why the unitary group occurs so frequently in applications. It could happen, of course, that the unitary group is a fundamental (or global) symmetry of the many-body Hamiltonian; this is clearly the case for the quantal angular momentum group, $SU(2)$. But far more frequently, unitary symmetry involves a *restricted solution manifold* (such as in the Hückel-Hubbard case), and this can occur in many ways. For atoms where the $f$-shell is filling, one may restrict the solution manifold to the $f$-shell alone; the basis states are then seven-fold degenerate and this restricted manifold thus has the unitary symmetry $SU(7)$, which Racah analyzed by the group chain $SU(7) \supset SO(7) \supset G(2) \supset SO(3)$. Similarly in nuclear physics—based on a harmonic oscillator Hamiltonian (which has $U(3)$ global symmetry)—the $s, d$ shell is degenerate. If we truncate the solution manifold to this $s$-$d$ shell, one has $SU(6)$ as the appropriate symmetry. Taking this $SU(6)$ symmetry to be realized in a more fundamental way (that is, postulating the symmetry and discarding the model) led to the famous Interacting Boson Model which is so surprisingly successful in nuclear theory.

The preceding descriptive results indicate the role of the unitary group in physical applications, but do not yet suggest the full breadth of the properties of the unitary group that are required. This paper is about the irreducible representations (irreps) of $U(n)$, its Wigner-Clebsch-Gordan (WCG) coefficients and associated operator algebras, general group-subgroup reductions, and Lie algebras. Why should one be interested in such results for physical applications? In order to see this, one must pursue further the role of simple physical systems in making up complex systems occurring in physics and chemistry. Let us then review the structure of a model of complex systems in order to show that one must go beyond the relatively simple procedures of finding irrep spaces and irreps of groups to obtain realistic descriptions.

Complex physical systems are generally viewed as composed of simpler systems whose properties are already understood. These "constituents" of the complex system are often "identical," which, for simplicity of our model, we shall assume to be the case.

We suppose that each constituent part is described by the Hamiltonian operator, $H$, whose state space is a Hilbert space $\mathcal{H}$. Thus, $H$ is a Hermitian operator mapping $H : \mathcal{H} \to \mathcal{H}$. We consider that the Hilbert space $\mathcal{H}$ is fully known. The Hamiltonian for the composite system, *without interactions*, is then

$$H_0 = \sum_{i=1}^{r} H_i, \tag{1.1a}$$

acting on the space

$$\mathcal{H}^r = \mathcal{H} \otimes \mathcal{H} \otimes \ldots \otimes \mathcal{H}, \tag{1.1b}$$

where

$$H_i = \mathbf{1} \otimes \ldots \otimes \mathbf{1} \otimes H \otimes \mathbf{1} \otimes \ldots \otimes \mathbf{1}, \text{ (H in position i).} \tag{1.1c}$$

Here $\otimes$ denotes the tensor product of vector spaces in Eq. (1.1b) and the tensor product of operators in Eq. (1.1c).

We further limit the discussion to the case where the Hamiltonian $H$ possesses a symmetry group $G$, which is taken to be a compact, semisimple Lie group. (This is for assuring that the finite-dimensional irreps of $G$ may be taken to be unitary matrices.) That $G$ is a symmetry group of the Hamiltonian $H$ means that there is defined an operator $\mathcal{U}_g$, that is, a unitary mapping

$$\mathcal{U}_g : \quad \mathcal{H} \to \mathcal{H}, \text{ each } g \in G \tag{1.2}$$

with the property

$$\mathcal{U}_g H \mathcal{U}_g^{-1} = H, \quad \text{each } g \in G, \tag{1.3a}$$

or, equivalently,

$$\mathcal{U}_g H - H \mathcal{U}_g = [\mathcal{U}_g, H] = 0, \quad \text{each } g \in G. \tag{1.3b}$$

The set of maps

$$\{\mathcal{U}_g | g \in G\} \tag{1.4a}$$

is then a *group of unitary operators* on $\mathcal{H}$:

$$\mathcal{U}_g \mathcal{U}_{g'} = \mathcal{U}_{gg'}. \tag{1.4b}$$

We suppose that the Hilbert space $\mathcal{H}$ of states of $H$ has been reduced into carrier spaces $\mathcal{H}_\sigma$ of unitary irreps $[\sigma] = \{\Gamma^\sigma(g) | g \in G\}$ of $G$. Here $[\sigma]$ is

a symbol that enumerates irreps of $G$ and its specific form is to be adapted to each specific group $G$. Various irreps are denoted $[\sigma_1], [\sigma_2], \ldots$. Thus, we can write $\mathcal{H}$ as a direct sum

$$\mathcal{H} = \sum_{\sigma} \oplus \mathcal{H}_{\sigma}, \tag{1.5}$$

where a given irrep $[\sigma]$ may be repeated. In the discussions of this section, we only consider the finite-dimensional tensor product subspace of $\mathcal{H}^r$ given by

$$\mathcal{H}(\sigma_1 \sigma_2 \ldots \sigma_r) = \mathcal{H}_{\sigma_1} \otimes \mathcal{H}_{\sigma_2} \otimes \ldots \otimes \mathcal{H}_{\sigma_r}. \tag{1.6}$$

The dimension of this space is

$$\dim \mathcal{H}(\sigma_1 \sigma_2 \ldots \sigma_r) = \prod_{i=1}^{r} \dim[\sigma_i], \tag{1.7}$$

where $\dim[\sigma]$ denotes the dimension of $\mathcal{H}_{\sigma}$.

We denote an orthonormal basis of $\mathcal{H}_{\sigma}$ by

$$B^{\sigma} = \left\{ \left| \begin{matrix} \sigma \\ m \end{matrix} \right\rangle \middle| \; m \text{ enumerates the vectors} \right\}, \tag{1.8a}$$

and, correspondingly, the basis of $\mathcal{H}(\sigma_1 \sigma_2 \ldots \sigma_r)$ by

$$B^{\sigma_1 \sigma_2 \ldots \sigma_r} = \left\{ \left| \begin{matrix} \sigma_1 \\ m_1 \end{matrix} \right\rangle \otimes \ldots \otimes \left| \begin{matrix} \sigma \\ m_r \end{matrix} \right\rangle \middle| \; \left| \begin{matrix} \sigma_i \\ m_i \end{matrix} \right\rangle \in B^{\sigma_i} \right\}. \tag{1.8b}$$

The action of $G$ on $\mathcal{H}_{\sigma}$ is given by

$$T_g : \quad \left| \begin{matrix} \sigma \\ m \end{matrix} \right\rangle \to T_g \left| \begin{matrix} \sigma \\ m \end{matrix} \right\rangle = \sum_{m'} \Gamma^{\sigma}_{m'm}(g) \left| \begin{matrix} \sigma \\ m' \end{matrix} \right\rangle. \tag{1.9}$$

Correspondingly, the action of $G$ on the tensor product space $\mathcal{H}(\sigma_1 \sigma_2 \ldots \sigma_r)$ is given by

$$T_g : \quad T_g \left| \begin{matrix} \sigma_1 \\ m_1 \end{matrix} \right\rangle \otimes \ldots \otimes T_g \left| \begin{matrix} \sigma_r \\ m_r \end{matrix} \right\rangle. \tag{1.10}$$

Thus, the tensor product space $\mathcal{H}(\sigma_1 \ldots \sigma_r)$ is the carrier space of the Kronecker product representation of $G$:

$$[\sigma_1] \times [\sigma_2] \times \ldots \times [\sigma_r] \tag{1.11}$$

The general transformation Eq. (1.10) corresponds to transforming the description of each elementary part of a composite physical system *in exactly the same way.* Indeed, the composite physical system would have the

symmetry of the direct product group $G \times G \times \ldots \times G$ *if there were no interactions between its parts.* The transformation $T_g$ in the right-hand side of (1.10) would be replaced successively by $T_{g_1}, T_{g_2}, \ldots, T_{g_r}$ thus defining $T_{g_1} \otimes \ldots \otimes T_{g_r} \in G \times \ldots \times G$. Composite systems acquire their individuality and richness of structure, thus becoming entities "on their own," precisely because of such interactions between their parts. Since in the present model all parts are equivalent, we can transform the description of no part separately, but must change the description of all parts *simultaneously*, in the same way. This means that the composite system, with interactions, must be invariant under the action of Eq. (1.10) of $G$; that is, every interaction must be itself a *G-invariant*, since $H_0$ already possesses this property. We conclude that an interaction $H'$ between identical parts of a composite system must be a Hermitian mapping $\mathcal{H}^r \to \mathcal{H}^r$ that is invariant under the action $\mathcal{T}_g$ of the group $G$:

$$[H', \mathcal{T}_g] = 0, \quad \text{each } g \in G. \tag{1.12a}$$

or, equivalently,

$$\mathcal{T}_g H' \mathcal{T}_g^{-1} = H'. \tag{1.12b}$$

An interaction term $H'$ is, in general, *not* a map of the tensor product subspace $\mathcal{H}(\sigma_1\sigma_2\ldots\sigma_r)$ into itself. It is often a useful *approximation* to consider the truncated problem in which one replaces the interaction $H'$ by its *restriction* $H'_R$ to the space $\mathcal{H}(\sigma_1\sigma_2\ldots\sigma_r)$. The Hermitian operator $H'_R$ is the map

$$H'_R: \quad \mathcal{H}(\sigma_1\sigma_2\ldots\sigma_r) \to \mathcal{H}(\sigma_1\sigma_2\ldots\sigma_r) \tag{1.13}$$

defined in the following way: For each pair of vectors $|\psi\rangle$, $|\psi'\rangle \in B^{(\sigma_1\sigma_2\ldots\sigma_r)}$, the basis of $\mathcal{H}(\sigma_1\sigma_2\ldots\sigma_r)$ defined by Eq. (1.8b), we calculate the matrix elements $\langle\psi'|H'|\psi\rangle$ of $H'$. Then $H'_R$ is defined by

$$H'_R|\psi\rangle = \sum_{\psi'} \langle\psi'|H'|\psi\rangle\, |\psi'\rangle, \quad \text{each } |\psi\rangle \in B^{(\sigma_1\sigma_2\ldots\sigma_r)}. \tag{1.14}$$

Since the interaction $H'$ commutes with the group of operators $\{\mathcal{T}_g | g \in G\}$ on the entire space $\mathcal{H}^r$, it commutes with its restriction to $\mathcal{H}(\sigma_1\sigma_2\ldots\sigma_r)$:

$$[H'_R, \mathcal{T}_g] = 0, \quad \text{each } g \in G. \tag{1.15}$$

There are many Hermitian operators satisfying the conditions (1.13) and (1.15): The only restriction on $H'_R$ coming from relation (1.15) is that $H'_R$ must be *unitarily equivalent* to a multiple of the unit matrix on each irrep space of $G$ (Schur's lemma) contained as a subspace in the tensor product space $\mathcal{H}(\sigma_1\sigma_2\ldots\sigma_r)$. Thus, one is led to the problem of reducing the tensor

product space $\mathcal{H}(\sigma_1\sigma_2\ldots\sigma_r)$ into the irrep spaces with respect to the action $\mathcal{T}_g$ of $G$:

$$\mathcal{H}(\sigma_1\sigma_2\ldots\sigma_r) = \sum_{\sigma}\sum_{\gamma}\oplus\mathcal{H}_{\sigma}^{(\gamma)}, \tag{1.16a}$$

where $\sigma$ is an irrep of $G$ occurring in the reduction of the Kronecker product:

$$[\sigma_1]\times[\sigma_2]\times\ldots\times[\sigma_r] = \sum_{\sigma} M_{\sigma}(\sigma_1\sigma_2\ldots\sigma_r)[\sigma]. \tag{1.16b}$$

Here $\gamma$ is a member of an indexing set $\Gamma_\sigma$ that distinguishes the multiple occurrences, $M_\sigma(\sigma_1\sigma_2\ldots\sigma_r)$ in number, of irrep $[\sigma]$ of $G$ in the $r$-fold Kronecker product of irreps of $G$. Each space $\mathcal{H}_\sigma^{(\gamma)}$ is the carrier space of one and the same irrep $[\sigma] = \{\Gamma^\sigma(g)|\ g\in G\}$ of $G$.

The interaction $H_R'$ in a specific problem may or may not have distinct eigenvalues on the various spaces $\mathcal{H}_\sigma^{(\gamma)}$. If all eigenvalues are distinct, then $H_0, H_R'$, and the symmetry group $G$ provide a complete description of the state space of the system; otherwise, one must seek further structure in the problem to resolve the degeneracy. It is useful to show how this works in special realizations of the above model.

It is instructive to consider a simple realization of the above structure which is provided by the coupling theory of $r$ angular momenta. This realization uses only well-known concepts from angular momentum theory, yet is already complicated enough to illustrate general features of interactions. The Hamiltonian $H$ given by $H = a\mathbf{J}\cdot\mathbf{J} = a\left(J_1^2 + J_2^2 + J_3^2\right)$, where $a$ is a constant and $J^2 = \mathbf{J}\cdot\mathbf{J}$ is the squared angular momentum of any object carrying angular momentum $\mathbf{J} = (J_1, J_2, J_3)$ relative to an inertial frame of reference. Each eigenspace of $H$ may be characterized as an irrep space $\mathcal{H}_j$ of $G = SU(2)$, where $j\in\{0, \frac{1}{2}, 1, \ldots\}$ with canonical basis $B^j = \{|jm\rangle|\ m = -j, -j+1, \ldots, j\}$ on which the components $J_i$ of the angular momentum $\mathbf{J} = (J_1, J_2, J_3)$ have the standard action. In particular, $J^2|jm\rangle = j(j+1)|jm\rangle, J_3|jm\rangle = m|jm\rangle$. The state space $\mathcal{H}$ of the elementary physical system is $\mathcal{H} = \sum_j \oplus\mathcal{H}_j$, where each irrep space $\mathcal{H}_j$ $(j = 0, \frac{1}{2}, 1, \ldots)$ occurs exactly once in the direct sum.

The total energy of the system composed of $r$ identical parts, without interaction, is given by

$$H_0 = a\sum_{\alpha=1}^{r} J^2(\alpha) \tag{1.17a}$$

with

$$J^2(\alpha) = \mathbf{1}\otimes\ldots\otimes\mathbf{1}\otimes J^2\otimes\mathbf{1}\otimes\ldots\otimes\mathbf{1}, \quad \alpha = 1, 2, \ldots, r, \tag{1.17b}$$

where $J^2$ is in position $\alpha$. Here we use the index $\alpha = 1,2,\ldots,r$ to label the parts of the system in order to free index $i$ for labelling components of angular momenta:

$$J_i(\alpha) = \mathbf{1} \otimes \ldots \otimes \mathbf{1} \otimes J_i \otimes \mathbf{1} \otimes \ldots \otimes \mathbf{1}, \quad i = 1,2,3, \tag{1.18a}$$

$$J^2(\alpha) = \sum_{i=1}^{3} J_i^2(\alpha), \quad \alpha = 1,2,\ldots,r. \tag{1.18b}$$

One now splits the tensor product space $\mathcal{H}^r = \mathcal{H} \otimes \ldots \otimes \mathcal{H}$ into a direct sum of spaces

$$\mathcal{H}_{(j_1 j_2 \ldots j_r)} = \mathcal{H}_{j_1} \otimes \mathcal{H}_{j_2} \otimes \ldots \otimes \mathcal{H}_{j_r}, \tag{1.19a}$$

where

$$\dim \mathcal{H}_{(j_1 j_2 \ldots j_r)} = \prod_{\alpha=1}^{r} (2j_\alpha + 1). \tag{1.19b}$$

The Hamiltonian $H_0$ is diagonal on $\mathcal{H}_{(j_1 j_2 \ldots j_r)}$ with eigenvalue:

$$H_0 \to a \sum_{r=1}^{r} j_r(j_r + 1). \tag{1.20}$$

One can consider a variety of exactly solvable interactions $H'$ in the above theory to illustrate various features. For example, the interaction given by

$$H' = b \sum_{\alpha<\beta} \mathbf{J}(\alpha) \cdot \mathbf{J}(\beta), \tag{1.21}$$

leaves the space $\mathcal{H}_{(j_1 j_2 \ldots j_r)}$ invariant; indeed, it has eigenvalues given by

$$H' \to (b/2) \left[ j(j+1) - \sum_{\alpha=1}^{r} j_\alpha(j_\alpha + 1) \right] \tag{1.22}$$

on the space $\mathcal{H}_{(j_1 j_2 \ldots j_r)}$, where for given $(j_1 j_2 \ldots j_r)$, each $j_i \in \{0, \frac{1}{2}1, \ldots\}$, the allowed $j$-values are such that $j \in [j_1] \times [j_2] \times \ldots \times [j_r]$. Here $j(j+1)$ is the eigenvalue of the square of the total angular momentum of the composite system:

$$J^2 = J_1^2 + J_2^2 + J_3^2; \quad J_i = \sum_{\alpha=1}^{r} J_i(\alpha). \tag{1.23}$$

Each value of $j$ occurs with multiplicity equal to $M_j(j_1 \ldots j_r)$, where this integer denotes the number of occurrences of $j$ in the reduction of the Kronecker product $[j_1] \times \ldots \times [j_r]$.

The vector space structure corresponding to the eigenvalues above is the following. The vector space $\mathcal{H}_{(j_1 j_2 \ldots j_r)}$ splits into a direct sum of orthogonal vector spaces $\mathcal{H}_j^{(\gamma)}$, each a carrier space of irrep $[j] = \{D^j(g) | \ g \in SU(2)\}$, where $(\gamma)$ is a member of an indexing set $\Gamma_j$ that distinguishes the orthogonal spaces $\mathcal{H}_j^{(\gamma)}$ carrying identical irreps $[j]$: Thus, $\mathcal{H}_{(j_1 j_2 \ldots j_r)} = \sum_j \oplus V_j$, where

$$V_j = \sum_{\gamma \in \Gamma_j} \oplus \mathcal{H}_j^{(\gamma)}. \tag{1.24}$$

The interaction $H'$ defined by Eq. (1.21) is, of course, degenerate on each space $\mathcal{H}_j^{(\gamma)}$, $\gamma \in \Gamma_j$; that is, has the eigenvalue (1.22) on each of these spaces.

The binary coupling theory of angular momenta (see Jucys *et al.*[2] and Ref. 3) leads to a unique determination of the indexing set $\Gamma_j$ corresponding to the eigenvalues of different *intermediate angular momentum operators* (squared). Different coupling schemes lead to different indexing sets, and in each case one solves uniquely the decomposition problem described by Eq. (1.24). For given $r$, the number of such coupling schemes is finite (see Ref. 3). Using the various squared intermediate angular momenta associated with a given coupling scheme, one could, of course, now construct interactions that have distinct eigenvalues on each subspace $H_j^{(\gamma)} \subset V_j$. The relations between these various coupling schemes leads to the theory of the so-called $3n-j$ coefficients ($r = n$). This is a fascinating, but incomplete theory leading into the classification of all cubic graphs of a certain type, which is itself an unsolved problem. All such unitary transformations between binary coupling schemes define unitary transformations $M_U$ of the space $V_j$ of the form:

$$\begin{aligned} M_U : \ & |(j_1 j_2 \ldots j_r); jm; (\gamma)\rangle \to M_U \, |(j_1 j_2 \ldots j_r); jm; (\gamma)\rangle \\ & = \sum_{\gamma' \in \Gamma'_j} U_{\gamma',\gamma} |(j_1 j_2 \ldots j_r); jm; (\gamma')\rangle, \text{ each } \gamma \in \Gamma_j. \end{aligned} \tag{1.25}$$

Such unitary relations between binary coupling schemes [essentially the $3n-j$ coefficients ($r = n$)] are but a finite subset of the group of all unitary transformations $\{M_U | U \in U(n_j)\}$, $n_j = |\Gamma_j| = |\Gamma'_j|$ of the form (1.25). One can ask whether or not there exists canonical or natural decompositions $\{\mathcal{H}_j^{(\gamma)} | \gamma \in \Gamma_j\}$ of $V_j$ in terms of which one should express all other bases of $V_j$. The results obtained in this paper suggest that properties of the multiplicity function $M_j$ defined by $M_j : \ (j_1 j_2 \ldots j_r) \to M_j(j_1 j_2 \ldots j_r)$, each $j_i \in \{0, \frac{1}{2}, 1, \ldots\}$ may be useful in such considerations.

Another interesting special case of the model theory outlined in Eqs. (1.1)-(1.16) in which the unitary group always has a role, in addition to the

symmetry group $G$, occurs when all irrep spaces $\mathcal{H}_{\sigma_i}$ in the tensor product space $\mathcal{H}(\sigma_1\sigma_2\ldots\sigma_r)$ are equal. Thus, in Eq. (1.6) defining $\mathcal{H}(\sigma_1\sigma_2\ldots\sigma_r)$, we take each $\sigma_i = \rho$ so that

$$V_\rho \;=\; \mathcal{H}_\rho \otimes \mathcal{H}_\rho \otimes \ldots \otimes \mathcal{H}_\rho \quad (r \text{ times}), \tag{1.26a}$$

where $\mathcal{H}_\rho$ is the carrier space of irrep $[\rho] = \{\Gamma^\rho(g) |\; g \in G\}$ of $G$. The dimension of $V_\rho$ is

$$\dim V_\rho \;=\; (\dim[\rho])^r. \tag{1.26b}$$

For each $U \in U(\dim[\rho])$ (the unitary group with $n = \dim[\rho]$), we define the transformation $T_U$ of $\mathcal{H}_\rho$ in terms of its basis $B^\rho$ by

$$T_U \Big| \begin{matrix} \rho \\ m \end{matrix} \Big\rangle \;=\; \sum_{m'} U_{m'm} \Big| \begin{matrix} \rho \\ m' \end{matrix} \Big\rangle, \tag{1.27}$$

where $U = (U_{m'm})$. Then with $\mathcal{T}_U$ defined by

$$\mathcal{T}_U \;=\; T_U \otimes T_U \ldots \otimes T_U \quad (r \text{ times}), \tag{1.28a}$$

the action of the unitary group $U(\dim[\rho])$ on $V_\rho$ yields the direct product representation:

$$U \times U \times \ldots \times U \quad (r \text{ times}). \tag{1.28b}$$

Since

$$[\mathcal{T}_U, H_0] \;=\; 0, \;\; \text{on } V_\rho, \tag{1.29}$$

*the unitary group $U(\dim[\rho])$ is a symmetry group of $H_0$ on the space $V_\rho$.* Moreover, the group of unitary matrices $[\sigma] = \{\Gamma^\sigma(g) | g \in G\}$ is a subgroup of $U(\dim[\rho])$:

$$[\sigma] \subset U(\dim[\rho]). \tag{1.30}$$

Accordingly, we may restrict the operators $T_U$ and $\mathcal{T}_U$ to $U = \Gamma^\sigma(g)$ in Eqs. (1.27)-(1.29). Corresponding to the reduction of the $r$-fold Kronecker product of fundamental irreps $[10\ldots0]$ of $U(\dim[\rho])$ into irreps $\{D^\lambda(U) | U \in U(\dim[\rho])\}$ of $U(\dim[\rho])$, one obtains the reducible representation

$$\{D^\lambda(\Gamma^\sigma(g)) | g \in G\} \tag{1.31}$$

of the symmetry group $G$. The reduction of these representations of $G$ into irreps of $G$, for all $\lambda \in [10\ldots0] \times \ldots \times [10\ldots0]$, must then agree with the reduction of $[\sigma]\times\ldots\times[\sigma]$ ($r$ times) into irreps of $G$. This structure generalizes Racah's result for $\ell^r$-configurations in atomic spectroscopy to what might be

called $[\rho]^r$-configurations for an arbitrary symmetry group $G$. This result illustrates the basic role of unitary groups in unexpected guises.

The interaction $H'_R$ itself need not commute with the group of operators $\{\mathcal{T}_U | U \in U(\dim[\rho])\}$ on the vector space $V_\rho$. In favorable circumstances, however, as we have noted at the beginning of the Introduction, the interaction can be approximated as a polynomial in the invariant operators associated with $U(\dim[\rho])$ and its subgroups.

From the examples given above, we see that a general theory of interactions deals with the construction of invariants with respect to the underlying symmetry group $G$. A standard approach to this problem uses the concept of an *irreducible tensor operator* with respect to $G$. One then uses the WCG-coefficients of $G$ to couple tensor operators to form invariants, from which model interactions are constructed.

We have shown in the preceding review that even for a model complex system one needs for a comprehensive study the full apparatus of irreps of groups, their WCG-coefficients, and the associated operator algebras (e.g., irreducible tensor operators). One would like to develop this apparatus in a natural way, independent of particular physical applications. This is done by the use of model spaces, which may or may not have direct relevance to a given physical system. The objective is to obtain a realization of the essential mathematics that is free of some of the complexities of real systems. The ultimate success of this procedure depends then on the adaptation of such "abstract" results to actual systems. This is not always a straightforward procedure; indeed, it is often in recognizing such adaptations that progress is made in understanding the physics and chemistry of real complex systems.

It is in the above spirit that we present the results of this paper with the focus on unifying principles and natural structures that underlie the mathematical apparatus itself. The emphasis is on the unitary groups with some attention to groups containing a unitary group as a subgroup and conversely. This is partly because the theory is most developed here, and partly because of the great generality of applications of the unitary groups.

Many insights and contributions of the sort alluded to above have already been made, not only in the spin-free quantum chemistry of Matsen, but in other directions as well. Our limited experience in these fields does not allow us to give a comprehensive overview; accordingly, we refer to several recent publications (and references therein) where group theoretical and Lie algebraic methods are used to confront and resolve problems in quantum chemistry: Iachello,[4] Hinze,[5] Iachello and Levine,[6] Levine,[7] Paldus,[7] Shavitt,[7] Kent and Schlesinger,[8] Li and Paldus,[9] Gould and Paldus.[10]

## 2. REVIEW OF GENERAL PRINCIPLES

In this section we review the concepts and techniques leading to canonical finite-dimensional irrep spaces and integral irreps of the general linear group $GL(n,\mathbb{C})$ of $n \times n$ complex, nonsingular matrices. These finite-dimensional irreps of $GL(n,\mathbb{C})$ remain irreducible when restricted to the unitary subgroup $U(n)$ of $n \times n$ unitary matrices. As we shall see, this general framework of $GL(n,\mathbb{C})$ leads to a richness of structure that would be bypassed should we confine our attention to $U(n)$ at the outset. Moreover, the irrep spaces and irreps considered are, in fact, isomorphic to the familiar boson calculus basis vectors and well-known boson polynomials often used in unitary group theory. This is because the complex variables of the theory may be considered to be indeterminates (or alphabets) in the spirit of Rota's umbral calculus.[11,12] Accordingly, if one wishes, these variables may be taken to be boson creation operators. Thus, in this section, we address (in the context of the family of unitary groups) the first part of the problem of dealing with complex systems, that of obtaining irrep spaces and irreps.

### 2.1. Left and Right Translations

Many applications of group theory to physical problems may be formulated in terms of the action of a matrix group on the set of complex matrices. Thus, let $G \subset GL(n,\mathbb{C})$ and $H \subset GL(m,\mathbb{C})$ denote arbitrary subgroups, respectively, of the general linear groups of $n \times n$ and $m \times m$ nonsingular matrices having complex elements, and let $M(n,m)$ denote the set of $n \times m$ complex matrices. The *left translation* of $G$ on $M(n,m)$ is defined by $L_g Z = gZ$, each $g \in G$, each $Z \in M(n,m)$. Similarly, the *right translation* of $H$ on $M(n,m)$ is defined by $R_h Z = Zh^T$, each $h \in H$, each $Z \in M(n,m)$. (Superscript $T$ denotes matrix transposition.) The most significant property of these left and right translations is that they commute; that is,

$$L_g(R_h Z) = R_h(L_g Z), \text{ each } g \in G,\ h \in H,\ Z \in M(n,m). \tag{2.1}$$

The transformation $Z \to Z' = L_g(R_h Z) = gZh^T$ can also be written as a linear transformation of vectors $z \in \mathbb{C}^{nm}$: one arranges the columns $Z^\alpha, \alpha = 1,2,\ldots,m$, of the $n \times m$ matrix $Z$ as successive entries in a single column vector $z \in \mathbb{C}^{nm}$. The transformation $Z' = gZh^T$ is then written in the equivalent form $z' = (g \times h)z$, where $\times$ denotes the direct product of matrices.

Let $f$ denote a complex function defined on $\mathbb{C}^{nm}$; that is, $f : z \to f(z) \in \mathbb{C}$, each $z \in \mathbb{C}^{nm}$. It is also convenient to express this relation as $f : Z \to f(Z) \in \mathbb{C}$, each $Z \in M(n,m)$.

Corresponding to the actions of the left and right translations $L_g$ and $R_h$ on matrices $Z \in M(n,m)$ (equivalently, on points of $\mathbb{C}^{nm}$), one defines the actions of $G$ and $H$ on functions defined on $\mathbb{C}^{nm}$:

$$(\mathcal{L}_g f)(Z) = f(g^T Z), \text{ each } g \in G, \tag{2.2a}$$
$$(\mathcal{R}_h f)(Z) = f(Zh), \text{ each } h \in H. \tag{2.2b}$$

Again one finds the commuting property for these group actions:

$$\mathcal{L}_g(\mathcal{R}_h f) = \mathcal{R}_h(\mathcal{L}_g f). \tag{2.3}$$

This latter result, when implemented on vectors $f \in \mathcal{H}$ of a Hilbert space $\mathcal{H}$, is an important group theoretical result for applications to quantum mechanics and has been employed in various guises by many authors.

## 2.2. Lie Algebras

Customarily, the emphasis in quantum mechanical applications is on the Lie algebras $L(G)$ and $L(H)$ of the groups $G$ and $H$, respectively. The *vector fields* corresponding to the group transformations (2.2a,b) are given, respectively, by

$$D_X = \mathrm{tr}(Z^T X \partial/\partial Z), \quad \text{each } X \in L(G), \tag{2.4a}$$
$$D^Y = \mathrm{tr}(Y^T Z^T \partial/\partial Z), \quad \text{each } Y \in L(H). \tag{2.4b}$$

In these relations $Z$ denotes the $n \times m$ complex matrix $Z = (z_i^\alpha)$ with element $z_i^\alpha \in \mathbb{C}$ in column $\alpha$ and row $i$ ($\alpha = 1,2,\ldots,m$; $i = 1,2,\ldots,n$), and $\partial/\partial Z = (\partial/\partial z_i^\alpha)$, the $n \times m$ matrix of corresponding derivatives. The matrix products are to be carried out keeping all derivatives to the right. (The symbol $\mathrm{tr}A$ denotes the trace of a matrix $A$.)

For $X, X' \in L(G)$, the differential operators defined by (2.4a) are *linear*, are *closed under commutation*, and are *derivations*; that is,

$$D_{\alpha X + \beta X'} = \alpha D_X + \beta D_{X'}, \ \alpha, \beta \in \mathbb{C}, \tag{2.5a}$$
$$[D_X, D_{X'}] = D_{[X,X']}, \tag{2.5b}$$
$$D_X(fg) = f D_X g + g D_X f, \ f, g \in \mathcal{H}. \tag{2.5c}$$

The differential operator $D_A$ ($X$ replaced by $A$) is defined for each $A \in M(n,m)$ so that $E_{\alpha X} = \alpha E_X$ is well-defined. Relations (2.5) are valid for this more general case with $X$ replaced by $A$ and $X'$ by $A'$. The restriction of (2.5) to the Lie algebra $L(G)$ assures that the commutator $[X, X']$ belongs to $L(G)$.

Properties analogous to relations (2.5) also hold for the vector fields $\{D^Y | Y \in L(H)\}$.

The commuting property (2.3) of the groups of operators $\{\mathcal{L}_g | g \in G\}$ and $\{\mathcal{R}_h | h \in H\}$ carries over to the Lie algebras $\{D_X | X \in L(G)\}$ and $\{D^Y | Y \in L(H)\}$; that is,

$$[D_X, D^Y] = 0, \quad \text{each } X \in L(G), \quad \text{each } Y \in L(H). \tag{2.6}$$

As discussed below, it is this commuting property of the vector fields $\{D_X\}$ and $\{D^Y\}$ which is the source of many applications of Lie algebras to quantum mechanics.

For $X = (x_{ij})$ $(i, j = 1, 2, \ldots n)$ and $Y = (y^{\alpha\beta})$ $(\alpha, \beta = 1, 2, \ldots, m)$, the explicit forms of the differential operators (2.4) are, respectively,

$$D_X = \sum_{i,j=1}^{n} x_{ij} D_{ij}, \tag{2.7a}$$

$$D^Y = \sum_{\alpha,\beta=1}^{m} y^{\alpha\beta} D^{\alpha\beta}. \tag{2.7b}$$

Here $D_{ij}$ and $D^{\alpha\beta}$ are the differential operators defined by

$$D_{ij} = \sum_{\alpha=1}^{m} z_i^\alpha (\partial/\partial z_j^\alpha), \quad i, j = 1, 2, \ldots n, \tag{2.8a}$$

$$D^{\alpha\beta} = \sum_{i=1}^{n} z_i^\alpha (\partial/\partial z_i^\beta), \quad \alpha, \beta = 1, 2, \ldots, m. \tag{2.8b}$$

The differential operators (2.8) satisfy the following commutation relations:

$$[D_{ij}, D_{k\ell}] = \delta_{jk} D_{i\ell} - \delta_{i\ell} D_{kj}, \tag{2.9a}$$

$$[D^{\alpha\beta}, D^{\gamma\epsilon}] = \delta^{\beta\gamma} D^{\alpha\epsilon} - \delta^{\alpha\epsilon} D^{\gamma\beta}, \tag{2.9b}$$

$$[D_{ij}, D^{\alpha\beta}] = 0, \tag{2.9c}$$

where $i, j, k, \ell = 1, 2, \ldots, n$ and $\alpha, \beta, \gamma, \epsilon = 1, 2, \ldots, m$. The operator sets $\{D_{ij}\}$ and $\{D^{\alpha\beta}\}$ are realizations of the Weyl generators of $GL(n, \mathbb{C})$ and $GL(m, \mathbb{C})$, respectively.

It is also useful to consider the Weyl generators of $G(nm, \mathbb{C})$ defined by

$$D_{ij}^{\alpha\beta} = z_i^\alpha \partial/\partial z_j^\beta. \tag{2.10a}$$

We then have

$$D_{ij} = \sum_{\alpha=1}^{m} D_{ij}^{\alpha\alpha}, \tag{2.10b}$$

$$D^{\alpha\beta} = \sum_{i=1}^{n} D_{ii}^{\alpha\beta}. \tag{2.10c}$$

## 2.3. Homogeneous Polynomial Spaces

In representation theory, one seeks the irreducible action of the operator sets $\{D_{ij}\}$ and $\{D^{\alpha\beta}\}$ on some appropriate space of functions $\{f(Z)\}$. For this, the most significant property of these operator sets is that they are *homogeneous of degree zero* in the variables $\{z_i^\alpha\}$. This means: *the space $\mathbb{P}_N$ of polynomials homogeneous of* (total) *degree $N$ in $\{z_i^\alpha\}$ is invariant under the action of the operators $D_X$ and $D^Y$:*

$$D_X : \ \mathbb{P}_N \to \mathbb{P}_N, \quad \text{each } X \in L(G), \tag{2.11a}$$

$$D^Y : \ \mathbb{P}_N \to \mathbb{P}_N, \quad \text{each } Y \in L(H). \tag{2.11b}$$

A second significant property of the operator sets $\{D_{ij}\}$ and $\{D^{\alpha\beta}\}$ is the fact that the invariant operators constructed separately from each of these operator sets are functionally dependent. These commuting invariants are given explicitly by

$$I_j^{(n)} = \sum_{(i_1 \cdots i_j)}^{n} D_{i_1 i_2} D_{i_2 i_3} \cdots D_{i_j i_1}, \quad j = 1, 2, \ldots n, \tag{2.12a}$$

$$I_{(m)}^{\beta} = \sum_{(\alpha_1 \cdots \alpha_\beta)}^{m} D^{\alpha_1 \alpha_2} D^{\alpha_2 \alpha_3} \cdots D^{\alpha_\beta \alpha_1}, \quad \beta = 1, 2, \ldots, m. \tag{2.12b}$$

(Casimir and Van der Waerden[13] defined the quadratic invariant only, and Gel'fand[14] extended this construction to a *complete set of invariant operators* for any classical group.) One has, for $m = n$, the relations

$$I_j^{(n)} = I_{(n)}^{j}, \quad j = 1, 2, \ldots, n; \tag{2.13a}$$

for $m < n$,

$$I_j^{(n)} = P_j \left( I_{(m)}^1, I_{(m)}^2, \ldots, I_{(m)}^m \right), \quad j = 1, 2, \ldots, n; \tag{2.13b}$$

and for $m > n$,

$$I_{(m)}^{\beta} = P^\beta \left( I_1^{(n)}, I_2^{(n)}, \ldots, I_n^{(n)} \right), \quad \beta = 1, 2, \ldots, m, \tag{2.13c}$$

where $P_j$ and $P^\beta$ are polynomials (see Ref. 15). The significance of these results for the invariant operators (2.12) of $GL(n,\mathbb{C})$ and $GL(m,\mathbb{C})$ is that each polynomial in the space $\mathbb{P}_N$ which is a simultaneous eigenpolynomial of the set of operators $\{I^\beta_{(m)}\}$ $(m \leq n)$ is also a simultaneous eigenpolynomial of the operators $\{I^{(n)}_j\}$ (a similar result holds for $m > n$). This property is important below in the discussion of the irreps of $GL(n,\mathbb{C})$ and $GL(m,\mathbb{C})$ carried by the space $\mathbb{P}_N$.

It is often useful to construct a separable Hilbert space $\mathcal{H}$ from the homogenous polynomial spaces $\mathbb{P}_N$ by forming the (infinite) direct sum

$$\mathcal{H} = \sum_{N=0}^{\infty} \oplus \mathbb{P}_N. \tag{2.14}$$

The inner product of two polynomials $p_N \in \mathbb{P}_N$ and $q_{N'} \in \mathbb{P}_{N'}$ is defined by (see, for example, Ref. 16)

$$(p_N, q_{N'}) = p^*_N(\partial/\partial Z) q_{N'}(Z)\big|_{Z=0}. \tag{2.15}$$

With respect to this inner product, $z^\alpha_i$ and $\partial/\partial z^\alpha_i$ are Hermitian conjugate operators, and, correspondingly, the operators $D_{ij}$ and $D^{\alpha\beta}$ satisfy the conjugation (†) relations

$$D^\dagger_{ij} = D_{ji}, \quad (D^{\alpha\beta})^\dagger = D^{\beta\alpha}. \tag{2.16}$$

The invariant operators $\{I^{(n)}_j\}$ and $\{I^\beta_{(m)}\}$ are then Hermitian and mutually commuting.

There are several ways of introducing an inner product into the space $\mathcal{H}$, one of the more often used being the Bargmann[17] inner product, which also gives $(\partial/\partial z^\alpha_i)^\dagger = z^\alpha_i$. The resulting Hilbert space is isomorphic to the space $\mathcal{H}$ defined above.

## 2.4. Boson Operator Realization

In many quantum mechanical applications of the theory outlined above, the complex variables $Z = (z^\alpha_i)$ and the derivatives $(\partial/\partial Z) = (\partial/\partial z^\alpha_i)$ are replaced by more general operators $A = (a^\alpha_i)$ and $\overline{A} = (\overline{a}^\alpha_i)$. These operators are then required to satisfy the commutation relations

$$[a^\alpha_i, a^\beta_j] = 0, \quad [\overline{a}^\alpha_i, \overline{a}^\beta_j] = 0, \tag{2.17a}$$

$$[\overline{a}^\alpha_i, a^\beta_j] = \delta^{\alpha\beta}\delta_{ij}, \tag{2.17b}$$

in analogy to the relations satisfied by the $\partial/\partial z_i^\alpha$ and $z_j^\beta$. The inner product (2.15) is then replaced by the numerically equal inner product.

$$\langle 0|p_N^*(\overline{A})q_{N'}(A)|0\rangle = (p_N, q_{N'}), \tag{2.18}$$

in which $|0\rangle$ is the (abstract) state defined by

$$\overline{a}_i^\alpha|0\rangle = 0, \quad i = 1,2,\ldots,n;\ \alpha = 1,2,\ldots m. \tag{2.19}$$

The vector space structure thus defined is isomorphic to the Hilbert space $\mathcal{H}$ defined by Eq. (2.14), hence also to the Bargmann space mentioned above.

This isomorphism of vector spaces is made more explicit by introducing the operators $\{E_{ij}\}$ and $\{E^{\alpha\beta}\}$ in analogy to the $\{D_{ij}\}$ and $\{D^{\alpha\beta}\}$ defined by Eqs. (2.8):

$$E_{ij} = \sum_{\alpha=1}^{m} a_i^\alpha \overline{a}_j^\alpha, \quad i,j = 1,2,\ldots,n, \tag{2.20a}$$

$$E^{\alpha\beta} = \sum_{i=1}^{n} a_i^\alpha \overline{a}_i^\beta, \quad \alpha,\beta = 1,2,\ldots,m. \tag{2.20b}$$

In consequence of the property $\overline{a}_i^\alpha|0\rangle = 0$, $i = 1,2,\ldots,n$; $\alpha = 1,2,\ldots m$, the action of the operators (2.20) on a general state $p_N(A)|0\rangle$, $p_N \in \mathbb{P}_N$, is given by commutation:

$$E_{ij}p_N(A)|0\rangle = [E_{ij}, p_N(A)]\,|0\rangle, \tag{2.21a}$$

$$E^{\alpha\beta}p_N(A)|0\rangle = [E^{\alpha\beta}, p_N(A)]\,|0\rangle. \tag{2.21b}$$

The commutators in relations (2.21) can also be expressed as

$$[E_{ij}, p_N(A)] = D_{ij}p_N(Z)\big|_{Z=A} = p'_N(A), \tag{2.22a}$$

$$[E^{\alpha\beta}, p_N(A)] = D^{\alpha\beta}p_N(Z)\big|_{Z=A} = p''_N(A), \tag{2.22b}$$

where, for each $p_N \in \mathbb{P}_N$, one has that $p'_N, p''_N \in \mathbb{P}_N$. Accordingly, the space of state vectors

$$\{p_N(A)|0\rangle\,|p_N \in \mathbb{P}_N\} \tag{2.23}$$

is invariant under the action of the operator sets $\{E_{ij}\}$ and $\{E^{\alpha\beta}\}$.

One may now proceed to duplicate for the boson operator sets $\{E_{ij}\}$ and $\{E^{\alpha\beta}\}$ the properties given in Section 2.2 for the Lie algebras $L(G)$ and $L(H)$ with basis sets $\{D_{ij}\}$ and $\{D^{\alpha\beta}\}$, respectively.

## 2.5. Irreducible Polynomial Spaces and Representations

It is well-known that the degree $N$ homogeneous polynomial *irreducible representations* of $GL(n,\mathbb{C})$ are in one-to-one correspondence with the partitions of $N$ into $n$ parts, including zero as a part. We denote such a partition by $[\lambda]$ and define it by

$$[\lambda] = [\lambda_1, \lambda_2, \ldots, \lambda_n], \quad \text{each } \lambda_i \in \mathbb{N}, \tag{2.24a}$$

where $\mathbb{N}$ denotes the set of nonnegative integers and

$$\lambda_1 \geq \lambda_2 \geq \ldots \geq \lambda_n \geq 0, \tag{2.24b}$$

$$\lambda_1 + \lambda_2 + \ldots + \lambda_n = N. \tag{2.24c}$$

It has been shown[15,16,18] that the space of homogeneous polynomials $\mathcal{P}_N$, whose domain is the set of $nm$ complex variables $Z = (z_i^\alpha)$, $i = 1,2,\ldots,n$; $\alpha = 1,2,\ldots,m$, splits under the action of the commuting operator sets $\{D_X | X \in g\ell(n,\mathbb{C})\}$ and $\{D^Y | Y \in g\ell(m,\mathbb{C})\}$ into a direct sum of invariant subspaces characterized by the partitions of $N$ into not more than $m$ parts (for $m \leq n$). Thus, let $[\lambda]$ and $[\lambda, 0^{n-m}]$ denote the partitions of $N$ as follows:

$$[\lambda] = [\lambda_1, \lambda_2, \ldots, \lambda_m], \tag{2.25a}$$

$$[\lambda, 0^{n-m}] = [\lambda_1, \ldots, \lambda_m, 0, \ldots, 0], \tag{2.25b}$$

where $0^{n-m}$ denotes $n-m$ repeated zeros. The parts $\lambda_i \in \mathbb{N}$ of the partition $[\lambda]$ are to satisfy

$$\lambda_1 \geq \lambda_2 \geq \ldots \geq \lambda_m \geq 0, \tag{2.26a}$$

$$\lambda_1 + \lambda_2 + \ldots + \lambda_m = N. \tag{2.26b}$$

Let $\mathbf{P}_N(m)$ denote the set of all such partitions of $N$ into $m$ parts. Then the space $\mathcal{P}_N$ may be written as a direct sum

$$\mathcal{P}_N = \sum_{[\lambda] \in \mathbf{P}_N(m)} \oplus \mathcal{P}_{[\lambda]}, \tag{2.27}$$

where each space $\mathcal{P}_{[\lambda]}$ occurs exactly once. Each of these spaces $\mathcal{P}_{[\lambda]}$ is invariant under $D_X$ and $D^Y$:

$$D_X : \ \mathcal{P}_{[\lambda]} \to \mathcal{P}_{[\lambda]}, \quad \text{each } X \in gl(n,\mathbb{C}), \tag{2.28a}$$

$$D^Y : \ \mathcal{P}_{[\lambda]} \to \mathcal{P}_{[\lambda]}, \quad \text{each } Y \in gl(m,\mathbb{C}). \tag{2.28b}$$

Indeed, the space $\mathbb{P}_{[\lambda]}$ is uniquely characterized by the fact that each vector in the space is an eigenpolynomial of the invariant operators $\{I_j^{(n)}\}$ and $\{I_{(m)}^{\beta}\}$ defined by (2.12).

The dimension of the space $\mathbb{P}_{[\lambda]}$, $[\lambda] \in \mathbf{P}_N(m)$, is given by

$$\mathrm{Dim}\mathbb{P}_\lambda \;=\; \mathrm{Dim}[\lambda]\,\mathrm{Dim}[\lambda, 0^{n-m}]. \tag{2.29}$$

The dimension factors on the right are given by Weyl's dimension formula for the irreps of the general linear group: $GL(k,\mathbb{C})$. For $[\mu] = [\mu_1, \mu_2, \ldots, \mu_k]$, each $\mu_i \in \mathbb{N}$, and $\mu_1 \geq \mu_2 \geq \ldots \geq \mu_k \geq 0$, the formula is

$$\mathrm{Dim}[\mu] \;=\; \prod_{r<s}^{k} {}_1 (\mu_r - \mu_s + r - s)/1!\,2! \ldots (k-1)!. \tag{2.30}$$

There is a close relationship between the vectors spanning the irreducible bases of the space $\mathbb{P}_N$ and the irreps of the group $GL(n,\mathbb{C})$. In order to describe this structure as succinctly as possible, it is convenient to take $m = n$, so that we are dealing with the space $\mathbb{P}_N^{(n^2)}$ of homogeneous polynomials of degree $N$ in the $n^2$ variables $z_i^j$ $(i,j = 1,2,\ldots,n)$. We shall see below that this is, in fact, no restriction.

Let us first describe a set of orthonormal basis vectors that span the irrep spaces that occur in the decomposition of $\mathbb{P}_N^{(n^2)}$ $(m = n)$. This is conveniently carried out by requiring that the basis vectors be simultaneous eigenvectors of the collection of operators (2.13a) associated with the unitary groups in the group-subgroup chain

$$U(n) \supset U(n-1) \supset \ldots \supset U(2) \supset U(1). \tag{2.31}$$

These operators are given by

$$\left\{ I_j^{(k)} \,|k = 1,2,\ldots,n;\;\; j = 1,2,\ldots,k \right\} \tag{2.32}$$

and are $n(n+1)/2$ in number, and they mutually commute. The set of simultaneous eigenvectors of these commuting, Hermitian operators is, in fact, a unique (up to arbitrary multiplicative constants) set of vectors spanning the space $\mathbb{P}_N^{(n^2)}$.

The description of the unique basis vectors described above may be given in terms of the so-called standard double-tableaux[12] or the associated double Weyl-Gel'fand-Zetlin patterns. We shall employ the latter. These patterns are triangular arrays of integers[19,20] that realize, by geometrical constraints,

the Weyl group-subgroup theorem enumerating the irreps of $U(n-1)$ contained in a given irrep of $U(n)$, when the latter is reduced, $U(n) \downarrow U(n-1)$, with respect to $U(n-1)$. Thus, the irreps of $U(n)$, $U(n-1)$, $U(n-2)$, $\ldots, U(1)$ are enumerated separately by partitions

$$\begin{aligned} [m]_n &= [m_{1n}, m_{2n}, \ldots, m_{nn}], \\ [m]_{n-1} &= [m_{1,n-1}, m_{2,n-1}, \ldots, m_{n-1,n-1}], \\ &\vdots \\ [m]_2 &= [m_{12}, m_{22}], \\ [m]_1 &= m_{11}. \end{aligned} \tag{2.33}$$

The Weyl-Gel'fand-Zetlin pattern places these irrep labels in a triangular array:

$$(m) = \begin{pmatrix} m_{1n} & m_{2n} & \cdots & & m_{nn} \\ & m_{1,n-1} & m_{2,n-1} & \cdots & m_{n-1,n-1} \\ & \ddots & & \iddots & \\ & & m_{12} & m_{22} & \\ & & & m_{11} & \end{pmatrix} \tag{2.34}$$

For a given irrep $[m]_n$ of $U(n)$, the Weyl reduction rules are realized as constraints on the remaining entries in the array (2.34). In detail, these constraints are the conditions

$$m_{1n} \geq m_{1,n-1} \geq m_{2n} \geq m_{2,n-1} \geq \ldots \geq m_{n-1,n} \geq m_{n-1,n-1} \geq m_{n,n} \tag{2.35a}$$

between row $n$ and row $n-1$; the conditions

$$m_{1,n-1} \geq m_{1,n-2} \geq m_{2,n-1} \geq \ldots \geq m_{n-2,n-1} \geq m_{n-2,n-2} \geq m_{n-1,n-1} \tag{2.35b}$$

between row $n-1$ and row $n-2$;

$\vdots$

the conditions

$$m_{12} \geq m_{11} \geq m_{22} \tag{2.35c}$$

between row 2 and row 1. Collectively, these constraints are called *betweenness conditions*. An array satisfying the betweenness conditions is called a *lexical* array, and one violating these conditions a *nonlexical* array. Lexical and nonlexical Gel'fand patterns, as we shall briefly refer to Weyl-Gel'fand-Zetlin patterns, are significant concepts in the sequel.

An important function defined on the set of Gel'fand patterns is the *weight function.* We denote the set of Gel'fand patterns having specified irrep labels $[m]_n$ by $G([m]_n)$:

$$G([m]_n) = \left\{ \begin{pmatrix} [m]_n \\ (m)_{n-1} \end{pmatrix} \middle| \, (m)_{n-1} \text{ is a lexical pattern} \right\}. \tag{2.36}$$

The weight of $(m) \in G([m]_n)$ is the row vector

$$w(m) = (w_1(m),\ w_2(m),\ \ldots,\ w_n(m)), \tag{2.37}$$

where $w_j(m)$ is defined to be the sum of the entries in row $j$ of $(m)$ minus the sum of the entries in row $j-1$:

$$w_j(m) = \sum_{i=1}^{j} m_{ij} - \sum_{i=1}^{j-1} m_{i,j-1}, \text{ with } w_1(m) = m_{11}. \tag{2.38}$$

We denote the set of all distinct weights of $G([m]_n)$ by $W([m]_n)$:

$$W([m]_n) = \left\{ w(m) \middle| (m) \in G([m]_n) \right\}. \tag{2.39}$$

Distinct patterns $(m), (m') \in G([m]_n)$ may have the same weight; we enumerate only distinct weights in the set $W([m]_n)$. The *multiplicity of a weight* $w \in W([m]_n)$ is the number of patterns $(m), (m'), \ldots$ that are mapped to $w$ by the rule (2.38). This multiplicity number is called a Kostka number and is denoted by $K([m]_n, w)$. Since the number of patterns in $G([m]_n)$ is given by the Weyl dimension formula, $\mathrm{Dim}[m]_n$, the following relation holds between Kostka numbers and the Weyl dimension number:

$$\mathrm{Dim}[m]_n = \sum_{w \in W([m]_n)} K([m]_n, w). \tag{2.40}$$

Using the above Gel'fand arrays, we can now describe a basis of the space $I\!P_N^{(n^2)}$ in terms of basis vectors of carrier spaces of irreps of $GL(n, \mathbb{C})$. This uses the notion of a *double Gel'fand pattern that shares the common irrep label* $[m]_n$:

$$\begin{pmatrix} (m')_{n-1} \\ [m]_n \\ (m)_{n-1} \end{pmatrix}. \tag{2.41a}$$

Here, for convenience of display, we invert the standard Gel'fand pattern

$$\begin{pmatrix} [m]_n \\ (m')_{n-1} \end{pmatrix} \tag{2.41b}$$

over the pattern

$$\begin{pmatrix} [m]_n \\ (m)_{n-1} \end{pmatrix}. \tag{2.41c}$$

For example, for $n = 3$, the double Gel'fand pattern is

$$\begin{pmatrix} & & m'_{11} & & \\ & m'_{12} & & m'_{22} & \\ m_{13} & & m_{23} & & m_{33} \\ & m_{12} & & m_{22} & \\ & & m_{11} & & \end{pmatrix}. \tag{2.42}$$

We frequently omit the subscripts $n$ and $n-1$ on $[m]_n$ and $(m)_{n-1}$ when the context is clear.

The basis vectors of the space $\mathbb{P}_N^{(n^2)}$ are labeled by double Gel'fand patterns (2.41a), where

(i) The partitions $[m]_n$ run over all partitions of $N$; that is, over all nonnegative integers $m_{in}$ such that

$$\begin{aligned} m_{1n} + m_{2n} + \ldots + m_{nn} &= N \\ m_{1n} \geq m_{2n} &\geq \ldots \geq m_{nn} \geq 0. \end{aligned} \tag{2.43}$$

(ii) For each partition $[m]_n$, the entries in the Gel'fand arrays $(m)_{n-1}$ and $(m')_{n-1}$ run independently over all values consistent with the betweenness conditions. Thus, for given $[m]_n$, there are, in all, (Dim $[m]_n)^2$ double Gel'fand patterns, where Dim $[m]_n$ denotes Weyl's dimension for irrep $[m]_n$ of $U(n)$.

We denote a basis vector of $\mathbb{P}_N^{(n^2)}$ labelled by the double Gel'fand pattern (2.41a) by the notation

$$P\begin{pmatrix} (m') \\ [m] \\ (m) \end{pmatrix} \in \mathbb{P}_N^{(n^2)} \tag{2.44a}$$

with values given by

$$P\begin{pmatrix} (m') \\ [m] \\ (m) \end{pmatrix}(Z) \in \mathbb{C}. \tag{2.44b}$$

These are, of course, homogeneous polynomials of total degree $N$ in the $n^2$ complex variables $z_i^j$ $(i,j = 1,2,\ldots,n)$.

We denote by $\mathbb{P}_N([m])$ the vector space spanned by the homogeneous polynomials (2.44a) for each partition $[m] \in \mathbf{P}_N(n)$. The set of polynomials

$$\left\{ P\begin{pmatrix}(m')\\ [m]\\ (m)\end{pmatrix} \Big| [m] \in \mathbf{P}_N(n);\ \text{all lexical patterns } (m'),(m) \right\} \tag{2.45}$$

is an orthonormal basis of $\mathbb{P}_N([m])$, each $[m] \in \mathbf{P}_N(n)$, with respect to the inner product (2.15). The orthogonality is a consequence of the fact that each polynomial in the set (2.45) is a simultaneous eigenvector of the complete set of commuting invariant operators (2.32); we also normalize these polynomials to unity. This normalization itself is achieved by normalizing the *highest weight vector* to unity. The highest weight vector in the set (2.45) is the one in which the entries $(m)$ and $(m')$ are chosen as large as possible for a prescribed partition $[m]$; that is,

$$m_{ij} = m'_{ij} = m_{in}, \quad i = 1,2,\ldots,n-1;\ j = 1,2,\ldots,i. \tag{2.46a}$$

We write

$$(m) = (\max), \quad (m') = (\max) \tag{2.46b}$$

for this *maximal set* of labels. The weight of a maximal Gel'fand pattern is found from definition (2.38) to be the irrep label $[m]$ itself. The explicit normalized highest weight vector in the set (2.45) is then given by

$$P\begin{pmatrix}(\max)\\ [m]\\ (\max)\end{pmatrix}(Z) = [\mathcal{M}([m])]^{-1/2} \prod_{i=1}^{n} \left(z_1^{1\,2\cdots i}\right)^{m_{in}-m_{i+1,n}}, \tag{2.47a}$$

where $m_{n+1,n} = 0$, and

$$z_{i_1 i_2 \cdots i_k}^{j_1 j_2 \cdots j_k} = \det \begin{pmatrix} z_{i_1}^{j_1} & \cdots & z_{i_1}^{j_k} \\ \vdots & & \vdots \\ z_{i_k}^{j_1} & \cdots & z_{i_k}^{j_k} \end{pmatrix}. \tag{2.47b}$$

The normalization factor $\mathcal{M}([m])$ is given by

$$\mathcal{M}([m]) = \prod_{i=1}^{n} p_{in}! \Big/ \prod_{i<j} (p_{in} - p_{jn}), \tag{2.48a}$$

where

$$p_{in} = m_{in} + n - i, \quad i = 1, 2, \ldots, n, \tag{2.48b}$$

and more generally

$$p_{ij} = m_{ij} + j - i, \quad j = 1, 2, \ldots; \quad i = 1, 2, \ldots j \tag{2.48c}$$

denote the so-called *partial hooks*. (The partial hooks are useful, since these are the *symmetric* variables for the eigenvalues of the invariants.)

The construction of the subspaces $\mathbb{P}_N([m]) \subset \mathbb{P}_N^{(n^2)}$, with orthonormal basis (2.45), solves completely the problem of splitting the space $\mathbb{P}_N^{(n_2)}$ of homogeneous polynomials of degree $N$ in the $n^2$ variables $(z_i^j)$ into subspaces that are carrier spaces of the irreps of $GL(n, \mathbb{C})$ under the left and right actions of this group defined by Eq. (2.2). The space splits according to the direct sum:

$$\mathbb{P}_N^{(n^2)} = \sum_{[m] \in \mathbf{P}_N(n)} \oplus \mathbb{P}_N([m]), \tag{2.49a}$$

where the summation extends over all partitions $[m]$ of $N$ into $n$ parts (including zeros). Moreover, the spaces in this direct sum are perpendicular in the inner product (2.15):

$$\mathbb{P}_N([m]) \perp \mathbb{P}_N([m']), \quad [m] \neq [m']. \tag{2.49b}$$

Before giving the explicit transformations of the space $\mathbb{P}_N([m])$ into itself under the action of the group $GL(n, \mathbb{C})$, it is convenient to introduce another notation for the basis vectors (2.45) that focuses on the fact that these basis vectors play a dual role: *Not only are they basis vectors of the space* $\mathbb{P}_N([m])$, *they are also irreducible representations of* $GL(n, \mathbb{C})$. To emphasize this property, we introduce a notation modelled after the Wigner D-function of $SU(2)$:

$$D^{[m]}_{(m)(m')}(Z) = [\mathcal{M}([m])]^{1/2} P \begin{pmatrix} (m') \\ [m] \\ (m) \end{pmatrix} (Z). \tag{2.50}$$

We have thus removed the normalization factor $\mathcal{M}([m])^{-1/2}$ from the polynomials $P([m])$. Thus, the D-functions (2.50) are not normalized in the inner product (2.15). This is deliberate so as to give these D-functions special properties that we now explain. The notation (2.50) is designed with the following properties in mind: The irrep labels $[m]$ label a matrix of dimension

Dim$[m]$, whose row labels are the Gel'fand patterns $(m)$ and column labels are the patterns $(m')$. We denote this matrix by

$$\mathbf{D}^{[m]}(Z). \tag{2.51a}$$

The polynomials defined by Eq. (2.50), with the factor $[\mathcal{M}([m])]^{1/2}$ multiplying the normalized basis vectors, now have the property that for $z_i^j = \delta_i^j$; that is, for $Z = I_n$, we have

$$\mathbf{D}^{[m]}(I_n) \;=\; I_{Dim[m]}, \tag{2.51b}$$

where $I_k$ $(k = 1, 2, \ldots)$ denotes the $k \times k$ unit matrix. The matrices (2.51a) have the group property

$$\mathbf{D}^{[m]}(Z)\mathbf{D}^{[m]}(Z') \;=\; \mathbf{D}^{[m]}(ZZ'); \tag{2.51c}$$

that is, the correspondence

$$Z \to \mathbf{D}^{[m]}(Z), \quad \text{each } Z \in GL(n, \mathbb{C}), \tag{2.51d}$$

is a *representation* of $GL(n, \mathbb{C})$.

Let us now summarize some of the more important properties of the space $\mathbb{P}_N([m])$, using either the language of basis vectors or of irrep functions, as appropriate to the stated property:

(i) The representation matrices $\mathbf{D}^{[m]}(Z)$ satisfy the transposition rule

$$\left[\mathbf{D}^{[m]}(Z)\right]^T \;=\; \mathbf{D}^{[m]}(Z^T). \tag{2.52}$$

(ii) The representation matrices satisfy the group-subgroup reduction rule

$$\mathbf{D}^{[m]_n}\begin{pmatrix} Z' & 0 \\ 0 & 1 \end{pmatrix} \;=\; \sum_{[m]_{n-1}} \oplus\, \mathbf{D}^{[m]_{n-1}}(Z'), \tag{2.53a}$$

where the direct sum of matrices is over all partitions

$$[m]_{n-1} \;=\; [m_{1,n-1}, \ldots, m_{n-1,n-1}] \tag{2.53b}$$

that obey the Weyl rule of betweenness:

$$m_{1n} \geq m_{1,n-1} \geq m_{2n} \geq \ldots \geq m_{n-1,n} \geq m_{n-1,n-1} \geq m_{nn}. \tag{2.53c}$$

(iii) Under the restriction $Z \to U \in U(n)$, the representation matrices $\mathbf{D}^{[m]}(U)$ are unitary:

$$[\mathbf{D}^{[m]}(U)]^\dagger = [\mathbf{D}^{[m]}(U)]^{-1}. \tag{2.54}$$

(iv) Under the left and right actions $\mathcal{L}_X$ and $\mathcal{R}_Y$ defined by Eqs. (2.2), for each $X, Y \in GL(n,\mathbb{C})$, the basis vectors $P([m])$ of $\mathbb{P}_N(n)$ are transformed irreducibly according to

$$\left[\mathcal{L}_X P\begin{pmatrix}(m')\\[m]\\(m)\end{pmatrix}\right](Z) = P\begin{pmatrix}(m')\\[m]\\(m)\end{pmatrix}(X^T Z)$$

$$= \sum_{(m'')} D^{[m]}_{(m'')(m)}(X) P\begin{pmatrix}(m')\\[m]\\(m'')\end{pmatrix}(Z); \tag{2.55a}$$

$$\left[\mathcal{R}_Y P\begin{pmatrix}(m')\\[m]\\(m)\end{pmatrix}\right](Z) = P\begin{pmatrix}(m')\\[m]\\(m)\end{pmatrix}(ZY)$$

$$= \sum_{(m'')} D^{[m]}_{(m'')(m')}(Y) P\begin{pmatrix}(m'')\\[m]\\(m)\end{pmatrix}(Z). \tag{2.55b}$$

For $Z \in GL(n,\mathbb{C})$ these relations are, of course, just expressions of the group property, accounting for the symmetry (2.52). It is important to observe that to each upper pattern $(m')$ in the basis vector (2.45) there corresponds a vector space

$$\mathbb{P}_N\begin{pmatrix}(m')\\[m]\end{pmatrix} \tag{2.56a}$$

with basis

$$\left\{ P\begin{pmatrix}(m')\\[m]\\(m)\end{pmatrix} \middle| (m) \text{ is lexical} \right\}. \tag{2.56b}$$

The dimension of this space is $\mathrm{Dim}([m])$, and each such space transforms into itself irreducibly under the left action of $GL(n,\mathbb{C})$. A similar result holds for the right action, where the vector space is denoted

$$\mathbb{P}_N\begin{pmatrix}[m]\\(m)\end{pmatrix} \tag{2.57a}$$

with basis

$$\left\{ P \begin{pmatrix} (m') \\ [m] \\ (m) \end{pmatrix} \middle| (m') \text{ is lexical} \right\}. \tag{2.57b}$$

(v) There is a duality between pattern restrictions and variable restrictions in the following sense: Write the matrix $Z$ in terms of its column matrices as $Z = [\mathbf{z}^1 \mathbf{z}^2 \dots \mathbf{z}^n]$. Then to the variable restriction given by

$$\mathbf{z}^j = 0, \quad j = k+1, \dots, n \; (1 \leq k < n), \tag{2.58a}$$

there corresponds the pattern restriction given by

$$\begin{pmatrix} (m') \\ [m] \\ (m) \end{pmatrix} \longrightarrow \begin{pmatrix} & & (m')_{k-1} & & & \\ & m_{1n} & \cdots & m_{kn} & & \\ & & & & 0 & \\ \iddots & & \iddots & \iddots & & \ddots \\ m_{1n} & \cdots & m_{kn} & 0 & \cdots & 0 \\ \ddots & & \ddots & \ddots & & \iddots \\ & & & & 0 & \\ & m_{1k} & \cdots & m_{kk} & & \\ & & (m)_{k-1} & & & \end{pmatrix} \tag{2.58b}$$

In the lower pattern, all lexical patterns are allowed that are consistent with $m_{in} = 0$, $i = k+1, \dots, n$; in the upper pattern, one has, in addition, that the labels in rows $k$, $k+1, \dots, n$ take on their maximum values. By *duality*, we mean that under the variable restriction (2.58a) in the basis polynomials (2.44b), one gets zero for the value unless one restricts the pattern to (2.58b). Conversely, if one makes the pattern restriction (2.58b) in the basis polynomials (2.44b), then the variables $\mathbf{z}^j$, $j = k+1, \dots, n$, do not appear in these polynomials. It is these properties that allow one to recover from the $n \times n$ matrix $Z$ and the associated polynomials (2.44b), the full theory of the irreps of $GL(n, \mathbb{C})$ and $GL(k, \mathbb{C})$ under the left and right actions of these groups on the $n \times k$ matrix $Z$ as presented in Section 2.1.

(vi) Each of the Lie algebras

$$\{E_X | X \in g\ell(n, \mathbb{C})\} \text{ and } \{E^Y | Y \in g\ell(n, \mathbb{C})\} \tag{2.59a}$$

acts irreducibly on the respective vector spaces

$$\mathbb{P}_N \begin{pmatrix} (m') \\ [m] \end{pmatrix} \quad \text{and} \quad \mathbb{P}_N \begin{pmatrix} [m] \\ (m) \end{pmatrix}. \tag{2.59b}$$

The matrices of the generators $\{D_{ij}\}$ and $\{D^{\alpha\beta}\}$ are the standard ones given by Gel'fand and Zetlin[19] and others.

We have emphasized above the fact that we may obtain the class of finite-dimensional irreps of the general linear group by considering spaces of homogeneous polynomials over the complex numbers and their transformation properties. This then gives all finite-dimensional unitary representations of $SU(n)$, and of $U(n)$, when properly extended by adjoining the invariant, $\det U$.

The family of polynomials

$$\left\{ P\begin{pmatrix}(m')\\ [m]\\ (m)\end{pmatrix} \;\middle|\; \text{all partitions } [m]\text{; all lexical patterns } (m),\ (m') \right\} \tag{2.60}$$

are objects of great significance, since *they span the space of all polynomials, in any number of variables and of arbitrary degree.* Their occurrences in many areas of mathematics and physics, in various guises, should come as no surprise. These interrelations are for the most part undeveloped. [See Refs. 19-24].

## 2.6. Algebras Associated with the General Linear Group

In the preceding subsections 2.1-2.5, we have reviewed how the left and right translation actions of the general linear group on the space of polynomials are used to determine canonically defined irrep spaces and the irreps themselves. We have pointed out in the Introduction the need to go beyond such constructions for addressing physical applications to complex systems and consider also the WCG-coefficients, Racah coefficients, and irreducible tensor operators of the underlying (compact) symmetry group. There is, of course, a vast literature on this subject with many approaches. For the unitary groups $U(n)$ we have found that a unifying viewpoint for this subject can be based on two algebraic structures, and it is the purpose of this section to outline these algebras. Not only are these algebras interesting in their own right, but they are highly suggestive of how natural or canonical methods come into play.

There are two important algebras associated with $GL(n,\mathbb{C})$. The first is that of the *representation functions* (homogeneous polynomials) defined by (2.50) above; and the second that of unit $U(n)$ *tensor operators*, which are defined below. The Wigner-Clebsch-Gordan (WCG) coefficients of $U(n)$, or equivalently of the *integral representations* (2.50) of $GL(n,\mathbb{C})$, have significant roles in each of these algebras. Accordingly, we next discuss how WCG-coefficients arise in the problem of reducing the Kronecker product (matrix direct product) of two integral irreps of $GL(n,\mathbb{C})$.

It is convenient to modify the earlier notation slightly so that the results given in this section parallel as much as possible the well-known results for $SU(2)$. We let $\mathbf{P}(n)$ denote the set of all partitions with $n$ parts, including 0 as a part. We denote such partitions by $\lambda, \mu, \nu, \ldots$. Thus, irrep labels $[m]_n$, $[m']_n, \ldots$ are now replaced by $\lambda, \mu, \ldots$. The double Gel'fand pattern (2.41a) is denoted by

$$\begin{pmatrix} m' \\ \lambda \\ m \end{pmatrix} = \begin{pmatrix} (m')_{n-1} \\ [m]_m \\ (m)_{n-1} \end{pmatrix}, \tag{2.61}$$

in which all subscripts on arrays symbols have been dropped. For example, the integral representation functions of $GL(n, \mathbb{C})$ defined by Eq. (2.50) are now denoted

$$D^{\lambda}_{mm'}(Z) = [M(\lambda)]^{1/2} P \begin{pmatrix} m' \\ \lambda \\ m \end{pmatrix} (Z). \tag{2.62}$$

The Kronecker product of two irreps $D^{\mu}$ and $D^{\nu}$ of $GL(n, \mathbb{C})$ is completely reducible into irreps of $GL(n, \mathbb{C})$:

$$D^{\mu} \times D^{\nu} = \sum_{\Delta \in W(\mu)} \oplus I(\mu \times \nu;\ \nu + \Delta) D^{\nu + \Delta}, \tag{2.63}$$

where the summation is over all distinct weights $\Delta$ of irrep $\mu$. The *intertwining numbers* $I(\mu \times \nu;\ \nu + \Delta)$ in this relation express the number of times irrep $\lambda = \nu + \Delta$ is contained in the direct product irrep $\mu \times \nu$. They are related to the Littlewood- Richardson numbers $g(\mu\nu\lambda)$ by $I(\mu \times \nu;\ \lambda) = g(\mu\nu\lambda)$ and have the property (see Ref. 25):

$$I(\mu \times \nu;\ \lambda) = g(\mu\nu\lambda) = 0, \text{ unless } \lambda = \nu + \Delta \text{ for some weight } \Delta \in W(\mu). \tag{2.64}$$

Indeed, the properties of these numbers when viewed as *functions over the set of all partitions* $\nu \in \mathbf{P}(n)$, that is,

$$I_{\mu,\Delta} : \quad \mathbf{P}(n) \longrightarrow L_{\mu,\Delta} = \{0, 1, \ldots, K(\mu, \Delta)\}, \tag{2.65}$$

with values $I_{\mu,\Delta}(\nu) = I(\mu \times \nu;\ \nu + \Delta)$ in the set $L_{\mu,\Delta}$, are crucial to the definition and construction of unit tensor (Wigner) operators in $U(n)$ (see below). The (Kostka) number $K(\mu, \Delta)$ is the multiplicity of $\Delta \in W(\mu)$. [See Eq. (2.38) for the definition of the weight of a Gel'fand pattern, which we denote here by $\Delta$.]

Using the above notations, we may now state the *product law for representation functions:*

$$D^{\mu}_{m_1 m_1'}(Z)\, D^{\nu}_{m_2 m_2'}(Z) = \sum_{\lambda,m,m'} \begin{bmatrix} m' & m_1' & m_2' \\ \lambda & \mu & \nu \\ m & m_1 & m_2 \end{bmatrix} D^{\lambda}_{mm'}(Z). \tag{2.66}$$

The summation is over all distinct irreps $\lambda$ that occur in the reduction of the Kronecker product $D^{\mu} \times D^{\nu}$, and, for each such $\lambda$, over all $m, m'$ giving lexical Gel'fand patterns. The coefficient [...] in Eq. (2.66) is a real number and is defined in terms of $U(n)$ WCG-coefficients by

$$\begin{bmatrix} m' & m_1' & m_2' \\ \lambda & \mu & \nu \\ m & m_1 & m_2 \end{bmatrix} = \sum_{\gamma} \left\langle \begin{matrix} \lambda \\ m \end{matrix} \middle| \left\langle \begin{matrix} \gamma \\ \mu \\ m_1 \end{matrix} \right\rangle \middle| \begin{matrix} \nu \\ m_2 \end{matrix} \right\rangle \left\langle \begin{matrix} \lambda \\ m' \end{matrix} \middle| \left\langle \begin{matrix} \gamma \\ \mu \\ m_1' \end{matrix} \right\rangle \middle| \begin{matrix} \nu \\ m_2' \end{matrix} \right\rangle. \tag{2.67}$$

The bracket notation

$$\left\langle \begin{matrix} \lambda \\ m \end{matrix} \middle| \left\langle \begin{matrix} \gamma \\ \mu \\ m_1 \end{matrix} \right\rangle \middle| \begin{matrix} \nu \\ m_2 \end{matrix} \right\rangle \tag{2.68}$$

for a WCG-coefficient is explained below.

The detailed form (2.67) of the coefficients occurring in relation (2.66) requires proof. That such a relation exists, however, follows already from the basis property noted in Eq. (2.60). We refer to the literature (for example, see Refs. 18,26-28) for the proof that relation (2.66) involves the WCG-coefficients as described in Eq. (2.67).

Relation (2.66) is one of the most important in all of unitary group theory since it relates WCG-coefficients to irreducible representation functions. Indeed, using the inner product (2.15), one has

$$\left(D^{\lambda'}, D^{\lambda}\right) = \delta_{\lambda'\lambda} \mathcal{M}(\lambda) \tag{2.69}$$

so that

$$\mathcal{M}(\lambda) \begin{bmatrix} m' & m_1' & m_2' \\ \lambda & \mu & \nu \\ m & m_1 & m_2 \end{bmatrix} = \left( D^{\lambda}_{mm'},\, D^{\mu}_{m_1 m_1'}\, D^{\nu}_{m_2 m_2'} \right). \tag{2.70}$$

Wigner[29] used this relation for $SU(2)$ to calculate explicitly the $SU(2)$ WCG-coefficients (with, however, a modified inner product). We outline in Section 3 how relation (2.70) may be used to calculate the $SU(3)$ WCG-coefficients.

We have formulated relation (2.66) in terms of polynomials over $Z = (z_i^j)$, instead of the usual way in terms of boson polynomials found in the physics and chemistry literature, in order to focus more clearly on the fact that we are dealing with *an algebra of the ring of polynomials over indeterminates*, in the spirit of Rota's umbral calculus.[24] Relation (2.66) may, in fact, be regarded as a natural generalization of the famous product rule for the set of all Schur functions $\{e_\lambda | \lambda \in \mathbf{P}(n)\}$ as expressed by

$$e_\mu(z)\, e_\nu(z) \;=\; \sum_\lambda g(\mu\nu\lambda) e_\lambda(z),\; z = (z_1, z_2, \ldots, z_n). \tag{2.71}$$

Indeed, this result for Schur functions is a special case of the general law (2.66) when one recognizes that

$$e_\lambda(z_1, z_2, \ldots, z_n) \;=\; \text{tr}\, D^\lambda(Z)\Big|_{z_{ij}=\delta_{ij} z_i}, \tag{2.72}$$

where tr denotes the trace of the matrix $D^\lambda(Z)$. The proof also requires using the orthogonality of the WCG-coefficients to obtain

$$\sum_{m_1, m_2} \begin{bmatrix} m' & m_1 & m_2 \\ \lambda & \mu & \nu \\ m & m_1 & m_2 \end{bmatrix} \;=\; \delta_{mm'} g(\mu\nu\lambda). \tag{2.73}$$

Let us next explain briefly the notation in Eq. (2.68) for a $U(n)$ WCG-coefficient. The patterns $\binom{\lambda}{m}$, $\binom{\mu}{m_1}$, $\binom{\nu}{m_2}$ are all Gel'fand patterns in which the labels in rows $n,\ n-1, \ldots, 1$ have the significance of group-subgroup reductions for the chain $U(n) \supset U(n-1) \supset \ldots \supset U(1)$, in accordance with the Weyl betweenness rule. The $n$-rowed inverted pattern $\binom{\gamma}{\mu}$, which appears in the notation (2.68) for a WCG-coefficient, has no such group-subgroup significance, although, by definition, its entries $\gamma_{ij}$ run over all values satisfying the betweenness relations. The discovery that patterns *numerically* identical to Gel'fand patterns enumerate all WCG-coefficients for $U(n)$ was one of the significant discoveries[30] in the early 1960's. It takes into account beautifully the fact that the intertwining function $I_{\mu,\Delta}$ takes on only values in the set $L_{\mu,\Delta}$. This accounting is made through the weight $\Delta = (\Delta_1, \Delta_2, \ldots, \Delta_n)$ of an operator pattern, where each $\Delta_j$ is defined in terms of the entries $\gamma_{ij}$ of the pattern exactly as in Eq. (2.38) for a Gel'fand pattern. A given weight $\Delta \in W(\mu)$ has a multiplicity $K(\mu, \Delta)$, and there are exactly this number of distinct operator patterns $\gamma$ having this weight. Thus, the WCG-coefficient (2.68) is, first of all, equal to zero, unless $\lambda = \nu + \Delta$, where $\Delta \in W(\mu)$ [the property of the intertwining number in Eq. (2.64)]; secondly,

there are exactly $K(\mu,\Delta)$ operator patterns $\gamma$ providing us with $K(\mu,\Delta)$ *sets* of orthogonal Wigner coefficients (this orthogonality is expressed in terms of summations over the Gel'fand patterns $m_1$ and $m_2$). These sets of orthogonal coefficients then effect completely the reduction of the direct product $(D^\mu \times D^\nu) \downarrow D^{\nu+\Delta}$, $\Delta \in W(\mu)$, in the region of maximal multiplicity; that is, for all $\mu,\nu$, and $\lambda = \nu + \Delta$ such that $I(\nu \times \nu;\ \nu+\Delta) = K(\nu,\Delta)$. The patterns $\gamma$ are referred to as *operator patterns* to distinguish them from the numerically identical Gel'fand patterns.

Operator patterns must have still further structure. This is because the intertwining number can assume each value in the set $L_{\mu,\Delta}$ for certain $\nu$. This means then that certain *whole sets* of WCG-coefficients must vanish. This property is best expressed through the notion of a Wigner operator and its *characteristic null space*. In its very conception, a $U(n)$ Wigner operator is to have certain mapping properties when acting in the Hilbert space over which it is defined. We take this Hilbert space $H$ to be a direct sum $H = \sum_{\lambda\in\mathbf{P}(n)} \oplus H_\lambda$, where $H_\lambda$ is the carrier space of irrep $\lambda$ of $U(n)$ [or $GL(n,\mathbb{C})$]; each such irrep space occurs exactly once in the direct sum, and the sum is over all $\lambda \in \mathbf{P}(n)$. (Such a space has been called a *model space* by Gel'fand.)

An abstract Wigner operator, denoted $\left\langle \begin{matrix} \gamma \\ \mu \\ m \end{matrix} \right\rangle$ below, is then a map $H \to H$ with the following specific properties[25-28] for each $\nu \in \mathbf{P}(n)$, where $\Delta$ denotes the weight of the operator pattern $\binom{\gamma}{\mu}$:

$$\left\langle \begin{matrix} \gamma \\ \mu \\ m \end{matrix} \right\rangle : \quad H_\nu \to \mathbf{0}, \text{ if } \nu+\Delta \notin \mu \times \nu; \tag{2.74a}$$

$$\left\langle \begin{matrix} \gamma \\ \mu \\ m \end{matrix} \right\rangle : \quad H_\nu \to \mathbf{0}, \text{ or } H_\nu \to H_{\nu+\Delta}, \text{ if } \nu+\Delta \in \mu \times \nu. \tag{2.74b}$$

The notation $\lambda \in \mu \times \nu$ denotes that $\lambda$ occurs as an irrep in the reduction of the Kronecker product $\mu \times \nu$. Among the $K(\mu,\Delta)$ unit tensor operators in the set

$$\left\{ \left\langle \begin{matrix} \gamma \\ \mu \\ m \end{matrix} \right\rangle \middle| \Delta\binom{\mu}{\gamma} = \Delta \in W(\mu) \right\}, \tag{2.75}$$

exactly $K(\mu,\Delta) - I(\mu\times\nu;\ \nu+\Delta)$ of them annihilate the irrep space $H_\nu$ [have the first property (2.74b)], while the remaining $I(\mu \times \nu;\ \nu+\Delta)$ operators effect maps $H_\nu \to H_{\nu+\Delta}$ [have the second property (2.74b)] as given explicitly

by the sets of orthogonal Wigner coefficients that effect the reduction $(D^{\mu} \times D^{\nu}) \downarrow D^{\nu+\Delta}$:

$$\left\langle \begin{matrix} \gamma \\ \mu \\ m_1 \end{matrix} \right\rangle \left| \begin{matrix} \nu \\ m_2 \end{matrix} \right\rangle = \sum_{m} \left\langle \begin{matrix} \nu+\Delta \\ m \end{matrix} \right| \left\langle \begin{matrix} \gamma \\ \mu \\ m_1 \end{matrix} \right\rangle \left| \begin{matrix} \nu \\ m_2 \end{matrix} \right\rangle \left| \begin{matrix} \nu+\Delta \\ m \end{matrix} \right\rangle. \tag{2.76}$$

Here the set of vectors $\{|\begin{smallmatrix} \nu \\ m_2 \end{smallmatrix}\rangle | m_2$ is a lexical Gel'fand pattern$\}$ is an orthonormal basis of $H_{\nu}$. As $\nu$ runs over all $\nu \in \mathbf{P}(n)$, these vectors are to be an orthonormal basis of the (separable) Hilbert space $H$.

Let us note also that under the unitary transformation $\mathcal{U}_U : H \to H$ given by

$$\mathcal{U}_U \left| \begin{matrix} \nu \\ m_2 \end{matrix} \right\rangle = \sum_{m_2'} D^{\nu}_{m_2' m_2}(U) \left| \begin{matrix} \nu \\ m_2' \end{matrix} \right\rangle, \tag{2.77a}$$

the unit tensor operators transform irreducibly according to

$$\mathcal{U}_U \left\langle \begin{matrix} \gamma \\ \mu \\ m_1 \end{matrix} \right\rangle \mathcal{U}_U^{-1} = \sum_{m_1'} D^{\mu}_{m_1' m_1}(U) \left\langle \begin{matrix} \gamma \\ \mu \\ m_1' \end{matrix} \right\rangle. \tag{2.77b}$$

This transformation property of a unit tensor operator is a direct consequence of definition (2.76), the transformation of basis states given by Eq. (2.77a), and relation (2.66) between $D$-functions and WCG-coefficients.

The concept of a general irreducible tensor operator $T\left(\begin{smallmatrix} \mu \\ m_1 \end{smallmatrix}\right)$ can be introduced at various levels of abstraction and generality. For our purposes here, it is sufficient to define $T\left(\begin{smallmatrix} \mu \\ m_1 \end{smallmatrix}\right)$ to be a mapping of $H \to H$ such that under the transformation of basis of $H$ given by (2.77a), the tensor operator undergoes the similarity transformation (2.77b) in the Gel'fand patterns $(m_1)$ and $(m_1')$. It is then a consequence of the generalized Wigner-Eckart theorem that one can express every such tensor operator as a linear combination of the unit tensor operators defined by (2.76); that is,

$$T\left(\begin{matrix} \mu \\ m_1 \end{matrix}\right) = \sum_{\gamma} I_{\gamma} \left\langle \begin{matrix} \gamma \\ \mu \\ m_1 \end{matrix} \right\rangle. \tag{2.78}$$

In this relation, the "scalars" $I_{\gamma}$ are to be invariant operators with respect to $U(n)$.

In view of the basis property (2.78), the algebra of unit tensor operators becomes the primary object of interest. Of the several ways of relating products of Wigner operators (see Refs. 26-28), we give here only two, the first of

which is the operator analogue of the product rule (2.66) for representation functions. This is the *product law for Wigner operators*:

$$\left\langle \begin{matrix} \gamma_1 \\ \mu \\ m_1 \end{matrix} \right\rangle \left\langle \begin{matrix} \gamma_2 \\ \nu \\ m_2 \end{matrix} \right\rangle = \sum_{\lambda,m,\gamma} \left\{ \begin{matrix} \gamma & \gamma_1 & \gamma_2 \\ \lambda & \mu & \nu \\ m & m_1 & m_2 \end{matrix} \right\} \left\langle \begin{matrix} \gamma \\ \lambda \\ m \end{matrix} \right\rangle, \tag{2.79}$$

where the summation is over all $\lambda \in \mu \times \nu$, and, for each such irrep label $\lambda$, over all Gel'fand patterns $m$ and all operator patterns $\gamma$. The curly-bracket object denotes an *operator* in $U(n)$, expressed in terms of *Racah invariant operators* and WCG-coefficients by

$$\left\{ \begin{matrix} \gamma & \gamma_1 & \gamma_2 \\ \lambda & \mu & \nu \\ m & m_1 & m_2 \end{matrix} \right\} = \sum_{\gamma_3} \left\langle \begin{matrix} \lambda \\ m \end{matrix} \middle| \left\langle \begin{matrix} \gamma_3 \\ \mu \\ m_1 \end{matrix} \right\rangle \middle| \begin{matrix} \nu \\ m_2 \end{matrix} \right\rangle \left\{ \begin{pmatrix} \lambda \\ \gamma \end{pmatrix} \begin{pmatrix} \gamma_3 \\ \mu \\ \gamma_1 \end{pmatrix} \begin{pmatrix} \nu \\ \gamma_2 \end{pmatrix} \right\}. \tag{2.80}$$

Here the curly-bracket symbol

$$\left\{ \begin{pmatrix} \lambda \\ \gamma \end{pmatrix} \begin{pmatrix} \gamma_3 \\ \mu \\ \gamma_1 \end{pmatrix} \begin{pmatrix} \nu \\ \gamma_2 \end{pmatrix} \right\} \tag{2.81}$$

denotes a Racah invariant operator. Its eigenvalue on a general irrep space $H_\rho \subset H$ are the Racah $(6j)$ coefficients of $U(n)$.[26,27]

The second useful form of Eq. (2.79) we wish to note shows how the Racah invariant operators are obtained in terms of WCG-coefficients and Wigner operators:

$$\left\{ \begin{matrix} \gamma & \gamma_1 & \gamma_2 \\ \lambda & \mu & \nu \\ m & m_1 & m_2 \end{matrix} \right\} = \left\langle \begin{matrix} \gamma_1 \\ \mu \\ m_1 \end{matrix} \right\rangle \left\langle \begin{matrix} \gamma_2 \\ \nu \\ m_2 \end{matrix} \right\rangle \left\langle \begin{matrix} \gamma \\ \lambda \\ m \end{matrix} \right\rangle^\dagger, \tag{2.82a}$$

$$\left\{ \begin{pmatrix} \lambda \\ \gamma \end{pmatrix} \begin{pmatrix} \gamma_3 \\ \mu \\ \gamma_1 \end{pmatrix} \begin{pmatrix} \nu \\ \gamma_2 \end{pmatrix} \right\} = \sum_{m_1 m_2} \left\langle \begin{matrix} \lambda \\ m \end{matrix} \middle| \left\langle \begin{matrix} \gamma_3 \\ \mu \\ m_1 \end{matrix} \right\rangle \middle| \begin{matrix} \nu \\ m_2 \end{matrix} \right\rangle \left\{ \begin{matrix} \gamma & \gamma_1 & \gamma_2 \\ \lambda & \mu & \nu \\ m & m_1 & m_2 \end{matrix} \right\}, \tag{2.82b}$$

where $m$ is arbitrary in the second expression.

It is particularly significant that Racah invariants are fully labelled by *operator patterns*. There are other important forms of Eqs. (2.79) and (2.82), derived from these relations by using the orthogonality relations for WCG-coefficients and Racah invariants (see Refs. 26-28).

Relation (2.70) for WCG-coefficients and relations (2.82) for Racah invariants are the principal results of this subsection. Relation (2.70) is a

general result on which the calculation of $U(n)$ WCG-coefficients can be based. With these coefficients determined, relations (2.82) then define fully the Racah coefficients.

It is useful to remark that the existence of the algebraic structures, relations (2.66) for functions and (2.79) for operators, is assured, since $D^{\mu} \times D^{\nu}$ is completely reducible. The important question is whether or not there exist canonical or natural realizations of these algebras, free of arbitrary choices. The answer for $U(2)$ and $U(3)$ is that the algebra of Wigner operators is canonically determined by characteristic null space alone, and is implied definitively by the intertwining number function. This structure is made precise for $U(2)$ in Ref. 3 and for $U(3)$ in numerous publications (see, for example, Refs. 31-36). Null space alone fails to give a complete classification of all Wigner operators for $n \geq 4$ (see Baclawski[37] and Ref. 25), but nonetheless must play a significant role in this classification.

## 3. CANONICAL $U(3)$ WCG-COEFFICIENTS

One method of calculating $U(n)$ WCG-coefficients takes Eq. (2.70) as the starting point, where we regard the irrep functions in this relation as fully known. [This assumption is justified, although these irreps are themselves quite complicated objects (see Ref. 23).] This relation, in itself, will, however, not yield the WCG-coefficients in the right-hand side of Eq. (2.67), since a summation over operator patterns $\gamma$ is present. However, for $U(2)$, the operator pattern is uniquely determined by $\lambda, \mu$, and $\nu$; that is, there is no summation in Eq. (2.67). In this case, relations (2.70) and (2.67) already determine uniquely (up to phase conventions) the normalized $SU(2)$ Wigner coefficients. Indeed, it was this structure, or more precisely one isomorphic to it, that Wigner used to calculate the $SU(2)$ coefficients. The details of this calculation are given in Ref. 3 (Vol. 8) in the language of the boson calculus. The general problem is to "take apart" the right-hand side of Eq. (2.67) in a canonical manner so that the resulting WCG-coefficients have properties that respect the null space constraints that a Wigner operator must possess in consequence of relations (2.74).

The splitting of the right-hand side of Eq. (2.67) has been solved canonically (see Refs. 18 and 30-36) for the unitary group $U(3)$, as well as the trivial $U(2)$ case mentioned above. The canonical solution for $U(3)$ is a (unique) consequence of properties of the intertwining function $I_{\mu,\Delta}$, its associated level sets, and the implied *characteristic null space* of a Wigner operator in the set

$$\left\{ \left\langle \begin{matrix} \gamma_t \\ \mu \\ m'' \end{matrix} \right\rangle \middle| \Delta \begin{pmatrix} \mu \\ \gamma_t \end{pmatrix} = (\Delta_1, \Delta_2, \Delta_3);\ t = 1, 2, \ldots, K(\mu, \Delta) \right\}. \tag{3.1a}$$

The Wigner operators in this set are enumerated by operator patterns

$$\begin{pmatrix} \mu \\ \gamma_1 \end{pmatrix}, \begin{pmatrix} \mu \\ \gamma_2 \end{pmatrix}, \ldots, \begin{pmatrix} \mu \\ \gamma_{K(\mu,\Delta)} \end{pmatrix}, \tag{3.1b}$$

which are $K(\mu, \Delta)$ in number, and which all have the same weight or shift pattern $\Delta = (\Delta_1, \Delta_2, \Delta_3)$. Each operator pattern $\gamma_t$ may be given explicitly in terms of $\Delta$ and the index $t$, but we do not require this detail here (see Ref. 35).

While the proof that a *canonical solution* exists requires a detailed analysis of the properties of the intertwining function $I_{\mu,\Delta,}$, the key result needed for the calculation of the canonical WCG-coefficients themselves is easily stated: It is that a certain class of WCG-coefficients, which are matrix elements of the Wigner operators in the set (3.1a), must be zero. Specifically, the following class of WCG-coefficients are zero in the canonical solution (see Ref. 33):

$$\left\langle \begin{matrix} \nu + \Delta \\ m'''_s \end{matrix} \middle| \left\langle \begin{matrix} \gamma_t \\ \mu \\ m'' \end{matrix} \right\rangle \middle| \begin{matrix} \nu \\ m' \end{matrix} \right\rangle = 0 \tag{3.2a}$$

for $t = s + 1,\ s + 2,\ \ldots,\ K(\mu, \Delta)$, where the initial (lexical) pattern $\begin{pmatrix} \nu \\ m' \end{pmatrix}$ is arbitrary, and the patterns

$$\begin{pmatrix} \nu + \Delta \\ m'''_s \end{pmatrix},\ s = 1, 2, \ldots, K(\mu, \Delta), \text{ and } \begin{pmatrix} \mu \\ m'' \end{pmatrix} \tag{3.2b}$$

are the *special lexical patterns* given by

$$\begin{pmatrix} \mu \\ m'' \end{pmatrix} = \begin{pmatrix} \mu_1 & \mu_2 & \mu_3 \\ & \mu_1 & \mu_3 \\ & m''_{11} & \end{pmatrix}, \tag{3.2c}$$

$$\begin{pmatrix} \nu + \Delta \\ m'''_s \end{pmatrix} = \begin{pmatrix} \nu_1 + \Delta_1 & & \nu_2 + \Delta_2 & & \nu_3 + \Delta_3 \\ & m'_{12} + \mu_1 - s + 1 & & m'_{22} + \mu_3 + s - 1 & \\ & & m'_{11} + m''_{11} & & \end{pmatrix}. \tag{3.2d}$$

Let us next show how the set of zero WCG-coefficients given by Eqs. (3.2) are used in relation (2.67) to obtain all $U(3)$ WCG-coefficients. The property that makes the system of relations (2.67) solvable is that the zeros (3.2) *triangularize* this set of equations. Thus, choosing $\lambda = \nu + \Delta$, $m' = m_s'''$, $m_1' = m''$, $m_2' = m'$, and $\gamma = \gamma_t$, relation (2.67) becomes

$$\sum_{t=1}^{s} \left\langle \begin{matrix} \nu+\Delta \\ m \end{matrix} \middle| \left\langle \begin{matrix} \gamma_t \\ \mu \\ m_1 \end{matrix} \right\rangle \middle| \begin{matrix} \nu \\ m_2 \end{matrix} \right\rangle \left\langle \begin{matrix} \nu+\Delta \\ m_s''' \end{matrix} \middle| \left\langle \begin{matrix} \gamma_t \\ \mu \\ m'' \end{matrix} \right\rangle \middle| \begin{matrix} \nu \\ m' \end{matrix} \right\rangle$$
$$= \begin{bmatrix} m_s''' & m'' & m' \\ \nu+\Delta & \mu & \nu \\ m & m_1 & m_2 \end{bmatrix}, \qquad s = 1, 2, \ldots, K(\mu, \Delta). \tag{3.3}$$

Since the right-hand side of Eq. (3.3) may be considered known, these relations solve fully the problem of constructing all $U(3)$ Wigner coefficients, up to phase conventions. Thus, one first chooses $s = 1$ in Eq. (3.3), reducing the left-hand side to one term. Choosing $m = m_1'''$, $m_1 = m''$, and $m_2 = m'$ then gives

$$\left\langle \begin{matrix} \nu+\Delta \\ m_1''' \end{matrix} \middle| \left\langle \begin{matrix} \lambda_1 \\ \mu \\ m'' \end{matrix} \right\rangle \middle| \begin{matrix} \nu \\ m' \end{matrix} \right\rangle = \begin{bmatrix} m_1''' & m'' & m' \\ \nu+\Delta & \mu & \nu \\ m_1''' & m'' & m' \end{bmatrix}^{1/2}. \tag{3.4a}$$

Using this back in the equation ($s = 1$) then gives the $U(3)$ Wigner coefficient

$$\left\langle \begin{matrix} \nu+\Delta \\ m \end{matrix} \middle| \left\langle \begin{matrix} \gamma_1 \\ \mu \\ m_1 \end{matrix} \right\rangle \middle| \begin{matrix} \nu \\ m_2 \end{matrix} \right\rangle \tag{3.4b}$$

for general labels. One next sets $s = 2$ in Eq. (3.3) and moves the $t = 1$ term to the right-hand side, since it is fully known from the $s = 1$ step. One then repeats the above process to obtain the general $U(3)$ Wigner coefficient

$$\left\langle \begin{matrix} \nu+\Delta \\ m \end{matrix} \middle| \left\langle \begin{matrix} \gamma_2 \\ \mu \\ m_1 \end{matrix} \right\rangle \middle| \begin{matrix} \nu \\ m_2 \end{matrix} \right\rangle. \tag{3.5}$$

Proceeding in the obvious way, one thus obtains all $U(3)$ Wigner coefficients

$$\left\langle \begin{matrix} \nu+\Delta \\ m \end{matrix} \middle| \left\langle \begin{matrix} \gamma_t \\ \mu \\ m_1 \end{matrix} \right\rangle \middle| \begin{matrix} \nu \\ m_2 \end{matrix} \right\rangle, \quad t = 1, 2, \ldots, K(k, \Delta). \tag{3.6}$$

The above procedure, while difficult to implement to obtain explicit algebraic expressions for the general coefficients (3.6), serves to illustrate nicely how the intertwining function, the associated characteristic null space, and the implied zero WCG-coefficients described in Eqs. (3.2) lead to a canonical set of coefficients.One of the nice features of the above method is its uniform approach to all $U(n)$: For $n = 2$, there is no multiplicity, that is, $\gamma$ in Eq. (2.67) is uniquely determined by the initial and final labels $\nu = [\nu_1, \nu_2]$, $\lambda = [\lambda_1, \lambda_2]$, and the method of solution reduces to Wigner's familiar one. For $n = 3$, the same type of procedure works when supplemented with zeros that are required by properties of the intertwining function (null space). Clearly, a similar procedure can work for $U(n)$ when supplemented with canonical conditions, if such exist. We will address the $U(n)$ problem in a future paper.

For comparison with subsequent results in Sections 4 and 5, it is useful to formulate the canonical solution outlined above in terms of the tensor product spaces $H \otimes H$, where $H$ is the Hilbert space described in Section 2.6. We first write $H \otimes H$ in the form

$$H \otimes H = \sum_{\mu,\nu} \oplus (H_\mu \otimes H_\nu), \tag{3.7}$$

where the summation is over all $\mu, \nu \in \mathbf{P}(n)$. The canonical basis of $H_\mu \otimes H_\nu$ is

$$B^{\mu,\nu} = \left\{ \left| \begin{matrix} \mu \\ m_1 \end{matrix} \right\rangle \otimes \left| \begin{matrix} \nu \\ m_2 \end{matrix} \right\rangle \middle| \, m_1 \text{ and } m_2 \text{ are Gel'fand patterns} \right\}. \tag{3.8}$$

The so-called *coupled basis* of $H \otimes H$ is now given by

$$\left| \begin{pmatrix} \mu \\ \gamma \end{pmatrix}^{\nu} \begin{pmatrix} \lambda \\ m \end{pmatrix} \right\rangle = \sum_{m_1, m_2} \left\langle \begin{matrix} \lambda \\ m \end{matrix} \middle| \left\langle \begin{matrix} \gamma \\ \mu \\ m_1 \end{matrix} \right\rangle \left| \begin{matrix} \nu \\ m_2 \end{matrix} \right\rangle \left| \begin{matrix} \mu \\ m_1 \end{matrix} \right\rangle \otimes \left| \begin{matrix} \nu \\ m_2 \end{matrix} \right\rangle. \tag{3.9}$$

In order to be precise in the description of this basis of $H \otimes H$ we define the vector space $H_\lambda(\mu, \nu; \gamma)$ to be the space with basis

$$B_\lambda(\mu, \nu; \gamma) = \left\{ \left| \begin{pmatrix} \mu \\ \gamma \end{pmatrix}^{\nu} \begin{pmatrix} \lambda \\ m \end{pmatrix} \right\rangle \middle| \, m \text{ is a Gel'fand pattern} \right\}. \tag{3.10}$$

Thus, the vector space $H_\lambda(\mu, \nu; \gamma)$ is either the zero vector space $\mathbf{0}$, or a nonzero vector space of dimension equal to $\mathrm{Dim}\lambda$. It is the zero vector space under either of the following conditions:

$$H_\lambda(\mu, \nu; \gamma) = \mathbf{0}, \text{ unless } \lambda = \nu + \Delta \in \mu \times \nu \text{ for some } \Delta \in W(\mu); \tag{3.11a}$$

$$H_\lambda(\mu, \nu; \gamma) = \mathbf{0}, \text{ if } H_\nu \text{ belongs to the characteristic null space of the Wigner operator } \begin{pmatrix} \gamma \\ \mu \end{pmatrix}. \tag{3.11b}$$

Otherwise, the vector space $H_\lambda(\mu,\nu;\gamma)$ is nonzero and $B_\lambda(\mu,\nu;\gamma)$ is an orthonormal basis of this space. The tensor product space $H_\mu \otimes H_\nu$ is thus split into a direct sum of perpendicular vector spaces:

$$H_\mu \otimes H_\nu = \sum_{\substack{\Delta \in W(\mu) \\ \nu+\Delta \in \mu \times \nu}} \sum_{t=1}^{K(\mu,\Delta)} \oplus H_{\nu+\Delta}(\mu,\nu;\gamma_t). \tag{3.12}$$

It is quite significant that the summation in Eq. (3.12) extends from $t = 1$ to $t = K(\mu,\Delta)$. This is because in the region of maximal multiplicity, that is, for values of $\nu \in \mathbf{P}(n)$ such that $I_{\mu,\Delta}(\nu) = K(\mu,\Delta)$, none of the vector spaces in the direct sum (3.12) is zero. A key feature of the canonical solution is that the vector space structure of Eq. (3.12) should "follow" the properties of the multiplicity function $I_{\mu,\Delta}$: Thus, for those $\nu \in \mathbf{P}(n)$ such that $I_{\mu,\Delta}(\nu) = K(\mu,\Delta)-1$, exactly one vector space in the direct sum (3.12) becomes and remains zero for all subsequently smaller values of $I_{\mu,\Delta}(\nu)$; for those $\nu \in \mathbf{P}(n)$ such that $I_{\mu,\Delta}(\nu) = K(\mu,\Delta) - 2$, exactly one more vector space in the direct sum becomes and remains zero for subsequently smaller values of $I_{\mu,\Delta}(\nu)$, etc.

There is, in fact, a natural ordering of the operator patterns $\gamma_t$ in Eq. (3.12) (see Ref. 35) given by

$$\gamma_1 > \gamma_2 > \ldots > \gamma_{K(\mu,\Delta)}. \tag{3.13}$$

This ordering identifies the precise way in which the vectors spaces in the direct sum (3.12) become the zero vector space, namely, first the one labelled $\gamma_1$, then the one labelled $\gamma_2$, etc.

The above results solve fully the problem of classifying the subspaces of $H \otimes H$ in terms of the irrep spaces of the unitary group $U(3)$ under the action of group of operators $\{\mathcal{U}_U \otimes \mathcal{U}_U | \, U \in U(3)\}$, where $\mathcal{U}_U$ is defined by Eq. (2.77a): Each vector space $H_\lambda(\mu,\nu;\gamma)$, when nonzero, is the carrier space of irrep $\{D^\lambda(U)|U \in U(3)\}$; that is, under the action of $\mathcal{U}_U \otimes \mathcal{U}_U$, the basis $B_\lambda(\mu,\nu;\gamma)$ undergoes the transformation

$$\mathcal{U}_U \otimes \mathcal{U}_U : \left| \begin{pmatrix} \mu \\ \gamma \end{pmatrix}^\nu \begin{pmatrix} \lambda \\ m \end{pmatrix} \right\rangle \longrightarrow \sum_{m'} D^\lambda_{m'm}(U) \left| \begin{pmatrix} \mu \\ \gamma \end{pmatrix}^\nu \begin{pmatrix} \lambda \\ m' \end{pmatrix} \right\rangle, \text{ each } U \in U(3). \tag{3.14}$$

The key role [noted in this section for $U(3) \times U(3) \downarrow U(3)$] played by the multiplicity function in defining canonical solutions of multiplicity problems associated with group-subgroup reductions has for the most part been overlooked in the literature.

## 4. FURTHER CANONICAL METHODS

### 4.1. Group-Subgroup Reductions: $G \downarrow U(n)$

Applications of symmetry techniques typically are based on exploiting the consequences of a chain of symmetry groups $G_1 \supset G_2 \supset \ldots \supset G_k$, where the final group $G_k$ is usually $SU(2)$ or $SO(3)$, using angular momentum symmetry. We wish to consider now what consequences we can obtain from the reduction $G \supset U(n)$, assuming that we know, in detail, the $U(n)$ tensor operator algebra, or more precisely the algebra generated by the unit tensor operators (Wigner operators) under the product rule (2.79). This is a very "large" algebra, but in practice it is useful to extend it by including as scalars all functions of invariant operators as well. The resulting algebra, call it $\mathcal{A}$, is a very general structure and includes, for example, the universal enveloping algebra of $U(n)$ as a subalgebra.

We wish to show now that *if $G \supset U(n)$, then the Lie algebra of $G$ can be imbedded in $\mathcal{A}$ as a subalgebra using the Lie product.*

This assertion is actually not difficult to prove. We remark first that the Lie algebra of $G$ is a tensor operator in $G$ carrying the adjoint representation. This representation splits under the Lie algebra of $U(n)$—by assumption a subalgebra of $G$—into a direct sum of unit tensor operators in $U(n)$, having as coefficients functions of invariant operators in $U(n)$. More generally a tensor operator in $G$ is also a tensor operator in a subgroup $H$, with $G \supset H$, which can be split into irreducible tensor operators in the subgroup. This suffices to prove the assertion.

### 4.2. Group-Subgroup Reductions: $U(n) \downarrow G$

We have shown in Section 4.1 how the generators of a group $G$ satisfying $G \supset U(n)$ may be classified as irreducible tensor operators with respect to $U(n)$, thus demonstrating the occurrence of the $U(n)$ WCG-coefficients in every such group $G$. Here we consider the case where $G$ is a subgroup of $U(n)$; that is, we address the problem of reducing a given irrep $\lambda = [\lambda_1, \lambda_2, \ldots, \lambda_n]$ of $U(n)$ into irreps of $G$. Let us denote an irrep of $G$ by the symbol $j$; that is, $j$ denotes an index or set of indices, say, $\langle j_1, j_2, \ldots \rangle$, such that the domain of definition of these indices enumerates the set of all irreps of $G$. Let us denote this set of all irrep labels by

$$J = \{ j \mid j \text{ is an irrep of } G \} . \tag{4.1}$$

The reduction of irrep $\lambda \in \mathbf{P}(n)$ of $U(n)$ into irreps $j \in J$ of $G$ is expressed abstractly by

$$\lambda = \sum_{j \in J} M(\lambda, j)\, j, \tag{4.2}$$

where $M(\lambda, j)$ denotes the number of times irrep $j$ of $G$ is contained in irrep $\lambda$ of $U(n)$, including 0. We call $M$ the ***multiplicity function*** for the group-subgroup reduction $U(n) \downarrow G$. The multiplicity function $M$ is a mapping of the Cartesian product $\mathbf{P}(n) \times J$ into the nonnegative integers $\mathbb{N} = \{0, 1, 2, \ldots\}$:

$$M: \quad \mathbf{P}(n) \times J \longrightarrow \mathbb{N}. \tag{4.3}$$

The multiplicity function for a given group-subgroup reduction carries valuable group theoretical information that has generally not been exploited because of the tendency to view it *numerically* (as a collection of integers) rather than *functionally*,[25] as described above. The fact that the multiplicity function is defined on infinitely many points is important for inferring properties of the $U(n) \downarrow G$ group-subgroup reduction problem, as we discuss below.

An important application of the group-subgroup reduction $U(n) \downarrow G$ is the case $U(n) \downarrow SO(n)$, for which we have

$$U(n) \supset SU(n) \supset SO(n), \tag{4.4}$$

where $SO(n) = SO(n, \mathbb{R})$ denotes the group of real, proper $n \times n$ orthogonal matrices. The first step in the reduction in $U(n) \downarrow SU(n)$ is easily made through the fact that irrep $[\lambda_1, \lambda_2, \ldots, \lambda_n]$ reduces to the unique irrep $[\lambda_1 - \lambda_n, \lambda_2 - \lambda_n, \ldots, \lambda_{n-1} - \lambda_n, 0]$ of $SU(n)$. In considering the reduction (4.4), we therefore restrict the discussion to

$$SU(n) \supset SO(n) \tag{4.5}$$

by taking the subset of $\mathbf{P}(n)$ corresponding to irreps of $SU(n)$ as given by $[\lambda_1, \lambda_2, \ldots, \lambda_{n-1}, 0]$, where

$$[\lambda_1, \lambda_2, \ldots, \lambda_{n-1}] \in \mathbf{P}(n-1). \tag{4.6}$$

It is well-known (see Ref. 16) that the irreps of $SO(n)$ are enumerated by partitions of the following type:

$$j = \langle j_1, j_2, \ldots, j_r \rangle, \tag{4.7a}$$

where

$$r = \left\{ \begin{matrix} n/2, & n \text{ even} \\ (n-1)/2, & n \text{ odd} \end{matrix} \right\}, \tag{4.7b}$$

and the $j_i$ are integers satisfying

$$j_1 \geq j_2 \geq \ldots \geq j_r \geq 0, \quad n \text{ odd}, \tag{4.7c}$$

$$j_1 \geq j_2 \geq \cdots \geq j_{r-1} \geq |j_r|, \quad n \text{ even}, \tag{4.7d}$$

where $j_{n/2}$ for $n$ even may be zero or a positive or negative integer. For example, the irreps of $SO(4)$ are enumerated by partitions

$$(j_1, j_2), \tag{4.8}$$

where $j_1$ and $|j_2|$ are any nonnegative integers satisfying $j_1 \geq |j_2| \geq 0$; the irreps $(j_1, j_2)$ and $(j_1, -j_2)(j_2 > 0)$ are inequivalent.

For the reduction $SU(n) \downarrow SO(n)$, we have for the multiplicity function (4.3):

$$J = \{j = (j_1, j_2, \ldots, j_r) | j \text{ is a partition (4.7)}\}, \tag{4.9a}$$

and $\mathbf{P}(n)$ is replaced by $\mathbf{P}(n-1)$. Thus, the multiplicity function $M$ is the map

$$M: \quad \mathbf{P}(n-1) \times J \longrightarrow \mathbb{N}. \tag{4.9b}$$

To our knowledge the general multiplicity function of $SU(n) \downarrow SO(n)$ described in Eqs. (4.9) has not been studied from the point of view adopted here, except for the case $n = 3$, with preliminary results in Ref. 16. This investigation has recently been completed (Ref. 38) and leads to the canonical solution for $SU(3) \downarrow SO(3)$ discussed in the following section. We believe that the canonical $SU(3) \downarrow SO(3)$ reduction can serve as a model for the general $SU(n) \downarrow SO(n)$ reduction problem, and that this general problem very likely also has a canonical solution.

## 4.3. The Canonical Solution of the $SU(3) \downarrow SO(3)$ Reduction Problem

**4.3.1.** The $SU(3) \downarrow SO(3)$ reduction problem is of considerable interest in atomic and nuclear physics. The symmetry $SU(3)$ has as (linear) irreps the set $\{[pq0] | p \geq q \geq 0 \text{ integers}\}$. In the subgroup chain $SU(3) \supset SU(2) \times U(1)$, there exists a canonical flag manifold labelled uniquely by $I, I_z$ (isospin $SU(2)$) and $Y$ (hypercharge $U(1)$). (This is the Gel'fand-Weyl basis which is the natural basis for high-energy (particle) physics.) In atomic and nuclear applications of $SU(3)$ symmetry, one is interested in a different subgroup chain: $SU(3) \supset SO(3)$, where the $SO(3)$ irrep in an $SU(3)$ irrep $[pq0]$—labelled by $L$ and $L_0$–may have multiple occurrences. This problem is also of group theoretic importance since the symmetry $SL(3, \mathbb{R})$—a noncompact real form of the complex $SU(3)$ group (denoted $A_2$)—enters in nuclear structure as an idealization for nonterminating rotational bands. For $SL(3, \mathbb{R})$ one has *only* the subgroup chain $SL(3, \mathbb{R}) \supset SO(3)$, or $SU(2)$ for the covering group $\overline{SL(3, \mathbb{R})}$. A canonical resolution has been shown[38] to exist for the $SU(3) \supset SO(3)$ problem and the discussion will be based on this reference.

**4.3.2.** Consider an irrep space of $SU(3)$ labelled by the partition $[pq0]$. Every basis vector in this space can be uniquely identified by operators whose eigenvalues give the canonical labels $(m_{ij})$, that is to say, every basis vector

$$|(m)\rangle = \left| \begin{pmatrix} p & q & 0 \\ m_{12} & m_{22} & \\ & m_{11} & \end{pmatrix} \right\rangle$$

can be uniquely determined operationally. (One says that the canonically labelled vectors form a "flag manifold.")

Now consider $SU(3) \supset SO(3)$. The $SO(3)$ subgroup can be embedded in $SU(3)$ using the canonical generators $\{E_{ij}\}$ by assigning:[15,16]

$$L_+ = \sqrt{2}(E_{32} - E_{13}), \tag{4.10a}$$

$$L_0 = E_{11} - E_{22}, \tag{4.10b}$$

$$L_- = \sqrt{2}(E_{23} - E_{31}). \tag{4.10c}$$

When acting on the canonical $SU(3)$ basis, the $SO(3)$ generator $L_0$ is sharp; that is:

$$L_0|(m)\rangle = (2m_{11} - m_{12} - m_{22})|(m)\rangle = M|(m)\rangle. \tag{4.11}$$

The *multiplicity problem* arises in this way: If we label vectors in the irrep space $[pq0]$ by the $SO(3)$ labels $(L, M)$, then we find that labelling is not in general unique; that is, distinct vectors having the same $(L, M)$-value may occur. A *resolution* of the multiplicity problem is the assignment, in some—possibly *ad hoc*—way, of additional labels specifying every vector uniquely. A *canonical* resolution of the multiplicity is a resolution which involves *no arbitrary choices whatsoever*, to within equivalence.

The set of all vectors in the irrep space $[pq0]$ having a specified $L$-value can be determined uniquely from the set of *highest weight (hw)* states with this specified $L$-value. This latter set can itself be uniquely determined by linear combinations over the canonical basis in this way: Let

$$|[pq0], L, hw\rangle \equiv \sum_{\alpha,\sigma} A^{[pq0],L}_{\alpha\sigma} \left| \begin{matrix} p & & q & & 0 \\ & \alpha & & \alpha - L - 2\sigma & \\ & & \alpha - \sigma & & \end{matrix} \right\rangle, \tag{4.12a}$$

where the $A^{[pq0],L}_{\alpha,\sigma}$ are numerical constants such that

$$L_+|[pq0], L, hw\rangle = 0, \tag{4.12b}$$

and the sum is over all $(\alpha, \sigma)$ such that the Gel'fand-Weyl patterns in Eq. (4.12a) are lexical.

There are $M_L(p,q)$—the multiplicity number—linearly independent orthonormal solutions to these conditions. As a *vector space* this is a unique determination. As *individual vectors*, however, there is no labelling whatsoever at this stage (since the set of solutions of Eq. (4.12b) is unchanged by any unitary transformation). Let us denote the vector space of solutions of Eq. (4.12b) as $V_L(p,q)$.

**4.3.3.** The key to the canonical resolution of the problem posed in §2, above, is the multiplicity function, $M_L(p,q,)$. This function, though not difficult to determine, is rather complicated in appearance (see §5) and this complication obscures the underlying simplicity of the key concepts. Let us therefore ignore these details, temporarily, and display the numerical answer graphically to illustrate the concepts.

We will graph the values $M_L(p,q)$ of the multiplicity function by fixing $L$, and using the Möbius plane for the irrep labels $p,q$, which are the variables for the function $M_L$. The Möbius plane is a description of the $I\!R^2$-plane obtained by using *three* axes $x_1,x_2,x_3$ with origin at (0,0,0) and positive directions at 120° as shown in Fig. 1. (The corresponding negative axes extend from the origin in the opposite direction, but are not shown.) The three Möbius coordinates (a,b,c) of an arbitrary point are obtained by perpendicular projection from the point onto each of the three axes. The geometry of equilateral triangles then assures that the Möbius coordinates $(x_1,x_2,x_3)$ of an arbitrary point sum to zero, that is, we have the constraint $x_1+x_2+x_3=0$. For the description of the multiplicity function, the irrep labels $[pq0]$ that correspond to the Möbius coordinates $(x_1,x_2,x_3)$ are

$$x_1=q, \qquad x_2=-p, \quad \text{and} \quad x_3=p-q. \tag{4.13}$$

Thus, the set of lexical irrep labels are in one-to-one correspondence with the lattice points belonging to the pie-shaped region with vertex at the origin and boundary lines $x_1=0$ and $x_3=0$ (see Fig. 2).

Figures 2-5 (taken from Ref. 38) display the level sets of the multiplicity function $M_L(p,q)$. The actual function displayed is: $M_{L=p-\Delta}(p,q) \equiv N_\Delta(p,q)$, that is, $\Delta \equiv p-L$ replaces $L$.

Level sets in the triangular regions denoted $T_\Delta$ in Figs. 2 and 4 are complicated to display, and we have chosen to give in Figs. 3 and 5 some examples, which illustrate the desired information.

*The critical information on the multiplicity function which these figures demonstrate is this:*

(a) The multiplicity function reaches a constant, maximum, value in the open triangular region having vertex $(\Delta,-2\Delta,\Delta)$.

(b) The multiplicity function *decreases monotonically* in directions perpendicular to (and toward) the $x_1$ and the $x_3$ axes.

(c) Every decrease is by exactly 1 unit.

**4.3.4.** We are now in a position to explain the concepts underlying the canonical resolution of the multiplicity. The basic problem is to identify uniquely each vector in a given multiplicity set, *without making any arbitrary choices*. The critical information on the multiplicity function, noted in (a)-(c) above, makes this task possible.

Suppose, for example, we are at a point $(q, -p, p-q)$ corresponding to the irrep $[pq0]$ in the maximal multiplicity region. Then our multiplicity set consists of precisely $N_\Delta$ vectors (with no distinguishing labels). Now move in a direction perpendicular, say, to $x_1$, out of the shaded region (referring to Fig. 2 or 4). At the boundary $x_3 = \Delta$ the multiplicity set loses *precisely one highest weight vector*. This unique vector can thus be given an identifying label. Proceeding to the next decrease, we label the next vector, etc. In this way all highest weight vectors in the multiplicity set receive labels. However, we *did* make arbitrary choices! We chose to move in an arbitrary direction, from an arbitrary initial point. To claim that the labelling is canonical we must show that *any* starting point, and moving in *any* direction out of the maximal region, identifies precisely the same vector. (This is done in Ref. 38.) Intuitively, one can see that this requirement of generality (independence of starting point, direction) leads to unlimitedly many zeros (on boundary lines) in the polynomial functions determining the individual vectors, and it is this information that uniquely determines the answer.

We remark that the canonical labelling of vectors in an irrep space $[pq0]$ can itself be posed as a reduction problem in group-subgroup form. This is the labelling problem: $SU(3) \downarrow (U(1) \times U(1))$, where the $U(1) \times U(1)$ group here is the Cartan subgroup. Using the multiplicity function for this problem, one can determine a canonical labelling (identical to the Gel'fand-Weyl labelling) from the above general procedure *without* any appeal to the existence of an intermediate group in the subgroup chain: $SU(3) \supset SU(2) \times U(1) \supset U(1) \times U(1)$.

*Remark:*

This informal discussion of the canonical labelling process is basically correct and capable of being formulated quite precisely. There is, however, one detail which should be cleared up even in this motivating discussion. In the argument given above, we spoke of identifying the unique vector that becomes the null vector as the multiplicity drops by unity. To identify this vector requires that we know the vectors in both the multiplicity set for $[pq0]$ and in the multiplicity set for $[p'q'0]$, (where $\Delta N$ decreases by unity). The problem is that these two sets of vectors *belong to different vector spaces*: how can this comparison be accomplished? It is essential to recognize that the singling out of one vector does *not* require that the two sets of vectors exist

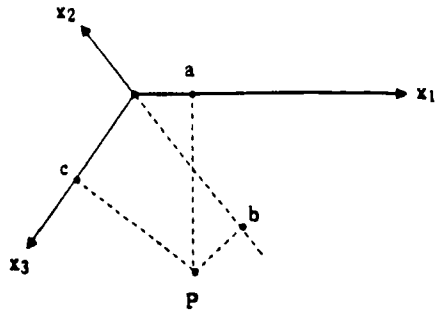



*Fig. 1. The Möbius coordinate description of the $\mathbf{R}^2$-plane.*

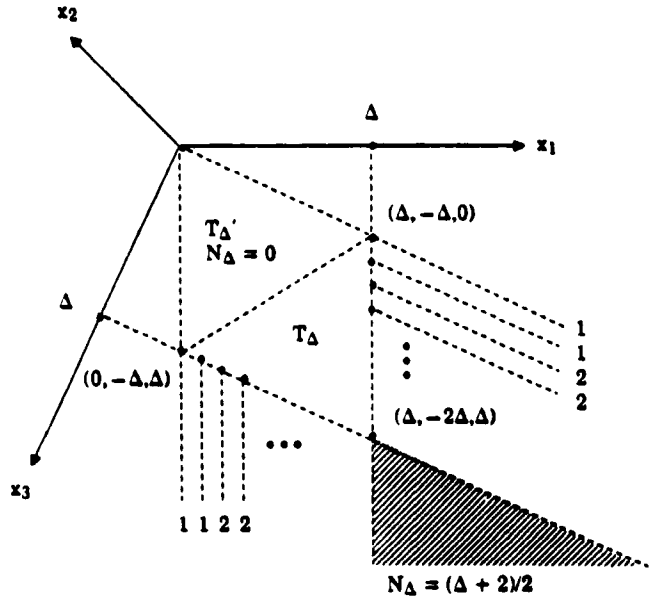



*Fig. 2. Level sets of the multiplicity function $N_{\Delta}(p,q) = k \in K_{\Delta}$ for $\Delta$ an even integer.*




*Fig. 3a. Value of $N_0$ on $T_0$.*

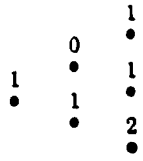



*Fig. 3b. Value of $N_2$ on $T_2$.*

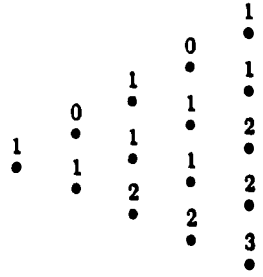



*Fig. 3c. Value of $N_4$ on $T_4$.*

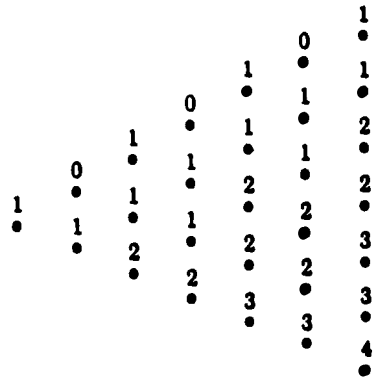



*Fig. 3d. Value of $N_6$ on $T_6$.*

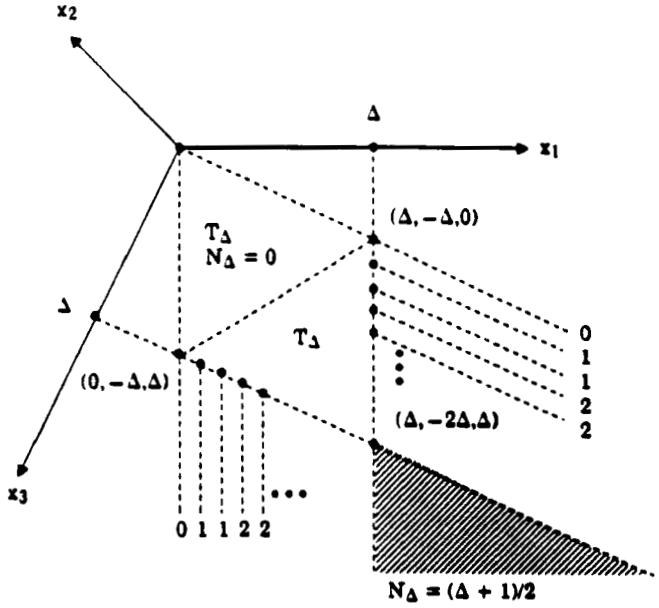



*Fig. 4. Level sets of the multiplicity function $N_\Delta(p,q) = k \in K_\Delta$ for $\Delta$ an odd integer.*




*Fig. 5a. Value of $N_1$ on $T_1$.*

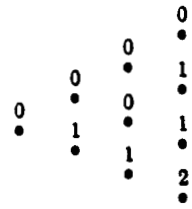



*Fig. 5b. Value of $N_3$ on $T_3$.*

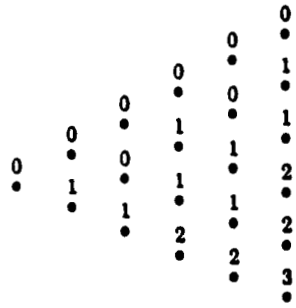



*Fig. 5c. Value of $N_5$ on $T_5$.*

in a common vector space—which cannot be achieved—but only that one be able to *correlate the vectors* in the two sets. In other words, one must be able to put the vectors in the two vector spaces in a one-to-one correspondence to identify that unique vector in the larger set which corresponds to the null vector in the smaller set.

To see that this correspondence can be accomplished consider Eqs. (4.12). Every vector in the highest weight space $V_L(p,q)$ is a linear combination over the set of vectors $\left\{\left|\begin{matrix} p & & q & & 0 \\ & \alpha & & 2\beta-\alpha-L & \\ & & \beta & & \end{matrix}\right\rangle\right\}$ belonging to the irrep space $[pq0]$. Every vector in this flag manifold of the irrep $[pq0]$ can, however, be uniquely identified by giving the Gel'fand-Weyl pattern labels $\begin{pmatrix} m_{12} & & m_{22} \\ & m_{11} & \end{pmatrix}$. Since these labels are common to the basis vectors in each $[pq0]$ flag manifold (though some may be the null vector), we can certainly put the vectors in the highest weight manifolds in 1-1 correspondence if the two vector spaces have the same dimension, and can identify the unique null vector if the dimensions differ by unity.

**4.3.5.** Let us now give the detailed form of the multiplicity function.[16,38] We use the notation $\langle L\rangle$ with $L \in \mathbb{N}$ to denote an irrep of $SO(3)$. The abstract reduction rule (4.2) then takes the following form for $SU(3) \downarrow SO(3)$:

$$[pq0] = \sum_{L\in\mathbb{N}} M_L(p,q)\langle L\rangle, \quad \text{each } [p,q] \in \mathbf{P}(2), \tag{4.14}$$

where $M_L(p,q)$ denotes the value of the multiplicity function $M_L : \mathbf{P}(2) \to \mathbb{N}$, yet to be explicitly determined. We next define for each $\Delta \in \mathbb{N}$ the function $N_\Delta$ with domain $\mathbf{P}(2)$ by

$$N_\Delta(p,q) = M_{p-\Delta}(p,q), \quad p \geq \Delta, \tag{4.15a}$$
$$N_\Delta(p,q) = 0, \quad 0 \leq p \leq \Delta - 1, \quad 0 \leq q \leq p. \tag{4.15b}$$

A basic result is that $N_\Delta$ is a map from $\mathbf{P}(2)$ onto the finite set $\mathbb{L}_\Delta$ defined by

$$\mathbb{L}_\Delta = \{0, 1, \ldots, \phi(\Delta+1)\}. \tag{4.16}$$

Here $\phi$ is the function defined for each $n \in \mathbb{N}$ by

$$\phi(n) = \begin{cases} n/2, & n \text{ even} \\ (n+1)/2, & n \text{ odd} \end{cases}. \tag{4.17}$$

We now give the multiplicity function $M_L(p,q)$:

$0 \leq p \leq L-1$ :

$$M_L(p,q) = 0, \quad 0 \leq q \leq p; \tag{4.18a}$$

$L \leq p \leq 2L$ :

$$M_L(p,q) = \begin{cases} \phi(p-L+1) - \phi(p-L-q), & 0 \leq q \leq p-L \\ \phi(p-L+1), & p-L \leq q \leq L \\ \phi(p-L+1) - \phi(q-L), & L \leq q \leq p \end{cases} ; \tag{4.18b}$$

$2L \leq p < \infty$ :

$$M_L(p,q) = \begin{cases} \phi(p-L+1) - \phi(p-L-q), & 0 \leq q \leq L \\ \phi(p-L+1) - \phi(p-L-q) - \phi(q-L), & L \leq q \leq p-L \\ \phi(p-L+1) - \phi(q-L), & p-L \leq q \leq p \end{cases} . \tag{4.18c}$$

In these expressions $\phi$ is the function defined in Eq. (4.17). The function $N_\Delta$ defined by Eq. (4.15) is obtained from the above relations to be:

$$\Delta = 0, 2, 4, \ldots,$$

$2\Delta \leq p \leq \infty$:

$$N_\Delta(p,q) = \begin{cases} \phi(q+1), & 0 \leq q \leq \Delta \\ \frac{\Delta}{2}+1, & \Delta \leq q \leq p-\Delta \\ \phi(p-q+1), & p-\Delta \leq q \leq p \end{cases} ; \tag{4.19a}$$

$\Delta \leq p \leq 2\Delta$:

$$N_\Delta(p,q) \equiv \begin{cases} \phi(q+1), & 0 \leq q \leq p-\Delta \\ -\frac{\Delta}{2}+1+\phi(p), & p \text{ even}, q \text{ even}, \quad p-\Delta \leq q \leq \Delta \\ -\frac{\Delta}{2}+\phi(p), & \text{otherwise}, \quad p-\Delta \leq q \leq \Delta \\ \phi(p-q+1), & \Delta \leq q \leq p \end{cases} . \tag{4.19b}$$

$$\Delta = 1, 3, 5, \ldots$$

$2\Delta \leq p < \infty$ :

$$N_\Delta(p,q) = \begin{cases} \phi(q), & 0 \leq q \leq p-\Delta \\ (\Delta+1)/2, & \Delta \leq q \leq p-\Delta \\ \phi(p-q), & p-\Delta \leq q \leq p \end{cases} ; \tag{4.20a}$$

$\Delta \leq p \leq 2\Delta$:

$$N_\Delta(p,q) = \begin{cases} \phi(q), & 0 \leq q \leq p-\Delta \\ -\frac{(\Delta+1)}{2} + 1 + \phi(p), & p \text{ even}, q \text{ even}, \quad p-\Delta \leq q \leq \Delta \\ -\frac{(\Delta+1)}{2} + \phi(p), & \text{otherwise}, \quad p-\Delta \leq q \leq \Delta \\ \phi(p-q), & \Delta \leq q \leq p \end{cases} . \tag{4.20b}$$

**4.3.6.** The structure of the multiplicity function $N_\Delta$ given in Figures 2-5 are strikingly similar to the graphs of the intertwining function $I_{\mu,\Delta}$ of the multiplicity problem for $U(3)$ WCG-coefficients; that is, the $(U(3) \times U(3)) \downarrow U(3)$ resolution.[31-33]

The principal difference is the assignment of numerical values to the triangular region $T_\Delta$. It is known[34-36] for $U(3)$ that the region $T_\Delta$ categorizes a certain class of $U(3)$ invariant polynomials characteristic of the $U(3)$ canonical solution, and one expects a distinction here between the $(U(3) \downarrow U(3)) \downarrow U(3)$ problem and the present one.

The semi-infinite lines of zeros are, however, of precisely the same structure, although the numerical assignments of multiplicities in the present case steps down by unity every *two* lines. Nonetheless, it is known from the $U(3)$ problem that the numerator pattern calculus (see below) describes precisely the zeros required for stepping down the number of nonzero vectors so as to match the intertwining number. This is a key observation for implementing the canonical structure.

Let us describe now the construction of the individual vectors in the multiplicity space $V_L(p,q)$ of highest weight vectors.

Each vector in $V_L(p,q)$ has the form given by Eq. (4.12); to denote an individual canonically labelled vector we rewrite Eq. (4.12) in a more explicit form as

$$|p,q;p-\Delta;\lambda\rangle = \sum_{\alpha,\sigma} \left\langle \begin{matrix} p & & q & & 0 \\ & \alpha & & \alpha-p+\Delta-2\sigma & \\ & & \alpha-\sigma & & \end{matrix} \middle| p,q;p-\Delta;\lambda \right\rangle$$

$$\times \left| \begin{matrix} p & & q & & 0 \\ & \alpha & & \alpha-p+\Delta-2\sigma & \\ & & \alpha-\sigma & & \end{matrix} \right\rangle, \tag{4.21}$$

where $\Delta = p - L$ and $\lambda$ is the multiplicity index.

*It is in the evaluation of the coefficients in the expansion* (4.21) *that the numerator pattern calculus factors of* $SU(3)$ *enter.* These coefficients can be

shown to factor in the form:

$$\left\langle \begin{matrix} p & & q & & 0 \\ & \alpha & & \alpha - p + \Delta - 2\sigma & \\ & & \alpha - \sigma & & \end{matrix} \middle| p, q; p - \Delta; \lambda \right\rangle =$$

$$\left[\frac{(L + 2\sigma + 1)(L + \sigma)!}{\sigma!}\right]^{\frac{1}{2}} P^{(\lambda)}_{p-\Delta}(\alpha, \sigma)$$

$$\times \left\langle \begin{matrix} p & & q & & 0 \\ & p - \Delta + 2\lambda & & \Delta - 2\lambda & \end{matrix} \middle| A\begin{pmatrix} 0\,0\,0 \\ \delta_1\ \delta_2 \end{pmatrix} \middle| \begin{matrix} p & & q & & 0 \\ & \alpha & & \alpha - p + \Delta - 2\sigma & \end{matrix} \right\rangle. \tag{4.22a}$$

In this expression the $P^{(\lambda)}_{p-\Delta}(\alpha, \sigma)$ are *polynomials* in the variables $(p, q)$ (suppressed in the notation), and *the bra-ket* factor $\langle \cdot | \cdots | \cdot \rangle$ is the *pattern calculus factor* in which $\delta_1$ and $\delta_2$ are the *shifts* defined by

$$\delta_1 \ = \ p - \alpha - \Delta + 2\lambda, \qquad \delta_2 \ = \ p - \alpha + 2\sigma - 2\lambda. \tag{4.22b}$$

The occurrence of the pattern calculus factor in Eq. (4.22a) is quite significant: *it is these factors that account for the lines of zeros in the graphs of the multiplicity function.* These zeros are determined by products of linear factors and the actual pattern calculus factor is the square root of this product of factors. The pattern calculus factors are accordingly a transcription of the structural information on the multiplicity function.

We discuss the pattern calculus in more detail in an appendix to this section.

It is through the zeros of the pattern calculus factor, and the zeros of the polynomial factor as well, in the coefficients (4.22a) that the vector $|pq; p - \Delta; \lambda\rangle$ becomes explicitly the zero vector when we go from $V_L(p, q)$ to $V_L(p', q')$ when $\Delta N$ decreases by unity.

The vectors in Eq. (4.21) are not normalized. We could, of course, normalize the vectors, since these vectors are all nonzero for $(p, q)$ in the maximal multiplicity region (where $N_\Delta(p, q) = \phi(\Delta + 1)$). The *norm of the vector* will then carry all the information as to when the vector is zero or not. This procedure has been successfully carried out for the $(U(3) \times U(3)) \downarrow U(3)$ problem[35,36,39], but has not yet been achieved for the present problem. It is then the properties (zeros) of these $SO(3)$ invariant norms that would uniquely characterize the above solution as canonical.

The explicit solution to the canonical construction given above requires the explicit construction of the polynomials $P(\ldots)$. This task has not yet been completed. What has been done[38] is to give the defining recursion

relation and boundary conditions for the $P(\ldots)$ along with a proof of the existence of solutions and a proof of the properties of these solutions (including the proof of the orthogonality relation).

Let us emphasize again the significance of the pattern calculus factor in the coefficients (4.22a). It is precisely this factor that renders the structure of the canonical solution comprehensible. Without knowledge of the elegant algebraic structure associated with the pattern calculus, relation (4.21) would be a hopelessly incomprehensible numerical result. It is precisely this calculus and the associated factorization of the coefficients for the $SU(3) \downarrow SO(3)$ problem into the form: (polynomial)$\times$ (pattern calculus factor) that brings a comprehensible structure to the multiplicity problem: the pattern calculus factor accommodates the lines of zeros and the polynomial factor the finite sets of zeros associated with the region $T_\Delta$ in just the right way so that the vector space structure follows the multiplicity number structure.

We believe these results for the numerator pattern calculus in the $SU(3) \downarrow SO(3)$ problem will extend to the general $U(n) \downarrow G$ reduction problem. Accordingly, the $U(n)$ numerator pattern calculus should be viewed as an important algebraic tool having potentially broad application. For this reason, we include a brief review of this subject in the appendix.

**4.3.7.** There is one property of the canonical resolution of the $SU(3) \downarrow SO(3)$ problem which was found to be valid in the explicit results of Ref. 31, and is a consequence of $M_L(p,q) = M_L(p,p-q)$.. This result has an interesting group theoretic interpretation.

It was found in Ref. 38 that the uniquely labelled vectors of the irrep space $[pq0]$ in the canonical resolution, that is, the set of vectors $\{|[pq0]; LM,\lambda\rangle\}$ with $L, M$ the usual $SO(3)$ labels and $\lambda = 0,1,\ldots$ the canonical multiplicity label obey the following "conjugation" relation:

$$|[pq0]; LM,\lambda\rangle \;=\; (-1)^\lambda |[p,p-q,0]; LM,\lambda\rangle. \tag{4.23}$$

To understand the group theoretic significance of this result consider the $SU(3) \supset SO(3)$ realization of the Lie algebra of $SU(3)$. The eight generators divide into two sets: three $L = 1$ (vector) generators ($\mathbf{L}$) and five $L = 2$ (quadruple) generators ($\mathbf{Q}$). The $SU(3)$ commutation relations take the symbolic form:

$$[\mathbf{L},\ \mathbf{L}] \subset \mathbf{L}, \qquad [\mathbf{L},\ \mathbf{Q}] \subset \mathbf{Q}, \qquad \text{and} \quad [\mathbf{Q},\ \mathbf{Q}] \subset \mathbf{L}. \tag{4.24}$$

In this form, the $SU(3) \downarrow SO(3)$ realization of the Lie algebra shows that there exists an involutary automorphism: $\mathbf{L} \rightarrow \mathbf{L}$, $\mathbf{Q} \rightarrow$ -$\mathbf{Q}$ which preserves the Lie algebra. (If the generators are realized as real, $3 \times 3$ matrices, the involution corresponds to matrix transposition.)

Applying this automorphism to the invariant operators[30] of $SU(3)$, one finds: $I_2 \to I_2$, and $I_3 \to -I_3$, where $I_2$ is the quadratic (or Casimir invariant) and $I_3$ is the cubic invariant (not given by Casimir). Solving for the irrep labels in terms of these two invariant operators, one finds that the irrep labels transform under the involution as: $p \to p$, $q \to p - q$. (This automorphism, found by Cartan, accordingly has the same effect on the set of unitary irreps $\{[pq0]\}$ as complex conjugation which carries $[pq0] \leftrightarrow [p, p-q, 0]$.)

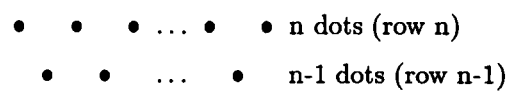
One sees that irreps of the form $[2k\ k\ 0]$ are invariant under this Cartan involution, and that for these self-conjugate irreps the Cartan involution implies that $(-1)^\lambda$ is a good quantum number.[41] For the generators, which belong to the irrep [210], the $SU(3) \downarrow SO(3)$ resolution is $(1^+, 2^-)$, as shown above for the Lie algebra. [The notations $L^+$ and $L^-$ denote that $(-1)^\lambda = +1$ and $(-1)^\lambda = -1$, respectively.] For the 27-plet (the self-conjugate irrep [420]) the resolution is $4^+, 3^-, 2^+, 2^-, 0^+$, which one recognizes to be precisely the canonical splitting. This "Cartan parity" label $(-1)^\lambda$ for self-conjugate irreps cannot, of itself, resolve the multiplicity completely, even for self-conjugate irreps. What this involution *does* accomplish, however, is a consistency check on any solution to the $SU(3) \downarrow SO(3)$ problem: ***if such solution claims to be canonical, then it must accord with this automorphism.*** It is gratifying that the solution discussed above does indeed have this property, which actually fails in some of the other, noncanonical resolutions.

## APPENDIX. The Pattern Calculus Rules

The pattern calculus rules were invented[40] to elucidate the structure of the matrix elements of the unit $U(n) \downarrow U(n-1)$ projective operators (reduced matrix elements) associated with $U(n)$ Wigner operators. The matrix elements of the $U(n)$ Wigner operators are the WCG-coefficients for the reduction of the direct product of two irreps of $U(n)$ into irreps of $U(n)$. These rules have been described in detail in Ref. 40. In particular, the so-called *numerator pattern calculus factor* has its origins in the decription of lines of zeros belonging to the null space of a Wigner operators. For convenience, we give the rules for the numerator pattern calculus in full generality.

Let $\Delta = (\Delta_1, \Delta_2, \ldots, \Delta_n)$, each $\Delta_i \in \mathbb{Z} = \{\ldots, -1, 0, 1, \ldots\}$ denote an arbitrary n-tuple of integers, and $\delta = (\delta_1, \delta_2, \ldots, \delta_{n-1})$, each $\delta_i \in \mathbb{Z}$, an arbitrary $(n-1)$tuple of integers. Then, we first form an *arrow-pattern* according to the following two rules:

*Rule 1:* Write out two rows of dots, as shown:



*Rule 2:* Draw arrows between dots as follows: Select a dot $i$ in row $n$ and a dot $j$ in row $n-1$. If $\Delta_i > \delta_j$, draw $\Delta_i - \delta_j$ arrows from dot $i$ to dot $j$; if $\delta_j > \Delta_i$, draw the arrows from dot $j$ to dot $i$. Carry out this procedure for all dots in rows $n$ and $n-1$. This yields a *numerator arrow-pattern* with arrows going *between* rows.

We denote this arrow-pattern by $A\binom{\Delta}{\delta}$. Next, let $\lambda = [\lambda_1, \lambda_2, \ldots, \lambda_n]$, each $\lambda_i \in \mathbb{N}$, with $\lambda_1 \geq \lambda_2 \geq \ldots \geq \lambda_n \geq 0$, denote a partition having $n$ parts (counting zeros), and $\mu = [\mu_1, \mu_2, \ldots, \mu_{n-1}]$, each $\mu_i \in \mathbb{N}$, with $\mu_1 \geq \mu_2 \geq \ldots \geq \mu_{n-1} \geq 0$, a partition having $n-1$ parts, such that the betweenness conditions

$$\lambda_1 \geq \mu_1 \geq \lambda_2 \geq \mu_2 \geq \ldots \geq \lambda_{n-1} \geq \mu_{n-1} \geq \lambda_n \geq 0 \qquad (A.1a)$$

are satisfied. We denote this by the symbol:

$$\binom{\lambda}{\mu} = \begin{pmatrix} \lambda_1 & & \lambda_2 & & \ldots & \lambda_{n-1} & & \lambda_n \\ & \mu_1 & & \mu_2 & \ldots & & \mu_{n-1} & \end{pmatrix}. \qquad (A.1b)$$

We also require the so-called partial hooks of the partitions $\lambda$ and $\mu$:

$$\begin{aligned} p_i &= \lambda_i + n - i, \quad i = 1, 2, \ldots, n \quad , \\ q_j &= \mu_j + n - 1 - j, \quad j = 1, 2, \ldots, n-1. \end{aligned} \qquad (A.2)$$

Finally, we associate with each arrow-pattern $A\binom{\Delta}{\delta}$ and each pair of partitions $\binom{\lambda}{\mu}$ a *nonnegative number*, denoted by (see Remark at end of this section)

$$\left\langle \begin{matrix} \lambda + \Delta \\ \mu + \delta \end{matrix} \middle| A\binom{\Delta}{\delta} \middle| \begin{matrix} \lambda \\ \mu \end{matrix} \right\rangle, \qquad (A.3)$$

where $\lambda + \Delta = (\lambda_1 + \Delta_1, \lambda_2 + \Delta_2, \ldots, \lambda_n + \Delta_n)$ and $\mu + \delta = (\mu_1 + \delta_1, \mu_2 + \delta_2, \ldots, \mu_{n-1} + \delta_{n-1})$. The symbol (A.3) is defined by the arrow-pattern $A\binom{\Delta}{\delta}$ and the following additional three rules:

*Rule 3:* In the arrow-pattern $A\binom{\Delta}{\delta}$ assign the partial hook $p_i$ to dot $i$ ($i = 1, 2, \ldots, n$) in row $n$, and $q_j$ to dot $j$ ($j = 1, 2, \ldots, n-1$) in row $n-1$.

*Rule 4:* In general, there will be several arrows going between dot $i$ in row $n$ and dot $j$ in row $n-1$. If $\Delta_i > \delta_j$ (downward going arrows), assign to the first arrow the factor $p_i - q_j$, to the second the factor $p_i - q_j + 1$, etc., until all arrows have been counted; if $\Delta_i < \delta_j$ (upward going arrows), assign to the first arrow the factor $q_j - p_i + 1$, to the second the factor $q_j - p_i + 2$, etc., until all arrows have been counted; if

$\Delta_i = \delta_j$, no arrows go between points $i$ and $j$, and the factor 1 is assigned.

*Rule 5:* Write out the product of all factors corresponding to $i = 1, \ldots, n$; $j = 1, 2, \ldots, n-1$ obtained in Rule 4, and take the square-root of the absolute value.

It is useful to use the following definitions of the rising factorial symbol for each $a \in \mathbb{Z}$ to give the explicit algebraic expression of the pattern calculus symbol:

$$\begin{aligned} (x)_a &= x(x+1)\ldots(x+a-1), \quad a \geq 1, \\ (x)_0 &= 1, \\ (x)_a &= (-x+1)_{-a}, \quad a \leq -1. \end{aligned} \tag{A.4}$$

These symbols obey the following useful and often used properties:

$$(-x)_a = (-1)^a (x-a+1)_a, \quad a \in \mathbb{Z}, \tag{A.5a}$$

$$(x)_a = (x)_b (x+b)_{a-b}, \quad a \geq b \geq 0, \quad a, b \in \mathbb{N}. \tag{A.5b}$$

The rules of the pattern calculus then assign the following value to the symbol (A.3):

$$\left\langle \begin{matrix} \lambda + \Delta \\ \mu + \delta \end{matrix} \middle| A\begin{pmatrix} \Delta \\ \delta \end{pmatrix} \middle| \begin{matrix} \lambda \\ \mu \end{matrix} \right\rangle = \left[ \left| \prod_{i=1}^{n} \prod_{j=1}^{n-1} (p_i - q_j)_{\Delta_i - \delta_j} \right| \right]^{\frac{1}{2}}. \tag{A.6}$$

We could, of course, have defined the symbol (A.3) by Eq. (A.6) at the outset (without reference to the pattern calculus), but the rules of the pattern calculus are a valuable aid to understanding the properties of this quantity. (The use of the absolute value sign in Eq. (A.6) is trivial, since all factors in the product are real, but some may be negative.)

The symbol (A.6) has two important properties:

*zeros of the symbol:*

$$\left\langle \begin{matrix} \lambda + \Delta \\ \mu + \delta \end{matrix} \middle| A\begin{pmatrix} \Delta \\ \delta \end{pmatrix} \middle| \begin{matrix} \lambda \\ \mu \end{matrix} \right\rangle = 0, \qquad \begin{matrix} \text{unless } \lambda' = \lambda + \Delta \text{ and } \mu' = \mu + \delta \\ \text{are partitions satisfying the} \\ \text{betweenness relations;} \end{matrix} \tag{A.7a}$$

and

$$\left\langle \begin{matrix} \lambda + \Delta \\ \mu + \delta \end{matrix} \middle| A\begin{pmatrix} \Delta \\ \delta \end{pmatrix} \middle| \begin{matrix} \lambda \\ \mu \end{matrix} \right\rangle \neq 0, \qquad \begin{matrix} \text{if } \lambda' = \lambda + \Delta \text{ and } \mu' = \mu + \delta \\ \text{are partitions satisfying the} \\ \text{betweenness relations.} \end{matrix} \tag{A.7b}$$

*multiplication of two symbols:*

$$\left\langle \begin{matrix} \lambda+\Delta'+\Delta \\ \mu+\delta'+\delta \end{matrix} \middle| A\begin{pmatrix} \Delta' \\ \delta' \end{pmatrix} \middle| \begin{matrix} \lambda+\Delta \\ \mu+\delta \end{matrix} \right\rangle \times \left\langle \begin{matrix} \lambda+\Delta \\ \mu+\delta \end{matrix} \middle| A\begin{pmatrix} \Delta \\ \delta \end{pmatrix} \middle| \begin{matrix} \lambda \\ \mu \end{matrix} \right\rangle$$
$$= I^{\Delta',\Delta}_{\delta',\delta}\begin{pmatrix} \lambda \\ \mu \end{pmatrix} \left\langle \begin{matrix} \lambda+\Delta'+\Delta \\ \mu+\delta'+\delta \end{matrix} \middle| A\begin{pmatrix} \Delta'+\Delta \\ \delta'+\delta \end{pmatrix} \middle| \begin{matrix} \lambda \\ \mu \end{matrix} \right\rangle, \quad (A.8a)$$

where the $I$-factor is defined by

$$I^{\Delta'\Delta}_{\delta',\delta}\begin{pmatrix} \lambda \\ \mu \end{pmatrix}$$
$$= \Big| \prod_{(ij)\in A_1} (-p_i - \Delta_i + q_j + \delta_j + 1)_{n_{ij}}$$
$$\times \prod_{(ij)\in A_2} (p_i + \Delta_i - q_j - \delta_j)_{m_{ij}} \Big|. \quad (A.8b)$$

The sets $A_1$ and $A_2$ are subsets of

$$A = \{(i,j) \,|\, i = 1,\ldots,n;\ j = 1,\ldots,n-1\}$$

defined by

$$A_1 = \{(i,j) \in A \mid \Delta_i > \delta_j,\ \Delta'_i < \delta'_j\},$$
$$A_2 = \{(i,j) \in A \mid \Delta_i < \delta_j,\ \Delta'_i > \delta'_j\}. \quad (A.9a)$$

The integers $n_{ij}$ and $m_{ij}$ are defined by

$$n_{ij} = \min(\Delta_i - \delta_j,\ \delta'_j - \Delta'_i),$$
$$m_{ij} = \min(\delta_j - \Delta_i,\ \Delta'_i - \delta'_j), \quad (A.9b)$$

where we note that $n_{ij} > 0$ for $(i,j) \in A_1$, and $m_{ij} > 0$ for $(i,j) \in A_2$. (If $A_1$ or $A_2$ is empty, the corresponding product in (A.8b) is unity.)

The proofs of relations (A.8) and (A.9) are direct consequences of the definition (A.6), where we recall that the partitions $\lambda$ and $\mu$ in the symbol are to satisfy the betweenness relations (A.1). This relation between $\lambda, \mu$, and the zeros of the rising factorial symbol given by $(m)_k = 0$ for $m, k \in \mathbb{N}$ and $k \geq m+1$, imply relations (A.8). The proofs of Eqs. (A.9) require attention to detail. The factor (A.8b) is called the *opposing arrow factor* between the arrow-patterns $A\binom{\Delta'}{\delta'}$ and $A\binom{\Delta}{\delta}$. This is because the numerical factor associated with the arrows going between point $i$ in row $n$ and point $j$ in row $n-1$ occurs in both factors in the left-hand side of Eq. (A.8a) if

and only if $A\binom{\Delta'}{\delta'}$ and $A\binom{\Delta}{\delta}$ have opposing arrows going between point $i$ and point $j$. There are four possible cases for each pair $(i,j)$: (a) $\Delta_i > \delta_j$, $\Delta_i' < \delta_j'$, $\Delta_i + \Delta_i' \geq \delta_j + \delta_j'$; (b) $\Delta_i > \delta_j$, $\Delta_i' < \delta_j'$, $\Delta_i + \Delta_i' \leq \delta_j + \delta_j'$; (c) $\Delta_i < \delta_j$, $\Delta_i' > \delta_j'$, $\Delta_i + \Delta_i' \geq \delta_j + \delta_j'$; and (d) $\Delta_i < \delta_j$, $\Delta_i' > \delta_j'$, $\Delta_i + \Delta_i' \leq \delta_j + \delta_j'$. For each pair of points $(i,j)$ for which (a) is satisfied, the pattern calculus factors for the product on the left-hand side of Eq. (A.8a) are

$$\left[\left|(q_j + \delta_j - p_i - \Delta_i + 1)_{\delta_j' - \Delta_i'}(p_i - q_j)_{\Delta_i - \delta_j}\right|\right]^{\frac{1}{2}}$$
$$= \left|(p_i + \Delta_i - q_j - \delta_j)_{\Delta_i' - \delta_j'}\right| \times \left[\left|(p_i - q_j)_{\Delta_i + \Delta_i' - \delta_j - \delta_j'}\right|\right]^{\frac{1}{2}}.$$

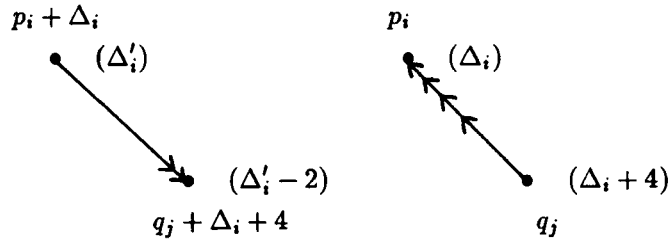
The square-root factor in this result is just that obtained for the arrow-pattern $A\binom{\Delta'+\Delta}{\delta'+\delta}$ for the point $(i,j)$ for the case at hand, while the first factor is the $(i,j)$-factor in Eq. (A.8b) for this case (a). Considering cases (b), (c), and (d), in turn, we complete the proof of Eqs. (A.9).

For simple numerical cases of the arrow-pattern $A\binom{\Delta}{\delta}$; that is, $\Delta$ and $\delta$ numerical, it is often easier to implement the pattern-calculus rules (1)-(5) directly for the evaluation of (A.6) rather than using the general result. This is also true for the verification of the properties (A.7) and (A.8). The general rule for writing out the opposing arrow factor (A.8b) is, however, easily given: *Draw the arrow-pattern for point $(i,j)$ for each of the patterns $A\binom{\Delta'}{\delta'}$ and $A\binom{\Delta}{\delta}$, and label it as shown:*

$$\begin{array}{ll} p_i + \Delta_i & p_i \\ \bullet \quad (\Delta_i') & \bullet \quad (\Delta_i) \\ \\ \bullet \quad (\delta_j') & \bullet \quad (\delta_j) \\ q_j + \delta_j & q_j \end{array} \qquad (A.10)$$

*Evaluate the pattern calculus factor in the usual way, either on the right pair or left pair of points, whichever has the fewer arrows, using the variables $(p_i, q_j)$ or the shifted variables $(p_i + \Delta_i,\ q_j + \delta_j)$, respectively, and square the result. Take the product of these factors over all pairs $(i,j)$.*

For example, the opposing arrow factor for the diagram




is

$$|(p_i - q_j - 4)(p_i - q_j - 3)|.$$

We have reviewed the above rules of the pattern calculus in full generality (for arbitrary $n$) although for the present problem of $SU(3) \downarrow SO(3)$, we require only the very special case $N = 3$ with $\Delta = (\Delta_1, \Delta_2, \Delta_3) = (0, 0, 0)$. To have given only the special cases required for the problem at hand would leave the impression that the rules are ad hoc. It is significant, we believe, to know that we are dealing here with special cases of *general rules.*

*Remark.* The Dirac bracket notation for the pattern calculus factor defined by the pattern calculus rules is deliberate: it is clear that relations (A.7) and (A.8) may be interpreted as an action of the *shift operator* $A\binom{\Delta}{\delta}$ on the *basis vector* $\left|\begin{smallmatrix}\lambda\\ \mu\end{smallmatrix}\right\rangle$ of a separable Hilbert space $\mathcal{H}$ having the orthonormal basis

$$\left\{\left|\begin{smallmatrix}\lambda\\ \mu\end{smallmatrix}\right\rangle \,\middle|\, \lambda, \mu \text{ are partitions having } n \text{ and } n-1 \text{ parts with } \binom{\lambda}{\mu} \text{lexical}\right\}. \tag{A.11}$$

Thus, we have

$$A\binom{\Delta}{\delta}\left|\begin{smallmatrix}\lambda\\ \mu\end{smallmatrix}\right\rangle = \#\left|\begin{smallmatrix}\lambda+\Delta\\ \mu+\delta\end{smallmatrix}\right\rangle, \tag{A.12a}$$

where # is given by the pattern calculus rules; that is, by Eq. (A.6). Property (A.7a) then assures that the operator $A\binom{\Delta}{\delta}$ maps each vector in $\mathcal{H}$ to a new vector in $\mathcal{H}$. Relations (A.8) then define the product of two such operators:

$$A\binom{\Delta'}{\delta'} A\binom{\Delta}{\delta} = A\binom{\Delta'+\Delta}{\delta'+\delta} I_{\delta',\delta}^{\Delta',\Delta}, \tag{A.12b}$$

where $I_{\delta,\delta}^{\Delta',\Delta}$ is a $U(n) : U(n-1)$ invariant operator (effects no shifts) with eigenvalue on the state $\left|\begin{smallmatrix}\lambda\\ \mu\end{smallmatrix}\right\rangle$ given by Eq. (A.8b). Such operator actions and relations can be useful for simplifying and suggesting many results.

## 5. NONCANONICAL METHODS: THE $SU(3) \supset SO(3)$ EXAMPLE

### 5.1. The Build-Up Principle

The essence of a canonical procedure is that the construction is *free of all arbitrary choices* to within equivalence. Thus the construction—if a canonical procedure exists!—is *unique* and inherently *nonarbitrary*. By contrast, noncanonical methods are far from unique (as we shall show below), arbitrary, and correspondingly *ad hoc*. One can not expect to be able to systematize such procedures, but in the methods we shall survey here we have been able to identify one principle—call it the "build-up principle"—which we now discuss.

The build-up principle for noncanonical methods of resolving $SU(3) \supset SO(3)$ is based on the fact that a carrier space of irrep $[pq0]$ of $SU(3)$ can be spanned by homogeneous polynomials of fixed degree (here $p+q$). Clearly one can construct polynomial realizations having sharp $SO(3)$ labels. Using Weyl's theorems on polynomial invariants, these arbitrary polynomial $SO(3)$ vectors can be multiplied by invariants to obtain the correct degree $(p+q)$ for an irrep $[pq0]$.

For this set of polynomials—carrying definite $SO(3)$ labels and of fixed homogeneity $p+q$—to span precisely the carrier space of irrep $[pq0]$ of $SU(3)$ is a result that must be proved. This can be done directly via laborious Lie algebraic techniques (as in the very large literature on this problem—see Refs. 43-48 and references therein) or *a priori* by global constraints, as we shall show.

We emphasize that such procedures for identifying vectors in the carrier space for irrep $[pq0]$ are inherently *ad hoc*, since it is clear that once having achieved such a set of linearly independent basis vectors—almost always nonorthogonal—one could construct an orthogonal basis set in arbitrarily many ways using these vectors, or indeed any linearly independent combination of these vectors respecting the good (canonical) quantum numbers.

There is nothing intrinsically noncanonical about the build-up principle, if it is effected in a manner that respects an underlying, identifiable canonical principle that dictates without free choice the $G \downarrow H$ reduction.

### 5.2. The Weyl Theorems

There are two fundamental theorems, both due to Weyl,[42] which are basic to the subsequent results:

(i) Every polynomial in the vectors $\mathbf{a}^\alpha = col(a_1^\alpha, a_2^\alpha, a_3^\alpha)(\alpha = 1,2)$ invariant under the left action $\mathbf{a}^\alpha \to L_R\mathbf{a}^\alpha = R\mathbf{a}^\alpha$, $R \in SO(3)$, is a polynomial in the three *basic invariants*

$$\mathbf{a}^1 \cdot \mathbf{a}^1, \quad \mathbf{a}^2 \cdot \mathbf{a}^2, \quad \mathbf{a}^1 \cdot \mathbf{a}^2, \tag{5.1}$$

where $\cdot$ denotes the usual scalar (dot) product.

(ii) Every polynomial in the vectors $\mathbf{a}_i = (a_i^1, a_i^2)(i = 1,2,3)$ invariant under the right action $\mathbf{a}_i \to R_U\mathbf{a}_i = \mathbf{a}_i\tilde{U}$, $U \in SU(2)$, is a polynomial in the three basic invariants

$$u_1 = a_{23}^{12}, \quad u_2 = a_{31}^{12}, \quad u_3 = a_{12}^{12}, \tag{5.2a}$$

where

$$u_i = (a_j^1 a_k^2 - a_k^1 a_j^2) = (\mathbf{a}^1 \times \mathbf{a}^2)_i, \tag{5.2b}$$

with $(i,j,k)$ cyclic in $(1,2,3)$. (Here $\times$ denotes the vector cross product and $\tilde{}$ denotes matrix transposition.)

Under the transformation $\mathbf{u}_i \to \mathbf{u}_i\tilde{U}$, each $U \in U(2)$, the $\mathbf{u}_i$ undergo the transformation

$$\mathbf{u}_i \to (\det U)\mathbf{u}_i. \tag{5.3}$$

Since $\det U$ appears to the power 1, each $\mathbf{u}_i$ $(i = 1,2,3)$ is called a $U(2)$ invariant of *index* 1. This property of the vector cross product under $U(2)$ transformations is generally not pointed out.

It is an obvious, but nonetheless important, observation that the vectors $\mathbf{a}^\alpha$ and $\mathbf{a}_i$ are but different names for the two-index indeterminates $a_i^\alpha$, carrying commuting left $(SO(3))$ and right $(U(2))$ actions. Thus we may classify the invariants (i) and (ii) in one group by transformation properties under the other group. This yields:

(i)* Under the transformation $\mathbf{a}_i \to \mathbf{a}_i\tilde{U}$, each $U \in U(2)$, the quantities $Z_\mu$ $(\mu = +1, 0, -1)$ defined by

$$Z_{+1} = (\mathbf{a}^1 \cdot \mathbf{a}^1)/\sqrt{2},\ Z_0 = \mathbf{a}^1 \cdot \mathbf{a}^2,\ Z_{-1} = \mathbf{a}^2 \cdot \mathbf{a}^2/\sqrt{2} \tag{5.4a}$$

undergo the transformation

$$Z_\mu \to \sum_\nu D^1_{\mu\nu}(U)Z_\nu, \quad U \in U(2), \tag{5.4b}$$

where $\mathbf{D}^1(U)$ is obtained explicitly for $U \in U(2)$ from Eq. (3.86) of Ref. 3.

(ii)* Under the transformation $\mathbf{a}^\alpha \to R\mathbf{a}^\alpha$ $(\alpha = 1,2)$, $R \in SO(3)$, the quantities $u_i$ defined by

$$u_1 = a_{23}^{12}, \quad u_2 = a_{31}^{12}, \quad u_3 = a_{12}^{12}, \tag{5.5a}$$

undergo the transformation

$$\mathbf{u} \rightarrow R\mathbf{u}, \quad \mathbf{u} = col(u_1, u_2, u_3). \tag{5.5b}$$

The transformation property (5.4b) of scalar products of two vectors under $U(2)$ transformations is easily verified directly—though infrequently stated. Property (5.5b) is, of course, just the familiar transformation of the vector cross product under proper orthogonal transformations.

It follows from the transformation properties (5.3) and (5.5b) that the following quantity is a *joint invariant* of $U(2)$ and $SO(3)$:

$$(\mathbf{a}^1 \times \mathbf{a}^2) \cdot (\mathbf{a}^1 \times \mathbf{a}^2) = \left(a_{23}^{12}\right)^2 + \left(a_{31}^{12}\right)^2 + \left(a_{12}^{12}\right)^2. \tag{5.6}$$

It is an invariant of index 2 of $U(2)$.

## 5.3. $SO(3)$ and $SU(2)$ Irreducible Polynomial Sets

The strategy for building-up solutions of the $SU(3) \downarrow SO(3)$ problem is first to construct explicit polynomial sets (containing $2L + 1$ independent functions) that transform among themselves according to an irrep $[L]$ of $SO(3)$ under the action of the group of operators $\{\mathcal{L}_R | R \in SO(3)\}$, and then to "lift" these polynomials to the irrep space $[pq0]$ of $SU(3)$ by multiplying by appropriate powers of the $SO(3)$ invariants (5.1). We can, of course, employ this same strategy for the construction of polynomial sets transforming irreducibly according to irrep $[pq]$ of $U(2)$ under the action of the group of operators $\{\mathcal{R}_U | U \in U(2)\}$.

In order to implement this "build-up principle" for constructing a basis of the irrep space for $[pq0]$, it is useful to recall some well-known results on polynomial functions over the $\mathbf{a}^\alpha$ $(\alpha = 1, 2)$ [equivalently, over the $\mathbf{a}_i$ $(i = 1, 2, 3)$] that have definite transformation properties under the actions of either the set of operators $\{\mathcal{L}_R | R \in SO(3)\}$ or $\{\mathcal{R}_U | U \in U(2)\}$, or both (see Section 2.1).

*(1) Solid harmonics in a vector under $SO(3)$ transformations*

The most familiar objects transforming irreducibly under the action of the operator $\mathcal{L}_R$ are the *solid harmonics*, which are defined on the components of an arbitrary vector $\mathbf{u} = (u_1, u_2, u_3)$ by

$$\begin{aligned} \mathcal{Y}_{\ell m}(\mathbf{u}) &= \left[2^\ell \ell!(\ell + m)!(\ell - m)!/(2\ell)!\right]^{1/2} \\ &\times \sum_k \frac{(-u_1 - iu_2)^{k+m}(u_1 - iu_2)^k u_3^{\ell - m - 2k}}{2^{2k+m}(k + m)!k!(\ell - m - 2k)!}, \end{aligned} \tag{5.7}$$

where $\ell = 0,1,2,\ldots$; $m = -\ell,\ -\ell+1,\ldots,\ell$; and the summation is over all integer $k$ for which the factorials are nonnegative. The normalization in definition (5.7) has been chosen such that $\mathcal{Y}_{\ell m}(\mathbf{u})$ is normalized to unity in the inner product (2.15). The explicit transformation under $\mathcal{L}_R$ is given by

$$(\mathcal{L}_R\mathcal{Y}_{\ell m})(\mathbf{u}) \;=\; \mathcal{Y}_{\ell m}(\tilde{R}\mathbf{u}) \;=\; \sum_{m'} \mathcal{D}^{\ell}_{m'm}(R)\mathcal{Y}_{\ell m'}(\mathbf{u}), \tag{5.8}$$

where $\mathcal{D}^{\ell}(R)$ denotes the standard irrep $[\ell]$ of $SO(3)$ (see Ref. 3).

The vector $\mathbf{u}$ in Eq. (5.7) is generic and may be replaced by any other quantity transforming according to $\mathbf{u} \to L_R\mathbf{u} = R\mathbf{u}$ under $R \in SO(3)$. This includes, for example, quantities such as: $\mathbf{u} = \mathbf{a}^1$ or $\mathbf{a}^2$, $\mathbf{v} = \mathbf{a}^1 \times \mathbf{a}^2$, $\mathbf{w} = \mathbf{a}^1 \times (\mathbf{a}^1 \times \mathbf{a}^2)$; where the $a^{\alpha}_i (\alpha = 1,2; i = 1,2,3)$ are boson operators (see Section 2.4). For example, the solid harmonics $\mathcal{Y}_{\ell m}(\mathbf{a}^1)$ undergo exactly the transformation (5.8) under the left action $\mathcal{L}_R$. Indeed, the polynomials $\mathcal{Y}_{\ell m}(\mathbf{a}^1)$ are orthonormal in the boson inner product;[16] that is,

$$\langle 0|\, Y^*_{\ell m}(\mathbf{a}^1)\mathcal{Y}_{\ell' m'}(\mathbf{a}^1)\,|0\rangle \;=\; \delta_{\ell'\ell}\delta_{m'm}. \tag{5.9}$$

The solid harmonics $\mathcal{Y}_{\ell m}(\mathbf{v})$ or $\mathcal{Y}_{\ell m}(\mathbf{w})$ also transform exactly as in Eq. (5.8), even though these polynomials are *not* orthogonal in the boson inner product. The linear independence of these polynomials is, however, unaffected. The transformation property (5.8) for an *arbitrary* vector $\mathbf{u}$ is a consequence of the fact that this relation is algebraic in structure; that is, it depends only on the *algebraic relation* between the polynomials $\{\mathcal{Y}_{\ell m}(\tilde{R}\mathbf{u})|m = -\ell, -\ell+1,\ldots,\ell\}$ and $\{\mathcal{Y}_{\ell m}(\mathbf{u})|m = -\ell, -\ell+1,\ldots,\ell\}$ and *not* on the nature of $\mathbf{u}$ itself, nor on the notion of inner product.

We introduce the special notation $Q_{\ell m}$ for the boson polynomials in $\mathbf{v} = \mathbf{a}^1 \times \mathbf{a}^2$. To emphasize that two vectors $\mathbf{a}^1$ and $\mathbf{a}^2$ enter, we write the argument as the $3 \times 2$ matrix $A = (a^{\alpha}_i) = (\mathbf{a}^1\mathbf{a}^2)$. The $2\ell+1$ polynomials in the set $\{Q_{\ell m}(A)|m = -\ell, -\ell+1,\ldots,\ell\}$ are linearly independent and are homogeneous of degree $2\ell$. They are *not* orthogonal, as noted earlier, with respect to the standard boson inner product. Their transformation properties under the actions $\{\mathcal{L}_R|R \in SO(3)\}$ and $\{\mathcal{R}_U|U \in U(2)\}$ are given by

$$Q_{\ell m}(\tilde{R}A) \;=\; \sum_{m'} \mathcal{D}^{\ell}_{m'm}(R)Q_{\ell m'}(A), \tag{5.10}$$

$$Q_{\ell m}(AU) \;=\; (\det U)^{\ell} Q_{\ell m}(A). \tag{5.11}$$

Thus, the $Q_{\ell m}$ transform irreducibly according to irrep $[\ell]$ of $SO(3)$ under the action of $\mathcal{L}_R$, and are invariants of index $\ell$ under the action of $\mathcal{R}_U$.

*(2) Coupled solid harmonics*

Let $\mathbf{u} = (u_1, u_2, u_3)$ and $\mathbf{v} = (v_1, v_2, v_3)$ denote arbitrary vectors; that is, $\mathbf{u}$ and $\mathbf{v}$ are vectors under orthogonal transformations $R \in SO(3)$. Then the *coupled solid harmonics* defined by

$$\mathcal{Y}_{(\ell_1\ell_2)\ell m}(\mathbf{u},\mathbf{v}) = \sum_{m_1 m_2} C^{\ell_1\ell_2\ell}_{m_1 m_2 m} \mathcal{Y}_{\ell_1 m_1}(\mathbf{u}) \mathcal{Y}_{\ell_2 m_2}(\mathbf{v}), \tag{5.12a}$$

also transform irreducibly (by construction):

$$\mathcal{Y}_{(\ell_1\ell_2)\ell m}(\tilde{R}\mathbf{u}, \tilde{R}\mathbf{v}) = \sum_{m'} \mathcal{D}^{\ell}_{m'm}(R) \mathcal{Y}_{(\ell_1\ell_2)\ell m'}(\mathbf{u},\mathbf{v}). \tag{5.12b}$$

In this result, $C^{\ell_1\ell_2\ell}_{m_1 m_2 m}$ denotes a Wigner-Clebsch- Gordan coefficient in which $(\ell_1, \ell_2, \ell_3)$ and $(m_1, m_2, m)$ satisfy the usual triangle rule and sum rule, respectively, of angular momentum coupling theory.[3]

We introduce the special notation

$$P_{(\ell_1\ell_2)\ell m}(A) = \mathcal{Y}_{(\ell_1\ell_2)\ell m}(\mathbf{a}^1, \mathbf{a}^2) \tag{5.13}$$

for the coupled spherical harmonics in the two vector bosons $\mathbf{a}^1$ and $\mathbf{a}^2$. These polynomials are orthonormal in the labels $(\ell_1\ell_2)\ell m$ using the standard boson inner product. In particular, for $\ell_1$ and $\ell_2$ given nonnegative integers, the $(2\ell_1 + 1)(2\ell_2 + 1)$ polynomials in the set

$$\left\{P_{(\ell_1\ell_2)\ell m}(A) \middle| \ell = |\ell_1 - \ell_2|,\ |\ell_1 - \ell_2| + 1, \ldots, \ell_1 + \ell_2;\ m = -\ell, \ldots, \ell\right\} \tag{5.14}$$

are orthonormal and are homogeneous of degree $\ell_1 + \ell_2$.

Under the action of the operators $\{\mathcal{L}_R | R \in SO(3)\}$, the polynomials in the set (5.14) transform (by construction) irreducibly according to irrep $[\ell]$:

$$P_{(\ell_1\ell_2)\ell m}(\tilde{R}A) = \sum_{m'} \mathcal{D}^{\ell}_{m'm}(R) P_{(\ell_1\ell_2)\ell m'}(A), \tag{5.15}$$

but in general have no simple transformation properties under $\mathcal{R}_U$. There is, however, a notable exception to this general property that occurs for

$$\ell_1 = \tfrac{1}{2}L + K, \quad \ell_2 = \tfrac{1}{2}L - K \tag{5.16a}$$

with

$$K \in \{-\tfrac{1}{2}L,\ -\tfrac{1}{2}L + 1, \ldots, \tfrac{1}{2}L\}. \tag{5.16b}$$

Here $L$ is an arbitrary nonnegative integer, and $\ell_1, \ell_2$ are still integers.

For $L \in \{0,1,2,\ldots\}$ and $M = -L, -L+1, \ldots, L$, it is convenient to define

$$\Psi_{(\frac{1}{2}L,K)(L,M)}(A) = P_{(\frac{1}{2}L+K,\frac{1}{2}L-K)LM}(A). \tag{5.17}$$

Then these boson polynomials have the transformation properties under the groups of operators $\{\mathcal{L}_R | R \in SO(3)\}$ and $\{\mathcal{R}_U | U \in U(2)\}$ given by

$$\mathcal{L}_R : \Psi_{(\frac{1}{2}L,K)(L,M)}(A) \to \Psi_{(\frac{1}{2}L,K)(L,M)}(\tilde{R}A) = \sum_{M'} \mathcal{D}^L_{M'M}(R)\Psi_{(\frac{1}{2}L,K)(L,M')}(A), \tag{5.18a}$$

$$\mathcal{R}_U : \Psi_{(\frac{1}{2}L,K)(L,M)}(A) \to \Psi_{(\frac{1}{2}L,K)(L,M)}(AU) = \sum_{K'} D^{\frac{1}{2}L}_{K'K}(U)\Psi_{(\frac{1}{2}L,K')(L,M)}(A). \tag{5.18b}$$

Here $\{\mathbf{D}^j(U)\}$ denotes the standard irrep $[j]$ of $U(2)$, or of $SU(2)$ under the restriction $U(2) \downarrow SU(2)$. [See Ref. 3 for the relation between irreps of $SU(2)$ and those of $SO(3)$, denoted $\{\mathcal{D}^l(R)\}$.] Relation (5.18a) is just a restatement of the general property (5.15) applied to the case at hand. Property (5.18b) requires proof. Since $\mathcal{L}_R$ and $\mathcal{R}_U$ commute, it is sufficient to prove (5.18b) for $M = L$. In this case, we have

$$\Psi_{(\frac{1}{2}L,K)(L,L)}(A) = \mathcal{Y}_{(\frac{1}{2}L+K,\frac{1}{2}L+K)}(\mathbf{a}^1)\mathcal{Y}_{(\frac{1}{2}L-K,\frac{1}{2}L-K)}(\mathbf{a}^2) = (-1)^L \frac{b_1^{\frac{1}{2}L+K} b_2^{\frac{1}{2}L-K}}{[(\frac{1}{2}L+K)!(\frac{1}{2}L-K)!]^{1/2}}, \tag{5.19a}$$

where

$$b_1 = (a_1^1 + ia_2^1)/\sqrt{2}, \quad b_2 = (a_1^2 + ia_2^2)/\sqrt{2}. \tag{5.19b}$$

Since for $A \to AU$, we have $(b_1 b_2) \to (b_1 b_2)U$, and since the polynomials (5.19a) are in standard spinor form, we must have exactly the required transformation property (5.18b).

The coupled solid harmonics given generally by Eq. (5.13) are orthonormal in the quantum numbers $(\ell_1, \ell_2)\ell m$ in the boson inner product, and in consequence so are the special polynomials (5.17). The construction of the orthonormal polynomial set

$$\left\{ \Psi_{(\frac{1}{2}L,K)(L,M)}(A) \middle| L = 0,1,\ldots; \begin{matrix} K = -\frac{1}{2}L, \ldots, \frac{1}{2}L \\ M = -L, \ldots, L \end{matrix} \right\} \tag{5.20}$$

with the transformation properties (5.18a,b) is a key result for understanding the structure of the noncanonical basis in Section 5.5 below.

*(3) Solid harmonics in* $\mathbf{Z} = (Z_1, Z_2, Z_3)$

The components of the 3-tuple $\mathbf{Z} = (Z_1, Z_2, Z_3)$ are defined in terms of the $Z_\mu$ given by Eq. (5.4a) by

$$Z_1 = -(Z_{+1} - Z_{-1})/\sqrt{2}, \quad Z_2 = i(Z_{+1} + Z_{-1})/\sqrt{2}, \quad Z_3 = Z_0. \tag{5.21a}$$

Under the transformation of the $Z_\mu$ ($\mu = +1, 0, -1$) given by (5.4b), the column vector $\mathbf{Z} = \text{col}\,(Z_1, Z_2, Z_3)$ undergoes the transformation

$$\mathbf{Z} \to \mathbf{Z}' = R(U)\mathbf{Z}, \tag{5.21b}$$

where the transformation

$$R(U) = A_0 D^1(U) A_0^\dagger, \tag{5.21c}$$

effects the change from a complex to a real basis (see Ref. 3, Vol. 8, Eq. (3.30) for the definition of the numerical unitary matrix $A_0 = A^*$).

We define the boson polynomials $T_{\ell m}(A)$ with $A = (\mathbf{a}^1 \mathbf{a}^2)$ by

$$T_{\ell m}(A) = \mathcal{Y}_{\ell m}(\mathbf{Z}), \text{ with } \ell = 0, 1, \ldots; \; m = -\ell, \ldots, \ell, \tag{5.22}$$

where the $Z_i$ are now defined by Eqs. (5.21a) and (5.4a) in terms of bosons. The polynomials in the set

$$\{T_{\ell m}(A) |\, m = -\ell, -\ell + 1, \ldots, \ell\} \tag{5.23}$$

are linearly independent and belong to the homogeneous polynomial space of degree $2\ell$. Their transformation properties under the action $\{\mathcal{L}_R | R \in SO(3)\}$ and $\{\mathcal{R}_U | U \in U(2)\}$ are given by

$$\mathcal{L}_R: \quad T_{\ell m}(A) \to T_{\ell m}(\tilde{R}A) = T_{\ell m}(A), \tag{5.24a}$$

$$\mathcal{R}_U: \quad T_{\ell m}(A) \to T_{\ell m}(AU) = \sum_{m'} D^\ell_{m'm}(U) T_{\ell m'}(A). \tag{5.24b}$$

## 5.4. Nonorthogonal Basis I

Using the constructions of Sections 5.2 and 5.3, we can now build up a variety of bases of the carrier space of all irreps $[L]$ contained as subspaces in the carrier space of irrep $[pq0]$ of $SU(3)$.

Let us define the $3 \times 2$ matrix boson polynomials $P_{LM;\lambda}$ by

$$P_{LM;\lambda}(A) = \mathcal{Y}_{(\lambda,L-\lambda)LM}(\mathbf{a}^1, \mathbf{a}^1 \times \mathbf{a}^2). \tag{5.25}$$

Here we have $\mathbf{u} = \mathbf{a}^1$, $\mathbf{v} = \mathbf{a}^1 \times \mathbf{a}^2$, $\ell_1 = \lambda$, $\ell_2 = L - \lambda$, $\ell = L$, $m = M$ in the general definition (5.12). Accordingly, we have

$$P_{LM;\lambda}(\tilde{R}A) = \sum_{M'} \mathcal{D}^L_{M'M}(R) P_{LM';\lambda}(A) \tag{5.26a}$$

for each

$$\lambda \in \{0, 1, \ldots, L\}. \tag{5.26b}$$

Each polynomial in the set

$$\{P_{LM;\lambda}(A) | M = -L, -L+1, \ldots, L\} \tag{5.27}$$

is homogeneous of degree $2L - \lambda$ and linearly independent, but nonorthogonal in the boson inner product.

There are precisely $L + 1$ sets of polynomials (5.25) corresponding to $\lambda = 0, 1, \ldots, L$, each set transforming as irrep $[L]$ of $SO(3)$ under the action of the group of operators $\{\mathcal{L}_R | R \in SO(3)\}$. These polynomials $P_{LM;\lambda}(A)$ are the basic ingredients for constructing a polynomial basis for the $SU(3)$ irrep $[pq0]$, but, in order to lift these polynomials to the required homogeneous space of degree $p + q$, we must appeal to the Weyl theorems and multiply by the appropriate invariants. There are only two invariants available (i) $(\mathbf{a}^1 \cdot \mathbf{a}^1)$ and (ii) $(\mathbf{a}^1 \times \mathbf{a}^2) \cdot (\mathbf{a}^1 \times \mathbf{a}^2)$, since the third possible invariant: $\mathbf{a}^1 \cdot (\mathbf{a}^1 \times \mathbf{a}^2)$ vanishes identically.

It follows that the polynomials based on (5.25) carrying $SO(3)$ irreps $[L]$ and homogeneous of degree $p$ in $\mathbf{a}^1$ and of degree $q$ in $\mathbf{a}^2$ are necessarily of the form:

$$B_{[pq0];LM;\lambda}(A) = (\mathbf{a}^1 \cdot \mathbf{a}^1)^{\frac{1}{2}(p-q-\lambda)} [(\mathbf{a}^1 \times \mathbf{a}^2) \cdot (\mathbf{a}^1 \times \mathbf{a}^2)]^{\frac{1}{2}(q-L+\lambda)} \times P_{LM;\lambda}(A), \quad p - L \text{ even}. \tag{5.28a}$$

To be well-defined as a polynomial the exponents of the two integrity basis invariants must be *nonnegative integers*; that is, we have the explicit conditions:

(i) $p - q - \lambda$ is a *nonnegative, even integer*,
(ii) $q - L + \lambda$ is a *nonnegative, even integer*, and
(iii) $\lambda \in \{0, 1, \ldots L\}$, from (5.25). (5.28b)

The vectors found so far cannot span the complete carrier space for the irrep $[pq0]$, since (i) and (ii) imply that $p - L$ is a nonnegative even integer, and there are vectors having $p - L$ odd.

It is not difficult to introduce these additional vectors using coupled solid harmonics. They are obtained by replacing $L$ and $\lambda$ in Eq. (5.25) by $L - 1$ and $\lambda - 1$ and then coupling with the solid harmonics $\mathcal{Y}_{1,\mu}(\mathbf{w})$, with $\mathbf{w} = \mathbf{a}^1 \times (\mathbf{a}^1 \times \mathbf{a}^2)$:

$$P'_{LM;\lambda}(A) = \sum_{M'\mu} C \begin{matrix} L-1 & 1 & L \\ M' & \mu & M \end{matrix} P_{L-1,M';\lambda-1}(A)\mathcal{Y}_{1,\mu}(\mathbf{w}). \tag{5.29}$$

These are homogeneous polynomials of degree $L+1$ in $\mathbf{a}^1$ and degree $L+1-\lambda$ in $\mathbf{a}^2$. In this definition of $P'_{LM;\lambda}$, we must have $L \geq 1$ and hence

$$\lambda \in \{1, 2, \ldots, L\}. \tag{5.30}$$

Again, we have the transformation property

$$P'_{LM;\lambda}(\tilde{R}A) = \sum_{M'} \mathcal{D}^L_{M'M}(R) P'_{LM';\lambda}(A). \tag{5.31}$$

Each polynomial in the set

$$\{P'_{LM;\lambda} | M = -L, -L+1, \ldots, L\} \tag{5.32}$$

is homogeneous of degree $2L-\lambda+2$ and linearly independent, but nonorthogonal in the boson inner product.

Just as before we lift these polynomials to the space of $p + q$ degree polynomials by multiplying by the two integrity invariants such that the degree is exactly $p$ in $\mathbf{a}^1$ and $q$ in $\mathbf{a}^2$. We find, necessarily, the following result:

$$\begin{aligned} B'_{[pq0];LM;\lambda}(A) &= (\mathbf{a}^1 \cdot \mathbf{a}^1)^{\frac{1}{2}(p-q-\lambda)}[(\mathbf{a}^1 \times \mathbf{a}^2) \cdot (\mathbf{a}^1 \times \mathbf{a}^2)]^{\frac{1}{2}(q-L+\lambda-1)} \\ &\quad \times P'_{LM;\lambda}(A), \quad \text{for } p - L \text{ odd.} \end{aligned} \tag{5.33a}$$

Again, we must assure that the exponents of the invariants in (5.33) are nonnegative integers; this imposes the conditions:

(i) $p - q - \lambda$ is a *nonnegative, even integer*
(ii) $q - L + \lambda - 1$ is a *nonnegative, even integer*, and
(iii) $\lambda \in \{1, 2, \ldots, L\}$, from (5.30). (5.33b)

To show that the polynomials in the sets (5.28) and (5.33) are, in fact, the Bargmann-Moshinsky basis one need only set $M = L$ in which case the polynomials reduce to the monomial highest weight vectors given in Refs. 43 and 46, after accounting for notational differences.

The natural question at this point is: why does this procedure work? The original construction of this noncanonical basis used rather involved Lie algebraic techniques designed to ensure the $SU(3)$ representation property, but our global construction uses none of this heavy machinery. What is behind it?

The answer lies in the canonical realization (using the matrix boson $A$) of the Gel'fand-Weyl basis vectors of the carrier space of irrep $[pq0]$. This realization uses $(p-q)$ bosons $\mathbf{a}^1$ and $q$ matrix bosons $a_i^1{}_j^2$. Since $(p-q)$ bosons $\mathbf{a}^1$ generate (uniquely) the irrep $[p-q,0,0]$ and since $q$ matrix bosons generate (again uniquely) the irrep $[qq0]$, the vectors in the noncanonical construction above must lie in the space of homogeneous polynomials of degree $p$ in $\mathbf{a}^1$ and $q$ in $\mathbf{a}^2$, carrying the direct product representation $[p-q,0,0] \times [qq0]$. Abstractly, this space has the reduction into irreducible components given by:

$$[p-q00]\times[qq0] \;=\; [pq0]\oplus[p-2,q-1,0]\oplus\ldots\oplus\left\{\begin{array}{l}[p-2q,0,0]\\ [2q-p,2q-p,0].\end{array}\right. \tag{5.34}$$

Except for the first term, all the other terms in Eq. (5.34) involve powers of an invariant [111], accounting for the change in the number of quanta.

Observe now that the only $SU(3)$ invariant available in the construction above is the scalar $\mathbf{a}^1 \cdot [\mathbf{a}^1 \times \mathbf{a}^2]$, which vanishes identically. *It is this constraint that forces the construction to yield the unique irrep* $[pq0]$ *using only degree considerations in the space of coupled harmonics.*

This global realization of a noncanonical nonorthogonal $SU(3)$ basis has the merit of showing in an elementary way just how arbitrary any noncanonical realization actually is. It has the additional merit that the coupled harmonics show that it is this coupling property that accounts for the fact that the multiplicity index $\lambda$ is an angular momentum quantum number and explains moreover why the further conditions of parity on $\lambda$ (even or odd) are imposed.

We remark that the nonorthogonality of the basis vectors described above stems from the quadratic bosons in the vector quantity $\mathbf{a}^1 \times \mathbf{a}^2$.

## 5.5. Nonorthogonal Basis II

There is another construction of a noncanonical solution[45–47] of the $SU(3) \downarrow SO(3)$ problem, this time based on the fact that the $U(2)$ operators $\mathcal{R}_U$ commute with the $SO(3)$ operators $\mathcal{L}_R$. This solution shares many of the

features of the previous construction and, likewise, can be derived using only global considerations and global transformations of well-known polynomials.

In this method, one begins with the boson polynomials $T_{\ell m}(A)$ defined by Eq. (5.22) with $\mathbf{Z}$ given by Eqs. (5.21a) and (5.4a). These polynomials are $SO(3)$ invariants and transform irreducibly as irrep $[\ell]$ of $U(2)$. These polynomials can be coupled with the polynomials $\Psi_{(\frac{1}{2}L,K)(L,M)}(A)$ defined by Eqs. (5.17) and (5.13). These $\Psi$-polynomials transform as irrep $[L]$ of $SO(3)$ and as irrep $[\frac{1}{2}L]$ of $U(2)$. Accordingly, the coupling will leave the $SO(3)$ transformation properties intact, but yield polynomials transforming under $U(2)$ according to the coupled irrep, call it $[j]$, of $U(2)$: we thus define the $3 \times 2$ matrix boson polynomials $Q$ by

$$Q_{(\frac{1}{2}L,\ell)jm;LM}(A) = \sum_{Km'} C^{\frac{1}{2}L\,\ell\,j}_{K,m',m}\, \Psi_{(\frac{1}{2}L,K)(L,M)}(A)\, T_{\ell m'}(A). \tag{5.35}$$

Since the $T_{\ell m'}(A)$ are $SO(3)$ invariants, these polynomials still have exactly the transformation property (5.18a) under the action of $\mathcal{L}_R$; that is,

$$\mathcal{L}_R : Q_{(\frac{1}{2}L,\ell)jm;LM}(A) \to Q_{(\frac{1}{2}L,\ell)jm;LM}(\tilde{R}A) = \sum_{M'} \mathcal{D}^L_{M'M}(R) Q_{(\frac{1}{2}L,\ell)jm;LM'}(A), \tag{5.36}$$

but now have the following transformation property under $\mathcal{R}_U$, each $U \in U(2)$:

$$\mathcal{R}_U : \quad Q_{(\frac{1}{2}L,\ell)jm;LM}(A) \to Q_{(\frac{1}{2}L,\ell)jm;LM}(AU) = \sum_{m'} D^j_{m'm}(U)\, Q_{(\frac{1}{2}L,\ell)jm';LM}(A). \tag{5.37}$$

Now we impose a requirement whose meaning will be discussed below. We require that the polynomials for the $SU(3) \downarrow SO(3)$ problem must transform under $\mathcal{R}_U$ according to irrep $[pq]$ of $U(2)$, so that we must choose

$$j = (p-q)/2 \tag{5.38}$$

in Eq. (5.37). Accordingly, for prescribed $[pq]$ and $L \in \{0, 1, \ldots\}$, the values of $\ell$ are restricted to those consistent with the triangle conditions; that is, $\ell$ must satisfy

$$\text{(i)} \qquad \ell \in \{|\tfrac{1}{2}L - j|, \ldots, \tfrac{1}{2}L + j\} \tag{5.39}$$

with the additional condition that $\frac{1}{2}L$ and $j$ must both be half-integral or both integral so that $\ell$ is integral.

For prescribed $\ell$, with $L \in \{0,1,\ldots\}$, the $Q$-polynomials defined by (5.35) are homogeneous of degree $L+2\ell$, this result being true independently of $j$. These polynomials are now lifted to the space of homogeneous polynomials of degree $p+q$ by multiplication with the unique joint $SO(3) : U(2)$ invariant defined in Eq. (5.6). We thus obtain a new basis of the carrier space of irrep $[pq0]$ of $SU(3)$:

$$Q_{[pq0];jm;LM;\ell}(A) = \left[\sqrt{(\mathbf{a}^1 \times \mathbf{a}^2)\cdot(\mathbf{a}^1 \times \mathbf{a}^2)}\right]^{\frac{1}{2}(p+q-L)-\ell} Q_{(\frac{1}{2}L,\ell)jm;LM}(A) \tag{5.40}$$

in which $j = (p-q)/2$. The exponent of the invariant in (5.40) is uniquely determined by the requirement that these polynomials be homogeneous of degree $p+q$. The conditions that $\ell$ be integral in the triangle conditions (5.39), and that the invariant in definition (5.40) be polynomial are that

$$\begin{aligned} &\text{(ii)} \quad p+q-L, \quad \text{and} \\ &\text{(iii)} \quad \tfrac{1}{2}(p+q-L)-\ell \text{ are both } \textit{nonnegative even integers.} \end{aligned} \tag{5.41}$$

The transformation property of the polynomials (5.40) under the action of the operators $\{\mathcal{R}_U | U \in U(2)\}$ is given by

$$\begin{aligned} \mathcal{R}_U : \; & Q_{[pq0];jm;LM;\ell}(A) \rightarrow Q_{[pq0];jm;LM;\ell}(AU) \\ & = (\det U)^{\frac{1}{2}(p+q-L)-\ell} \sum_{m'} D^j_{m'm}(U)\, Q_{[pq0];jm';LM;\ell}(A). \end{aligned} \tag{5.42}$$

Of course, the transformation property (5.36) still holds true for these polynomials under the action of $\mathcal{L}_R$.

The constraints imposed on the index $\ell$ by conditions (i) and (iii) above admit exactly $M_L(p,q)$ values of this index. Since the corresponding polynomials are clearly linearly independent (though nonorthogonal in the boson inner product), the polynomials $Q_{[pq0];jm;LM;\ell}$ are a noncanonical resolution of the multiplicity problem $SU(3) \downarrow SO(3)$ for the case $p+q-L$ *an even integer.* If we set $m = j$ and $M = L$, these polynomials reduce to the simultaneous highest weight polynomials given in Ref. 46.

*For $p+q-L$ an odd positive integer*, the polynomials given above must be modified slightly, along lines similar to the case $p-L$ an odd integer in the previous construction. Thus, we go back to the $\Psi$-polynomials defined by (5.17) and couple in the special solid harmonic $\mathcal{Y}_{1,\mu}(\mathbf{v})$, $\mathbf{v} = \mathbf{a}^1 \times \mathbf{a}^2$, after shifting $L$ down to $L-1$ in the $\Psi$-polynomials:

$$\Psi'_{(\frac{1}{2}(L-1),K)(L,M)}(A) = \sum_{M'\mu} C^{L-1\;1\;L}_{M'\mu M}\, \Psi_{(\frac{1}{2}(L-1),K)(L-1,M')}(A)\, \mathcal{Y}_{1,\mu}(\mathbf{v}), \tag{5.43}$$

where we now require $L \geq 1$. These polynomials have transformation properties exactly as given by (5.18) upon replacing $\frac{1}{2}L$ by $\frac{1}{2}(L-1)$ in the pair $(\frac{1}{2}L, K)$ only, adjoining a prime to $\Psi$, and replacing $\mathbf{D}^{\frac{1}{2}L}(U)$ in (5.18b) by $(\det U)\,\mathbf{D}^{\frac{1}{2}(L-1)}(U)$. (The extra factor $(\det U)$ comes from $\mathbf{v} \to (\det U)\mathbf{v}$ in $\mathcal{Y}_{1,\mu}(\mathbf{v})$ under $U(2)$ transformations.) We remark that the presence of $\mathcal{Y}_{1,\mu}(\mathbf{v})$ in these $\Psi'$-polynomials spoils their general orthogonality.

We now proceed just as before in going from (5.36) to the final result (5.40). Thus, we obtain the polynomial bases for $p+q-L$ *odd* to be

$$Q'_{[pq0];jm;LM;\ell}(A) = \left[\sqrt{(\mathbf{a}^1 \times \mathbf{a}^2)\cdot(\mathbf{a}^1 \times \mathbf{a}^2)}\right]^{\frac{1}{2}(p+q-L-1)-\ell} \times Q'_{(\frac{1}{2}(L-1),\ell)jm;LM}(A), \tag{5.44a}$$

where $Q'$ on the right is defined by the coupling analogous to Eq. (5.35):

$$Q'_{(\frac{1}{2}(L-1),\ell)jm;LM}(A) = \sum_{K\mu} C^{\frac{1}{2}(L-1)\,\ell\,j}_{K,m',m}\, \Psi'_{(\frac{1}{2}(L-1),K)(L,M)}(A)\, T_{\ell m'}(A). \tag{5.44b}$$

Once again, we have $j = (p-q)/2$, and the conditions that must be satisfied by the index $\ell$ are

$$\begin{aligned} &\text{(i)} \quad \ell \in \left\{\left|\frac{1}{2}(L-1)-j\right|, \ldots, \frac{1}{2}(L-1)+j\right\}, \\ &\text{(ii)} \quad p+q-L-1, \quad \text{and} \\ &\text{(iii)} \quad \frac{1}{2}(p+q-L-1)-\ell \quad \text{are both } \textit{nonnegative even integers.} \end{aligned} \tag{5.44c}$$

The polynomials $Q'$ defined by the above equations transform as irrep $\mathcal{D}^L(R)$ of $SO(3)$ in the $(LM)$ labels under the action of $\mathcal{L}_R$. Similarly, they transform as irrep $(\det U)^{\frac{1}{2}(p+q-L+1)-\ell}\mathbf{D}^j(U)$ of $U(2)$ in the $(jm)$ labels under the action of $\mathcal{R}_U$. Since the number of values of $\ell$ that satisfy conditions (i), (ii) and (iii) is equal to the multiplicity number $M_L(p,q)$ for $p+q-L$ odd, and since the corresponding $Q'$-polynomials are linearly independent, we thus obtain the full solution of the $SU(3) \downarrow SO(3)$ problem for $p+q-L$ even as well as odd. If we set $m=j$ and $M=L$, the $Q'$ polynomials reduce to the simultaneous highest weight polynomials given in Ref. 46.

The question as to why this construction, based as it is on global considerations such as polynomial degree, should work is easier to answer now than for the previous noncanonical construction, since this time the basic results discussed in Section 2.5 is involved. The construction of the noncanonical $Q$-polynomials is based on the $3 \times 2$ matrix boson $A = (a^\alpha_i)$, $\alpha = 1,2$ and

$i = 1, 2, 3$, whose components enter homogeneously. According to the results in Section 2.5, the homogeneous polynomials of degree $p + q$ in the matrix boson $A$ split into a direct sum of $SU(3) \times U(2)$ irreps whose vectors have the double Gel'fand-Weyl pattern: $\begin{pmatrix} & & \bullet & & \\ & p+q-k & & k & \\ p+q-k & & k & & 0 \\ & \bullet & & \bullet & \\ & & \bullet & & \end{pmatrix}$, for $k = 0, 1, \ldots, \left[\frac{p+q}{2}\right]$.

Accordingly, we see that *the requirement that the $U(2)$ irreps have $j = \frac{p-q}{2}$ is precisely the requirement that selects the $SU(3)$ irrep* $[pq0]$. Since the matrix boson realization of $SU(3) \times U(2)$ is adapted to the flag manifold of the canonical chain $SU(3) \supset SU(2) \times U(1)$, and not to the $SU(3) \supset SO(3)$ chain, Lie algebraic methods to construct these noncanonical $Q$-polynomials prove much more cumbersome than the direct global approach given above. The global approach shows quite clearly the *ad hoc* nature of the construction, which, in contrast to a canonical approach, arbitrarily identifies vectors in the manifold for which any linear combination (with the same $L$-values) would serve as well.

**Acknowledgments**: Work performed under the auspices of the U.S. Department of Energy. One of the authors (JDL) expresses his thanks to H. W. Galbraith for the benefit of numerous discussions on the topics of this paper. We also thank the referee for a careful reading of the manuscript and suggestions for improvements.

## References

1. F. A. Matsen and R. Paunz, *The Unitary Group in Quantum Chemistry, Studies in Physical and Theoretical Chemistry*, Elsevier, New York, 1987.

2. A. P. Jucys, I. B. Levinson, and V. V. Vanagas, *The Theory of Angular Momentum, (Mathematischeskii apparat teorii momenta kolichestva dvizheniya)*, Vilnius, USSR, 1960. Translated from the Russian by A. Sen and A. R. Sen, Jerusalem, Israel (1962).

3. L. C. Biedenharn and J. D. Louck, *Angular Momentum in Quantum Physics, Encyclopedia of Mathematics and Its Applications*, Vol. 8; *The Racah-Wigner Algebra in Quantum Theory*, Vol. 9, edited by G.-C. Rota, Addison-Wesley, Reading, MA, 1981. (Reissued: Cambridge University Press, London and New York, 1985).

4. F. Iachello, "Algebraic methods for molecular rotation-vibration spectra," *Chem. Phy. Letters* **78** (1981), 581-585.

5. J. Hinze, ed., *The Unitary Group for the Evaluation of Electronic Energy Matrix Elements*, Lecture Notes in Chemistry, Vol. 22, Springer-Verlag, Berlin, 1981.

6. F. Iachello and R. D. Levine, "Algebraic approach to molecular rotation-vibration spectra. I. Diatomic molecules," *J. Chem. Phys.* **77** (1982), 3046-3055.

7. R. D. Levine, "*Lie Algebraic Approach to Molecular Structure and Dynamics*," in Mathematical Frontiers in Computational Chemical Physics (D. G. Truhlar, ed.), The IMA Volumes in Mathematics and Its Applications, Vol. 15, Springer-Verlag, Berlin, 1988, 245-261; J. Paldus, "*Lie Algebraic Approach to the Many-Electron Correlation Problem*, *ibid*, 262-299; I. Shavitt, "*Unitary Group Approach to Configuration Interaction Calculations of the Electronic Structure of Atoms and Molecules*," *ibid*, 300-349.

8. R. D. Kent and M. Schlesinger, "Graphical approach to the U(n) Racah-Wigner theory of angular momentum," *Phys. Rev. A* **40** (1989), 536-544.

9. X. Li and J. Paldus, "Tensor operator algebra for many-electron systems. I. Clebsch-Gordon and Racah coefficients," *J. Math. Chem.* **4** (1990), 295-353.

10. M. D. Gould and J. Paldus, "Spin-dependent unitary group approach I. General formalism," *J. Chem. Phys.* **92** (1990), 7394-7401.

11. G.-C. Rota, *Finite Operator Calculus*, Academic Press, New York, 1975.

12. J. Desarmenien, J. P. S. Kung, and G.-C. Rota, "Invariant theory, Young bitableaux, and combinatorics," *Advan. in Math.* **27** (1978), 63-92.

13. H. Casimir and B. L. van der Waerdan, "Algebraischer Beweis der vollständigen Reduzibilität der Darstellungen halbeinfacher Lieschen Gruppen," *Math. Ann.* **111** (1935), 1-12.

14. I. M. Gel'fand, "The center of an infinitesimal group ring," *Math. Sb.* **26** (1950), 103-112 (in Russian).

15. J. D. Louck, "Group theory of harmonic oscillators in $n$-dimensional space," *J. Math. Phys.* **6** (1965), 1786-1804.

16. J. D. Louck and H. W. Galbraith, "Application of orthogonal and unitary group methods to the $n$-body problem," *Rev. Mod. Phys.* **44** (1972), 540-601.

17. V. Bargmann, "On a Hilbert space of analytic functions and an associated integral transform," *Commun. Pure Appl. Math.* **14** (1961), 187-214.

18. L. C. Biedenharn, A. Giovannini, and J. D. Louck, "Canonical definition of Wigner operators in $U_n$," *J. Math. Phys.* **8** (1967), 691-700.

19. I. M. Gel'fand and M. L. Zetlin, "Finite Representations of the group of unimodular matrices," *Doklady Akad. Nauk* **71** (1980), 825-28. (Appears in translation in: I. M. Gel'fand, R. A. Minlos, and Z. Ya. Shapiro, *Representations of the Rotation and Lorentz Groups and Their Applications*, Pergamon, New York, 1963. Translated from the Russian by G. Cummins and T. Boddington); I. M. Gel'fand and M. I. Graev, "Finite-dimensional irreducible representations of the unitary and full linear groups, and related special functions," *Izv. Akad. Nauk SSSR Ser. Mat.* **29** (1965), 1329-1356 *[Am. Math. Soc. Transl.* **64** (1967), Ser. 2, 116-146].

20. G. E. Baird and L. C. Biedenharn, "On the representations of semisimple Lie groups," *J. Math. Phys.* **4** (1963), 1449-1466.

21. M. Ciftan and L. C. Biedenharn, "Combinatorial structure of state vectors in $U_n$. I. Hook patterns for maximal and semimaximal states in $U_n$," *J. Math. Phys.* **10** (1969), 221-232.

22. A. C. T. Wu, "Structure of the combinatorial generalization of hypergeometric functions for $SU(n)$ states," *J. Math. Phys.* **12** (1971), 437-440.

23. J. D. Louck and L. C. Biedenharn, "The structure of the canonical tensor operators in the unitary groups. III. Further developments of the boson polynomials and their implications," *J. Math. Phys.* **14** (1973), 1336-1357.

24. J. P. S. Kung, and G.-C. Rota, "The invariant theory of binary forms," *Bull. Am. Math. Soc.* **10** (1984), 27-85.

25. J. D. Louck and L. C. Biedenharn, "Some properties of the intertwining number of the general linear group," *Science and Computers, Adv. Math. Suppl. Studies* **10**, Academic Press, New York, 1986, 265-311.

26. J. D. Louck, "Recent progress toward a theory of tensor operators in the unitary groups," *Amer. J. Phys.* **26** (1970), 3-42.

27. J. D. Louck and L. C. Biedenharn, "Canonical unit adjoint tensor operators in $U(n)$," *J. Math. Phys.* **11** (1970) 2368-2414.

28. W. J. Holman and L. C. Biedenharn, "The representations and tensor operators of the unitary groups $U(n)$," *Group Theory and Its Applications* (E. M. Loebl., ed.), Vol. II, Academic Press, New York, 1971, 1-73.

29. E. P. Wigner, *Group Theory and Its Application to the Quantum Mechanics of Atomic Spectra*, Academic Press, New York, 1959. Translation by J. J. Griffin of the 1931 German edition.

30. G. E. Baird and L. C. Biedenharn, "A canonical classification for tensor operators in $SU_3$," *J. Math. Phys.* **5** (1965) 1730-1747.

31. L. C. Biedenharn, J. D. Louck, and E. Chacon, and M. Ciftan, "On the structure of the canonical tensor operators in the unitary groups. I. An extension of the pattern calculus rules and the canonical splitting in $U(3)$," *J. Math. Phys.* **13**, (1972), 1957-1984.

32. L. C. Biedenharn and J. D. Louck, "On the structure of the canonical tensor operators in the unitary groups. II. The tensor operators in $U(3)$ characterized by maximal null space," *J. Math. Phys.* **13** (1972), 1985-2001.

33. J. D. Louck, M. A. Lohe, and L. C. Biedenharn, "Structure of the canonical $U(3)$ Racah functions and the $U(3) : U(2)$ projective functions," *J. Math. Phys.* **16** (1975), 2408-2426.

34. M. A. Lohe, L. C. Biedenharn, and J. D. Louck, "Structural properties of the self-conjugate $SU(3)$ tensor operators," *J. Math. Phys.* **18** (1977), 1883-1891.

35. L. C. Biedenharn, M. A. Lohe, and J. D. Louck, "On the denominator function for canonical $SU(3)$ tensor operators," *J. Math. Phys.* **26** (1985), 1458-1492.

36. L. C. Biedenharn, M. A. Lohe, and J. D. Louck, "On the denominator function for canonical $SU(3)$ tensor operators. II. Explicit polynomial form," *J. Math. Phys.* **29** (1988), 1106-1117.

37. K. Baclawski, "A new rule for computing Cleʋsch-Gordan series," *Adv. Appl. Math.* **5** (1984), 418-432.

38. H. W. Galbraith and J. D. Louck, "Canonical solution of the $SU(3) \downarrow SO(3)$ reduction problem from the $SU(3)$ pattern calculus," (to appear in *Acta Applicandoe Mathematicae*, 1991).

39. L. C. Biedenharn, A. M. Bincer, M. A. Lohe, and J. D. Louck," New relations and identities for generalized hypergeometric coefficients," (to appear in *Adv. Appl. Math.)*

40. L. C. Biedenharn and J. D. Louck, "A pattern calculus for tensor operators in the unitary groups," *Commun. Math. Phys.* **8** (1968), 80-131.

41. L. C. Biedenharn, "Are the rotational bands assigned correctly in the nuclear $SU_3$ model?," *Phys. Lett.* **28** (1969), 537-538.

42. H. Weyl, *The Classical Groups. Their Invariants and Representations*, Princeton Univ. Press., Princeton, NJ, 1946.

43. V. Bargmann and M. Moshinsky, "Group theory of harmonic oscillators (I). The collective modes," *Nucl. Phys.* **18** (1960), 697-712; "(II). The integrals of motion for the quadrupole-quadrupole interaction," *ibid.* **23** (1961), 177-199.

44. G. Racah, "Lectures on Lie Groups," *Group Theoretical Concepts and Methods in Elementary Particle Physics* (F. Gürsey, ed.), Gordon and Breach, New York, 1962, 1-36.

45. J. Deenen and C. Quesne, "Canonical solution of the state labelling problem for $SU(n) \supset SO(n)$ and Littlewood's branching rule: I. General formulation," *J. Phys. A: Math. Gen.* **16** (1983), 2095-2104.

46. C. Quesne, "Canonical solution of the state labelling problem for $SU(n) \supset SO(n)$ and Littlewood's branching rule: II. Use of modification rules," *J. Phys. A: Math. Gen.* **17** (1984), 777-789; "III. $SU(3) \supset SO(3)$ case," *ibid.* **17** (1984), 791-799.

47. R. Le Blanc and D. J. Rowe, "Canonical orthonormal basis for $SU(3) \supset SO(3)$. I. Construction of the basis," *J. Phys. A: Math. Gen.* **18** (1985), 1891-1904; "II. Reduced matrix elements of the $SU(3)$ generators," *ibid.* (1985), 1905-1914; "III. Complete set of $SU(3)$ tensor operators," *ibid.* **19** (1986), 1093-1110.

48. M. Moshinsky, J. Patera, R. T. Sharp, and P. Winternitz, "Everything you always wanted to know about $SU(3) \supset O(3)$," *Ann. Phys.* **95** (1975), 139-169.

# ANALYTICAL ENERGY GRADIENTS IN MØLLER-PLESSET PERTURBATION AND QUADRATIC CONFIGURATION INTERACTION METHODS:

# THEORY AND APPLICATION

*Jürgen Gauss*[‡] *and Dieter Cremer*

Theoretical Chemistry,
University of Göteborg, Kemigården 3,
S-41296 Göteborg, Sweden

1. Introduction

2. Comparison of Møller-Plesset and Quadratic Configuration Interaction Electron Correlation Theories

2.1 Møller-Plesset (MP) Perturbation Theory

2.2 Quadratic Configuration Interaction (QCI) Theory

2.3 The Relationship between QCISD and MP Perturbation Theory

3. Energy Gradients

3.1 Derivatives of Two-Electron Integrals and Orbital Energies

3.2 Gradients in MP Perturbation Theory

[‡] *present address: Lehrstuhl für Theoretische Chemie, Institut für Physikalische Chemie und Elektrochemie der Universität Karlsruhe, D-7500 Karlsruhe, Federal Republic of Germany*

ADVANCES IN QUANTUM CHEMISTRY
VOLUME 23



Copyright © 1992 By Academic Press, Inc.
All rights of reproduction in any form reserved.

3.3 Gradients in QCI Theory
3.4 The Relationship between MP and QCI Energy Gradients
3.5 General Theory of MPn and QCI Gradients

4. Implementation of Analytical MPn and QCI Gradients
4.1 The Program System COLOGNE
4.2 MPn Calculations
4.3 QCI Calculations
4.4 MPn Gradient Calculations
4.5 QCI Gradient Calculations

5. Calculation of Molecular Properties at MPn and QCI Using Analytical Gradients
5.1 Response Densities and other One-Electron Properties
5.2 Equilibrium Geometries
5.3 Vibrational Spectra

6. Concluding Remarks

Appendix 1
Appendix 2
References

## 1. Introduction

During the last decades, quantum chemistry has become a rapidly expanding field of active research with many applications to pending chemical problems [1]. The breath-taking progress in quantum chemistry is strongly coupled to the successful construction of high speed computers, and, in particular, to the recent development of vector and parallel processors [2]. Their enormous computational capacity provides the basis to routinely apply quantum chemical methods to interesting chemical problems [3] thus revealing more and more the importance and relevance of quantum chemistry to all fields of chemistry. Of course, all the accomplishments in computer technology could only have such a large impact on quantum chemistry, because

quantum chemical methods have been improved at the same rapid pace leading to more efficient and more accurate algorithms almost on a daily basis. Thus, progress in computer technology and improvement of quantum chemical methods have gone hand in hand pushing quantum chemical research projects forward. High speed computers have provided for the first time the possibility of going right away from the pencil-and-paper work of method development to the reality of computational work.

One field of quantum chemistry, which has strongly contributed to the current popularity and efficiency of quantum chemical calculations, is the field of analytical energy derivative methods [4,5]. The importance of these methods results from the fact that many characteristic features of molecules depend on the variation of the energy with respect to nuclear coordinates or some external perturbation parameter such as a static electric or magnetic field. When specifying the dependence of the energy on these parameters the corresponding derivatives of the energy play a key role. For example, derivatives of the energy with respect to nuclear coordinates are used to explore the potential energy surface of a molecule and to search for equilibrium geometries and transition states along reaction paths [6]. Both equilibrium geometries and transition states represent stationary points on the potential energy surface for which the forces on the nuclei, i.e. the first derivatives of the energy with respect to the nuclear coordinates, vanish. Stationary points on an energy surface can be further characterized by the Hesse matrix which comprises the second derivatives of the energy with respect to nuclear coordinates [6]. Second and higher derivatives are also used to calculate harmonic and anharmonic frequencies [7,8].

Variation of the energy with respect to an external electric or magnetic field provides the possibility of calculating molecular properties such as dipole moment, quadrupole moment, octupole moment, polarizabilities, magnetic moments, etc. [9]. Differentiating dipole moment and polarizability with respect to nuclear coordinates leads to IR and Raman intensities [10,11] which have turned out to be very useful when assigning vibrational modes to observed IR and Raman bands. Such an assignment just on the basis of vibrational frequencies is in most cases very difficult or even impossible and, therefore, additional information such as calculated intensities is needed [7].

In principle, it is possible to calculate all properties just mentioned with the aid of finite differentiation procedures. However, there are two arguments that suggest the use of analytical derivatives rather than finite differentiation methods [12,13]. First, the accuracy of the finite differentiation scheme is not very high and calculating higher derivatives in this way can be very troublesome. Analytical methods avoid these difficulties and provide sufficient

accuracy for all derivatives. Secondly, if the number of perturbation parameters increases (in a polyatomic molecule with K atoms there are 3K forces), the numerical procedures will become very expensive. The computational costs of numerical methods directly scale with the number of perturbations, while the costs of analytical derivative methods are more or less independent of the number of perturbation parameters [5,14]. Therefore, use of analytical methods is advantageous, especially when investigating larger molecules. Compared to numerical differentiation procedures, time savings by analytical methods are considerable.

The impact of analytical derivative methods in quantum chemistry is clearly demonstrated by the fact that nowadays most quantum chemical studies include (at least at all lower levels of theory) optimization of geometries by utilizing analytically evaluated forces.

Historically, Pulay [12,14] was the first who implemented an analytical derivative scheme for a quantum chemical ab initio method. As early as 1969, he presented analytical gradients for the Hartree-Fock (HF) energy and used them to calculate equilibrium geometries, and, by numerical differentiation of the analytically evaluated gradients, force constants [14,15]. However, it should be mentioned that during this time one of the major problems of analytical derivative methods was the evaluation of the derivatives of the one-electron and two-electron integrals over AO basis functions. A major step in direction of a more efficient implementation of analytical derivatives was done when new techniques for the evaluation of electron integrals were introduced into quantum chemistry. In this context, the gaussian quadrature based on the use of Rys polynominals [16] has to be mentioned. This new technique for evaluating electron integrals was especially designed to calculate integrals over higher order Cartesian gaussian functions and this feature could be used with great advantage when computing integral derivatives [17].

In 1979, Pople and co-workers [18] implemented analytical second derivatives for HF energies thus significantly reducing the computational costs for the calculation of HF force constants. The key to their successful implementation of analytical second derivatives was the development of an efficient scheme to solve the Coupled-perturbed HF (CPHF) equations [19-21] in order to get perturbed orbitals. These are not needed for HF energy gradients but they become necessary for HF second derivatives. Pople and co-workers also presented for the first time analytical first derivatives for a correlation method, namely for second order Møller-Plesset (MP2) perturbation theory. Again, the solution of the CPHF equations was an important prerequisite for the calculation of analytical derivatives. This is due to the fact that all correlation methods, which do not optimize orbitals, require the derivatives

of the MO coefficients (given in form of perturbed orbitals) or at least some equivalent information in form of the so-called z-vector [22].

In the following, analytical first derivatives of the energy were coded for CI methods with single (S) and double (D) excitations (CISD) with respect to a HF reference function [23,24] and for the MCSCF ansatz [25,26]. Also, analytical methods for higher derivatives, which are of special interest for the calculation of vibrational spectra, were developed. For example, analytical HF third derivatives [27], analytical MCSCF- [28,29] and CI second derivatives [30] as well as analytical dipole [31] and polarizability derivatives [32,33] were coded and successfully applied in a large number of calculations.

After these developments had taken place, it was clear that the main thrust of any further developments in analytical gradient techniques would concentrate on more sophisticated electron correlation methods. Especially attractive were three groups of single determinant based correlation methods, namely the many-body perturbation techniques in the form introduced by Møller and Plesset (MP) [34], the CI methods [35] and, finally, the coupled cluster (CC) methods [36,37]. MPn methods with n = 3 and 4 were implemented by the Pople and co-workers in the late seventies [38-40] and after generally usable MP3 and MP4 programs had been released by Pople group in the early eighties [41], perturbation methods became soon very popular. The main advantage of the MP methods in particular and many-body perturbation theory in general results from the fact that these methods are size-consistent [38] (or size-extensive [37]) thus allowing a consistent description of molecules independent of size and number of electrons. Contrary to perturbation methods, CI methods truncated to single and double excitations are not size-consistent and, therefore, a CI description of chemical reaction systems has to be corrected in most cases by some empirical correction terms [42].

Apart from being size-consistent, MP methods are attractive since they can be used to investigate electron correlation in a systematic way. MP2 is certainly the simplest method of treating dynamical correlation. Of course, MP2 often exaggerates effects of D excitations, i.e. electron pair correlation, but this is largely corrected at third order MP (MP3) perturbation theory, which introduces coupling between D excitations. Fourth order MP (MP4) perturbation theory provides a simple way of including effects of higher order excitations, namely (beside those of S and D excitations) those of triple (T), and quadruple (Q) excitations [40]. T excitations can be handled at the MP4 level in a routine way even when calculating larger molecules [43]. This, however, is very difficult at the CI level [44].

Since many-body perturbation theory is not a variational theory, it does

not lead to an upper bound for the energy and this may be considered as a disadvantage of MP methods. However, in practise it turns out that lack of the variational property does not lead to serious problems. A much more severe restriction of MP methods is the fact that they are based on the single determinant ansatz of HF theory. In this context, new developments such as spin projected MP [45,46], MP with GVB [47] or CASSCF reference function [48] have to be mentioned since they may be considered as promising generalizations of the MP approach.

The CC approach [37] is related to MP perturbation theory but, although a non-variational method, it is iterative and, therefore, more expensive to carry out. Within CC theory, the wave function is written in exponential form, namely as exp(T) acting on a reference wave function where T is the excitation operator covering all possible excitations of a given type. Restricting excitations to, e.g., S and D and projecting the Schrödinger equation on all S- and D-excited forms of the reference wave function leads to a closed set of equations which can be solved iteratively [49-51]. The CC approach is size-consistent and is invariant with regard to unitary transformations among occupied (virtual) orbitals [37]. Furthermore, it seems to be applicable on a larger scale than MP theory. At least in some cases, CC methods turned out to provide reasonable descriptions of molecular systems that actually require a multi-determinant approach.

Recently, Pople, Head-Gordon, and Raghavachari [52] introduced a modified method for calculating correlation energies starting from a HF wave function. Their method corrects CI for its size-consistency error by adding to the CI equations new terms, which are quadratic in the CI coefficients. Therefore, the method was coined, perhaps unfortunately [54], quadratic CI (QCI). Alternatively, the QCI method may be considered as an approximate CC method [52-54], but since the general strategy of QCI differs from that of CC, QCI results are not necessarily inferior to those obtained with the CC methods. Both CC and QCI are correct to the same order of perturbation theory if the same excitations are considered. Thus, QCISD, i.e. QCI with S and D excitations, is correct in the SDQ space of MP4 and QCISD(T), which also considers triple excitations in an approximated way, is fully correct in fourth order perturbation theory. The more recent QCISD(TQ) method is even fully correct in fifth order perturbation theory [55]. Work carried out with the QCI methods clearly shows that these methods will establish themselves beside MP and CC methods as promising ways of getting electron correlation corrections.

During the eighties, work on analytical energy derivatives was aimed at getting appropriate formulas and efficient computer programs for MP,

CC, and QCI methods. In 1983, Jørgensen and Simons worked out the formulas for the analytical MP3 and CCD energy gradient [56]. A first attempt to implement analytical MP3 gradients was made in 1985 by Bartlett and co-workers [57]. The computer program these authors developed was not very efficient and, certainly, was not intended for routine applications. The main drawback of their program was that it required a full transformation of the two-electron integral derivatives from AO to MO basis which is a very expensive and unnecessary step [58,59]. An implementation of analytical MP3 energy gradients for routine calculations was presented by Gauss and Cremer in 1987 [58], followed shortly afterwards by a similar implementation by Bartlett's group [60]. Later, Alberts and Handy extended analytical MP3 gradient methods to unrestricted HF (UHF) reference wave functions [61].

In 1986, Fitzgerald, Harrison, and Bartlett formulated the theory for analytical MP4 energy gradients [62]. The first computer implementation of the analytical MP4 gradient restricted to S, D, and Q excitations was published by Gauss and Cremer in 1987 [58]. Full MP4 gradient calculations including T excitations were reported by Gauss and Cremer [63] and, independently, by Bartlett and co-workers [64,65] in 1988.

In the early eighties, analytical gradients for CC methods seemed to be more complicated than either MP or CI gradients. Due to the nonvariational character of the CC method the derivatives of the excitation amplitudes seemed to be needed for the CC energy gradient. In 1985, Bartlett and co-workers succeeded in solving the Coupled-perturbed CC (CPCC) equations for CCD to determine the derivatives of the D excitation amplitudes [66]. This, however, was not the final solution of the CC gradient problem. In 1984, Handy and Schaefer showed that in all gradient expressions perturbation dependent quantities which have to be determined by some additional set of equations, e.g. by the CPHF or CPCC equations, can be replaced by a vector z [22]. The z-vector is the solution of only one set of equations that does not depend on the perturbation. Adamowicz, Laidig, and Bartlett [67] applied the z-vector method to derive expressions for the analytical CCSD energy gradient. In 1987, Schaefer and co-workers presented the first computer implementation of analytical CCSD gradients based on these ideas [68]. Later, Scuseria and Schaefer extended this work by including T excitations via the CCSDT-1 ansatz [69,70]. However, most of these developments were restricted so far to RHF reference functions. A generalization to UHF and ROHF reference functions as well as some special classes of non-HF reference functions in the case of the CCSD method was recently carried out by Gauss, Stanton, and Bartlett [71].

In 1988, the theory of analytical QCISD energy gradients as well as the

first computer implementation for routine calculations was reported by Gauss and Cremer [72]. In this work, the z-vector method was used to determine the derivatives of the QCI amplitudes. Recently, Gauss and Cremer were also able to derive the analytical energy gradient for QCISD(T) [73] utilizing techniques which had previously been developed to handle T excitations at the MP4 level [63]

## 2. Comparison of Møller-Plesset and Quadratic CI Electron Correlation Theories

### 2.1 Møller-Plesset Perturbation theory

In Møller-Plesset (MP) perturbation theory [34] the unperturbed Hamiltonian $\mathbf{H}_0$ is chosen as a sum of Fock operators $\mathbf{F}$

$$\mathbf{H}_0 = \sum_{\xi} \mathbf{F}(\xi). \tag{2.1}$$

and the perturbed Hamiltonian $\mathbf{H}'$ is given as the difference between the exact Hamiltonian $\mathbf{H}$ and the zeroth order Hamiltonian $\mathbf{H}_0$. The Fock operator $\mathbf{F}(\xi)$ of the $\xi$th electron in eq.(2.1) is defined as

$$\mathbf{F}(\xi) = \mathbf{h}(\xi) + \sum_{\tau} (\mathbf{J}_\tau(\xi) - \mathbf{K}_\tau(\xi)), \tag{2.2}$$

where $\mathbf{h}(\xi)$ denotes the one-electron part of the Hamiltonian and $\mathbf{J}_\tau(\xi)$ and $\mathbf{K}_\tau(\xi)$ are the Coulomb and exchange operators which describe two-electron interactions between the $\tau$th and the $\xi$th electron. For the perturbation expansion the Hartree-Fock (HF) wave function is used as zeroth order function. In the following the HF spin orbitals are denoted by $\varphi_p$. It is assumed that they are eigen functions of the Fock operator $\mathbf{F}$ with eigen value $\varepsilon_p$. Following a widespread convention we will use indices $i, j, k, \ldots$ to label occupied orbitals and indices $a, b, c, \ldots$ to label unoccupied (virtual) orbitals. In cases where the formulas hold for both type of orbitals indices $p, q, r, \ldots$ are used.

The energy corrections are calculated in MP theory using the Rayleigh-Schrödinger expansion. At second order, this gives the following energy contribution [34,38]

$$\mathrm{E(MP2)} = \frac{1}{4} \sum_{i,j} \sum_{a,b} a(ij, ab) \langle ij \| ab \rangle, \tag{2.3}$$

where $a(ij,ab)$ denotes the first order correction to the wave function

$$a(ij,ab) = \langle ij\|ab\rangle/(\varepsilon_i + \varepsilon_j - \varepsilon_a - \varepsilon_b) \tag{2.4}$$

and $\langle pq\|rs\rangle$ is the usual anti-symmetrized two-electron integral

$$\langle pq\|rs\rangle = \int \varphi_p(1)\varphi_q(2)\frac{1}{|\mathbf{r_1}-\mathbf{r_2}|}[\varphi_r(1)\varphi_s(2) - \varphi_s(1)\varphi_r(2)]d\tau_1 d\tau_2. \tag{2.5}$$

At third order the energy correction is given by [38]

$$\mathrm{E(MP3)} = \frac{1}{4}\sum_{i,j}\sum_{a,b} a(ij,ab)w(ij,ab) \tag{2.6}$$

with

$$\begin{aligned} w(ij,ab) = {} & \frac{1}{2}\sum_{k,l}\langle kl\|ij\rangle a(kl,ab) + \frac{1}{2}\sum_{c,d}\langle ab\|cd\rangle a(ij,cd) \\ & - \sum_k\sum_c\{\langle ka\|ic\rangle a(kj,cb) + \langle ka\|jc\rangle a(ik,cb) \\ & + \langle kb\|ic\rangle a(kj,ac) + \langle kb\|jc\rangle a(ik,ac)\}. \end{aligned} \tag{2.7}$$

While second and third order MP perturbation theory include only double(D) excitations with respect to the HF reference function, fourth order MP theory considers in addition single(S), triple(T), and quadruple(Q) excitations [39]. The energy correction at this level of theory is usually given as [39,40]

$$\begin{aligned} \mathrm{E(MP4)} = {} & \sum_i\sum_a w(i,a)d(i,a) + \frac{1}{4}\sum_{i,j}\sum_{a,b} w(ij,ab)d(ij,ab) \\ & + \frac{1}{36}\sum_{i,j,k}\sum_{a,b,c} w(ijk,abc)d(ijk,abc) \\ & + \frac{1}{4}\sum_{i,j}\sum_{a,b} a(ij,ab)v_q(ij,ab). \end{aligned} \tag{2.8}$$

In eq.(2.8), the first term denotes the energy correction due to S, the second due to D, the third due to T, and the fourth due to Q excitations. The various arrays in eq.(2.8) are defined as

$$w(i,a) = \frac{1}{2}\sum_j\sum_b\Big(\sum_c\langle aj\|cb\rangle a(ij,cb) - \sum_k\langle ib\|kj\rangle a(kj,ab)\Big), \tag{2.9}$$

$$d(i,a) = w(i,a)/(\varepsilon_i - \varepsilon_a), \tag{2.10}$$

$$d(ij,ab) = w(ij,ab)/(\varepsilon_i + \varepsilon_j - \varepsilon_a - \varepsilon_b), \tag{2.11}$$

$$\begin{aligned} w(ijk,abc) = \sum_d \{ & a(ij,ad)\langle bc\|dk\rangle + a(ij,bd)\langle ca\|dk\rangle + a(ij,cd)\langle ab\|dk\rangle \\ & + a(ki,ad)\langle bc\|dj\rangle + a(ki,bd)\langle ca\|dj\rangle + a(ki,cd)\langle ab\|dj\rangle \\ & + a(jk,ad)\langle bc\|di\rangle + a(jk,bd)\langle ca\|di\rangle + a(jk,cd)\langle ab\|di\rangle \} \\ + \sum_l \{ & a(il,ab)\langle cl\|jk\rangle + a(il,bc)\langle al\|jk\rangle + a(il,ca)\langle bl\|jk\rangle \\ & + a(jl,ab)\langle cl\|ki\rangle + a(jl,bc)\langle al\|ki\rangle + a(jl,ca)\langle bl\|ki\rangle \\ & + a(kl,ab)\langle cl\|ij\rangle + a(kl,bc)\langle al\|ij\rangle + a(kl,ca)\langle bl\|ij\rangle \}, \end{aligned} \tag{2.12}$$

$$d(ijk,abc) = w(ijk,abc)/(\varepsilon_i + \varepsilon_j + \varepsilon_k - \varepsilon_a - \varepsilon_b - \varepsilon_c), \tag{2.13}$$

and

$$\begin{aligned} v_q(ij,ab) = \frac{1}{4} \sum_{k,l} \sum_{c,d} \langle kl\|cd\rangle \big[ & a(ij,cd)a(kl,ab) \\ & - 2\{a(ij,ac)a(kl,bd) + a(ij,bd)a(kl,ac)\} \\ & - 2\{a(ik,ab)a(jl,cd) + a(ik,cd)a(jl,ab)\} \\ & + 4\{a(ik,ac)a(jl,d) + a(ik,bd)a(jl,ac)\}\big]. \end{aligned} \tag{2.14}$$

Note that in order to reduce computational costs the formula for the energy contribution due to quadruple excitations has been rearranged [39] and combined with the renormalization term.

An alternative formula which turns out to be useful when deriving formulas for the energy gradient with respect to some external perturbation (see chapter 3), is given by eq.(2.15) [58] :

$$\begin{aligned} \mathrm{E(MP4)} = \frac{1}{4} \sum_{i,j} \sum_{a,b} a(ij,ab) \{ & v_s(ij,ab) + v_d(ij,ab) \\ & + v_t(ij,ab) + v_q(ij,ab)\}, \end{aligned} \tag{2.15}$$

where the various $v$-arrays are defined by [58,63]

$$\begin{aligned} v_s(ij,ab) = \sum_c \{ & \langle ab\|cj\rangle d(i,c) + \langle ab\|ic\rangle d(j,c)\} \\ & - \sum_k \{\langle kb\|ij\rangle d(k,a) + \langle ka\|ji\rangle d(k,b)\}, \end{aligned} \tag{2.16}$$

$$v_d(ij,ab) = \frac{1}{2}\sum_{k,l}\langle kl\|ij\rangle d(kl,ab) + \frac{1}{2}\sum_{c,d}\langle ab\|cd\rangle d(ij,cd) - \sum_k\sum_c\{\langle ka\|ic\rangle d(kj,cb) + \langle ka\|jc\rangle d(ik,cb) + \langle kb\|ic\rangle d(kj,ac) + \langle kb\|jc\rangle d(ik,ac)\}. \quad (2.17)$$

$$v_t(ij,ab) = \frac{1}{2}\sum_k\sum_{c,d}\{\langle cd\|bk\rangle d(ijk,acd) - \langle cd\|ak\rangle d(ijk,bcd)\} + \frac{1}{2}\sum_{k,l}\sum_c\{\langle cj\|kl\rangle d(ikl,abc) - \langle ci\|kl\rangle d(jkl,abc)\}. \quad (2.18)$$

Recently, also formulas for the energy correction at fifth order MP theory have been given and implemented [55,74,75]. Compared to MP4, no additional excitations are included and only couplings between S, T, and Q excitations, respectively, are introduced in MP5. However, since MP5 is computationally very expensive (the evaluation of the T-T coupling terms requires $O(N^8)$ operations compared to the most expensive $O(N^7)$ step in MP4), it is not expected that MP5 will be in the near future a standard method for large scale calculations.

## 2.2 Quadratic Configuration Interaction Theory

The coupled cluster (CC) [36] ansatz for the description of electron correlation is based on the following exponential form of the wave function

$$\Psi = \exp(\mathbf{T})\Psi_0, \quad (2.19)$$

where $\Psi_0$ denotes a single determinant reference function, usually the HF wave function, and $\mathbf{T}$ denotes a general excitation operator which considers all possible types of excitations up to n-tuple excitations when n is the number of electrons. Equations for the energy and for the amplitudes of the various excitations are obtained in CC theory by projecting the Schrödinger equation with $\Psi$ given by eq. (2.19) onto the various determinants, namely $\Psi_0$, the singly excited determinants $\Psi_i^a$, etc. [36,37].

Similar to the CI method [35] CC calculations including all possible types of excitations are not feasible in most cases and several restrictions have to be imposed. Limitation of $\mathbf{T}$ to double excitations yields the CC doubles (CCD) method [49,50], additional inclusion of single excitations leads to the CC singles and doubles (CCSD) method [51] and so on.

The QCI approach of Pople and co-workers [52] can be regarded as an approximate CC method in which only those of the non linear terms are kept which are needed to guarantee size consistency. QCID including only double excitations is identical with CCD, while QCISD including single and double excitations neglects all cubic and quartic terms compared to CCSD [52].

With single and double excitation amplitudes denoted by $a_i^a$ and $a_{ij}^{ab}$ respectively, projection of the Schrödinger equation onto $\Psi_0$, $\Psi_i^a$, and $\Psi_{ij}^{ab}$ yields for the QCISD correlation energy [52]

$$\mathrm{E(QCISD)} = \frac{1}{4}\sum_{i,j}\sum_{a,b} a_{ij}^{ab}\langle ij\|ab\rangle \tag{2.20}$$

and for the equations, which determine the amplitudes $a_i^a$ and $a_{ij}^{ab}$ [52]

$$(\varepsilon_a - \varepsilon_i)a_i^a + w_i^a + v_i^a = 0, \tag{2.21}$$

$$(\varepsilon_a + \varepsilon_b - \varepsilon_i - \varepsilon_j)a_{ij}^{ab} + w_{ij}^{ab} + v_{ij}^{ab} + \langle ij\|ab\rangle = 0. \tag{2.22}$$

The arrays $w_i^a$ and $w_{ij}^{ab}$ depend linearly on the configuration coefficients $a_i^a$ and $a_{ij}^{ab}$,

$$w_i^a = -\sum_j\sum_b \langle ja\|ib\rangle a_j^b - \frac{1}{2}\sum_j\sum_{b,c}\langle ja\|bc\rangle a_{ij}^{bc} - \frac{1}{2}\sum_{j,k}\sum_b \langle jk\|ib\rangle a_{jk}^{ab} \tag{2.23}$$

and

$$\begin{aligned} w_{ij}^{ab} = {} & \sum_c\{\langle ab\|cj\rangle a_i^c - \langle ab\|ci\rangle a_j^c\} + \sum_k\{-\langle kb\|ij\rangle a_k^a + \langle ka\|ij\rangle a_k^b\} \\ & + \frac{1}{2}\sum_{k,l}\langle kl\|ij\rangle a_{kl}^{ab} + \frac{1}{2}\sum_{c,d}\langle ab\|cd\rangle a_{ij}^{cd} - \sum_k\sum_c\{\langle kb\|jc\rangle a_{ik}^{ac} \\ & + \langle ka\|jc\rangle a_{ik}^{cb} + \langle kb\|ic\rangle a_{kj}^{ac} + \langle ka\|ic\rangle a_{kj}^{cb}\}, \end{aligned} \tag{2.24}$$

while $v_i^a$ and $v_{ij}^{ab}$ are quadratic in the amplitudes :

$$v_i^a = \frac{1}{2}\sum_{j,k}\sum_{b,c}\langle jk\|bc\rangle\{a_i^b a_{jk}^{ca} + a_j^a a_{ik}^{cb} + 2a_j^b a_{ik}^{ac}\} \tag{2.25}$$

and

$$v_{ij}^{ab} = \frac{1}{4}\sum_{k,l}\sum_{c,d}\langle kl\|cd\rangle[a_{ij}^{cd}a_{kl}^{ab} - 2\{a_{ij}^{ac}a_{kl}^{bd} + a_{ij}^{bd}a_{kl}^{ac}\} - 2\{a_{ik}^{ab}a_{jl}^{cd} + a_{ik}^{cd}a_{jl}^{ab}\} + 4\{a_{ik}^{ac}a_{jl}^{bd} + a_{ik}^{bd}a_{jl}^{ac}\}]. \quad (2.26)$$

The QCISD equations are solved iteratively via eq.s (2.27) and (2.28)

$$a_i^{a(n+1)} = [w_i^{a(n)} + v_i^{a(n)}]/(\varepsilon_i - \varepsilon_a), \quad (2.27)$$

$$a_{ij}^{ab(n+1)} = [\langle ij\|ab\rangle + w_{ij}^{ab(n)} + v_{ij}^{ab(n)}]/(\varepsilon_i + \varepsilon_j - \varepsilon_a - \varepsilon_b), \quad (2.28)$$

using as initial guess for the amplitudes

$$a_i^{a(0)} = 0, \quad (2.29)$$

$$a_{ij}^{ab(0)} = \langle ij\|ab\rangle/(\varepsilon_i + \varepsilon_j - \varepsilon_a - \varepsilon_b). \quad (2.30)$$

Convergence is usually significantly accelerated by applying extrapolation schemes of the DIIS type [76-79].

Since an explicit treatment of triple excitations in QCI theory is in most cases impractical [80] but on the other side often necessary, Pople and coworkers [52] proposed an useful approximation for treating them within the QCI approach. Their approximation is based on the assumption that triple excitations are small perturbations on the solution obtained at the QCISD level. Perturbation theory yields then for the energy correction due to triples [52]

$$\Delta E(T) = \frac{1}{36}\sum_{i,j,k}\sum_{a,b,c} d_{ijk}^{abc}(w_{ijk}^{abc} + 2\tilde{w}_{ijk}^{abc}) \quad (2.31)$$

with

$$\begin{aligned} w_{ijk}^{abc} = &\sum_d \{a_{ij}^{ad}\langle bc\|dk\rangle + a_{ij}^{bd}\langle ca\|dk\rangle + a_{ij}^{cd}\langle ab\|dk\rangle + a_{ki}^{ad}\langle bc\|dj\rangle \\ &+ a_{ki}^{bd}\langle ca\|dj\rangle + a_{ki}^{cd}\langle ab\|dj\rangle + a_{jk}^{ad}\langle bc\|di\rangle + a_{jk}^{bd}\langle ca\|di\rangle + a_{jk}^{cd}\langle ab\|di\rangle\} \\ &+ \sum_l \{a_{il}^{ab}\langle cl\|jk\rangle + a_{il}^{bc}\langle al\|jk\rangle + a_{il}^{ca}\langle bl\|jk\rangle + a_{jl}^{ab}\langle cl\|ki\rangle \\ &+ a_{jl}^{bc}\langle al\|ki\rangle + a_{jl}^{ca}\langle bm\|ki\rangle + a_{kl}^{ab}\langle cl\|ij\rangle + a_{kl}^{bc}\langle al\|ij\rangle + a_{kl}^{ca}\langle bm\|ij\rangle\}, \end{aligned} \quad (2.32)$$

$$\tilde{w}_{ijk}^{abc} = a_i^a\langle jk\|bc\rangle + a_i^b\langle jk\|ca\rangle + a_i^c\langle jk\|ab\rangle + a_j^a\langle ki\|bc\rangle + a_j^b\langle ki\|ca\rangle + a_j^c\langle ki\|ab\rangle + a_k^a\langle ij\|bc\rangle + a_k^b\langle ij\|ca\rangle + a_k^c\langle ij\|ab\rangle, \quad (2.33)$$

and

$$d_{ijk}^{abc} = w_{ijk}^{abc}/(\varepsilon_i + \varepsilon_j + \varepsilon_k - \varepsilon_a - \varepsilon_b - \varepsilon_c). \quad (2.34)$$

In these equations, $a_i^a$ and $a_{ij}^{ab}$ denote the converged QCISD amplitudes of single and double excitations, respectively. It has been demonstrated [52,83-86] that this approximate treatment of triple excitations leads to highly accurate results, which are in many cases comparable to those of full CI calculations.

Recently, Raghavachari et. al. [55] proposed a new non-iterative correction to the QCISD approach which considers beside triple excitations also connected quadruple excitations [87]. This method, which was named QCISD(TQ) is correct to fifth order of MP theory [55,74,75] and should yield as long as the single reference ansatz is appropriate, excellent result. However, since this method contains a $O(N^8)$ step which should be compared with the most expensive $O(N^7)$ of the QCISD(T) method, it is certainly not a method which can routinely be applied in large scale calculations.

## 2.3 The Relationship between QCISD Theory and MP Perturbation Theory

As it has been shown by several authors [74,76] there is a close relation between MP perturbation theory on one side and CC and QCI theory on the other side. The results of MP perturbation theory can be recovered by collecting various terms of the first iterations of QCISD (and as well as CCSD), which in the language of perturbation theory is a method that sums up several terms to infinite order [74,76].

When we write the MPn energy contribution in n-th order in the form

$$\mathrm{E(MPn)} = \frac{1}{4}\sum_{i,j}\sum_{a,b} a_{ij}^{ab}(\mathrm{MPn})\langle ij\|ab\rangle, \quad (2.35)$$

we obtain for the amplitudes $a_{ij}^{ab}(\mathrm{MPn})$ in second, third, and fourth order

$$a_{ij}^{ab}(\mathrm{MP2}) = a(ij,ab), \quad (2.36)$$

$$a_{ij}^{ab}(\mathrm{MP3}) = d(ij,ab), \quad (2.37)$$

and

$$a_{ij}^{ab}(\mathrm{MP4}) = \{v_s(ij,ab) + v_d(ij,ab) + v_t(ij,ab) + v_q(ij,ab)\}/(\varepsilon_i + \varepsilon_j - \varepsilon_a - \varepsilon_b). \quad (2.38)$$

The first iteration of QCISD yields (with $a_i^a$ and $a_{ij}^{ab}$ set to zero in the initial guess)

$$a_{ij}^{ab}(\mathrm{QCISD, 1.Iteration}) = \langle ij \| ab \rangle / (\varepsilon_i + \varepsilon_j - \varepsilon_a - \varepsilon_b) \quad (2.39)$$

and, therefore, recovers the MP2 result. The second iteration gives

$$a_{ij}^{ab}(\mathrm{QCISD, 2.Iteration}) = a(ij,ab) + d(ij,ab) + v_q(ij,ab)/(\varepsilon_i + \varepsilon_j - \varepsilon_a - \varepsilon_b) \quad (2.40)$$

and produces the MP3 amplitudes as well as those due to the quadruple part of MP4. Note that while $d(ij,ab)$ is linear in the amplitudes $a(ij,ab)$ ( see eq.s (2.7) and (2.8)) and thus a third order term, $v_q(ij,ab)$ is quadratic in $a(ij,ab)$ and hence a fourth order term. The third iteration of the QCISD method finally yields

$$a_{ij}^{ab}(\mathrm{QCISD, 3.Iteration}) = a(ij,ab) + d(ij,ab) + \{v_s(ij,ab) + v_d(ij,ab) + v_q(ij,ab)\}/(\varepsilon_i + \varepsilon_j - \varepsilon_a - \varepsilon_b) + \textit{higher order terms}. \quad (2.41)$$

Beside several higher order terms the third iteration gives the remaining single and double excitation terms of MP4. However, a theory which includes only single and double excitations cannot account for the triple excitation terms in MP4 and, therefore, is not exact to fourth order. The triple term in MP4 on the other side is closely related to the additional terms in QCISD(T) theory which are obtained in the perturbational treatment of triple excitations. The differences are that the fully converged QCISD amplitudes rather than $a(ij,ab)$ are used to calculate the triple corrections, and, second, that an additional coupling of single and double excitations which corresponds to a fifth order term in MP theory is introduced. The recently introduced QCISD(TQ) method [55] is finally correct to fifth order of MP theory.

## 3. Energy gradients

Analytical expressions for the energy gradients in MP and QCI theory with respect to an external perturbation $\lambda$ such as the displacements of nuclear coordinates, or the components of a static electric (magnetic) field are easily derived by straightforward differentiation of the energy formulas discussed in the previous paragraph. Since the energy formulas are given in terms of two-electron integrals and orbital energies, we first discuss (section 3.1) the derivatives of these quantities. This requires some discussion of the theory of energy derivatives in HF theory, in particular of the so called coupled-perturbed HF theory. After this we will derive formulas for MP2, MP3, MP4 (section 3.2), QCISD and QCISD(T) (section 3.3) energy gradients and discuss the relations between the various gradient formulas (section 3.4). Finally, these formulas are condensed into a form which is useful for the implementation of analytical gradient methods within computer programs (section 3.5).

### 3.1 Derivatives of Two-electron Integrals and Orbital Energies

Differentiation of the two-electron integrals $\langle pq\|rs\rangle$ and the orbital energies $\varepsilon_p$ with respect to an external perturbation $\lambda$ is straightforward. The HF orbitals are given by

$$\varphi_p = \sum_\mu c_{\mu p}\chi_\mu, \tag{3.1}$$

where the $\chi_\mu$ are the AO basis functions and the $c_{\mu p}$ the usual MO coefficients as determined in the SCF procedure. The derivatives of the orbitals are usually given in terms of the derivatives $\partial c_{\mu p}/\partial\lambda$ of the MO coefficients. Within standard Coupled-perturbed HF (CPHF) theory [18,21]), the derivatives $\partial c_{\mu p}/\partial\lambda$ are expanded in terms of the unperturbed coefficients $c_{\mu p}$ [18]

$$\frac{\partial c_{\mu p}}{\partial\lambda} = \sum_q U^\lambda_{qp} c_{\mu q}, \tag{3.2}$$

where the $U^\lambda_{qp}$ are the perturbation dependent expansion coefficients. Orthonormality of the perturbed orbitals requires further that

$$U^\lambda_{qp} + U^\lambda_{pq} + S^\lambda_{qp} = 0 \tag{3.3}$$

with

$$S^\lambda_{qp} = \sum_{\mu,\nu} c_{\mu p}\frac{\partial S_{\mu\nu}}{\partial\lambda}c_{\nu q} \tag{3.4}$$

and $S_{\mu\nu}$ being the overlap matrix of the AO basis functions. Note that the dependence of the AO basis functions on the perturbation $\lambda$ is usually included into the derivatives of the one- and two-electron operators of the Hamiltonian within the AO representation, e.g.

$$\frac{\partial h_{\mu\nu}}{\partial\lambda} = \langle\frac{\partial\chi_\mu}{\partial\lambda}|\mathbf{h}|\chi_\nu\rangle + \langle\chi_\mu|\frac{\partial\mathbf{h}}{\partial\lambda}|\chi_\nu\rangle + \langle\chi_\nu|\mathbf{h}|\frac{\partial\chi_\mu}{\partial\lambda}\rangle \tag{3.5}$$

and

$$\begin{aligned}\frac{\partial\langle\mu\nu\|\sigma\rho\rangle}{\partial\lambda} = &\langle\frac{\partial\chi_\mu}{\partial\lambda}\chi_\nu\|\chi_\sigma\chi_\rho\rangle + \langle\chi_\mu\frac{\partial\chi_\nu}{\partial\lambda}\|\chi_\sigma\chi_\rho\rangle \\ &+ \langle\chi_\mu\chi_\nu\|\frac{\partial\chi_\sigma}{\partial\lambda}\chi_\rho\rangle + \langle\chi_\mu\chi_\nu\|\chi_\sigma\frac{\partial\chi_\rho}{\partial\lambda}\rangle.\end{aligned} \tag{3.6}$$

The coefficients $U_{pq}^{\lambda}$ are determined by solving the CPHF equations [19-21] which are obtained by differentiating the HF equations with respect to $\lambda$. However, there exists some ambiguity with respect to the definition of the perturbed orbitals in a similar way as it exists for the unperturbed orbitals. Energy gradients and perturbed wave function are invariant to rotations among the perturbed occupied (virtual) orbitals. There is no unique choice for the corresponding mixing coefficients $U_{ij}^{\lambda}$ and $U_{ab}^{\lambda}$ [88]. The selection of canonical orbitals which turns out to be advantageous in the case of the unperturbed orbitals and which would diagonalize the matrix $\partial\varepsilon_{pq}/\partial\lambda$ of the derivatives of the Lagrangian multipliers is not the best choice. Computation of the mixing coefficients $U_{ij}^{\lambda}$ and $U_{ab}^{\lambda}$ within this specific choice of perturbed orbitals causes numerical difficulties as soon as degenerate or nearly degenerate orbitals are encountered [18,88]. It is more advantageous to fix the coefficients $U_{ij}^{\lambda}$ and $U_{ab}^{\lambda}$ to

$$U_{ij}^{\lambda} = -\frac{1}{2}S_{ij}^{\lambda} \tag{3.7}$$

and

$$U_{ab}^{\lambda} = -\frac{1}{2}S_{ab}^{\lambda} \tag{3.8}$$

respectively [89]. In this way, one avoids all numerical difficulties although one has to deal now with the off-diagonal elements of the $\partial\varepsilon_{pq}/\partial\lambda$ matrix [88]. The only derivatives $U_{pq}^{\lambda}$ that have not been defined so far are the derivatives $U_{ai}^{\lambda}$ which describe the mixing between occupied and virtual orbitals. They are determined by the CPHF equations [18,21]

$$\sum_b\sum_j(A_{aibj} + (\varepsilon_a - \varepsilon_i)\delta_{ab}\delta_{ij})U_{bj}^{\lambda} = B_{ai}^{\lambda} \tag{3.9}$$

which are obtained by differentiating the HF equations with respect to $\lambda$. The various terms in eq. (3.9) are defined as

$$A_{pqrs} = \langle pr \| qs \rangle + \langle ps \| qr \rangle \tag{3.10}$$

and

$$B_{ai}^{\lambda} = -F_{ai}^{(\lambda)} + \varepsilon_i S_{ai}^{\lambda} + \frac{1}{2} \sum_{k,l} A_{klai} S_{kl}^{\lambda}, \tag{3.11}$$

where $F_{ai}^{(\lambda)}$ denotes the following derivative of the Fock matrix $F_{\mu\nu}$ transformed to the MO basis

$$\begin{aligned} F_{ai}^{(\lambda)} &= \sum_{\mu,\nu} c_{\mu a} F_{\mu\nu}^{(\lambda)} c_{\nu i} \\ &= \sum_{\mu,\nu} c_{\mu a} \{ \frac{\partial h_{\mu\nu}}{\partial \lambda} + \sum_{k} \sum_{\sigma,\rho} c_{\sigma k} c_{\rho k} \frac{\partial \langle \mu\sigma \| \nu\rho \rangle}{\partial \lambda} \} c_{\nu i}. \end{aligned} \tag{3.12}$$

Although one can show that the solution of the CPHF equation is not required for the evaluation of analytical energy gradients in any of the methods considered [22,58,59], it is on the other side very convenient to use the derivatives $U_{pq}^{\lambda}$ in the derivation of the gradient formulas. The elimination of the coefficient $U_{ai}^{\lambda}$ from the gradient formulas is discussed later in chapter 3.5.

Using CPHF theory, we obtain the following expression for the derivatives of the two-electron integrals $\langle pq \| rs \rangle$ :

$$\begin{aligned} \frac{\partial \langle pq \| rs \rangle}{\partial \lambda} &= \sum_{\mu\nu\sigma\rho} c_{\mu p} c_{\nu q} c_{\sigma r} c_{\rho s} \frac{\partial \langle \mu\nu \| \sigma\rho \rangle}{\partial \lambda} + \sum_{t} U_{tp}^{\lambda} \langle tq \| rs \rangle \\ &\quad + \sum_{t} U_{tq}^{\lambda} \langle pt \| rs \rangle + \sum_{t} U_{tr}^{\lambda} \langle pq \| ts \rangle + \sum_{t} U_{ts}^{\lambda} \langle pq \| rt \rangle. \end{aligned} \tag{3.13}$$

Explicit specification of the orbitals $\varphi_p$, $\varphi_q$, $\varphi_r$, and $\varphi_s$ allows further simplification of eq. (3.13) using eq.s (3.3), (3.7), and (3.8). E.g., the derivatives of the integrals $\langle ij \| ab \rangle$ are given by

$$\begin{aligned} \frac{\partial \langle ij \| ab \rangle}{\partial \lambda} &= \sum_{\mu\nu\sigma\rho} c_{\mu i} c_{\nu j} c_{\sigma a} c_{\rho b} \frac{\partial \langle \mu\nu \| \sigma\rho \rangle}{\partial \lambda} \\ &\quad + \sum_{c} U_{ci}^{\lambda} \langle cj \| ab \rangle - \frac{1}{2} \sum_{k} S_{ki}^{\lambda} \langle kj \| ab \rangle \end{aligned}$$

$$+\sum_c U_{cj}^{\lambda}\langle ic\|ab\rangle - \frac{1}{2}\sum_k S_{kj}^{\lambda}\langle ik\|ab\rangle$$
$$-\sum_k\{U_{ak}^{\lambda}+S_{ak}^{\lambda}\}\langle ij\|kb\rangle - \frac{1}{2}\sum_c S_{ca}^{\lambda}\langle ij\|cb\rangle$$
$$-\sum_k\{U_{bk}^{\lambda}+S_{bk}^{\lambda}\}\langle ij\|ak\rangle - \frac{1}{2}\sum_c S_{cb}^{\lambda}\langle ij\|ac\rangle. \tag{3.14}$$

For the Lagrangian multipliers which are in HF theory given as

$$\varepsilon_{pq} = \sum_{\mu,\nu} c_{\mu p} F_{\mu\nu} c_{\nu q} \tag{3.15}$$

straightforward differentiation yields

$$\frac{\partial \varepsilon_{pq}}{\partial\lambda} = F_{pq}^{(\lambda)} + \sum_a\sum_i U_{ai}^{\lambda} A_{pqai} - \frac{1}{2}\sum_{k,l} S_{kl}^{\lambda} A_{pqkl} - \frac{1}{2} S_{pq}^{\lambda}(\varepsilon_p+\varepsilon_q). \tag{3.16}$$

By this, the derivatives of the orbital energies and two-electron integrals are given which are needed to derive analytic expressions for MP and QCI gradients.

## 3.2 Gradients in MP Perturbation Theory

In MP perturbation theory differentiation of the energy is straightforward, because the MP energies at all orders are given as "fixed" expressions in terms of two-electron integrals $\langle pq\|rs\rangle$ and orbital energies $\varepsilon_p$. Thus, the formulas for the energy gradients contain only derivatives of these quantities and beside the derivatives of one- and two-electron integrals as well as the derivatives of the MO coefficients no additional perturbation dependent quantities are required.

For second [18], third [58], and fourth order [58,63], one obtains

$$\frac{dE(\mathrm{MP2})}{d\lambda} = \frac{1}{2}\sum_{i,j}\sum_{a,b}\frac{\partial\langle ij\|ab\rangle}{\partial\lambda} a(ij,ab)$$
$$-\frac{1}{2}\sum_{i,j}\frac{\partial\varepsilon_{ij}}{\partial\lambda}\sum_k\sum_{a,b} a(ik,ab)a(jk,ab)$$
$$+\frac{1}{2}\sum_{a,b}\frac{\partial\varepsilon_{ab}}{\partial\lambda}\sum_c\sum_{i,j} a(ij,ac)a(ij,bc), \tag{3.17}$$

$$\frac{dE(\mathrm{MP3})}{d\lambda} = \frac{1}{2}\sum_{i,j}\sum_{a,b}\frac{\partial\langle ij\|ab\rangle}{\partial\lambda}d(ij,ab)$$
$$+\sum_{i,j}\sum_{a,b}a(ij,ab)\{\frac{1}{8}\sum_{k,l}\frac{\partial\langle kl\|ij\rangle}{\partial\lambda}a(kl,ab)$$
$$+\frac{1}{8}\sum_{c,d}\frac{\partial\langle ab\|cd\rangle}{\partial\lambda}a(ij,cd)-\sum_{k}\sum_{c}\frac{\partial\langle ka\|ic\rangle}{\partial\lambda}a(kj,cb)\}$$
$$-\sum_{i,j}\frac{\partial\varepsilon_{ij}}{\partial\lambda}\sum_{k}\sum_{a,b}a(ik,ab)d(jk,ab)$$
$$+\sum_{a,b}\frac{\partial\varepsilon_{ab}}{\partial\lambda}\sum_{c}\sum_{i,j}a(ij,ac)d(ij,bc), \qquad (3.18)$$

and

$$\frac{dE(\mathrm{MP4})}{d\lambda} = \frac{1}{2}\sum_{i,j}\sum_{a,b}\frac{\partial\langle ij\|ab\rangle}{\partial\lambda}\{e(ij,ab)+x(ij,ab)\}$$
$$+\sum_{i,j}\sum_{a,b}a(ij,ab)\{\frac{1}{4}\sum_{k,l}\frac{\partial\langle kl\|ij\rangle}{\partial\lambda}d(kl,ab)$$
$$+\frac{1}{4}\sum_{c,d}\frac{\partial\langle ab\|cd\rangle}{\partial\lambda}d(ij,cd)-\sum_{k}\sum_{c}\frac{\partial\langle ka\|ic\rangle}{\partial\lambda}d(kj,cb)\}$$
$$+\sum_{i,j}\sum_{a,b}a(ij,ab)\{\sum_{c}\frac{\partial\langle ab\|cj\rangle}{\partial\lambda}d(i,c)-\sum_{k}\frac{\partial\langle kb\|ij\rangle}{\partial\lambda}d(k,a)\}$$
$$+2\sum_{i,j,k}\sum_{a}\frac{\partial\langle ij\|ka\rangle}{\partial\lambda}r(ijk,a)+2\sum_{i}\sum_{a,b,c}\frac{\partial\langle ia\|bc\rangle}{\partial\lambda}s(i,abc)$$
$$-\sum_{i,j}\frac{\partial\varepsilon_{ij}}{\partial\lambda}\{\sum_{k}\sum_{a,b}a(ik,ab)\{e(jk,ab)+\frac{1}{2}x(jk,ab)\}$$
$$+\sum_{a}d(i,a)d(j,a)+\frac{1}{12}\sum_{k,l}\sum_{a,b,c}d(ikl,abc)d(jkl,abc)\}$$
$$+\sum_{a,b}\frac{\partial\varepsilon_{ab}}{\partial\lambda}\{\sum_{c}\sum_{i,j}a(ij,ac)\{e(ij,bc)+\frac{1}{2}x(ij,bc)\}$$
$$+\sum_{i}d(i,a)d(i,b)+\frac{1}{12}\sum_{i,j,k}\sum_{c,d}d(ijk,acd)d(ijk,bcd)\}$$
$$(3.19)$$

with

$$e(ij,ab) = \{v_s(ij,ab) + v_d(ij,ab) + v_t(ij,ab) + v_q(ij,ab)\}/(\varepsilon_i + \varepsilon_j - \varepsilon_a - \varepsilon_b), \tag{3.20}$$

$$\begin{aligned} x(ij,ab) = \frac{1}{4}\sum_{k,l}\sum_{c,d} a(kl,cd)\{&a(ij,cd)a(kl,ab) \\ &- 2\{a(ij,ac)a(kl,bd) + a(ij,bd)a(kl,ac)\} \\ &- 2\{a(ik,ab)a(jl,cd) + a(ik,cd)a(jl,ab)\} \\ &+ 4\{a(ik,ac)a(jl,bd) + a(ik,bd)a(jl,ac)\}\}, \end{aligned} \tag{3.21}$$

$$r(ijk,a) = \frac{1}{4}\sum_{l}\sum_{b,c} a(kl,bc)d(ijl,abc), \tag{3.22}$$

and

$$s(i,abc) = \frac{1}{4}\sum_{j,k}\sum_{d} a(jk,ad)d(ijk,bcd). \tag{3.23}$$

### 3.3 Gradients in QCI Theory

The calculation of QCISD energy gradients is somewhat more complicated, because straightforward differentiation of the QCISD energy expression (eq. (2.20)) with respect to $\lambda$ yields a formula (eq. (3.24)) which contains, in addition to the derivatives of the two-electron integrals $\langle pq\|rs\rangle$, derivatives of the double excitation amplitudes $a_{ij}^{ab}$ :

$$\frac{dE(\mathrm{QCISD})}{d\lambda} = \frac{1}{4}\sum_{i,j}\sum_{a,b}\frac{\partial\langle ij\|ab\rangle}{\partial\lambda}a_{ij}^{ab} + \frac{1}{4}\sum_{i,j}\sum_{a,b}\langle ij\|ab\rangle\frac{\partial a_{ij}^{ab}}{\partial\lambda}. \tag{3.24}$$

As has been shown in section 3.1, evaluation of the two-electron integral derivatives causes no serious problems. However, computation of the derivatives of $a_{ij}^{ab}$ requires the solution of the Coupled-perturbed QCISD (CPQCISD) equations which are obtained by differentiating the QCISD equations (eq.s (2.27) and (2.28)) with respect to $\lambda$. The CPQCISD equations can be written in the following form [72]

$$B_i^{a(\lambda)} = \sum_{j}\sum_{b} C_{i,j}^{a,b}\frac{\partial a_j^b}{\partial\lambda} + \sum_{j<k}\sum_{b<c} C_{i,jk}^{a,bc}\frac{\partial a_{jk}^{bc}}{\partial\lambda} \tag{3.25}$$

and

$$B_{ij}^{ab(\lambda)} = \sum_k \sum_c C_{ij,k}^{ab,c} \frac{\partial a_k^c}{\partial \lambda} + \sum_{k<l} \sum_{c<d} C_{ij,kl}^{ab,cd} \frac{\partial a_{kl}^{cd}}{\partial \lambda}. \tag{3.26}$$

For a definition of the various B and C terms see appendix I. Note that the C terms are independent of the perturbation $\lambda$, while the B terms contain derivatives of the two-electron integrals $\langle pq||rs\rangle$ and of the Lagrangian multipliers $\varepsilon_{pq}$ with respect to $\lambda$.

Explicit solution of the CPQCISD equations is very costly, since it requires for each perturbation parameter approximately the same time as needed for the solution of the corresponding QCISD equations. Computation of QCISD energy gradients by solving the CPQCISD equations (3.23) and (3.26) obviously presents no real advantage compared to a calculation via a numerical finite differentiation scheme. However, the explicit determination of the derivatives of $a_{ij}^{ab}$ can be avoided by using the z-vector method of Handy and Schaefer [22,67,68,72]. If we define the z-amplitudes $z_i^a$ and $z_{ij}^{ab}$ by [72]

$$\sum_j \sum_b z_j^b C_{j,i}^{b,a} + \sum_{j<k} \sum_{b<c} z_{jk}^{bc} C_{jk,i}^{bc,a} = 0, \tag{3.27}$$

$$\sum_k \sum_c z_k^c C_{k,ij}^{c,ab} + \sum_{k<l} \sum_{c<d} z_{kl}^{cd} C_{kl,ij}^{cd,ab} = \langle ij||ab\rangle, \tag{3.28}$$

the term in the QCISD energy gradient expression which contains the derivative of $a_{ij}^{ab}$, can be replaced using the following equality

$$\frac{1}{4} \sum_{i,j} \sum_{a,b} \langle ij||ab\rangle \frac{\partial a_{ij}^{ab}}{\partial \lambda} = \sum_i \sum_a B_i^{a(\lambda)} z_i^a + \frac{1}{4} \sum_{i,j} \sum_{a,b} B_{ij}^{ab(\lambda)} z_{ij}^{ab}. \tag{3.29}$$

The main advantage of the z-vector method is that it requires only the solution of one set of linear equations in order to determine the perturbation independent quantities $z_i^a$ and $z_{ij}^{ab}$. The corresponding costs are similar to those for the solution of the QCISD equations.

Using eq.(3.29) and the definition of $B_i^{a(\lambda)}$ and $B_{ij}^{ab(\lambda)}$ given in the appendix the QCISD energy gradient expression can be given in terms of derivatives of two-electron integrals $\langle pq||rs\rangle$ and the Lagrangian multipliers $\varepsilon_{pq}$ [72]

:

$$\frac{dE(\mathrm{QCISD})}{d\lambda} = \frac{1}{4}\sum_{i,j}\sum_{a,b}\frac{\partial\langle ij\|ab\rangle}{\partial\lambda}(a_{ij}^{ab} - z_{ij}^{ab} - x_{ij}^{ab})$$
$$- \sum_{i,j}\sum_{a,b} z_{ij}^{ab}\{\frac{1}{8}\sum_{c,d}\frac{\partial\langle ab\|cd\rangle}{\partial\lambda}a_{ij}^{cd} + \frac{1}{8}\sum_{k,l}\frac{\partial\langle kl\|ij\rangle}{\partial\lambda}a_{kl}^{ab}$$
$$- \sum_{k}\sum_{c}\frac{\partial\langle ka\|ic\rangle}{\partial\lambda}a_{kj}^{cb}\} + \sum_{i,j}\sum_{a,b}\frac{\partial\langle ja\|ib\rangle}{\partial\lambda}z_i^a a_j^b$$
$$+ \frac{1}{2}\sum_{i,j}\sum_{a,b,c}\frac{\partial\langle ja\|bc\rangle}{\partial\lambda}\{a_{ij}^{bc}z_i^a + z_{ij}^{bc}a_i^a\}$$
$$+ \frac{1}{2}\sum_{i,j,k}\sum_{a,b}\frac{\partial\langle jk\|ib\rangle}{\partial\lambda}\{a_{jk}^{ab}z_i^a + z_{jk}^{ab}a_i^a\}$$
$$+ \sum_{i,j}\frac{\partial\varepsilon_{ij}}{\partial\lambda}\{\sum_{a}a_i^a z_j^a + \frac{1}{2}\sum_{k}\sum_{a,b}a_{ik}^{ab}z_{jk}^{ab}\}$$
$$- \sum_{a,b}\frac{\partial\varepsilon_{ab}}{\partial\lambda}\{\sum_{i}a_i^a z_i^b + \frac{1}{2}\sum_{i,j}\sum_{c}a_{ij}^{ac}z_{ij}^{bc}\} \qquad (3.30)$$

with

$$x_{ij}^{ab} = \sum_{k}\sum_{c} z_k^c\{a_{ij}^{ca}a_k^b - a_{ij}^{cb}a_k^a + a_{jk}^{ab}a_i^c - a_{ik}^{ab}a_j^c$$
$$+ a_{jk}^{bc}a_i^a - a_{jk}^{ac}a_i^b - a_{ik}^{bc}a_j^a + a_{ik}^{ac}a_j^b\}$$
$$+ \frac{1}{4}\sum_{k,l}\sum_{c,d} z_{kl}^{cd}\{a_{ij}^{cd}a_{kl}^{ab} - 2(a_{ij}^{ac}a_{kl}^{bd} + a_{ij}^{bd}a_{kl}^{ac})$$
$$- 2(a_{ik}^{ab}a_{jl}^{cd} + a_{ik}^{cd}a_{jl}^{ab}) + 4(a_{ik}^{ac}a_{jl}^{bd} + a_{ik}^{bd}a_{jl}^{ac})\}. \qquad (3.31)$$

Differentiation of the perturbation correction due to triple excitation within the QCISD(T) approach yields [73]

$$\frac{\partial\Delta\mathrm{E}(\mathrm{T},\mathrm{QCISD(T)})}{\partial\lambda} = \frac{1}{2}\sum_{i,j}\sum_{a,b}\frac{\partial a_{ij}^{ab}}{\partial\lambda}v_{ij}^{ab} + 2\sum_{i,j,k}\sum_{a}\frac{\partial\langle ij\|ka\rangle}{\partial\lambda}r_{ijk}^{a}$$
$$+ 2\sum_{i}\sum_{a,b,c}\frac{\partial\langle ia\|bc\rangle}{\partial\lambda}s_i^{abc} + \sum_{i}\sum_{a}\frac{\partial a_i^a}{\partial\lambda}\tilde{v}_i^a + \frac{1}{2}\sum_{i,j}\sum_{a,b}\frac{\partial\langle ij\|ab\rangle}{\partial\lambda}u_{ij}^{ab}$$
$$+ \frac{1}{12}\sum_{a,b}\frac{\partial\varepsilon_{ab}}{\partial\lambda}\sum_{i,j,k}\sum_{c,d}d_{ijk}^{acd}\{d_{ijk}^{bcd} + \tilde{d}_{ijk}^{bcd}\}$$

$$-\frac{1}{12}\sum_{i,j}\frac{\partial\varepsilon_{ij}}{\partial\lambda}\sum_{k,l}\sum_{a,b,c}d_{ikl}^{abc}\{d_{jkl}^{abc}+\tilde{d}_{jkl}^{abc}\}. \tag{3.32}$$

The arrays $v$, $\tilde{v}$, $r$, $s$, and $u$ are defined as follows

$$\begin{aligned}v_{ij}^{ab}=&\frac{1}{2}\sum_{k}\sum_{c,d}\{\langle cd\|bk\rangle[d_{ijk}^{acd}+\tilde{d}_{ijk}^{acd}]-\langle cd\|ak\rangle[d_{ijk}^{bcd}+\tilde{d}_{ijk}^{bcd}]\}\\&+\frac{1}{2}\sum_{k,l}\sum_{c}\{\langle cj\|kl\rangle[d_{ikl}^{abc}+\tilde{d}_{ikl}^{abc}]-\langle ci\|kl\rangle[d_{jkl}^{abc}+\tilde{d}_{jkl}^{abc}]\},\end{aligned} \tag{3.33}$$

$$r_{ijk}^{a}=\frac{1}{4}\sum_{l}\sum_{b,c}a_{kl}^{bc}\{d_{ijl}^{abc}+\tilde{d}_{ijl}^{abc}\}, \tag{3.34}$$

$$s_{i}^{abc}=\frac{1}{4}\sum_{j,k}\sum_{d}a_{jk}^{ad}\{d_{ijk}^{bcd}+\tilde{d}_{ijk}^{bcd}\}, \tag{3.35}$$

$$u_{ij}^{ab}=\sum_{k}\sum_{c}a_{k}^{c}d_{ijk}^{abc}, \tag{3.36}$$

and

$$\tilde{v}_{i}^{a}=\frac{1}{2}\sum_{j,k}\sum_{b,c}\langle jk\|bc\rangle d_{ijk}^{abc}. \tag{3.37}$$

Compared to the QCISD gradient expression, eq. (3.30), two additional terms that involve derivatives of $a_i^a$ and $a_{ij}^{ab}$ appear. While the CPQCI equations are identical for QCISD and QCISD(T), the corresponding z-vector equations are not. Triple excitations when treated as a perturbative correction to the QCISD result do no affect the unperturbed as well as the perturbed amplitudes of single and double excitations. However, since several terms in $\partial E(\Delta\mathrm{E(T,QCISD(T))})/\partial\lambda$ depend on the derivatives of $a_i^a$ and $a_{ij}^{ab}$, the z-vector equations have to be modified in order to get rid of these terms in the final QCISD(T) energy gradient expression [73]. Thus, the z-vector equations in QCISD(T) theory are given by

$$\sum_{j}\sum_{b}z_{j}^{b}C_{j,i}^{b,a}+\sum_{j<k}\sum_{b<c}z_{jk}^{bc}C_{jk,i}^{bc,a}=\tilde{v}_{i}^{a}, \tag{3.38}$$

$$\sum_k \sum_c z_k^c C_{k,ij}^{c,ab} + \sum_{k<l} \sum_{c<d} z_{kl}^{cd} C_{kl,ij}^{cd,ab} = \langle ij \| ab \rangle + 2v_{ij}^{ab}. \tag{3.39}$$

The terms dependent on $\partial a_i^a / \partial \lambda$ and $\partial a_{ij}^{ab} / \partial \lambda$ in the QCISD(T) energy gradient expression, eq. (3.32) are now replaced by

$$\sum_i \sum_a \tilde{v}_i^a \frac{\partial a_i^a}{\partial \lambda} + \frac{1}{2} \sum_{i,j} \sum_{a,b} v_{ij}^{ab} \frac{\partial a_{ij}^{ab}}{\partial \lambda} + \frac{1}{4} \langle ij \| ab \rangle \frac{\partial a_{ij}^{ab}}{\partial \lambda}$$
$$= \sum_i \sum_a B_i^{a(\lambda)} z_i^a + \frac{1}{4} \sum_{i,j} \sum_{a,b} B_{ij}^{ab(\lambda)} z_{ij}^{ab}. \tag{3.40}$$

In the final formula for the QCISD(T) energy gradient [73],

$$\frac{dE(\mathrm{QCISD(T)})}{d\lambda} = \frac{dE(\mathrm{QCISD})}{d\lambda} + 2 \sum_{i,j,k} \sum_a \frac{\partial \langle ij \| ka \rangle}{\partial \lambda} r_{ijk}^a$$
$$+ 2 \sum_i \sum_{a,b,c} \frac{\partial \langle ia \| bc \rangle}{\partial \lambda} s_i^{abc} + \frac{1}{2} \sum_{i,j} \sum_{a,b} \frac{\partial \langle ij \| ab \rangle}{\partial \lambda} u_{ij}^{ab}$$
$$+ \frac{1}{12} \sum_{a,b} \frac{\partial \varepsilon_{ab}}{\partial \lambda} \sum_{i,j,k} \sum_{c,d} d_{ijk}^{acd} \{ d_{ijk}^{bcd} + \tilde{d}_{ijk}^{bcd} \}$$
$$- \frac{1}{12} \sum_{i,j} \frac{\partial \varepsilon_{ij}}{\partial \lambda} \sum_{k,l} \sum_{a,b,c} d_{ikl}^{abc} \{ d_{jkl}^{abc} + \tilde{d}_{jkl}^{abc} \}, \tag{3.41}$$

the contribution of the triple excitations appears in two different ways. First, the QCISD energy gradient terms in eq. (3.41) have to be calculated using the modified z-amplitudes determined by eq.s (3.38) and (3.39). Second, eq. (3.41) includes several additional terms containing derivatives of the two-electron integrals and the Lagrangian multipliers.

Similar to MPn and QCISD energy gradients, the QCISD(T) energy gradient can be written in a form which contains only derivatives of the two-electron integrals $\langle pq \| rs \rangle$ and of the Lagrangian multipliers $\varepsilon_{pq}$. The z-vector equations are independent of the perturbation $\lambda$ and have to be solved only once for all possible types of perturbations.

### 3.4 The Relationship between MP and QCI Energy Gradients

In the same way as there is a close relationship between the MP and QCI energy expressions, there also is a close connection between the energy gradient formulas of both methods. By expanding the QCISD amplitudes $a_i^a$

and $a_{ij}^{ab}$ (see section 2.3) as well as the z-vector amplitudes $z_i^a$ and $z_{ij}^{ab}$ up to fourth order

$$\begin{aligned} a_{ij}^{ab} &= a(ij,ab) && \text{(second order)} \\ &\quad + d(ij,ab) && \text{(third order)} \\ &\quad + \{v_s(ij,ab) + v_d(ij,ab) \\ &\qquad + v_q(ij,ab)\}/(\varepsilon_i + \varepsilon_j - \varepsilon_a - \varepsilon_b) && \text{(fourth order)} \\ &\quad + \ldots && (3.42) \end{aligned}$$

$$\begin{aligned} a_i^a &= 0 && \text{(second order)} \\ &\quad + d(i,a) && \text{(third order)} \\ &\quad + v(i,a)/(\varepsilon_i - \varepsilon_j) && \text{(fourth order)} \\ &\quad + \ldots && (3.43) \end{aligned}$$

$$\begin{aligned} z_{ij}^{ab} &= -a(ij,ab) && \text{(second order)} \\ &\quad - d(ij,ab) && \text{(third order)} \\ &\quad - \{v_s(ij,ab) \\ &\qquad + v_d(ij,ab) + v_q(ij,ab)\}/(\varepsilon_i + \varepsilon_j - \varepsilon_a - \varepsilon_b) && \text{(fourth order)} \\ &\quad - \ldots && (3.44) \end{aligned}$$

$$\begin{aligned} z_i^a &= 0 && \text{(second order)} \\ &\quad - d(i,a) && \text{(third order)} \\ &\quad - v(i,a)/(\varepsilon_i - \varepsilon_j) && \text{(fourth order)} \\ &\quad - \ldots && (3.45) \end{aligned}$$

the relationship between the various gradient formulas becomes obvious. By substituting eq.s (3.41) - (3.45) in eq. (3.30) for the QCISD energy gradient, we obtain

$$\begin{aligned} \frac{dE(\text{QCISD})}{d\lambda} &= \frac{dE(\text{MP2})}{d\lambda} + \frac{dE(\text{MP3})}{d\lambda} \\ &\quad + \frac{dE(\text{MP4(SDQ)})}{d\lambda} + \textit{higher order terms} \end{aligned} \qquad (3.46)$$

Considering also triple excitations, a comparison of the QCISD(T) (eq. (3.32)) and the MP4(T) gradient (eq. (3.19)) reveals their similarity. Again, additional terms ($\tilde{d}_{ijk}^{abc}$,$u_{ij}^{ab}$, and $\tilde{v}_i^a$) are due to the fifth order coupling between single and double excitations.

### 3.5 General theory of MPn and QCI Gradients

As has been shown in the previous sections, the energy gradient expression for all methods considered can be casted in a form which contains only derivatives of the two-electron integrals and of the Lagrangian multipliers. Therefore, a general formula for the energy gradient is given by

$$\begin{aligned}\frac{dE(\text{METHOD})}{d\lambda} = &\sum_{i,j}\sum_{a,b}\frac{\partial\langle ij\|ab\rangle}{\partial\lambda}X_1^{METHOD}(ijab)\\ &+\sum_{i,j,k,l}\frac{\partial\langle ij\|kl\rangle}{\partial\lambda}X_2^{METHOD}(ijkl)\\ &+\sum_{i,j}\sum_{a,b}\frac{\partial\langle ia\|jb\rangle}{\partial\lambda}X_3^{METHOD}(iajb)\\ &+\sum_{a,b,c,d}\frac{\partial\langle ab\|cd\rangle}{\partial\lambda}X_4^{METHOD}(abcd)\\ &+\sum_{i,j,k}\sum_{a}\frac{\partial\langle ij\|ka\rangle}{\partial\lambda}X_5^{METHOD}(ijka)\\ &+\sum_{i}\sum_{a,b,c}\frac{\partial\langle ia\|bc\rangle}{\partial\lambda}X_6^{METHOD}(iabc)\\ &+\sum_{i,j}\frac{\partial\varepsilon_{ij}}{\partial\lambda}Y_1^{METHOD}(ij)\\ &+\sum_{a,b}\frac{\partial\varepsilon_{ab}}{\partial\lambda}Y_2^{METHOD}(ab). \qquad (3.47)\end{aligned}$$

Appendix 2 summarizes for all methods discussed the explicit expressions of the various $X$ and $Y$ terms in eq.(3.47). It should be noted that eq. (3.47) also holds for gradients in CI [23,24] and CC theory [90] provided a single determinant reference function is used.

However, eq. (3.47) does not offer a convenient basis for implementation of computer programs for analytical calculation of energy gradients. In actual gradient calculations the derivatives $\partial\langle pq\|rs\rangle/\partial\lambda$ are never computed, since it is more advantageous to deal directly with the derivatives of the AO integrals and the derivatives of the MO coefficients. The computation of $\partial\langle pq\|rs\rangle/\partial\lambda$ would require for each perturbation a full transformation of the two-electron integral derivatives from the AO to the MO representation and, therefore, is too expensive.

An expression for the energy gradient in terms of the AO integral derivatives and the coefficients $U_{pq}^{\lambda}$ is obtained by substituting eq. (3.13) into

eq.(3.47) [58]

$$\frac{dE(\mathrm{METHOD})}{d\lambda} = \sum_{\mu\nu\sigma\rho} T_{\mu\nu\sigma\rho} \frac{\partial \langle \mu\nu \| \sigma\rho \rangle}{\partial \lambda} + \sum_i \sum_a U^{\lambda}_{ai} L'_{ai} + \sum_i \sum_a U^{\lambda}_{ia} L''_{ia} - \frac{1}{2} \sum_{i,j} S^{\lambda}_{ij} L'_{ij} - \frac{1}{2} \sum_{a,b} S^{\lambda}_{ab} L''_{ab} + \sum_{i,j} K'_{ij} \frac{\partial \varepsilon_{ij}}{\partial \lambda} + \sum_{a,b} K''_{ab} \frac{\partial \varepsilon_{ab}}{\partial \lambda} \tag{3.48}$$

with

$$\begin{aligned} T_{\mu\nu\sigma\rho} = & \sum_{i,j} \sum_{a,b} c_{\mu i} c_{\nu j} c_{\sigma a} c_{\rho b} X_1^{METHOD}(ijab) \\ & + \sum_{i,j,k,l} c_{\mu i} c_{\nu j} c_{\sigma k} c_{\rho l} X_2^{METHOD}(ijkl) \\ & + \sum_{i,j} \sum_{a,b} c_{\mu i} c_{\nu a} c_{\sigma j} c_{\rho b} X_3^{METHOD}(iajb) \\ & + \sum_{a,b,c,d} c_{\mu a} c_{\nu b} c_{\sigma c} c_{\rho d} X_4^{METHOD}(abc) \\ & + \sum_{i,j,k} \sum_{a} c_{\mu i} c_{\nu j} c_{\sigma k} c_{\rho a} X_5^{METHOD}(ijka) \\ & + \sum_{i} \sum_{a,b,c} c_{\mu i} c_{\nu a} c_{\sigma b} c_{\rho c} X_6^{METHOD}(iabc), \end{aligned} \tag{3.49}$$

$$\begin{aligned} L'_{pi} = & 2 \sum_{j} \sum_{a,b} \langle pj \| ab \rangle X_1^{METHOD}(ijab) \\ & + 4 \sum_{j,k,l} \langle pj \| kl \rangle X_2^{METHOD}(ijkl) \\ & + 2 \sum_{j} \sum_{a,b} \langle pa \| jb \rangle X_3^{METHOD}(iajb) \\ & + 2 \sum_{j,k} \sum_{a} \langle pj \| ka \rangle X_5^{METHOD}(ijka) \\ & + \sum_{j,k} \sum_{a} \langle jk \| pa \rangle X_5^{METHOD}(jkia) \\ & + \sum_{a,b,c} \langle pa \| bc \rangle X_6^{METHOD}(iabc), \end{aligned} \tag{3.50}$$

$$
\begin{aligned}
L''_{pa} = & 2\sum_{i,j}\sum_{b}\langle ij\|pb\rangle X_1^{METHOD}(ijab) \\
& + 2\sum_{i,j}\sum_{b}\langle ip\|jb\rangle X_3^{METHOD}(iajb) \\
& + 4\sum_{b,c,d}\langle pb\|cd\rangle X_4^{METHOD}(abcd) \\
& + \sum_{i,j,k}\langle ij\|kp\rangle X_5^{METHOD}(ijka) \\
& + \sum_{i}\sum_{b,c}\langle ip\|bc\rangle X_6^{METHOD}(iabc) \\
& + 2\sum_{i}\sum_{b,c}\langle ib\|pc\rangle X_6^{METHOD}(ibac),
\end{aligned}
\tag{3.51}
$$

$$
K'_{ij} = Y_1^{METHOD}(ij), \tag{3.52}
$$

and

$$
K''_{ab} = Y_2^{METHOD}(ab). \tag{3.53}
$$

Using further the orthonormality condition (eq. (3.3)) and the explicit expression for the derivatives of the Lagrangian multipliers, eq. (3.16), eq. (3.48) is rewritten as

$$
\begin{aligned}
\frac{dE(\text{METHOD})}{d\lambda} = & \sum_{\mu,\nu,\sigma,\rho} T_{\mu\nu\sigma\rho}\frac{\partial\langle\mu\nu\|\sigma\rho\rangle}{\partial\lambda} + \sum_{i}\sum_{a} L_{ai}U_{ai}^{\lambda} \\
& + \sum_{p,q} M_{pq}S_{pq}^{\lambda} + \sum_{p,q} N_{pq}F_{pq}^{(\lambda)}
\end{aligned}
\tag{3.54}
$$

with

$$
L_{ai} = L'_{ai} - L''_{ia} + 2\sum_{j,k} K'_{jk}\langle aj\|ik\rangle + 2\sum_{b,c} K''_{bc}\langle ab\|ic\rangle \tag{3.55}
$$

$$
M_{pq} = \begin{cases}
-\frac{1}{2}(L'_{ij} + (\varepsilon_i + \varepsilon_j)K'_{ij}) + 2\sum_{k,l} K'_{kl}\langle ik\|jl\rangle & \\
\qquad\qquad + 2\sum_{a,b} K''_{ab}\langle ia\|jb\rangle & \text{p = i, q = j} \\
-\frac{1}{2}(L''_{ab} + (\varepsilon_a + \varepsilon_b)K''_{ab}) & \text{p = a, q = b} \\
-\frac{1}{2}L''_{ia} & \text{p = i, q = a} \\
-\frac{1}{2}L''_{ia} & \text{p = a, q = i}
\end{cases}
$$

and

$$N_{pq} = \begin{cases} K'_{ij} & \text{p = i, q = j} \\ K''_{ab} & \text{p = a, q = b} \\ 0 & \text{otherwise} \end{cases} \tag{3.57}$$

Following Handy and Schaefer [22], the derivatives $U^{\lambda}_{ai}$ can be eliminated from the expression for the energy gradient (eq. (3.54)). By defining the Z-vector $Z_{bj}$ for the CPHF equations (3.9) :

$$\sum_b \sum_j (A_{aibj} + (\varepsilon_a - \varepsilon_i)\delta_{ab}\delta_{ij}) Z_{bj} = L_{ai} \tag{3.58}$$

the second term in eq. (3.54), which contains the derivative $U^{\lambda}_{ai}$, is replaced by

$$\sum_a \sum_i L_{ai} U^{\lambda}_{ai} = \sum_b \sum_j B^{(\lambda)}_{bj} Z_{bj}. \tag{3.59}$$

The main advantage of this approach is that only one set of equations, eq. (3.58), rather than M sets of linear equations with M as the number of perturbations has to be solved. The idea, which is used to eliminate here $U^{\lambda}_{ai}$ from the gradient expression, is actually the same which has been used to eliminate the derivatives of the excitation amplitudes from the gradient expression in QCI theory (see section 3.3). Both elimination procedures are based on the fact that the gradient expression is necessarily linear with respect to the perturbation $\lambda$. Thus, the original set of coupled perturbed QCI or HF equations can be replaced by one set of equations which is independent of $\lambda$. These equations are usually called the z-vector equations [22].

Using eq. (3.59) and transforming all remaining terms to the AO representation we get the following final formula for the energy gradient [58,59]

$$\frac{dE(\text{METHOD})}{d\lambda} = \sum_{\mu,\nu,\sigma,\rho} T_{\mu\nu\sigma\rho} \frac{\partial \langle \mu\nu \| \sigma\rho \rangle}{\partial \lambda} + \sum_{\mu,\nu} F^{(\lambda)}_{\mu\nu} D_{\mu\nu} + \sum_{\mu,\nu} S^{\lambda}_{\mu\nu} W_{\mu\nu}, \tag{3.60}$$

where $D_{\mu\nu}$ and $W_{\mu\nu}$ are defined as

$$D_{\mu\nu} = \sum_{p,q} N_{pq} c_{\mu p} c_{\nu q} - \frac{1}{2} \sum_i \sum_a Z_{ai} (c_{\mu a} c_{\nu i} + c_{\mu i} c_{\nu a}) \tag{3.61}$$

and

$$W_{\mu\nu} = \sum_{p,q} M_{pq} c_{\mu p} c_{\nu q} + \frac{1}{2} \sum_{i} \sum_{a} Z_{ai} \varepsilon_i (c_{\mu a} c_{\nu i} + c_{\mu i} c_{\nu a}) + \frac{1}{2} \sum_{i,j,k} \sum_{a} c_{\mu i} c_{\nu j} A_{akij} Z_{ak}. \quad (3.62)$$

The various quantities in eq. (3.60) might be interpreted as follows. $D_{\mu\nu}$ is a generalized density matrix which is usually called response density matrix [91-93]. $W_{\mu\nu}$ might be regarded as a generalized energy weighted density matrix and $T_{\mu\nu\sigma\rho}$ represents an effective two-particle density matrix.

Eq. (3.60) is a suitable basis for the implementation of computer programs for the calculation of analytical energy gradients within MP and QCISD theory.

## 4. Implementation of Analytical MPn and QCI Gradients

### 4.1 The Program System COLOGNE

The MPn and QCI gradient methods discussed in the previous section have been implemented into the ab initio program package COLOGNE [94]. The present version of COLOGNE has been developed at Cologne University and at the University of Göteborg during the years 1985 to 1990. While earlier versions of COLOGNE developed in the time period 1974 - 1984 [95] exclusively run on a CDC Cyber 176, the present version also runs on a CRAY XMP/48. COLOGNE is constantly improved and new features are added on a regular basis. Besides the MPn and QCI gradient methods, COLOGNE offers some other features not generally available in ab initio programs:

a) the calculation of IR and Raman intensities at the HF level [96] using analytically evaluated dipole and polarizability derivatives,

b) a direct and semi-direct SCF approach for calculation of large molecules [97-99],

c) a GVB program for calculating nondynamic correlation effects [100],

d) a pseudo-potential ansatz for calculation on transition metal compounds [101],

e) the use of puckering coordinates for optimizing and analyzing the geometries of ring compounds [102] ,

f) the calculation of CI, MPn, QCI, and CC response properties [93],

g) a topological analysis of the electron density [103-105] either for HF or correlated wave functions [93],

h) the PISA solvent model [122],

i) the IGLO- program for calculating magnetic properties of molecules [123],

j) determination of correlation energies with the LSD approach [124], and

k) graphics software for plotting molecular geometries, normal modes, IR and Raman spectra as well as various properties of the one-electron density.

In the following we will discuss only the implementation of MPn and QCI methods which are the focus of this review. Other features of COLOGNE are described in detail elsewhere [96,99].

### 4.2 MPn Calculations

MP calculations are carried out along the lines described by Pople and co-workers [41]. After the SCF part, first a partial integral transformation from the AO to the MO basis is performed. Single point energy calculations require in the case of second order MP theory the integrals of the type $\langle ij\|ab\rangle$, in third order integrals of the type $\langle ij\|kl\rangle$, $\langle ij\|ab\rangle$, $\langle ia\|jb\rangle$ and in fourth order integrals of the type $\langle ij\|ab\rangle$, $\langle ij\|ka\rangle$, $\langle ij\|ab\rangle$, $\langle ia\|jb\rangle$, and $\langle ia\|bc\rangle$. In MP3 and MP4 calculations a full transformation is avoided by evaluating the term, which requires in principle integrals of the type $\langle ab\|cd\rangle$,

$$w_3(ij,ab) = \frac{1}{2}\sum_{c,d}\langle ab\|cd\rangle a(ij,cd), \tag{4.1}$$

with the help of the AO integrals [38]. Therefore, the amplitudes $a(ij,ab)$ are partially transformed from the MO to the AO basis

$$\overline{a}(ij,\mu\nu) = \sum_{a,b} c_{\mu a}c_{\nu b}a(ij,ab), \tag{4.2}$$

then multiplied by the AO integrals,

$$\overline{w}_3(ij,\sigma\rho) = \frac{1}{2}\sum_{\mu,\nu}\langle\mu\nu\|\sigma\rho\rangle\overline{a}(ij,\mu\nu), \tag{4.3}$$

and, finally, transformed back to the MO basis

$$w_3(ij,ab) = \sum_{\sigma,\rho} c_{\sigma a}c_{\rho b}\overline{w}_3(ij,\sigma\rho). \tag{4.4}$$

The evaluation of the contribution (4.1) to the second order amplitude $w(ij,ab)$ with the AO integrals requires $O(n_{occ}^2 n_{vir}^2 n_{basis}^2)$ operations for the two transformations (eq.s (4.2) and (4.4)) and $O(n_{occ}^2 n_{basis}^4)$ operations for the multiplication (4.3). Computation of the term (4.1) using the MO integrals $\langle ab \| cd \rangle$ requires first $O(n_{basis}^5)$ multiplications for the full transformation instead of $O(n_{occ} n_{basis}^4)$ multiplication for the partial transformation and then $O(n_{occ}^2 n_{vir}^4)$ operations for multiplying the amplitudes $a(ij,ab)$ with the MO integrals. The AO algorithm as it has been suggested by Pople and coworkers [38] turns out to be very efficient when the number of virtual orbitals is large compared to the number of occupied orbitals. This condition is fulfilled in nearly all large scale calculations. In these calculations, the reduced disk space requirements of the AO algorithm are also of advantage and extend the applicability of the MPn methods significantly. All other terms, which contribute either to the amplitudes $w(ij,ab)$, $w(i,a)$, $w(ijk,abc)$, or $v_q(ij,ab)$, are calculated directly using the MO-integrals $\langle pq \| rs \rangle$ and first order amplitudes $a(ij,ab)$.

While in MP2 calculations the partial integral transformation is with $O(n_{occ} n_{vir}^4)$ operations the most expensive step, in MP3 and MP4(SDQ) calculations the multiplication of the amplitudes $a(ij,ab)$ with the two-electron integrals requires $O(n_{occ}^3 n_{vir}^3)$ and $O(n_{occ}^2 n_{vir}^4)$ operations, respectively. The additional inclusion of triple excitations increases the CPU requirements of a MP calculation further, since the evaluation of the triple amplitudes requires $O(n_{occ}^3 n_{vir}^4)$ multiplications. So far, symmetry is not used in the MP and QCI programs. It can only be exploited prior to the MPn calculation, namely in the AO integral evaluation, in the solution of the SCF problem [106], and in the integral transformation [107], in order to reduce mass storage and CPU requirements.

## 4.3 QCI calculations

The QCI method has been implemented in COLOGNE following the outline given by Pople and coworkers [52]. Contrary to the original implementation by Pople and coworkers, the simple iterative scheme based on eq.s ( 2.27), (2.28) together with a geometric extrapolation has been replaced by the more efficient DIIS method [76]. While for single point energy calculations a convergence threshold of $10^{-5}$ for the amplitudes is sufficient, higher accuracy is necessary in gradient calculations in order to get reliable results for the forces. Our experience shows that a convergence threshold of $10^{-8}$ is usually sufficient. However, due to the more stringent convergence threshold gradient calculations usually require more iterations to reach convergence in the QCI step than simple energy calculations. Therefore, methods to improve

convergence such as the DIIS method [76,77] are important and save a lot of computer time. The DIIS method is the optimal choice since it is ideally suited to speed up convergence in the last part of an iterative calculation, especially when high accuracy is required.

In most cases, the QCISD equations are solved up to the desired accuracy of $10^{-8}$ within 10 to 15 iterations. Only, in notorious cases where the single reference ansatz yields an insufficient description for the wave function, more iteration, usually up to 20 or 30, are necessary to reach convergence. However, this is not due to a failure of the QCI method itself, which has been proven successful to describe these systems (i.e. ozone [84] and carbonyl oxide [73]). It turns out that the slower convergence is more or less due to the insufficient MP2 guess for the amplitudes $a_{ij}^{ab}$ used in the first iteration. In these cases MP2 usually exaggerates the influence of correlation effects by a large amount and leads to an insufficient description of the molecular wave function.

Contrary to MPn calculations, it is more advantageous in QCI calculations to perform a full integral transformation and to calculate the term (4.5)

$$w_3{}_{ij}^{ab} = \frac{1}{2}\sum_{c,d}\langle ab\|cd\rangle a_{ij}^{cd}, \tag{4.5}$$

using the transformed integrals $\langle ab\|cd\rangle$. The AO algorithm of Pople and coworkers, which has been originally designed for MP3 calculations is more expensive since it would require a large number of two-index transformation with a total of $n_{iteration}O(n_{occ}^2 n_{basis}^4)$ multiplications. The additional costs of the AO algorithm scale with the number of iterations required for convergence while the additional amount for the full integral transformation required for the MO algorithm is independent of the number of iterations. Only, if disk space is the bottleneck of a QCI calculation, the AO algorithm of Pople and co-workers will be more advantageous due to its reduced disk space requirements. Calculation of all other terms is carried out with the same algorithm as for MP3 and MP4 calculations, except that some additional terms have to be considered in the QCI approach [52].

As in MP3 and MP4(SDQ) calculations the most expensive steps in one QCI iteration are several multiplications of the amplitudes $a_{ij}^{ab}$ with the two-electron integrals with $O(n_{occ}^3 n_{vir}^3)$ and $O(n_{occ}^2 n_{vir}^4)$ operations respectively. However, QCISD calculations are much more expensive than MP3 and MP4(SDQ) calculations since the computational costs scale with the number of iterations. The non-iterative inclusion of triple excitations requires $O(n_{occ}^3 n_{vir}^4)$ multiplications, which is a modest amount of additional

CPU time and can be routinely included in most cases. A thorough analysis of the computational costs of the QCISD and CCSD methods has recently been presented by Scuseria and Schaefer [53]. They showed that QCISD and CCSD actually require the same amount of computer time. Also, these authors suggested some improvements to the original QCI algorithm of Pople and coworkers. A similar analysis including also MPn methods and explicitly considering UHF reference functions has recently been carried out by Stanton and coworkers [108], who presented also a new efficient implementation of both the QCISD and CCSD method.

## 4.4 MPn Gradient Calculations

In principle, MP gradient calculations require the following additional steps compared to a single point energy calculation :

a) calculation of the perturbation independent matrices $L_{pq}$,$M_{pq}$, and $N_{pq}$ as well as of the two-particle density matrix $T_{\mu\nu\sigma\rho}$,

b) solution of the Z-vector equation within CPHF theory and the construction of the response density $D_{\mu\nu}$ as well as the energy-weighted response density matrix $W_{\mu\nu}$,

c) evaluation of the one- and two-electron integral derivatives, which are multiplied with the corresponding density matrix elements in order to obtain the desired forces.

We will discuss the various steps now in some more detail.

**Integral transformations required for MPn gradient calculations.** MPn gradient calculations require a larger subset of MO integrals than the corresponding MPn energy calculation. In second order, the formula for the gradients involves integrals of the type $\langle ij\|ka\rangle$ and $\langle ia\|bc\rangle$ in addition to the integrals $\langle ij\|ab\rangle$, which are sufficient to calculate the MP2 energy. Third-order gradient calculations require in addition to the integrals $\langle ij\|kl\rangle$, $\langle ij\|ab\rangle$, and $\langle ia\|jb\rangle$ also those of the type $\langle ij\|ka\rangle$ and $\langle ia\|bc\rangle$. As in the MP3 energy calculation all terms in the MP3 gradient expression, which involve the integrals $\langle ab\|cd\rangle$ can be evaluated with the AO procedure of Pople and co-workers. Fourth-order gradient calculations require the full set of MO integrals since the term involving triple amplitudes and the two-electron integrals $\langle ab\|cd\rangle$ can only be calculated efficiently in the MO basis. Only, when the MP4 ansatz is restricted to single, double, and quadruple excitations, MP4(SDQ), the full integral transformation might be avoided and these critical tems are evaluated in the same way as in third-order calculations.

The solution of the Z-vector equation requires integrals of the type $\langle ij\|ab\rangle$ and $\langle ia\|jb\rangle$. In principle, all terms needed for solving the Z-vector

equations might be computed using AO integrals (compare for example the AO-CPHF method [109,110]), but this offers in MPn gradient calculations no advantages. On the one hand, usually the MO integrals are available and, on the other hand, the AO-CPHF algorithm turns out to be more expensive than the MO-CPHF approach.

**Calculation of $L_{pq}$, $M_{pq}$, and $N_{pq}$.** The computation of the $L_{pq}$, $M_{pq}$, and $N_{pq}$ matrices is straightforward with the formulas given in section 3.5 and in appendix 2. In second- and third-order, these formulas are solely given in terms of the MO integrals and the first (MP2) or first and second order amplitudes (MP3), respectively. The formulas in fourth-order are more advantageously written in a form which contains in addition to these quantities the third-order amplitudes $v_s(ij,ab)$, $v_d(ij,ab)$, $v_t(ij,ab)$, and $x(ij,ab)$, which are actually required for the first time in MP5 energy evaluations. However, calculation of these terms is straightforward. The array $v_d(ij,ab)$ is computed in the same way as $w(ij,ab)$ using only the second-order amplitudes $w(ij,ab)$ as input rather than the first-order amplitudes $a(ij,ab)$. $v_s(ij,ab)$ is evaluated in a similar way as the contributions of the singles to the array $w_{ij}^{ab}$ in QCI theory using only $w(i,a)$ instead of $a_i^a$. The computation of $x(ij,ab)$ follows the same line as that of $v_q(ij,ab)$, the only difference being that the two-electron integrals $\langle pq\|rs\rangle$ are substituted by the amplitudes $a(ij,ab)$.

The treatment of the triples in fourth-order theory, i.e. the calculation of $v_t(ij,ab)$, $r(ijk,a)$, $s(i,abc)$, but also the computation of the contributions of the triples to $Y_1(i,j)$ and $Y_2(a,b)$,

$$t_1(i,j) = \frac{1}{12} \sum_{k,l} \sum_{a,b,c} d(ikl,abc) d(jkl,abc), \tag{4.6}$$

$$t_2(a,b) = \frac{1}{12} \sum_{i,j,k} \sum_{c,d} d(ijk,acd) d(ijk,bcd), \tag{4.7}$$

poses much severe problems. In MP4 energy calculations, the contribution due to triple excitations is evaluated using a direct algorithm, where the amplitudes are never stored on disk [40]. This procedure ensures that the full MP4 method can be applied without any restriction in large-scale calculations. The storage of the triple amplitudes would require about $n_{occ}^3 n_{vir}^3$ words of disk space and thus be a serious bottleneck in large scale calculations. For example, a calculation with about 60 basis function (e.g DZ+P calculation on a molecule with three heavy atoms) would require about 10 to 50 Mwords, while a calculation with up to 100 and more basis functions (e.g. a TZ+2P calculation on a molecule with three, four and more heavy

atoms) would require several hundreds of Mwords of disk space and, thus, they would be prohibitive even on the largest available super computer. In addition, storage of the triple amplitudes if possible would increase the I/O significantly and, therefore, slow down the performance of a MP4 gradient calculation by several orders of magnitude.

A direct algorithm for the calculation of the triple amplitudes and their contribution to the gradients is more or less mandatory [63]. However, the implementation of such an algorithm is more complicated than in MP4 energy calculations, since there are five different terms which contain the triples either in a linear or quadratic way. The terms linear in the triple excitation amplitudes, actually the arrays $v_t(ij,ab)$, $r(ijk,a)$, and $s(i,abc)$, are relatively easy to handle, since all corresponding contributions can be immediately formed when the triple amplitudes are evaluated. More difficult are the quadratic terms, $t_1(i,j)$ and $t_2(a,b)$, since two different amplitudes $d(ijk,abc)$ are required simultaneously in order to evaluate the corresponding contribution. Fortunately, the required amplitudes differ only in one index, either in one of the labels of the occupied or the virtual orbitals and a direct computation of the two $t$-terms is possible. In the original implementation of MP4(T) energy calculation of Pople and co-workers [40], all triple amplitudes for fixed labels $a$, $b$, and $c$ are calculated and processed together. Hence, computation of $t_1(i,j)$ causes no problems. To overcome the difficulties in calculating the second $t$-matrix, $t_2(a,b)$, where amplitudes differing in one virtual orbital index are multiplied, one recalculates the triple amplitudes in such a way that now all amplitudes with fixed labels $i$, $j$, and $k$ [63] are obtained together. This recalculation of the triple amplitudes with a reversed loop structure ensures that a direct algorithm can be applied in full MP4 gradient calculation. However, it increases the computational costs by the order of $n_{occ}^3 n_{vir}^4$ operations. Nevertheless, the analytical procedure remains to be more efficient than the corresponding finite differentiation scheme.

**Calculation of the two-particle density matrix $T_{\mu\nu\sigma\rho}$.** In all MPn gradient calculations the two-particle density matrix $T_{\mu\nu\sigma\rho}$ is first evaluated in the MO basis using the MO integrals and the various amplitudes and, then, transformed to the AO basis. The expensive transformation step requires $O(n_{basis}^5)$ operations, but is independent of the number of perturbations. The alternative choice to multiply the two-particle density matrix in the MO basis with the integral derivatives includes a full transformation of the AO integral derivatives to the MO basis. It scales with the number of perturbations, is more expensive, requires in addition the storage of integral derivatives on disk, and, therefore, is not recommended.

MP3 and MP4 gradient calculations require for $T_{\mu\nu\sigma\rho}$ a full transforma-

tion from the MO to the AO basis and $O(n_{basis}^5)$ multiplications. In MP2 gradient calculations, a partial transformation with $O(n_{occ}n_{basis}^4)$ operations is sufficient, since the indices p,q (r,s) of $T_{pqrs}$ run only over occupied (virtual) orbitals.

The transformed two-particle density matrix $T_{\mu\nu\sigma\rho}$ is stored on disk for latter use in the integral derivative calculation to form the appropriate contribution to the forces. In order to use a direct algorithm, which avoids the storage of the integral derivatives on disk, it must be ensured that the elements of $T_{\mu\nu\sigma\rho}$ are stored in the same (or at least a similar) order as the integral derivatives are evaluated. The transformation step produces an ordered list of $T_{\mu\nu\sigma\rho}$ elements with $\mu \geq \nu$, $\sigma \geq \rho$ and $[\mu\nu] \geq [\sigma\rho]$, while the integral derivatives are calculated in batches where all integral with indices belonging to the same shell combinations are computed together. In small calculations, the whole $T_{\mu\nu\sigma\rho}$-matrix can be kept in core memory and no problem exists to pick up the required $T_{\mu\nu\sigma\rho}$ elements. In large scale calculations, the whole $T_{\mu\nu\sigma\rho}$-matrix does no longer fit into core memory. However, it is sufficient that only this part of the $T_{\mu\nu\sigma\rho}$-matrix is kept in the core which contains for the indices $\mu$ of the first shell $I$ all possible indices $\nu$, $\sigma$, and $\rho$. With at most 6 or 10 basis functions per shell (i.e, 6 d- or 10 f-functions) such a procedure requires approximately $6n_{basis}^3/2$ or $10n_{basis}^3/2$ words of core memory, an amount, which on modern super computers is available even in large scale calculations. In this case, no preprocessing of the ordered list of $T_{\mu\nu\sigma\rho}$ elements is necessary. However, if there is not enough core memory for this procedure, the only solution will be a sort of the $T_{\mu\nu\sigma\rho}$ elements prior to the integral derivative calculation. By using an algorithm due to Yoshimine [111] this sort requires two additional reads and writes of the $T_{\mu\nu\sigma\rho}$ matrix. Since the sort of the $T_{\mu\nu\sigma\rho}$ elements increases the I/O requirements of a MPn gradient calculation, it should be avoided, whenever possible.

**Solution of the z-vector equations in CPHF theory.** The z-vector equations are solved using a procedure Pople and coworkers [18] originally developed for the solution of the CPHF equations. The z-vector $Z_{ai}$ is expanded in a set of orthonormal vectors which are obtained by multiplying $L_{ai}/(\varepsilon_i - \varepsilon_a)$ n times with $A_{aibj}/(\varepsilon_i - \varepsilon_a)$ and then performing a Schmidt-orthogonalization. The expansion coefficients are determined by solving a small set of linear equations. The required accuracy of $10^{-8}$ for the z-vector is usually achieved in 10 to 15 iterations. The converged z-vector is used to construct the response density and energy weighted response density matrices in the MO representation. Both matrices are transformed in the AO representation which is needed for multiplication with the AO integral derivatives

to obtain the corresponding contributions to the energy gradients.

**Evaluation of the integral derivatives.** The contribution of integral derivatives to the forces are calculated using a direct algorithm. The one-electron integral derivatives $h^{\lambda}_{\mu\nu}$ and $S^{\lambda}_{\mu\nu}$ are multiplied with the total density and the total energy weighted matrix, respectively, while the two-electron integral derivatives are multiplied with the corresponding elements of the $T_{\mu\nu\sigma\rho}$ matrix and are used to build the two-electron contribution of the Fock-matrix derivatives $F^{(\lambda)}_{\mu\nu}$. Note that all contributions to the forces including the HF contribution must be considered in order to get the total force. When one-electron properties are evaluated, only the response density matrix $D_{\mu\nu}$ is multiplied with the corresponding property integrals, provided the basis is chosen to be independent of the corresponding perturbation.

The costs of an analytical evaluation of energy gradients at the various levels of MP theory are independent of the number of perturbations. They scale in a similar way with the number of occupied and virtual orbitals as the energy calculations and usually a gradient calculation requires about 2-3 times the costs of the foregoing energy evaluation.

## 4.5 QCI Gradient Calculations

QCISD and QCISD(T) gradient calculations are carried out using the same strategies as in the case of MPn gradient calculations. The only additional step is the solution of the z-vector equations within CPQCISD theory. Detailed formulas for the z-vector equations are given in appendix 2. However, evaluation of most arrays needed is straightforward and can be carried out with the same programs used for the solution of the QCI equations. The arrays $w[z]^a_i$ and $w[z]^{ab}_{ij}$ are calculated in the same way as $w^a_i$ and $w^{ab}_{ij}$, only with the z-amplitudes $z^a_i$ and $z^{ab}_{ij}$ as input instead of the QCISD amplitudes $a^a_i$ and $a^{ab}_{ij}$. $v[z]^a_i$ and $v[z]^{ab}_{ij}$ are closely related to the quadratic arrays $v^a_i$ and $v^{ab}_{ij}$. Note that $v^a_i$ and $v^{ab}_{ij}$ are quadratic arrays, while $v[z]^a_i$ and $v[z]^{ab}_{ij}$ are actually linear with respect to the z-amplitudes. Therefore, it is possible to precalculate and store some intermediate arrays in order to reduce the computational requirements. The only new term in the z-vector equation is $y[z]^{ab}_{ij}$ , but computation of this term causes no severe problems.

The z-vector equations within CPQCISD theory are solved in the same way as the QCISD equations. Again, convergence is accelerated using a DIIS procedure. As initial guess either the negative MP2 amplitudes or the negative QCISD amplitudes might be used.

$$z^{a\,(0)}_i = 0 \qquad \text{or} \qquad z^{a\,(0)}_i = -a^a_i \tag{4.8}$$

$$z_{ij}^{ab(0)} = -a(ij,ab) \qquad \text{or} \qquad z_{ij}^{ab(0)} = -a_{ij}^{ab}. \tag{4.9}$$

Our experience shows that the latter choice is more advantageous and saves usually a few iterations compared to the MP2 guess. When triple excitations are considered, the initial guess must be modified by subtracting $\tilde{v}_i^a$ and $\tilde{v}_{ij}^{ab}$, respectively

$$z_i^{a(0)} = -a_i^a - \tilde{v}_i^a/(\varepsilon_i - \varepsilon_a), \tag{4.10}$$

$$z_{ij}^{ab(0)} = -a_{ij}^{ab} - \tilde{v}_{ij}^{ab}/(\varepsilon_i + \varepsilon_j - \varepsilon_a - \varepsilon_b). \tag{4.11}$$

Since the z-vector equations are linear their solution usually requires less operations than the solution of the corresponding QCISD equations. The array $x_{ij}^{ab}$ which includes both QCISD and z-amplitudes is evaluated after the solution of the z-vector equation using an algorithm similar to the evaluation of $v_{ij}^{ab}$ and $y[z]_{ij}^{ab}$.

The calculation of the matrices $L_{pq}$, $M_{pq}$, $N_{pq}$, and $T_{\mu\nu\sigma\rho}$, the solution of the z-vector equation in CPHF theory and the integral derivative calculation are carried out after the z-amplitudes have been determined, since in this case both the QCISD amplitudes and the z-amplitudes are required.

As in MPn gradient calculations the costs of a QCISD gradient calculation are very similar to those of the corresponding energy evaluation. Actually, since the equations for the z-amplitudes are only linear in $z_{ij}^{ab}$ while the original QCI equations are quadratic in $a_{ij}^{ab}$, the ratio of the computational costs for energy and gradient calculations are for the QCISD method usually more favorable than for MPn methods. Gradient calculations at the QCISD level usually require about 1-2 times the expenses of a single QCISD energy calculation thus proving the efficiency of analytical gradient methods for this type of quantum chemical methods.

## 5. Calculation of Molecular Properties at MPn and QCI Using Analytical Gradients

### 5.1 Response Densities and other One-Electron Properties

A one-electron property $O$ of a molecule can be defined as the response of the molecule to an external perturbation $\lambda$. The Hamiltonian $\hat{\mathbf{H}}$ under

the impact of the perturbation has to be corrected by the term $\lambda\hat{O}$ where $\hat{O}$ is the quantum mechanical operator which corresponds to the property $O$

$$\hat{\mathbf{H}}(\lambda) = \hat{\mathbf{H}}(0) + \lambda\hat{\mathbf{O}}. \tag{5.1}$$

The energy in the presence of the perturbation depends on $\lambda$ and, therefore, it can be expanded for small $\lambda$ in a power series

$$E(\lambda) = E(\lambda = 0) + \lambda\frac{dE}{d\lambda}|_{\lambda=0} + \frac{1}{2}\lambda^2\frac{d^2E}{d\lambda^2}|_{\lambda=0} + \ldots \tag{5.2}$$

Applying the Hellmann-Feynman theorem leads to

$$\frac{dE}{d\lambda}|_{\lambda=0} = \langle\Psi|\hat{\mathbf{O}}|\Psi\rangle. \tag{5.3}$$

Eq. (5.3) shows that the definition of an one-electron property $O$ as a response to an external perturbation requires the evaluation of an energy derivative, namely the derivative of the energy with respect to the external perturbation. The value obtained for $O$ in this way will be identical to the expectation value $\langle\Psi|\hat{\mathbf{O}}|\Psi\rangle$ of the corresponding operator $\hat{O}$ as long as the Hellmann-Feynman theorem is satisfied. In cases where the Hellmann-Feynman theorem does not hold, the energy derivative approach should be the preferred way of calculating one-electron properties. In addition, the energy derivative approach offers the possibility to calculate one-electron properties even for methods for which a wave function is not defined and expectation values cannot be evaluated.

The total electron density distribution $\rho(\mathbf{r_p})$ at a point $\mathbf{r_p}$ is the response of the molecule to a perturbation $\lambda$ that corresponds to the one-electron operator $\delta(\mathbf{r_p} - \mathbf{r})$, which is the Dirac delta operator.

$$\frac{dE(\lambda)}{d\lambda}|_{\lambda=0} = \langle\Psi|\delta(\mathbf{r_p} - \mathbf{r})|\Psi\rangle = \rho(\mathbf{r_p}). \tag{5.4}$$

When $\rho(\mathbf{r})$ is expanded in terms of basis functions used to calculate energy and wave function eq. (5.4) leads to

$$\frac{dE(\lambda)}{d\lambda}|_{\lambda=0} = \rho(\mathbf{r}) = \sum_{\mu\nu}\mathbf{D}_{\mu\nu}\chi_\mu(\mathbf{r})\chi_\nu(\mathbf{r}), \tag{5.5}$$

where $\mathbf{D}$ defines the response density matrix according to eq. (3.61) in Section 3. For a correlated wave function $\mathbf{D}$ can be decomposed into

$$\mathbf{D} = \mathbf{D}^{\mathbf{SCF}} + \mathbf{D}^{\mathbf{corr}} \tag{5.6}$$

indicating that **D** contains a SCF and a correlation part. In the same way $\rho(\mathbf{r_p})$ is expressed as a sum of the SCF density and a correlation correction

$$\rho(\mathbf{r})^{res} = \rho(\mathbf{r})^{SCF} + \rho(\mathbf{r})^{corr} \tag{5.7}$$

Using eq. (3.60) it is easily shown that one-electron properties calculated as energy derivatives are closely related to the response density. Provided that the basis set chosen is independent of the perturbation $\lambda$ the corresponding one-electron property is simply given as the product of the response density matrix **D** with the corresponding property integrals.

$$O = \frac{dE(\lambda)}{d\lambda}|_{\lambda=0} = \sum_{\mu\nu} \mathbf{D}_{\mu\nu}\langle\chi_\mu|\hat{\mathbf{O}}|\chi_\nu\rangle. \tag{5.8}$$

In the following $\rho(\mathbf{r})$ and one-electron properties are investigated at various levels of theory using basis sets of valence DZ+P and valence TZ+2P quality [118]. As suitable test molecule carbon monosulfide, CS, has been chosen since its electron density distribution is sensitive to correlation effects. However, similar effects have been found for other molecules investigated recently [93].

For CS, one may expect that C carries a small negative and S a small positive charge in accordance with the fact that the electronegativity of C is slightly larger than that of S (2.50 vs. 2.44 on the Allred-Rochow scale). On the other hand, bonding in CS may be close to a triple bond since one of the electron lone pairs of S can be shared between the two atoms thus establishing a semipolar bond beside the two normal bonds.

$$C^{\delta-} \equiv S^{\delta+}$$

If this is true , C will carry a much larger negative charge and S a much larger positive charge as it can be expected from comparision of the electronegativities. However, HF theory predicts relatively small partial charges for C and S suggesting that there is no or only weak semipolar bonding. As a consequence the calculated dipole moment of CS is just 1.77 Debye (HF/MC-311G(2d)) while the experimental one is 1.98 Debye [112] (compare with Table 1). Obviously, HF underestimates the extent of semipolar bonding.

In Figure 1, $\rho(\mathbf{r})^{corr}(\mathrm{MP2}) = \rho(\mathbf{r})^{res}(\mathrm{MP2}) - \rho(\mathbf{r})^{res}(\mathrm{HF})$ of carbon monsulfide, CS, calculated with a VTZ + 2P basis set is given in form of a contour line diagram. Solid (dashed) contour lines are in regions of positive (negative) response densities. Obviously, correlation corrections at the MP2

**Table 1.** Energies, bond lengths, charges, dipole moments, and quadrupole moments of CS calculated with the MC-311G(2d) Basis.[a]

| Method | Energy | R(CS) | Charge at S | Dipole Moment | Quadrupole Moment $Q_{xx} = Q_{yy}$ | $Q_{zz}$ |
|---|---|---|---|---|---|---|
| HF | -435.341729 | 1.5132 | 188.3 | -1.773 | -18.64 | -20.33 |
| MP2 | -435.758863 | 1.5413 | 273.4 | -2.308 | -18.38 | -21.04 |
| MP3 | -435.767744 | 1.5269 | 253.2 | -2.111 | -18.45 | -20.75 |
| MP4(DQ) | -435.767665 | 1.5295 | 249.5 | -2.106 | -18.44 | -20.68 |
| MP4(SDQ) | -435.775175 | 1.5418 | 238.8 | -2.063 | -18.44 | -20.72 |
| MP4(SDTQ) | -435.797700 | 1.5646 | 240.3 | -2.111 | -18.42 | -20.92 |
| CCD | -435.768000 | 1.5298 | 248.4 | -2.086 | -18.45 | -20.73 |
| QCISD | -435.775721 | 1.5421 | 235.3 | -2.010 | -18.46 | -20.66 |
| QCISD(T) | -435.793730 | 1.5506 | 239.5 | -2.028 | -18.45 | -20.73 |

[a] Energy in Hartree, bond length in Å, charge in melectron, dipole moment in Debye, quadrupole moment in Debye Å.

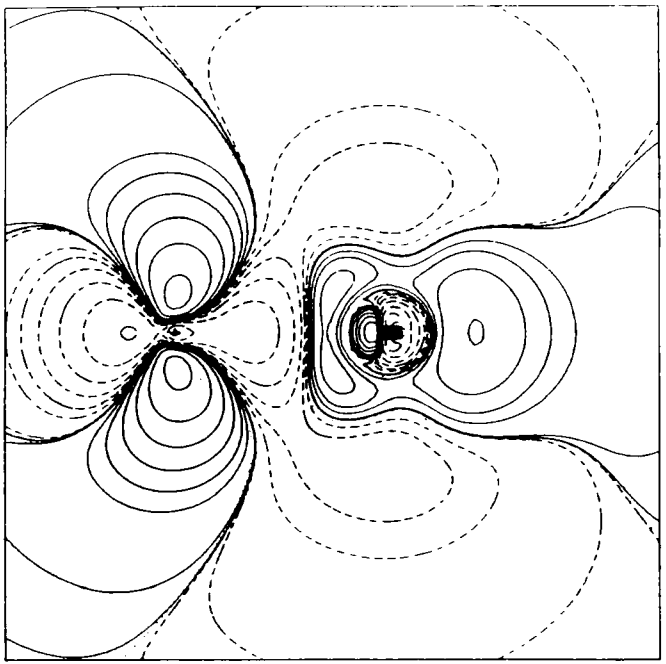



**Figure 1.** Contour line diagram of the difference electron density distribution $\Delta\rho(\mathbf{r})^{res}(MP2) = \rho(\mathbf{r})^{res}(MP2) - \rho(\mathbf{r})HF = \rho(\mathbf{r})^{corr}(MP2)$ of CS calculated with the 6-311G(2d) basis. Solid (dashed) contour lines are in regions of positive (negative) difference densities. The positions of the C and the S nucleus are indicated.

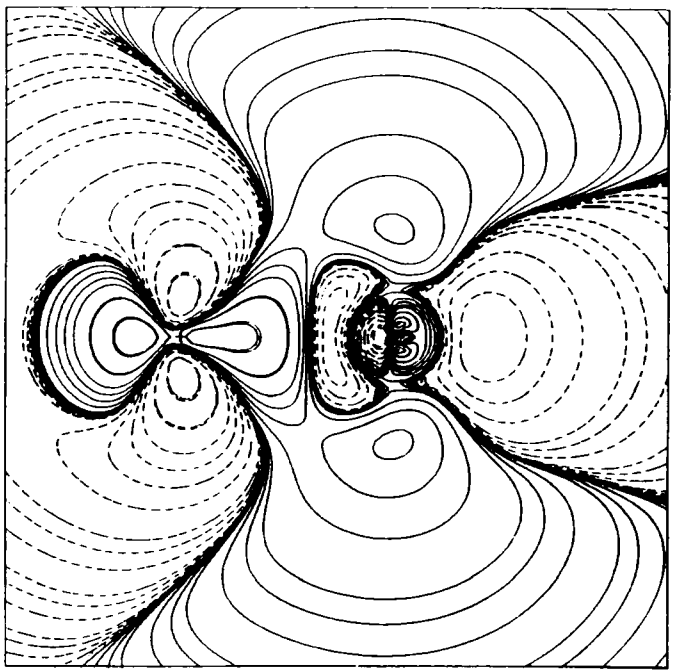



**Figure 2.** Contour line diagram of the difference electron density distribution $\Delta\rho(\mathbf{r})^{res}(MP3) = \rho(\mathbf{r})^{res}(MP3) - \rho(\mathbf{r})^{res}(MP2)$ of CS calculated with the 6-311G(2d) basis. Solid (dashed) contour lines are in regions of positive (negative) difference densities. The positions of the C and the S nucleus are indicated.

level lead to a transfer of $\pi$ electronic charge from the sulfur to the carbon atom. At the same time, $\sigma$ electronic charge is decreased at the C atom while it is increased in the valence shell of the S atom, both in the bonding and the lone pair region. Closer inspection of diagram 1 as well as an analysis of the corresponding Mulliken population values reveals that the transfer of $\pi$-charge from S to C depopulates the valence region of S. However in the $2p\pi$ core region of S, there is a build up of $\pi$-charge which envelopes another region of charge decrease. Thus, a complex pattern of alternating charge decrease and increase from valence to inner core region of S and from left to right along the CS bond axis results (Figure 1).

From inspection of Figure 1 and analysis of the response density contributions to the orbital populations it becomes clear that left-right correlation of $p\pi$ electrons is the most important correction of the HF electron distribution at the MP2 level of theory. They lead to an increase (decrease) of the negative (positive) charge at C (S). Less important but substantial are angular and in-out correlation.

The same features of $\rho(\mathbf{r})^{res}$ are found at the MP3, MP4(SDQ), MP4(SD TQ), CCD, QCISD, and QCISD(T) level. Qualitatively, there are no differences in the corresponding response densities which means that MP2 already includes the most important correlation corrections. In order to analyze the different correlation effects covered by the various methods difference response density plots have to be investigated.

In Figure 2, the difference density $\Delta\rho(\mathrm{MP3}) = \rho^{res}(\mathrm{MP3}) - \rho^{res}(\mathrm{MP2}) = \rho^{corr}(\mathrm{MP3}) - \rho^{corr}(\mathrm{MP2})$ is shown. It reveals that MP3 correlation corrections reduce MP2 effects, i.e. the MP2 response density is slightly changed back in the direction of the HF electron density distribution. Changes comprise a $\pi$ electron transfer from C to S, transfer of $\sigma$ electrons from outer valence functions to inner valence functions at C and vice versa at S, a transfer of $\sigma$ electronic charge from S to C and depopulation (population) of the lone-pair region at S (C). These changes lead to a decrease of the CS bond polarity and decreased atomic charges relative to MP2. (Table 1)

Clearly, at MP3 the correlation effects of the double excitations are reduced relative to those calculated at the MP2 level. As has been outlined before this is due to the fact that at MP3 couplings between double excitations are introduced and, therefore, correlation between two electrons is no longer independent of the correlation between other electron pairs. At MP2 only interactions of the double excitations with the ground state wave function are considered and, as a consequence, correlation between two electrons is exaggerated.

In Figure 3, the calculated difference response density $\Delta\rho(\mathrm{MP4(SDQ)}) =$

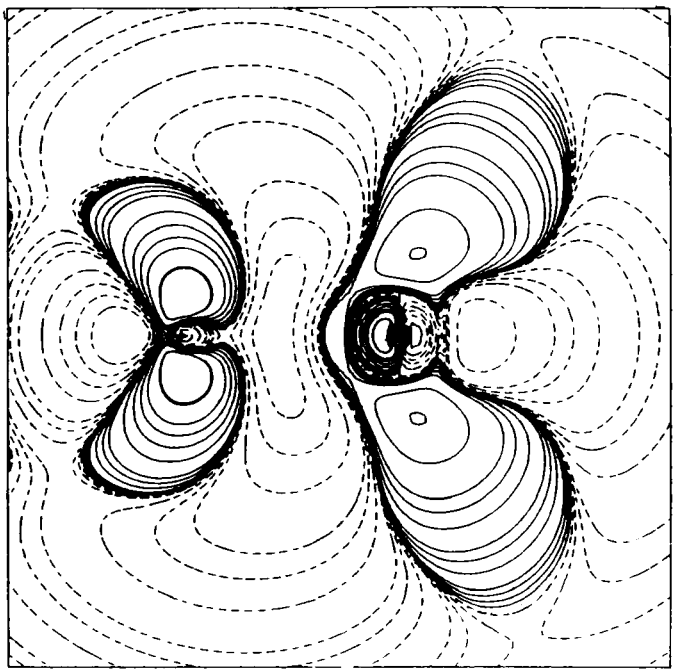



**Figure 3.** Contour line diagram of the difference electron density distribution $\Delta\rho(\mathbf{r})^{res}(MP4(SDQ)) = \rho(\mathbf{r})^{res}(MP4(SDQ)) - \rho(\mathbf{r})^{res}(MP3)$ of CS calculated with the 6-311G(2d) basis. Solid (dashed) contour lines are in regions of positive (negative) difference densities. The positions of the C and the S nucleus are indicated.

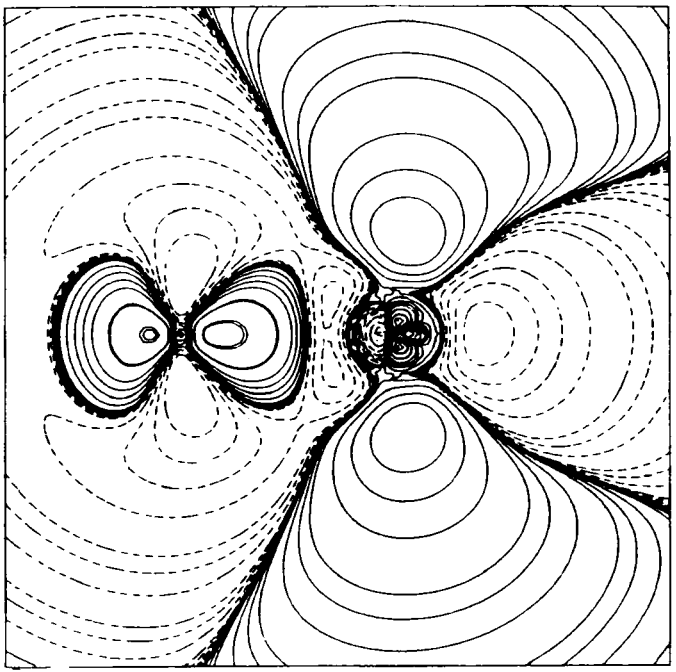



**Figure 4.** Contour line diagram of the difference electron density distribution $\rho(\mathbf{r})^{res}(MP4(SDQ)) - \rho(\mathbf{r})^{res}(MP2)$ of CS calculated with the 6-311G(2d) basis. Solid (dashed) contour lines are in regions of positive (negative) difference densities. The positions of the C and the S nucleus are indicated.

$\rho^{res}(\text{MP4(SDQ)}) - \rho^{res}(\text{MP3})$ of CS is given. Its general features are similar to those of the MP2 response density, which means that MP4(SDQ) correlation corrections are in the same direction than MP2 correlation corrections. As a consequence, correlation corrections to charges, dipole moment, and other molecular properties are larger than those calculated at the MP3 level of theory. Apart from this, there are significant differences in the charge distribution at the MP4(SDQ) level. Both bonding and lone pair regions are depopulated relative to the MP3 charge distribution. Charge concentrates in the C $2p\pi$ and S $2p\pi$ and $3p\pi$ region in such a way that electron repulsion is minimized (see Figure 3).

The charge distribution at the MP4(SDQ) level is even better understood when comparing it with the MP2 charge distribution with the help of the difference response density $\rho^{res}(\text{MP4(SDQ)}) - \rho^{res}(\text{MP2})$ shown in Figure 4. There, one sees that at MP4(SDQ) the charge transfer to the C $2p\pi$ orbitals is smaller than at MP2. Hence, the pattern of changes is similar to that obtained at the MP3 level. Obviously, corrections due to single, double, and quadruple excitations at the MP4 level are between those obtained at the MP2 and the MP3 level.

Figure 5 gives the changes in the response density distribution that are due to triple excitations at the MP4 level of theory. They are in the same direction than those obtained from S, D, and Q excitations, i.e. they increase the charge transfer from the S to the C atom. A detailed analysis of calculated charges and dipole moments shows that the changes due to triples are larger than those of the S, D, and Q excitations at the MP4 level thus proving the importance of T excitations for multiple bonded systems.

The MP4 level is as far as we can go in MP perturbation theory. The results obtained clearly indicate that still considerable changes have to be expected for MP5, possibly correcting the MP4 response density back into the direction of the MP3 response density. This prediction is partially confirmed by the response density obtained at the QCISD and QCISD(T) level of theory. QCI is correct to fourth order perturbation theory in the space of the S, D, and Q excitations while QCISD(T) is correct to fourth order in the complete space of S, D, T, and Q excitations. Apart from that both methods contain important terms that first appear at MP5 [55]. Hence, they should indicate whether correlation effects are overestimated at MP4.

Figure 6 gives the difference response density $\Delta\rho(\text{QCISD}) = \rho^{res}(\text{QCISD}) - \rho^{res}(\text{MP4(SDQ)})$. It indicates that the MP4(SDQ) response density is primarily corrected by a transfer of $\pi$ electrons from C to S. As a consequence, the QCISD atomic charge of S is less positive, the bond polarity and, thereby, the CS dipole moment smaller than that obtained at the MP4(SDQ) level.

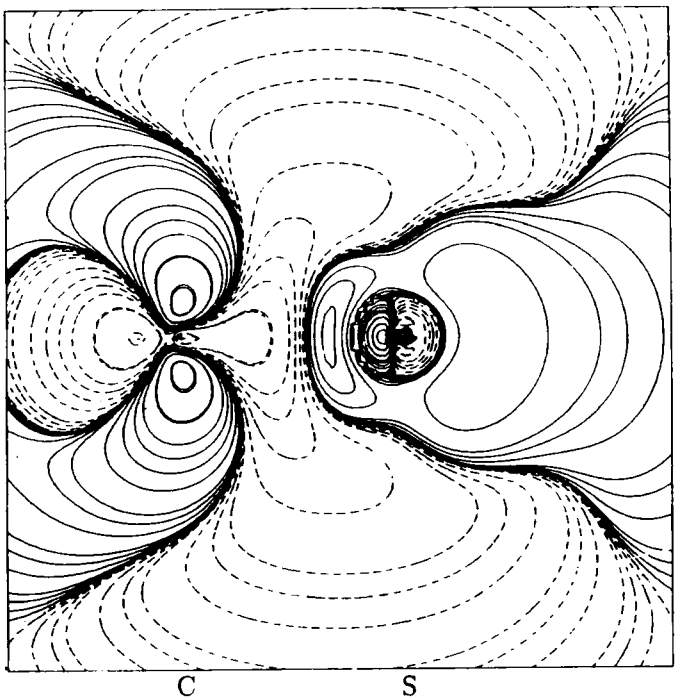



**Figure 5.** Contour line diagram of the difference electron density distribution $\Delta\rho(\mathbf{r})^{res}(MP4(SDQT)) = \rho(\mathbf{r})^{res}(MP4(SDQT)) - \rho(\mathbf{r})^{res}(MP4(SDQ))$ of CS calculated with the 6-311G(2d) basis. Solid (dashed) contour lines are in regions of positive (negative) difference densities. The positions of the C and the S nucleus are indicated.

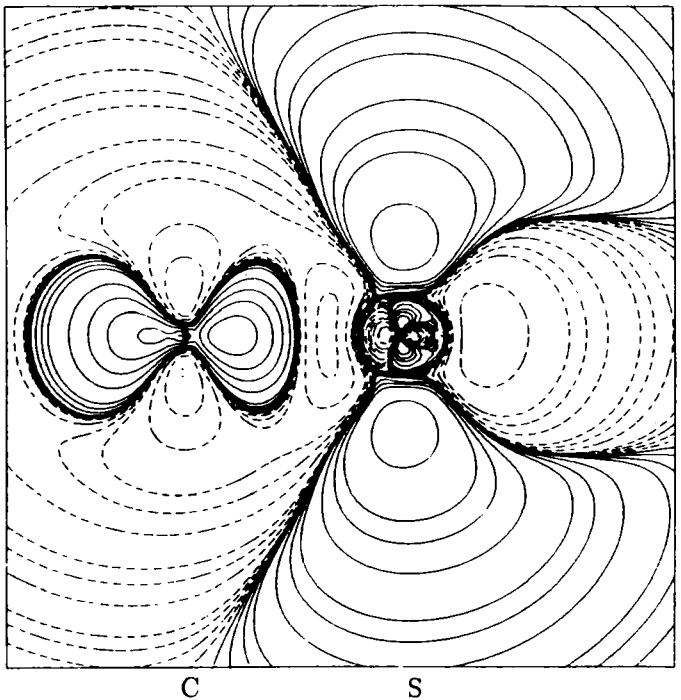



**Figure 6.** Contour line diagram of the difference electron density distribution $\Delta\rho(\mathbf{r})^{res}(QCISD) = \rho(\mathbf{r})^{res}(QCISD)) - \rho(\mathbf{r})^{res}(MP4(SDQ))$ of CS calculated with the 6-311G(2d) basis. Solid (dashed) contour lines are in regions of positive (negative) difference densities. The positions of the C and the S nucleus are indicated.

The difference response density shown in Figure 6 is similar to that obtained for MP3 (Figure 2) and, therefore, it is reasonable to conclude that the coupling of S, D, and Q excitations at MP5 as well as the infinite order effects contained in QCISD lead to a correction of MP4(SDQ) back in the direction of MP3. The same conclusion is also true for the response density calculated at the QCISD(T) level as can be seen from the difference response density $\Delta\rho(\mathrm{QCISD(T)}) = \rho^{res}(\mathrm{QCISD(T)}) - \rho^{res}(\mathrm{MP4(SDTQ)})$ shown in Figure 7. As a matter of fact the contour line diagrams in Figures 6 and 7 are very similar.

Nevertheless, the T corrections both at MP4 and at QCI are in the same direction which is reflected by the difference response density $\Delta\rho(\mathrm{QCISD(T)}) = \rho^{res}(\mathrm{QCISD(T)}) - \rho^{res}(\mathrm{QCISD})$ given in Figure 8. They lead to transfer of $\pi$ charge from S to C thus increasing gross atomic charges, bond polarity and dipole moment. Obviously, T effects are exaggerated at the MP4 level (compare Figure 7). A better account of T effects is given at QCISD(T).

The changes in the response density distribution of CS are parallel to calculated changes in atomic charges, dipole moment, quadrupole moment, and other one-electron properties, some of which are listed in Table 1. Figure 9 and 10 depict changes in atomic charge, dipole moment, and components of the quadrupole moment in dependence of the method. The multipole moments of CS oscillate in dependence of the order of perturbation theory applied where HF and MP2 results often represent upper and lower bound of computed values. Oscillations in calculated properties are observed in many cases [93]. Figure 11 gives as another example computed values of the CO dipole moment obtained at different levels of theory for a VDZ+P and a VTZ+2P basis set. Figure 11 also indicates that oscillations are largely independent of the basis set used.

Comparison of Figure 9, 10 and 11 leads to the following conclusions:

(1) The largest part of the correlation corrections to response properties is recovered at the MP2 level, but higher order effects are still considerable and cannot be neglected if accurate one-electron properties are needed.

(2) Correlation corrections due to D excitations are exaggerated at the MP2 level. They are reduced at the MP3 level where couplings between D excitations are first introduced.

(3) Single excitations lead only to relatively small changes in calculated response properties. This is opposite to the importance of S excitations when calculating one-electron properties as expectation values at the CI level [113]. There, S excitations are important to account for orbital relaxation effects which are covered within the energy derivative approach by solving the CPHF equations or the corresponding z-vector equation.

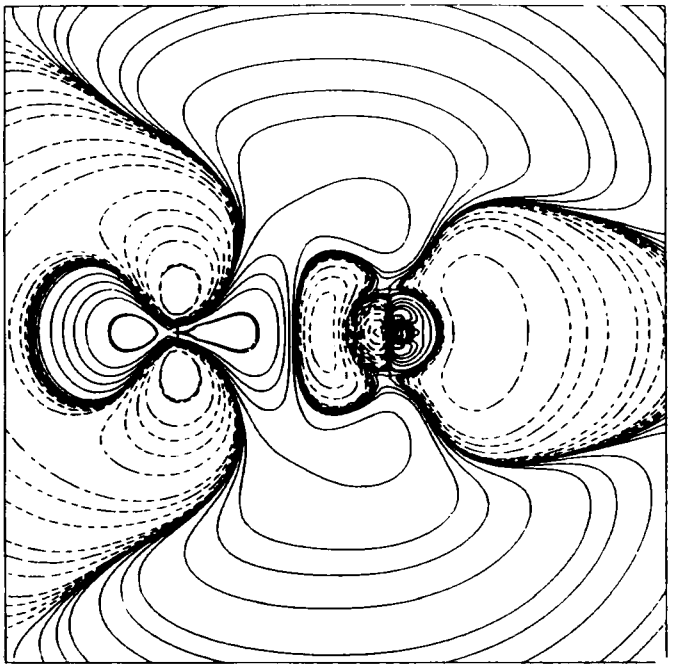



**Figure 7.** Contour line diagram of the difference electron density distribution $\Delta\rho(\mathbf{r})^{res}(QCISD(T)) = \rho(\mathbf{r})^{res}(QCISD(T)) - \rho(\mathbf{r})^{res}(MP4(SDQT))$ of CS calculated with the 6-311G(2d) basis. Solid (dashed) contour lines are in regions of positive (negative) difference densities. The positions of the C and the S nucleus are indicated.

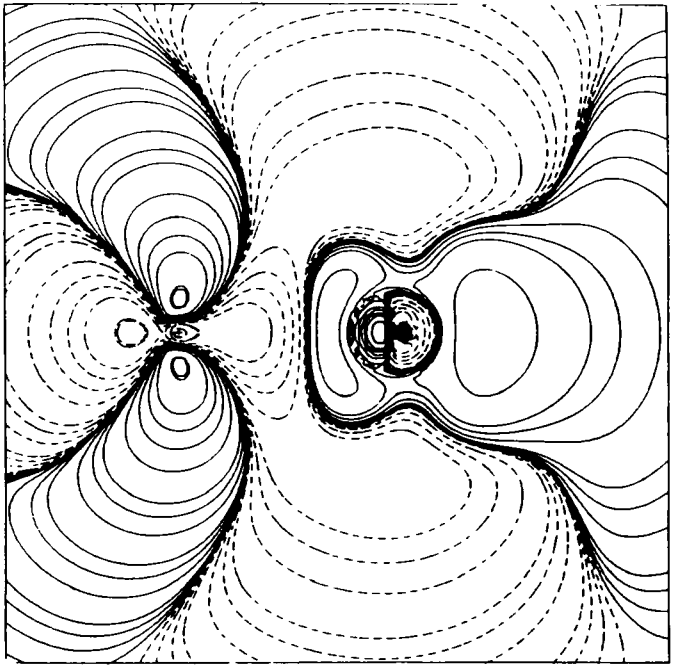



**Figure 8.** Contour line diagram of the difference electron density distribution $\rho(\mathbf{r})^{res}(QCISD(T)) - \rho(\mathbf{r})^{res}(QCISD)$ of CS calculated with the 6-311G(2d) basis. Solid (dashed) contour lines are in regions of positive (negative) difference densities. The positions of the C and the S nucleus are indicated.

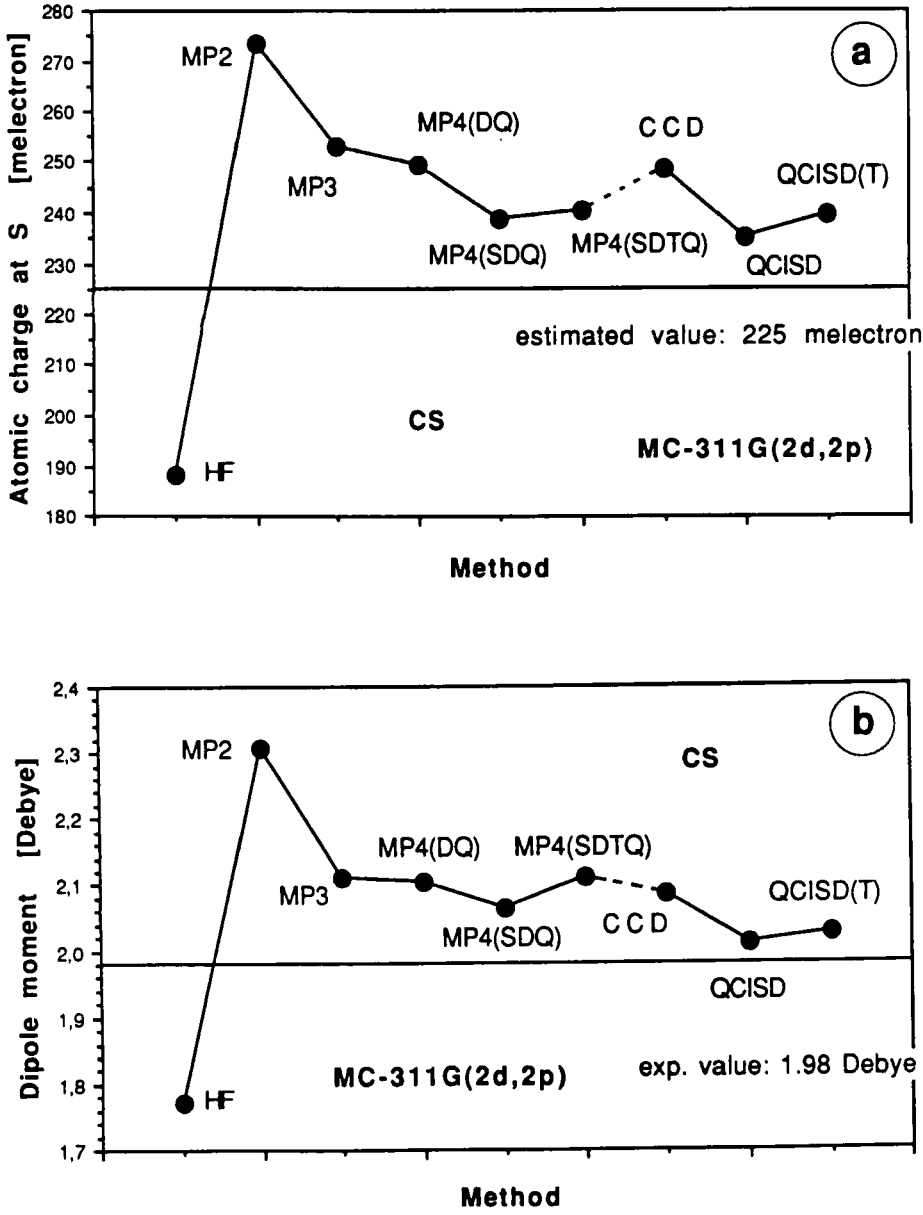



**Figure 9.** Dependence of calculated one-electron properties on the method used. (a) Charge of the S atom in carbon monosulfide. (b) Dipole moment of carbon monosulfide (6-311G(2d,2p) calculations).

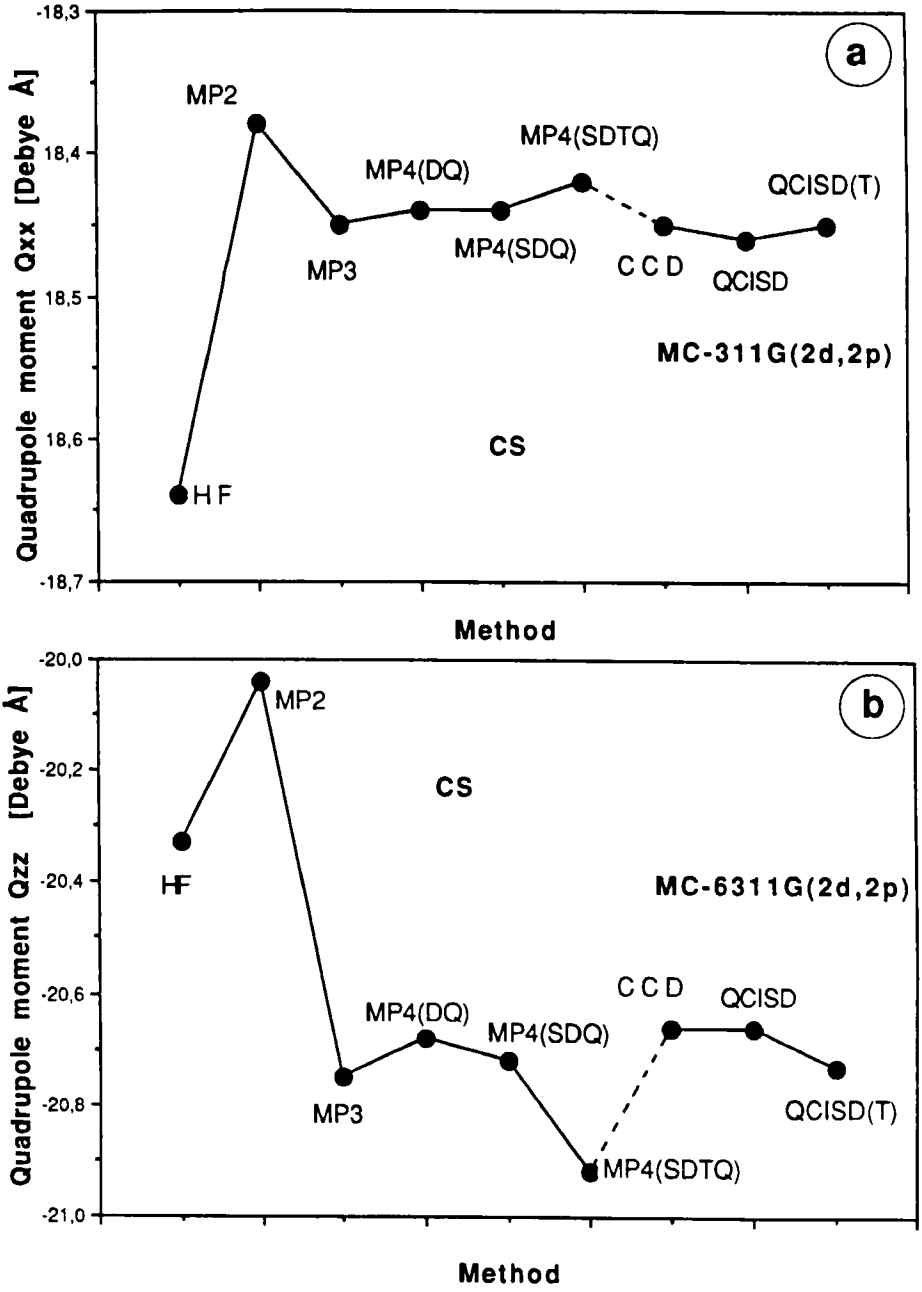



**Figure 10.** Dependence of calculated quadrupole moment Q of carbon monosulfide, CS, on the method used. (a) $Q_{xx}$. (b) $Q_{zz}$ (6-311G(2d,2p) calculations; z-axis is identical with molecular axis).

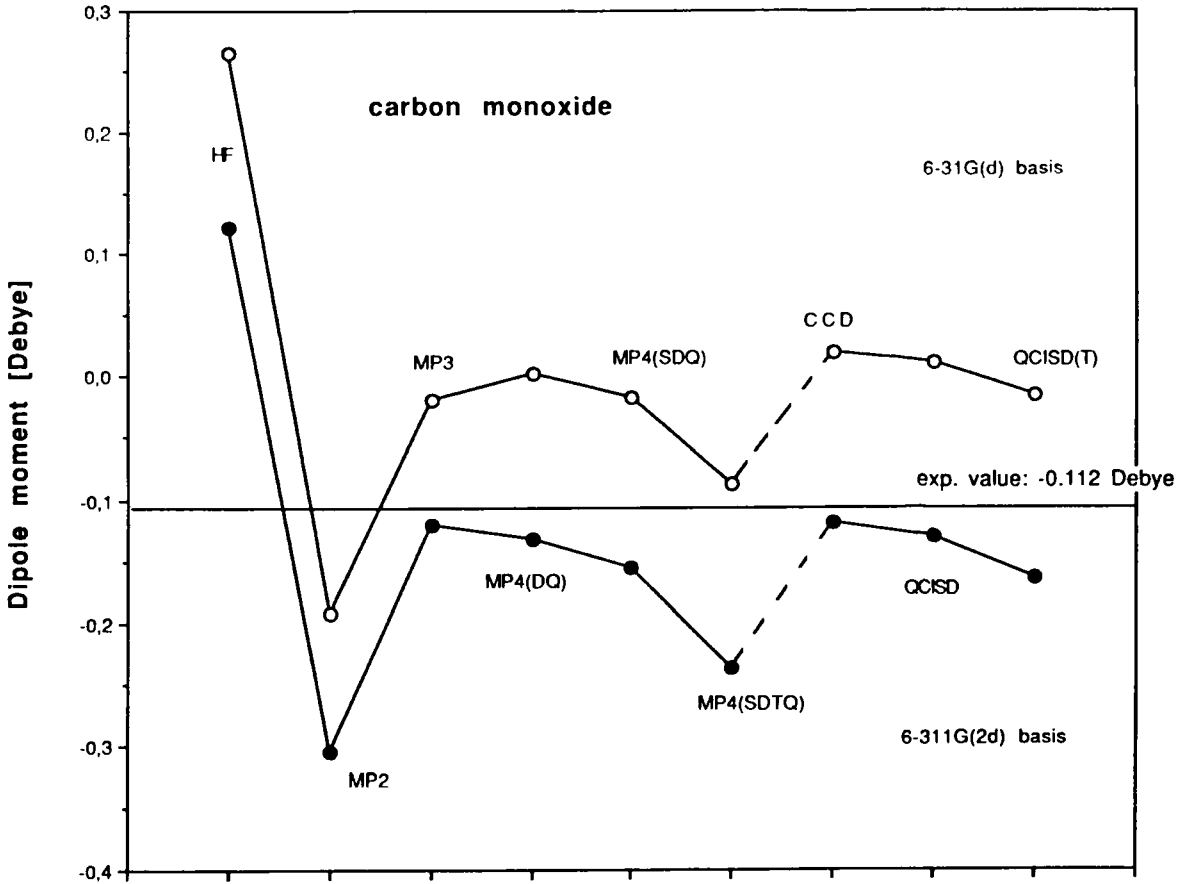



**Figure 11.** Dependence of the dipole moment of carbon monoxide, CO, on method and basis set.

(4) The influence of T excitations at MP4 is relatively large, at least for molecules with multiple bonds. However, comparison with QCISD(T) suggests that T effects are somewhat exaggerated at the MP4 level. This may also be true for S and Q effects at MP4 since couplings between these excitations are not considered at this level of theory.

(5) It is most likely that MP5, which introduces couplings between SDTQ excitations corrects MP4 values back in the direction of the MP3 result. On the other hand, MP6, which introduces P and H excitations may lead to response properties closer to MP4 than MP3 values. In other words, oscillations of response property values may only slowly damp out at the MPn level.

(6) Calculated response property values from CC and QCI methods that contain infinite order effects seem to converge to a limiting value rather than to oscillate in dependence of the excitation effects included. At least, this is suggested by the calculated CCD, QCISD, and QCISD(T) results. In any case the changes in the CC and QCI values are much smaller than those observed for the MPn results.

It is clear that changes in the response property that lead to an increase or decrease of the atomic charges (bond polarity) will also lead to similar changes in dipole moment and higher multipole moments. However, similar oscillations in the calculated values are also obtained for other properties such as for example nuclear quadrupole moments [114]. Figure 12 gives calculated values of the $^{14}$N nuclear quadrupole moment $Q$ of HCN. Actually, $Q(^{14}\mathrm{N})$ is largely independent of the molecular structure. Experimental and theoretical investigations have led to $Q(^{14}\mathrm{N})$ values of 19.3 $\pm$ 0.8 [115] and 20.5$\pm$0.5 mbarn [116], respectively. Theoretically, $Q(^{14}\mathrm{N})$ is derived from the computed electric field gradient $q$ and the experimentally known nuclear quadrupole coupling constant $\chi$ according to

$$Q = 4.256\chi/q \tag{5.9}$$

with $\chi$ given in MHz and q in atomic units both determined for a particular molecule. Since the component of the nuclear quadrupole coupling constant of HCN along the molecular axis is accurately known ($\chi_{aa}$ = -4.7091(13) MHz) [117], calculated values of $Q(^{14}\mathrm{N})$ reflect the accuracy of computed electric field gradients $q_{aa}$.

The diagram in Figure 12 indicates that correlation corrections for $Q(^{14}\mathrm{N})$ calculated with a basis set of TZ+2P quality are substantial increasing the HF value by 3 to 5 mbarn. Again, the MP2 and (less strongly) the MP4 value are too large while the MP3 value is too small compared to the accepted $Q(^{14}\mathrm{N})$ value. Hence, MPn results oscillate between $Q(^{14}\mathrm{N})$ values

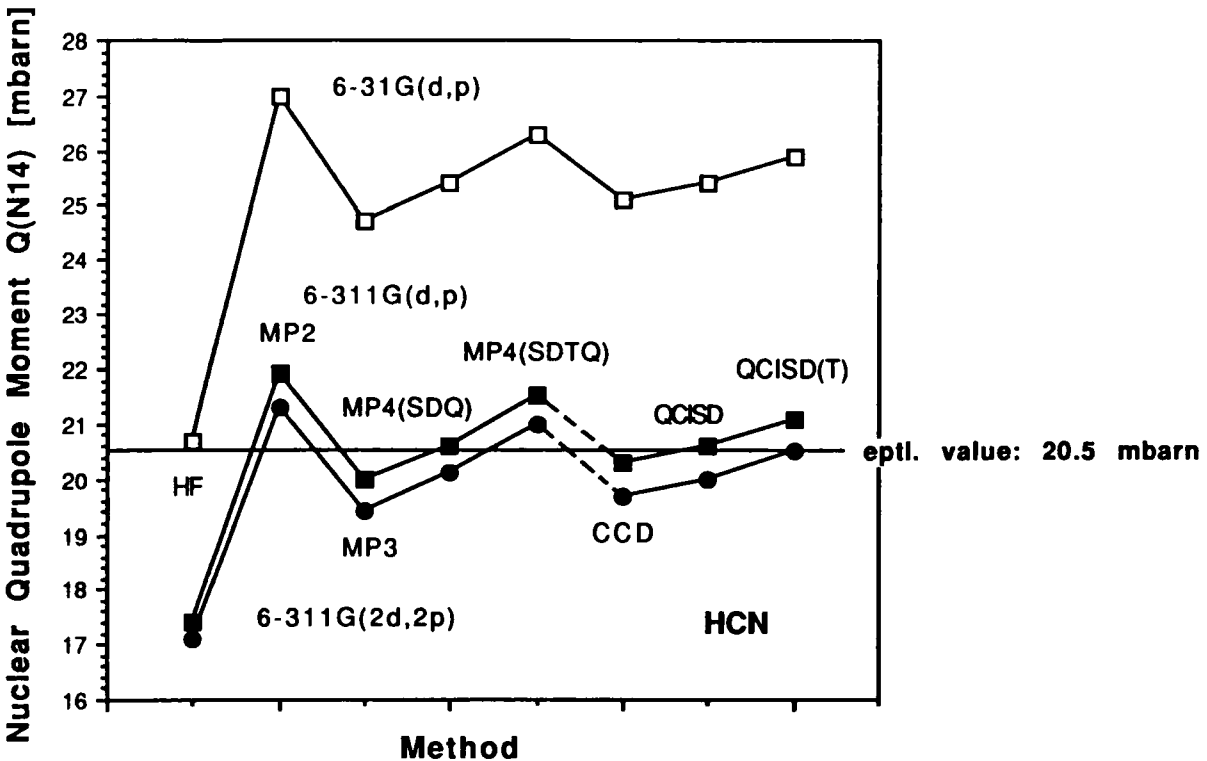



**Figure 12.** Dependence of the nuclear quadrupole moment $Q(^{14}N)$ of HCN on method and basis set.

obtained at the HF and MP2 level. CC and QCI values of $Q(^{14}N)$ quickly converge to the correct value of 20.5 mbarn (see Figure 12). Both at the MP and at the CC (QCI) level, the inclusion of T excitations has a substantial effect on the $Q(^{14}N)$ value.

The same trends have been found for electric field gradients and $^{14}N$ nuclear quadrupole moments of other molecules. In all cases investigated, correlation corrections are almost independent of the basis set used (compare with Figure 12).

In conclusion we stress the following points:

(1) Calculated MPn, CC, and QCI one-electron properties follow calculated changes in response densities due to correlation corrections. These changes are almost independent of the basis set used provided the basis is sufficiently large (at least DZ+P quality).

(2) At the MPn level of theory correlation corrections to response properties oscillate where in most cases the maximal values of the oscillation are given by HF and MP2. Oscillations clearly depend on the fact that at even orders of perturbation theory new types of correlation effects are included (D at MP2, STQ at MP4, etc.) while at odd orders these effects are reduced by introducing couplings between excitations included at the previous order (coupling between D excitations at MP3, between STQ excitations at MP5, etc.).

(3) Analysis of calculated response properties suggests that oscillations persist at MP5 and probably also at higher orders of MP theory. Convergence to a limiting MPn value seems to be much slower as one generally tends to believe. In many cases, MP4 is not sufficient to obtain an accurate value of the response property in question.

(4) CC and QCI values of response properties seem to converge very fast to a limiting value which in most cases is already reached when T excitations are included. This is due to the fact that CC and QCI methods contain infinite order effects that prevent overestimation (underestimation) of a particular correlation effect. Hence, CC and QCI methods are clearly superior to MP methods. If high accuracy is needed, QCISD(T) or CC methods including triple corrections such as CCSD(T) or even CCSDT will definitely be the methods of choice.

In the following we will investigate whether similar trends can be observed for other molecular properties calculated at either MP, CC or QCI.

### 5.2 Equilibrium Geometries

In Figure 13 calculated and experimental $r_e$ geometries (compare with

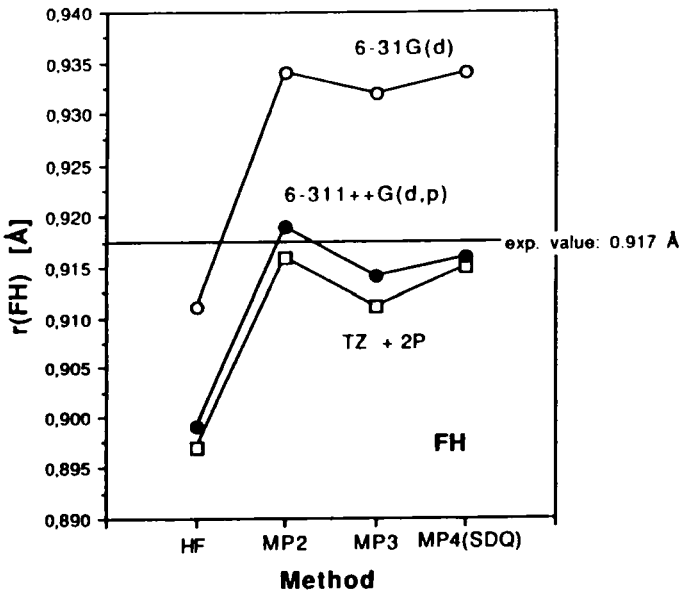



**Figure 13a.** Dependence of calculated equilibrium geometries on method and basis set. FH, bond length.

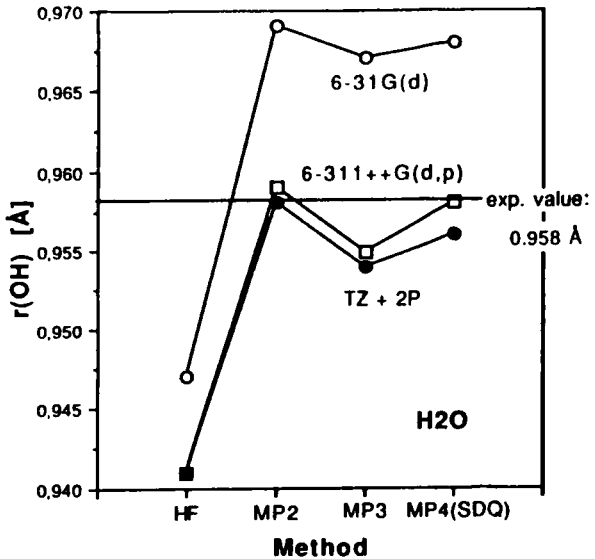



**Figure 13b.** Dependence of calculated equilibrium geometries on method and basis set. $H_2O$, bond length $OH$.

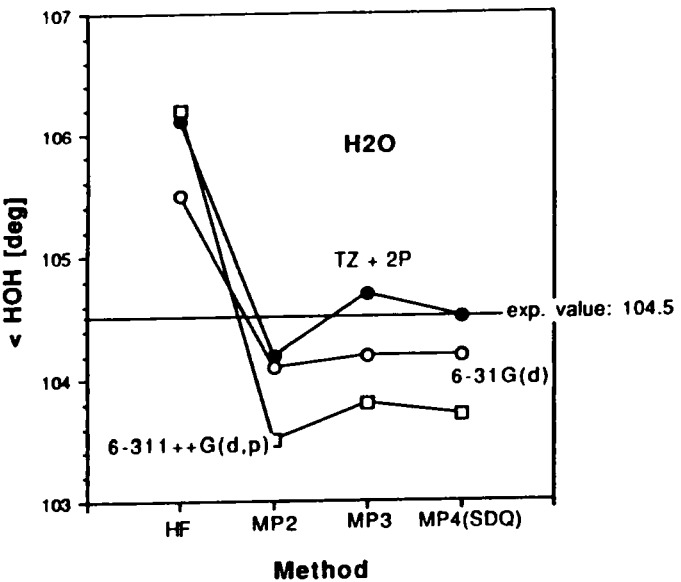



**Figure 13c.** Dependence of calculated equilibrium geometries on method and basis set. $H_2O$, bond angle $HOH$.

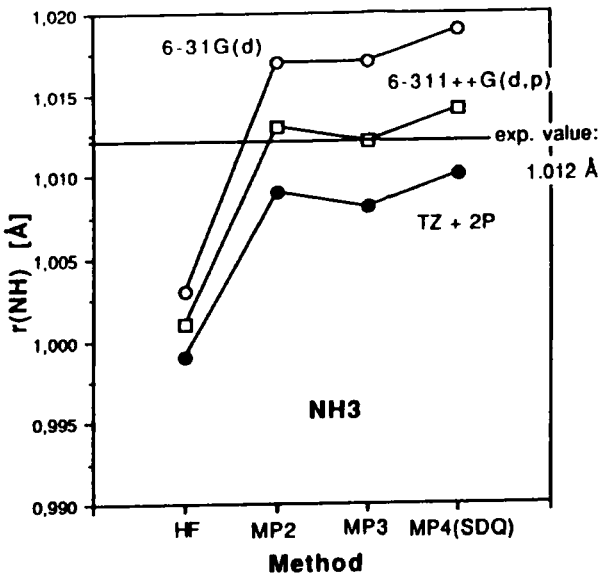



**Figure 13d.** Dependence of calculated equilibrium geometries on method and basis set. $NH_3$, bond length $NH$.

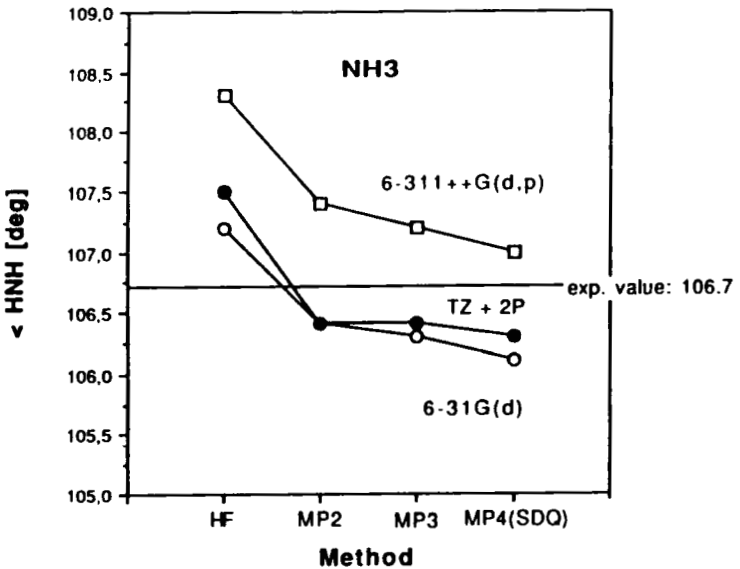



**Figure 13e.** Dependence of calculated equilibrium geometries on method and basis set. $NH_3$, bond angle $HNH$.

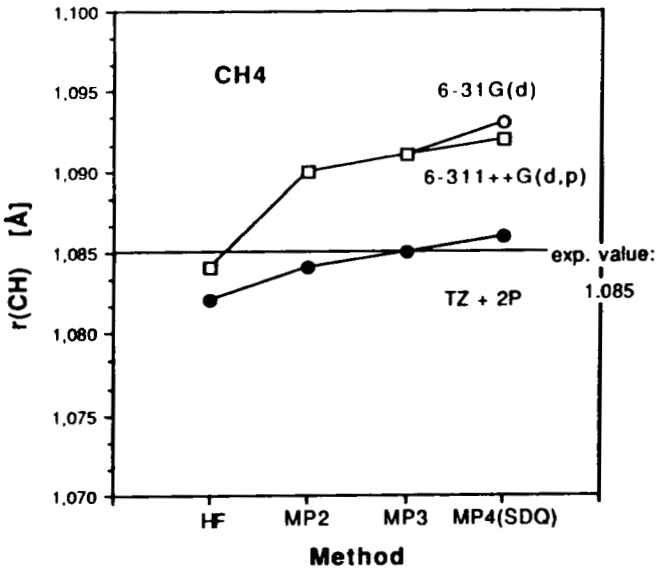



**Figure 13f.** Dependence of calculated equilibrium geometries on method and basis set. $CH_4$, bond length $CH$.

Tables 2 and 3) of FH (Figure 13a), $H_2O$ (Figure 13b and c), $NH_3$ (Figure 13d and e) and $CH_4$ (Figure 13f) are shown. Theoretical values have been obtained with three different basis sets, 6-31G(d), 6-311++G(d,p) and (9s5p2d/5s2p)[5s3p2d/3s2p], which are of VDZ+(P), VTZ+P+diff, and VTZ +2P quality [118]. The diffuse basis functions added to the second basis are used to describe the distribution of the lone pair electrons at F, O, and N more accurately. Calculations have been carried out at the HF, MP2, MP3, and MP4 level of theory, where in the later case only SDQ excitations have been considered since T excitations are known to be of minor importance for molecules with just single bonds [119].

For all $AH_n$ molecules investigated, similar trends in calculated equilibrium geometries are found. Trends in calculated AH bond lengths are opposite to trends in calculated HAH bond angles, i.e. a large bond length implies a small HAH bond angle and vice versa. As in the case of the response properties discussed in the previous section, correlation corrections to the calculated geometrical parameters depend only slightly on the basis set used.

Typical of all calculations is that HF underestimates the AH bond length by 0.01 - 0.02 Å. Two observations can be made in this connection. (a) Compared to the experimental value the HF value of $r_e$(AH) is the smaller, the larger the difference in the electronegativities between A and H and, hence, the AH bond polarity is. (b) With increasing size of the basis set the HF value decreases thus increasing the difference between experimental and theoretical $r_e$ value.

MP2 leads to an increase of the AH bond length by 0.01-0.02 Å. In this way VTZ+P+diff or VTZ+2P values come close to the experimental $r_e$ value while VDZ+P values become clearly too large. MP3 on the other hand reduces the value of the AH bond length back in the direction of the HF value. However, the reduction of $r_e$(AH) is much smaller than the increase calculated at the MP2 level. Also, the reduction of the AH bond length becomes the smaller the smaller the AH bond polarity and the smaller the basis set is. The MP3/6-31G(d) result for $NH_3$ and all the MP3 results for $CH_4$ already lead to a slight increase of the AH bond length.

At MP4(SDQ), again an increase of the calculated AH bond length is obtained. Since this increase is almost as large as the relative changes obtained at the MP3 level, MP4(SDQ) values are close to MP2 ones (exceptions: $CH_4$ and MP4(SDQ)/6-31G(d) result for $NH_3$). As a consequence, most MP4(SDQ) bond lengths obtained with the two VTZ basis sets agree with the experimental $r_e$ values.

It would be difficult to distinguish between the quality of MP2 and

**Table 2.** Calculated equilibrium geometries, dipole moments, harmonic vibrational frequencies, and infrared intensities for HF, $H_2O$, $NH_3$, and $CH_4$. Bond lengths are given in Å, angles in deg, dipole moments ($\mu$) in Debye, frequencies ($\omega$) in $cm^{-1}$, and intensities ($I$) in km/mol.

| Basis | HF | MP2 | MP3 | MP4(SDQ) | HF | MP2 | MP3 | MP4(SDQ) | HF | MP2 | MP3 | MP4(SDQ) | exp. |
|---|---|---|---|---|---|---|---|---|---|---|---|---|---|
| | | 6-31G(d) | | | | 6-311++G(d,p) | | | | | TZ2P | | |
| Hydrogen Fluoride(HF) | | | | | | | | | | | | | |
| r(FH) | 0.911 | 0.934 | 0.932 | 0.934 | 0.897 | 0.916 | 0.911 | 0.915 | 0.899 | 0.919 | 0.914 | 0.916 | 0.917[a] |
| $\mu$ | 1.972 | 1.948 | 1.941 | 1.935 | 2.026 | 1.969 | 1.857 | 1.954 | 1.934 | 1.860 | 1.862 | 1.853 | 1.819[b] |
| $\nu$ | 4357 | 4042 | 4071 | 4031 | 4493 | 4202 | 4286 | 4219 | 4471 | 4153 | 4229 | 4181 | 4139[c] |
| $I$ | 141.4 | 91.3 | 84.6 | 77.8 | 191.7 | 142.0 | 131.3 | 124.4 | 149.5 | 102.9 | 100.5 | 93.9 | 99.8[d] |
| Water ($H_2O$) | | | | | | | | | | | | | |
| r(OH) | 0.947 | 0.969 | 0.967 | 0.968 | 0.941 | 0.959 | 0.955 | 0.958 | 0.941 | 0.958 | 0.954 | 0.956 | 0.958[e] |
| $\alpha$(HOH) | 105.5 | 104.1 | 104.2 | 104.2 | 106.2 | 103.5 | 103.8 | 103.7 | 106.1 | 104.2 | 104.7 | 104.5 | 104.5[e] |
| $\mu$ | 2.199 | 2.199 | 2.188 | 2.179 | 2.196 | 2.189 | 2.164 | 2.164 | 2.020 | 1.984 | 1.977 | 1.971 | 1.855[f] |
| $\nu_1$ | 4189 | 3919 | 3930 | 3893 | 4244 | 4007 | 4053 | 4005 | 4228 | 3980 | 4018 | 3980 | 3943[e] |
| $\nu_2$ | 4071 | 3778 | 3809 | 3765 | 4143 | 3889 | 3960 | 3900 | 4128 | 3861 | 3921 | 3876 | 3832[e] |
| $\nu_3$ | 1827 | 1734 | 1750 | 1745 | 1727 | 1627 | 1665 | 1653 | 1760 | 1657 | 1686 | 1680 | 1649[e] |
| $I_1$ | 58.1 | 39.2 | 31.3 | 26.3 | 87.9 | 63.5 | 52.0 | 47.6 | 68.6 | 49.8 | 42.8 | 38.1 | 44.6[g] |
| $I_2$ | 18.2 | 5.6 | 4.9 | 3.2 | 25.5 | 13.2 | 11.2 | 9.2 | 14.3 | 5.9 | 5.5 | 4.2 | 2.2[g] |
| $I_3$ | 107.3 | 88.9 | 89.8 | 86.3 | 85.4 | 57.7 | 59.3 | 56.9 | 98.7 | 74.7 | 77.7 | 74.9 | 53.6[g] |

[a] K.P. Huber and G. Herzberg, *Constants of Diatomic Molecules* (Van Nostrand Reinhold, New York 1979).
[b] A.L. McCellan, *Tables of Experimental Dipole Moments* (Freeman, San Francisco, 1963).
[c] D.R. Stull and H. Prophet, *JANAF Thermochemical Tables* (NBS, Washington, 1971).
[d] A.S. Pine, A. Fried, and J.W. Elkins, *J. Mol. Spectrosc.* **109** (1985) 30.
[e] A.R. Hoy, I.M. Mills, and G. Strey, *Mol. Phys.* **24** (1972) 1265.
[f] S.A. Clough, Y. Beers, G.P. Klein, and L.S. Rothman, *J. Chem. Phys.* **59** (1973) 2254.
[g] B. A. Ziles and W.B. Person, *J. Chem. Phys.* **59** 2254 (1973).

Continuation of Table 2.

| Basis | HF | MP2 | MP3 | MP4(SDQ) | HF | MP2 | MP3 | MP4(SDQ) | HF | MP2 | MP3 | MP4(SDQ) | exp. |
|---|---|---|---|---|---|---|---|---|---|---|---|---|---|
| | | 6-31G(d) | | | | 6-311++G(d,p) | | | | TZ2P | | | |
| Ammonia ($NH_3$) | | | | | | | | | | | | | |
| r(NH) | 1.003 | 1.017 | 1.017 | 1.019 | 1.001 | 1.013 | 1.012 | 1.014 | 0.999 | 1.009 | 1.008 | 1.010 | 1.013[a] |
| $\alpha$(HNH) | 107.2 | 106.4 | 106.3 | 106.1 | 108.3 | 107.4 | 107.2 | 107.0 | 107.5 | 106.4 | 106.4 | 106.3 | 106.7[a] |
| $\mu$ | 1.920 | 1.965 | 1.955 | 1.958 | 1.723 | 1.733 | 1.736 | 1.736 | 1.682 | 1.718 | 1.703 | 1.703 | 1.472[b] |
| $\nu_1$ | 3822 | 3661 | 3648 | 3611 | 3825 | 3689 | 3672 | 3659 | 3808 | 3672 | 3694 | 3642 | 3577[c] |
| $\nu_2$ | 3689 | 3504 | 3519 | 3470 | 3696 | 3537 | 3555 | 3523 | 3689 | 3538 | 3562 | 3524 | 3506[c] |
| $\nu_3$ | 1850 | 1756 | 1758 | 1753 | 1793 | 1666 | 1719 | 1678 | 1800 | 1705 | 1680 | 1716 | 1691[c] |
| $\nu_4$ | 1209 | 1160 | 1172 | 1178 | 1098 | 1065 | 1107 | 1095 | 1135 | 1088 | 1090 | 1110 | 1022[c] |
| $I_1$ | 0.9 | 1.4 | 0.0 | 0.3 | 10.7 | 12.5 | 5.5 | 3.5 | 6.9 | 8.3 | 3.5 | 1.9 | 3.8[d] |
| $I_2$ | 0.3 | 0.1 | 0.3 | 0.7 | 0.2 | 1.5 | 1.9 | 2.7 | 0.0 | 0.1 | 0.4 | 0.7 | 7.6[d] |
| $I_3$ | 42.7 | 39.9 | 39.3 | 36.2 | 55.2 | 49.7 | 45.1 | 43.4 | 39.1 | 31.6 | 31.1 | 29.4 | 25[d] |
| $I_4$ | 218.3 | 188.3 | 183.8 | 174.3 | 232.4 | 208.8 | 197.5 | 192.2 | 192.9 | 159.6 | 156.4 | 152.1 | 127[d] |
| Methane ($CH_4$) | | | | | | | | | | | | | |
| r(CH) | 1.084 | 1.090 | 1.091 | 1.093 | 1.084 | 1.090 | 1.091 | 1.092 | 1.082 | 1.084 | 1.085 | 1.086 | 1.086[e] |
| $\nu_1$ | 3301 | 3251 | 3230 | 3203 | 3252 | 3217 | 3204 | 3183 | 3254 | 3218 | 3199 | 3177 | 3157[e] |
| $\nu_2$ | 3197 | 3113 | 3104 | 3079 | 3150 | 3079 | 3079 | 3060 | 3153 | 3085 | 3080 | 3061 | 3026[e] |
| $\nu_3$ | 1703 | 1625 | 1614 | 1607 | 1667 | 1570 | 1567 | 1566 | 1672 | 1605 | 1603 | 1600 | 1583[e] |
| $\nu_4$ | 1488 | 1413 | 1409 | 1403 | 1453 | 1361 | 1367 | 1367 | 1457 | 1375 | 1381 | 1380 | 1367[e] |
| $I_1$ | 119.5 | 58.0 | 67.0 | 75.1 | 125.8 | 60.0 | 71.6 | 79.2 | 82.9 | 27.9 | 38.5 | 45.1 | 64[f] |
| $I_4$ | 30.8 | 48.8 | 48.3 | 44.7 | 35.9 | 44.8 | 39.5 | 36.2 | 35.8 | 47.0 | 42.1 | 38.9 | 33[f] |

[a] W.S. Benedict and E.K. Pyler, *Can. J. Phys.* **35** (1957) 1235.
[b] M.D. Marshall and J.S. Muenter, *J. Mol. Spetrosc.* **85** (1981) 322.
[c] J.L. Duncan and I.M. Mills, *Spectrochim. Acta* **29** (1964) 523.
[d] K. Kim, *J. Quant. Spectrosc. Radiat. Trans.* **33** (1985) 611; T. Koops, T. Visser, and W.M.A. Smith, *J. Mol. Struct.* **44** (1966) 3561.
[e] D.L. Gray and A.G. Robiette, *Mol. Phys.* **37** (1979) 1901.
[f] D.E. Jennings and A.G. Robiette, *J. Mol. Spectrosc.* **94** (1982) 369; M. Dang-Nhu, A.S. Pine, and A.G. Robiette, *J. Mol. Spectrosc.* **77** (1979) 57.

**Table 3.** Calculated geometrical parameters for various multiple bonded molecules. Bond distances are given in Å, and angles in deg.

| Basis | HF | MP2 | MP3 | MP4(SDQ) | HF | MP2 | MP3 | MP4(SDQ) | exp. |
|---|---|---|---|---|---|---|---|---|---|
| | | | 6-31G(d) | | | | TZ2P | | |
| Acetylen($C_2H_2$) | | | | | | | | | |
| r(CC) | 1.185 | 1.216 | 1.205 | 1.211 | 1.180 | 1.208 | 1.197 | 1.201 | 1.203[a] |
| r(CH) | 1.057 | 1.066 | 1.066 | 1.068 | 1.054 | 1.060 | 1.059 | 1.062 | 1.061[a] |
| Carbon Monoxide (CO) | | | | | | | | | |
| r(CO) | 1.114 | 1.150 | 1.134 | 1.146 | 1.104 | 1.137 | 1.121 | 1.133 | 1.128[b] |
| Formaldehyde ($H_2CO$) | | | | | | | | | |
| r(CO) | 1.184 | 1.220 | 1.209 | 1.216 | 1.178 | 1.211 | 1.198 | 1.206 | 1.203[c] |
| r(CH) | 1.092 | 1.104 | 1.103 | 1.107 | 1.092 | 1.098 | 1.098 | 1.100 | 1.099[c] |
| $\alpha$(HCH) | 115.7 | 115.6 | 115.9 | 115.6 | 116.1 | 116.4 | 116.4 | 116.3 | 116.5[c] |
| Hydrogen Cyanide (HCN) | | | | | | | | | |
| r(CN) | 1.133 | 1.176 | 1.157 | 1.166 | 1.124 | 1.164 | 1.145 | 1.153 | 1.153[d] |
| r(CH) | 1.059 | 1.069 | 1.069 | 1.071 | 1.057 | 1.062 | 1.061 | 1.063 | 1.065[d] |
| Fluorine ($F_2$) | | | | | | | | | |
| r(FF) | 1.345 | 1.421 | 1.414 | 1.425 | 1.335 | 1.414 | 1.402 | 1.415 | 1.412[e] |
| Hydrogen Peroxide ($H_2O_2$) | | | | | | | | | |
| r(OO) | 1.397 | 1.468 | 1.452 | 1.464 | 1.390 | 1.459 | 1.440 | 1.451 | 1.464 [f] |
| r(OH) | 0.949 | 0.976 | 0.971 | 0.974 | 0.943 | 0.964 | 0.958 | 0.961 | 0.965 [f] |
| $\alpha$(OOH) | 102.1 | 98.7 | 99.7 | 99.3 | 102.8 | 99.4 | 100.7 | 100.2 | 99.4[f] |
| $\theta$(HOOH) | 116.0 | 121.2 | 121.1 | 120.9 | 109.4 | 110.8 | 110.8 | 110.9 | 111.8[f] |

[a] A. Baldacci, S. Ghersetti, S.C. Hurlock, and K.N. Rao, *J. Mol. Spectrosc.* **59** (1976) 116.
[b] K.P. Huber and G. Herzberg, *Constants of Diatomic Molecules* (Van Nostrand Reinhold, New York 1979).
[c] K. Yamada, T. Nakagawa, K. Kuchitsu, and Y. Morino, *J. Mol. Spectrosc.* **38** (1971) 70.
[d] G. Winnewisser, A.G. Maki, and R.D. Johnson, *J. Mol. Spectrosc.* **39** (1971) 149.
[e] E.A. Colbourn, M. Dagenais, A.E. Douglas, and J.W. Raymonds, *Can. J. Phys.* **54** (1976) 1343.
[f] J. Koput, *J. Mol. Spectrosc.* **115** (1986) 438.

MP4(SDQ) results on the one side and between 6-311++G(d,p) and TZ+2P results on the other side if just the bond lengths of $AH_n$ molecules would be considered. However, comparison of the calculated HAH angles with experimental values clearly reveals that the best results are obtained at the MP4(SDQ) level using the TZ+2P basis set. For a reliable description of bond angles a second set of polarization function seems to be more important than diffuse functions. This is also true in the case of the CH bond length of $CH_4$ where the VTZ+2P values are slightly better than the VTZ+P+diff values.

The relative changes of the calculated geometrical parameters can easily be understood when considering the extent of electron correlation included at the different levels of theory. For example, at the HF level only exchange correlation is considered. Accordingly, electrons can concentrate around the nuclei and in the bonding region thus increasing electron-nucleus attraction and, thereby, the stability of the molecule. In the case of an $AH_n$ molecule with a strongly electronegative atom A electrons accumulate in the nuclear region of A. As a consequence, nucleus A is largely shielded by the surrounding negative charge, nuclear repulsion between A and the H atom(s) is decreased, and a relatively short internuclear AH distance results. This effect is the more pronounced the larger the electronegativity of A is and the more negative charge can be concentrated in the nuclear region. Also, concentration of electronic charge is limited by the number of basis functions describing the region around the nuclei. Accordingly, the underestimation of the $r_e$ value of polar AH bonds depends on the bond polarity and the basis set employed.

If electron correlation is considered, negative charge is no longer concentrated around the nuclei and in the bonding region. These areas are depleted relative to the HF electron distribution. As a consequence, the nuclei are partially deshielded, nuclear repulsion is increased, and longer AH bond lengths result. Of course, the extent of depletion of electronic charge and the increase of nuclear repulsion depend on how many correlation effects are included in the calculation. Electron pair correlation dominates these effects and, therefore, MP2 leads to the strongest corrections. Coupling of pair correlations at MP3 reduces MP2 corrections. MP4(SDQ) brings in new correlation effects due to S, D, and Q excitations thus increasing correlation corrections back to the MP2 values.

Obviously, trends in geometrical parameters are similar to those observed for multipole moments and other one-electron properties. This is not astonishing since the equilibrium geometry is defined by vanishing forces on the nuclei. These, on the other hand, are response properties which depend

on the changes in the response density. However, since the basis set depends on the position of the nuclei, additional terms have to be considered when calculating forces (compare e.g. eq. (3.60)).

Explanation of the trends in calculated bond lengths can easily be extended to those obtained for computed bond angles. In Figure 14, theoretical values of the HOH bond angle are plotted against the corresponding values of the OH bond length. There is a linear relationship between the two geometrical parameters in the way that the larger bond length implies a smaller bond angle. A similar relationship can also be found for $NH_3$ and other $AH_n$ molecules. According to the electrostatic model of charge distribution used to explain trends in calculated bond lengths, accumulation of charge in the nuclear region of A is accompanied by a short bond length. It also leads to a relatively large positive charges at the H atoms. As a consequence, Coulomb repulsion between the H atoms becomes large thus forcing the HAH angle to widen. Accordingly, a short AH bond length implies a large HAH bond angle and vice versa.

The same explanations can be used to discuss trends in calculated geometrical parameters of two-heavy atoms. Figure 15 gives results for acetylene, $C_2H_2$, Figure 16 for formaldehyde, $CH_2O$, Figure 17 for hydrogen cyanide, HCN, Figure 18 for hydrogen peroxide, $H_2O_2$, and Figure 19 for $F_2$. In all these cases, bond lengths AH and AB as well as bond angles ABH show the same dependence on method and basis set as the geometrical parameters of molecules $AH_n$ do. Apart from this, the following additional observations can be made:

(1) Changes due to the inclusion of correlation effects are now much stronger, namely up to 0.08 Åfor bonds OO and FF, up to 0.03 Åfor the OH bond in $H_2O_2$, and $3-4°$ for the angle OOH. This can be explained by considering the fact that now two heavy atoms rather than one concentrate negative charge around their nuclei thus leading to a relative strong change in nuclear repulsion between them.

(2) Geometrical parameters such as dihedral angles depend strongly on the basis set but not so much on the method used (Figure 18d). In the case of $H_2O_2$, a basis set such as 6-31G(d) which leads to more positively charged H atoms, predicts a larger dihedral angle while a more balanced charge distribution obtained with the TZ+2P basis predicts a smaller dihedral angle. On the other hand, changes in the distribution of electronic charge due to correlation effects seem to be too small to strongly affect H,H interactions that are more than 2 bonds apart.

(3) Equilibrium geometries depicted in Figures 15 to 17 clearly indicate the superiority of the MP4(SDQ) method compared to MP3 or MP2. Also,

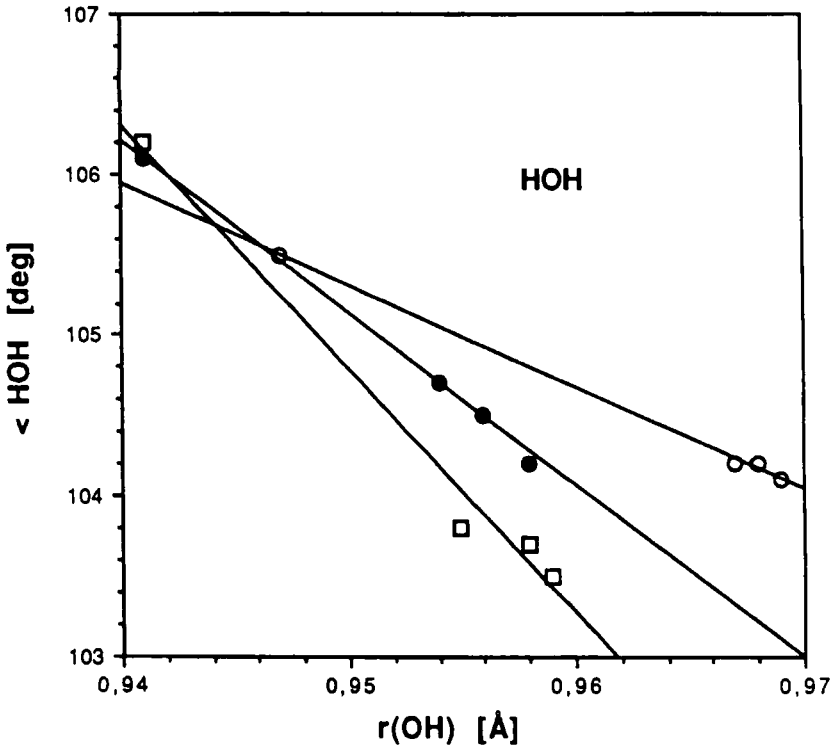



**Figure 14.** Relationship between geometrical parameters: $H_2O$ - Calculated values of the bond angles HOH vs. calculated bond lengths OH.

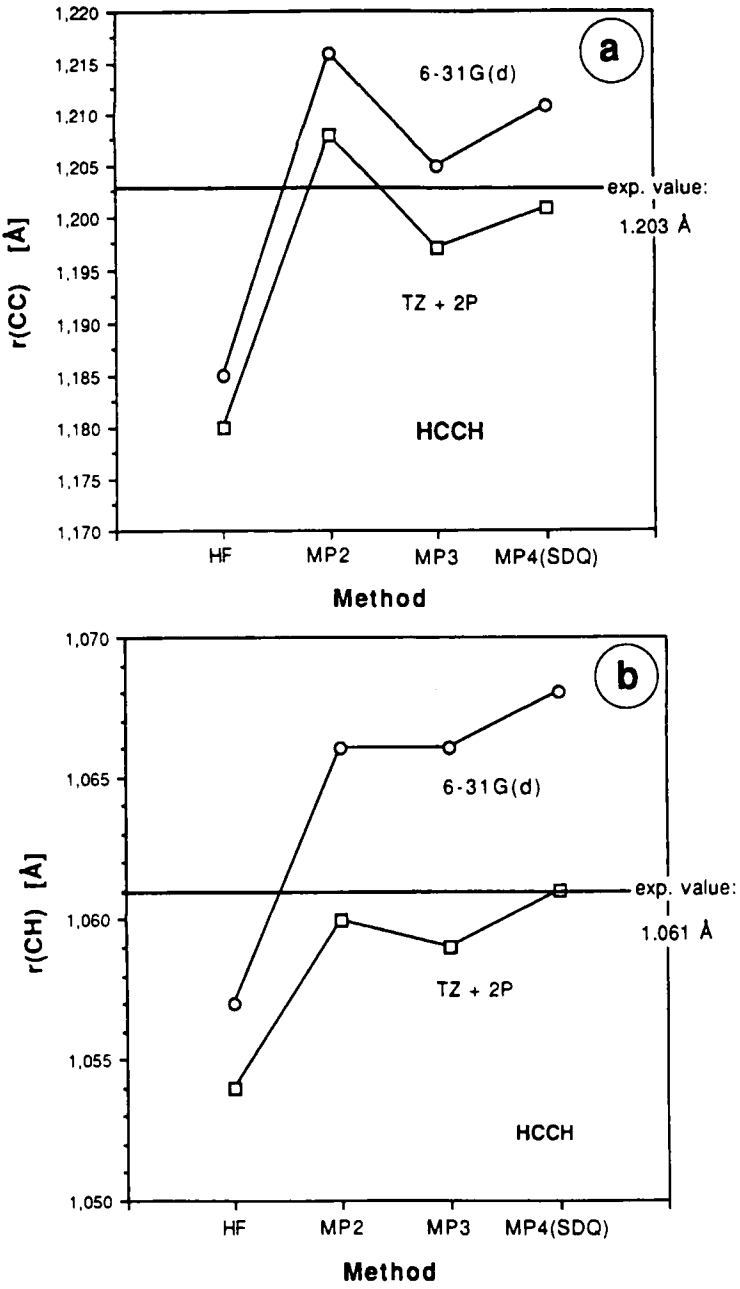



**Figure 15.** Dependence of calculated equilibrium geometries on method and basis set. Acetylene, HCCH: (a) CC bond length. (b) CH bond length.

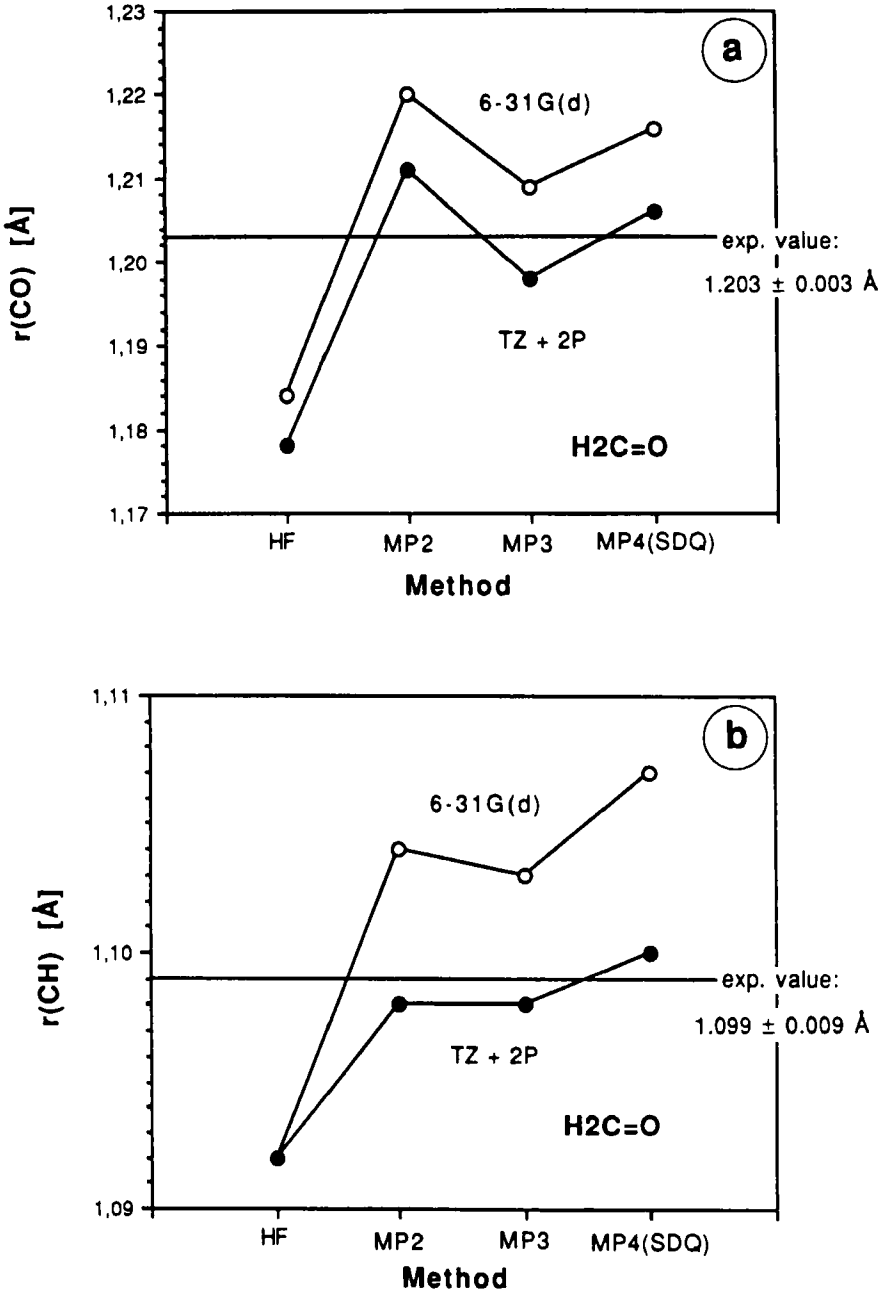



**Figure 16.** Dependence of calculated equilibrium geometries on method and basis set. Formaldehyde, $CH_2O$: (a) CO bond length. (b) CH bond length.

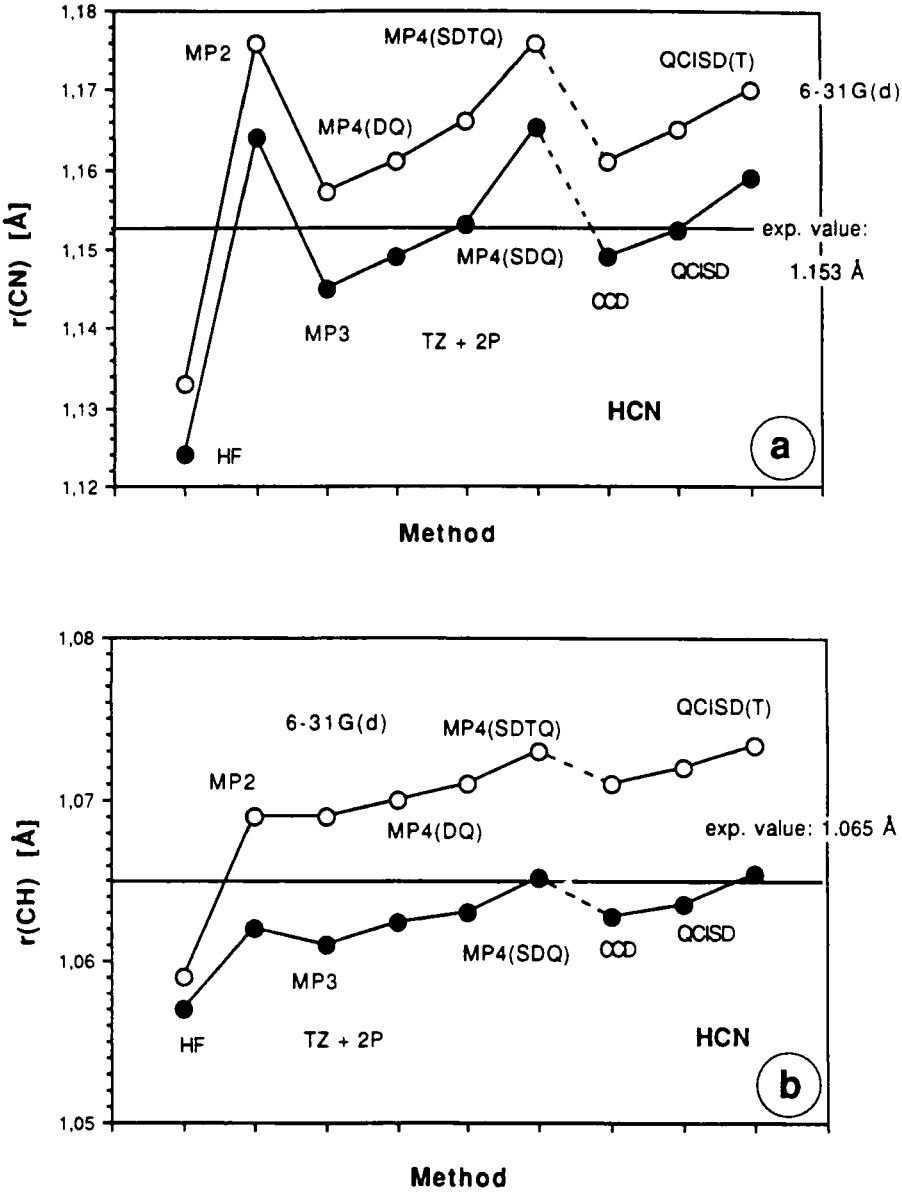



**Figure 17.** Dependence of calculated equilibrium geometries on method and basis set. Hydrogen cyanide, HCN: (a) CN bond length. (b) CH bond length.

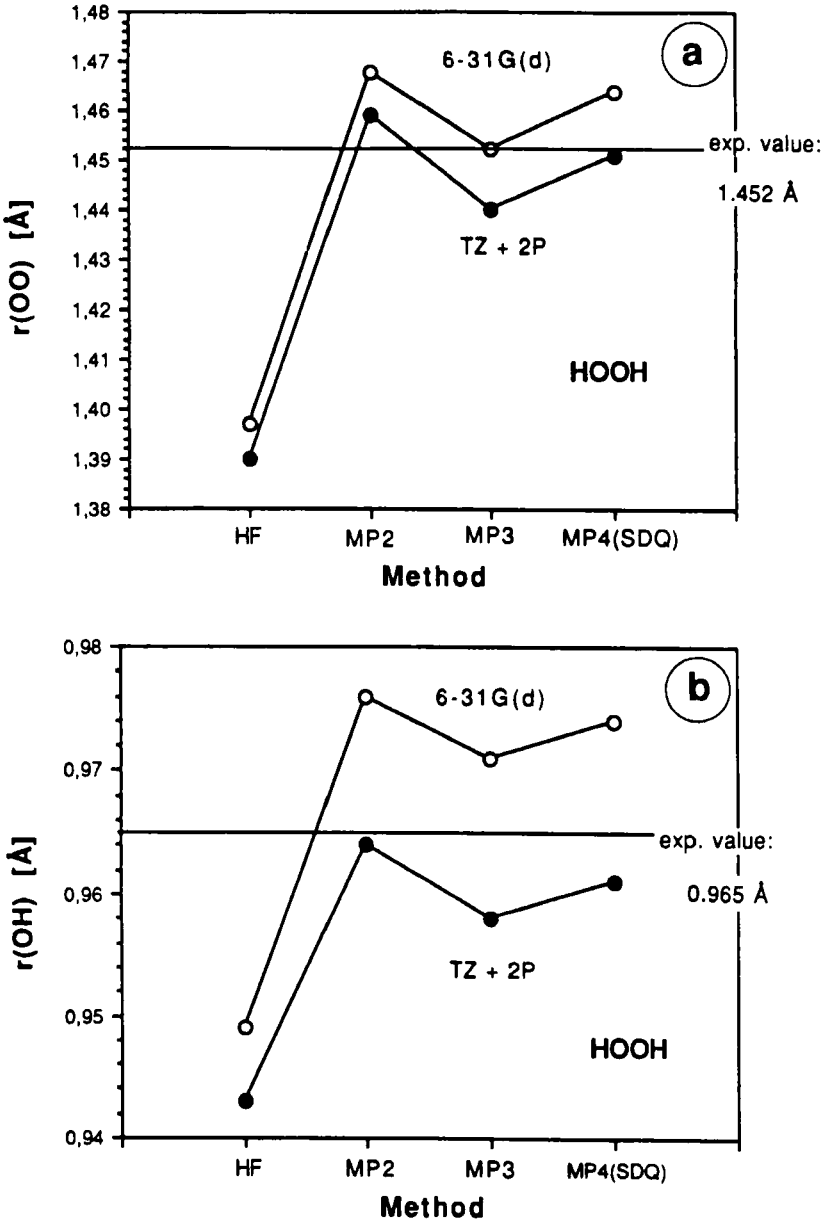



**Figure 18.** Dependence of calculated equilibrium geometries on method and basis set. Hydrogen peroxide, HOOH: (a) OO bond length. (b) OH bond length.

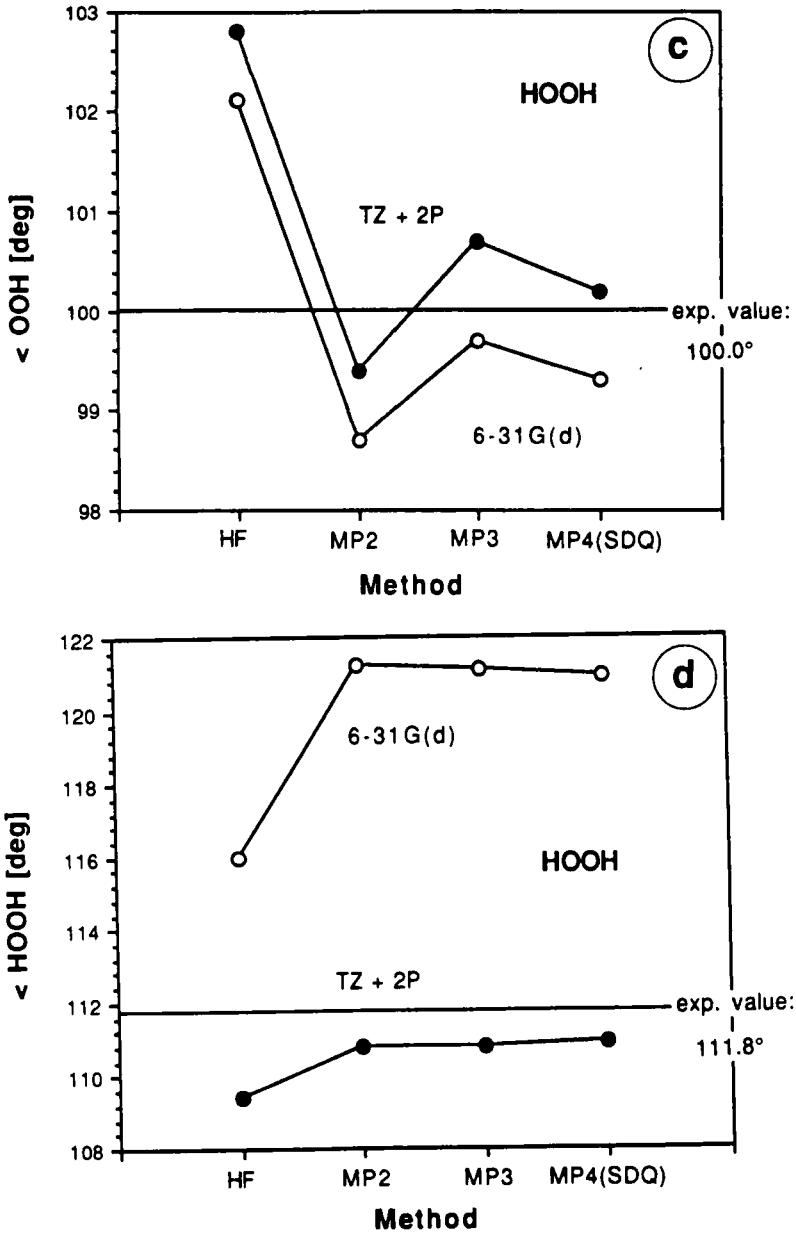



**Figure 18.** Dependence of calculated equilibrium geometries on method and basis set. Hydrogen peroxide, HOOH: (c) OOH bond angle. (d) HOOH dihedral angle.

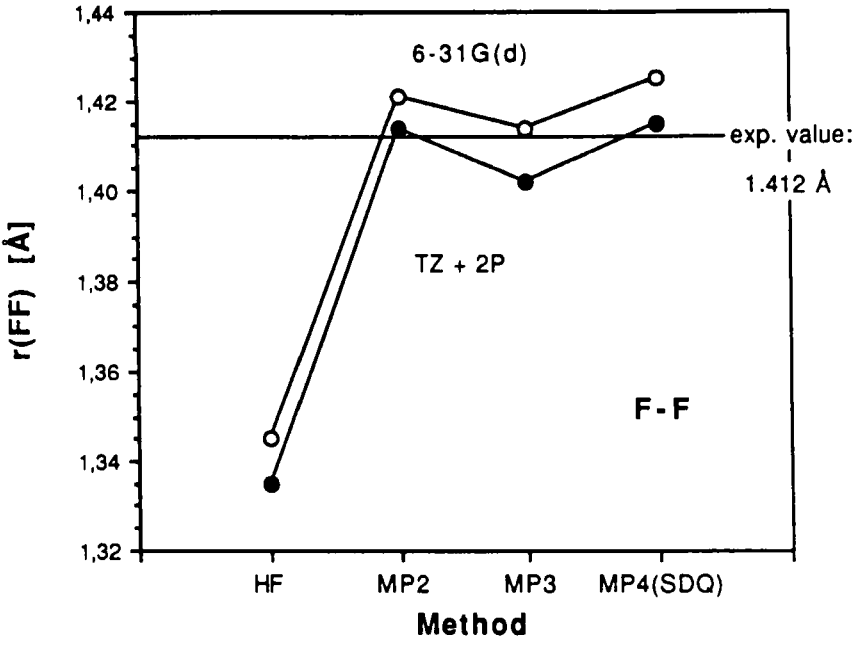



**Figure 19.** Dependence of calculated equilibrium geometries on method and basis set. $F_2$: FF bond length.

results underline the necessity of using a TZ+2P basis set to obtain accurate geometrical parameters. Previous investigations that have stressed the accuracy of MP3 or MP2 results [120] are misleading since they were due to a fortuitous cancellation of basis set and correlation errors. Of course, an even higher accuracy of calculated geometrical parameters is obtained by applying higher orders of MP perturbation theory or using CC or QCI methods.

For HCN (Figure 17), results obtained with methods that account for T effects, namely MP4(SDTQ) and QCISD(T), are also shown. It is well-known that T effects are important in the case of multiple bonds [119] and, therefore, one would expect an improvement of calculated geometries when going from MP4(SDQ) to MP4(SDTQ) or from QCISD to QCISD(T). Surprisingly, this is not the case. The CN bond length is predicted too long when T excitations are included. One could interpret this result as reflecting deficiencies of the TZ+2P basis set used. On the other hand, it has been found that T effects are significantly overestimated at the MP4(SDTQ) level of theory [93]. Furthermore, a detailed analysis of QCI in terms of perturbation theory reveals that the same is true to some extent with regard to QCISD(T) results [121]. The calculated values for the CN bond length reflect this as do the results shown in Figures 9 (charge and dipole moment of CS) and 11 (dipole moment of CO). Therefore, precautions have to be taken when accounting for T effects. A more balanced assessment of T effects is obtained at the CCSD(T), QCISD(TQ), CCSD(TQ) or CCSDT level of theory [121].

In Figure 20, the computed LiH bond length in dependence of method and basis set is shown as an example of a geometrical parameter that follows not the usual trends discussed above. The 6-31G(d) values of r(LiH) increase from HF to MP4(SDQ) while the 6-311++G(d,p) values decrease in the same direction. The LiH bond possesses partial ionic character according to the charge distribution $Li^+H^-$. At the HF/6-311++G(d,p) level of theory the ionicity of the LiH bond is exaggerated leading to a rather long bond distance of 1.61 Å(see Figure 20). At the MP level covalent biradical structures $Li{\cdot}H{\cdot}$ are mixed into the ground state wave function thus leading to a shorter bond length close to the experimental value (Figure 20). Clearly, the 6-31G(d) basis set is not sufficient to describe these changes correctly. This basis assigns 15 basis functions to Li and just 2 to H even though both atoms possess the same number of electrons (2) in an ionic structure, and, therefore, leads to an unbalanced description of the electron density distribution.

In summary all trends in calculated equilibrium geometries can be easily understood on the basis of changes in the response densities and on the basis of simple electrostatic models. As with other response properties, at

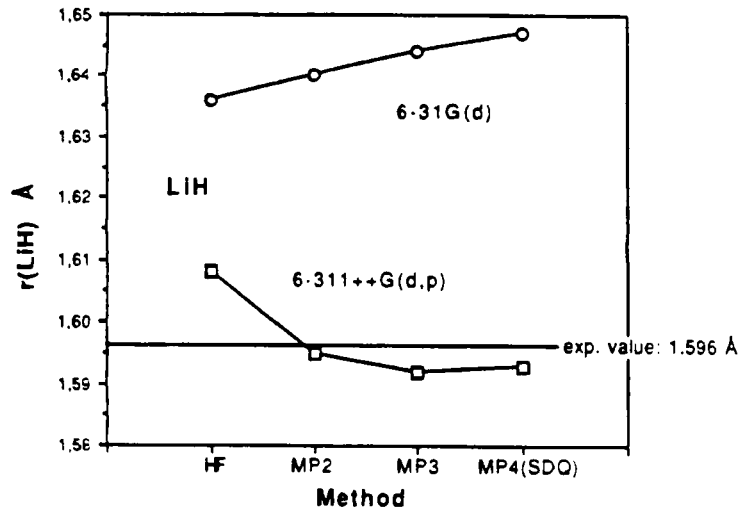



**Figure 20.** Dependence of calculated equilibrium geometries on method and basis set. LiH bond length.

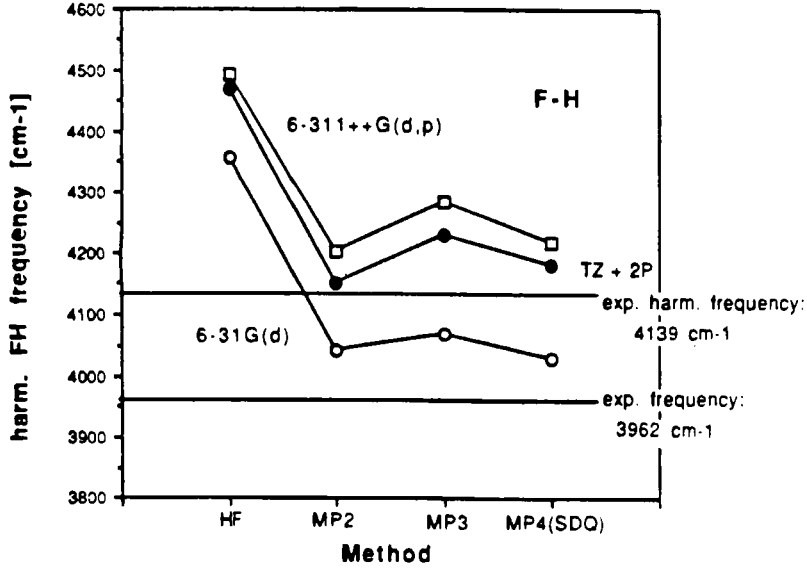



**Figure 21.** Dependence of calculated harmonic frequencies on method and basis set. FH stretching frequency.

least MP4(SDQ) and a TZ+P basis set is required to calculate accurate geometrical parameters.

### 5.3 Vibrational Spectra

In Figures 21, 22, 23, and 24 calculated harmonic frequencies $\omega$ of FH, $H_2O$, $NH_3$, and $CH_4$ are compared with experimental ones. Clearly, the theoretical $\omega$ values reflect a strong dependence on the computed equilibrium geometries.

(1) A short (long) bond length implies a large (small) value for the corresponding stretching frequency(ies) (compare Figures 13a and 21, 13b, 22a, and 22b, 13d and 23a, 13f and 24a).

(2) A large (small) bond angle, which can be considered to be the result of a short (large) bond length, implies a large (small) value of the corresponding bending frequency(ies) (compare Figures 13c and 22c, 13e, 23b, and 23c).

The harmonic frequency is proportional to the curvature of the potential surface at the equilibrium geometry in the direction of the corresponding internal coordinate. Therefore, on first sight it may be surprising that calculated frequencies directly depend on the theoretical values of the geometrical parameters. However, the potential surface in the direction of a bond distance AB (AH) becomes steeper if the AB (AH) distance is shortened and, hence, the corresponding bond strengthened. Accordingly, the stretching frequencies increase with a shortening of the bond. Widening of an angle ABC (HAH), on the other hand, indicates that there is increased electrostatic repulsion between A and C (or the H atoms) which makes the angle stiffer and, thereby, increases the bending frequency.

Figures 21 - 24 also show that MP4(SDQ)/TZ+2P is not sufficient to get accurate harmonic frequencies. In most cases calculated values are still too large. Obviously, higher order correlation effects have to be included to improve the accuracy of calculated values.

Finally, in Figure 25 theoretical and experimental IR intensities of the three vibrational modes of $H_2O$ are compared. Since, there are not so many accurately determined IR intensities available from experiment the discussion is limited here to one example. This example, however, shows that agreement of calculated data with experimental values is even poorer as in the case of the harmonic frequencies. HF intensities are too large by up to 50 km/mol and more. Stepwise inclusion of correlation effects leads to a continuous decrease of intensities. Similar trends are also observed for other molecules. However, dependence on method and basis set may change more strongly

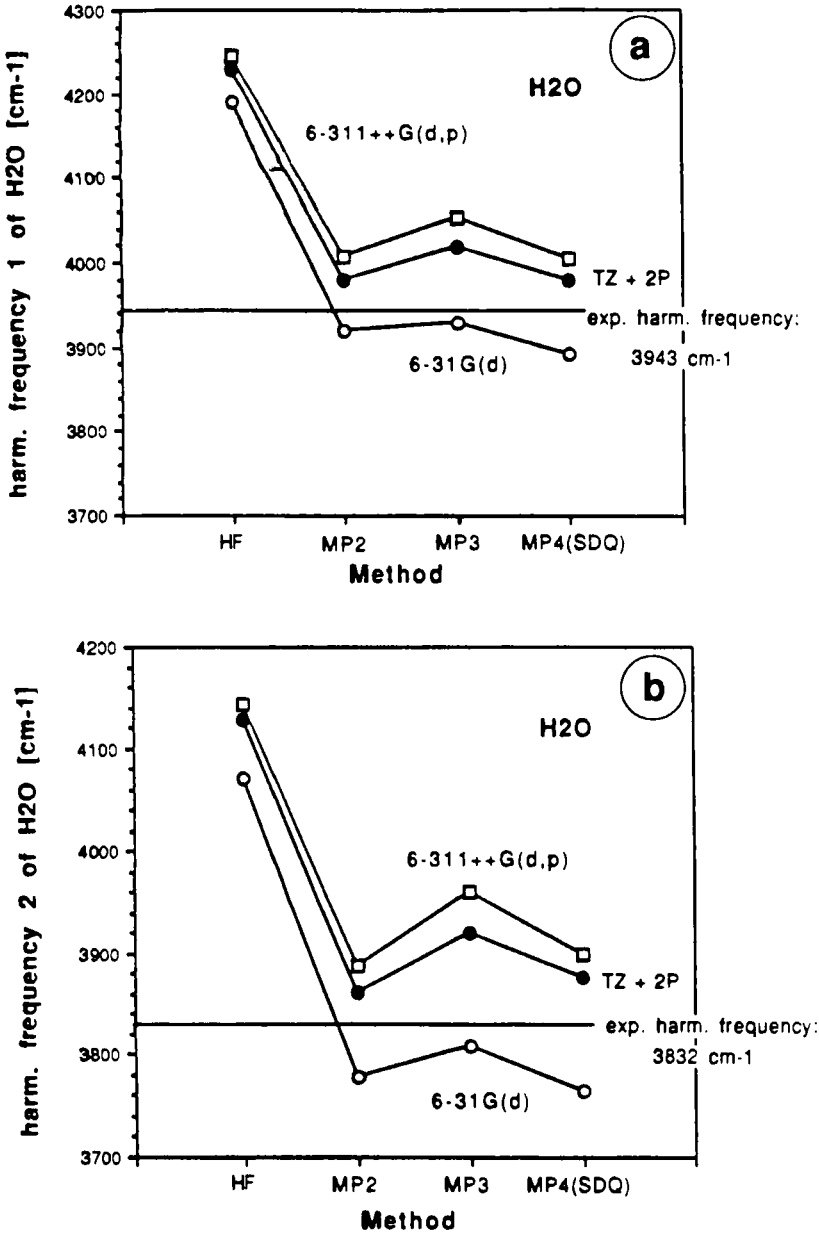



**Figure 22.** Dependence of calculated harmonic frequencies on method and basis set. $H_2O$ : (a) asymmetric OH stretching frequency. (b) symmetric OH stretching frequency.

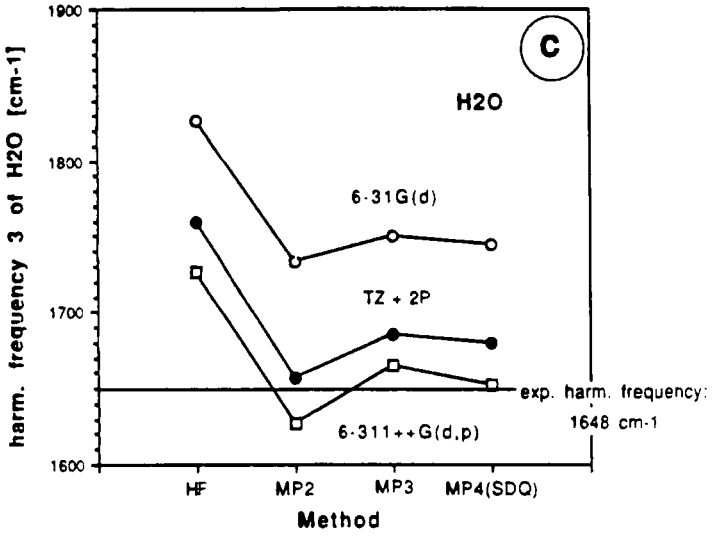



**Figure 22.** Dependence of calculated harmonic frequencies on method and basis set. $H_2O$ : (c) HOH bending frequency.

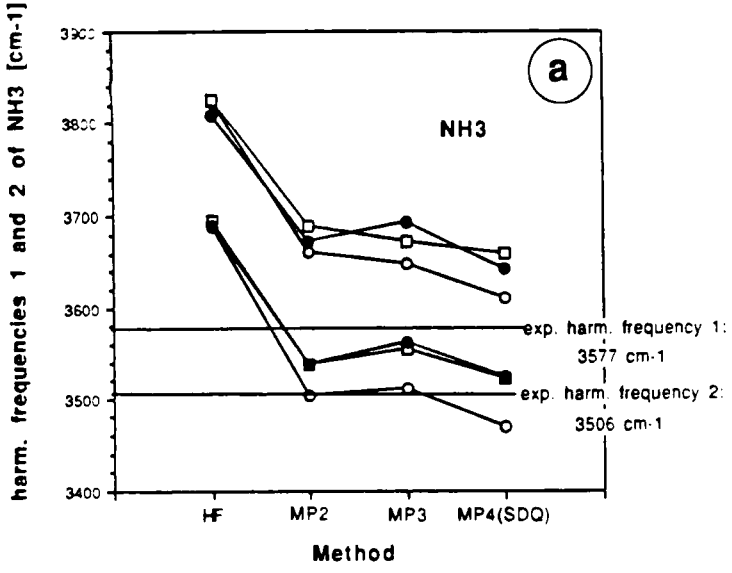



**Figure 23.** Dependence of calculated harmonic frequencies on method and basis set. $NH_3$ : (a) asymmetric and symmetric NH stretching frequency.

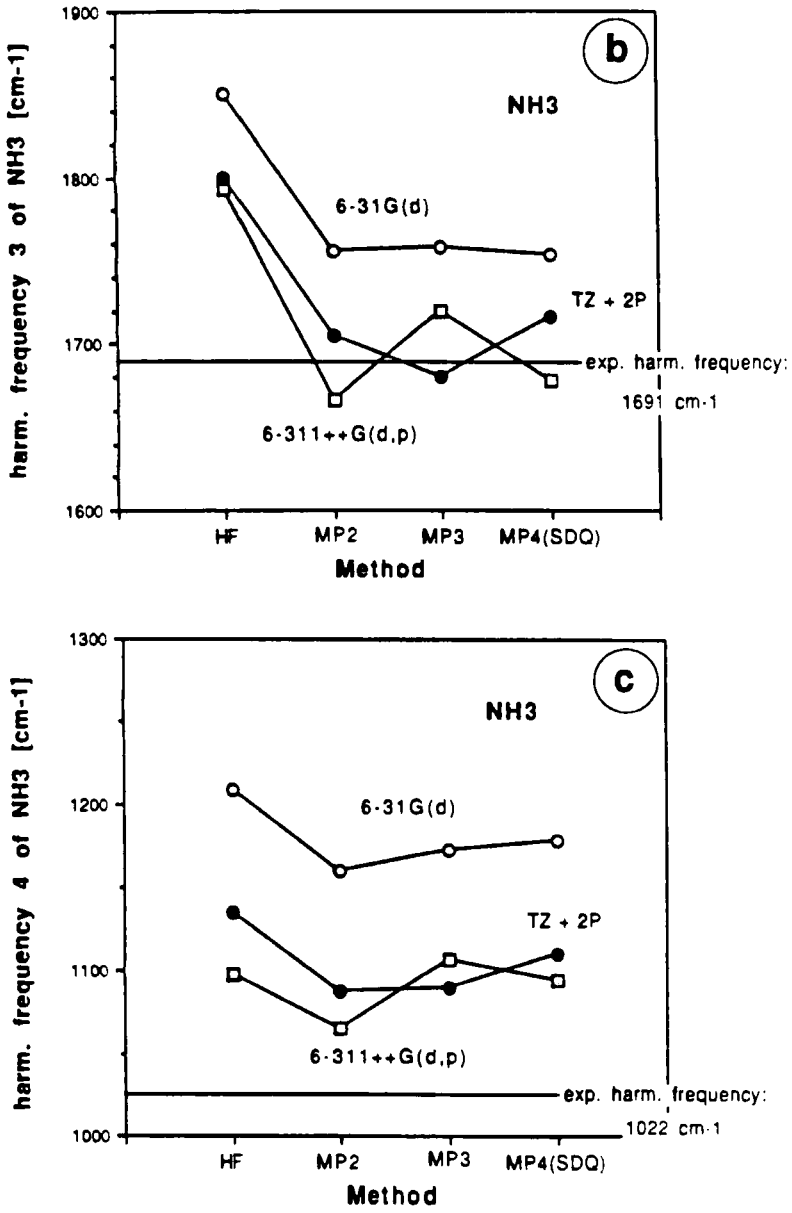



**Figure 23.** Dependence of calculated harmonic frequencies on method and basis set. $NH_3$ : (b) asymmetric HNH bending frequency. (c) symmetric HNH bending frequency.

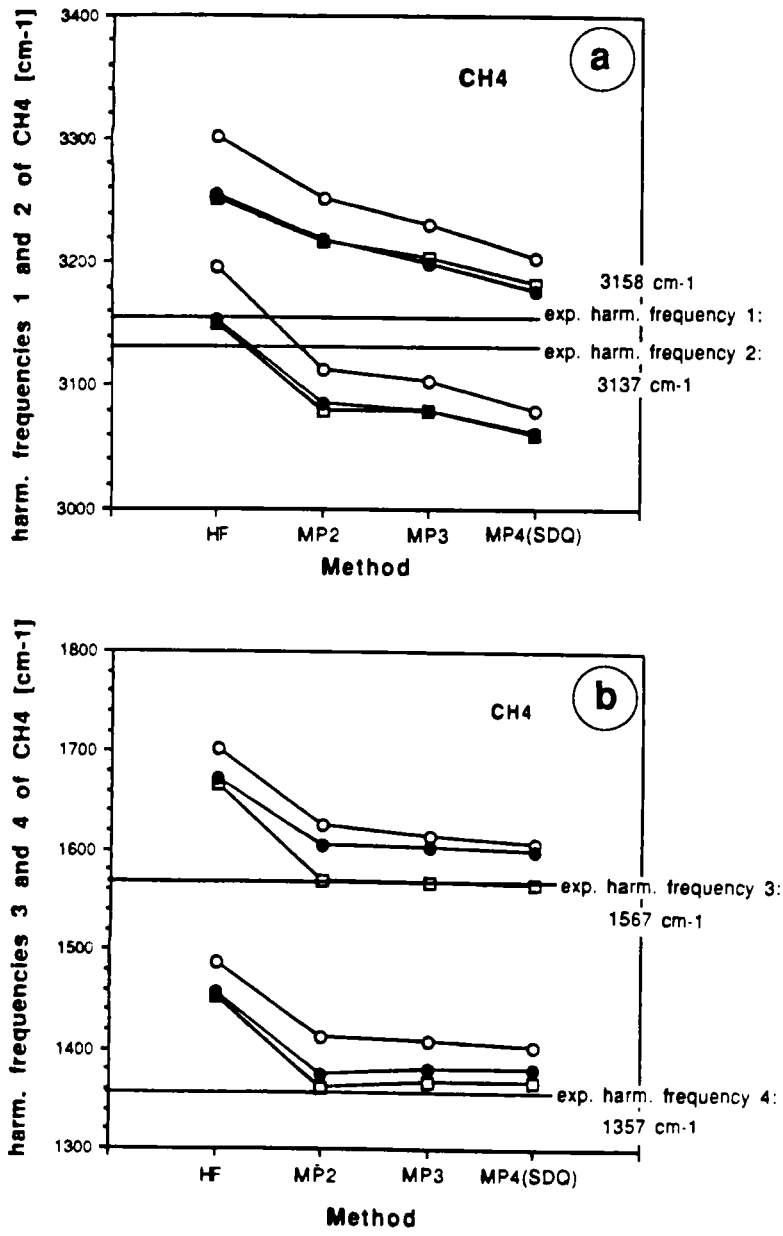



**Figure 24.** Dependence of calculated harmonic frequencies on method and basis set. $CH_4$ : (a) asymmetric and symmetric CH stretching frequency. (b) asymmetric and symmetric HCH bending frequency.

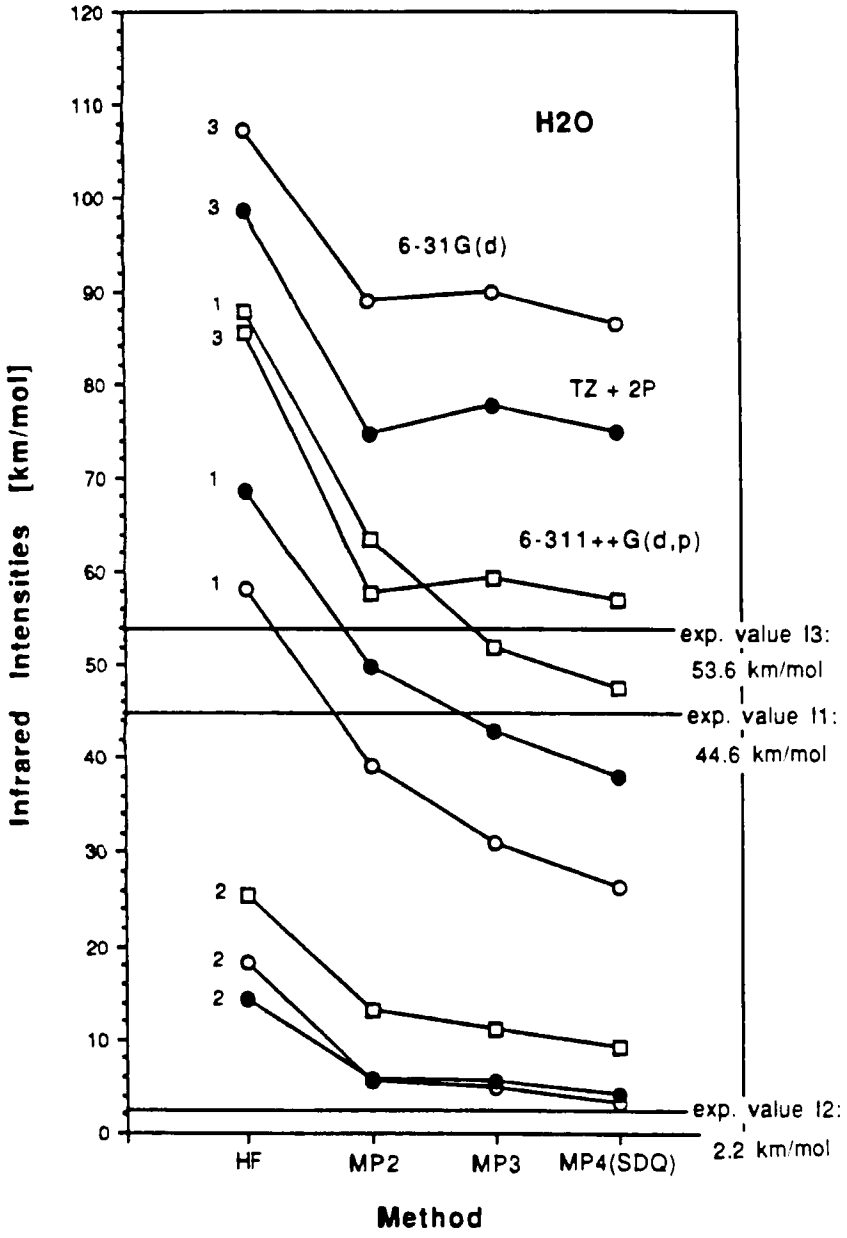



**Figure 25.** Dependence of calculated infra red (IR) intensities on method and basis set. $H_2O$.

than observed for geometrical parameters and vibrational frequencies. In any case, it seems that diffuse basis functions are probably more important than a second set of polarization functions (see Figure 25).

IR intensities are derived from dipole moment derivatives with regard to Cartesian coordinates. Assuming that dipole moment derivatives change similarly as dipole moments with method and basis set, HF and MP intensities can be discussed. At the HF level, the OH bond polarity and, thereby, the molecular dipole moment are exaggerated, obviously causing also enlarged IR intensities (Figure 25). Correlation effects reduce bond polarities and molecular dipole moment. The same is reflected by the computed IR intensities. In the case of $H_2O$, the best values are obtained at the MP4(SDQ)/6-311++G(d,p) level of theory. However, this may change from molecule to molecule as is shown by Figure 26 which compares calculated and experimental intensities for $CH_4$. Clearly, for harmonic frequencies and IR intensities it is much more difficult to predict trends in calculated ab initio data from response densities.

## 6. Concluding Remarks

Analytical energy gradients have opened a new avenue for the routine calculation of many molecular properties. They are particularly important for correlation corrected ab initio methods since they provide the basis for an understanding of the influence of correlation effects on calculated one-electron properties, geometries, vibrational spectra, etc.. In this article we have sketched the development of the theory of analytical gradients where we have put special emphasis on single-determinant ab initio methods. On first sight it may look as a demanding and tedious enterprise to develop for each method analytical derivatives of the molecular energy. However, as we have shown in this article, there are many similarities and relationships between the analytical derivatives for the various methods that can be used to reach a unified theory of analytical derivatives. Further developments in the area of analytical derivatives can be expected and are needed. One can predict that an important criterion of ab initio methods to be developed in the future will be the availability and the economy of analytical gradient calculations for the method in question.

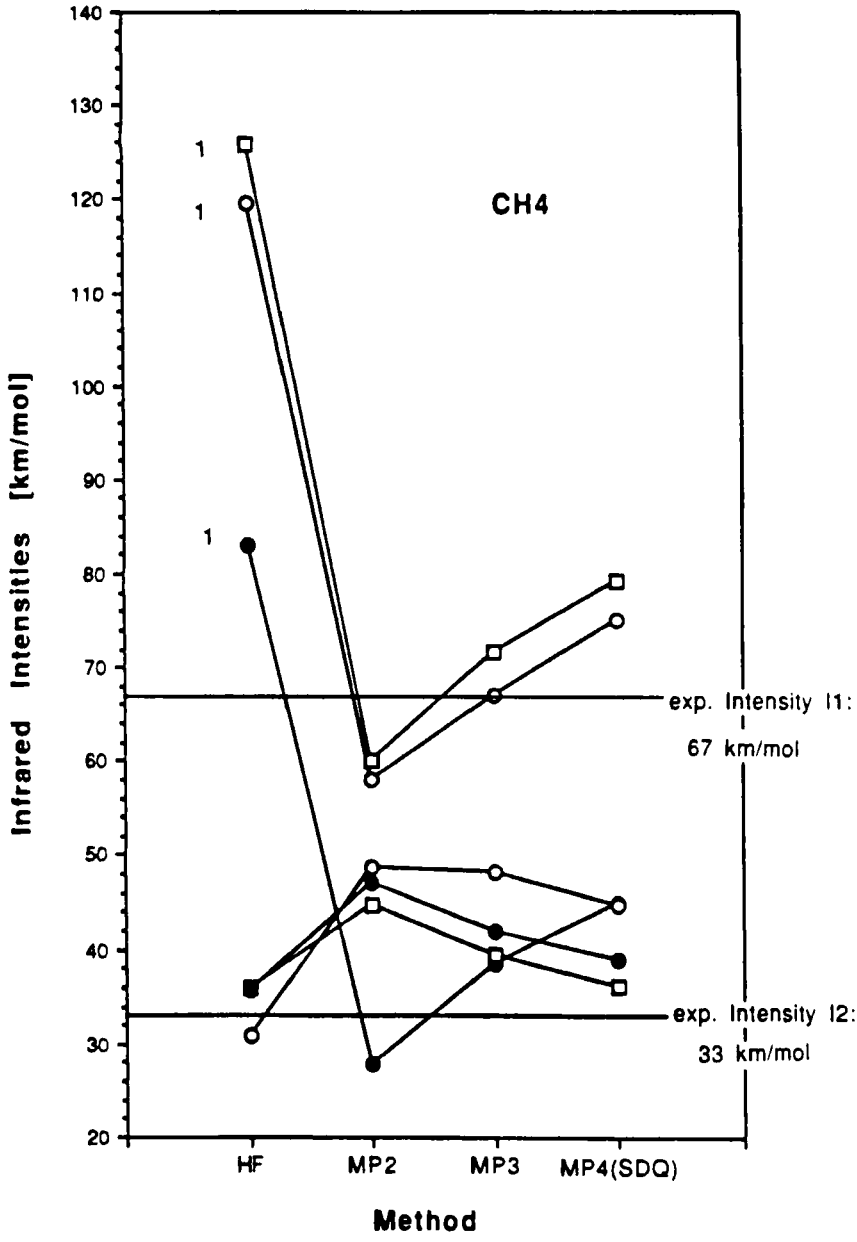



**Figure 26.** Dependence of calculated infra red (IR) intensities on method and basis set. $CH_4$.

## Acknowledgement

The authors acknowledge helpful discussions with Dr. Elfi Kraka and Mrs. Zhi He. This work was supported by the Swedish Natural Science Research Council (NFR), Stockholm, Sweden. Calculations have been carried out with the CRAY XMP/48 of the Nationellt Superdatorcentrum (NSC), Linköping, Sweden. DC thanks the NSC for a generous allotment of computer time.

## Appendix 1

The B and C terms in the CPQCISD equations are given by [72] :

$$
\begin{aligned}
B_i^{a(\lambda)} = &- \sum_b \frac{\partial \varepsilon_{ab}}{\partial \lambda} a_i^b + \sum_j \frac{\partial \varepsilon_{ij}}{\partial \lambda} a_j^a + \sum_j \sum_b \frac{\partial \langle ja \| ib \rangle}{\partial \lambda} a_j^b \\
&+ \frac{1}{2} \sum_j \sum_{b,c} \frac{\partial \langle ja \| bc \rangle}{\partial \lambda} a_{ij}^{bc} + \frac{1}{2} \sum_{j,k} \sum_b \frac{\partial \langle jk \| ib \rangle}{\partial \lambda} a_{jk}^{ab} \\
&- \frac{1}{2} \sum_{j,k} \sum_{b,c} \frac{\partial \langle jk \| bc \rangle}{\partial \lambda} \{ a_i^b a_{jk}^{ca} + a_j^a a_{ik}^{cb} + 2 a_j^b a_{ik}^{ac} \}, \qquad \text{(A1.1)}
\end{aligned}
$$

$$
\begin{aligned}
B_{ij}^{ab(\lambda)} = &- \frac{\partial \langle ij \| ab \rangle}{\partial \lambda} - \sum_c \{ \frac{\partial \varepsilon_{ac}}{\partial \lambda} a_{ij}^{cb} + \frac{\partial \varepsilon_{bc}}{\partial \lambda} a_{ij}^{ac} \} \\
&+ \sum_k \{ \frac{\partial \varepsilon_{ik}}{\partial \lambda} a_{kj}^{ab} + \frac{\partial \varepsilon_{jk}}{\partial \lambda} a_{ik}^{ab} \} - \frac{1}{2} \sum_{c,d} \frac{\partial \langle ab \| cd \rangle}{\partial \lambda} a_{ij}^{cd} - \frac{1}{2} \sum_{k,l} \frac{\partial \langle kl \| ij \rangle}{\partial \lambda} a_{kl}^{ab} \\
&+ \sum_k \sum_c \{ \frac{\partial \langle kb \| jc \rangle}{\partial \lambda} a_{ik}^{ac} + \frac{\partial \langle ka \| jc \rangle}{\partial \lambda} a_{jk}^{cb} + \frac{\partial \langle kb \| ic \rangle}{\partial \lambda} a_{kj}^{ac} + \frac{\partial \langle ka \| ic \rangle}{\partial \lambda} a_{kj}^{cb} \} \\
&- \frac{1}{4} \sum_{k,l} \sum_{c,d} \frac{\partial \langle kl \| cd \rangle}{\partial \lambda} \{ a_{ij}^{cd} a_{kl}^{ab} - 2[a_{ij}^{ac} a_{kl}^{bd} + a_{ij}^{bd} a_{kl}^{ac}] \\
&\qquad - 2[a_{ik}^{ab} a_{jl}^{cd} + a_{ik}^{cd} a_{jl}^{ab}] + 4[a_{ik}^{ac} a_{jl}^{bd} + a_{ik}^{bd} a_{jl}^{ac}] \} \\
&- \sum_c \{ \frac{\partial \langle ab \| cj \rangle}{\partial \lambda} a_i^c - \frac{\partial \langle ab \| ci \rangle}{\partial \lambda} a_j^c \} \\
&- \sum_k \{ - \frac{\partial \langle kb \| ij \rangle}{\partial \lambda} a_k^a + \frac{\partial \langle ka \| ij \rangle}{\partial \lambda} a_k^b \}, \qquad \text{(A1.2)}
\end{aligned}
$$

$$\sum_j \sum_b C_{i,j}^{a,b} \frac{\partial a_j^b}{\partial \lambda} = (\varepsilon_a - \varepsilon_i) \frac{\partial a_i^a}{\partial \lambda} - \sum_j \sum_b \langle ja \| ib \rangle \frac{\partial a_j^b}{\partial \lambda} + \frac{1}{2} \sum_{j,k} \sum_{b,c} \langle jk \| bc \rangle \{ a_{jk}^{cd} \frac{\partial a_i^b}{\partial \lambda} + a_{ik}^{cb} \frac{\partial a_j^a}{\partial \lambda} + 2 a_{ik}^{ac} \frac{\partial a_j^b}{\partial \lambda} \}, \tag{A1.3}$$

$$\sum_{j<k} \sum_{b<c} C_{i,jk}^{a,bc} \frac{\partial a_{jk}^{bc}}{\partial \lambda} = -\frac{1}{2} \sum_j \sum_{b,c} \langle ja \| bc \rangle \frac{\partial a_{ij}^{bc}}{\partial \lambda} - \frac{1}{2} \sum_{j,k} \sum_b \langle jk \| ib \rangle \frac{\partial a_{jk}^{ab}}{\partial \lambda} + \frac{1}{2} \sum_{j,k} \sum_{b,c} \langle jk \| bc \rangle \{ \frac{\partial a_{jk}^{ca}}{\partial \lambda} a_i^b + \frac{\partial a_{ik}^{cb}}{\partial \lambda} a_j^a + 2 \frac{\partial a_{ik}^{ac}}{\partial \lambda} a_j^b \}, \tag{A1.4}$$

$$\sum_k \sum_c C_{ij,k}^{ab,c} \frac{\partial a_k^c}{\partial \lambda} = \sum_c \{ \langle ab \| cj \rangle \frac{\partial a_i^c}{\partial \lambda} - \langle ab \| ci \rangle \frac{\partial a_j^c}{\partial \lambda} \} + \sum_k \{ -\langle kb \| ij \rangle \frac{\partial a_k^a}{\partial \lambda} + \langle ka \| ij \rangle \frac{\partial a_k^b}{\partial \lambda} \}, \tag{A1.5}$$

$$\begin{aligned} \sum_{k<l} \sum_{c<d} C_{ij,kl}^{ab,cd} \frac{\partial a_{kl}^{cd}}{\partial \lambda} = {} & (\varepsilon_a + \varepsilon_b - \varepsilon_i - \varepsilon_j) \frac{\partial a_{ij}^{ab}}{\partial \lambda} + \frac{1}{2} \sum_{c,d} \langle ab \| cd \rangle \frac{\partial a_{ij}^{cd}}{\partial \lambda} \\ & + \frac{1}{2} \sum_{k,l} \langle kl \| ij \rangle \frac{\partial a_{kl}^{ab}}{\partial \lambda} - \sum_k \sum_c \{ \langle kb \| jc \rangle \frac{\partial a_{ik}^{ac}}{\partial \lambda} \\ & + \langle ka \| jc \rangle \frac{\partial a_{ik}^{cb}}{\partial \lambda} + \langle kb \| ic \rangle \frac{\partial a_{kj}^{ac}}{\partial \lambda} + \langle ka \| ic \rangle \frac{\partial a_{kj}^{cb}}{\partial \lambda} \} \\ & + \frac{1}{4} \sum_{k,l} \sum_{c,d} \langle kl \| cd \rangle \{ \frac{\partial a_{ij}^{cd}}{\partial \lambda} a_{kl}^{ab} + a_{ij}^{cd} \frac{\partial a_{kl}^{ab}}{\partial \lambda} \\ & - 2[a_{ij}^{ac} \frac{\partial a_{kl}^{bd}}{\partial \lambda} + a_{ij}^{bd} \frac{\partial a_{kl}^{ac}}{\partial \lambda} + \frac{\partial a_{ij}^{ac}}{\partial \lambda} a_{kl}^{bd} + \frac{\partial a_{ij}^{bd}}{\partial \lambda} a_{kl}^{ac}] \\ & - 2[a_{ik}^{ab} \frac{\partial a_{jl}^{cd}}{\partial \lambda} + a_{ik}^{cd} \frac{\partial a_{jl}^{ab}}{\partial \lambda} + \frac{\partial a_{ik}^{ab}}{\partial \lambda} a_{jl}^{cd} + \frac{\partial a_{ik}^{cd}}{\partial \lambda} a_{jl}^{ab}] \\ & + 4[a_{ik}^{ac} \frac{\partial a_{jl}^{bd}}{\partial \lambda} + a_{ik}^{bd} \frac{\partial a_{jl}^{ac}}{\partial \lambda} + \frac{\partial a_{ik}^{ac}}{\partial \lambda} a_{jl}^{bd} + \frac{\partial a_{ik}^{bd}}{\partial \lambda} a_{jl}^{ac}] \}, \end{aligned} \tag{A1.6}$$

The final z-vector equations within QCISD theory are given by

$$(\varepsilon_a - \varepsilon_i) z_i^a + w[z]_i^a + v[z]_i^a = 0 \tag{A1.7}$$

and

$$(\varepsilon_a + \varepsilon_b - \varepsilon_i - \varepsilon_j) z_{ij}^{ab} + w[z]_{ij}^{ab} + v[z]_{ij}^{ab} + y[z]_{ij}^{ab} = \langle ij \| ab \rangle, \tag{A1.8}$$

that means by a form which is very similar to the original QCISD equations. The arrays $w[z]_i^a$ and $w[z]_{ij}^{ab}$ are very similar to the arrays $w_i^a$ and $w_{ij}^{ab}$. The only difference is that while $w_i^a$ and $w_{ij}^{ab}$ are calculated using the amplitudes $a_i^a$ and $a_{ij}^{ab}$ the arrays $w[z]_i^a$ and $w[z]_{ij}^{ab}$ are evaluated using the z-amplitudes $z_i^a$ and $z_{ij}^{ab}$ :

$$\begin{aligned} w[z]_i^a = &- \sum_j \sum_b \langle ja \| ib \rangle z_i^b - \frac{1}{2} \sum_j \sum_{b,c} \langle ja \| bc \rangle z_{ij}^{bc} \\ &- \frac{1}{2} \sum_{j,k} \sum_b \langle jk \| ib \rangle z_{jk}^{ab}, \end{aligned} \tag{A1.9}$$

$$\begin{aligned} w[z]_{ij}^{ab} = &\sum_c \{ \langle ab \| cj \rangle z_i^c - \langle ab \| ci \rangle z_j^c \} + \sum_k \{ - \langle kb \| ij \rangle z_k^a + \langle ka \| ij \rangle z_k^b \} \\ &+ \frac{1}{2} \sum_{c,d} \langle ab \| cd \rangle z_{ij}^{cd} + \frac{1}{2} \sum_{k,l} \langle kl \| ij \rangle z_{kl}^{ab} - \sum_k \sum_c \{ \langle kb \| jc \rangle z_{ik}^{ac} \\ &+ \langle ka \| jc \rangle z_{ik}^{cb} + \langle kb \| ic \rangle z_{kj}^{ac} + \langle ka \| ic \rangle z_{kj}^{cb} \}. \end{aligned} \tag{A1.10}$$

The array $v[z]_i^a$ is obtained from $v_i^a$ by substituting the two-electron integrals by the double excitation amplitudes $a_{ij}^{ab}$, the double excitation amplitudes by the two-electron integrals $\langle ij \| ab \rangle$ and by replacing the single excitation amplitudes $a_i^a$ by $z_i^a$ :

$$v[z]_i^a = \frac{1}{2} \sum_{j,k} \sum_{b,c} a_{jk}^{bc} \{ z_i^b \langle jk \| ca \rangle + z_j^a \langle ik \| cb \rangle + 2 z_j^b \langle ik \| ac \rangle \}. \tag{A1.11}$$

The array $v[z]_{ij}^{ab}$ is derived in a similar way from the quadratic array $v_{ij}^{ab}$ :

$$\begin{aligned} v[z]_{ij}^{ab} = \frac{1}{4} \sum_{k,l} \sum_{c,d} a_{kl}^{cd} \{ &\langle ij \| cd \rangle z_{kl}^{ab} + z_{ij}^{cd} \langle kl \| ab \rangle \\ &- 2[\langle ij \| ac \rangle z_{kl}^{bd} + \langle ij \| bd \rangle z_{kl}^{ac} + z_{ij}^{ac} \langle kl \| bd \rangle + z_{ij}^{bd} \langle kl \| ac \rangle] \\ &- 2[\langle ik \| ab \rangle z_{jl}^{cd} + \langle ik \| cd \rangle z_{jl}^{ab} + z_{ik}^{ab} \langle jl \| cd \rangle + z_{ik}^{cd} \langle jl \| ab \rangle] \\ &+ 4[\langle ik \| ac \rangle z_{jl}^{bd} + \langle ik \| bd \rangle z_{jl}^{ac} + z_{ik}^{ac} \langle jl \| bd \rangle + z_{ik}^{bd} \langle jl \| ac \rangle]] \}. \end{aligned} \tag{A1.12}$$

The only new term in the z-vector equations in comparision with the original QCISD equation is the array $y[z]_{ij}^{ab}$ which is defined as

$$y[z]_{ij}^{ab} = \sum_k \sum_c a_k^c \{\langle ij\|ca\rangle z_k^b + \langle ij\|bc\rangle z_k^a + \langle kj\|ba\rangle z_i^c + \langle ik\|bc\rangle z_j^c + \langle kj\|cb\rangle z_i^a + \langle kj\|ac\rangle z_i^b + \langle ik\|cb\rangle z_j^a + \langle ik\|ac\rangle z_j^b\}. \tag{A1.13}$$

There is no corresponding term to $y[z]_{ij}^{ab}$ in the QCISD equations. This is because the excitations $\mathbf{T_1T_2}$ are only included in the equations for the singles, but not considered in the equations for the doubles.

## Appendix 2

Here, formulas for the arrays $X_1$, $X_2$, ... ,$X_6$, $Y_1$, and $Y_2$ are given.

$$\text{MP2}: X_1^{MP2}(ijab) = \frac{1}{2}a(ij,ab)$$

$$Y_1^{MP2}(ij) = -\frac{1}{2}\sum_k \sum_{a,b} a(ik,ab)a(jk,ab)$$

$$Y_2^{MP2}(ab) = \frac{1}{2}\sum_{i,j} \sum_c a(ij,ac)a(ij,bc)$$

$$\text{MP3}: X_1^{MP3}(ij,ab) = \frac{1}{2}d(ij,ab)$$

$$X_2^{MP3}(ijkl) = \frac{1}{8}\sum_{a,b} a(ij,ab)a(kl,ab)$$

$$X_3^{MP3}(iajb) = -\sum_k \sum_c a(jk,ac)a(ik,bc)$$

$$X_4^{MP3}(abcd) = \frac{1}{8}\sum_{i,j} a(ij,ab)a(ij,cd)$$

$$Y_1^{MP3}(ij) = -\frac{1}{2}\sum_k \sum_{a,b} \{a(ik,ab)d(jk,ab) + d(ik,ab)a(jk,ab)\}$$

$$Y_2^{MP3}(ab) = \frac{1}{2}\sum_{i,j} \sum_c \{a(ij,ac)d(ij,bc) + d(ij,ac)a(ij,bc)\}$$

$$\text{MP4}: X_1^{MP4}(ij,ab) = \frac{1}{2}\{e(ij,ab) + x(ij,ab)\}$$

$$X_2^{MP4}(ijkl) = \frac{1}{8}\sum_{a,b}\{a(ij,ab)d(kl,ab) + d(ij,ab)a(kl,ab)\}$$

$$X_3^{MP4}(iajb) - \sum_{k}\sum_{c}\{a(jk,ac)d(ik,bc) + d(jk,ac)a(ik,bc)\}$$

$$X_4^{MP4}(abcd) = \frac{1}{8}\sum_{i,j}\{a(ij,ab)d(ij,cd) + d(ij,ab)a(ij,cd)\}$$

$$X_5^{MP4}(ijka) = -\sum_{b} d(k,b)a(ij,ba) + 2r(ijk,a)$$

$$X_6^{MP4}(iabc) = \sum_{j} d(j,a)a(ji,bc) + 2s(i,abc)$$

$$\begin{aligned} Y_1^{MP4}(ij) = -\frac{1}{2}\sum_{k}\sum_{a,b}\{&a(ik,ab)[e(jk,ab) + \frac{1}{2}x(jk,ab)] \\ &+[e(ik,ab) + \frac{1}{2}x(ik,ab)a(jk,ab)\} \\ &-\sum_{a} d(i,a)d(j,a) - \frac{1}{2}\sum_{k}\sum_{a,b} d(ik,ab)d(jk,ab) \\ &-\frac{1}{12}\sum_{k,l}\sum_{a,b,c} d(ikl,abc)d(jkl,abc) \end{aligned}$$

$$\begin{aligned} Y_2^{MP4}(ab) = \frac{1}{2}\sum_{i,j}\sum_{c}\{&a(ij,ac)[e(ij,bc) + \frac{1}{2}x(ij,bc)] \\ &+[e(ij,ac) + \frac{1}{2}x(ij,ac)]a(ij,bc)\} \\ &+\sum_{i} d(i,a)d(i,b) + \frac{1}{2}\sum_{i,j}\sum_{c} cd(ij,ac)d(ij,bc) \\ &+\frac{1}{12}\sum_{i,j,k}\sum_{c,d} d(ijk,acd)d(ijk,bcd) \end{aligned}$$

$$\text{QCISD}: X_1^{QCISD}(ijab) = \frac{1}{4}\{a_{ij}^{ab} - z_{ij}^{ab} - x_{ij}^{ab}\}$$

$$X_2^{QCISD}(ijkl) = -\frac{1}{16}\sum_{a,b}\{z_{ij}^{ab}a_{kl}^{ab} + z_{kl}^{ab}a_{ij}^{ab}\}$$

$$X_3^{QCISD}(iajb) = \frac{1}{2}\sum_{k}\sum_{c}\{a_{jk}^{ac}z_{ik}^{bc} + z_{jk}^{ac}a_{ik}^{bc}\} + \frac{1}{2}\{z_i^b a_j^a + a_i^b z_j^a\}$$

$$X_4^{QCISD}(abcd) = -\frac{1}{16}\sum_{i,j}\{z_{ij}^{ab}a_{ij}^{cd} + z_{ij}^{cd}a_{ij}^{ab}\}$$

$$X_5^{QCISD}(ijka) = \frac{1}{2}\sum_{b}\{a_{ij}^{ba}z_k^b + z_{ij}^{ba}a_k^b\}$$

$$X_6^{QCISD}(iabc) = \frac{1}{2}\sum_{j}\{a_{ji}^{bc}z_j^a + z_{ji}^{bc}a_k^b\}$$

$$Y_1^{QCISD}(ij) = -\frac{1}{2}\sum_{a}\{a_i^a z_j^a + a_j^a z_i^a\} - \frac{1}{4}\sum_{k}\sum_{a,b}\{a_{ik}^{ab}z_{jk}^{ab} + z_{ik}^{ab}a_{jk}^{ab}\}$$

$$Y_2^{QCISD}(ab) = \frac{1}{2}\sum_{i}\{a_i^a z_i^b + z_i^a a_i^b\} + \frac{1}{4}\sum_{i,j}\sum_{c}\{a_{ij}^{ac}z_{ij}^{bc} + z_{ij}^{ac}a_{ij}^{bc}\}$$

$$\text{QCISD(T)}: X_1^{QCISD(T)}(ijab) = X_1^{QCISD}(ijab) + \frac{1}{2}u_{ij}^{ab}$$

$$X_2^{QCISD(T)}(ijkl) = X_2^{QCISD}(ijkl)$$

$$X_3^{QCISD(T)}(iajb) = X_3^{QCISD}(iajb)$$

$$X_4^{QCISD(T)}(abcd) = X_4^{QCISD}(abcd)$$

$$X_5^{QCISD(T)}(ijka) = X_5^{QCISD}(ijka) + 2r_{ijk}^a$$

$$X_6^{QCISD(T)}(iabc) = X_6^{QCISD}(iabc) + 2s_i^{abc}$$

$$Y_1^{QCISD(T)}(ij) = Y_1^{QCISD}(ij) + \frac{1}{24}\sum_{k,l}\sum_{a,b,c}\{d_{ijk}^{acd}[d_{ijk}^{bcd} + \tilde{d}_{ijk}^{bcd}] + d_{jkl}^{abc}[d_{ikl}^{abc} + \tilde{d}_{ikl}^{abc}]\}$$

$$Y_2^{QCISD(T)}(ab) = Y_2^{QCISD}(ab) + \frac{1}{24}\sum_{i,j,k}\sum_{c,d}\{d_{ijk}^{acd}[d_{ijk}^{bcd} + \tilde{d}_{ijk}^{bcd}] + d_{ijk}^{bcd}[d_{ijk}^{acd} + \tilde{d}_{ijk}^{acd}]\}.$$

All formulas are given here in such a way that symmetries between the four indices $p$, $q$, $r$, and $s$ of the corresponding integral derivative can be used. For example, in the case of the integral $\langle ij\|ab\rangle$ the following symmetry relations hold

$$\langle ij\|ab\rangle = -\langle ji\|ab\rangle = -\langle ij\|ba\rangle = \langle ji\|ba\rangle$$

and in the same way

$$X_1(ijab) = -X_1(jiab) = -X_1(ijba) = X_1(jiba).$$

## References


[1] See, e.g. (a) H.F. Schaefer III, *Quantum Chemistry, the Development of Ab initio Methods in Molecular Electronic Structure Theory* (Clarendon Press, Oxford, 1984); (b) C.E. Dykstra, *Ab initio Calculations of the Structures and Properties of Molecules* (Elsevier, Amsterdam, 1988); (c) R.S. Mulliken and W.C. Ermler, *Polyatomic Molecules, Results of ab initio Calculations* (Academic Press, New York, 1981); (d) R.S. Mulliken and W.C. Ermler, *Diatomic Molecules, Results of ab initio Calculations* (Academic Press, New York, 1977)

[2] See, for example, *Theoret. Chim. Acta* **71** (1987) 89 - 245 ; **72** (1987) 71-173, where papers from the Symposium on Computational Quantum Chemistry and Parallel Processors held in Edmonton, Canada, were published.

[3] W.J. Hehre, L. Radom, P.v. R. Schleyer, and J.A. Pople. *Ab Initio Molecular Orbital Theory* (Wiley, New York, 1986).

[4] P.Jørgensen and J. Simons, eds. *Geometrical Derivatives of Energy Surfaces and Molecular Properties* (Reidel, Dordrecht, 1986).

[5] (a) H.F. Schaefer and Y. Yamaguchi *J. Mol. Struct. (THEOCHEM)* **135** (1986) 369; (b) P. Pulay, *Adv. Quant. Chem.* **67** (1987) 241.

[6] H.B. Schlegel, *Adv. Quant. Chem.* **67** (1987) 249.

[7] B.A. Hess Jr., L.J. Schaad, P. Carsky, and R. Zahradnik, *Chem. Rev.* **86** (1986) 709.

[8] J.F. Gaw and N.C. Handy in *Geometrical Derivatives of Energy Surfaces and Molecular Properties*,P.Jørgensen and J. Simons, eds. (Reidel, Dordrecht, 1986), p. 79.

[9] R.D. Amos, *Adv. Quant. Chem.* **67** (1987) 99.

[10] S. Califano, *Vibrational States* (Wiley, New York, 1976).

[11] E.B. Wilson, J.C. Decius, P.C. Cross, *Molecular Vibrations* (Dover, New York, 1981 ).

[12] P. Pulay in *Modern Theoretical Chemistry, Vol. 3*, ed. H.F. Schaefer III (Plenum Press, New York, 1977).

[13] P. Pulay in *The Force Concept in Chemistry*, ed. B.M. Deb (van Nostrand Reinhold, New York 1983).

[14] P. Pulay, *Mol. Phys.* **17** (1969) 197.

[15] P. Pulay, *Mol. Phys.* **18** (1970) 473.

[16] H.F. King and M. Dupuis, *J. Comp. Phys.* **21** (1976) 144; M. Dupuis, J. Rys, and H.F. King, *J. Chem. Phys.* **65** (1976) 111.

[17] H.B. Schlegel, J.S. Binkley, and J.A. Pople, *J. Chem. Phys.* **80** (1984) 1976.

[18] J.A. Pople, R. Krishnan, H.B. Schlegel, and J.S. Binkley, *Intern. J. Quantum Chem. Symp.* **13** (1979) 225.

[19] R. McWeeny, *Rev. Mod. Phys.* **32** (1960) 335; R. McWeeny, *Phys.Rev.* **126** 1028.

[20] R.M. Stevens, R.M. Pitzer, and W.N. Lipscomb, *J. Chem. Phys.* **38** (1963) 550.

[21] J. Gerratt and I.M. Mills, *J. Chem. Phys.* **49** (1968) 1719.

[22] N.C. Handy and H.F. Schaefer III, *J. Chem. Phys.* **81** (1984) 5031.

[23] B.R. Brooks, W.D. Laidig, P. Saxe, J.D. Goddard, Y.Yamaguchi, and H.F. Schaefer III, *J. Chem. Phys.* **72** (1980) 4652.

[24] R. Krishnan, H.B. Schlegel, and J.A. Pople, *J. Chem. Phys.* **72** (1980) 4654.

[25] J.D. Goddard, N.C. Handy, and H.F. Schaefer III, *J. Chem. Phys.* **71** (1979) 1525.

[26] S. Kato and K. Morokuma, *Chem. Phys. Letters* **65** (1979) 19.

[27] J.F. Gaw, Y. Yamaguchi, and H.F. Schaefer III, *J. Chem. Phys.* **81** (1984) 6395.

[28] R.N. Camp, H.F. King, J.W. McIver, and D Mullally, *J. Chem. Phys.* **79** (1983) 1088.

[29] Y. Yamaguchi, Y. Osamura, G. Fitzgerald, and H.F. Schaefer III, *J. Chem. Phys.* **78** (1983) 1607.

[30] D.J. Fox, Y. Osamura, M.R. Hoffmann, J.F. Gaw, G. Fitzgerald, Y. Yamaguchi, and H.F. Schaefer III, *Chem. Phys. Letters* **102** (1983) 17.

[31] R.D. Amos, *Chem. Phys. Letters* **108** (1985) 185.

[32] R.D. Amos, *Chem. Phys. Letters* **124** (1986) 376.

[33] M.J. Frisch, Y. Yamaguchi, J.F. Gaw, H.F. Schaefer III, and J.S. Binkley, *J. Chem. Phys.* **84** (1986) 531.

[34] C. Møller and M.S. Plesset, *Phys. Rev.* **46** (1934) 618.

[35] I. Shavitt, in *Modern Theoretical Chemistry, Vol. 3*, ed. H.F. Schaefer III (Plenum Press, New York, 1977).

[36] J. Čížek, *J. Chem. Phys.* **45** (1966) 4256; *Advan. Chem. Phys.* **14** (1966) 35.

[37] R.J. Bartlett, *Ann. Rev. Phys. Chem.* **32** (1981) 359; J. Paldus in *New Horizons of Quantum Chemistry*; R.J. Bartlett, C.E. Dykstra, and J. Paldus in *Advanced Theories and Computational Approaches to the Electronic Structure of Molecules*; R.J. Bartlett, J. Phys. Chem. **93** (1989) 1697.

[38] J.A. Pople, J.S. Binkley, and R. Seeger, *Intern. J. Quantum Chem. Symp.* **10** (1976) 1.

[39] R. Krishnan and J.A. Pople, *Intern. J. Quantum Chem.* **14** (1978) 91.

[40] R. Krishnan, M.J. Frisch, and J.A. Pople, *J. Chem. Phys.* **72** (1980) 4244.

[41] J.S. Binkley, M.J. Frisch, D.J. DeFrees, K. Raghavachari, R.A. Whiteside, H.B. Schlegel, E.M. Fluder, and J.A. Pople, *GAUSSIAN82*, Carnegie-Mellon University, Pittsburgh (1985).

[42] S.R. Langhoff and E.R. Davidson, *Intern. J. Quantum Chem.* **8** (1974) 61.

[43] (a) C.W. Gillies, J.Z. Gillies, R.D. Suenram, F.J. Lovas, E. Kraka, D. Cremer, *J. Am. Chem. Soc.* **113** (1991) 2412; (b) D. Cremer, to be published.

[44] See for example T.J. Lee, R.B. Remington, Y. Yamaguchi, and H.F. Schaefer III, *J. Chem. Phys.* **89** (1988) 408.

[45] H.B. Schlegel, *J. Chem. Phys.* **84** (1986) 4530; H.B. Schlegel, *J. Phys. Chem.* **92** (1988) 3075.

[46] P.J. Knowles and N.C. Handy, *J. Chem. Phys.* **88** (1988) 6991.

[47] K. Wolinski and P. Pulay, *J. Chem. Phys.* **90** (1989) 3647.

[48] K. Anderssen, P. Å. Malmqvist, B.O. Roos, A.J. Sadlej, and K. Wolinski, *J. Phys. Chem.* **94** (1990) 5403.

[49] J.A. Pople, R. Krishnan, H.B. Schlegel, and J.S. Binkley, *Intern. J. Quantum Chem.* **14** (1978) 545.

[50] R.J. Bartlett and G.D. Purvis III, *Intern. J. Quantum Chem.* **14** (1978) 561.

[51] G.D. Purvis III and R.J. Bartlett, *J. Chem. Phys.* **76** (1982) 1910.

[52] J.A. Pople, M. Head-Gordon, and K. Raghavachari, *J. Chem. Phys.* **87** (1987) 5968.

[53] G.E. Scuseria and H.F. Schaefer III, *J. Chem. Phys.* **90** (1989) 3700.

[54] J. Paldus, J.Čížek, and B. Jeziorski, *J. Chem. Phys.* **90** (1989) 4356.

[55] K. Raghavachari, J.A. Pople, E.S. Replogle, and M. Head-Gordon, *J. Phys. Chem.* **94** (1990) 5579.

[56] P. Jørgensen and J. Simons, *J. Chem. Phys.* **79** 91983) 334.

[57] G. Fitzgerald, R. Harrison, W.D. Laidig, and R.J. Bartlett, *J. Chem. Phys.* **82** (1985) 4379.

[58] J. Gauss and D. Cremer, *Chem. Phys. Letters* **138** (1987) 131.

[59] J.E. Rice and R.D. Amos, *Chem. Phys. Letters* **122** (1985) 585.

[60] E.A. Salter, G.W. Trucks, G. Fitzgerald, and R.J. Bartlett, *Chem. Phys. Letters* **141** (1987) 61.

[61] I.L. Alberts and N.C. Handy, *J. Chem. Phys.* **89** (1988) 2107.

[62] G. Fitzgerald, R.J. Harrison, and R.J. Bartlett, *J. Chem. Phys.* **85** (1986) 5143.

[63] J. Gauss and D. Cremer, *Chem. Phys. Letters* **153** (1988) 303.

[64] G.W. Trucks, J.D. Watts, E.A. Salter, and R.J. Bartlett, *Chem. Phys. Letters* **153** (1988) 490.

[65] J.D. Watts, G.W. Trucks, and R.J. Bartlett, *Chem. Phys. Letters* **164** (1989) 502.

[66] G. Fitzgerald, R.J. Harrison, W.D. Laidig, and R.J. Bartlett, *Chem. Phys. Letters* **117** (1985) 433.

[67] L. Adamowicz, W.D. Laidig, and R.J. Bartlett, *Intern. J. Quantum Chem. Symp.* **18** (1984) 245.

[68] A.C. Scheiner, G.E. Scuseria, J.E. Rice, T.J. Lee, and H.F. Schaefer III, *J. Chem. Phys.* **87** (1987) 433.

[69] Y.S. Lee and R.J. Bartlett, *J. Chem. Phys.* **80** (1983) 4371; Y.S. Lee, S.A. Kucharski, and R.J. Bartlett, *J. Chem. Phys.* **81** (1984) 5906; *J. Chem. Phys.* **82** (1984) 5761.

[70] G.E. Scuseria and H.F. Schaefer III, *Chem. Phys. Letters* **146** (1988) 23.

[71] J. Gauss, J.F. Stanton, and R.J. Bartlett, *J. Chem. Phys.*, in press.

[72] J. Gauss and D. Cremer, *Chem. Phys. Letters* **150** (1988) 280.

[73] J. Gauss and D. Cremer, *Chem. Phys. Letters* **163** (1989) 549.

[74] S. Kucharski and R.J. Bartlett, *Adv. Quant. Chem.* **18** (1986) 281.

[75] S. Kucharski, J. Noga, and R.J. Bartlett, *J. Chem. Phys.* **90** (1989) 7282.

[76] P. Pulay, *Chem. Phys. Letters* **73** (1980) 393; *J. Comp. Chem.* **3** (1982) 556.

[77] G.D. Purvis and R.J. Bartlett, *J. Chem. Phys.* **75** (1981) 1284; G.W. Trucks, J. Noga, and R.J. Bartlett, *Chem. Phys. Letters* **145** (1988) 548.

[78] C.E. Dykstra and J.D. Augspurger, *Chem. Phys. Letters* **145** (1988) 545.

[79] G.E. Scuseria, T.J. Lee, and H.F. Schaefer III, *Chem. Phys. Letters* **130** (1986) 236.

[80] It should be noted that QCISDT is no longer a size consistent method (see e.g. ref [54]) Therefore, an iterative inclusion of triple excitations in QCI theory is not as straightforward as in CC theory, where the full CCSDT model [81] and various approximations to it [82] can be easily formulated in a size consistent way.

[81] J. Noga and R.J. Bartlett, *J. Chem. Phys.* **86** (1987) 7041; J.D. Watts and R.J. Bartlett, *J. Chem. Phys.* **93** (1990) 6104.

[82] J. Noga, R.J. Bartlett, and M. Urban, *Chem. Phys. Letters* **134** (1987) 126.

[83] K. Raghavachari, G.W. Trucks, J.A. Pople, and M. Head-Gordon, *Chem. Phys. Letters* **157** (1989) 479.

[84] K. Raghavachari, G.W. Trucks, J.A. Pople, and E. Replogle, *Chem. Phys. Letters* **158** (1989) 207.

[85] L.A. Curtiss and J.A. Pople, *J. Chem. Phys.* **90** (1989) 2833.

[86] L.A. Curtiss and J.A. Pople, *J. Chem. Phys.* **90** (1989) 2522; *J. Chem. Phys.* **90** (1989) 4314; *J. Chem. Phys.* **91** (1989) 4189.

[87] For other CC methods, which include connected quadruple excitations, see for example S. Kucharski and R.J. Bartlett, *Chem. Phys. Letters* **158** (1989) 550.

[88] N.C. Handy, R.D. Amos, J.F. Gaw, J.E. Rice, and E.D. Simandiras, *Chem. Phys. Letters* **120** (1985) 151.

[89] R. Moccia, *Chem. Phys. Letters* **5** (1970) 260.

[90] E.A. Salter, G.W. Trucks, and R.J. Bartlett, *J. Chem. Phys.* **90** (1989) 1752.

[91] G.W. Trucks, E.A. Salter, J. Noga, and R.J. Bartlett, *Chem. Phys. Letters* **150** (1988) 37.

[92] G.W. Trucks, E.A. Salter, C. Sosa, and R.J. Bartlett, *Chem. Phys. Letters* **147** (1988) 359.

[93] E. Kraka, J. Gauss, and D. Cremer, *J. Mol. Struct. (THEOCHEM)* , in

press.

[94] J. Gauss, E. Kraka, F. Reichel, and D. Cremer, *COLOGNE*, University of Cologne, Cologne (1989) and University of Göteborg, Göteborg (1990).

[95] D. Cremer and E. Kraka, *COLOGNE84*, University of Cologne, Cologne (1984).

[96] J. Gauss, Ph.D. Thesis, University of Cologne, Cologne (1988).

[97] J. Almlöf, K. Faegri,Jr., and K. Korsell, *J. Comp. Chem.* **3** (1982) 385.

[98] D. Cremer and J. Gauss, *J. Comp. Chem.* **7** (1986) 274.

[99] F. Reichel, Diploma Thesis, University of Cologne, Cologne (1988).

[100] F.W. Bobrowicz and W.A. Goddard III, *Modern Theoretical Chemistry Vol.3*, ed. H.F. Schaefer III (Plenum Press, New York, 1977).

[101] L.R. Kahn, P. Baybutt, and D.G. Truhlar, J. Chem. Phys. **65** (1976) 3826.

[102] D. Cremer, *J. Phys. Chem.* **94** (1990) 5502.

[103] R.F.W. Bader, T.S. Slee, D. Cremer, and E. Kraka, *J. Am. Chem. Soc.* **105** (1985) 5061.

[104] D. Cremer and E. Kraka, *Croat. Chem. Acta* **57** (1985) 1265.

[105] D. Cremer in *Modelling of Structure and Properties of Molecules*, ed. Z.B. Maksic (Ellis Horwood, Chichester, 1988).

[106] M. Dupuis and H.F. King, *Int. J. Quant. Chem.*, **11** (1977) 613.

[107] P. Carsky, B.A. Hess, Jr., and L.J. Schaad, *J. Comp. Chem.* **5** (1984) 280.

[108] J.F. Stanton, J. Gauss, J.D. Watts, and R.J. Bartlett, *J. Chem. Phys.* **94** (1991) 4334.

[109] Y. Osamura, Y. Yamaguchi, P. Saxe, D.J. Fox, M.A. Vincent, and H.F. Schaefer III, *J. Mol. Struct. (THEOCHEM)* **103** (1983) 183.

[110] P. Pulay, *J. Chem. Phys.* **78** (1983) 5043.

[111] M. Yoshimine, *J. Comp. Phys.* **11** (1973) 449.

[112] R.D. Nelson, Jr., D.R. Lide, Jr., and A.A. Maryott, *Selected Values of Electric Dipole Moments for Molecules in the Gas Phase*, NSRDS-NBS **10**, Washington 1967.

[113] A.K. Siu and E.R. Davidson, *Intern. J. Quantum Chem.* **4** (1970) 233; S. Green *Chem. Phys.* **54** (1971) 827; S. Green, *Adv. Chem. Phys.* **25** (1974) 179.

[114] D. Cremer, M. Krüger, and H. Dreizler, to be published.

[115] N. Ensllin, W. Bertozzi, S. Kowalski, C.P. Sargent, W. Turchinetz, C.F. Williamson, S.P. Fivozinsky, J.W. Lightbody, and S. Penner, *Phys. Rev. (C)* **9** (1974) 1705; H. Winter and H.J. Andr, *Phys. Rev. (A)* **21** (1980) 581.

[116] D. Sundholm, P. Pyykkö, L.Laakoonen, and A.J. Sadlej, *Chem. Phys.* **101** (1986) 219; I. Cernusak, G.H.F. Diercksen, and A.J. Sadlej, *Chem. Phys.* **101** (1986) 45; S. Gerber and H. Huber, *Chem. Phys.* **134** (1989) 279.

[117] F.C. de Lucia and W. Gordy, *Phys. Rev.* **187** (1969) 58.

[118] 6-31G(d) and 6-31G(d,p): P.C. Hariharan and J.A. Pople, *Theoret. Chim. Acta* **28** (1973) 213. 6-311G(d,p): R. Krishnan, J.S. Binkley, R. Seeger, and J.A. Pople, *J. Chem. Phys.* **72** (1980) 650; MC-311G(d,p): A.D. McLean and G.S. Chandler, *J. Chem. Phys.* **72** (1980) 5639. 6-311++G(d,p): T. Clark, J. Chandrasekhar, G.W. Spitznagel, and P. v. R. Schleyer, *J. Comp. Chem.* **4** (1983) 294. [5s3p2d/3s2p]: T. Dunning, Jr., *J. Chem. Phys.* **53** (1970) 2823. Exponents of the polarisation functions: K. Somasundram, R.D. Amos, and N.C. Handy, *Theoret. Chim. Acta* **69** (1986) 491.

[119] T.J. Lee, R.B. Remington, Y. Yamaguchi, and H.F. Schaefer III, *J. Chem. Phys.* **89** (1988) 408. R. Krishnan, M.J. Frisch and J. A. Pople, *J. Chem. Phys.* **72** (1980) 4244.

[120] See, e.g., W.J. Hehre, L. Radom, P.v. R. Schleyer, and J. A. Pople, *Ab Initio Molecular Orbital Theory*, (John Wiley, New York, 1986) and references cited therein.

[121] Zhi He and D. Cremer, *Intern. J. Quantum Chem. Symp.*, in press.

[122] S. Miertus and J. Tomasi, *Chem. Phys.* **65** (1982) 239.

[123] M. Schindler and W. Kutzelnigg, *J. Chem. Phys.* **76** (1982) 1919.

[124] E. Kraka, D. Cremer, and S. Nordholm in *Molecules in Science and Biomedicine*, Z. Maksic, Edt., Ellis Horwood, 1991, in press.

# AB INITIO MOLECULAR ORBITAL CALCULATIONS OF BOND INDEX AND VALENCY

A. B. Sannigrahi

Department of Chemistry
Indian Institute of Technology
Kharagpur - 721302
India

1. INTRODUCTION
2. DEFINITIONS OF BOND INDEX AND VALENCY FOR SINGLE DETERMINANT SCF WAVEFUNCTIONS
2.1 Heuristic Definition
2.2 Exchange Part of the Second Order Density Matrix and Bond Index
2.3 Statistical Interpretation of Bond Index
3. DEFINITIONS OF BOND INDEX AND VALENCY FOR CORRELATED WAVEFUNCTIONS
4. APPLICATIONS OF THE CONCEPTS OF BOND INDEX AND VALENCY
4.1 Results of Calculations using Single Determinant SCF Wavefunctions

ADVANCES IN QUANTUM CHEMISTRY
VOLUME 23

Copyright © 1992 By Academic Press, Inc.
All rights of reproduction in any form reserved.

4.2. Results of Calculations using Correlated Wavefunctions
5. SUMMARY AND CONCLUSIONS

## 1. INTRODUCTION

The Molecular Orbital (MO) theory,[1-3] since its inception, has been receiving overwhelming attention in the theoretical studies of electronic structure and spectra of molecules. Nearly all current quantum chemical calculations are based on the Hartree-Fock self-consistent-field (SCF)[4,5] theory recast by Roothaan[6] and others[7,8] in the framework of the LCAO (linear combination of atomic orbitals) approximation. Ab initio SCF wavefunctions using basis sets of moderate size can be obtained now-a-days for a wide variety of molecules without prohibitive computational efforts and expenses. For small molecules, calculations beyond the SCF level yielding results in very good agreement with experiment, are being meticulously performed by several investigators.[9] Ab initio quantum chemical calculations[9] taking relativistic effects into account have also been an active field of research since last 15 years or so. The basic mathematical structure, applications and limitations of various ab initio methods currently in use in quantum chemistry have recently been reviewed[9] by pioneering workers in the respective field.

Unfortunately, contemporary molecular wavefunctions emerging from the computer are usually too complicated to be directly amenable to simple chemical interpretations. It is, therefore, not possible to get an insight into the structure and properties of a molecule merely by calculating its wavefunction. What is needed, is to derive from the wavefunction a set of simple quantities which will be intuitively appealing to the chemists. The charge of an atom in a molecule or the atomic charge is one such quantity.

This is a local quantity and a measure of the number of electrons associated with a particular atom in a molecule. Since the atoms do not strictly retain their individual identities in the molecular environment, the atomic charge does not correspond to any observable within the framework of quantum mechanics, and cannot be measured experimentally. The observable quantity which is of direct relevance in this context is the three dimensional probability distribution function, $\rho(r) = \psi(r)\,\psi^{*}(r)$. It provides the basis for almost all the definitions[10-41] of atomic charge that have been proposed from time to time.

Besides atomic charge, the other useful local quantities that have been defined directly from the density matrix of a molecule are bond order, bond index and valency. According to the simple MO theory the bond order in homonuclear diatomics is defined to be equal to half the difference between the number of electrons in bonding and anti-bonding MOs. However, for heteronuclear diatomics and polyatomics, it is not possible to define bond order in such a simple manner. The definition of bond order in a polyatomic molecule was first given by Coulson[11] in the context of Hückel MO theory.[42] These bond orders are the off-diagonal elements ($P_{ab}$) of the first order density matrix, P. More explicitly,

$$P_{ab} = \sum_{i} n_i\, C_{ia}\, C^{*}_{ib} \qquad (1.1)$$

where $n_i$ is the occupation number of the ith MO, and $C_{ia}$ is the coefficient of the ath atomic orbital in the ith MO. Coulson's bond order is a measure of the degree of $\pi$-bonding of a given bond. It correlates well with the observed bond length[11] in conjugated systems. From a knowledge of bond order, one can also calculate the free valence index i.e., the residual $\pi$-bonding power of an atom in a molecule. This definition of bond order is applicable when the AOs are assumed to be mutually orthogonal, and only one AO is considered per center. These approximations are usually invoked in the $\pi$-electron theories of Hückel[42] and of Pariser, Parr and Pople.[43,44]

For an overlapping basis set Chirgwin and Coulson[12] proposed the following definition for bond order (henceforth it is denoted by the elements of B matrix).

$$B_{ab} = \frac{1}{2}[(PS)_{ab} + (SP)_{ab}] \tag{1.2}$$

where $P = 2CC^{+}$ (C is the coefficient matrix of the doubly occupied MOs, and $C^{+}$ is the adjoint of C) and S is the AO overlap matrix. In Eq.(1.2) the symmetrized sum of PS and SP matrices is used in order to ensure that the bond order matrix is symmetric. Using Löwdin's symmetrically orthogonalized orbitals,[13] McWeeny[14] defined bond order as the off-diagonal elements of the $(S^{1/2}PS^{1/2})$ matrix.

$$B_{ab} = (S^{1/2}\,PS^{1/2})_{ab} \tag{1.3}$$

Mulliken[15] chose to define bond order in a somewhat different manner. For an overlapping basis he proposed that

$$B_{ab} = P_{ab}(S_{ab} + 1) \tag{1.4}$$

Equations (1.2) - (1.4) reduce to Coulson's bond order [ Eq.(1.1)] when S = I, the identity matrix.

The above definitions of bond order are restricted to cases where only one AO is considered per atom. For a general case, when more than one AO is considered per atomic center, one may try to define bond order as follows.

$$B_{AB} = \sum_{a}^{A}\sum_{b}^{B} B_{ab} \tag{1.5}$$

where summation is taken over all the orbitals centered on A and B respectively. A relation of this type was used by a few investigators[45-48] for the calculation of bond order in polyatomic molecules.

Cohen[49] proposed the following definition of bond order for an overlapping basis set.

$$B_{AB} = \sum_{a}^{A}\sum_{b}^{B} (P_{ab}S_{ab} + P_{ab}f_{ab}\bar{z}_{ab}) \tag{1.6}$$

where $f_{ab}$ is a long range factor and defined by

$$f_{ab} = S_{ab} / S^{R}_{ab} \qquad (1.7)$$

The superscript R indicates that the overlap integrals are taken at the reference bond distance. For neighboring pairs of atoms, $f_{ab}$ is set equal to one. For a nonbonded pair, he defined the reference bond distance as the sum of the covalent bond radii. Then, $f_{ab}$ is less than one and this ratio becomes an additional long range factor. The term $g_{ab}$ in Eq.(1.6) is an atomic hybridization and nonorthogonality factor. It is defined by

$$g_{ab} = h_a h_b$$

where,

$$h_a = \frac{\sum_c (P_{cc}\ S_{ac})^{1/2}}{(\sum_{cd} P_{cc}^{1/2}\ P_{dd}\ S_{cd}^{1/2})^{1/2}}$$

Cohen showed that definition (1.6) reduces in the appropriate special cases to Coulson and Mulliken bond orders. Presumably due to its complicated nature and concurrent availability of simpler expressions, Cohen's bond order has received very little attention.[50]

Following the observation of Salem[51] that the elements of the Hückel charge-bond order matrix for closed-shell systems obey the relation,

$$\sum_b P^2_{ab} = 2P_{aa} - P^2_{aa} \qquad (1.8)$$

Wiberg[52] proposed the following definition for bond order in the case of an orthonormal set of atomic orbitals (AO).

$$B_{AB} = \sum_a^A \sum_b^B P^2_{ab} \qquad (1.9)$$

In order to distinguish it from Coulson's bond order, which is linear in $P_{ab}$, Wiberg called $B_{AB}$ defined by Eq.(1.9), bond index, which is quadratic in $P_{ab}$. Using CNDO/2[53] density matrix he calculated $B_{AB}$ for several hydrocarbons and observed that the calculated quantities are almost identical with the corresponding bond multiplicity expected from classical consideration.

Deviations from classical integral values are ascribed to the ionic character of the bonds. Several definitions of $B_{AB}$ which are either quadratic or bilinear in the off-diagonal elements of the first order density matrix, have subsequently been proposed. They have been variously called bond order, bond valency, bond index, bond order index, degree of bonding etc. Of these, the term bond valency or bond valence is the most appropriate one. However, in order to give due recognition to the pioneering work of Wiberg we shall henceforth use the term bond index. It is a measure of the number of electrons of an atom A engaged in covalent bonding with another atom B.

Using Wiberg's definition of bond index and making use of the fact that the P matrix corresponding to closed-shell systems is duodempotent, i.e., $P^2 = 2P$ [Eq.(1.8) is a consequence of this property], Armstrong *et al.*[54] proposed the following definition for the valency ($V_A$) of an atom.

$$V_A = \sum_{B \neq A} B_{AB} \qquad (1.10)$$

which implies that the valency of an atom is a sum of the multiplicities of all bonds (these include also nonbonded pairs of atoms) formed by A. The same definition of valency had been given slightly earlier by Borisova and Semenov.[55]

In the framework of the extended Hückel theory[56] where a nonorthogonal basis set of AOs are used, Giambiagi *et al.*[57] proposed the following definition of bond index for a closed-shell molecule.

$$B_{AB} = \sum_{a}^{A} \sum_{b}^{B} (PS)_{ab} (PS)_{ba} \qquad (1.11)$$

In contrast to Wiberg's definition, Eq.(1.11) is bilinear in density matrix elements. They defined valency in the same manner as in Eq.(1.10). Among other earlier works dealing with the basic definitions of bond index and valency, mention may be made of those by Jug[58,59] which appeared in the late 1970s.

The definitions of bond index and valency mentioned thus far were proposed rather heuristically, and their applications were

made using semiempirical SCF wavefunctions.[52,60-69] The famous 1983-paper of Mayer[64] where he studied the decomposition of the LCAO Hamiltonian into terms of different physical significance, and the related energy partitioning scheme for the wavefunctions, marked the beginning of ab initio calculations in this field. Since then a large number of papers dealing with the definitions, interpretations and applications of bond index and valency calculated from both ab initio and semiempirical wavefunctions (SCF and correlated) have appeared in the literature.[65-136] The purpose of the present article is to critically analyze these definitions (sections 2 and 3) and review their applications (section 4). As the title of the article indicates, we are primarily concerned with the ab initio calculations. The results of semiempirical calculations are also included, but discussed rather briefly. The main conclusions of the present review have been summarized in section 5.

## 2. DEFINITIONS OF BOND INDEX AND VALENCY FOR SINGLE DETERMINANT SCF WAVEFUNCTIONS

In this section we shall present various definitions of bond index and valency for single determinant SCF wavefunctions. A statistical interpretation of bond index has also been given.

### 2.1 Heuristic Definition

It is well known that the restricted HF (RHF) wavefunction for a closed-shell system and the unrestricted HF (UHF) wavefunction for an open-shell system are both described by a single Slater determinant, and the latter reduces to the former when the number of electrons, $N^{\alpha}$ with $\alpha$-spin, is equal to the number of electrons, $N^{\beta}$ with $\beta$-spin. For a UHF wavefunction, we have (in matrix form)

$$\psi^{\sigma} = \chi\, C^{\sigma} \quad (\sigma = \alpha, \beta) \tag{2.1.1}$$

$$P^{\sigma} = C^{\sigma}\, C^{\sigma +} \tag{2.1.2}$$

$$P = P^{\alpha} + P^{\beta} \tag{2.1.3}$$

$$(P^{\sigma})^2 = P^{\sigma} \tag{2.1.4}$$

where $\{\psi_i^{\sigma}\}$ is the orthonormal set of MOs, and $\{\chi_a\}$ is the nonorthogonal set of AOs with the overlap matrix, $S = \chi^{+}\chi$. Let us denote by D the first order density matrix corresponding to the UHF wavefunction for $N = N^{\alpha} + N^{\beta}$ electrons. Then from Eq.(2.1.1) - (2.1.3) we have,

$$\begin{aligned} tr(D) &= \sum_{\sigma} \sum_{i}^{N} \langle \psi_i^{\sigma} | \psi_i^{\sigma} \rangle \\ &= \sum_{\sigma} \sum_{i}^{N^{\sigma}} \sum_{a} \sum_{b} C_{ia}^{\sigma}\, C_{ib}^{\sigma *} \langle \chi_b | \chi_a \rangle \\ &= \sum_{\sigma} \sum_{a} \sum_{b} (P^{\sigma})_{ab}\, S_{ba} \\ &= \sum_{a} (PS)_{aa} \\ &= tr(PS) \\ &= N \end{aligned} \tag{2.1.5}$$

This implies that for a nonorthogonal basis set the first order density matrix is D = PS. Equation (2.1.5) forms the basis of Mulliken's population analysis (MPA)[15], according to which the orbital population ($q_a$), the total number of electrons ($Q_A$) on the atom A, and the overlap population ($OP_{AB}$) of the bond AB are given by

$$q_a = D_{aa} \tag{2.1.6}$$

$$Q_A = \sum_{a}^{A} q_a \tag{2.1.7}$$

$$OP_{AB} = \sum_{a}^{A} \sum_{b}^{B} P_{ab}\, S_{ba} \tag{2.1.8}$$

Now it can be shown in a straightforward manner that

$$D^2 = (D^{\alpha} + D^{\beta})^2 = 2D - (P^{s}S)^2 = 2D - (D^{s})^2 \tag{2.1.9}$$

where $D^s = (P^\alpha - P^\beta)S$ is the spin density matrix. In the derivation of Eq.(2.1.9) it has been assumed for the sake of generality that $\alpha$- and $\beta$- MOs are not orthogonal. Since tr(D) = N, it follows from Eq.(2.1.9) that

$$N = \frac{1}{2}\ tr[\ D^2 + (D^s)^2] = \frac{1}{2}\sum_a \sum_b (D_{ab}\ D_{ba} + D^s_{ab}\ D^s_{ba}) \qquad (2.1.10)$$

Separating the R.H.S. of Eq.(2.1.10) into atomic and diatomic parts we get

$$N = \frac{1}{2}\sum_A (B_{AA} + \sum_{B \neq A} B_{AB}) \qquad (2.1.11)$$

where,

$$B_{AB} = \sum_a^A \sum_b^B (D_{ab}\ D_{ba} + D^s_{ab}\ D^s_{ba}) \qquad (2.1.12)$$

provides the definition of bond index. An alternative but equivalent expression for $B_{AB}$ that can be derived from Eq.(2.1.10) is

$$B_{AB} = 2 \sum_a^A \sum_b^B \sum_\sigma D^\sigma_{ab}\ D^\sigma_{ba} \qquad (2.1.13)$$

where

$$D^\sigma = P^\sigma S.$$

For a closed-shell system $N^\alpha = N^\beta$, $P^\alpha = P^\beta = P/2$, $D^s = 0$ and $D^2 = 2D$. Thus,

$$B_{AB} = \sum_a^A \sum_b^B D_{ab}\ D_{ba} \qquad (2.1.14)$$

which is identical with the definition [Eq.(1.11)] of Giambiagi *et al*.[57] Now valency ($V_A$) is defined as

$$V_A = \sum_{B \neq A} B_{AB} = 2\ Q_A - B_{AA} \qquad (2.1.15)$$

which is same as that proposed by Armstrong *et al*.[52]

In order to define valency for a UHF wavefunction we rewrite Eq.(2.1.10) as

$$2N = \sum_A^A \sum_a 2\ D_{aa} = \sum_A [\sum_a^A \sum_b^A (D_{ab}\ D_{ba} + D^s_{ab}\ D^s_{ba}) + \sum_{B \neq A} \sum_a^A \sum_b^B (D_{ab}\ D_{ba} + D^s_{ab}\ D^s_{ba})]$$

which on rearrangement gives

$$2\sum_{a}^{A} D_{aa} - \sum_{a}^{A}\sum_{b}^{A} D_{ab}\, D_{ba} = \sum_{B\neq A}\sum_{a}^{A}\sum_{b}^{B} (D_{ab}\, D_{ba} + D^{e}_{ab}\, D^{e}_{ba})$$

$$+ \sum_{a}^{A}\sum_{b}^{A} D^{e}_{ab}\, D^{e}_{ba} \qquad (2.1.16)$$

The L.H.S. of Eq.(2.1.16) is identified with the total (potential) valency in the spirit of Eq.(2.1.15) for a closed-shell case. The first term in the R.H.S. of Eq.(2.1.16) is $\sum_{B\neq A} B_{AB}$ (active valency) and the second term is called the free (inactive) valency ($F_A$).

Thus,

$$V_A = 2\sum_{a}^{A} D_{aa} - \sum_{a}^{A}\sum_{b}^{A} D_{ab}\, D_{ba} \qquad (2.1.17)$$

$$F_A = \sum_{a}^{A}\sum_{b}^{A} D^{e}_{ab}\, D^{e}_{ba} = V_A - \sum_{B\neq A} B_{AB} \qquad (2.1.18)$$

The derivation outlined above follows closely that given by Mayer.[70,73,74,76,77] The duodempotency of the D matrix for a closed-shell system plays the key role in this derivation. In the case of an open-shell system, the deviation of the D matrix from idempotency determines free valency, which is bilinear in the off-diagonal elements of the spin density matrix. This should not be confused with the free valence index ($F_r$) introduced by Coulson in the context of the Hückel theory. For a closed-shell SCF wavefunction $F_A = 0$ which indicates that the pertinent molecule is totally unreactive, which is obviously not true. The $F_r$ index is free from this shortcoming, and is not zero even for a closed-shell molecule [it is well known that the outer carbon atoms ($C_1$ and $C_4$) of butadiene are more reactive than the inner ones ($C_2$ and $C_3$) towards radical attack, since $F_1 > F_2$]. Thus the $F_A$ index proposed by Mayer, although it carries some sense in the case of a UHF wavefunction ($F_A$ may be regarded as the effective number of unpaired electrons on A), is totally misleading in the context of a closed-shell RHF wavefunction.

Recently Kar *et al.*[127,128] have defined bond index within the framework of the general nonsingular transformation of the AO basis set, which is of the form,

$$\phi = S^{-n} \tag{2.1.19}$$

where n can take any finite value. Now the density matrix for a closed-shell system is given by

$$D = S^{n} P S^{1-n} \tag{2.1.20}$$

which, as can be easily verified, is duodempotent. In the case of an open-shell system, we have

$$D^{\sigma} = S^{n} P^{\sigma} S^{1-n} \tag{2.1.21}$$

$$(D^{\sigma})^{2} = D^{\sigma} \tag{2.1.22}$$

$$D^{\beta} = S^{n} P^{\beta} S^{1-n} \tag{2.1.23}$$

Now using Eq.(2.1.9) and (2.1.21)-(2.1.23) one can define expressions for bond index, valency and free valency in a straightforward manner. It may be noted that in Eq.(2.1.19) n = 0 corresponds to the standard nonorthogonal basis set, n = 0.5 to the Löwdin-orthogonalized[13] functions and n = 1.0 to the biorthogonal basis set[64]. The density matrix corresponding to n = 0.5 is given by

$$D = S^{1/2} P S^{1/2} \tag{2.1.24}$$

which forms the basis of the Löwdin population analysis (LPA).[14]

Natiello and Medrano[110] proposed the definitions of $B_{AB}$ and $V_A$ in terms of the above density matrix [Eq.(2.1.24)] for a closed-shell system. The same definitions had, however, been proposed by Borisova and Semenov[111] as early as in 1976. In the case of a UHF wavefunction Natiello *et al.*[112] defined $B_{AB}$ after substituting $P = P^{\alpha}+P^{\beta}$ in Eq.(2.1.24), which is obviously wrong, since $\langle \psi_i^{\alpha} \mid \psi_j^{\beta} \rangle \neq \delta_{ij}$, in general. Later, Medrano and Bochicchio[114] suggested a modified definition which is too complicated, and predicts sometimes unphysical negative free valency. The definitions for bond index and valency applied by Gopinathan and coworkers (following Gopinathan and Jug[92] they

called it bond valency) in their ab initio calculations[98-100,102-105] on closed-shell systems are same as those proposed by Natiello and Medrano,[110] although the method of derivation[92-94] is somewhat different.

## 2.2 Exchange Part of the Second Order Density Matrix and bond Index

According to the CNDO energy partitioning scheme[59] the exchange part of the diatomic energy component is connected with the Wiberg bond index by means of the following relation.

$$E_{AB}^{exch} = - B_{AB} \gamma_{AB} /2 \qquad (2.2.1)$$

where $\gamma_{AB}$ is the diatomic Coulomb integral. This result indicates that besides the accumulation of electron density between the atoms, the nonclassical exchange effect also plays an important role in chemical bonding. Based on this observation Mayer[73,74,76,77] provided a definition of bond index from the exchange part of the second order density matrix. His derivation is outlined below.

It is well known that for a single determinant wavefunction

$$\rho_2(X_1,X_2;X_1',X_2') = \rho_1(X_1;X_1')\,\rho_1(X_2;X_2') - \rho_1(X_2;X_1')\,\rho_1(X_1;X_2') \qquad (2.2.2)$$

where $\rho_2$ is the second order density matrix, $\rho_1$ is the first order one (we have deviated for the time being from our previous notation D for the first order density matrix) and X's stand collectively for the space coordinates r and spin coordinates s. Using McWeeny's normalization[197] we have

$$\int \rho_2(X_1,X_2;X_1',X_2')\, d\tau_1\, d\tau_2 = N^2-N \qquad (2.2.3)$$

$$\int \rho_1(X_1;X_1')\,\rho_1(X_2;X_2')\, d\tau_1\, d\tau_2 = N^2 \qquad (2.2.4)$$

$$\int \rho_1(X_2;X_1')\,\rho_1(X_1;X_2')\, d\tau_1\, d\tau_2 = N \qquad (2.2.5)$$

In terms of $P^{\sigma}$ matrices defined earlier we can write

$$\rho_1 (X_1;X_2') = \sum_{\sigma} \sum_{ab} [P^{\sigma}_{ab} \chi_a(r_1) \chi^*_b (r_2) \sigma(s_1) \sigma^*(s_2)] \tag{2.2.6}$$

$$\rho_1 (X_2;X_1') = \sum_{\sigma} \sum_{cd} [P^{\sigma}_{cd} \chi_c(r_2) \chi^*_d (r_1) \sigma(s_2) \sigma^*(s_1)] \tag{2.2.7}$$

Substituting Eq.(2.2.6) and (2.2.7) into (2.2.5) and performing the integration we get,

$$\begin{aligned} N &= \sum_{abcd} \sum_{\sigma} P^{\sigma}_{ab} P^{\sigma}_{cd} S_{bc} S_{da} \\ &= \sum_{ac} \sum_{\sigma} D^{\sigma}_{ac} D^{\sigma}_{ca} \\ &= \frac{1}{2} \sum_{ab} [D_{ab} D_{ba} + D^{\alpha}_{ab} D^{\alpha}_{ba}] \end{aligned} \tag{2.2.8}$$

which is same as Eq.(2.1.10). Thus expressions for bond index and hence of valency and free valency can be derived as has been done in section 2.1.

## 2.3 Statistical Interpretation of Bond Index

According to the second quantization formalism the operator for the number of electrons, $Q_A$ on atom A in the LCAO-SCF theory is given[138,139] by

$$\hat{N}_A = \sum_{a}^{A} \phi^+_a \phi^-_a \tag{2.3.1}$$

where $\phi^+_a$ and $\phi^-_a$ are respectively the creation and annihilation operators corresponding to the orthonormal set of AOs, $\{\phi_a\}$. For an overlapping basis set, $\{\chi_a\}$

$$\{ \chi^+_a, \chi^-_b \} = S_{ab} \tag{2.3.2}$$

and $\chi^-_a$ is not the true annihilation operator adjoint to $\chi^+_a$. Thus it is not possible to define an expression for $\hat{N}_A$ in the $\{\chi_a\}$ basis. Mayer[64,70] circumvented the problem by using the biorthogonal set $\{\phi_a\}$, where $\phi = \chi S^{-1}$. Using $\phi^-_a$ as the annihilation operator adjoint to $\chi^+_a$ he derived

$$\hat{N}_A = \sum_{a}^{A} \chi^+_a \phi^-_a \tag{2.3.3}$$

which is the operator for the atomic charge in the the MPA scheme.

Then performing some lengthy but simple algebra Mayer showed that

$$\langle \hat{N}_A \rangle = \sum_a^A \langle \chi_a^+ \phi_a^- \rangle = \sum_a^A (PS)_{aa} = Q_A \qquad (2.3.4)$$

$$\langle \hat{N}_A \hat{N}_B \rangle = \sum_a^A \sum_b^B [(PS)_{aa} (PS)_{bb} - (PS)_{ab} (PS)_{ba}] \qquad (2.3.5)$$

Then,

$$\langle \hat{N}_A \hat{N}_B \rangle - \langle \hat{N}_A \rangle \langle \hat{N}_B \rangle = - \sum_a^A \sum_b^B [(PS)_{ab} (PS)_{ba}] = -B_{AB} \qquad (2.3.6)$$

Again,

$$\langle \hat{N}_A \hat{N}_B \rangle - \langle \hat{N}_A \rangle \langle \hat{N}_B \rangle = \langle (\hat{N}_A - \langle \hat{N}_A \rangle)(\hat{N}_B - \langle \hat{N}_B \rangle)$$

which shows that the bond index is a measure of the correlation between the fluctuations of $Q_A$ and $Q_B$ from their average values. It vanishes when the motion of the electrons on A is independent of the motion of that on B. Thus a statistical interpretation of bond index is provided by Eq.(2.3.6).

Equation (2.3.6) has been derived independently by Mayer[76,77] and Giambiagi and coworkers.[84-88] Using compact tensorial notation the latter authors showed that the bond index is an invariant associated with the second order density matrix, while atomic charge is an invariant built from the first order density matrix of a molecule.

## 3. DEFINITIONS OF BOND INDEX AND VALENCY FOR CORRELATED WAVEFUNCTIONS

For a correlated wavefunction it is not possible to define bond index from the second order density matrix, since it cannot be factorized into Coulomb and exchange components. Moreover, the first order density matrix corresponding to an approximate correlated wavefunction is not idempotent. Mayer,[77] therefore, suggested to use the SCF definition of bond index in the case of

correlated wavefunction also after suitably modifying the P matrix. Essentially the same approach was used by other investigators.[97,119] We present here the derivation of Medrano *et al*.[119] who used an orthogonalized set of AOs. We shall, however, use the standard nonorthogonal basis set $\{\chi_a\}$ for the sake of generality.

The most commonly used method for obtaining correlated wavefunctions is the configuration interaction (CI) technique. The CI wavefunction can be written as

$$\Psi_{CI} = \sum_K C_K \psi_K \tag{3.1}$$

where $\psi_K$ is a Slater determinant corresponding to a given electronic configuration. The associated density operator is given by

$$\hat{D} = \Psi_{CI}\, \Psi^*_{CI} = \sum_K \sum_L C_K\, C^*_L\, \hat{D}_{KL} \tag{3.2}$$

After reduction to first order, the elements of the $\hat{D}$ matrix can be written as

$$\hat{D}_{KK}(1;1') = \sum_i^N \psi_{Ki}(1)\, \psi^*_{Ki}(1') \tag{3.3}$$

$$\hat{D}_{KL}(1;1') = (-1)^q\, \psi_{Ki}(1)\, \psi^*_{Lj}(1') \tag{3.4}$$

where $\psi_{Ki}$ is the ith molecular spinorbital in $\psi_K$. and q is the number of permutations needed to bring $\psi_K$ and $\psi_L$ into maximum coincidence. In terms of $\{\chi_a\}$ the density matrix elements are given by

$$\begin{aligned}(\hat{D}_{KK})_{ab} &= \sum_i \sum_c \sum_d C_{Ki_c}\, C_{Ki_d}\, S_{ac}\, S_{db} \\ &= \sum_c \sum_d (P_{KK})_{cd}\, S_{ac} S_{db} \\ &= (P_{KK}\, S)_{ab}\end{aligned} \tag{3.5}$$

$$(\hat{D}_{KL})_{ab} = (-1)^q \sum_c \sum_d C_{Ki_c}\, C^*_{Lj_d}\, S_{ac}\, S_{db} \tag{3.6}$$

Once the matrix elements are known the bond index, valency and free valency can be calculated as in the case of single determinant SCF wavefunction. It may be noted that since the D

matrix corresponding to an approximate CI wavefunction is not idempotent the frre valency index does not vanish even in the case of a closed-shell molecule.

## 4. APPLICATIONS OF THE CONCEPTS OF BOND INDEX AND VALENCY

This section is devoted to the applications of the quantitative definitions of bond index and valency given in sections 2 and 3. The results corresponding to SCF and correlated wavefunctions are discussed separately. In order to save space we have not reproduced extensive tables, unless these are considered essential.

### 4.1 Results of Calculations using Single Determinant SCF Wavefunctions

Wiberg[52] was the first to calculate chemically acceptable values of bond indices in polyatomic molecules taking a number of hydrocarbons as the test cases and using CNDO/2 wavefunctions.[52] He also estimated the hybridization of carbon in methane from the calculated bond index. This idea was extended by Trindle and Sinanoglu,[62] who estimated the hybridization of carbon in a number of alkanes, alkenes, alcohols, ethers and carboxylic acids from CNDO/2 canonical MOs (CMO) using Wiberg's definition of bond index, and from localized MOs (LMO). They observed that when an LMO description is possible, a situation which allows an unambigious definition of hybridization, the two methods give identical results. Trindle[64] suggested a bond index characterization of the extent of delocalization in LMOs.

Armstrong *et al.*[54] calculated bond indices and valencies for a number of hydrocarbons and boron compounds using CNDO/2 wavefunctions, and successfully interpreted their results in terms of classical valence theory. In this context they proposed a quantitative definition for the deviation of electron distribution around an atom in a molecule from the spherical symmetry. They termed this deviation as `anisotropy' and defined it as follows.

$$L_A = B_{AA} - \sum_{l=0}^{K} \left( \sum_{a=l^2+1}^{(l+1)^2} P_{aa} \right)^2 / (2^l+1) \qquad (4.1.1)$$

They showed that the local anisotropy ($L_A$) of an atom serves as a useful index for the study of reaction mechanism. In the case of molecules containing second-row atoms, they observed that inclusion of d orbitals causes a significant increase in bond indices and valencies.

Lipscomb and Coworkers[62,63] studied the nature of bonding in a number of molecules containing fractionally bonded atoms (an atom is said to be fractionally bonded when it forms more bonds than the number of available orbitals), on the basis of their LMOs, bond indices and valencies calculated from PRDDO[140,141] wavefunctions. Almost similar type of calculations were carried out by Sannigrahi and coworkers[65-69] on a number of cumulated multiple-bonded systems, sulfidoborons, interhalogens and hydrogen-bonded complexes using CNDO/2 wavefunctions. They observed that : 1. In sulfidoborons the BS bond index lies between 2.Ø and 3.Ø indicating S $\longrightarrow$ B back donation. 2. The sum of the atomic valencies in a molecule is a useful index to compare the relative stability of its conformers. They postulated that higher is the total valency, more stable is the conformer. On this basis the preferred conformations for $F_2Cl^+$, $F_2Cl^-$, $Cl_2F^+$ and $Cl_2F^-$ were predicted to be $(FClF)^+$, $(FClF)^-$, $(ClClF)^+$ and $(ClClF)^-$ respectively. 3. The H-bond energy in a series of complexes varies qualitatively as the H...X bond index.

Mayer[70] initiated the ab initio calculations of bond index (he used the term bond order) and valency using definitions based on MPA. He used a number of basis sets and observed that the split-valence double-zeta (3-21G, 4-31G etc.) basis sets are not adequate inasmuchas they generally underestimate bond indices and valencies. In the case of open-shell systems like $CH_3$ and CN, $F_C$ = 1 in $CH_3$ and $F_C > F_N$ in CN. The latter is in conformity with the structure of the $(CN)_2$ molecule which contains a CC bond rather than an NN bond. In subsequent papers[73,74,76,77] Mayer elaborated the physical significance of bond index at great length. A linear relationship between overlap population and bond index of the NO bonds in some nitrogen oxide molecules and ions, calculated using the STO-3G basis set, was observed by Mayer.[74] For sulfur atoms with formal valency of 4 (as in $SO_2$) and 6 (as in $H_2SO_4$) Mayer and coworkers[71,72,75,77,78] recommended to include d orbitals on S in order to obtain chemically reasonable bond index and valency. Comparing the results of STO-3G, STO-3G* (STO-3G + d on S), 3-21G and 4-31G calculations they concluded that the inclusion of d orbitals in the basis set of S could not be averted by using more flexible sp basis sets. In a recent paper Mayer[79] reported analytical calculations of bond indices in two- and four-electron three-center model molecules, and showed that the presence of the two 3c-2e bonds in diborane leads to bond indices of about Ø.5, not only between the bridging hydrogens and each boron atom, but also between the two borons. The stability of $B_2H_6$ against the dissociation into two $BH_3$ molecules was attributed to the attractive boron-boron exchange interaction.

Yadav and coworkers[80-83] applied Mayer's definition of bond index and valency to a large number of substituted benzenes, phenols, toluenes etc. and obtained results in accordance with classical concept.

In the framework of the extended Hückel theory[56] de Giambiagi *et al.*[84] calculated bond indices and valencies of a wide variety of molecules, hydrogen-bonded species and transition metal

complexes. They also proposed the following intuitive definition of oxidation number (ON) of an atom in a molecule.

$$ON_A = (|q_A|/q_A) \; / \; \sum_B B_{AB} \qquad (4.1.2)$$

where $q_A$ is the atomic charge ($q_A = Z_A - Q_A$, where Z stands for atomic number), and the summation is taken over the atoms with polarity different from that of A. Their calculated oxidation numbers are almost equal to the integral values predicted by classical consideration. There is, however, an important point to note. In the molecule like $O_3$ where the classical theory assigns equal oxidation number (zero) to all three oxygen atoms, definition (4.1.2) predicts two different values for this quantity (one value for the terminal oxygens and another for the central one). Yadav *et al.*[81] also applied this definition to calculate oxidation numbers in mono and disubstituted chlorobenzenes. As it has already been mentioned in section 2.3 Giambiagi and coworkers[84-88] provided a statistical interpretation of bond index in terms of the charge fluctuation between the two atoms forming the bond. Further, on the basis of statistical thermodynamical arguments, Pitanga *et al.*[86] established a relation between the self-charge of an atom ($B_{AA}$) and the local softness parameter.[142] The relation proposed by them is as follows.

$$S_A = - B_{AA} \; / \; kT \qquad (4.1.3)$$

where $S_A$ is the softness parameter for atom A, k is the Boltzmann constant and T is the absolute temperature. Jorge and Batista[89] contradicted the above definition and suggested that $S_A$ is linearly dependent not on $B_{AA}$ but on $V_A$ i.e.,

$$S_A = - V_A \; / \; kT \qquad (4.1.4)$$

The authors of the original work, however, pointed out[90] that the mathematical derivation of Jorge and Batista leading to Eq.(4.1.4) is wrong. Relation (4.1.3) was recently applied[91] to calculate the $S_A$ values of a number of simple molecules. The calculated values, however, seem to be far from convincing.

Gopinathan and Jug[93] calculated the valency of Be, B, C, N and O in a number of compounds using SINDO1 wavefunctions.[143] The $\pi$-electron concept of free valency was extended by them to $\sigma$-systems. Atoms in a molecule were classified as subvalent, normal and hypervalent by comparing the calculated valency with a reference value. The refenence values were chosen to be the integral ones around which the computed values are distributed in a large number of molecules. From these results they found a correlation between the free valency (difference between the reference and actual values) of atoms and their affinity for covalent bond formation with other reagents. They also hypothesized that in a chemical reaction, an atom in a molecule would make further covalent bonds or break or weaken the existing ones so as to convert its sub or hypervalency to the normal one.

Jug[93] pointed out that hypervalency in molecules containing atoms with normal valency, is an artifact of extended basis sets (this is not true in the case of real hypervalency, e.g., S in $SO_3$, P in $PCl_5$ etc.), while subvalency can result both from ionic and zwitterionic contributions, and from radical and diradical (note that Jug did not use the term free valency even in the case of open-shell systems) contributions.

Since Wiberg's bond index is incapable of describing an antibonding interaction that might take place between nonbonded atoms, Gopinathan and Jug[93] proposed to define this quantity in a different manner. Following Jug[58] they first projected the eigenvalues ($\lambda_i$) of the bond orbitals[59] into its bonding and antibonding components. Then using a projection factor, $f_i$ which is given by the cosine of the angle between these components, they defined bond index as follows.

$$B_{AB} = \sum_{i}^{+ve} f_i \lambda_i^2 \,(AB) \qquad (4.1.5)$$

They further partitioned the bond index into $\sigma$ (along the AB axis) and $\pi$ (perpendicular to the AB axis) components by transforming the two-center density matrix to a local coordinate system. The

bond indices calculated using SINDO1 wavefunctions for various organic and inorganic molecules are generally in agreement with the chemical concepts such as bent bonds, unsaturation, antibonding interaction etc.

Jug[94] demonstrated that the contribution to the total valency of an atom in a molecule is additive at the MO level, and defined the total electron sharing in a molecule as half of the sum of atomic valencies, i.e.,

$$M = \left( \sum_{A} V_A \right) / 2 \qquad (4.1.6)$$

He also discussed the application of M as a useful index in the interpretation of photoelectron spectra of some simple molecules, and reactivity of a number of subvalent and hypervalent systems. Jug and coworkers[96,97] used ΔM values to study the rotation about single and double bonds in several molecules containing central single and double bonds. They observed that the rotation about single bonds (free rotation) is accompanied by only a marginal change in M, whereas that about double bonds (restricted rotation) involves substantial changes.

The quantity M defined by Eq.(4.1.6) was called molecular valency ($V_M$) by Gopinathan *et al.*[98] Decomposing $V_M$ into its MO components ($V_M = \sum_{i}^{occ} V_i$, where $V_i$ is the MO valency) and making use of the relation,

$$V_M = \left( \sum_{A} \sum_{B \neq A} B_{AB} \right) / 2 \qquad (4.1.7)$$

they derived an expression for $V_i$ in terms of $n_i$, the occupation number of the MO, $\psi_i$, and the AO coefficients. Using the Löwdin-orthogonalized STO-3G basis set they calculated MO valencies of a number of simple molecules, which were found to correlate qualitatively with the degree of bonding of an MO as predicted by the photoelectron spectra. Siddarth and Gopinathan[99,100] showed that the MO valencies satisfy the criteria to be used as the ordinate in a quantitative Mulliken-Walsh[144,145] diagram. They further postulated that $V_M$ reaches a maximum value

at the equilibrium bond angle of a molecule. This postulate was verified to hold good in a number of cases. However, as pointed out by Jug,[101] it is doubtful whether such a postulate is theoretically sound.

Siddarth and Gopinathan[102] calculated strain energy (SE) from bond index using the following semiempirical relation.

$$SE_{AB} = [\,(B^{\sigma}_{AB})^{ref} - B^{\sigma}_{AB}\,]\; E^{\sigma}_{AB} - [\,(B^{\pi}_{AB})^{ref} - B^{\pi}_{AB})\; E^{\pi}_{AB}] \qquad (4.1.8)$$

where $B^{ref}_{AB}$ is the strain-free integral reference value of the bond index, $B_{AB}$ is the corresponding calculated value in the strained molecule and $E_{AB}$ is the empirical bond energy. They calculated the strain energies of a number of hydrocarbons using ab initio and INDO wavefunctions.[53] In the former they applied Löwdin-orthogonalized STO-3G basis set. The calculated values were obtained, in general, in good agreement with experiment. The same authors[103] successfully applied the above method for the calculation of strain energies of a number of heterocyclic compounds. Attempts were also made to estimate bond energy from bond index.[104]

Another interesting application of molecular valency was reported by Jug and Gopinathan[105] using SINDO1 wavefunctions. In the case of concerted reactions like cyclobutene $\longrightarrow$ butadiene, they found that the Woodward - Hoffmann allowed conrotatory transition is accompanied by only marginal (Ø.1) reduction of valency, whereas for the forbidden disrotatroy transitions the corresponding reduction is about 2 units of valency (interestingly only the valency of the terminal C-atom is reduced almost by one unit and the transition state may be called a diradical). From this study they concluded that the reaction pathway which involves the minimum reduction in valency is the preferred one. They also studied some nonconcerted thermal reactions and found that the radical, biradical and zwitterion nature of the transition states and intermediates could be deduced from the claculated valency reduction.

Siddarth and Gopinathan[100] used the concept of molecular valency to predict the equilibrium bond angle of the excited/ ionized states of small molecules. For this purpose they performed the ground state SCF calculations of a molecule at various bond angles using STO-3G Löwdin-orthogonalized basis functions and calculated $V_M$ as a sum of the occupied MO valencies corresponding to any desired electronic configuration. Then the equilibrium bond angle of the excited/ionized state was predicted to be the one at which $V_M$ is maximum. Taking a number of simple molecules they showed that the geometries thus predicted agree reasonably well with those obtained from ab initio CI calculations and/or experiment. The drawback of this approach is that the geometry is predicted only for the state with the highest spin multiplicity arising out of a given electronic configuration.

Following Foster and Weinhold,[146] Gopinathan[106] used the concept of valency to determine atomic hybridization from the MO theory. He estimated the contributions of s, p and d orbitals to the total valency of the atom and these contributions were taken to be the same as that of the corresponding orbitals to the atomic hybrid. Taking a few simple molecules and using STO-3G, 4-31G and 6-31G* basis sets the author showed that the calculation of hybridization by the above scheme yields results similar to those obtained by other MO methods.[146]

Natiello and Medrano[110] defined bond index and valency in the framework of LPA, where the first order density matrix is $S^{1/2}PS^{1/2}$. Nateillo *et al.*[112] calculated these quantities using MNDO,[147] PRDDO and ab initio (STO-3G, 4-31G, DZ and DZP basis sets) wavefunctions for a number of closed-shell molecules. They also calculated bond indices and valencies for a few open-shell systems using MNDO-UHF and PRDDO - UHF wavefunctions, and a wrong expression for $B_{AB}$. In a latter work, Medrano and Bochicchio[114] rectified the error committed by Natiello *et al.*[112] They, however, landed up with unphysical negatgive values of $F_A$, the free valency in a few cases. Stradella *et al.*[115] proposed the following

definition for free electron index.

$$N_A^c = \frac{1}{2}(V_A + B_{AA}) - \sum_{B \neq A} B_{AB} \qquad (4.1.9)$$

From the results of their MNDO calculations on some simple molecules, they concluded that the free electron index is a more useful quantity than the local anisotropy [Eq.(4.1.1)] for predicting the chemical reactivity of an atom in a molecule.

Angyan *et al.*[116] considered a series of model compounds of the type X-S-A = B-Y(Z) = O(X = F, OH, $NH_2$, $CH_3$ and SH; A = CH; B = CH and N; Y = CH and N; Z = H, O and lone pairs) and investigated the intramolecular 1,5 sulfur(II)-oxygen interaction using STO-3G, 3-21G and 3-21G* basis sets. They optimized the geometries of the two basic planar conformations of these compounds, s-cis/s-trans (CT) and s-trans/s-trans (TT) resulting from the internal rotation about the B-Y and S-C bonds. These energy minimum conformations represent respectively the optimum geometries with and without S..O interaction. In order to measure the extent of S..O interaction they used four quantities, namely, the lengthening of the Y = O bond [ $\Delta R$ (Y = O)] on going from TT to CT, the shortening of the SO distance [ $\Delta R$ (S..O)] , the energy difference between TT and CT [ $\Delta E$ (S..O)] and the Mayer-type bond index of the S..O bond ($B_{S..O}$) in the CT conformations. The linear interdependence of these four quantities indicated that each of them was about equally good measure of the strength of the S..O interaction. Depending upon the nature of the individual compounds studied, the covalent character of the S..O bond was found to be 10-30% of a normal single bond when S d orbitals were included in the basis set.

In a subsequent paper Angyan *et al.*[117] investigated the nature and the strength of SO bonding in a series of sulfonic acids ($X_2S(OH)_2$), sulfoxides ($X_2SO$), sulfones ($X_2SO_2$) and sulfuranes ($X_2SOH$). The substituent X was varied to assess the influence of the additional ligand on the valency of S. The authors observed that the Mayer bond index is just as convenient as the bond length for the characterization of the SO linkage. They used STO-3G,

STO-3G* and 3-21G* basis sets, and provided further evidence for the necessity of using S d orbitals in compounds with hypervalent sulfur. They also observed a correlation between SO bond indices and bond lengths, and between valencies and 2p ionization potentials of S in different molecules.

Villar and Dupuis[118] calculated atomic charges, bond indices, valencies and spin densities for the prototypical molecules $CH_3$, $C_2H_4$, $C_2H_2$, $H_2O$ and HF using Mayer's definition and the 6-31G basis set. They obtained results in agreement with the classical chemical concept. The authors defined the free electron number as

$$N_A = \sum_a^A \sum_b^A [(PS)_{ab}(PS)_{ba} + (P^\alpha S)_{ab}(P^\alpha S)_{ba}]$$
$$= \frac{1}{2}[(V_A + B_{AA}) - \sum_a^A \sum_b^A (P^\alpha S)_{ab}(P^\alpha S)_{ba} \qquad (4.1.10)$$

which differs from the formulation [Eq.(4.1.9)] of Stradella *et al.*[115] who called it free electron index ($N_A^\alpha$). Further they calculated the CC bond lengths and bond indices in the closed-shell polyene cation, $C_{21}H_{22}^+$ and the neutral species, $C_{22}H_{24}$ using the 6-31G basis set. Comparing their valencies, bond indices and atomic charges the authors concluded that the extent of defect in alternancy in the charged polyene is about 15 CC units.

Lendvay[119] calculated bond indices free valencies and spin densities of the transition states of various simple reactions using Mayer's definition and the STO-3G basis. He found that the principle of conservation of bond index holds good for the transition state. The author also made an interesting observation that the calculated bond indices reflect the trend suggested by Hamond's principle:[148] In an exothermic reaction the transition state resembles more to the products than to the reactants, while the reverse is true for an endothermic reaction. The free valencies of the atoms in the transition state were found to correlate very well with their spin densities. This indicates that Mayer's free valency indices represent an appropriate measure of the chemically unsaturated nature of the atoms not only in the free molecule but also during chemical reactions. Further he

calculated bond index at different stages of the metathetic reaction, $Cl + HH' \longrightarrow ClH + H'$, and the bimolecular nucleophilic substitution reaction, $CH_3F' + F^- \longrightarrow FCH_3 + (F')^-$ along the minimum energy path (MEP), and found that the sum of the bond indices of the bond being broken and the bond being formed is very close to unity at all stages of the reaction.

Balban *et al.*[120] calculated the bond length, bond index, overlap population and force constant of $O_2$, SO, $S_2$, $C_2H_2$ and the corresponding mono and dications using STO-3G, 3-21G and 6-31G* basis sets. Their results tally with the qualitative predictions based on simple MO theory of bonding. In the three isovalent diatomic species the highest occuied MO ($\pi^*$) is an antibonding one. Removal of electrons from the $\pi^*$ MO to form the mono and dication results in an increase in bond order, overlap population and force constant. The bond length progressively decreases under the same situation. For acetylene the HOMO ($\pi_u$) is bonding, and an opposite trend was observed. Now the bond order, overlap population and the force constant decrease from $C_2H_2$ to $C_2H_2^{2+}$ and the lengths of both CH and CC bonds increase.

Very recently, Somogui and Tamas[136] have calculated the Mayer bond indices in cyclodisiloxane ($Si_2O_2H_4$), cyclodisilathiane ($Si_2S_2H_4$) and 1,3 dioxetane ($C_2O_2H_4$) using several basis sets. On the basis of these quantities they concluded that a weak covalent Si..Si bond exists in cyclodisiloxane. They also observed that Si d orbitals are needed to describe this weak interaction.

The results of calculations of bond index, valency and related quantities reviewed thus far indicate that three types of density matrices were used in such calculations. For NDO-type wavefunctions D = P and for ab initio wavefunctions either D = PS (MPA scheme) or $D = S^{1/2} P S^{1/2}$ (LPA scheme) were used. Baker[121] compared the performance of these two schemes by calculating atomic charges, bond indices and valencies in a variety of simple molecules, and concluded that LPA is far more satisfactory than MPA. However, his conclusion was not based on any sound

theoretical reasoning but rather on some bizarre results (negative $q_\alpha$, $B_{AB}$ and $V_A$) obtained for the $C_3H_3^-$ ion using the 3-21+G basis set, which contains a set of diffuse s and p functions on C.

The protagonists of LPA[101,114] and NPA[122] schemes take this as an authentic example in support of their method of calculation. Although we could not repeat the calculations of Baker on $C_3H_3^-$ using 3-21+G and 3-21+G* basis sets due to the convergence problem, we thought that the absurd results obtained in the case of $C_3H_3^-$ might be an artifact of the 3-21+G basis set. We, therefore, undertook a more systematic comparative study[123-127] of the MPA and LPA schemes.

Kar *et al.*[123] made a comparative study of H-, Li- and Na-bonding in the X...M-Y ( X = $H_2O$, $NH_3$; M = H, Li, Na; Y = F, Cl) complexes on the basis of atomic charges, valencies, bond indices and overlap populations calculated from Mulliken and Löwdin density matrices using the STO-3G basis set. In contrast to the observation made by Baker[121] they observed that the Löwdin scheme yields quite unrealistic charge distributions (like halogens being more positive than Li) and overwhelmingly underestimates the bond ionicities. The linear relationship between overlap population and bond index as observed for the first time by Mayer[74] holds for the X..M (X = O,N; M = H, Li, Na) bonds in the above mentioned complexes.

In a subsequent work Kar *et al.*[124] employed the MPA and LPA schemes to study the nature of bonding in some normal and strong H-bonded complexes using 4-31G, 6-31G* and 6-31G** basis sets. They observed that the local quantities calculated using the 6-31G* basis set and the MPA scheme were obtained in conformity with classical valence theory. The LPA scheme overestimates the covalent bonding. The authors attributed this to the fact that the AOs in this scheme, due to their nonlocal character, fail to localize the electrons in a classically expected manner, and overemphasize nonbonded interaction. They also observed that compared to MPA, the LPA scheme predicts considerably higher

values for the ratio $|\Delta q|/|\Delta E|$, where $\Delta q$ is the population of an added orbital to a given basis set, and $|\Delta E|$ is the correspoonding lowering in the SCF energy. Ideally this ratio should be[98] of the order unity.

Kar and Sannigrahi[125] made further comparative studies of the MPA and LPA schemes by applying them to some highly ionic (LiH, LiF) and polar covalent (HF, $H_2O$, $NH_3$) molecules. They used minimal as well as extended basis sets for the calculation of various local quantities. It was observed by them that for predominantly ionic molecules MPA performs far more satisfactorily than LPA. With decreasing ionicity the performance of the two schemes becomes comparable. Atomic charge, valency, bond index etc. are highly sensitive to basis sets. They observed that variation of the geometrical parameters of a molecule within a small range does not have any appreciable effect on its charge distribution and related local quantities.

Since the classical picture of bonding is retrieved from the MO theory in a straightforward manner by localized molecular orbital (LMO) studies, Sannigrahi and Kar[126] performed LMO calculations on a number of LiX (X = H, BeH, $BH_2$, $CH_3$ $NH_2$, OH and F) dimers. They observed that the LMO picture of bonding is supported by the changes in bond indices and valencies occuring upon dimerization, and in this respect MPA provides a more consistent picture of bonding in the dimers than LPA.

The comparative study of the MPA and LPA schemes made by Sannigrahi and coworkers[123-126] was certainly more systematic (with respect to the choice of both basis sets and molecules) and revealing than that made by Baker. It has nevertheless, several limitations, some of which are as follows.

1. The authors did not make any attempt to provide a theoretical basis for the discrepancy between MPA and LPA atomic charges and valencies.

2. They considered molecules containing only first-row atoms and hydrogen. Thus their conclusions are somewhat of restricted validity.
3. They did not consider any basis set which includes diffuse functions. It may be recalled that the bizarre results obtained by Baker in the case of $C_3H_3^-$ was attributed by them to the use of diffuse functions in the basis set.
4. Some interesting aspects of the MO calculations of valency such as the valency correlation diagram and the variation of molecular valency with bond angle were overlooked by them.
5. They did not examine the effect of basis set superpositon error (BSSE)[149] in the calculation of atomic charges and valencies in intermolecular complexes.

Sannigrahi and coworkers[128-133] made further studies to critically examine the above aspects of MO calculations of atomic charges and valencies. Instead of confining their attention to Mulliken and Löwdin density matrices, they considered a more general density matrix, $D = S^n P S^{1-n}$ where n can take any finite value.

The density matrices of the MPA and LPA schemes correspond respectively to n = Ø.Ø and Ø.5 in this generalized density matrix. Kar *et al.*[128,129] calculated atomic charges, bond indices, valencies and MO valencies of a number of simple molecules containing first- and second-row atoms by varying n within the range $-Ø.5Ø \leq n \leq Ø.5$ (this is same as the range, $Ø.5Ø \leq n \leq 1.5Ø$) and using basis sets ranging from STO-3G to 6-31G**. They observed that apart from a few molecules with a second-row atom and basis sets like 6-31G*, 6-31G** etc. the lowest values of atomic charges are obtained for n = Ø.5Ø. This value of n predicts maximum valencies in all cases. It is an expected result since only for n = Ø.5 the D matrix is symmetric and all the matrix elements appear as squared terms in the expression for $B_{AB}$. With the exception of highly ionic molecules, quite absurd values of atomic charges and valencies were obtained for $n < Ø.Ø$. Interestingly, for such

molecules the values of atomic charges for n = -Ø.25 compare favorably with the corresponding NPA values.[98] The plots of $V_M$ vs $\theta$ in linear triatomic molecules showed maxima at $\theta = 180^{\circ}$ for all values of n and the minimal basis set. Exceptions occured in a few cases for negative values of n and higher basis sets. In the case of nonlinear molecules the $\theta$ values corresponding to maximum $V_M$ deviate considerably from those obtained by minimizing energy. In many cases well-defined minima did not occur. This is at variance with the findings of Siddarth and Gopinathan.[100] Mulliken-Walsh type diagrams (valency correlation diagrams) were plotted for a few molecules using MO valencies as the ordinate. The slopes of these plots were observed to be quite sensitive to basis sets and n. For n < Ø.Ø these plots generally showed very erratic behaviour. Finally, the LMO valencies of a number of molecules were calculated for n = Ø and their possible usefulness was discussed. From the above study Kar *et al.*[128,129] concluded that use of n in the range Ø.Ø ≤ n ≤ Ø.5 will lead to generally acceptable results for molecular charge distribution and related local quantities. However, apart from n = Ø.Ø and Ø.5, other values of n do not have any physical significance.

For the sake of ready reference calculated values of atomic charges, bond indices and valencies of a number of simple molecules are summarized in Table 4.1.1 for a variety of basis sets and n = Ø.ØØ (MPA) and Ø.5 (LPA). The molecules are so chosen that one can assess the reliability of their calculated local quantities in the light of classical theory of bonding. Let us first confine our attention to atomic charge. As can be seen from Table 4.1.1 for molecules without a second-row atom, $|q_A|_L < |q_A|_M$ for all the basis sets. Exceptions to this general trend

Table 4.1.1: MPA(M) and LPA(L) atomic charges ($q_A$), bond indices ($B_{AB}$) and valencies ($V_A$) of some simple molecules.

| Molecule[a] | Calculated quantity | STO-3G | | 4-31G | | 6-31G*[b] | |
|---|---|---|---|---|---|---|---|
| | | M | L | M | L | M | L |
| $F_2$ | $V_F$ | 1.000 | 1.000 | 0.942 | 1.139 | 0.965 | 1.378 |
| $Cl_2$ | $V_{Cl}$ | 1.000 | 1.000 | 0.970 | 1.069 | 0.884 | 1.197 |
| CO | $q_C$ | 0.199 | 0.047 | 0.394 | 0.163 | 0.287 | 0.053 |
| | $B_{CO}$ | 2.514 | 2.605 | 2.140 | 2.871 | 2.299 | 2.991 |
| $CO_2$ | $q_C$ | 0.444 | 0.323 | 0.964 | 0.467 | 0.892 | 0.352 |
| | $q_O$ | -0.222 | -0.162 | -0.482 | -0.234 | -0.446 | -0.178 |
| | $B_{CO}$ | 1.967 | 1.979 | 1.799 | 2.173 | 1.957 | 2.377 |
| | $B_{OO}$ | 0.386 | 0.396 | 0.234 | 0.359 | 0.174 | 0.251 |
| | $V_C$ | 3.934 | 3.958 | 3.598 | 4.345 | 3.914 | 4.754 |
| | $V_O$ | 2.353 | 2.376 | 2.033 | 2.532 | 2.132 | 2.628 |
| $CH_4$ | $q_C$ | -0.262 | -0.144 | -0.611 | -0.420 | -0.678 | -0.518 |
| | | | | | | -0.472 | -0.277 |
| | $q_H$ | 0.066 | 0.036 | 0.153 | 0.105 | 0.169 | 0.129 |
| | | | | | | 0.118 | 0.069 |
| | $B_{CH}$ | 0.991 | 0.998 | 0.963 | 0.986 | 0.959 | 0.980 |
| | | | | | | 0.978 | 0.990 |
| | $B_{HH}$ | 0.001 | 0.000 | -0.009 | 0.008 | -0.010 | 0.007 |
| | | | | | | -0.008 | 0.018 |
| | $V_C$ | 3.965 | 3.991 | 3.851 | 3.944 | 3.836 | 3.918 |
| | | | | | | 3.911 | 3.959 |
| | $V_H$ | 0.996 | 0.999 | 0.936 | 1.009 | 0.930 | 1.002 |
| | | | | | | 0.953 | 1.043 |
| HF | $q_H$ | 0.192 | 0.141 | 0.479 | 0.364 | 0.544 | 0.405 |
| | | | | | | 0.402 | 0.192 |
| | $B_{HF}$ | 0.963 | 0.980 | 0.745 | 0.892 | 0.683 | 0.858 |
| | | | | | | 0.848 | 1.120 |
| HCl | $q_H$ | 0.174 | 0.115 | 0.231 | 0.146 | 0.245 | 0.197 |
| | | | | | | 0.193 | 0.109 |
| | $B_{HCl}$ | 0.970 | 0.987 | 0.911 | 1.004 | 0.902 | 0.986 |
| | | | | | | 0.946 | 1.071 |
| $H_2O$ | $q_H$ | 0.165 | 0.116 | 0.402 | 0.290 | 0.450 | 0.325 |
| | | | | | | 0.339 | 0.161 |
| | $q_O$ | -0.330 | -0.232 | -0.804 | -0.580 | -0.900 | -0.650 |
| | | | | | | -0.678 | -0.322 |
| | $B_{OH}$ | 0.964 | 0.986 | 0.796 | 0.929 | 0.768 | 0.907 |
| | | | | | | 0.882 | 1.071 |
| | $B_{HH}$ | 0.008 | 0.000 | 0.006 | 0.009 | -0.004 | 0.008 |
| | | | | | | -0.002 | 0.034 |
| | $V_H$ | 0.973 | 0.987 | 0.802 | 0.938 | 0.764 | 0.914 |
| | | | | | | 0.880 | 1.105 |
| | $V_O$ | 1.929 | 1.973 | 1.592 | 1.858 | 1.536 | 1.814 |
| | | | | | | 1.764 | 2.141 |

"Table 4.1.1 (Continued)"

| Molecule[a] | Calculated quantity | STO-3G | | 4-31G | | 6-31G*[b] | |
|---|---|---|---|---|---|---|---|
| | | M | L | M | L | M | L |
| $H_2S$ | $q_H$ | -Ø.Ø36 | -Ø.Ø62 | Ø.Ø96 | Ø.Ø44 | Ø.111 | Ø.12Ø |
| | | | | | | Ø.Ø67 | Ø.Ø66 |
| | $q_S$ | Ø.Ø72 | Ø.123 | -Ø.191 | -Ø.Ø89 | -Ø.222 | -Ø.241 |
| | | | | | | -Ø.134 | -Ø.132 |
| | $B_{HS}$ | Ø.991 | Ø.995 | Ø.944 | 1.Ø14 | Ø.947 | Ø.998 |
| | | | | | | Ø.969 | 1.Ø35 |
| | $B_{HH}$ | Ø.ØØ7 | Ø.ØØ2 | Ø.ØØ7 | Ø.ØØ6 | -Ø.ØØ2 | Ø.ØØ5 |
| | | | | | | -Ø.ØØ6 | Ø.Ø1Ø |
| | $V_H$ | Ø.999 | Ø.996 | Ø.951 | 1.Ø2Ø | Ø.945 | 1.ØØ3 |
| | | | | | | Ø.968 | 1.Ø46 |
| | $V_S$ | 1.983 | 1.99Ø | 1.887 | 2.Ø28 | 1.893 | 1.996 |
| | | | | | | 1.938 | 2.Ø71 |
| $NH_3$ | $q_H$ | Ø.147 | Ø.Ø95 | Ø.321 | Ø.213 | Ø.341 | Ø.234 |
| | | | | | | Ø.263 | Ø.124 |
| | $q_N$ | -Ø.44Ø | -Ø.286 | -Ø.964 | -Ø.683 | -1.Ø24 | -Ø.7Ø1 |
| | | | | | | -Ø.79Ø | -Ø.373 |
| | $B_{NH}$ | Ø.962 | Ø.99Ø | Ø.866 | Ø.958 | Ø.857 | Ø.951 |
| | | | | | | Ø.919 | 1.Ø24 |
| | $B_{HH}$ | Ø.ØØ8 | Ø.ØØØ | -Ø.ØØ2 | Ø.ØØ9 | -Ø.ØØ7 | Ø.ØØ8 |
| | | | | | | -Ø.ØØ5 | Ø.Ø26 |
| | $V_H$ | Ø.978 | Ø.991 | Ø.862 | Ø.977 | Ø.843 | Ø.966 |
| | | | | | | Ø.9Ø9 | 1.Ø76 |
| | $V_N$ | 2.885 | 2.971 | 2.597 | 2.874 | 2.572 | 2.852 |
| | | | | | | 2.757 | 3.Ø72 |
| $PH_3$ | $q_H$ | -Ø.115 | -Ø.127 | -Ø.Ø21 | -Ø.Ø9Ø | -Ø.Ø13 | Ø.Ø27 |
| | | | | | | -Ø.Ø54 | -Ø.ØØ7 |
| | $q_P$ | Ø.346 | Ø.381 | Ø.Ø64 | Ø.269 | Ø.Ø38 | -Ø.Ø81 |
| | | | | | | Ø.161 | Ø.Ø23 |
| | $B_{PH}$ | Ø.973 | Ø.983 | Ø.945 | 1.ØØ4 | Ø.967 | 1.ØØ6 |
| | | | | | | Ø.974 | 1.Ø14 |
| | $V_H$ | Ø.987 | Ø.984 | Ø.96Ø | 1.Ø12 | Ø.963 | 1.Ø15 |
| | | | | | | Ø.97Ø | 1.Ø3Ø |
| | $V_P$ | 2.919 | 2.941 | 2.835 | 3.Ø12 | 2.9Ø2 | 3.Ø18 |
| | | | | | | 2.923 | 3.Ø43 |
| LiH | $q_{Li}$ | -Ø.Ø16 | -Ø.Ø13 | Ø.263 | Ø.15Ø | Ø.169 | Ø.Ø86 |
| | | | | | | Ø.189 | Ø.Ø92 |
| | $B_{LiH}$ | 1.ØØØ | 1.ØØØ | Ø.931 | Ø.985 | Ø.972 | 1.ØØØ |
| | | | | | | Ø.965 | Ø.999 |
| NaH | $q_{Na}$ | Ø.583 | Ø.535 | Ø.329 | 2.Ø4 | 2.63Ø | Ø.Ø77 |
| | | | | | | Ø.271 | Ø.Ø77 |
| | $B_{NaH}$ | Ø.66Ø | Ø.714 | Ø.89Ø | Ø.964 | Ø.93Ø | Ø.999 |
| | | | | | | Ø.926 | 1.ØØØ |

"Table 4.1.1 (Continued)"

| Molecule[a] | Calculated quantity | STO-3G M | STO-3G L | 4-31G M | 4-31G L | 6-31G*[b] M | 6-31G*[b] L |
|---|---|---|---|---|---|---|---|
| LiF | $q_{Li}$ | 0.228 | 0.093 | 0.719 | 0.577 | 0.691 | 0.351 |
| | $B_{LiF}$ | 1.346 | 1.537 | 0.536 | 0.820 | 0.548 | 1.206 |
| LiCl | $q_{Li}$ | 0.379 | 0.100 | 0.561 | 0.299 | 0.502 | 0.198 |
| | $B_{LiCl}$ | 1.110 | 1.480 | 0.803 | 1.230 | 0.885 | 1.390 |
| HCN | $q_H$ | 0.150 | 0.102 | 0.326 | 0.171 | 0.312 | 0.229 |
| | $q_C$ | 0.012 | -0.009 | 0.011 | -0.109 | 0.067 | -0.132 |
| | $q_N$ | -0.161 | -0.093 | -0.337 | -0.062 | -0.380 | -0.097 |
| | $B_{HC}$ | 0.968 | 0.979 | 0.859 | 0.919 | 0.863 | 0.901 |
| | $B_{CN}$ | 2.989 | 3.005 | 2.921 | 3.314 | 2.934 | 3.286 |
| | $B_{HN}$ | 0.010 | 0.010 | 0.008 | 0.063 | 0.012 | 0.057 |
| | $V_H$ | 0.978 | 0.990 | 0.868 | 0.982 | 0.875 | 0.959 |
| | $V_C$ | 3.957 | 3.948 | 3.780 | 4.233 | 3.797 | 4.187 |
| | $V_N$ | 2.999 | 3.015 | 2.929 | 3.377 | 2.946 | 3.344 |
| HCP | $q_H$ | 0.067 | 0.041 | 0.242 | 0.138 | 0.240 | 0.212 |
| | $q_C$ | -0.407 | -0.313 | -0.693 | -0.583 | -0.374 | -0.424 |
| | $q_P$ | 0.340 | 0.273 | 0.451 | 0.445 | 0.134 | 0.213 |
| | $B_{HC}$ | 0.981 | 0.989 | 0.933 | 0.966 | 0.893 | 0.914 |
| | $B_{CP}$ | 2.914 | 2.964 | 2.781 | 3.099 | 2.929 | 3.124 |
| | $B_{HP}$ | 0.014 | 0.009 | 0.009 | 0.042 | 0.013 | 0.055 |
| | $V_H$ | 0.995 | 0.998 | 0.942 | 1.008 | 0.906 | 0.970 |
| | $V_C$ | 3.895 | 3.953 | 3.714 | 4.065 | 3.821 | 4.038 |
| | $V_P$ | 2.928 | 2.974 | 2.970 | 3.141 | 2.942 | 3.179 |
| HNO | $q_H$ | 0.135 | 0.080 | 0.322 | 0.176 | 0.328 | 0.238 |
| | $q_N$ | -0.062 | -0.029 | -0.002 | 0.009 | -0.058 | -0.078 |
| | $q_O$ | -0.073 | -0.051 | -0.320 | -0.185 | -0.270 | -0.160 |
| | $B_{HN}$ | 0.933 | 0.956 | 0.820 | 0.938 | 0.826 | 0.903 |
| | $B_{NO}$ | 2.009 | 2.023 | 1.683 | 2.282 | 1.844 | 2.412 |
| | $B_{HO}$ | 0.048 | 0.038 | 0.018 | 0.069 | 0.007 | 0.066 |
| | $V_H$ | 0.982 | 0.994 | 0.839 | 1.007 | 0.833 | 0.970 |
| | $V_N$ | 2.942 | 0.978 | 2.503 | 3.220 | 2.670 | 3.315 |
| | $V_O$ | 2.057 | 2.061 | 1.701 | 2.351 | 1.851 | 2.478 |
| HOP | $q_H$ | -0.157 | -0.167 | -0.054 | -0.135 | -0.131 | -0.050 |
| | $q_P$ | 0.534 | 0.489 | 0.864 | 0.822 | 0.714 | 0.606 |
| | $q_O$ | -0.378 | -0.322 | -0.810 | -0.688 | -0.583 | -0.556 |
| | $B_{HP}$ | 0.924 | 0.926 | 0.911 | 0.949 | 0.886 | 0.958 |
| | $B_{PO}$ | 1.934 | 1.971 | 1.537 | 1.901 | 1.882 | 2.144 |
| | $B_{HO}$ | 0.050 | 0.046 | 0.037 | 0.058 | 0.025 | 0.055 |
| | $V_H$ | 0.975 | 0.972 | 0.948 | 1.006 | 0.911 | 1.013 |
| | $V_P$ | 2.859 | 2.897 | 2.449 | 2.850 | 2.768 | 3.102 |
| | $V_O$ | 1.985 | 2.017 | 1.574 | 1.959 | 1.906 | 2.199 |

"Table 4.1.1 (Continued)"

| Molecule[a] | Calculated quantity | STO-3G | | 4-31G | | 6-31G*[b] | |
|---|---|---|---|---|---|---|---|
| | | M | L | M | L | M | L |
| HOF | $q_H$ | Ø.196 | Ø.139 | Ø.453 | Ø.3Ø7 | Ø.476 | Ø.383 |
| | $q_O$ | -Ø.148 | -Ø.Ø97 | -Ø.351 | -Ø.162 | -Ø.268 | -Ø.239 |
| | $q_F$ | -Ø.Ø48 | -Ø.Ø41 | -Ø.2Ø2 | -Ø.145 | -Ø.2Ø7 | -Ø.144 |
| | $B_{HO}$ | Ø.946 | Ø.971 | Ø.748 | Ø.915 | Ø.74Ø | Ø.853 |
| | $B_{OF}$ | Ø.99Ø | Ø.997 | Ø.878 | 1.11Ø | Ø.923 | 1.234 |
| | $B_{HF}$ | Ø.Ø15 | Ø.Ø1Ø | Ø.ØØ9 | Ø.Ø27 | Ø.ØØ4 | Ø.Ø26 |
| | $V_H$ | Ø.962 | Ø.981 | Ø.757 | Ø.942 | Ø.745 | Ø.879 |
| | $V_O$ | 1.936 | 1.968 | 1.626 | 2.Ø28 | 1.664 | 2.Ø87 |
| | $V_F$ | 1.ØØ5 | 1.ØØ8 | Ø.888 | 1.137 | Ø.928 | 1.26Ø |
| HOCl | $q_H$ | Ø.228 | Ø.168 | Ø.44Ø | Ø.3Ø2 | Ø.48Ø | Ø.384 |
| | $q_O$ | -Ø.155 | -Ø.1ØØ | -Ø.57Ø | -Ø.431 | -Ø.69Ø | -Ø.577 |
| | $q_{Cl}$ | -Ø.Ø74 | -Ø.Ø68 | Ø.13Ø | Ø.129 | Ø.21Ø | Ø.193 |
| | $B_{HO}$ | Ø.941 | Ø.969 | Ø.759 | Ø.923 | Ø.741 | Ø.85Ø |
| | $B_{OCl}$ | Ø.987 | Ø.995 | Ø.934 | 1.Ø6Ø | Ø.885 | 1.155 |
| | $B_{HCl}$ | Ø.ØØ7 | Ø.ØØ3 | Ø.ØØ8 | Ø.Ø2Ø | -Ø.ØØ5 | Ø.Ø26 |
| | $V_H$ | Ø.948 | Ø.972 | Ø.766 | Ø.943 | Ø.736 | Ø.875 |
| | $V_O$ | 1.928 | 1.964 | 1.693 | 1.983 | 1.626 | 2.ØØ5 |
| | VCl | Ø.994 | Ø.998 | Ø.942 | 1.Ø8Ø | Ø.88Ø | 1.181 |
| $SO_2$ | $q_S$ | Ø.9Ø2 | Ø.874 | | | 1.Ø76 | 1.129 |
| | $q_O$ | -Ø.451 | -Ø.437 | | | -Ø.538 | -Ø.564 |
| | $B_{SO}$ | 1.462 | 1.473 | | | 1.741 | 2.Ø49 |
| | $B_{OO}$ | Ø.5Ø4 | Ø.49Ø | | | Ø.115 | Ø.222 |
| | $V_S$ | 2.925 | 2.946 | | | 3.482 | 4.Ø98 |
| | $V_O$ | 1.966 | 1.963 | | | 1.857 | 2.271 |

[a]For the diatomics, $V_A = V_B = B_{AB}$. For NaH the entries under the 4-31G basis set were obtained using the 6-31G basis.

[b]The second entries udner 6-31G* refer to the 6-31G** basis.

occur in some molecules with a second-row atom [$H_2S$ (all but 4-31G), $PH_3$ (STO-3G and 4-31G), HCP (6-31G*), HPO (STO-3G and 4-31G) and $SO_2$ (6-31G*)]. For molecules like $H_2S$ and $PH_3$ where the electronegative difference between the constituent atoms is small, and in some other cases like HCN, MPA and LPA predict different polarity. The minimal basis set (STO-3G) generally underestimates charge separation or polarization. In the case of

NaH, however, the same basis set predicts maximum polarization which is an unexpected result. Inclusion of a set of polarization p functions on the basis set of H (6-31G$^{**}$) increases its populationin in an expected manner. Apart from this, no well-defined trend is followed by atomic charges with regard to the extension of basis sets.

Let us now turn our attention to the bond indices and valencies (Table 4.1.1), with which we are primarily concerned in this article. Without any exception the LPA values for these quantities are overwhelmingly overestimated in comparison to the corresponding MPA values. In a large number of cases the LPA scheme predicts very unrealistic bond indices especially for higher basis sets. For example. the HF bond is predicted to be less ionic than HCl, both LiH and NaH bonds are purely covalent, and so on. In contrast to atomic charges, certain well-defined trend is observed in the bond indices and valencies with respect to their variation with basis sets. The MPA bond indices for the STO-3G basis are always higher than the 4-31G values (we have already remarked that the 4-31G basis has a pronounced overpolarizing tendency). With further extension of basis sets the bond indices and valencies increase slowly. The LPA values do not always follow this trend.

The results of calcualtions given in Table 4.1.1 were obtained for basis sets which do not contain any diffuse functions. Behera *et al.*[130] therefore made a comparative study of the MPA and LPA schemes taking $SN_2$, $SN_2^{2+}$, $SN_2^{2-}$, $S_2N^+$ and $S_2N^-$ as the test molecules and using 4-31G, 3-21G$^*$, 3-21+G$^*$ and 3-21++G$^*$ (only for the negatively charged species) basis sets. The geometries of the molecules were optimized using first three basis sets, all of which predict a linear asymmetric ($C_{\infty v}$) structure for $SN_2$, a linear symmetric structure ($D_{\infty h}$) for $S_2N^+$ and a bent structure ($C_{2v}$) for the remaining species (the geometry of $SN_2^{2+}$could not be optimized using the 4-31G basis). The atomic charges of these molecules calculated at the respective equilibrium geometry (for

the negatively charged species 3-21++G** calculations were made at the 3-21+G* optimized geometry) are given in Table 4.1.2. Table 4.1.3 contains the calculated values of their bond indices and valencies. A survey of the results of Table 4.1.2 indicates that

Table 4.1.2: Calculated atomic charges ($q_A$) of $SN_2^{2+}$, $SN_2$, $SN_2^{2-}$, $S_2N^-$ and $S_2N^+$.

| System | Atom | Basis set[a] | | | | | |
|---|---|---|---|---|---|---|---|
| | | 4-31G | | 3-21G | | 3-21+G* | |
| | | M | L | M | L | M | L |
| $SN_2^{2+}$ | S | | | +1.508 | +1.216 | +1.370 | +1.488 |
| | N | | | +0.246 | +0.392 | +0.315 | +0.256 |
| $SN_2$ | S | +0.128 | -0.058 | 0.000 | -0.244 | +0.052 | +0.110 |
| | N1[b] | -0.075 | +0.089 | +0.069 | +0.092 | -0.184 | +0.093 |
| | N2 | -0.052 | -0.031 | -0.069 | +0.153 | +0.132 | -0.203 |
| $SN_2^{2-}$ | S[c] | +0.426 | +0.469 | +0.083 | -0.142 | +0.647 | +0.663 |
| | | | | | | -0.336 | +0.209 |
| | N[c] | -1.213 | -1.234 | -1.042 | -0.928 | -1.323 | -1.331 |
| | | | | | | -0.832 | -1.104 |
| $S_2N^+$ | S | +0.955 | +0.710 | +0.649 | +0.420 | +0.612 | +0.654 |
| | N | -0.911 | -0.420 | +0.298 | +0.160 | -0.224 | -0.308 |
| $S_2N^-$ | S[c] | -0.139 | -0.242 | -0.274 | -0.438 | -0.186 | -0.106 |
| | | | | | | -0.419 | -0.238 |
| | N[c] | -0.721 | -0.516 | -0.451 | -0.124 | -0.629 | -0.785 |
| | | | | | | -0.162 | -0.524 |

[a] M and L refer to MPA and LPA respectively.
[b] Terminal nitrogen atom.
[c] The second entries under 3-21+G* refer to the 3-21++G* basis.

in a few cases the sign of MPA and LPA atomic charges is reversed. For $SN_2^{2-}$ the 3-21+G* values are almost identical for the two schemes. However on adding a set of diffuse sp functions on S also (3-21++G*) its MPA atomic charge decreases by about 0.7 unit while the corresponding LPA value decreases by about 0.4 unit. A similar effect, although to a lesser extent, is also observed in

Table 4.1.3: Calculated bond indices ($B_{AB}$) and valencies ($V_A$) of $SN_2^{2+}$, $SN_2$, $SN_2^{2-}$, $S_2N^+$ and $S_2N^-$.

| System | Calculated quantity | Basis set | | | | | |
|---|---|---|---|---|---|---|---|
| | | 4-31G | | 3-21G | | 3-21+G* | |
| | | M | L | M | L | M | L |
| $SN_2^{2+}$ | $B_{NN}$ | | | 1.229 | 1.520 | 1.641 | 1.833 |
| | $B_{NS}$ | | | 1.394 | 1.641 | 1.312 | 1.724 |
| | $V_N$ | | | 2.622 | 3.161 | 2.954 | 3.557 |
| | $V_S$ | | | 2.787 | 3.282 | 2.625 | 3.448 |
| $SN_2$[a] | $B_{NN}$ | 2.603 | 3.148 | 2.451 | 2.917 | 2.705 | 3.117 |
| | $B_{N1S}$ | 2.260 | 0.332 | 0.346 | 0.417 | 0.477 | 0.508 |
| | $B_{N2S}$ | 0.426 | 0.946 | 0.828 | 1.160 | 0.764 | 1.542 |
| | $V_{N1}$ | 2.863 | 3.480 | 2.797 | 3.334 | 3.182 | 3.625 |
| | $V_{N2}$ | 3.029 | 4.094 | 3.279 | 4.077 | 3.469 | 4.659 |
| | $V_S$ | 0.686 | 1.278 | 1.174 | 1.577 | 1.241 | 2.050 |
| $SN_2^{2-}$[b] | $B_{NN}$ | 0.620 | 0.654 | 0.442 | 0.516 | 0.211 | 0.587 |
| | | | | | | 0.267 | 0.521 |
| | $B_{NS}$ | 1.305 | 1.580 | 1.928 | 2.184 | 1.668 | 2.240 |
| | | | | | | 1.519 | 2.430 |
| | $V_N$ | 1.925 | 2.234 | 2.370 | 2.700 | 1.880 | 2.827 |
| | | | | | | 1.252 | 2.950 |
| | $V_S$ | 2.610 | 3.161 | 3.856 | 4.368 | 3.337 | 3.479 |
| | | | | | | 3.038 | 4.859 |
| $S_2N^+$ | $B_{NS}$ | 1.315 | 1.991 | 1.683 | 1.967 | 1.537 | 2.221 |
| | $B_{SS}$ | 0.857 | 0.888 | 0.831 | 0.874 | 0.848 | 0.943 |
| | $V_N$ | 2.631 | 3.823 | 3.366 | 3.934 | 3.075 | 4.423 |
| | $V_S$ | 2.172 | 2.780 | 2.515 | 2.841 | 2.385 | 3.155 |
| $S_2N^-$[b] | $B_{NS}$ | 1.155 | 1.521 | 1.295 | 1.571 | 1.337 | 1.975 |
| | | | | | | 0.931 | 1.884 |
| | $B_{SS}$ | 0.234 | 0.275 | 0.208 | 0.296 | 0.204 | 0.360 |
| | | | | | | 0.200 | 0.487 |
| | $V_N$ | 2.311 | 3.042 | 2.589 | 3.143 | 2.647 | 3.950 |
| | | | | | | 1.861 | 3.768 |
| | $V_S$ | 1.390 | 1.796 | 1.502 | 1.867 | 1.541 | 2.335 |
| | | | | | | 1.130 | 2.371 |

[a] In $SN_2$ N1 and N2 refer to the terminal and central nitrogen atoms, respectively.
[b] The second entries under 3-21+G* refer to the 3-21++G* basis.

$SN_2^-$. Thus no significant abnormality is noted in the MPA scheme when diffuse functions are added to the basis set. So far the bond

indices and valencies (Table 4.1.3) are concerned, the LPA values are always appreciably exaggerated compared to the MPA values.

Sannigrahi *et al.*[139] have recently analyzed the causes of discrepancy between MPA and LPA atomic charges. They showed that

$$S^{1/2}PS^{1/2} = PS - \frac{1}{2}[P,d] + \frac{1}{8}[d,[P,d]] - \frac{1}{16}[d,[P,d^2]] + \ldots \quad (4.1.11)$$

or

$$D_L = D_M + \sum_{i=1}^{i} R_i \quad (4.1.12)$$

where $d = S - I$ and $R_i$ is a residual term of ith degree in $d$. Equation (4.1.12) implies that

$$(Q_A)_L = (Q_A)_M + \sum_{i=1}^{i} (R_i)_A \quad (4.1.13)$$

where

$$(R_i)_A = \sum_{\alpha}^{A} (R_i)_{\alpha\alpha}$$

Since $d$ is a symmetric matrix with all diagonal elements equal to zero, and $P$ is also a symmetric matrix, the diagonal terms of $Pd$ and $dP$ matrices are identical. Thus Eq.(4.1.13) becomes

$$(Q_A)_L = (Q_A)_M + \sum_{i=2}^{i} (R_i)_A \quad (4.1.14)$$

It is obvious from Eq.(4.1.11) - (4.1.14) that

$$(Q_A)_L = (Q_A)_M$$

when $[P,d] = \emptyset$. Sannigrahi *et al.*[139] showed that even when $[P,S]$ or $[P,d]$ does not vanish (for example, in homonuclear diatomics) the MPA and LPA may give identical charges because the residual terms $R_2$, $R_3$ etc. do not contribute to $Q_A$. They also observed that the discrepancy between MPA and LPA atomic charges could be qualitiatively explained on the basis of the diagonal terms of the $R_2$ matrix which is a multiple of the commutator of $d$ and $[P,d]$ matrices.

The effect of basis set superposition (BSS)[140] on the MPA and LPA atomic charges, bond indices and valencies was studied by Sannigrahi *et al.*[141] for six H-bonded ($HF_2^-$, $HFCl^-$, $HCl_2^-$ and $H_3N$/

$H_2O$ / HF..HF) and two Li-bonded ($H_3N$ / $H_2O$ ..LiF) complexes using 6-31G, 6-31G* and 6-31G** basis sets and employing counterpoise (CP)[150] and polarization counterpoise (PCP)[151,152] correction methods. Their results indicate that both MPA and LPA schemes exaggerate BSS effects. The former predicts unphysical negative population on the ghost centers in a few cases, and the latter generally gives very high values of spurious bond indices and electron populations. The changes in $q_A$ and $V_A$ due to CP correction do not follow any well-defined trend with respect to the extension of basis sets. Overcorrection of BSSE by the CP method is considerably reduced when the PCP correction is applied, but the corrected values obtained thereby do not differ significantly from the uncorrected ones. So far the uncorrected values are concerned the MPA scheme predicts more consistent result than LPA. Thus unlike in the case of complexation energy, BSSE correction for $\Delta q$, $\Delta V$ etc. is not warranted, especially when MPA- and LPA-like schemes are used.

Sannigrahi and Kar[132] have, recently extended the definition of bond index to multi-center cases. For closed-shell SCF wavefunctions the D matrix is $2^{K-1}$-potent. Using this property they derived the following expression for a K- center bond index.

$$B_{AB\ldots K} = \sum_{a}^{A} \sum_{b}^{B} \ldots \sum_{k}^{K} D_{ab} D_{bc} \ldots D_{ka} \qquad (4.1.15)$$

Using Eq.(4.1.15) one can derive in a straightforward manner that

$$Q_A = 2^{1-K} \sum_{B} \ldots \sum_{K} B_{AB..K} \qquad (4.1.16)$$

$$B_{AB} = 2^{2-K} \sum_{C} \ldots \sum_{K} B_{AB\ldots K} \qquad (4.1.17)$$

$$B_{ABC} = 2^{3-K} \sum_{D} \ldots \sum_{K} B_{AB\ldots K} \qquad (4.1.18)$$

Now, using the relation,

$$B_{ABC} = \sum_{a}^{A} \sum_{b}^{B} \sum_{c}^{C} D_{ab} D_{bc} D_{ca} \qquad (4.1.19)$$

they calculated MPA and LPA 3-center bond indices in a number of molecules using several basis sets, and observed that $B_{ABC}$ is positive and appreciably high ( $\geq$ Ø.1) only for those 3-center

bonds which can be obtained from LMO calculations. In other cases $B_{ABC}$ is either very close to zero or negative. A comprehensive study of this delocalized MO approach for the detection of multi-center bonding is in progress.

Before closing this subsection we would like to make some comments on a recent method[122] suggested by Reed and Schleyer for the calculation of bond index (it was called bond order by them) in the framework of NPA. They proposed (without derivation) that

$$B_{AB} = \sum_{i}^{occ} b_{iAB} \qquad (4.1.20)$$

where

$$b_{iAB} = \text{sgn}\,(S_{iAB})\ \min\,(n_{iA}, n_{iB}) \qquad (4.1.21)$$

In Eq.(4.1.21) $S_{iAB}$ is the overlap between the natural atomic orbitals forming the bond AB and $n_{iA}$ is the number of electrons associated with A due to the occupation of the ith LMO. The authors applied this scheme to calculate the CC bond indices in ethane, ethene and ethyne. The values thus obtained (1.02, 2.03 and 3.01) tally with the classically expected ones. The excess values are attributed to hyperconjugation. They also calculated the XA, AY and XY bond indices, and atomic valencies of a series of compounds of the $X_3AY$ type (X = H,F; A = C, N, P, S and Y = O, S, N) using the 6-31G* basis set, and obtained results which are consistent with the hypervalent nature of atom A and the antibonding interaction between X and Y. The expression for bond index in the NPA scheme is a linear function of the diagonal elements of the first order density matrix, while those in the MPA and LPA schemes are quadratic functions of $D_{ab}$. The latter definitions are in conformity with the covalent sharing of electrons between a pair of atoms, and is thus theoretically sound and falls in line with the chemist's concept of a bond. The Reed-Schleyer definition on the other hand is completely heuristic and in no way related to electron sharing.

## 4.2 Results of Calculations using Correlated Wavefunctions

Only a few calculations of bond index and valency using correlated wavefunctions have been reported. Taking the Weinbaum type wavefuction for $H_2$ which corresponds to full CI in the minimal basis, Mayer[77] showed that with increasing internuclear distance, the bond index decreases and the free valency of each atom increases. In the limit of infinite internuclear separation $B_{AB} = V_A = 0$ and $F_A = 1$. It may be noted in this context that for a single determinant wavefunction for $H_2$, $B_{AB} = V_A = 1.0$ and $F_A = 0$ at all internuclear distances.

Villar and Dupuis[118] investigated the nature of bonding in $O_3$ using GVB / PP wavefunctions and the 3-21G basis set. They observed that the biradical character of the molecule is reflected from the spin density values at the terminal oxygens. Using CASSCF wavefunction[9] and the 6-31G basis set they calculated various geometrical parameters of the $C_5H_7$, $C_7H_9$, $C_9H_{11}$ and $C_{11}H_{13}$ radicals. Their results indicate that the spin density is more or less localized around the central carbon atom and decreases appreciably towards the end of the molecule, which is in contrast to the UHF results.

Lendvay[194] investigated the variation of bond indices with bond lengths using MCSCF wavefunctions. He considered the diatomic species $H_2$, HF, OH and CN which are representative of different bonding situations. On the basis of chemical intuition one would expect the bond index of a diatomic molecule to decrease from the appropriate integral value at the equilibrium distance down to zero at very large internuclear separation. The total valency of the atom is expected to be invariant with respect to bond length while the free valency of the atom should increase from zero to the total valency. Using STO-3G and 6-311G* basis sets the author found the above trend to be followed by $H_2$. For the other diatomics he used STO-3G and 4-31G basis sets and noted some discrepancy at internuclear distances smaller than the equilibrium

bond length. However, at greater distances the expected trend was observed. Lendvay also observed that the ab initio bond indices calculated using Mayer's definition follow a more consistent trend than that observed using 'chemist's bond order' of Pauling.[152] The latter is defined by

$$B = \exp [-b (R_{AB} - R^{o}_{AB})] \qquad (4.2.1)$$

where $R_{AB}$ is the actual interatomic distance, $R^{o}_{AB}$ is the equilibrium bond length of the single bond, and b = 3.85 $\mathring{A}^{-1}$ is an empirical constant. Lendvay also tested the principle of conservation of bond index along the MEP of the metathetic reaction, $H^1 + H^2H^3 \longrightarrow H^1H^2 + H^3$ using STO-3G and 6-311G* basis sets and MCSCF wavefunctions.

Johnston[154] suggested the following empirical relation between bond energy and Pauling's bond order.

$$V = D B^{p} \qquad (4.2.2)$$

where V is the binding energy, D is the dissociation energy of the molecule and p is a constant. Parr and Johnston[155] noted that the value of p is often close to unity. However, when ab initio bond indices were used in Eq.(4.2.2) the log-log plot of bond index and binding energy was curved instead of being a straight line. Using Eq.(4.2.2) as a nonlinear fitting function for the data at extended bond lengths Lendvay found that the p values significantly differ from unity. He used this semiquantitative relation between bond energy and bond index to construct a model of the potential profile for the atom-transfer reactions of the type, A + BC $\longrightarrow$ AB + C. According to this model, as it was shown by Lendvay, the degree of reaction is uniquely determined by $B_{AB}$.

Maity and Bhattacharyya[195] studied the photochemical decomposition of XNO ( X = H, Li, F etc.) type of molecules using bond energy - bond index relation and INDO-MCSCF wavefunctions. For the isomerization of HNO to NOH in the lowest $^3A''$ state, they observed that the potential energy when plotted as a function of

<HNO predicted a value of 55.5° for the HNO angle in the transition state. When the OH and NH bond indices were plotted against <HNO the inflection points for both the curves were obtained at exactly identical HNO angle (55.5°). Thus the point of inflection noted in the bond index plot was identified with the actual saddle point revealed in the energy profile. The authors also studied the bond index profile of the NH bond in HNO in the photochemical decomposition of the molecule (HNO ⟶ H + NO). They pointed out that it is difficult to trace the bond breaking point in the above reaction as the energy profile is rather flat around the transition point. The bond index method, on the other hand, locates the bond breaking point rather sharply.

Medrano *et al.*[113] calculated bond indices and valencies of a number of closed-shell systems at their equilibrium configuration using CI and GVB + CI wavefuctions, and Löwdin-orthogonalized basis sets. Their results showed that the CI bond indices are smaller than the corresponding SCF values in most cases.

Following Jug,[94] Siddarth and Gopinathan[108] have recently extended the definition of atomic valency to CI wavefunctions. Using their definition in conjunction with INDO CI wavefunction the authors reaffirmed their earlier assertion that the molecular valency reaches a maximum near the equilibrium bond angle. Barring $H_2$, they obtained a well-defined maximum in the $V_M$ vs R (bond length) curves at or around the equilibrium bond length for all other diatomics like $N_2$, $F_2$ etc. studied by them. For the heteronuclear diatomics also, the CI moelcular valency generally reaches a maximum value in the vicinity of the equilibrium bond length. The exceptions were attributed to the appreciable variation of atomic charge with bond length. They also partitioned the CI molecular valency into contributions from MOs and used the resulting MO valencies as the ordinates in quantitative Mulliken-Walsh diagrams as had been done previously at the SCF level. This is, however, a wrong procedure since the identity of the individual MOs is not retained in the CI wavefunction.

Quite recently, Jug and Poredda[100] proposed a valency partitioning scheme for the characterization of radicals and zwitter ions. According to this scheme a molecule is said to be a diradical when the following condition is satisfied.

$$\emptyset << \Delta V_M^{CI} \sim 2 \qquad (4.2.3)$$

where

$$\Delta V_M = \sum_A^M | \Delta V_A | \qquad (4.2.4)$$

with $\Delta V = V_A - V_A$ ($V_A$ is the calculated atomic valency and $V_A^O$ is the corresponding reference value which is 4.Ø for C, 3.Ø for N etc.). For the zwitter ion the following condition is satisfied.

$$\emptyset << \Delta V_M^{RHF} \sim 2 \qquad (4.2.5)$$

Using SINDO1 wavfunction they applied this scheme to a large number of small neutral molecules and classified them into five groups, namely, covalent molecules, diradicals, zwitter ions, 1,n-dipolar molecules and diradicals with ionic character.

## 5. SUMMARY AND CONCLUSIONS

The results of the calculations reviewed herein indicate that at the ground state equilibrium geometry of a molecule the SCF wavefunction is adequate for the study of its nature of bonding on the basis of bond indices and valencies. The latter quantities are sensitive to basis sets and the population analysis schemes. Generally basis sets of double-zeta quality augmented with a set of polarization and a set of diffuse functions (only in the case of highly ionic and/or negatively charged species) on highly eleectronegative centers should be employed in these calculations.

Of the two schemes of population analysis (MPA and LPA) that are currently in use, the MPA generally gives a more consistent picture of bonding.

The important qauantities related to bond index and valency are the molecular valency ($V_M$) and the MO valency ($V_i$). The $V_M$ index can be used to understand the changes in bonding occuring with geometrical distortion, to follow chemical reaction along various possible reaction pathways, to provide an insight into the causes of difference in the stability of various conformers of a molecule, and so on. The principle of conservation of bond index during the course of simple (metathetic, $S_N2$ etc.) reactions is an important concept. The similarity between Mulliken-Walsh and valency correlation diagrams (plots of $V_i$ vs $\theta$) leads to many interesting applications of the valence concept. The free valency ($F_A$) proposed by Mayer, although it has some significance in the context of a UHF wavefunction, is rather misleading and can be confused with the $F_r$ index of Coulson. The delocalized MO approach for the study of multi-center bonding on the basis of bond index is an interesting and useful outcome of bond index and valency calculations. Since SCF bond indices are rather insensitive to bond length, CI calculations must be performed in order to understand the course of a reaction caused mainly by deformation of bonds. Further calculations are needed in order to explore the full potential of such calculations. The existing methods for the calculation of bond indices and valency fail conspicuously in the case of predominantly ionic molecules. The applicability of these methods to molecules containing third- and higher-row elements has not yet been tested at the ab initio level. A few limitations notwithstanding, quantification of the concepts of bond index and valency by means of rigorous quantum mechanical calculations has opened up new vistas in the realm of chemical bonding.

**ACKNOWLEDGEMENTS**

My sincere thanks are due to my Ph.D. students Mr. L. Behera and Mr. P.K. Nandi, to my eldest daughter, Miss Soma Sannigrahi, and to Mr. P.K. Halder for their invaluable help in the preparation of this manuscript.

**REFERENCES**

1. R.S. Mulliken, Phys. Rev. 32, 186 (1928); 32, 388 (1928).
2. F. Hund, Z. Physik 51, 759 (1928).
3. J.E. Lennard-Jones, Trans. Faraday Soc. 25, 668 (1929).
4. D.R. Hartree, Proc. Cambridge Phil. Soc. 24, 89 (1928).
5. V. Fock, Z. Physik 61, 126 (1930).
6. C.C.J. Roothaan, Rev. Mod. Phys. 23, 69 (1951); 32, 179 (1960).
7. G.G. Hall, Proc. Roy. Soc. (London) A205, 541 (1951).
8. J.A. Pople and R.K. Nesbet, J.Chem. Phys. 22, 571 (1954).
9. K.P. Lawley, Ed. *Ab Initio Methods in Quantum Chemistry* : Parts I and II. Adv. Chem. Phys. Vol. XXLVII and XXL (John Wiley, New York, 1987).
10. R.S. Mulliken, J. Chem. Phys. 3, 573 (1935).
11. C.A. Coulson, Proc. Roy. Soc. (London) A169, 413 (1939).
12. B.H. Chirgwin and C.A. Coulson, Proc. Roy Soc. (London) A201, 196 (1950).
13. P.-O. Löwdin, J. Chem. Phys. 18, 365 (1950); 21, 374 (1953).
14. R. McWeeny, J. Chem. Phys. 19, 164 (1951); 20, 920 (1960).
15. R.S. Mulliken, J. Chem. Phys. 23, 1833 (1955); 23, 1841 (1955).
16. R.S. Ross and G.C.A. Schmit, Theor. Chim. Acta 4, 1 (1966).
17. E.R. Davidson, J. Chem. Phys. 46, 3319 (1967).
18. E.W. Stout and P. Politzer, Theor. Chim, Acta 12, 379 (1968).
19. G. Dogget, J. Chem. Soc. A, 229 (1969).
20. I.H. Hiller and J.P. Wyatt, Int. J. Quantum Chem. 3, 67 (1969).
21. P. Politzer and R.R. Harris, J. Am. Chem. Soc. 92, 6 (1970).
22. R.E. Christoffersen and K.A. Baker, Chem. Phys. Lett. 8, 4 (1971).
23. R.F.W. Bader, P.M. Beddall and P.E. Cade, J. Am. Chem. Soc. 93, 3095 (1971).

24. R.C.A.R. Maclagon, Chem. Phys. Lett. 8, 114 (1971).
25. C. Aslangul, R. Constanciel, R. Daudel and P. Kottis, Adv. Quantum Chem. 6, 94 (1972).
26. R.F.W. Bader and P.M. Beddall, J. Chem. Phys. 56, 3320 (1972).
27. R. Rein, Adv. Quantum Chem. 7, 335 (1973).
28. R.F.W. Bader, P.M. Beddall and J. Peslak, Jr., J. Chem. Phys. 58, 557 (1973).
29. K.R. Roby, Mol. Phys. 27, 81 (1974); 28, 1441 (1974).
30. R.F.W. Bader and M.E. Stevens, J. Am. Chem. Soc. 97, 7391 (1975).
31. J. Rys, H.F. King and P. Coppens, Chem. Phys. Lett. 41, 383 (1976).
32. P. Kollman, J. Am. Chem. Soc. 100, 2974 (1978).
33. E. Scrocco and J. Tomasi, Adv. Quantum Chem. 11, 115 (1978).
34. C. Etchebest, R. Lavery and A. Pullman, Theor. Chim. Acta 62, 17 (1982).
35. D.W.J. Cruickshank and E.J. Avramides, Phil, Roy. Soc. A304, 533 (1982).
36. G.G. Hall, Adv. At. Mol. Phys. 20, 41 (1985).
37. J. B. Collins and A. Streitwieser, J. Comp. Chem. 1, 81 (1980).
38. A.E. Reed, R.B. Weinstock and F. Weinhold, J. Chem. Phys. 83, 735 (1985).
39. C.M. Smith and G.G. Hall, Int. J. Quantum Chem. 31, 685 (1987).
40. J. Cioslowski, J. Am. Chem. Soc. 22, 8333 (1989).
41. K. Jug, E. Fasold and M.S. Gopinathan, J. Comp. Chem. 10, 965 (1989).
42. E. Hückel, Z. Physik 70, 204 (1942); 72, 310 (1931); 76, 628 (1932).
43. R. Pariser and R.G. Parr, J. Chem. Phys. 21, 466 (1953); 21, 767 (1953).
44. J.A. Pople, Trans. Faraday Soc. 49, 1375 (1953).
45. P.C. Misra and D.K. Rai, Mol. Phys. 23, 631 (1972).
46. J.S. Yadav, P.C. Misra and D.K. Rai, Mol. Phys. 26, 193 (1973).
47. O.P. Singh and J.S. Yadav, Int. J. Quantum Chem. 29, 1283 (1986).
48. L.S. Yadav, O.P. Singh and J.S. Yadav, J. Mol. Struct. (THEOCHEM) 149, 121 (1987) and refernces cited therein.
49. I. Cohen, J. Chem. Phys. 57, 5076 (1972).
50. B. Dick and H.-J. Freund, Int. J. Quantum Chem. 24, 747 (1983).
51. L. Salem, *Molecular Orbital Theory of Conjugatged Systems*, p.39 (Benjamin, New York, 1966).
52. K.Wiberg, Tetrahedron 24, 1083 (1968).
53. J. A. Pople and D.L. Beveridge, *Approximate Molecular Orbital Theory* (McGraw-Hill, New York, 1970).
54. D.A. Armstrong, P.G. Perkins and J.J.P. Stewart, J. Chem. Soc. (Dalton). 838 (1973); 2273 (1973).

55. N.P. Borisova and S.G. Semenov, Vestn. Leningrad Univ. **16**, 119 (1973).
56. R. Hoffmann, J. Chem. Phys., **39**, 1379 (1963).
57. M. Giambiagi, M.S. de Giambiagi, D.R. Grempel and C.D. Heymann, J. Chim. Phys. **72**, 15 (1975).
58. K. Jug, J. Am. Chem. Soc. **99**, 7800 (1977); **100**, 6581 (1978).
59. K. Jug, Theor. Chim. Acta **51**, 331 (1979).
60. C. Trindle and O. Sinanoglu, J. Am. Chem. Soc. **91**, 853 (1969).
61. C. Trindle, J. Am. Chem. Soc. **91**, 219 (1969).
62. L.D. Brown and W.N. Lipscomb, J. Am. Chem. Soc. **99**, 3968 (1977).
63. T.A. Halgren, L.D. Brown, D.A. Kleier and W.N. Lipscomb, J.Am. Chem. Soc. **99**, 6793 (1977).
64. I. Mayer, Int. J. Quantum Chem. **23**, 341 (1983).
65. S. Bhattacharjee and A.B. Sannigrahi, Ind. J. Chem. **23A**, 285 (1984).
66. S. Bhattacharjee and A.B. Sannigrahi, Ind. J. Chem. **23A**, 707 (1984).
67. S. Bhattacharjee, T. Kar and A.B. Sannigrahi, Ind. J. Chem. **24A**, 173 (1985).
68. S. Bhattacharjee, T. Kar and A.B. Sannigrahi, Ind. J. Chem. **24A**, 276 (1985).
69. T.Kar and A.B. Sannigrahi, Bull. Chem. Soc. Japan **39**, 1283 (1986).
70. I. Mayer, Chem. Phys. Lett. **97**, 270 (1983); addendum, **117**, 396 (1985).
71. I. Mayer, M. Revesz and I. Hargittai, Acta Chim. Hung. **115**, 159 (1983).
72. I. Mayer and M. Revesz, Inorg. Chim. Acta **77**, L205 (1983).
73. I. Mayer, Chem. Phys. Lett. **110**, 440 (1984).
74. I. Mayer, Int. J. Quantum Chem. **26**, 151 (1984); addendum, **28**, 419 (1985).
75. I. Mayer and P.R. Surjan, Acta Chim. Hung. **117**, 85 (1984).
76. I. Mayer, Theor. Chim. Acta **67**, 315 (1985).
77. I. Mayer, Int. J. Quantum Chem. **29**, 73 (1986); **29**, 477 (1986).
78. I. Mayer, J. Mol. Struct. (THEOCHEM) **149**, 81 (1987).
79. I. Mayer, J. Mol. Struct. (THEOCHEM) **186**, 43 (1989).
80. O.P. Singh and J.S. Yadav, J. Mol. Struct. (THEOCHEM) **124**, 287 (1985); **149**, 91 (1987).
81. L.S. Yadav, O.P. Singh, P.N.S. Yadav and J.S. Yadav, J. Mol. Struct. (THEOCHEM) **151**, 227 (1987).
82. A. Yadav, P.R. Surjan and R.P. Poierier, J.Mol. Struct. (THEOCHEM) **165**, 297 (1988).
83. L.S. Yadav and J.S. Yadav, J. Mol. Struct. (THEOCHEM) **165**, 289 (1988).
84. M.S. de Giambiagi, M. Gaimbiagi and F.E. Jorge, Z. Naturforsch. **39a**, 1259 (1984).
85. M.S. de Giambiagi, M. Giambiagi and F.E. Jorge, Theor. Chim. Acta **68**, 337 (1985).
86. P. Pitanaga, M. Giambiagi and M.S. de Giambiagi, Chem. Phys. Lett. **128**, 411 (1986).

87. M. S. de Giambiagi, M.Giambiagi and P. Pitanga, Chem. Phys. Lett. **129**, 367 (1986).
88. P. Pitanga, M.S. de Giambiagi and M. Giambiagi, Quimica Nova **11**, 90 (1988).
89. F.E. Jorge and A.B. Batista, Chem. Phys. Lett. **138**, 115 (1987).
90. M.S. de Giambiagi, M. Giambiagi and P. Pitanga, Chem. Phys. Lett. **141**, 466 (1987).
91. M. Giambiagi, M.S. de Giambiagi, J.M. Pires and P. Pitanga, J. Mol. Struct. (THEOCHEM) **180**, 223 (1988).
92. M.S. Gopinathan and K. Jug, Theor. Chim. Acta **63**, 497 (1983).
93. M. S. Gopinathan and K. Jug, Theor. Chim. Acta **63**, 511 (1983).
94. K. Jug, J. Comp. Chem. **5**, 555 (1984).
95. K. Jug, Tetrahedron Lett. **26**, 1439 (1985).
96. K. Jug and S. Buss, J. Comp. Chem. **6**, 507 (1985).
97. K. Jug, N.D. Epiotis and S. Buss, J. Am. Chem. Soc. **108**, 3640 (1986).
98. M.S. Gopinathan, P. Siddarth and C. Ravimohan, Theor. Chim. Acta. **70**, 303 (1986).
99. P. Siddarth and M.S. Gopinathan, Proc. Ind. Acad. Sc. (Chem. Sc.) **99**, 91 (1987).
100. P. Siddarth and M.S. Gopinathan, J. Am. Chem. Soc. **110**, 96 (1988).
101. K. Jug, in *Topics in Molecular Organization and Engineering*, J. Maruani, Ed. Vol.3, p.149 (Reidel, Dordrecht, 1988).
102. P. Siddarth and M. S. Gopinathan, J. Mol. Struct. (THEOCHEM) **148**, 101 (1986).
103. P. Siddarth and M.S. Gopinathan, J. Mol. Struct. (THEOCHEM) **187**, 169 (1989).
104. P. Siddarth and M.S. Gopinathan, Proc. Ind. Acad. Sc. (Chem. Sc.) **101**, 37 (1989).
105. K. Jug and M.S. Gopinathan, Theor. Chim. Acta, **68**, 343 (1985).
106. M. S. Gopinathan, J. Mol. Struct. (THEOCHEM) **169**, 379 (1988).
107. K. Jug and M.S. Gopinathan, in *Theoretical Models of Chemical Bonding*: Part 2. *The Concept of the Chemical Bond*, Z.B. Makzic, Ed. p.77 (Springer-Verlag, Berlin, 1990).
108. P. Siddarth and M. S. Gopinathan, Int. J. Quantum Chem. **37**, 685 (1990).
109. K. Jug. and A. Poredda, Chem. Phys. Lett. **171**, 394 (1990).
110. M. A. Natiello and J.A. Medrano, Chem. Phys. Lett. **105**, 180 (1984); **110**, 446 (1984).
111. N.P. Borisova and S.G. Semenov, Vestn. Leningrad Univ. **16**, 98 (1976).
112. M. A. Natiello, H.F. Reale and J.A. Medrano, J. Comp. Chem. **6**, 108 (1985).
113. J. A. Medrano, H.F. Reale and R.C. Bochicchio, J. Mol. Struct. (THEOCHEM) **135**, 117(1986).
114. J. A. Medrano and R.C. Bochicchio, J. Mol. Struct. (THEOCHEM) **200**, 463 (1989).

115. O.G. Stradella, H.O. Villar and E.A. Castro, Theor. Chim. Acta 70, 67 (1986).
116. J.G. Angyan, R.A. Poirier, A. Kucsman and I.G. Csizamadia, J. Am. Chem. Soc. 109, 2237 (1987).
117. J. G. Angyan, C. Bonnelle, R. Daudel, A. Kucsman and I.G. Csizmadia, J. Mol. Struct. (THEOCHEM) 165, 273 (1988).
118. H.O. Villar and M. Dupuis, Chem. Phys. Lett. 142, 59 (1987).
119. G. Lendvay, J. Mol. Struct. (THEOCHEM) 167, 331 (1988).
120. A.T. Balban, G.R.De Mare and R. Poirier, J. Mol. Struct. (THEOCHEM) 183, 103 (1989).
121. J. Baker, Theor. Chim. Acta 68, 221 (1985).
122. A. E. Reed and P.v.R. Schleyer, J.Am. Chem. Soc. 112, 1434 (1990).
123. T. Kar, A.B. Sannigrahi and D.C. Mukherjee, J. Mol. Struct. (THEOCHEM) 153, 93 (1987).
124. T. Kar, A.B. Sannigrahi and B.C. Guha Niyogi, Ind. J. Chem. 26A, 989 (1987).
125. T. Kar and A.B. Sannigrahi, J. Mol. Struct. (THEOCHEM) 165, 47 (1988).
126. T. Kar and A.B. Sannigrahi, J. Mol. Struct. (THEOCHEM) 180, 149 (1988).
127. A.B. Sannigrahi and T. Kar, J. Chem. Educn. 65, 675 (1988).
128. T. Kar, A.B. Sannigrahi and L. Behera, Chem. Phys. Lett. 163, 157 (1989).
129. T. Kar, L. Behera and A.B. Sannigrahi, J. Mol. Struct. (THEOCHEM) 209, 45 (1990).
130. L. Behera, T. Kar and A.B. Sannigrahi, J. Mol. Struct. (THEOCHEM) 209, 111 (1990).
131. A.B. Sannigrahi, T. Kar and L. Behera, Chem. Phys. Lett. 172, 487 (1990).
132. A. B. Sannigrahi and T. Kar, Chem. Phys. Lett.173, 569 (1990).
133. A. B. Sannigrahi, P. K. Nandi, T. Kar and L. Behera, J. Mol. Struct. (THEOCHEM) (In press).
134. G. Lendvay, J. Phys. Chem. 93, 4422 (1989).
135. D.K. Maity and S.P. Bhattacharyya, J. Am. Chem. Soc. 112, 3223 (1990).
136. A. Somogui and J. Tamas, J. Phys. Chem. 94, 5554 (1990).
137. R. McWeeny and B.T. Sutcliffe, *Methods of Molecular Quantum Mechanics* (Academic Press, New York, 1969).
138. H. C. Longuet-Higgins, in *Quantum Theory of Atoms, Molecules and the Solid State*, P,O-. Lowdin, Ed. p.106 (Academic Press, New York, 1986).
139. A. B. Sannigrahi, Chemistry Education 3, 5 (1986); 3, 18 (1986).
140. T. A. Halgren and W.N. Lipscomb, Proc. Natl. Acad. Sc. 69, 652 (1972).
141. T. A. Halgren and W.N. Lipscomb, J. Chem. Phys. 58, 1569 (1973).
142. R.G. Parr and R.G. Pearson, J. Am. Chem. Soc. 105, 7512 (1983).

143. D. N. Nanda and K. Jug, Theor, Chim. Acta 57, 95 (1980).
144. R.S. Mulliken, Rev. Mod. Phys. 14, 204 (1942).
145. A.D. Walsh, J. Chem. Soc. 2260, 2321 (1953).
146. J. P. Foster and F. Weinhold, J. Am. Chem. Soc. 102, 7211 (1980).
147. M. J. S. Dewar and W. Thiel, J. Am. Chem. Soc. 99, 4899 (1977).
148. G. S. Hammond, J. Am. Chem. Soc. 77, 334 (1955).
149. R. K. Kestner, J. Chem. Phys. 48, 252 (1968).
150. S. F. Boys and F. Bernardi, Mol. Phys. 19, 553 (1970).
151. D.W. Schwenke and D.G. Truhlar, J. Chem. Phys. 82, 2418 (1985).
152. F.J. Olivares del Valle, S. Tolosa, J.J. Esperilla, E.A. Ojalvo and A. Requena, J. Chem. Phys. 84, 5077 (1986).
153. L. Pauling, J.Am. Chem. Soc. 69, 542 (1947).
154. H. S. Johnston, *Gas Phase Reaction Rate Theory* (Ronald Press, New York, 1966).
155. C. Parr and H.S. Johnston, J. Am. Chem. Soc. 85, 2544 (1963).

# Index

## A


Abstract Hilbert space
  notations, 85
  projector, 85
  properties, 86–87
  realizations, 84–85
Acetylene, Auger spectra, 60, 64–65
Acetylene (HCCH), 269, 271
ALCHEMY, 47
Algebraic diagrammatic construction (ADC) scheme, 56–57
Ammonia ($NH_3$), 262–263, 265–266, 269, 273, 281–282
Analytical MPn and QCI gradients, *See* MPn and QCI gradients
Analytical energy derivative methods, 206–212
  coupled cluster (CC), 209–212
  coupled-perturbed Hartree-Fock equations (CPHF), 208
  electron correlation, 209–212
  finite differentiation methods, 207–208
  Hartree-Fock (HF) energy, 208
  history of, 208–212
  impact, 208
  importance, 207
  Møller-Plesset (MP) perturbation theory, 209–212
  quadratic configuration interaction (QCI) theory, 210–212
Angular momentum (J), 133–134
Angular momentum operators, 135
Approximate linear dependencies, 108–111
  approximate hyperplanes, 110
  canonical orthonormalization, 108–110
  linear independence, measure of, 109
  minor theorems, 110–111
  symmetric orthonormalization, 108–110
Auger continuum function, 35–36
Auger cross section, direct contributions, 10–13
Auger cross section, resonant contributions, 13–15
Auger decay, 18, 29, 37
Auger effect, 7, 19
Auger electron emission, 5, 15–17, 19, 21, 25
Auger electron functions, 35–37
Auger emission, 4, 40
Auger initial state, *See* Core hole states
Auger intensities, 33–34
Auger lineshape, 60, 62, 67
Auger overlap amplitude, generalized (GOA), 33, 43, 49
Auger satellites, 58
Auger spectra, chemical information in, 60–65
  fingerprinting, 61–62
  functional groups, 61
  hybridization, 60–61
  solid state spectra, relation to, 63
  symmetry, 62
Auger spectral function, 25
Auger spectra, *See* Molecular auger spectra
Auger spectra, vibronic interactions, 21–28
  Born-Oppenheimer potential energy, 21–22
  decay processes, line profile, 24–25
  electronic transition energy, 22–23
  Franck-Condon factors, 25–28
  Franck-Condon zone, 22
  initial state nuclear motion, 21–22
  multidimensional Hermite polynomials, 26–28
  vibronic profiles, 22–23
Auger states, 33, 38–39
Auger transition amplitude, 32
Auger transition energies, 48
Auger transition moment, 32–33, 35–37

Auger transition rates
annihilation operators, 31–32
Auger continuum function, 35–36
general equations, 34–35
general many-electron wave functions, 29–32
general scattering formulation, 29
Lippmann-Schwinger solution, 29
$L^2$ methods, applications using, 35–36
relaxation, effect of, 34–35
single channel description, 31
theoretical studies, 29–32
transition amplitude, 31
transition probability, 30
Auger transition, 6

## B

Bargmann-Moshinsky basis, 196
Bargmann space, 143
Basis set superposition (BSS), 338–339
Becker's lemma, 105
Bessel's inequality, 93
Bethe-Salpeter equation, 52–54
Binary coupling theory of angular momenta, 135
Bond index and valency, ab initio calculations
bond indices ($B_{ab}$), 331–334, 337
concepts, applications of, 316–344
correlated wavefunctions, results using, 341–344
SCF wavefunctions, results using, 316–340
conclusions, 344–345
correlated wavefunctions, definitions for, 314–316
introduction, 302–307
LPA (L) atomic charges ($q_a$), 331–334, 336
MPA (M) atomic charges ($q_a$), 331–334, 336
references, 346–350
SCF wavefunctions, definitions for, 307–314
bond index, exchange part, 312–313
bond index, statistical interpretation, 313–314
density matrix, second order, 312–313
heuristic, 307–312
valencies ($V_a$), 331–334, 337
Born-oppenheimer approximation, 10, 12, 50, 74
Born perturbation expansion, 11
Boson operator realization, 142–143
Boson polynomials, 194, 196–197, 199
Brillouin theorem, 47
Build-up principle, 187, 189

## C

Canonical finite-dimensional spaces, *See* Finite-dimensional spaces
Canonical labelling process, 171, 176
Carbon monosulfide (CS), 246–256
Carbon monoxide, Auger spectra, 66–73
assignment, 71–72
carbon k-11 Auger, 69
hole-mixing states, 66–70
oxygen k-11 Auger, 70
satellites, 72–73
Carbon monoxide (CO), 253, 257
Carbon monoxide, KVV spectrum, 72
CAS wave function, 47, 49, 57
Channel scattering theory, *See* Many channel scattering theory
Charge-stripping mass (CSM) spectroscopy, 5
$CN^-$, Auger data, 60
CO, Auger data, 39, 60
CO, Auger energies, 46
COLOGNE, 235–237
Configurational state function (CSF), 33, 47–49, 66
Configuration interaction (CI), 43–45, 48–50, 63–64, 67, 71
Core hole processes, 19–20
Core hole states, 9, 16, 18, 24–25, 41
Core type spectra, 5
Correlated wavefunctions, 314–316
calculations, 341–344
Mulliken-Walsh diagrams, 343, 345
Weinbaum type, 341
Correlation state satellites, 39–40
Coster-Kronig structure, 29
Coulson's bond order, 304–305
Counterpoise (CP) correction methods, 339–340
Coupled cluster (CC), 59, 209–212, 215–216, 218

Coupled-perturbed HF (CPHF) theory, 220–223, 242

## D

DIIS method, 237–238
Dimethyl ether, Auger spectra, 60
Dirac bracket notation, 186
Dirac delta operator, 245
Dirac notation, 35
Double-charge-transfer spectroscopy (DCT), 5, 65
Double hole states, 6, 48
Double ionization potentials (DIP:s), 51, 54, 56, 58, 64
Dyson equation, 53
Dyson orbitals (DO:s), 40

## E

Effective interaction matrix, 56
Electron correlation, methods and theories
  appendices, 287–292
  bond lengths, 247
  charges, 247, 255
  comparisons, 212–219
    Møller-Plesset (MP) perturbation theory, 212–215
    QCISD and MP perturbation theory, relationship, 218–219
    Quadratic Configuration Interaction (QCI) theory, 215–218
  conclusion, 285
  dipole moments, 247, 255, 257, 265–266
  electron density distribution, 248, 250, 252, 254
  energies, 247
  energy gradients, 220–235
    MP and QCI gradients, relationship, 229–230
    MPn and QCI gradients, general theory, 231–235
    in MP perturbation theory, 223–225
    orbital energies, 220–223
    in QCI theory, 225–229
    two-electron integrals, derivatives, 220–223
  equilibrium geometries, 261–263, 265–266, 271–276, 278
  geometrical parameters, 267, 270
  harmonic vibrational frequencies, 265–266, 278, 280–283
  infrared intensities, 265–266, 284, 286
  introduction, 206–212
  molecular properties, calculation, 244–285
    ammonia ($NH_3$), measurements, 265–266
    carbon monosulfide (CS), electron density distribution, 248, 250, 252, 254
    carbon monosulfide (CS), measurements, 247
    dipole moment, method dependence, 257
    equilibrium geometries, 260–279
    equilibrium geometries, method dependence, 261–263, 271–276, 278
    geometrical parameters, 267
    geometrical parameters, HOH vs. OH, 270
    harmonic frequencies, method dependence, 278, 280–283
    $H_2O$, measurements, 265–266
    hydrogen fluoride (HF), measurements, 265–266
    infrared (IR) intensities, method dependence, 284, 286
    methane ($CH_4$), measurements, 265–266
    multiple bonded molecules, 267
    nuclear quadrapole moment, method dependence, 259
    one-electron properties, 244–260
    one-electron properties, method dependence, 255
    quadrapole moment (Q), method dependence, 256
    response densities, 244–260
    vibrational spectra, 279–285
  MPn and QCI gradients, implementation, 235–244
    COLOGNE, 235–236
    MPn calculations, 236–237
    MPn gradient calculations, 239–243
    QCI calculations, 237–239
    QCI gradient calculations, 243–244
  nuclear quadrapole moments, 259
  quadrapole moments, 247, 256
  references, 293–299

Energy gradients
analytical expressions, 220
coupled-perturbed HF (CPHF) theory, 220–223
Fock matrix, 222
Lagrangian multipliers, 223, 231, 233
MP and QCI, relationship between, 229–230
MPn and QCI gradients, general theory of, 231–235
orbital energies, 220–223
perturbation dependent expansion coefficients, 220–221
two-electron integrals, derivatives of, 220–223
Equilibrium geometries, 260–279
Ethylene, Auger spectra, 60, 64–65

## F

$F_2$, 269, 276
Fermi golden rule, 4, 29, 38, 41
Final state correlation, 42, 44
Final state correlation effects, 6
Finite-dimensional spaces, 138–161
Bargmann space, 143
betweenness conditions, 146
Boson operator realization, 142–143
commuting property, 139–140
differential operator (D), 139–144
double Gel'fand number, 147, 155–156
general linear group algebras, 154–161
general linear group (GL), 138, 140, 142, 144, 150, 158
highest weight vector normalization, 149
homogeneous polynomial space, properties of, 151–153
homogeneous polynomial spaces, 141–142
irreducible polynomial spaces, 144–154
Kostka number, 147
left translations, 138–139
Lie algebras, 139–141, 153
partial hooks, 150
right translations, 138–139
weight function, 147
Weyl dimension formula, 145
Weyl-Gel'fand-Zetlin patterns, 145–149, 151, 155, 157, 159–160
Weyl generator, 140–141
Weyl reduction rules, 146
Wigner D-function, 150–152, 155–156
Fluorine, Auger spectra, 64
Fock matrix, 222
Formaldehyde (CHO), 269, 272
Franck-Condon factors, 25–28
Franck-Condon zone, 12, 22
Frozen orbital approximation, 32–34

## G

Gel'fand pattern, 154–160, 164
Gel'fand-Weyl basis, 196
Generalized least squares method, 102–108
alternative formulation, 105–107
Becker's lemma, 105
inner projection, properties of, 108
Kalman construction, 105–107
Kalman filter, 107
main component, 103
projectors, 102–104
Given's method, 123
Gramm's determinant, 95
Green's function, 4, 7, 30, 51–58, 63, 71
Bethe-Salpeter equation, 52–54
double ionization potentials (DIP:s), 51, 54, 56, 64
higher order irreducible vertex parts, 54–56
three-particle functions, 57–58
two-particle functions, 51–52, 56–57
Group-subgroup reductions, 129, 145
Group-subgroup reductions, G $\downarrow$ U(n), 166
Group-subgroup reductions, U(n) $\downarrow$ G, 166–168
multiplicity function, 167
Group theory applications
canonical methods, further, 166–186
G $\downarrow$ U(n) reductions, 166
Möbius coordinate description, 172
multiplicity function, level sets of, 172–174
SU(3) $\downarrow$ SO(3) reductions, 168–181
U(n) $\downarrow$ G reductions, 166–168
canonical U(3) WCG–coefficients, 161–165
general principles, 138–161
boson operator realization, 142–143
general linear group, algebras associated with, 154–161
homogeneous polynomial spaces, 141–142

irreducible polynomial spaces, 144–154
left translations, 138–139
Lie algebras, 139–140
right translations, 138–139
introduction, 129–137
noncanonical methods, 187–200
pattern calculus rules, 181–186
references, 201–204
SU(3) ⊃ SO(3), 187–200
build-up principle, 187
nonorthogonal basis, 193–200
SO(3) and SU(2), irreducible polynomial sets, 189–193
Weyl theorems, 187–189

## H

Hadamard circle, 122–123
Hadamard radius, 123
Hadamatd's inequality, 122
Hamiltonian harmonic oscillator, 129
Hamiltonian operator (H), 130, 133–134
Hamiltonian operator (H), symmetry group (G) of, 130–133, 136–138
HAM/3 method, 59, 64
Hamond's principle, 325
Hankel matrix, 122
Hartree-Fock ground state, 53
Hartree-Fock (HF) energy, 208
Hartree-Fock (HF) wave function, 212–213
Hartree-Fock, Open-shell Restricted (OSRHF), 4, 7, 47, 51, 53
Hartree-Fock orbitals (CMO:s), 40
Hartree-Fock self consistent field (SCF) theory, 302, 307
Hartree-Fock spin orbitals, 51, 53, 55
Hellmann-Feynman theorem, 245
Hermitian operator, 130, 132, 142
Hexamethyldisilane, Auger spectra, 61
Hilbert-Schmidt binary product, 88
Hilbert-Schmidt operator space, 88
Hilbert space, 130–131, 133–136, 139, 142–143, 164, 186
Hilbert space, orthonormal basis of (B), 131, 133
$H_2O$, 261–262, 265–266, 280–281, 284
$H_2O$ Auger spectrum, DIPs for, 64
$H_2O$, Auger transitions in, 37
Hole-mixing Auger states, 66–70
Hole-particle excitations, 39
Homogeneous polynomial spaces, 141–142
Hückel-Hubbard approach, 129
Hückel theory, 303, 306, 310, 318
Hydrogen cyanide, Auger spectra, 61
Hydrogen cyanide (HCN), 258–259, 277
Hydrogen fluoride (HF), 253, 260–261, 265–266, 278
Hydrogen peroxide ($H_2O_2$), 269, 274–275
Hyperplanes, 100–102

## I

Initial state correlation (ISCI), 42–43
Irreducible polynomial sets, 189–193
coupled solid harmonics, 190–193
solid harmonics, 189–190, 193
Irreducible polynomial spaces, 144–154
Irreducible tensor operator, 137, 154, 159

## K

Kalman construction, 105–107
KLM spectra, 5
Koopmans double-hole states, 38–40, 44–45
Koopmans theorem, 38–40
Kostka number, 147, 155
Kronecker product representation, 131, 133–134, 136, 154–155
Kryloff basis, 121

## L

Lagrangian multipliers, 223, 231, 233
Lanczos method, 49
Least squares method, 91–97
approximate linear dependencies, 91, 100
Bessel's inequality, 93
concept of the norm, 94–96
covariant representations, 92
Gramm's determinant, 95
linear relations, importance of, 91–92
partitioning technique, 96–97, 119–120, 124
set of elements, geometrical structure of, 94–96
subspace projector, 92–94
Lehman representation, 51
Levy-Hadamard-Gerschgoring theorem, 122
Lie algebras, 129, 137, 139–141, 153, 166, 180
Lie group, 130

LiF, Auger transition energies of, 48
Lifetime-vibrational interference, *See* Vibrational-lifetime interference
LiH, 278
Linear combination of atomic orbitals (LCAO), 302, 307
Linear dependencies, *See* Approximate linear dependencies
Linear group algebras
  Gel'fand pattern, 154–160
  Littlewood-Richardson numbers, 155
  operator patterns, 158
  product law for representation functions, 156
  product law for Wigner operators, 160
  Racah invariants, 160–161
  representation functions, 150, 154
  Schur functions, 157
  unit U(n) tensor operators, 154–155
  Weyl betweenness rule, 157
  Wigner coefficients, 159
  Wigner-Eckart theorem, 159
Linear operators, properties of, 87–88, 97–102
  characteristic polynomial, 98–101, 120–122
  fundamental invariants, 99
  Hankel matrix, 122
  hyperplanes, point deviation from, 101–102
  Kryloff basis, 121
  matrix representation, 97–98
  principal minors, 98–99
Linear relations, search for, 111–119
  error evaluation, 118–119
  numerical example, 117–118
  probability assumptions, 111
  regressands, 112
  regression analysis, canonical, 114–118
  regression analysis, democratic, 113–114
  regression analysis, principles of, 111–113
  regressors, 112
  system analysis, 118–119
Lippmann-Schwinger solution, 29
Littlewood-Richardson numbers, 155
Localized molecular orbital, 328, 330
Lorentzian profile, 19
LPA scheme, 326–340

## M

Many-body factor, 38–40
Many channel scattering theory, 8–20
  Auger cross section, 10–15
  Auger decay, 18
  continuum functions, electronic-vibrational, 10–12
  coordinate representation, 9–10
  core-hole molecular species, 9
  electronic Hamiltonian matrix, 17–18
  generalized transition matrix, 11–12
  Lorentzian profile, 19
  non-adiabatic corrections, 11–12
  nuclear motion, 15–16
  nuclear wave function, 13
  post-collision interaction (PCI), 9, 19–20, 29
  resonant scattering processes, 16–17
  resonant-transition matrix, 13–14, 17–18
  resonant wave function, 9–10
  Rydberg series, 9
  scattering functions, 9–10, 13
  state interference effects, 16–19
  state vector space, 9
  transition amplitude, 11–13, 15–16, 18
Mayer bond indices, 326
McWeeny's normalization, 312–313
Methane, 263–266, 283
Methane, Auger spectra, 60, 64
Methanol, Auger spectra, 60
Methyl cyanide, Auger spectra, 61
MNDO, 323
Möbius coordinates, 170
Möbius plane, 170
Molecular auger spectra
  algebraic diagrammatic construction (ADC) scheme, 56–57
  analysis of, 5, 38–44
    auger and photoelectron spectra, comparative analysis, 41–44
    many-body factor, 38–40
    molecular orbital factor, 40–41
  applications, 60–65
    chemical information, 60
    fingerprinting, 61–62
    functional groups, 61
    $H_2O$ spectrum, DIPs for, 64
    hybridization, 60–61
    Ne and $NH_3$, comparison, 62
    solid state spectra, relation to, 63
    symmetry, 62
  applications, survey of, 63–65
  basic overlap integrals, 25–28
  Born-Oppenheimer (BO) approximation, 10, 12, 50, 74

Born pertubation expansion, 11
Brillouin theorem, 47
CAS wave function, 47, 49, 57
charge-stripping mass (CSM) spectroscopy, 5
computational methods, 7
conclusions, 64–75
configurational state function (CSF), 33, 47–49, 66
configuration interaction theory, 8, 16–17
*conjugate transitions, neglect of*, 41, 43
core excited initial states, structures, 72–73
core-hole states, 9, 16, 18, 24–25
Coster-Kronig structure, 29
coupled cluster method, 59
decay processes, 24–25, 29
double charge transfer (DCT) spectroscopy, 5
double coincidence, 5
double hole states, 6–7
double ionization potential (DIP:s), 51, 54, 56, 64
Dyson orbitals (DO:s), 40
early investigations, 6–7
electron emission, 5
electronic transition matrix, 26, 41
"electron rich" molecules, 7
Fermi's golden rule, 29, 38, 41–42
final state correlation (FSCI), 6, 42, 44
Franck-Condon analyses, 12, 22, 25–28
frozen orbital description, 30, 35
generalized overlap amplitude (GOA), 33, 43, 49
Green's function methods, 7, 30, 51–58
  Bethe-Salpeter equation, 52–54
  higher order irreducible vertex parts, 54–56
  three-particle functions, 57–58
  two-particle functions, 51–52
  two-particle functions, other treatments, 56–57
HAM/3 method, 59, 64
Hartree-Fock equation, 32
Hartree-Fock orbitals (CMO:s), 40
Hartree-Fock spin orbitals, 51, 53, 55
Hermite polynomials, 26–28
initial state correlation (ISCI), 42–43
*intermediate state Hamiltonian operator*, 15
introduction, 5–7
KLM spectra, 5
Koopmans double-hole states, 38–40, 44–45
Lanczos method, 49
Lehmann representation, 51
$L^2$ methods, 36
many-channel resonant scattering theory, 8–10, 16–19
molecular orbital (MO) analysis, 38–40, 45–46
molecular valence spectra (CVV), 5
moment theory, 36
natural orbitals (NO:s), 40
*non-local vs. local operator*, 15
nuclear kinetic energy operator, 8–9
one-center model, 40–41
one-particle calculations, Auger energies, 6, 46
one-particle methods, 5–6, 45–46
one-step resonant scattering, 7
orbital orthogonality, 42, 44
orbital transition matrix elements, 41, 43
other methods, 59
outgoing electron approximation, 41, 43
photoelectron-photoelectron (PEPECO) methods, 5
photoelectron-photoion (PEPICO) methods, 5
photoionization, 13–19, 43–44
photo-induced, 8
Racah coefficient, 33
radiative (non-radiative) transitions, 41–43
RAS wave function, 47, 49
references, 76–82
resonant-transition matrix, 14, 17
Roothaan many operator, 47
sample analysis: carbon monoxide, 66–73
  assignment, 71–72
  carbon k-11 auger, 69
  CO dication, breakdown effects, 71
  hole-mixing auger states, 66–70
  KVV peak assignments, 72
  oxygen k-11 auger, 70
  satellites, 72–73
  $\Sigma^+$ states, 67
satellite transitions, 72–73
scanning techniques, 5
scattering process, as a, 8–20
  auger cross section, resonant contributions, 13–15
  channel scattering theory, 8–10
  post-collision interaction (PCI), 9, 19–20, 29
  state interference effects, 16–19

Molecular auger spectra (*continued*)
scattering process, as a
auger cross section, direct contributions, 10–13
nuclear motion, local approximation, 15–16
scattering transition amplitude, 14, 16
Slater determinant (SD), 33, 47, 54
spin-restricted theory, 40–41
state interference effects, 19
Stieltjes imaging method, 36–37
surface imaging techniques, 5
theoretical research, 5–7
transition amplitude, 31–32
transition operator **T**, 15
transition rates, 29–37
electron functions, 35–37
frozen orbital approximation, 32–34
general many-electron wave functions, 29–32
relaxation, role of, 34–35
transition moments, 35–37
water molecule intensities, 37
transitions, final states of, 6
types of, 5–6
vibronic coupling constant, 15
vibronic interaction, 21–28
approaches, adiabatic, 21–23
approaches, vertical, 21–23
Franck-Condon factors, 25–28
lifetime-vibrational interference effects, 24–25
vibronic profiles, 22
vibronic transitions, 24–25
wave function methods, 7, 47–50
LiF, MCSCF Auger transition energies of, 48
multi-configuration self-consistent field (MCSCF), 7, 47–48
open-shell restricted Hartree-Fock (OSRHF), 7, 47, 51, 53
semi-internal configuration interaction (SEMICI), 7, 48–50
Wentzels ansatz, 29–30, 33
Wick's time ordering operator, 51
Molecular orbital calculations, *See* bond index and valency
Molecular orbital factor, 40–41
Molecular orbital (MO) theory, 302–307
Molecular valence spectra (CVV), 5
Møller-Plesset (MP) perturbation theory, 209–215, 223–225
energy gradients in, 220, 223–225
Hartree-Fock (HF) wave function, 212–213
Rayleigh-Schrödinger expansion, 212–213
relationship to QCISD theory, 218–219
MPA scheme, 326–340
MPn and QCI gradients, 235–285
COLOGNE, 235–237
DIIS method, 237–238
equilibrium geometries, 260–279
implementation of, 235–244
molecular property calculations, 244–285
carbon monosulfide (CS), 246–256
difference response density, 251–252
Dirac delta operator, 245
electron density distribution, 245–246, 249–254
equilibrium geometries, 260–279
harmonic frequencies, 278, 280–283
Hellmann-Feynman theorem, 245
infrared intensities, 284, 286
one electron properties, 244–260
response densities, 244–260
vibrational spectra, 279–285
MPn calculations, 236–237
MPn gradient calculations, 239–243
amplitude calculations, 241
integral derivatives, evaluation of, 243
integral transformations required, 239–240
two-particle density matrix, 241–242
Z-vector equation, 239, 242–243
QCI calculations, 237–239
QCI gradient calculations, 243–244
vibrational spectra, 279–285
Mulliken bond order, 305
Mulliken notation, 35
Mulliken's population analysis, 308–309
Mulliken-Walsh diagrams, 343, 345
Multi-configuration self-consistent field (MCSCF), 7, 47–48
Multiplicity function ($M_t(p, q)$), 170–171, 176–179

## N

Natural orbitals (NO:s), 40
$N_2$, Auger data, 60
$NH_4Cl$, Auger spectra, 63
Nitrogen, Auger spectra, 63–64
Nuclear approximation, local motion, 15–16
Numerator pattern calculus factors, 178–181

## O

One-center model, 40–41
One-particle approach, 4, 6
One-particle methods, 5–6, 45–46
Open-Shell Self Consistent Field (OSSCF), 7
Orthonormality property, 86

## P

Partitioning technique, 96–97, 119–120, 124
*Pattern calculus rules, 181–186*
Photoelectron-photoelectron (PEPECO) experiments, 5
Photoelectron-photoion (PEPICO) experiments, 5
Photoelectron spectra, analysis of, 41–44
Photoelectron transition moment, 42–43
Photoion-photoion (PIPICO) experiments, 5
Polarization counterpoise (CP) correction methods, 339–340
Post-collision interaction (PCI), 9, 19–20, 29
PRDDO, 323
*Product law for representation functions, 156*
Product law for Wigner operators, 160
Projectors, 85, 88, 102–104, 115

## Q

QCI gradients, *See* MPn and QCI gradients
Quadrapole moments, 247, 256, 259
Quadratic configuration interaction (QCI) theory, 210–212, 215–218, 225–229
  approach, 216–218
  coupled cluster (CC), 215–218
  energy gradients in, 220, 225–229
  excitation amplitudes, 216–218
  relationship to MP perturbation theory, 218–219
Quantum chemistry, linear algebra usage in appendices
  characteristic polynomial calculation, 120–122
  eigenvalue evaluation by partitioning, 124
  eigenvalues of **T** estimates, 122–123
  matrix inversion by partitioning, 119–120
  approximate linear dependencies, 108–111
  minors, theorems, 110–111
  orthonormalization procedures, 108–110
  generalized least squares method, 102–108
  generalization, 102–105
  inner projection, properties, 108
  Kalman construction, 105–107
  introduction, 84–91
  abstract Hiller space, 84–85
  abstract Hiller space, properties, 86–87
  linear operators, properties, 87–88
  matrix inequalities, 88–89
  operator inequalities, 88–89
  quantum theory problems, 89–91
  useful notations, 85
  least squares method
  geometrical structure, 94–96
  linear relations, importance, 91–92
  partitioning technique, 96–97
  subspace, projector on, 92–94
  linear operators, properties, 97–102
  characteristic polynomial, 98–101
  hyperplanes, deviations of points, 101–102
  matrix representation, 97–98
  linear relations, search for, 111–119
  econometrics, numerical example, 117–118
  error evaluation, 118–119
  regression analysis, canonical, 114–117
  regression analysis, "democratic," 113–114
  regression analysis, principles of, 111–113
  system analysis, 118–119
  references, 125–126
Quantum theory
  general uncertainty relations, 90
  matrix inequalities, 88–89
  mean quadratic deviation, 90
  operator inequalities, 88–89
  problems, 89–91

## R

Racah coefficient, 33, 154, 160
Racah invariants, 160–161
Radiative (non-radiative) transitions, 41–43
RAS wave function, 47, 49
Rayleigh-Schrödinger expansion, 212–213
Regressands, 112
Regression analysis, 111–117
Regressors, 112
Response densities, 244–260

Restricted solution manifold, 129
Roothaan many operator, 47
Rota's umbral calculus, 138, 157

## S

Schmidt's successive orthonormalization procedure, 84
Schrödinger equation, 129
Schur functions, 157
Schur's lemma, 132
Self-Consistent Field, Multi-Configuration (MCSCF), 4, 7, 47–48
Semi-Internal Configuration Interaction (SEMICI), 4, 7, 48–50
SIND01 wavefunctions, 320–322, 344
Single determinant SCF wave functions, 307–314
  basis set superposition (BSS), 338–339
  bond index, 312–314
  bond indices and valences, 331–335, 337
  calculated atomic charges, 336
  calculations, 316–340
  counterpoise (CP) correction methods, 339–340
  Hamond's principle, 325
  heuristic definition, 307–312
  localized molecular orbital, 328, 330
  LPA scheme, 326–340
  Mayer bond indices, 326
  McWeeny's normalization, 312–313
  MNDO, 323
  molecular valency, 321–323
  MPA scheme, 326–340
  Mulliken's population analysis, 308–309
  polarization counterpoise (CP) correction methods, 339–340
  PRDDO, 323
  second order density matrix, exchange part, 312–313
  SIND01 wavefunctions, 320–322
  Wiberg bond index, 320–321
Slater-Condon rules, 43
Slater determinant (SD), 33, 47, 54, 307, 315
Spin-free quantum chemistry, 129
Spin-restricted theory, 40
Stieltjes imaging method, 36–37
SU(3) ⊃ SO(3) example, 187–200
  Bargmann-Moshinsky basis, 196
  boson polynomials, 194, 196–197, 199
  build-up principle, 187, 189
  Gel'fand-Weyl basis, 196
  irreducible polynomial sets, 189–193
  $L_R$ operator, 189–192, 198
  nonorthogonal basis I, 193–196
  nonorthogonal basis II, 196–200
  Weyl theorems, 187–189
SU(3) ↓ SO(3) reduction, 168–181
  canonical generators, 169
  canonical labelling process, 171, 176
  highest weight (hw) states, 169
  L-value, 169–170
  Möbius coordinate description of $R^2$ plane, 171, 176172
  Möbius coordinates, 170
  Möbius plane, 170
  multiplicity function ($M_L(p,q)$), 170–171, 176–180
  multiplicity function ($M_L(p,q)$), level sets of, 172, 174
  multiplicity problem, 169–170
  multiplicity space $V_L(p,q)$, 178
  numerator pattern calculus factors, 178–180

## T

Tensor product space ($T_g$), 130, 132–134, 136
Tetramethylsilane, Auger spectra, 61
Trinitrobenzene, Auger spectra, 61
Trinitrotoluene, Auger spectra, 61
Triple ionization potentials (TIP:s), 58

## U

Unitary equivalence, 132
Unitary group techniques, 129, 135
Unitary group (U), 135–136, 138, 145, 154
Unitary transformations, 135

## V

Vibrational-lifetime interference, 16, 24–25

## W

Wave function approach, 4, 7
Wave function methods, 7, 47–50
Weinbaum type wavefunction, 341
Weinstein radius, 123
Wentzel's ansatz, 29–30, 33
Weyl betweenness rule, 157

Weyl dimension formula (Dim[m]$_n$), 145, 147–148, 152
Weyl-Gel'fand-Zetlin patterns, 145–149, 151, 155, 157, 159–160
Weyl generator, 140–141
Weyl reduction rules, 146
Weyl theorems, 187–189
Wiberg bond index, 320–321
Wick's time ordering operator, 51
Wigner-Clebsch-Gordan (WCG) coefficients, 129, 137, 154, 156–165
  calculating, methods of, 161–162
  Wigner operator, 161–165
Wigner coefficients, 159, 163
Wigner D-function, 150–152, 155–156
Wigner-Eckart theorem, 159
Wigner operator, 161–166, 181

## Z

Z-vector equation, 239, 242–243